Zootaxa 5554 (1): 001–306
https://www.mapress.com/zt/

Monograph

ISSN 1175-5326 (print edition)
ZOOTAXA
ISSN 1175-5334 (online edition)

https://doi.org/10.11646/zootaxa.5554.1.1
http://zoobank.org/urn:lsid:zoobank.org:pub:26D520E1-4A81-42FC-B9D5-5056605586A1

ZOOTAXA

5554

A new forest lizard fauna from Caribbean islands (Squamata, Diploglossidae, Celestinae)

MOLLY SCHOOLS[1] & S. BLAIR HEDGES[2]
Department of Biology, Center for Biodiversity, 1925 N 12th St Suite 502, Philadelphia, PA 19122, USA
[1]*Corresponding author. molly.schools@temple.edu, https://orcid.org/0000-0002-2687-7885*
[2] *sbh@temple.edu, https://orcid.org/0000-0002-0652-2411*

Magnolia Press
Auckland, New Zealand

Accepted by M. Heinicke: 5 Nov. 2024; published: 16 Dec. 2024

MOLLY SCHOOLS & S. BLAIR HEDGES
A new forest lizard fauna from Caribbean islands (Squamata, Diploglossidae, Celestinae)
(*Zootaxa* 5554)

306 pp.; 30 cm.

16 Dec. 2024

ISBN 978-1-77973-229-3 (paperback)

ISBN 978-1-77973-230-9 (Online edition)

FIRST PUBLISHED IN 2024 BY

Magnolia Press

P.O. Box 41-383

Auckland 1041

New Zealand

e-mail: magnolia@mapress.com

https://www.mapress.com/zt

ISSN 1175-5326 (Print edition)

ISSN 1175-5334 (Online edition)

Table of Contents

Abstract

The taxonomy of Neotropical forest lizards (Diploglossidae) has been the subject of controversy because of a paucity of diagnostic characters and genetic data. Recent molecular studies have produced phylogenies that are highly supported but have few individuals represented for each species. These studies have corrected generic names and defined new genera and subfamilies in Diploglossidae. However, they have shown that multiple species are not monophyletic or have high levels of genetic divergence, indicating the need to define new species. Three subfamilies, 12 genera, and 56 species of diploglossid lizards are currently recognized; 25 of these are in the subfamily Celestinae. We conducted a systematic revision of Caribbean celestine forest lizards (from the Cayman Islands, Jamaica, and Hispaniola) using DNA sequence data from 372 individuals, supplemented by both conventional and unconventional morphological characters from 958 preserved specimens. In some cases, we obtained DNA sequence data from museum specimens, including types, nearly 200 years old. We propose and use a new species delimitation method based on time of divergence. We define 17 new species, elevate 17 subspecies, and elevate one species from synonymy, resulting in 35 newly recognized species. Additionally, we synonymize two pairs of previously recognized subspecies and one pair of species. This increases the number of celestine species from 25 to 59 and raises the total number of diploglossids to 90 species. Of those, 63 occur on Caribbean islands and all are endemic to those islands. Fourteen Caribbean celestine species (24%) are Critically Endangered, 17 species (29%) are Endangered, and 1 species (2%) is Vulnerable, resulting in a proportion of threatened species (54%) more than twice as high as the average for reptiles, based on IUCN Redlist criteria. Three of the Critically Endangered species are possibly extinct because of human activities during the last two centuries. Several of the surviving species are near extinction and in need of immediate protection. Extensive forest loss on Caribbean islands has led to the decline of Caribbean forest lizards, which rely on forests as their primary habitat. In addition to deforestation, the introduction of the Small Indian Mongoose is in part responsible for the decline of Caribbean diploglossid lizards. That invasive predator was introduced as a biological control of rats in sugar cane fields in the late 19th Century (1872–1900), immediately resulting in a mass extinction of reptiles. The ground-dwelling and diurnal habits of diploglossids have made them particularly susceptible to mongoose predation.

Key words: evolution, systematics, biogeography, taxonomy, lizard, Reptilia, Caribbean, West Indies, Jamaica, Hispaniola, deforestation, mongoose, historical DNA

Introduction

Neotropical forest lizards (Diploglossidae) are distributed throughout the Neotropics, including the Caribbean islands, Middle America, and South America. Previously referred to as galliwasps, these smooth-scaled, forest-dwelling lizards have been assigned to 56 species in 12 genera and three subfamilies (Schools & Hedges 2021). Until recently, the taxonomy had been a subject of controversy because of conflicting morphological characteristics and a lack of genetic data. A well-supported molecular phylogeny then formed the basis of a new taxonomy that defined three new subfamilies (Celestinae, Diploglossinae, and Siderolamprinae), resurrected four genera (*Panolopus* Cope, 1862b, *Sauresia* Gray, 1852, *Siderolamprus* Cope, 1861, and *Wetmorena* Cochran 1927), defined four new genera (*Advenus* Schools & Hedges 2021, *Caribicus* Schools & Hedges 2021, *Comptus* Schools & Hedges 2021, and *Mesoamericus* Schools & Hedges 2021), and recognized two previously defined species (*Celestus striatus* and *Celestus macrolepis*) to better account for the diversity in this family (Schools & Hedges 2021). We defined these genera and subfamilies based on traditional and nontraditional morphological characteristics. More recently, a new genus and species of celestine, *Guarocuyus jaraguanus* Landestoy *et al.* 2022 was discovered and described based on genetic and morphological data (Landestoy *et al.* 2022). The discovery of *Guarocuyus* rendered several of the diagnostic characteristics at the subfamilial level (Schools & Hedges 2021) obsolete. Furthermore, an increased sample size of the species *Celestus macrotus* rendered the diagnostic characteristic of axilla-to-groin distance obsolete at the generic level (Landestoy *et al.* 2022).

Previous studies of diploglossid lizards that used genetic and genomic data have indicated that several Caribbean species are either not monophyletic or have high levels of genetic divergence warranting the definition of new species (Schools & Hedges 2021; Landestoy *et al.* 2022; Schools *et al.* 2022). Our objective was to address this this question by conducting a comprehensive revision of the Caribbean species of Celestinae using molecular and morphological data. To do this, we used conventional and unconventional morphological traits together with molecular and geographic data. The results revealed a surprising hidden diversity of species, some of which are likely extinct because of human-mediated alterations of habitat and invasive species. Using molecular data from 372 diploglossids and examining 958 preserved specimens, we have identified and described 17 new diploglossid species and elevated 17 subspecies to species. Two sets of subspecies and one set of species were synonymized based on low levels of genetic divergence and a lack of diagnostic characters. In addition, we analyzed the impact of deforestation on Caribbean forest lizards. Remaining primary forest in Haiti accounts for <1% of the total land area, whereas remaining primary forest in the Dominican Republic is estimated to be ~5% (Hedges & Conn 2012; Hedges *et al.* 2018). We consider this extreme habitat destruction a threat to nearly all Caribbean diploglossid lizards. Finally, we reviewed and analyzed historical collection data and present evidence that implicates a single introduced predator, the Small Indian Mongoose, *Urva auropunctata* (Hodgson), in several likely extinctions of Caribbean forest lizards.

Materials and Methods

Molecular Analyses

The molecular dataset comprised 372 individuals (Appendix 1) and 6,948 total aligned nucleotide sites from mitochondrial genes (CytB, ND2, 12S rRNA, and 16S rRNA) and nuclear genes (AMEL, BDNF, PRLR, RAG1, and ZFP36). We contributed 586 new sequences from 284 samples, which were included together with sequences already deposited in Genbank from earlier studies (Schools & Hedges 2021; Landestoy *et al.* 2022; Schools *et al.* 2022), and those generated earlier in the laboratory of SBH (e.g., Dennison 2010) but never formally published. We performed DNA extractions with the DNeasy Blood and Tissue kit (Qiagen, Massachusetts, USA), and we used phenol chloroform extractions for degraded samples and those with a low yield. We performed PCR amplification under standard reaction conditions as outlined elsewhere (Hedges *et al.* 2008). Localities, Genbank accession numbers, and museum numbers (if applicable) for all sequences used are in Appendix 1. We performed alignments with MUSCLE in MEGA X (Kumar *et al.* 2018).

Historical DNA. We also used shotgun genomic sequencing with samples from old museum specimens that were important for taxonomic purposes. These included (age of specimen noted in brackets, from museum data and type catalogs) *Celestus crusculus* (holotype = MCZ R-6051 [1878]), *C. fowleri* (holotype = MCZ R-125601 [1970]), *C. macrolepis* (holotype = BMNH 1946.8.3.82 [1845 or earlier]), *C. occiduus* (holotype = BMNH XV.115a [1802

or earlier], syntype of *Diploglossus shawii* (synonymized with *C. occiduus*) = MNHN 0.1227 [1802 or earlier], and MNHN 0.2855 [1834 or earlier]), *C. striatus* (holotype = BMNH 1946.8.8.3 [1839 or earlier]), and *Sauresia sepsoides* (holotype = BMNH 1946.8.29.29 [1852 or earlier]).

Libraries were sequenced on a partial lane of an Illumina NovaSeq 6000 PE150 S4 v1.5 run, by Daicel Arbor Biosciences. Data were demultiplexed on-board into raw FASTQs using the unique combinations of i7 and i5 index sequences for each library. These FASTQs were transferred to the Daicel Arbor Biosciences analysis platform and analyzed with FastQC. Trimmomatic (v0.39, with parameters ILLUMINACLIP:TruSeq3-PE.fa:2:30:10 LEADING:20 TRAILING:20 MINLEN:50 SLIDINGWINDOW:4:20) was used to trim low-quality bases and putative adapter sequence, followed by FastQC analysis of the trimmed reads. To improve mapping, R1 and R2 reads were merged using Flash (version 1.2.11, with parameters -r 151 -f 200 -s 55). The merged and unmerged reads were then combined and mapped to appropriate mitochondrial genomes/genes using bwa mem (version 0.7.17, default parameters) and sorted according to genomic coordinates using SAMtools (v1.15.1). PCR duplicates were removed using GATK MarkDuplicates (http://broadinstitute.github.io/picard/, v4.2.5.0) applying the STRICT validation stringency and the REMOVE_DUPLICATES parameter. Mapping statistics for the original and the deduplicated bam files were collected using SAMtools stats and the unmapped reads were subsequently removed. In the final step, consensus sequences were generated using bcftools (version 1.16, using the --ploidy-file option to set the ploidy to 1 for mitogenomes and mt genes and 2 for nuclear genes) and converted to FASTA format using seqtk (version 1.3-r106).

Of the eight samples, two (*C. crusculus* and *C. occiduus*-MNHN 0.1227) did not yield useful sequences of any kind, and no useful nuclear gene sequences were obtained using references for 11 nuclear genes. However, the remaining six samples yielded ~4400 bp of aligned mitochondrial DNA sequence (12S, 16S, ND2, and CytB). The Genbank accession numbers of the mitochondrial references are EU747729.1 (*Ophisaurus attenuatus*) for all four genes, with additional references of MW824915.1 (*Celestus crusculus*) for 12S and 16S, MW824727.1 (*Celestus duquesneyi*) for ND2, and MW824664.1 (*Celestus barbouri*) for CytB. During the bioinformatics stage, we found that using "bwa mem" (>70 bp) and high-quality nucleotides helped avoid reference bias, as opposed to "bwa aln" and low-quality nucleotides. In addition, we found that using two different references (but not too distant) for each target was useful as a check for reference bias and to capture different regions of the target, generating a more complete consensus sequence.

Molecular phylogenetics and time estimation. We used Maximum Likelihood (ML) and Bayesian methods to conduct phylogenetic analyses, with *Pseudopus apodus* (Anguidae) as the outgroup. We generated our ML phylogeny using IQ-tree v2.1.2 (Minh *et al.* 2020) and assessed branch support with 2000 ultrafast bootstrap replicates. ModelFinder identified the GTR + F + I + G4 model as the optimal substitution model for our analysis. We used a GTR + Γ + I model in Bayesian analyses performed with MrBayes 3.2.7 (Ronquist *et al.* 2012). We ran four chains for one million generations each, with a 25% burn-in and sampling every 100 generations. We quantified nodal support for Bayesian trees with posterior probabilities (PP) and assessed convergence by monitoring the standard deviation of split frequencies (<0.01 in all cases).

With our ML tree, we generated a timetree using RelTime (Tamura *et al.* 2012), as this program outperforms many other dating methods while using less computational power (Barba-Montoya *et al.* 2021; Kumar 2022). As calibrations, we used a bounded uniform distribution with the 95% confidence intervals from internal nodes as maxima and minima from the secondary calibrations (calibrations derived from other molecular dating studies) used in Schools & Hedges (2021). For this analysis, we used a local clock type along with a GTR + Γ + I model.

Species delimitation using time of divergence. Besides using morphology and phylogeny as means of delimiting species, we estimated times of divergence from a molecular-clock analysis. We preferred time of divergence over the commonly used percent genetic divergence because time is universal whereas genetic divergence varies with taxon, gene, and rate correction used. Hedges *et al.* (2015) showed that diverse species of organisms were separated by a modal time of about 1–3 million years. For vertebrates, they obtained a modal time of 2.1 Ma with a confidence interval of 2.55–1.74 Ma. However, for species delimitation, we are more interested in the minimum time of speciation, rather than the mode. Unfortunately, the data for speciation time come from intervals between crown and stem times, not actual speciation times, which are otherwise difficult to estimate (Hedges *et al.* 2015). The speciation time is estimated for taxonomic groups by overlapping intervals and calculating the mode.

Crown times and stem times are often more practical to use for delimitation. If we calculate modal confidence intervals (Hedges & Shah 2003) for vertebrate crown and stem times from the same data (Hedges *et al.* 2015: supplementary data), we get: 0.20–0.68 (Hedges & Shah mode, 0.41) Ma for crown time and 0.85–3.16 (Hedges &

Shah mode, 1.91) Ma for stem time. For further reference, using data from Hedges *et al.* 2015, the modal confidence interval for vertebrate populations (within species) is 0.03–0.09 Ma, much lower than either crown or stem time. Therefore, we can evaluate any single stem or crown time estimate in the context of those intervals, but especially considering the CI of the speciation interval's maximum crown time (0.68 Ma) and minimum stem time (0.85 Ma), which are similar, providing a delimitation boundary. Although speciation typically takes 1–3 million years, two lineages separated by < 0.7 Ma are more likely to be populations of the same species rather than different species. Because speciation time varies, this should not be taken as a precise cutoff but instead used together with other data such as phenotype and distribution.

As a secondary means of species delimitation for comparison, we used the ASAP method (Puillandre *et al.* 2021; ASAP 2023). For this, we used the mitochondrial genes from our nine-gene alignment (CytB, ND2, 12S rRNA, and 16S rRNA) because the nuclear gene sequences were not available for many samples. ASAP functions by applying different partition schemes to the provided data and taking both the probability that each partition represents a species and the barcode gap width between the different partition schemes into account when determining the optimal partitioning scheme. This analysis was performed using the Simple Distance model and the result with the lowest ASAP score was considered to be the optimal group number.

Morphological Analyses

We identified non-overlapping, diagnostic, morphological characters that distinguish species in the majority of pairwise comparisons after examining representatives of 58 different species (Appendix 2). To determine diagnostic characters, we initially grouped specimens known to be conspecific based on genetic data and subsequently analyzed their morphological traits for diagnostic consistency. We scored a primary suite of 31 morphological traits used in the diagnoses including four of pattern, four of scalation, and 23 of body proportions (Figs. 1–2). Those characters included some used in past studies of diploglossid lizards (Schools & Hedges 2021; Landestoy *et al.* 2022) as well as non-conventional characters not used previously or commonly. Scale terminology was adapted from the descriptions and definitions of Savage *et al.* (2008) and revised for consistency (Fig. 1). Most celestine species have two loreal scales, comparable to those designated as loreal 2 and loreal 3 by Savage *et al.* (2008). We retained this numbering scheme as this will make our head scale terminology applicable to mainland diploglossids that have three loreal scales (loreals 1, 2, and 3); however, in the descriptions we often reference loreal scales in the order of their appearance (1st loreal, 2nd loreal, etc.), not to be confused with loreals 1–3.

All measurements were taken with digital calipers (Mitutoyo; 0.01 mm accuracy). Although we could diagnose some new taxa by conventional characters alone, the non-conventional characters also proved useful. These non-conventional measurements included: presence of dots arranged in bars in the lateral line, total lamellae counted on one forelimb, total strigae counted on ten scales, relative length of digits on one hindlimb, relative distance between angled subocular and mouth, relative eye length, relative mental width, relative postmental width, relative cloacal width, relative prefrontal width, relative largest supraocular width, relative longest finger length, relative distance between the ear and eye, relative frontal width, relative nasal scale height, relative angled subocular height, relative distance between the eye and nostril, relative canthal iii width, relative angled subocular width, and the relative nasal width.

To avoid bias from allometric growth differences in quantitative traits, we used only sexually mature individuals. Because many specimens were inaccessible for gonadal examination, including types and those in museums with restrictions on dissection, direct observation of sexual maturity was not possible. Therefore, we inferred sexual maturity for each species using body size, including only individuals that were within 25% of the largest individual of that species for body proportion measurements (Wiens *et al.* 2006). Because of the limited data on specimen sex, males and females are not differentiated in the following list of measurements. From a taxonomic standpoint, this means that our diagnoses are more inclusive because they separate all individuals and not just one sex.

Pattern. We scored the following four pattern characters (Fig. 2). *Dorsal pattern*: absent (a), bands (b), irregular flecks (if), flecks in series (fis), irregular dots (id), dots in series (dis), mottled (m), lineate (l), chevrons (c), dots in chevrons (dic), and bicolored (bi). *Head markings*: present is the form of a dark outline around head scales or irregular dark markings on the head (p), absent (a). *Longitudinal paramedian markings*: present (p), absent (a). *Dots in bars in the lateral line*: present (p), absent (a). Variations in pattern exist within each species but usually are less than variation among species. Therefore, characterizing the typical (representative) pattern for each species is possible, while recognizing that each animal can differ from that pattern in some respects.

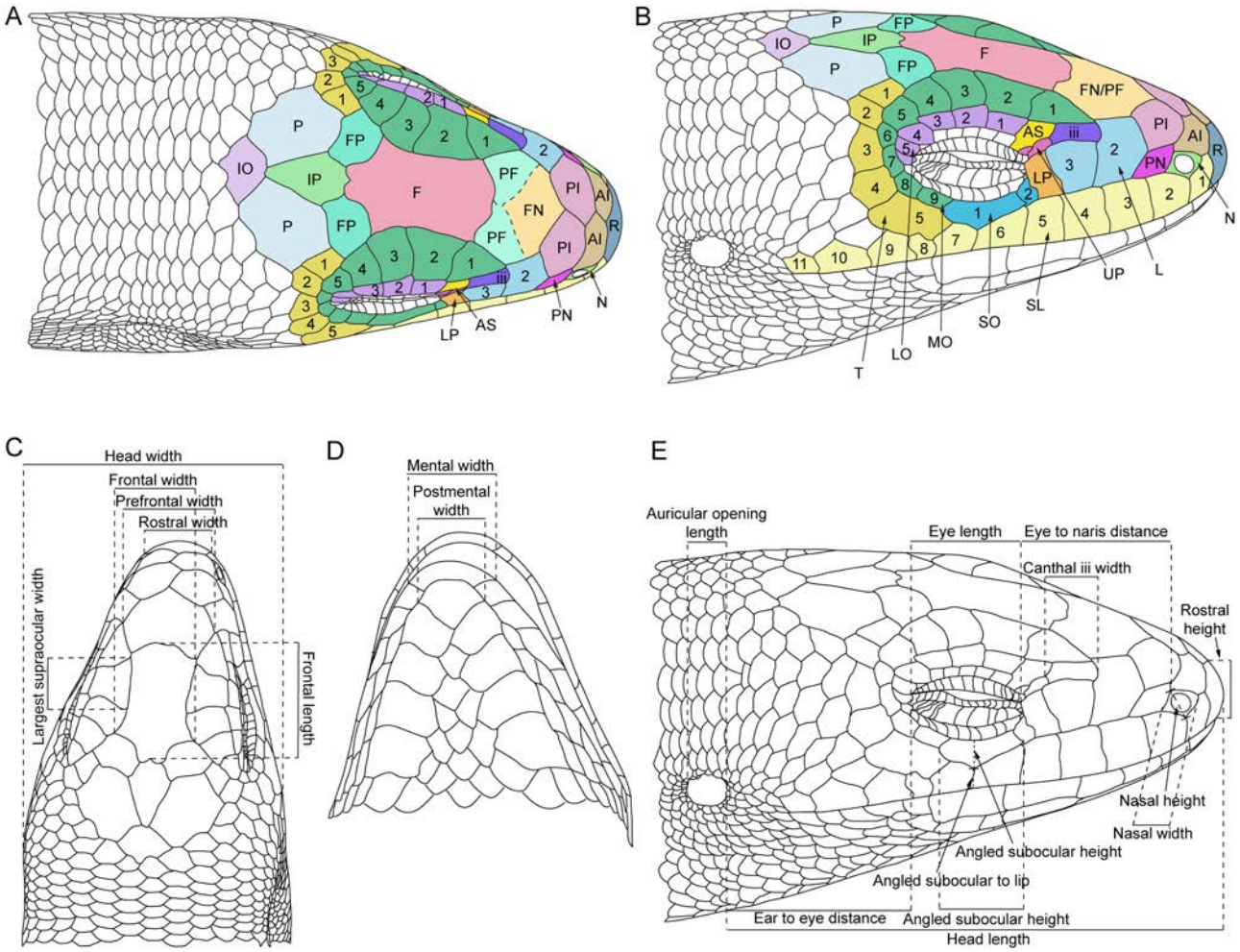

FIGURE 1. Head scalation of diploglossid lizards. Locations and names of scales on top (A) and side (B). Measurements taken on top (C), bottom (D), and side (E). Key is as follows: AI (anterior internasal), AS (anterior supraciliary), F (frontal), FN (frontonasal), FP (frontoparietal), IO (interoccipital), IP (interparietal), L (loreal), LO (lateral ocular), LP (lower preocular), MO (median ocular), N (nasal), P (parietal), PN (postnasal), PF (prefrontal), PI (posterior internasal), R (rostral), SL (supralabial), SO (subocular), T (temporal), UP (upper preocular), and iii (canthal three).

Scalation. Our suite of scale characters included four counts. Midbody scale rows were counted around the body midway between the forelimbs and hindlimbs. Ventral scales were counted in a line from (and including) the chin scale (mental) to the vent. Lamellae were counted on all digits of one forelimb and added together. Strigae were counted on ten scales in the longitudinal paramedian region and added together.

Body Proportions. We measured the following characters: snout-vent length (SVL; tip of snout to vent opening), toe length (TL; length of all toes on one hindlimb added together), distance between the angled subocular and the mouth (ASO; the closest distance between the two features), eye length (EL; distance between anterior and posterior edges of ocular opening), forelimb length (FL; distance from where the forelimb meets the body to the tip of the longest digit), auricular length (AL; distance between anterior and posterior edges of auricular opening), rostral height (RH; vertical height of the rostral scale at the tallest point), head length (HL; tip of snout to anterior edge of auricular opening), mental width (MW; width of the mental scale at the widest point), postmental width (PMW; width of the postmental scale at the widest point), cloacal width (CW; width of the cloaca at the widest point), prefrontal width (PFW; width of the prefrontal scale at the widest point), largest supraocular width (SOW; width of the largest supraocular scale at the widest point), longest forelimb digit length (LFDL; length of the longest forelimb digit from the base to the tip), distance between the ear and eye (EED; distance between the anterior border of the auricular opening and the posterior border of the ocular opening), head width (HW; head width at the widest point of the head), frontal width (FW; width of the frontal scale at the widest point), nasal height (NH; height of the nasal scale at the largest point), angled subocular height (ASOH; height of the angled subocular at the largest

point), distance between the eye and naris (END; distance between the anterior border of the eye and the posterior border of the naris), the width of canthal iii (C3W; width of canthal iii at the widest point), angled subocular width (ASOW; width of the angled subocular at the widest point), and the width of the nasal scale (NW; width of the angled subocular at the widest point). All character measurements except for RH, HW, and FW were divided by SVL to produce relative sizes that would allow comparison among adult individuals of different body sizes. RH was divided by rostral width (RW), HW was divided by head length (HL), and FW was divided by frontal length (FL) to allow comparisons.

Museum abbreviations are: AMNH (American Museum of Natural History, New York, New York, USA), ANSP (Academy of Natural Sciences, Philadelphia, Pennsylvania, USA), BMNH (Natural History Museum, London, England, UK), KU (The University of Kansas Biodiversity Institute and Natural History Museum, Lawrence, Kansas, USA), MALT (Private collection of Miguel T. Landestoy, Bani, Dominican Republic), MCZ (Museum of Comparative Zoology, Harvard University, Cambridge, Massachusetts, USA), MNHN (National Museum of Natural History, Paris, France), MNHNSD (Museo Nacional de Historia Natural Prof. Eugenio de Jesús Marcano, Santo Domingo, Dominican Republic), SBH (Frozen tissue and voucher collection, S. Blair Hedges, Temple University, Philadelphia, Pennsylvania, USA), USNM (National Museum of Natural History, Smithsonian Institution, Washington, D.C., USA), ZMB (Museum für Naturkunde, Berlin, Germany).

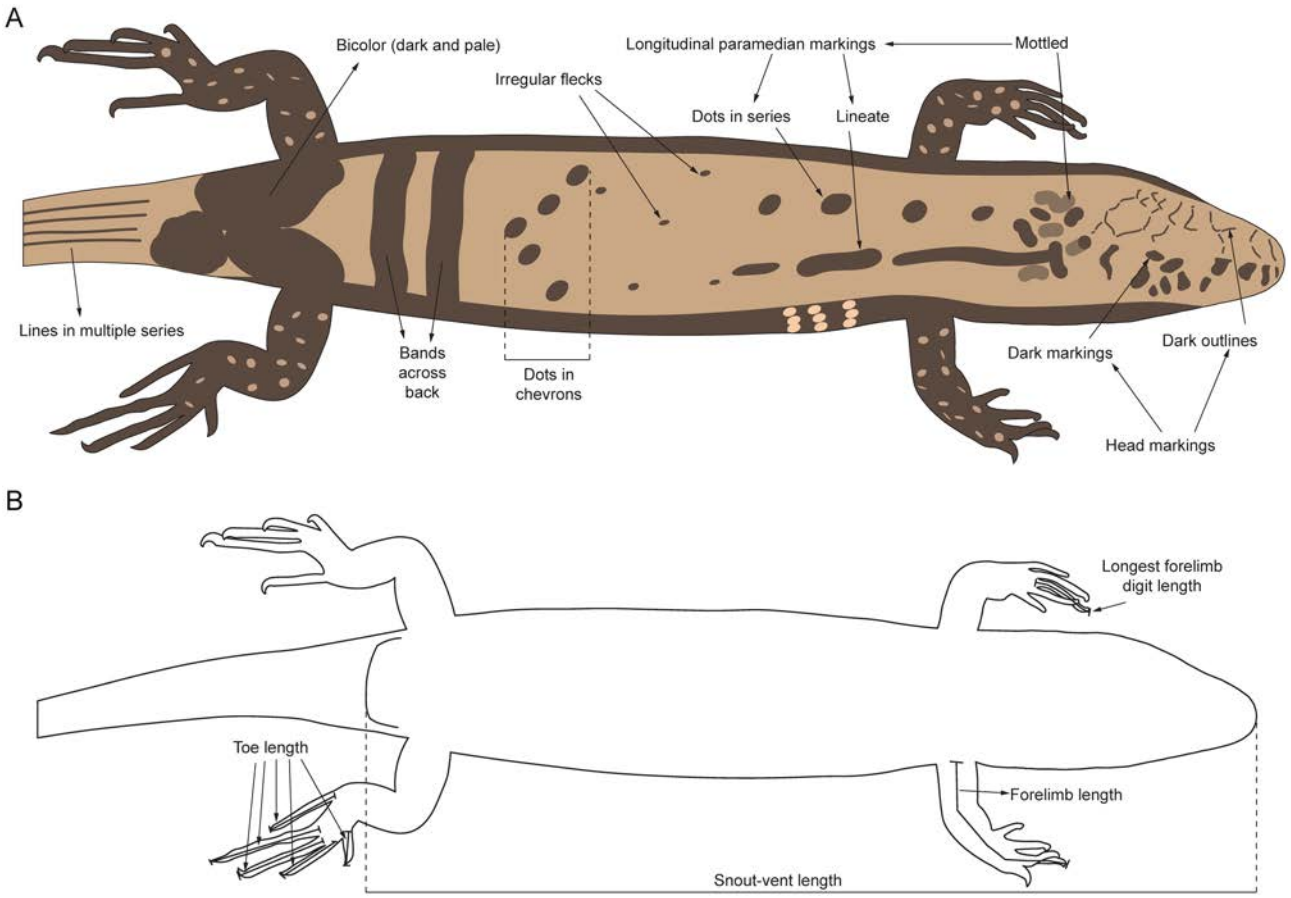

FIGURE 2. Characterization of pattern elements in diploglossid lizards of the subfamily Celestinae (top, dorsal view) (A). Measurements taken shown on the venter (B).

Distribution Maps

We constructed distribution maps for diploglossid species using the localities of specimens that were included in our genetic and morphological datasets. If samples used in these datasets did not have coordinates provided, we georeferenced them carefully with Google Earth and by using topographic and historical maps in the Caribmap database (Hedges 2013). Species range polygons were constructed using mapping software (QGIS 2020). In addition to our specimens examined, we included museum-only datapoints from GBIF (2022). Samples marked with an empty symbol indicate records that were not included in our genetic or morphological datasets. All coordinates used were reported in decimal degrees and WGS84 datum. The coordinates we generated were (usually) two decimal places

for localities in a city, three for a small town, or greater precision if warranted. Other coordinates used had the precision as provided by the source dataset (e.g., GBIF), although corrections were necessary in some cases.

As a cautionary note, we found that different museums (especially KU, but also MCZ and USNM) frequently georeferenced specimens incorrectly, considering precision and accuracy, including those collected at the same time and the same location. As just one example, all known specimens of *Panolopus emys* were collected in 1969–1970 at Palmiste, Haiti, a village that we georeference in Google Earth as 20.018, -72.725, 320 m elevation. However, KU georeferences it precisely as 20.016666, -72.73333 (264 m), which is 0.9 km from Palmiste. In contrast, MCZ georeferences it precisely as 20.0452041, -72.790504 (247 m), which is 7.5 km from Palmiste. Finally, USNM georeferences it imprecisely as 20.02, -72.73 (310 m), which is 0.6 km from Palmiste. All three museums georeferenced the location at different levels of precision and accuracy. Another major problem that we encountered in museum georeferencing was interpreting distances measured from towns and villages as straight-line rather than path. Collectors nearly always describe distances as path (by road, as measured by odometers on vehicles) and rarely by straight line. If they do intend the measurement to be straight line, it is usually indicated by the word "airline" (or "straight line"). Nonetheless, museums usually interpret locations as straight line, probably because it is faster and simpler to do so. But this can lead to an error of dozens of kilometers and we encountered a number of museum-georeferenced locations in the ocean. Although we have corrected most of these problems, we regret that some have likely entered this work.

Ecology and Conservation

We took information on habitats and natural history from the literature, if it was possible to associate them with a restricted taxon recognized here. For some species, we took this information from the field notes of one of us (SBH). The vast majority of forest lizards have been collected under objects (rocks, logs, and rotting vegetation) on the ground in open areas next to wooded areas. This is because open areas are easier to access by collectors than closed forest, and the animals find humidity and abundant insect food, albeit temporarily, in those situations. This is a type of "extinction debt," a future ecological cost of current habitat destruction (Tilman *et al.* 1994). We mention it here because many collection localities of fragile species restricted to primary forest were from habitats destroyed at the time of collection, and can mislead some researchers (and species distribution models) into classifying such species as disturbance-tolerant simply because of a GPS location that is adjacent to but not precisely within primary forest.

Similarly, rotting vegetation, especially coconut husks and fronds under palm trees, is often referred to by herpetologists as "trash" even if naturally occurring (e.g., Grant 1940a; Schwartz & Henderson 1991). Although a handful of experts know what it means, this can give a false impression (e.g., in scientific summary volumes and in IUCN Redlist accounts) that trash piles and open areas represent the habitat of the species, although in reality they are simply accessible areas for collectors. Without adjacent forested areas (the natural habitat), many of the species would not survive long in exposed "trash" piles.

For the new species described here and for many others where distributions have changed by our taxonomic decisions, we have re-evaluated the extinction threat using IUCN Redlist criteria (IUCN 2023).

Systematic Accounts

For species, we identified 31 key (diagnostic) characters (Table 1) including: dorsal pattern, head markings, longitudinal paramedian markings, dots in bars in the lateral line, SVL in mm, ventral scale rows, midbody scale rows, total lamellae counted on one hindlimb, total strigae counted on ten scales, relative TL (% TL/SVL), relative ASO (% ASO/SVL), relative EL (% EL/SVL), relative FL (% FL/SVL), relative AL (% AL/SVL), relative RH (% RH/RW), relative HL (% HL/SVL), relative MW (% MW/SVL), relative PMW (% PMW/SVL), relative PFW (% PFW/SVL), relative CW (% CW/SVL), relative SOW (% SOW/SVL), relative LFDL (% LFDL/SVL), relative EED (% EED/SVL), relative HW (% HW/HL), relative FW (% FW/FL), relative NH (% NL/SVL), relative ASOH (% ASOH/SVL), relative END (% END/SVL), relative C3W (% C3W/SVL), relative ASOW (5ASOW/SVL), and relative NW (%NW/SVL). Pattern-based characters, ventral scale rows, midbody scale rows, and total lamellae counted on one hindlimb are listed for all specimens examined. All other characters are listed for adults (specimens within 25% SVL of the largest measured individual), unless a juvenile is the only known representative of the species (*Celestus oligolepis* **sp. nov.**). Characters that have only been measured in one individual are reported but are only regarded as diagnostic when they differ by more than 1.5X when compared to one another or when compared to other traits for which n=2.

TABLE 1. Taxonomic summary of diagnostic morphological variation for Caribbean lizards of the subfamily Celestinae. The traits are: (1) dorsal pattern, (2) head markings, (3) longitudinal paramedian markings, (4) dots in bars in the lateral area, (5) SVL, (6) ventral scale rows, (7) midbody scale rows, (8) total lamellae on one forelimb, (9) total strigae on ten scales, (10) relative TL, (11) relative ASO, (12) relative EL, (13) relative FL, (14) relative AL, (15) relative RH, (16) relative HL, (17) relative MW, (18) relative PMW, (19) relative CW, (20) relative PFW, (21) relative SOW, (22) relative LFDL, (23) relative EED, (24) relative HW, (25) relative FW, (26) relative NH, (27) relative ASOH, (28) relative END, (29) relative C3W, (30) relative ASOW, and (31) relative NW. Abbreviations: a (absent), b (stripes across back), c (chevrons), dic (dots in chevrons), dis (dots in series), bi (bicolored), if (irregular flecks), fis (flecks in series), id (irregular dots), l (lineate), m (mottled), na (not applicable), and p (present).

Name	1	2	3	4	5	6	7
Caribicus anelpistus	b	p	a/p	a	279	81–107	33–40
Caribicus darlingtoni	l	a/p	a/p	a/p	61.1–74.9	69–92	33–39
Caribicus warreni	a/b	a/p	p	a/p	227–300	78–98	33–43
Celestus barbouri	c	a/p	a	a	78.4–93.6	118–151	47–56
Celestus capitulatus **sp. nov.**	id/dic	a/p	a/p	a/p	62.1–81.8	97–121	37–47
Celestus crusculus	a/fis/dic	a/p	p	a	59.6–77.6	98–114	37–44
Celestus duquesneyi	b	a	a	a	62.1	na	48
Celestus hesperius **sp. nov.**	dic	a	a/p	a	54.0–62.3	111–114	39–44
Celestus hewardi	m/b	a	a/p	a/p	129–171	113–137	43–59
Celestus jamesbondi **sp. nov.**	a/id/dic	a/p	a/p	a/p	54.7–72.0	91–112	35–44
Celestus macrolepis	bi	a	a	a	254–316	112–116	46–48
Celestus macrotus	c/b	a/p	p	p	60.0–86.1	87–93	41–45
Celestus microblepharis	c	a	a	a	96.4	109	43
Celestus molesworthi	dic	a/p	a/p	a/p	78.1–103	102–125	41–49
Celestus occiduus	a	a	a	a	269–367	109–134	46–56
Celestus oligolepis **sp. nov.**	dic	p	p	a	30.7	98	35
Celestus striatus	a/c	a/p	a/p	a	145	101–109	41–43
Comptus alloeides	id/dis/dic	a/p	p	a/p	124–161	84–109	36–44
Comptus arboreus **sp. nov.**	dis/dic	a/p	p	p	93.2–123	102–110	41–44
Comptus badius	id/m	a/p	p	a/p	78.2–99.1	94–109	39–44
Comptus maculatus	a/c	a/p	a/p	a/p	60.1–81.3	94–108	37–41
Comptus stenurus	dis/dic	a/p	p	a/p	121–146	87–110	38–45
Comptus weinlandi	id/dis/dic	a/p	a/p	a/p	101–133	81–105	37–44
Guarocuyus jaraguanus	m/c/b	p	p	a	84.6–110	100–114	40
Panolopus aenetergum	id	a	a	p	83.0–92.0	80–86	35–36
Panolopus aporus	a/if/id/dic	a	a/p	p	77.8–100	85–102	37–42
Panolopus chalcorhabdus	a/if/id	a/p	a/p	p	71.9–95.4	88–97	36–41
Panolopus costatus	a/id/dis/dic	a/p	a/p	p	83.6–107	89–106	39–43
Panolopus curtissi	a/if	a	a/p	a	64.1–85.5	90–103	32–38
Panolopus diastatus	a/if	a	a	a/p	66.1–83.7	86–114	33–39
Panolopus emys	a/if	a	a/p	p	99.0–113	89–104	34–40
Panolopus hylonomus	a/if	a	a/p	a	59.3–76.5	80–97	33–39
Panolopus lanceolatus **sp. nov.**	a/id/dis/dic	a/p	p	p	78.5–104	93–102	37–43
Panolopus lapierrae **sp. nov.**	a/dic	a/p	a/p	a/p	72.6–88.3	90–98	33–38
Panolopus leionotus	a/id/dis/dic	a	a/p	p	86.3–105	84–101	35–40
Panolopus marcanoi	id/dic	p	p	p	64.6–85.8	89–102	38–45

.....continued on the next page

TABLE 1. (Continued)

Name	1	2	3	4	5	6	7
Panolopus melanchrous	a/if/id/dic	a/p	p	p	93.2–124	89–113	35–42
Panolopus neiba	if/dic	a	a/p	p	77.9–102	84–102	35–43
Panolopus nesobous	id/dis	a	p	p	82.3–108	77–96	38–43
Panolopus oreistes	id/dis/dic	a/p	p	p	77.3–103	80–104	35–43
Panolopus psychonothes	id/dis/dic	a/p	a/p	a/p	70.9–97.2	88–109	36–42
Panolopus saonae	a	a	a	a/p	90.9–98.3	92–95	35–39
Panolopus semitaeniatus **sp. nov.**	a/id/dic	a/p	a/p	a/p	84.1–109	81–101	36–41
Panolopus unicolor **sp. nov.**	a	a	p	p	67.6	93	40
Sauresia agramma **sp. nov.**	a	a/p	a/p	a	53.8–69.1	121–127	37–39
Sauresia cayemitae **sp. nov.**	a/if/l	a/p	p	a	47.8–58.1	101–119	31–37
Sauresia gracilis **sp. nov.**	m/l	a	p	a	51.1	103	36
Sauresia habichi	a/l	p	a/p	a	51.9–63.3	122–125	38–41
Sauresia manicula **sp. nov.**	a	a/p	p	a	59.6–69.0	121–129	37–38
Sauresia pangnolae **sp. nov.**	a/id	a/p	a/p	a	53.8–66.7	104–119	35–42
Sauresia sepsoides	a/m/if	a/p	a/p	a	50.7–65.9	104–119	34–37
Sauresia synoria **sp. nov.**	a	a/p	p	a	53.5–72.0	114–127	34–36
Wetmorena agasepsoides	a	a/p	a/p	a	49.1–58.6	110–121	27–31
Wetmorena haetiana	a/id/l	a/p	a/p	a	78.3–102	100–126	34–39
Wetmorena mylica	a/id	a/p	a/p	a	76.0–98.2	112–126	37–41
Wetmorena obscura **sp. nov.**	l	p	p	a	46.9–61.1	108–111	35–36
Wetmorena orosaura **sp. nov.**	l/id	a/p	p	a	59.6–68.0	110–125	33–41
Wetmorena surda	id/dis/l	a/p	p	a	62.5–81.9	100–124	31–43

TABLE 1. (Continued)

Name	8	9	10	11	12	13
Caribicus anelpistus	43–48	471	24.6	1.24	3.69	21.0
Caribicus darlingtoni	33–39	90–120	26.1–31.9	0.768–1.13	3.45–3.92	20.2–23.3
Caribicus warreni	41–47	458–500	27.0–27.3	1.51–1.57	3.43–3.54	19.8–22.0
Celestus barbouri	36–49	105–136	18.2–23.5	0.437–0.556	2.87–3.63	15.4–19.0
Celestus capitulatus **sp. nov.**	25–38	105–192	17.6–22.3	0.525–1.17	2.75–3.80	14.3–18.1
Celestus crusculus	30–39	106–194	18.7–24.7	0.339–0.884	2.93–3.61	12.8–20.7
Celestus duquesneyi	64	130	31.4	0.644	4.36	24.4
Celestus hesperius **sp. nov.**	29–34	95–122	21.7–26.2	0.594–0.648	3.61–3.74	18.6–21.3
Celestus hewardi	50–61	164–315	24.1–30.6	0.744–1.40	2.98–4.05	22.2–24.6
Celestus jamesbondi **sp. nov.**	30–36	101–173	19.8–26.3	0.363–1.01	2.94–4.06	14.4–19.9
Celestus macrolepis	52–54	398	27.5–28.0	1.39–1.66	3.63–3.70	26.1–26.7
Celestus macrotus	39–40	64–115	30.2–31.2	0.640–0.983	3.79–5.17	22.4–25.0
Celestus microblepharis	30	165	16.6	0.820	1.83	14.2
Celestus molesworthi	32–44	138–159	22.4–29.4	0.653–0.845	3.28–3.70	17.5–24.2
Celestus occiduus	50–66	374	24.4–29.7	1.26–1.27	2.87–3.33	23.5–23.9
Celestus oligolepis **sp. nov.**	30	83	34.6	0.651	4.85	21.4
Celestus striatus	59–66	279	37.8	0.710	3.85	26.1
Comptus alloeides	43–58	237–323	23.8–35.2	0.587–1.03	3.16–3.90	21.4–25.3

.....continued on the next page

TABLE 1. (Continued)

Name	8	9	10	11	12	13
Comptus arboreus **sp. nov.**	48–54	143–207	37.4–39.7	0.723–0.923	3.46–4.18	24.1–25.3
Comptus badius	40–45	203–241	23.4–33.9	0.403–0.866	2.83–3.53	19.6–23.0
Comptus maculatus	32–37	149–201	24.8–27.0	0.556–0.849	3.51–3.91	19.3–21.6
Comptus stenurus	47–57	176–234	29.2–37.1	0.676–1.12	2.99–3.92	22.3–27.5
Comptus weinlandi	43–55	167–236	24.5–36.5	0.449–0.901	3.33–4.43	20.1–27.9
Guarocuyus jaraguanus	na	na	na	na	na	na
Panolopus aenetergum	40	267	26.8	0.717	3.34	20.6
Panolopus aporus	36–48	150–235	27.7–33.7	0.441–0.669	2.91–3.76	19.3–26.4
Panolopus chalcorhabdus	40–52	184–233	31.3–36.0	0.481–0.818	3.07–3.71	20.4–23.7
Panolopus costatus	49–58	158–217	31.5–37.8	0.582–0.916	2.52–3.73	19.9–24.2
Panolopus curtissi	32–39	165–260	20.8–28.1	0.393–0.587	2.66–4.01	15.1–20.5
Panolopus diastatus	35–41	169–234	21.5–27.4	0.00–0.614	2.71–3.32	16.2–20.1
Panolopus emys	39–54	238–311	28.9–35.2	0.533–0.826	2.87–3.40	18.5–23.4
Panolopus hylonomus	34–47	169–222	22.8–28.2	0.424–0.873	2.78–3.72	17.1–20.7
Panolopus lanceolatus **sp. nov.**	41–52	186–234	28.4–35.9	0.567–0.704	3.01–3.51	17.4–23.9
Panolopus lapierrae **sp. nov.**	38–47	228–231	24.3–30.9	0.620–0.725	2.88–3.67	18.5–20.6
Panolopus leionotus	43–48	191–266	25.4–34.1	0.524–1.17	2.36–3.75	18.6–23.5
Panolopus marcanoi	36–44	141–254	26.3–31.9	0.451–0.755	3.03–3.93	19.9–23.6
Panolopus melanchrous	47–58	168–413	30.7–41.3	0.442–0.883	2.78–3.97	19.5–27.6
Panolopus neiba	45–49	179–239	29.5–36.6	0.670–0.747	2.95–3.93	19.8–25.7
Panolopus nesobous	50–59	155–222	35.1	0.486–0.843	3.41–3.63	23.3–25.1
Panolopus oreistes	39–55	155–267	31.2–40.1	0.406–0.865	3.03–3.67	20.1–24.9
Panolopus psychonothes	37–44	172–244	26.5–33.1	0.505–1.03	2.74–3.87	17.4–23.8
Panolopus saonae	40–42	212–284	26.5–29.8	0.517–0.630	3.06–3.20	19.0–20.2
Panolopus semitaeniatus **sp. nov.**	34–51	156–204	30.4–37.0	0.666–0.826	3.38–3.77	20.8–25.6
Panolopus unicolor **sp. nov.**	48	144	36.8	0.533	3.38	23.5
Sauresia agramma **sp. nov.**	17	103–138	11.3–14.9	0.217–0.262	2.30–3.16	10.2–13.6
Sauresia cayemitae **sp. nov.**	15–19	84–104	11.5–14.0	0.0558–0.473	2.14–2.90	9.65–12.5
Sauresia gracilis **sp. nov.**	18	100	13.8	0.254	2.97	10.8
Sauresia habichi	18–19	89–113	11.2–13.1	0.000594–0.201	2.22–2.95	9.84–13.1
Sauresia manicula **sp. nov.**	15–17	119–150	11.2–12.1	0.168–0.188	2.29–2.32	11.5–11.9
Sauresia pangnolae **sp. nov.**	14–19	78–109	11.6–14.3	0.129–0.259	2.56–3.02	11.4–12.6
Sauresia sepsoides	14–19	83–119	10.6–15.1	0.00–0.427	2.46–3.40	9.48–12.5
Sauresia synoria **sp. nov.**	16–18	84–111	10.5–12.3	0.0561–0.472	2.47–2.94	9.14–11.9
Wetmorena agasepsoides	14–17	94–153	9.44–11.2	0.00–0.224	2.22–3.11	8.05–9.58
Wetmorena haetiana	18–26	96–144	13.0–18.2	0.135–0.600	2.53–3.74	12.4–15.7
Wetmorena mylica	16–23	84–105	9.62–15.5	0.00–0.504	2.13–2.97	10.5–14.3
Wetmorena obscura **sp. nov.**	20–21	73–83	13.8–16.2	0.295–0.426	2.65–3.13	13.6–16.3
Wetmorena orosaura **sp. nov.**	22–26	92–98	18.6–19.7	0.206–0.285	3.04–3.56	16.9–17.2
Wetmorena surda	18–21	84–123	10.7–14.4	0.0151–0.520	2.07–2.83	11.3–13.9

.....continued on the next page

TABLE 1. (Continued)

Name	14	15	16	17	18	19
Caribicus anelpistus	1.15	2.03	23.8	1.82	3.87	10.8
Caribicus darlingtoni	1.17–1.85	1.76–2.22	17.4–20.0	2.05–2.52	2.70–3.21	7.08–8.48
Caribicus warreni	1.20–1.88	1.55–1.99	19.1–22.1	1.46–1.87	2.73–3.32	9.33–10.3
Celestus barbouri	0.810–1.86	1.41–1.66	14.6–16.6	1.51–1.85	2.51–3.29	7.64–8.26
Celestus capitulatus **sp. nov.**	0.671–2.04	1.51–2.03	15.1–17.7	1.28–1.84	2.62–2.97	7.84–8.67
Celestus crusculus	0.716–2.00	1.62–2.04	15.5–20.3	1.37–2.31	2.73–3.37	6.89–8.77
Celestus duquesneyi	2.45	2.14	21.6	2.35	3.19	9.98
Celestus hesperius **sp. nov.**	1.52–1.59	1.60–1.77	15.7–17.7	1.51–1.78	2.87–2.92	7.99–8.55
Celestus hewardi	1.40–1.82	1.50–1.76	16.8–21.5	1.75–1.81	2.84–3.44	8.81–9.89
Celestus jamesbondi **sp. nov.**	0.917–2.18	1.62–2.35	15.1–20.4	1.59–2.01	2.61–2.92	6.59–9.08
Celestus macrolepis	0.760–1.43	1.53–1.75	19.2–22.9	1.87	3.81	11.2
Celestus macrotus	1.75–2.08	1.61–1.95	18.2–20.5	1.77	3.00	7.80–9.48
Celestus microblepharis	0.446	1.71	14.7	1.44	2.47	8.02
Celestus molesworthi	1.37–1.50	1.72–1.81	17.2–20.0	1.81–2.00	2.97–3.08	8.73–9.35
Celestus occiduus	0.948–1.39	1.60–1.83	20.4–20.6	1.86	3.57	9.00
Celestus oligolepis **sp. nov.**	2.28	2.11	19.5	2.28	4.20	8.95
Celestus striatus	1.30	1.94	18.9	na	na	7.93
Comptus alloeides	0.710–1.83	1.52–1.99	15.5–20.0	0.840–1.95	2.54–2.97	8.86–10.3
Comptus arboreus **sp. nov.**	1.22–1.60	1.53–1.85	15.5–18.0	1.54–1.74	2.95–3.01	9.05–9.51
Comptus badius	1.34–1.75	1.83–2.42	14.7–18.3	1.38	2.39	7.92–9.30
Comptus maculatus	0.993–1.70	1.67–1.88	16.6–18.3	1.69–1.85	2.32–2.86	8.29–9.23
Comptus stenurus	0.451–1.87	1.68–2.03	15.8–18.9	1.52–1.78	2.61–3.05	8.73–10.3
Comptus weinlandi	0.802–2.18	1.46–1.86	15.8–18.5	1.41–1.90	2.57–2.91	8.76–10.1
Guarocuyus jaraguanus	2.33–2.90	1.55–1.85	18.6	na	na	na
Panolopus aenetergum	1.29	2.09	17.5	1.63	2.62	7.60
Panolopus aporus	1.06–1.88	2.01–2.40	10.2–18.6	1.72–2.08	2.42–2.92	7.92–8.86
Panolopus chalcorhabdus	1.26–1.65	1.85–2.24	16.6–18.8	1.47–2.00	2.38–3.31	7.74–9.08
Panolopus costatus	0.590–2.07	1.78–2.26	16.3–20.0	1.66–2.00	2.29–2.92	7.27–8.51
Panolopus curtissi	0.827–2.09	1.77–2.66	13.6–17.9	1.60–2.09	2.07–2.72	7.49–8.61
Panolopus diastatus	0.667–1.43	1.89–2.45	14.2–18.8	1.51–2.00	2.43–3.17	7.15–8.06
Panolopus emys	0.756–1.75	2.10–2.37	14.5–18.6	1.49–2.01	2.20–2.87	8.24–8.96
Panolopus hylonomus	0.902–2.08	1.72–2.28	15.1–18.5	1.63–2.11	2.67–2.89	7.98–8.57
Panolopus lanceolatus **sp. nov.**	0.770–1.35	1.78–2.28	15.2–18.2	1.45–1.96	2.36–2.66	8.01–8.76
Panolopus lapierrae **sp. nov.**	0.929–1.58	1.86–2.06	17.0–18.7	1.92–1.94	2.68–3.58	8.55–8.81
Panolopus leionotus	1.06–2.24	1.79–2.36	14.6–19.7	1.67–2.02	2.43–3.18	8.03–8.69
Panolopus marcanoi	0.936–2.25	1.96–2.38	15.7–19.9	1.75–2.33	2.46–3.24	7.18–9.56
Panolopus melanchrous	0.569–2.39	1.40–2.75	15.2–22.5	1.33–2.06	2.71–3.38	7.61–9.20
Panolopus neiba	0.966–1.97	1.75–2.23	15.4–19.8	1.66–2.36	2.27–3.29	7.58–8.77
Panolopus nesobous	1.39–1.60	2.26–2.38	17.9–19.8	1.96–2.18	2.82–3.02	8.11–8.21
Panolopus oreistes	0.558–1.79	1.82–2.88	15.3–19.8	1.54–1.90	2.18–3.19	7.13–8.78
Panolopus psychonothes	0.954–2.31	1.80–2.32	15.9–19.5	1.47–2.91	2.46–3.34	7.56–8.53
Panolopus saonae	0.880–1.35	2.15–2.46	15.4–17.5	1.52	2.43	8.20
Panolopus semitaeniatus **sp. nov.**	1.47–1.90	1.67–1.72	16.3–17.9	1.65–1.75	2.50–3.10	8.22–9.65
Panolopus unicolor **sp. nov.**	1.60	2.23	17.8	1.73	2.80	7.61

.....continued on the next page

TABLE 1. (Continued)

Name	14	15	16	17	18	19
Sauresia agramma **sp. nov.**	0.576–0.709	1.92–2.12	13.6–15.2	1.61–2.05	2.30–2.70	6.09–6.82
Sauresia cayemitae **sp. nov.**	0.294–1.17	1.65–2.73	13.0–15.6	1.46–1.78	2.27–2.51	5.59–6.24
Sauresia gracilis **sp. nov.**	0.665	1.90	15.7	1.76	2.76	7.18
Sauresia habichi	0.364–0.996	1.83–2.42	13.3–15.0	1.49–1.82	2.11–2.34	5.86–6.68
Sauresia manicula **sp. nov.**	0.604–0.870	1.89–1.90	13.1–14.3	1.48–1.67	2.13–2.16	5.30–6.41
Sauresia pangnolae **sp. nov.**	0.681–1.11	1.73–2.27	13.0–15.4	1.23–1.90	2.04–2.47	6.07–6.81
Sauresia sepsoides	0.428–1.01	1.45–2.49	13.1–16.3	1.32–1.97	1.92–2.61	5.11–6.77
Sauresia synoria **sp. nov.**	0.361–0.670	1.82–1.94	12.3–15.9	1.21–1.70	2.09–2.75	5.62–6.94
Wetmorena agasepsoides	0.292–0.634	1.58–2.58	12.1–14.4	1.40–1.66	1.75–2.30	4.69–6.57
Wetmorena haetiana	0.00	1.62–2.48	na	1.45–1.78	2.16–2.82	6.26–7.64
Wetmorena mylica	0.00	1.76–2.37	na	1.34–1.95	2.02–2.91	5.90–7.07
Wetmorena obscura **sp. nov.**	0.00	1.72–2.22	na	1.72–2.24	2.49–3.05	6.26–6.69
Wetmorena orosaura **sp. nov.**	0.00	1.85–2.31	na	1.61–1.93	2.31–2.68	6.69–6.88
Wetmorena surda	0.00	1.72–2.28	na	1.49–1.96	1.81–2.93	5.89–7.23

TABLE 1. (Continued)

Name	20	21	22	23	24	25
Caribicus anelpistus	5.38	2.31	4.98	10.6	77.0	89.3
Caribicus darlingtoni	4.51–7.09	2.70–3.12	4.86–6.14	6.83–8.58	72.5–93.4	74.3–80.7
Caribicus warreni	4.65–7.41	1.95–2.79	3.41–4.71	5.96–9.08	71.4–83.7	82.3
Celestus barbouri	3.97–4.33	1.92–2.74	2.92–3.81	6.23–7.15	73.8–81.7	65.6–82.1
Celestus capitulatus **sp. nov.**	4.30–4.72	2.03–2.61	3.45–3.75	6.45–7.84	71.6–78.6	78.1–81.6
Celestus crusculus	3.93–4.67	1.97–2.65	2.94–4.10	6.07–8.61	72.1–76.4	82.6–91.1
Celestus duquesneyi	5.41	2.66	6.52	7.68	64.6	75.2
Celestus hesperius **sp. nov.**	4.65–5.02	1.91–2.22	3.50–4.04	6.74–7.53	76.5–79.8	80.5–86.1
Celestus hewardi	4.18–4.80	2.43–2.96	5.03–5.66	6.72–8.73	68.4–77.1	57.3–75.3
Celestus jamesbondi **sp. nov.**	4.29–5.09	2.16–2.79	3.66–4.33	6.92–7.80	76.0–80.8	70.5–77.6
Celestus macrolepis	3.94	2.64–3.01	5.47–5.51	8.02–10.9	80.5	78.4
Celestus macrotus	4.87–5.55	2.96–4.03	6.43–6.67	7.58–8.02	67.6–80.6	57.6–66.1
Celestus microblepharis	4.37	2.06	3.11	7.05	75.4	na
Celestus molesworthi	4.44–4.90	1.69–2.80	4.28–5.19	7.97–8.83	69.1–76.5	75.9–95.5
Celestus occiduus	4.76	2.27–3.02	4.77–5.46	8.98–10.9	73.8	63.8
Celestus oligolepis **sp. nov.**	6.41	4.03	5.14	9.14	78.3	74.3
Celestus striatus	5.68	2.63	7.48	9.00	82.1	76.5
Comptus alloeides	4.25–5.07	2.66–2.95	5.32–5.95	6.43–8.53	70.0–74.2	64.9–75.1
Comptus arboreus **sp. nov.**	4.50–4.82	2.61–3.05	6.01–6.37	6.45–7.03	71.7–80.3	62.6–71.4
Comptus badius	4.59–5.47	2.57–2.74	4.38–5.04	6.99–9.51	62.8–69.3	71.3–86.5
Comptus maculatus	3.95–4.73	2.23–2.74	4.14–5.01	6.93–7.60	69.6–80.0	66.6–81.9
Comptus stenurus	4.32–4.71	2.53–3.11	5.89–7.19	6.18–7.42	70.2–74.2	68.0–79.2
Comptus weinlandi	4.29–4.88	2.31–3.49	5.08–6.31	6.03–7.95	73.6–82.2	58.8–84.6
Guarocuyus jaraguanus	na	na	na	na	74.5	na
Panolopus aenetergum	4.15	2.49	4.83	8.40	76.4	88.2
Panolopus aporus	4.18–4.53	2.74–3.62	4.57–5.72	6.73–8.49	71.4–83.2	61.7–75.1

.....continued on the next page

TABLE 1. (Continued)

Name	20	21	22	23	24	25
Panolopus chalcorhabdus	4.37–4.93	2.52–2.86	5.29–6.97	6.82–8.58	65.0–76.3	62.5–80.8
Panolopus costatus	3.97–4.67	1.93–3.01	5.53–6.66	7.32–8.89	68.3–76.8	56.2–67.4
Panolopus curtissi	3.96–4.68	1.88–2.98	3.59–4.54	5.36–7.71	68.3–78.1	65.4–83.1
Panolopus diastatus	3.74–4.61	1.88–2.57	3.48–4.87	6.32–8.58	69.4–74.8	57.4–86.2
Panolopus emys	3.99–4.36	2.01–2.89	5.15–5.83	7.03–8.44	71.1–78.7	67.7–74.5
Panolopus hylonomus	4.23–4.87	2.65–2.90	4.47–5.27	6.78–8.05	73.8–76.4	64.0–74.5
Panolopus lanceolatus **sp. nov.**	3.97–4.55	2.20–2.71	4.76–6.36	6.45–7.70	68.0–77.6	63.1–72.1
Panolopus lapierrae **sp. nov.**	4.73–4.75	1.91–2.77	4.49–4.55	7.78–8.43	77.7–78.1	77.6–79.0
Panolopus leionotus	4.06–5.21	1.94–2.50	4.58–6.10	6.78–8.80	67.3–82.9	68.7–81.2
Panolopus marcanoi	4.19–5.19	2.47–3.33	4.75–6.68	7.02–8.81	68.4–77.9	59.0–73.0
Panolopus melanchrous	4.21–5.06	2.39–3.26	5.76–7.09	6.70–9.14	68.3–83.6	61.3–71.4
Panolopus neiba	4.41–5.49	2.06–3.04	5.61–6.66	6.69–8.66	67.9–78.4	63.3–74.0
Panolopus nesobous	4.74–4.81	2.85–3.11	6.19–6.33	7.91–10.0	71.2–76.4	60.8–63.5
Panolopus oreistes	4.18–4.96	2.28–3.23	5.27–7.23	6.29–9.50	66.1–85.0	61.6–76.9
Panolopus psychonothes	3.89–4.75	1.92–2.68	4.89–5.81	6.79–8.29	68.4–78.6	66.5–81.0
Panolopus saonae	4.14	2.77	5.01	7.63	73.5	72.5
Panolopus semitaeniatus **sp. nov.**	4.38–4.81	2.59–2.96	5.17–6.72	6.69–7.42	63.8–74.6	71.0–76.5
Panolopus unicolor **sp. nov.**	4.69	3.12	6.65	7.61	70.8	58.2
Sauresia agramma **sp. nov.**	3.02–3.98	1.87–2.47	2.11–2.86	6.93–7.86	69.7–74.6	80.2–81.9
Sauresia cayemitae **sp. nov.**	3.11–3.64	1.67–2.25	2.36–2.65	6.02–6.88	68.5–77.1	71.3–83.1
Sauresia gracilis **sp. nov.**	3.81	2.44	1.96	7.63	67.6	82.9
Sauresia habichi	3.39–3.96	1.96–2.23	2.26–2.71	6.64–7.30	77.7–78.6	71.8–77.5
Sauresia manicula **sp. nov.**	3.32–3.62	1.86–2.01	2.20–2.21	6.76–7.49	72.9–82.8	81.5
Sauresia pangnolae **sp. nov.**	3.70–3.83	1.77–2.63	2.29–2.54	6.94–7.46	70.8–78.2	69.6–81.5
Sauresia sepsoides	3.02–4.29	1.61–2.48	1.69–2.37	6.13–8.03	64.7–83.1	69.1–93.3
Sauresia synoria **sp. nov.**	3.01–3.30	1.57–1.91	1.75–2.52	5.91–7.81	70.8–76.0	82.0–94.4
Wetmorena agasepsoides	2.77–3.35	1.66–2.07	1.44–2.01	5.80–6.61	64.0–77.5	74.9–94.4
Wetmorena haetiana	3.44–4.60	1.99–2.38	2.65–3.63	na	na	75.6–97.3
Wetmorena mylica	3.26–4.01	1.62–2.97	2.43–2.95	na	na	84.8–114
Wetmorena obscura **sp. nov.**	4.03–4.58	1.70–2.54	4.08–5.35	na	na	73.6–81.9
Wetmorena orosaura **sp. nov.**	3.85–4.11	2.27–2.39	3.86–4.46	na	na	80.0–84.6
Wetmorena surda	3.47–3.91	1.73–2.06	2.12–2.98	na	na	81.1–89.7

TABLE 1. (Continued)

Name	26	27	28	29	30	31
Caribicus anelpistus	1.11	1.89	5.23	1.64	2.27	1.80
Caribicus darlingtoni	1.14–1.45	0.810–1.05	4.38–5.61	1.68–2.03	2.24–2.81	1.63–1.92
Caribicus warreni	1.06	0.652–1.34	5.42–6.27	1.90–2.17	2.13–2.91	1.49
Celestus barbouri	0.930–1.12	0.553–1.16	4.68–4.83	1.54–1.93	1.97–2.52	1.38–1.65
Celestus capitulatus **sp. nov.**	0.953–1.42	0.586–1.01	4.57–5.03	1.61–1.70	1.93–2.32	1.40–1.84
Celestus crusculus	0.925–1.37	0.953–1.21	4.31–4.86	1.59–2.07	2.03–2.43	1.27–1.60
Celestus duquesneyi	na	1.61	5.46	1.59	2.90	2.01
Celestus hesperius **sp. nov.**	1.09–1.44	0.963–1.24	4.70–5.28	1.77–1.93	2.01–2.48	1.52–1.78

.....continued on the next page

TABLE 1. (Continued)

Name	26	27	28	29	30	31
Celestus hewardi	1.21–1.24	0.918–1.30	5.00–5.60	1.70–2.12	1.63–2.23	1.56–1.88
Celestus jamesbondi **sp. nov.**	1.12–1.21	0.893–1.18	4.25–5.54	1.75–2.16	2.09–2.76	1.42–1.75
Celestus macrolepis	1.18	1.17	6.02	1.99	2.57	1.75
Celestus macrotus	1.15–1.62	1.00–1.07	5.48–5.60	1.85	2.77–2.83	2.08–2.33
Celestus microblepharis	0.726	0.778	4.79	1.74	2.90	1.11
Celestus molesworthi	1.17–1.26	1.11	5.32–5.50	1.99–2.09	2.09–2.48	1.55–1.72
Celestus occiduus	1.16	1.30	6.51	na	2.52	1.83
Celestus oligolepis **sp. nov.**	2.34	1.89	5.63	2.77	3.12	2.44
Celestus striatus	1.08	1.12	6.16	2.12	2.29	1.59
Comptus alloeides	0.863–1.30	0.733–1.23	4.82–6.77	1.60–2.20	2.26–3.01	1.46–2.03
Comptus arboreus **sp. nov.**	1.03–1.20	0.929–0.992	5.11–5.52	1.86–1.94	2.82–3.28	1.47–1.99
Comptus badius	0.999–1.06	0.691–1.33	4.96–5.24	1.45–2.42	1.91–2.31	1.54–1.82
Comptus maculatus	0.873–1.11	0.815–1.05	4.81–5.20	1.73–1.85	2.25–2.52	1.50–1.77
Comptus stenurus	0.992–1.17	0.697–0.893	4.38–5.53	1.37–1.97	2.31–2.85	1.39–1.82
Comptus weinlandi	0.965–1.32	0.568–1.23	4.67–5.72	1.65–2.08	1.64–3.36	1.48–1.95
Guarocuyus jaraguanus	na	na	na	na	na	na
Panolopus aenetergum	1.15	1.08	4.35	1.86	2.07	1.92
Panolopus aporus	1.08–1.23	0.638–1.02	4.69–5.44	1.85–1.96	2.32–2.73	1.56–1.78
Panolopus chalcorhabdus	0.854–1.55	0.739–0.854	4.93–5.62	1.98–2.05	2.36–2.71	1.70–2.01
Panolopus costatus	1.02–1.28	0.562–0.886	5.08–5.50	1.82–1.90	2.36–2.81	1.58–1.74
Panolopus curtissi	1.04–1.25	0.708–1.19	4.02–5.03	1.75–1.93	2.26–2.76	1.44–1.82
Panolopus diastatus	0.913–1.19	0.564–1.08	4.06–4.94	1.21–2.70	1.93–2.86	1.41–1.77
Panolopus emys	0.963–1.10	0.696–0.981	4.37–5.19	1.54–2.01	2.12–2.20	1.23–1.58
Panolopus hylonomus	0.961–1.37	0.690–1.13	4.03–4.98	1.95–2.03	1.61–2.75	1.48–2.01
Panolopus lanceolatus **sp. nov.**	0.904–1.06	0.484–0.854	4.58–4.98	1.73–2.00	2.38–3.09	1.48–1.95
Panolopus lapierrae **sp. nov.**	1.06–1.09	0.838–0.978	5.21	1.54–1.86	2.71	1.81
Panolopus leionotus	0.971–1.18	0.750–1.33	4.46–5.61	1.55–1.89	2.48–2.95	1.59–2.01
Panolopus marcanoi	1.07–1.28	0.505–0.793	4.68–5.82	1.60–2.23	2.19–3.14	1.64–1.96
Panolopus melanchrous	0.897–0.952	0.680–0.856	4.89–5.59	1.67–1.94	2.28–2.82	1.44–2.09
Panolopus neiba	0.963–1.08	0.713–0.885	4.51–5.01	1.51–1.95	2.34–2.83	1.67–1.92
Panolopus nesobous	1.12–1.14	0.669–0.750	5.62–5.73	2.01–2.12	2.61–2.82	1.69–1.71
Panolopus oreistes	0.878–1.06	0.737–0.978	5.01–5.63	1.61–2.16	2.13–3.04	1.37–1.65
Panolopus psychonothes	1.12–1.32	0.803–0.952	4.00–5.62	1.16–2.01	2.01–2.44	1.68–1.94
Panolopus saonae	1.01	0.847	6.43	1.99	2.31	1.69
Panolopus semitaeniatus **sp. nov.**	1.04–1.18	0.654–0.844	4.61–5.61	1.80–1.98	2.45–2.71	1.46–1.62
Panolopus unicolor **sp. nov.**	1.15	0.814	5.52	1.79	2.90	2.00
Sauresia agramma **sp. nov.**	0.883–1.02	0.912–1.13	2.98–3.75	1.17–1.30	2.07–2.47	1.36–1.57
Sauresia cayemitae **sp. nov.**	0.792–0.951	0.740–1.02	2.86–3.51	1.07–1.30	1.88–2.17	1.06–1.46
Sauresia gracilis **sp. nov.**	0.998	0.958	3.15	1.82	1.96	1.33
Sauresia habichi	0.890–1.11	0.909–1.42	3.04–3.59	1.10–1.41	1.67–2.03	0.942–1.12
Sauresia manicula **sp. nov.**	0.772–1.09	0.923–1.25	2.89–3.17	1.06–1.43	1.81–2.01	1.19–1.29
Sauresia pangnolae **sp. nov.**	0.945–1.05	0.862–1.64	2.86–3.70	1.09–1.51	2.16–2.39	1.38–1.62
Sauresia sepsoides	0.706–1.17	0.778–1.25	2.99–3.77	0.943–1.62	1.54–2.55	1.16–1.60

.....continued on the next page

TABLE 1. (Continued)

Name	26	27	28	29	30	31
Sauresia synoria **sp. nov.**	0.754–1.09	0.880–1.22	2.67–3.61	0.943–1.31	1.82–2.30	1.13–1.35
Wetmorena agasepsoides	0.712–0.933	0.851–1.09	2.25–3.27	0.481–0.970	1.55–2.36	0.803–1.55
Wetmorena haetiana	0.777–1.19	0.940–1.52	3.02–5.20	0.800–1.14	1.71–2.39	1.47–1.92
Wetmorena mylica	0.850–1.13	1.09–1.50	3.10–3.67	0.956–1.15	1.74–2.29	1.23–1.65
Wetmorena obscura **sp. nov.**	0.753–1.24	0.999–1.29	3.68–5.01	0.835–0.980	1.82–2.17	1.41–1.57
Wetmorena orosaura **sp. nov.**	1.07–1.16	1.22–1.45	3.37–3.91	1.14–1.26	2.21–2.47	1.50–1.95
Wetmorena surda	0.828–1.06	0.944–1.52	3.04–3.71	1.17–1.33	1.93–2.31	1.26–1.54

All new species are assigned to genera and described. Following the numbered diagnoses, we describe characters that distinguish the new taxon from other taxa within each genus. In some cases, damage to specimens precluded scoring of a character or specific characters that were not mentioned in species descriptions, and therefore the total number scored for that character was fewer than the total number of specimens listed as examined (Table 2). In addition, we recorded characters through a combination of measurements, pictures, and primary literature, resulting in varying sample sizes for each trait. Because organisms are three-dimensional objects, the rulers or scale bars that accompany some of the photographs and illustrations should not be used for precise measurements, but rather for general guidance in overall dimension.

TABLE 2. Sample sizes used for each corresponding trait value in Table 1. An asterisk indicates that juveniles were used to determine the given trait value.

Name	1	2	3	4	5	6	7	8	9	10	11	12	13	14	15
Caribicus anelpistus	8*	8*	8*	8*	1	8*	8*	8*	1	1	1	1	1	1	1
Caribicus darlingtoni	4*	6*	6*	4*	9	5*	5*	5*	4	4	4	4	4	9	7
Caribicus warreni	5*	5*	4*	3*	11	7*	7*	5*	2	3	2	2	4	9	7
Celestus barbouri	5*	6*	6*	5*	8	6*	6*	6*	5	5	5	8	8	8	5
Celestus capitulatus **sp. nov.**	34*	35*	35*	35*	25	35*	35*	35*	23	22	25	25	25	25	24
Celestus crusculus	13*	21*	21*	18*	20	20*	21*	21*	15	10	16	20	20	20	15
Celestus duquesneyi	1	1	1	1	1	0	1	1	1	1	1	1	1	1	1
Celestus hesperius **sp. nov.**	3*	3*	3*	3*	2	3*	3*	3*	2	2	2	2	2	2	2
Celestus hewardi	10*	18*	18*	14*	4	18*	18*	18*	4	4	4	4	4	4	4
Celestus jamesbondi **sp. nov.**	32*	37*	37*	31*	35	35*	37*	37*	31	22	31	35	35	35	31
Celestus macrolepis	2	2	2	2	2	2	2	2	1	2	2	2	2	2	2
Celestus macrotus	2*	3*	3*	3*	6	3*	3*	3*	2	2	2	2	2	6	6
Celestus microblepharis	1	1	1	1	1	1	1	1	1	1	1	1	1	1	1
Celestus molesworthi	7*	11*	11*	10*	3	11*	11*	10*	3	3	3	3	3	3	3
Celestus occiduus	3*	6*	5*	4*	2	6*	6*	6*	1	2	2	2	2	2	2
Celestus oligolepis **sp. nov.**	1	1	1	1	1	1	1	1	1	1	1	1	1	1	1
Celestus striatus	2*	2*	2*	2*	1	2*	2*	2*	1	1	1	1	1	1	1
Comptus alloeides	37*	44*	44*	42*	10	42*	44*	43*	9	5	10	10	9	10	9
Comptus arboreus **sp. nov.**	9*	9*	9*	9*	5	9*	9*	9*	5	5	5	5	5	5	5
Comptus badius	3*	5*	5*	5*	4	5*	6*	6*	3	4	4	4	4	4	3
Comptus maculatus	8*	9*	9*	8*	5	8*	8*	8*	5	5	5	5	5	5	5
Comptus stenurus	14*	14*	14*	10*	9	14*	14*	14*	9	9	9	9	8	9	9
Comptus weinlandi	52*	53*	53*	44*	17	53*	53*	51*	17	17	17	17	17	16	17
Guarocuyus jaraguanus	19*	9*	9*	9*	13	19	1	0	0	0	0	0	0	14	14
Panolopus aenetergum	1	1	1	1	1	1	1	1	1	1	1	1	1	1	1

.....continued on the next page

TABLE 2. (Continued)

Name	1	2	3	4	5	6	7	8	9	10	11	12	13	14	15
Panolopus aporus	23*	23*	23*	23*	15	23*	23*	23*	6	6	6	13	15	13	6
Panolopus chalcorhabdus	8*	8*	8*	8*	6	8*	8*	8*	6	6	6	6	6	6	6
Panolopus costatus	14*	14*	14*	10*	15	14*	14*	12*	9	6	9	15	13	15	8
Panolopus curtissi	12*	18*	18*	18*	9	18*	18*	17*	9	7	7	9	9	9	9
Panolopus diastatus	16*	16*	16*	16*	14	16*	16*	16*	14	14	14	14	14	14	14
Panolopus emys	17*	20*	20*	16*	9	20*	20*	20*	9	7	9	9	9	9	9
Panolopus hylonomus	11*	12*	12*	9*	10	12*	12*	12*	10	9	10	10	10	10	10
Panolopus lanceolatus **sp. nov.**	9*	9*	9*	9*	8	9*	9*	9*	7	8	8	8	8	8	8
Panolopus lapierrae **sp. nov.**	5*	5*	5*	5*	2	5*	5*	5*	2	2	2	2	2	2	2
Panolopus leionotus	16*	17*	17*	17*	12	17*	17*	17*	10	8	10	12	12	12	9
Panolopus marcanoi	23*	23*	23*	23*	21	23*	23*	23*	20	19	21	21	21	21	21
Panolopus melanchrous	76*	79*	80*	80*	46	79*	79*	68*	46	39	46	46	44	46	43
Panolopus neiba	13*	13*	13*	11*	20	13*	13*	12*	10	9	10	17	19	17	9
Panolopus nesobous	8*	8*	8*	8*	2	6*	8*	8*	2	2	2	2	2	2	2
Panolopus oreistes	53*	53*	53*	51*	23	53*	53*	53*	19	19	19	19	19	19	19
Panolopus psychonothes	19*	19*	19*	19*	10	19*	19*	19*	10	10	10	10	10	10	10
Panolopus saonae	3	3	3	3	3	3	3	2	3	2	3	3	2	3	2
Panolopus semitaeniatus **sp. nov.**	8*	8*	8*	7*	3	8*	8*	8*	3	3	3	3	3	3	2
Panolopus unicolor **sp. nov.**	1	1	1	1	1	1	1	1	1	1	1	1	1	1	1
Sauresia agramma **sp. nov.**	4*	4*	4*	4*	3	4*	4*	4*	3	3	3	3	3	3	3
Sauresia cayemitae **sp. nov.**	12*	12*	12*	12*	11	11*	11*	11*	8	11	11	11	10	11	11
Sauresia gracilis **sp. nov.**	1	1	1	1	1	1	1	1	1	1	1	1	1	1	1
Sauresia habichi	11	11	11	11	11	10	10	11	4	10	11	11	10	11	11
Sauresia manicula **sp. nov.**	4*	4*	4*	4*	2	4*	4*	4*	2	2	2	2	2	2	2
Sauresia pangnolae **sp. nov.**	11*	11*	11*	11*	6	11*	11*	11*	5	6	6	6	6	6	6
Sauresia sepsoides	40*	41*	41*	41*	33	41*	41*	41*	32	23	33	33	33	33	33
Sauresia synoria **sp. nov.**	4	4	4	2	4	4	4	4	3	4	4	4	4	4	4
Wetmorena agasepsoides	9	10	10	10	10	10	10	10	10	8	10	10	10	10	10
Wetmorena haetiana	36*	38*	38*	38*	14	37*	38*	37*	13	13	14	14	14	38*	14
Wetmorena mylica	11*	15*	15*	15*	14	15*	15*	15*	7	6	7	14	14	26*	7
Wetmorena obscura **sp. nov.**	3	3	3	3	3	3	3	3	3	3	3	3	3	3	3
Wetmorena orosaura **sp. nov.**	4*	4*	4*	4*	3	4*	4*	4*	3	3	3	3	3	4*	3
Wetmorena surda	23*	32*	32*	32*	22	32*	32*	32*	22	17	22	22	22	22	22

TABLE 2. (Continued)

Name	16	17	18	19	20	21	22	23	24	25	26	27	28	29	30	31
Caribicus anelpistus	1	1	1	1	1	1	1	1	1	1	1	1	1	1	1	1
Caribicus darlingtoni	4	4	4	4	4	4	4	4	4	4	4	4	4	4	4	4
Caribicus warreni	2	2	2	2	2	2	2	2	2	1	1	2	2	2	2	1
Celestus barbouri	8	5	5	5	5	5	5	5	5	5	5	5	5	5	5	5
Celestus capitulatus **sp. nov.**	25	3	3	3	3	5	5	5	3	3	3	3	3	2	3	3
Celestus crusculus	16	5	5	5	5	9	9	9	2	5	5	5	5	5	5	5
Celestus duquesneyi	1	1	1	1	1	1	1	1	1	1	0	1	1	1	1	1

.....continued on the next page

TABLE 2. (Continued)

Name	16	17	18	19	20	21	22	23	24	25	26	27	28	29	30	31
Celestus hesperius **sp. nov.**	2	2	2	2	2	2	2	2	2	2	2	2	2	2	2	2
Celestus hewardi	4	3	3	3	3	4	4	4	3	3	3	3	3	3	3	3
Celestus jamesbondi **sp. nov.**	31	5	5	5	5	5	5	5	5	5	5	5	5	4	5	5
Celestus macrolepis	2	1	1	1	1	2	2	2	1	1	1	1	1	1	1	1
Celestus macrotus	2	1	1	2	2	2	2	2	2	2	2	2	2	1	2	2
Celestus microblepharis	1	1	1	1	1	1	1	1	1	0	1	1	1	1	1	1
Celestus molesworthi	3	2	2	2	2	2	2	2	2	2	2	2	2	2	2	2
Celestus occiduus	2	1	1	1	1	2	2	2	1	1	1	1	1	0	1	1
Celestus oligolepis **sp. nov.**	1	1	1	1	1	1	1	1	1	1	1	1	1	1	1	1
Celestus striatus	1	0	0	1	1	1	1	1	1	1	1	1	1	1	1	1
Comptus alloeides	10	5	5	5	5	5	5	5	5	5	5	5	5	5	5	5
Comptus arboreus **sp. nov.**	5	4	4	4	4	4	4	4	4	3	4	4	4	4	4	4
Comptus badius	3	1	1	3	3	3	3	3	2	3	2	3	2	3	2	2
Comptus maculatus	5	5	5	5	5	5	5	5	5	5	5	5	5	5	5	5
Comptus stenurus	9	5	5	5	5	7	7	7	5	5	5	5	5	5	5	5
Comptus weinlandi	17	15	15	15	15	15	15	15	15	14	15	15	15	15	15	15
Guarocuyus jaraguanus	1	0	0	0	0	0	0	0	1	0	0	0	0	0	0	0
Panolopus aenetergum	1	1	1	1	1	1	1	1	1	1	1	1	1	1	1	1
Panolopus aporus	10	5	5	5	5	5	5	5	5	5	5	5	5	5	3	3
Panolopus chalcorhabdus	6	6	6	6	6	6	6	6	6	5	5	5	5	5	5	5
Panolopus costatus	9	5	5	5	5	5	5	5	5	5	5	5	5	5	6	5
Panolopus curtissi	9	7	7	7	7	7	7	7	7	7	5	5	5	8	5	5
Panolopus diastatus	14	10	10	10	10	10	10	10	10	9	10	10	10	10	10	10
Panolopus emys	9	5	5	5	5	5	5	5	5	5	5	5	5	5	2	2
Panolopus hylonomus	10	6	6	6	6	6	6	6	6	6	3	3	3	5	3	3
Panolopus lanceolatus **sp. nov.**	8	8	8	8	8	8	8	8	8	8	7	8	8	8	7	7
Panolopus lapierrae **sp. nov.**	2	2	2	2	2	2	2	2	2	2	2	2	1	2	1	1
Panolopus leionotus	9	7	7	7	7	7	7	7	6	5	7	7	7	7	7	7
Panolopus marcanoi	19	17	18	18	18	18	18	18	16	16	18	18	18	17	18	18
Panolopus melanchrous	46	9	9	9	9	9	8	9	9	8	5	5	5	7	5	4
Panolopus neiba	10	5	6	6	6	6	5	6	6	5	5	5	5	5	5	5
Panolopus nesobous	2	2	2	2	2	2	2	2	2	2	2	2	2	2	2	2
Panolopus oreistes	19	15	14	15	15	15	14	15	15	15	14	14	14	17	14	14
Panolopus psychonothes	10	6	6	6	6	6	6	6	6	6	5	5	5	5	5	5
Panolopus saonae	3	1	1	1	1	1	1	1	1	1	1	1	1	1	1	1
Panolopus semitaeniatus **sp. nov.**	3	3	3	3	3	3	3	3	3	3	1	1	1	1	1	1
Panolopus unicolor **sp. nov.**	1	1	1	1	1	1	1	1	1	1	1	1	1	1	1	1
Sauresia agramma **sp. nov.**	3	3	3	3	3	3	3	3	3	2	3	3	2	3	3	3
Sauresia cayemitae **sp. nov.**	11	7	7	7	7	7	7	7	7	7	7	7	7	7	7	7
Sauresia gracilis **sp. nov.**	1	1	1	1	1	1	1	1	1	1	1	1	1	1	1	1
Sauresia habichi	11	9	9	8	9	8	8	9	9	8	9	9	9	9	3	3
Sauresia manicula **sp. nov.**	2	2	2	2	2	2	2	2	2	1	2	2	2	2	2	2
Sauresia pangnolae **sp. nov.**	6	4	4	4	3	4	4	4	4	4	4	4	4	3	4	4

.....continued on the next page

TABLE 2. (Continued)

Name	16	17	18	19	20	21	22	23	24	25	26	27	28	29	30	31
Sauresia sepsoides	33	31	31	31	32	32	32	32	32	31	33	33	33	33	33	33
Sauresia synoria **sp. nov.**	4	4	4	4	4	4	4	4	4	2	4	4	4	4	4	4
Wetmorena agasepsoides	10	7	7	8	8	8	8	8	8	8	8	8	8	8	8	8
Wetmorena haetiana	na	12	12	12	12	12	12	na	na	11	12	12	12	11	12	12
Wetmorena mylica	na	5	5	5	5	5	5	na	na	5	5	5	5	5	5	5
Wetmorena obscura **sp. nov.**	na	3	3	3	3	3	3	na	na	3	3	3	3	3	3	3
Wetmorena orosaura **sp. nov.**	na	3	3	3	3	3	3	na	na	2	3	3	3	3	3	3
Wetmorena surda	na	6	6	6	6	6	6	na	na	6	5	5	5	5	5	5

Results

Molecular Analyses

Twenty-one of the previously recognized Caribbean celestine species are represented in our phylogeny and 13 of the previously recognized subspecies are represented in our phylogeny (Fig. 3). Of the 39 Caribbean celestine species that we recognize after our genetic and morphological analyses with more than one representative in the tree, all had ML support values at the crown node ≥ 95% and 37 had Bayesian support values ≥ 95%. The molecular timetree (Fig. 4) uses the same nine-gene dataset and topology of Fig. 3. Divergences (stem times) between genera were 10.5–7.50 Ma, whereas divergences of species (stem times) within genera were 6.83–0.74 Ma.

Previous authors have attempted to explain the relationships of Caribbean celestine lizards. One idea was proposed by Grant (1940a), which suggested a short-legged and a long-legged group of Jamaican celestines. The long-legged group according to Grant (1940a) included *Celestus duquesneyi*, *C. occiduus*, and *C. hewardi*, whereas the short-legged group included *C. barbouri* and *C. crusculus* (including *C. crusculus crusculus*, *C. crusculus cundalli*, and *C. crusculus molesworthi*). The short-legged group was later expanded to include members of *Diploglossus* and *Comptus* (Grant 1951). Our molecular phylogeny does not support these groups, notably placing *C. duquesneyi* and *C. hewardi* as closer relatives to *C. molesworthi* than to *C. occiduus.* Specimens that were previously considered *C. crusculus* fall outside of this grouping in non-monophyletic groups throughout the genus.

Schwartz (1964) attempted to categorize the relationships among the Hispaniolan celestines, and introduced numerous subspecies within *Comptus stenurus*, *Panolopus costatus*, and *P. curtissi*. Of the subspecies in *Comptus*, low levels of genetic divergence and a lack of diagnostic characters observed between *C. stenurus weinlandi* and *C. stenurus rugosus* caused us to synonymize these two subspecies under the species *C. weinlandi.* Within *Panolopus*, the subspecies that Schwartz (1964) introduced were placed in either *P. costatus* or *P. curtissi* based on "size, coloration and pattern, and general habitus." In our molecular analyses (Fig. 3), neither *P. costatus* nor *P. curtissi* were monophyletic.

The ASAP delimitation analysis identified the best partition scheme for the mitochondrial data (CytB, ND2, 12S rRNA, and 16S rRNA) as 55 groups (ASAP-Score = 7.50; p = 0.00408; W-rank = 0.0000328; and threshold distance = 0.028509). The second-best partition scheme identified by ASAP had 64 groups (ASAP-Score = 8.50; p = 0.0321; W-rank = 0.0000356; and threshold distance = 0.022327).

In most cases, ASAP correctly identified groups that are clearly different species based on several other methods. However, it failed to identify some clades that, according to morphological data and our divergence time criterion, are valid species, and identified yet other clades as species that are, by all other indications, not valid species (see accounts below). Part of this problem is that any delimitation method based on gaps, including coalescent methods, identifies isolated clades but they cannot distinguish actual species (Sukumaran & Knowles 2017). Our time-based method is better in that regard. Therefore, although we present the ASAP results in each account, we do not place much weight on those results.

We report the stem time of each species and compare this time to the 0.7 Ma species delimitation time boundary calculated above from data in Hedges *et al.* (2015) for separating vertebrate species.

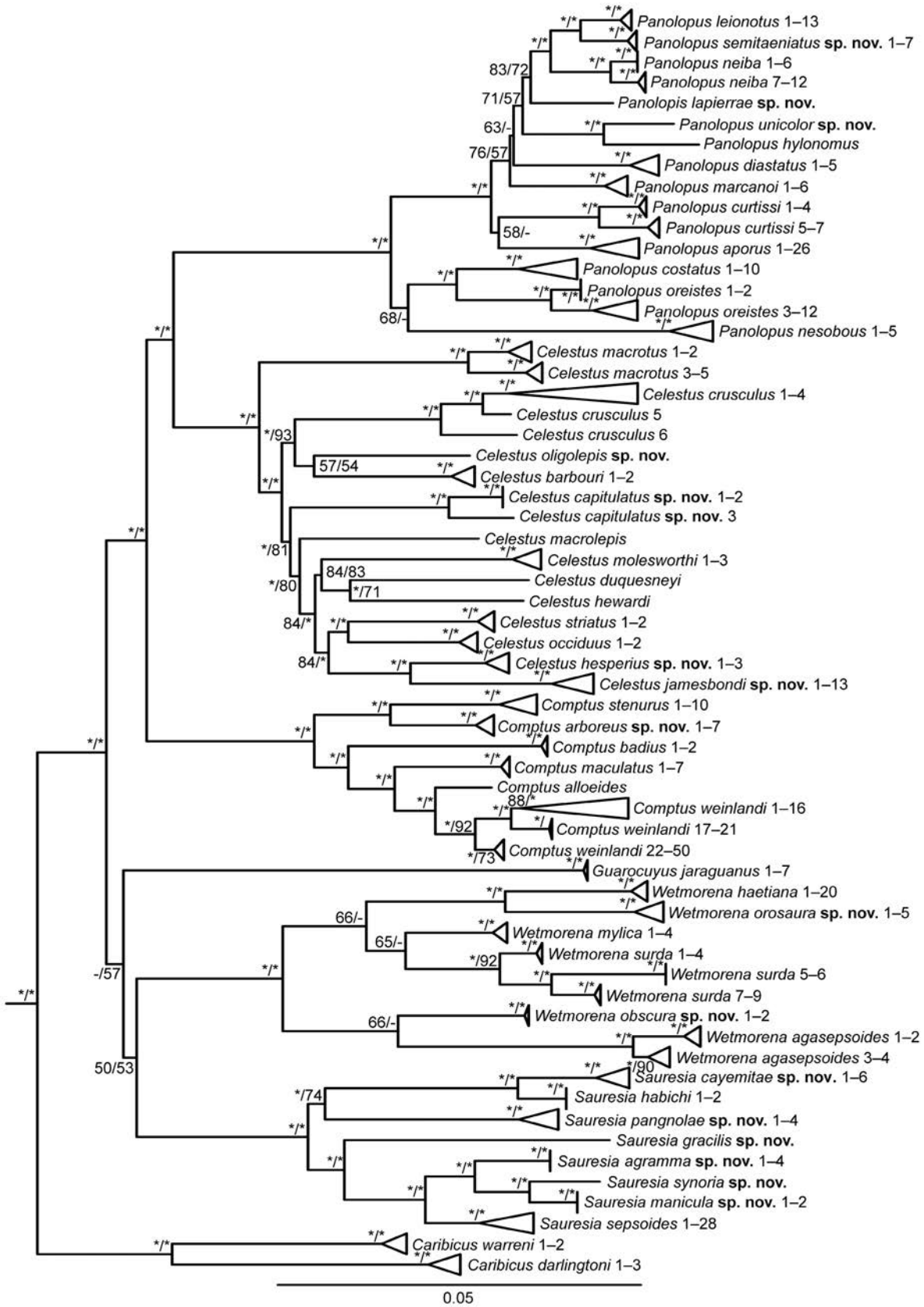

FIGURE 3. Pruned phylogenetic tree of celestine lizards based on sequences of nine genes: four mitochondrial genes (CytB, ND2, 12S rRNA, and 16S rRNA) and five nuclear genes (AMEL, BDNF, PLPR, RAG1, and ZFP36). Maximum likelihood tree obtained from the nine-gene dataset (357 individuals; 6,949 sites). A scale bar indicates 5% sequence divergence. The numbers at nodes are ML bootstrap values, followed by Bayesian posterior probabilities; asterisks indicate significant (≥ 95%) support, and a dash or zero value indicates weak (< 50%) support. The tree is rooted with *Pseudopus apodus* (Anguidae).

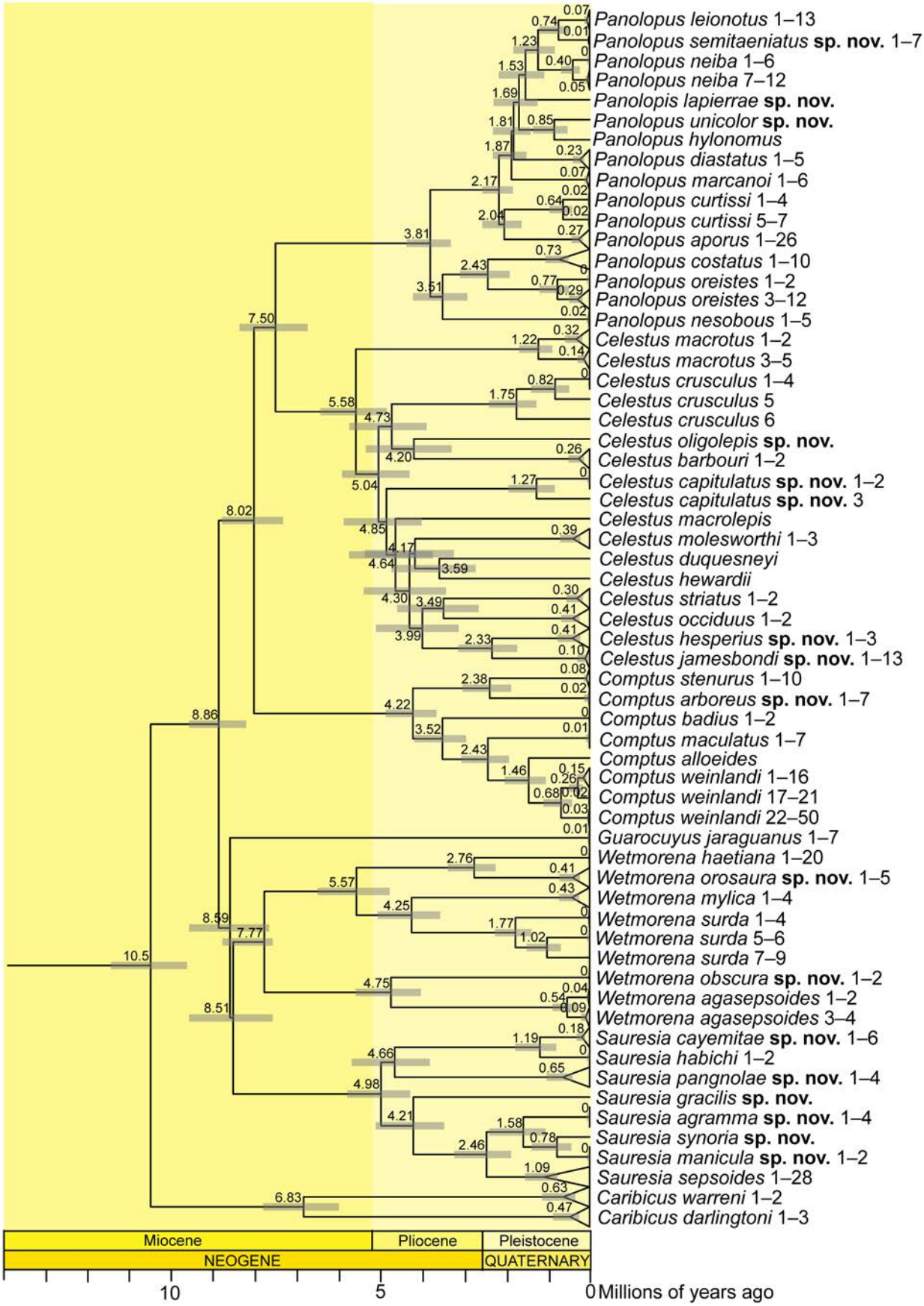

FIGURE 4. Pruned timetree of celestine lizards based on sequences of nine genes: four mitochondrial genes (CytB, ND2, 12S rRNA, and 16S rRNA) and five nuclear genes (AMEL, BDNF, PLPR, RAG1, and ZFP36). Nodes show divergence times in millions of years. We show Bayesian credibility ranges as gray bars at nodes.

Systematic Accounts

Order Squamata Oppel, 1811
Toxicofera Vidal & Hedges, 2005
Anguimorpha Fürbringer, 1900
Neoanguimorpha Vidal & Hedges, 2009
Superfamily Anguioidea Gray, 1825
Family Diploglossidae Cope, 1865

Subfamily Celestinae Schools & Hedges, 2021
Caribbean Forest Lizards

Genus *Caribicus* Schools & Hedges, 2021
Hispaniolan Giant Forest Lizards

Type species. *Celestus darlingtoni* Cochran, 1939:2.

Diagnosis. Species of *Caribicus* have (1) a dorsal pattern of absent/lineate/bands, (2) head markings absent/present, (3) markings in the longitudinal paramedian area absent/present, (4) dots arranged in bars in the lateral band absent/present, (5) a maximum SVL of 61.1–300 mm, (6) ventral scale rows, 69–107, (7) midbody scale rows, 33–43, (8) total lamellae on one hand, 33–48, (9) total strigae on ten scales, 90–500, (10) relative length of all digits on one hindlimb, 24.6–31.9 %, (11) relative distance between the angled subocular and mouth, 0.768–1.57 %, (12) relative eye length, 3.43–3.92 %, (13) relative forelimb length, 19.8–23.3 %, (14) relative ear width, 1.15–1.88 %, (15) relative rostral height, 1.55–2.22 %, (16) relative head length, 17.4–23.8 %, (17) relative mental width, 1.46–2.52 %, (18) relative postmental width, 2.70–3.87 %, (19) relative cloacal width, 7.08–10.8 %, (20) relative prefrontal width, 4.51–7.41 %, (21) relative largest supraocular width, 1.95–3.12 %, (22) relative longest finger length, 3.41–6.14 %, (23) relative distance between the ear and eye, 5.96–10.6 %, (24) relative head width, 71.4–93.4 %, (25) relative frontal width, 74.3–89.3 %, (26) relative nasal height, 1.06–1.45 %, (27) relative angled subocular height, 0.652–1.89 %, (28) relative distance between the eye and naris, 4.38–6.27 %, (29) relative canthal iii length, 1.64–2.17 %, (30) relative angled subocular width, 2.13–2.91 %, and (31) relative nasal width, 1.49–1.92 %.

Content. Three species (Table 3): *Caribicus anelpistus*, *C. darlingtoni*, and *C. warreni*.

Distribution. *Caribicus* occurs primarily on the geological North Island of Hispaniola and adjacent Île-de-la-Tortue, although two old records are from the South Island (Fig. 5).

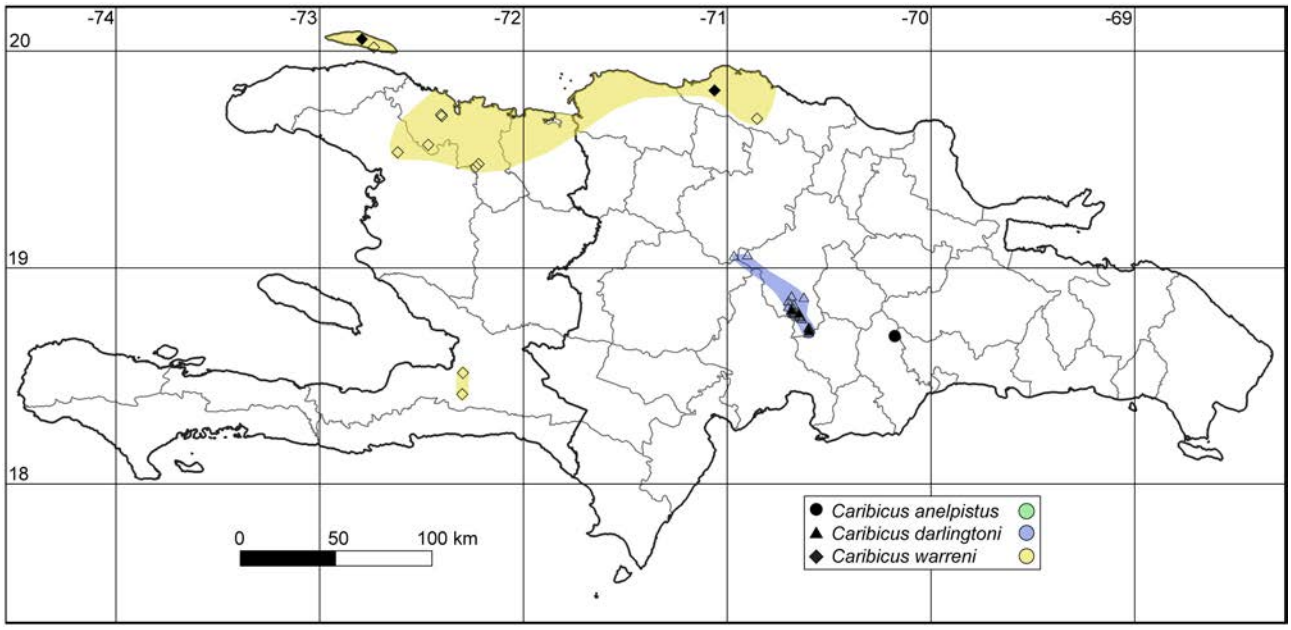

FIGURE 5. Map showing the distribution of *Caribicus*. Hollow symbols indicate unexamined records assignable to species.

TABLE 3. Classification and IUCN threat level of the Caribbean species of the subfamily Celestinae. Additional details on distribution are provided in the text. Bold text in the IUCN Threat Level column indicates a threat level assessment recommended herein.

Species	Common Name	IUCN Threat Level	Distribution
Caribicus anelpistus	Altagracia Giant Forest Lizard	Critically Endangered(Possibly Extinct) B1ab(iii)	Hispaniola
Caribicus darlingtoni	Hispaniolan Striped Forest Lizard	Endangered B1ab(iii)	Hispaniola
Caribicus warreni	Hispaniolan Giant Forest Lizard	Vulnerable B1ab(iii)	Hispaniola
Celestus barbouri	Jamaican Chevronate Forest Lizard	Endangered B1ab(i,iii,v)	Jamaica
Celestus capitulatus **sp. nov.**	Southwestern Jamaican Forest Lizard	**Least Concern**	Jamaica
Celestus crusculus	Common Jamaican Forest Lizard	**Least Concern**	Jamaica
Celestus duquesneyi	Jamaican Blue-tailed Forest Lizard	Critically Endangered B1ab(iii,v)	Jamaica
Celestus hesperius **sp. nov.**	Western Jamaican Forest Lizard	**Endangered B1ab(iii)**	Jamaica
Celestus hewardi	Red-spotted Forest Lizard	Endangered B1ab(iii,v)	Jamaica
Celestus jamesbondi **sp. nov.**	James Bond Forest Lizard	Least Concern	Jamaica
Celestus macrolepis	Black Giant Forest Lizard	**Critically Endangered (Possibly Extinct) C2a(i,ii); D**	Jamaica
Celestus macrotus	Laselle-Baoruco Forest Lizard	Endangered B1ab(i,iii)	Hispaniola
Celestus microblepharis	Small-eyed Forest Lizard	Critically Endangered B1ab(iii,v)	Jamaica
Celestus molesworthi	Eastern Jamaican Forest Lizard	Endangered B1ab(iii,v)	Jamaica
Celestus occiduus	Yellow Giant Forest Lizard	Critically Endangered (Possibly Extinct) C2a(i,ii); D	Jamaica
Celestus oligolepis **sp. nov.**	Jamaican Few-scaled Forest Lizard	**Critically Endangered B1ab(iii)**	Jamaica
Celestus striatus	Golden Forest Lizard	**Critically Endangered B1ab(iii)**	Jamaica
Comptus alloeides	Samana Keeled Forest Lizard	**Least Concern**	Hispaniola
Comptus arboreus **sp. nov.**	Tiburon Keeled Forest Lizard	**Least Concern**	Hispaniola
Comptus badius	Navassa Forest Lizard	Least Concern	Navassa Island
Comptus maculatus	Lesser Cayman Forest Lizard	Endangered B1ab(iii)+2ab(iii)	Cayman Islands
Comptus stenurus	Macaya Keeled Forest Lizard	**Least Concern**	Hispaniola
Comptus weinlandi	Hispaniolan Keeled Forest Lizard	**Least Concern**	Hispaniola
Guarocuyus jaraguanus	Jaragua Forest Lizard	Critically Endangered (CR B2a)	Hispaniola
Panolopus aenetergum	Isla Catalinita Forest Lizard	**Least Concern**	Isla Catalinita
Panolopus aporus	Barahona Smooth-scaled Forest Lizard	**Least Concern**	Hispaniola
Panolopus chalcorhabdus	Big-nosed Smooth-scaled Forest Lizard	**Least Concern**	Hispaniola
Panolopus costatus	Tiburon Smooth-scaled Forest Lizard	**Least Concern**	Hispaniola
Panolopus curtissi	Hispaniolan Khaki Forest Lizard	**Least Concern**	Hispaniola
Panolopus diastatus	Northwestern Smooth-scaled Forest Lizard	**Least Concern**	Hispaniola
Panolopus emys	Tortue Smooth-scaled Forest Lizard	**Least Concern**	Tortue Island
Panolopus hylonomus	Southeastern Smooth-scaled Forest Lizard	**Least Concern**	Hispaniola
Panolopus lanceolatus **sp. nov.**	Westcentral Smooth-scaled Forest Lizard	**Least Concern**	Hispaniola
Panolopus lapierrae **sp. nov.**	Lapierre Forest Lizard	**Critically Endangered B1ab(iii)**	Hispaniola
Panolopus leionotus	Pale Neiba Forest Lizard	**Least Concern**	Hispaniola

.....continued on the next page

TABLE 3. (Continued)

Species	Common Name	IUCN Threat Level	Distribution
Panolopus marcanoi	Pico Duarte Forest Lizard	Least Concern	Hispaniola
Panolopus melanchrous	Hispaniolan Chevronate Forest Lizard	**Least Concern**	Hispaniola
Panolopus neiba	Dark Neiba Forest Lizard	**Least Concern**	Hispaniola
Panolopus nesobous	Ile-a-Vache Forest Lizard	**Least Concern**	Hispaniola
Panolopus oreistes	Dark Spotted Forest Lizard	**Least Concern**	Hispaniola
Panolopus psychonothes	Constanza Forest Lizard	**Endangered B1ab(iii)**	Hispaniola
Panolopus saonae	Saona Forest Lizard	**Least Concern**	Hispaniola
Panolopus semitaeniatus **sp. nov.**	Haitian Half-striped Forest Lizard	**Endangered B1ab(iii)**	Hispaniola
Panolopus unicolor **sp. nov.**	Unicolored Forest Lizard	**Least Concern**	Hispaniola
Sauresia agramma **sp. nov.**	Denfer Four-toed Forest Lizard	**Critically Endangered B1ab(iii)**	Hispaniola
Sauresia cayemitae **sp. nov**.	Cayemite Four-toed Forest Lizard	**Endangered B1ab(iii)**	Hispaniola
Sauresia gracilis **sp. nov.**	Slender Four-toed Forest Lizard	**Critically Endangered B1ab(iii)**	Hispaniola
Sauresia habichi	Stout Four-toed Forest Lizard	**Endangered B1ab(iii)**	Hispaniola
Sauresia manicula **sp. nov.**	Small-footed Four-toed Forest Lizard	**Critically Endangered B1ab(iii)**	Hispaniola
Sauresia pangnolae **sp. nov.**	Pangnol Four-toed Forest Lizard	**Endangered B1ab(iii)**	Hispaniola
Sauresia sepsoides	Eastern Four-toed Forest Lizard	**Least Concern**	Hispaniola
Sauresia synoria **sp. nov.**	Borderland Four-toed Forest Lizard	**Endangered B1ab(iii)**	Hispaniola
Wetmorena agasepsoides	Serpentine Forest Lizard	Endangered B1ab(iii)	Hispaniola
Wetmorena haetiana	Stout Earless Forest Lizard	**Endangered B1ab(iii)**	Hispaniola
Wetmorena mylica	Barahona Earless Forest Lizard	**Endangered B1ab(iii)**	Hispaniola
Wetmorena obscura **sp. nov.**	Long-fingered Earless Forest Lizard	**Critically Endangered B1ab(iii)**	Hispaniola
Wetmorena orosaura **sp. nov.**	Denfer Earless Forest Lizard	**Critically Endangered B1ab(iii)**	Hispaniola
Wetmorena surda	Striped Earless Forest Lizard	**Endangered B1ab(iii)**	Hispaniola

***Caribicus anelpistus* (Schwartz *et al.* 1979)**

Altagracia Giant Forest Lizard
(Fig. 6)

Diploglossus anelpistus Schwartz *et al.*, 1979:3. Holotype: USNM 197336, collected by Miguel A. Jardines at Ingenio Catarey, San Cristobal, Dominican Republic, on 21 July 1977 (18.686, -70.178; 172 m).
Diploglossus anelpistus—Schwartz & Henderson, 1991:402.
Celestus anelpistus—Powell *et al.*, 1996:65.
Celestus warreni anelpistus—Hallermann & Böhme, 2002:169.
Celestus anelpistus—Hedges *et al.*, 2019:16.
Caribicus anelpistus—Schools & Hedges, 2021:218.
Caribicus anelpistus—Landestoy *et al.*, 2022:204.

Material examined (n=8). DOMINICAN REPUBLIC. **San Cristobal**. KU 227505, KU 227506–11, USNM 197336, Miguel A. Jardines, Villa Altagracia, Ingenio Catarey, 'Come Hombre,' 21 July 1977.

Diagnosis. *Caribicus anelpistus* has (1) a dorsal pattern of bands, (2) head markings present, (3) markings in the longitudinal paramedian area absent/present, (4) dots arranged in bars in the lateral band absent, (5) an adult SVL of 279 mm, (6) ventral scale rows, 81–107, (7) midbody scale rows, 33–40, (8) total lamellae on one hand, 43–48, (9) total strigae on ten scales, 471, (10) relative length of all digits on one hindlimb, 24.6 %, (11) relative distance between the angled subocular and mouth, 1.24 %, (12) relative eye length, 3.69 %, (13) relative forelimb length, 21.0 %, (14) relative ear width, 1.15 %, (15) relative rostral height, 2.03 %, (16) relative head length, 23.8 %, (17) relative mental width, 1.82 %, (18) relative postmental width, 3.87 %, (19) relative cloacal width, 10.8 %, (20) relative prefrontal width, 5.38 %, (21) relative largest supraocular width, 2.31 %, (22) relative longest finger

length, 4.98 %, (23) relative distance between the ear and eye, 10.6 %, (24) relative head width, 77.0 %, (25) relative frontal width, 89.3 %, (26) relative nasal height, 1.11 %, (27) relative angled subocular height, 1.89 %, (28) relative distance between the eye and naris, 5.23 %, (29) relative canthal iii length, 1.64 %, (30) relative angled subocular width, 2.27 %, and (31) relative nasal length, 1.80 %. No genetic data are available for estimating the species stem time or crown time.

Caribicus anelpistus has the smallest relative length of digits on one hindlimb (24.6), relative auricular length (1.15), and relative canthal iii length (1.64) of the genus. This species also has the largest relative head length (23.8), relative postmental width (3.87), relative cloacal width (10.8), relative distance between the ear and eye (10.6), relative frontal width (89.3), and relative angled subocular height (1.89) of the genus.

From *Caribicus darlingtoni*, we distinguish *C. anelpistus* by the dorsal pattern (bands versus lineate), the adult SVL (279 versus 61.1–74.9), the total lamellae on one hand (43–48 versus 33–39), the total strigae on ten scales (471 versus 90–120), the relative length of digits on one hindlimb (24.6 versus 26.1–31.9), the relative distance between angled subocular and mouth (1.24 versus 0.768–1.13), the relative ear width (1.15 versus 1.17–1.85), the relative head length (23.8 versus 17.4–20.0), the relative mental width (1.82 versus 2.05–2.52), the relative postmental width (3.87 versus 2.70–3.21), the relative cloacal width (10.8 versus 7.08–8.48), the relative largest supraocular width (2.31 versus 2.70–3.12), the relative distance between the ear and eye (10.6 versus 6.83–8.58), the relative frontal width (89.3 versus 74.3–80.7), the relative nasal height (1.11 versus 1.14–1.45), the relative angled subocular height (1.89 versus 0.810–1.05), and the relative width of canthal iii (1.64 versus 1.68–2.03). From *C. warreni*, we distinguish *C. anelpistus* by the relative length of digits on one hindlimb (24.6 versus 27.0–27.3), the relative ear width (1.15 versus 1.20–1.88), and the relative rostral height (2.03 versus 1.55–1.99).

Description of holotype. USNM 197336. An adult male; SVL 279 mm; tail laterally compressed, broken in life and partially regenerated, 109 mm (39.1% SVL); axilla-to-groin distance 158 mm (56.6% SVL); forelimb length 58.6 mm (21.0% SVL); hindlimb length 78.5 mm (28.1% SVL); head length 66.5 mm (23.8% SVL); head width 51.2 mm (18.4% SVL); head width 77.0% head length; diameter of orbit 10.3 mm (3.69% SVL); horizontal diameter of ear opening 3.20 mm (1.15% SVL); vertical diameter of ear opening 3.17 mm (1.14% SVL); length of all toes on one foot 68.7 mm (24.6% SVL); shortest distance between angled subocular and lip 3.46 mm (1.24% SVL); shortest distance between the ocular and auricular openings 29.6 mm (10.6% SVL); longest finger length 13.9 mm (4.98% SVL); largest supraocular width 6.45 mm (2.31% SVL); cloacal width 30.1 mm (10.8% SVL); mental width 5.09 mm (1.82% SVL); postmental width 10.8 mm (3.87% SVL); prefrontal width 15.0 mm (5.38% SVL); frontal width 89.3% frontal length; nasal height 3.10 mm (1.11% SVL); angled subocular height 5.26 mm (1.89% SVL); shortest distance between the eye and naris 14.6 mm (5.23% SVL); canthal iii width 4.57 mm (1.64% SVL); angled subocular width 6.32 mm (2.27% SVL); nasal width 5.01 mm (1.80% SVL); rostral width 2.03X as wide as high, barely visible from above, not in contact with nasals, in contact with 1st supralabial and anterior internasal (left)/(right); anterior internasals are narrower than posterior ones; frontonasals and prefrontal fused into a single large plate with a straight posterior margin, much wider than long, bordered by posterior internasals, additional scale separating the postnasal and the 1st loreal (left), 1st loreals, canthal iii, 1st median oculars, and the frontal; frontal barely longer than wide; a pair of frontoparietals, separated by the posterior prolongation of the frontal and the interparietal plate; interparietal plate much smaller than parietals and separating them, posteriorly touching the interoccipital, which is approximately as wide as long; parietal separated from supraoculars by 1st and 2nd temporals and frontoparietal (left)/(right); nasal single; nostril above suture between 1st and 2nd supralabials (left)/(right); 1 postnasal (left)/(right); 2 (left)/3 (right) loreals; 1st loreal higher than wide (left)/(right), in contact with postnasal, two smaller scales separating it from the postnasal, prefrontal/frontonasal complex, canthal iii, 2nd loreal, and two additional scales that separate the tops of the 3rd–5th supralabials (left)/postnasal, posterior internasal, prefrontal/frontonasal complex, canthal iii, 2nd and 3rd loreal, supralabial 3, and an additional scale that separates the 3rd–4th supralabials (right); 2nd loreal shorter than 1st, higher than wide (left)/shorter than 1st, irregular (right), excluded from contact with supraocular by canthal iii (left); 3rd loreal irregular, excluded from contact with supraocular by canthal iii (right); final loreal posteriorly bordering the upper and lower preoculars (left)/(right); canthal iii wider than high (left)/(right), contacting 1st median ocular, anterior supraciliary, upper preocular, prefrontal/frontonasal complex, and 1st–2nd loreals (left)/1st median ocular, anterior supraciliary, upper preocular, prefrontal/frontonasal complex, and the 1st–3rd loreals (right); 9 median oculars (left)/(right), 1st contacting the prefrontal (left)/(right); 1 upper preocular (left)/(right); an irregular anterior supraciliary (left)/(right); 6 (left)/7 (right) lateral oculars; 5 temporals (left)/(right);

2 suboculars (left)/(right); posterior subocular large and elongate (left)/(right); anterior subocular small (left)/(right); 11 (left)/9 (right) supralabials, 7 (left)/6 (right) to level below center of eye; 12 (left)/10 (right) infralabials, 6–7 (left)/6 (right) to level below center of eye; mental small, followed by a single, slightly larger postmental; 4 pairs of enlarged chin shields; 1st pair in contact with one another; 2nd–4th pairs separated by 1–4 scales; 93 transverse rows of dorsal scales from interoccipital to base of tail; 93 transverse rows of ventral scales from mental to vent; 40 scales around midbody; 5 digits; finger lengths 3>4>2>5>1; 11 lamellae under longest finger (left)/(right); 45 total lamellae on one hand; toe lengths 4>3>5>2>1; 17 lamellae under longest toe (left)/(right); striate with a median keel on dorsal body and caudal scales; smooth ventral scales; 471 total strigae counted on ten scales.

Color (in alcohol): dorsal surface of head medium brown with darker brown areas on scale borders; lateral surfaces of head grading from medium brown to pale gray-brown with darker brown mottling; dorsal surfaces of the body have darker markings on the neck in longitudinal paramedian lines, rest of body has darker brown bands; on the dorsal surface of tail the dark brown bands of body become one and the predominant color of the tail; lateral areas medium brown with continuations of the darker brown bands; dorsal surfaces of the limbs are dark brown with some even darker mottling; lateral and ventral areas of the limbs grade to yellow-green with darker brown mottling; ventral surfaces of the head, body, and tail are yellow-green with dark brown mottling that becomes the predominant color on the tail.

Variation. The patterns of the juveniles examined resemble that of the holotype with dark bands extending across their backs. The pale areas between the bands on the juveniles are much paler than those areas on the adult holotype. All the juveniles have darker outlines on the borders of their head scales with KU 227505 exhibiting this trait in its most reduced form. The lateral areas exhibit continuations of the dorsal pattern. Several specimens exhibit markings in the longitudinal paramedian area as faded streaks or the beginnings of longitudinal paramedian lines (KU 227505, 227507, and 227511). Measurements and other morphological data for the holotype and other examined material are presented in Table 1.

Distribution. *Caribicus anelpistus* is known only from the region of Villa Altagracia, San Cristóbal Province, Dominican Republic (Fig. 5).

Ecology and conservation. No information is available on the ecology of this species, other than what was recorded for the type series. The type locality was an area of broadleaf lowland forest near a creek (Schwartz *et al.* 1979) that was approximately 1 km x ¼ km before clearing began. The holotype and three other adults from the type locality were collected by a bulldozer crew from the root system of a "jabilla" tree (*Hura crepitans*) as the bulldozer knocked it down; the workers and many locals reported that they had never seen these lizards before the clearing began. The living animals were reported to have been most active at night (Schwartz *et al.* 1979). The bulldozer crew that unearthed the type specimen said that some locals referred to this species as "*lucias grandotas.*"

Recently, *Caribicus anelpistus* was rediscovered 7 km SW of Villa Altagracia (De Jesus *et al.* 2023). The discovery of a single specimen occurred as farmers were clearing land to plant Cacao Trees. Locals from the area also reported seeing additional animals of the same species in the area, particularly at night. Surveys should be conducted in an effort to preserve any remaining individuals.

The IUCN Redlist (IUCN 2023) considers the conservation status of *Caribicus anelpistus* to be Critically Endangered (Possibly Extinct) B1ab(iii) because "of its limited extent of occurrence (being known from a single locality) and it occurs in a single location, and any surviving population is presumed to be undergoing a continuing decline in the extent and quality of its habitat. Natural habitat at the type locality has been essentially destroyed, although if the species occurred more widely a continuing decline in the extent and quality of its habitat can be inferred." The holotype description states that locals killed some of the lizards found with the type series (Schwartz *et al.* 1979), indicating that this species may face persecution from humans. Studies are needed to determine the health of any remaining populations and threats to the survival of the species. Captive-breeding programs should be undertaken, because eradication of introduced mammalian predators is currently not possible on large islands. All mongoose-free islets of Hispaniola need to be thoroughly surveyed for the possible presence of this species.

Reproduction. Ovoviviparous. Two wild-caught females gave birth to a total of 42 young between 16 July and 3 August (Schwartz *et al.* 1979).

Etymology. The species name is derived from the Greek word for "unexpected."

FIGURE 6. (A–F) *Caribicus anelpistus* (USNM 197336, holotype), SVL 279 mm.

Remarks. When this species was described, it was designated as a full species, rather than a subspecies of *Caribicus warreni*, based on morphological traits and a distance of ~300 km between the type locality and the nearest *C. warreni* population (Schwartz *et al*. 1979). *Caribicus anelpistus* was later designated as a subspecies of *C. warreni*, along with *C. carraui* (Hallermann & Böhme 2002). Later, *C. anelpistus* was elevated again to a full species, whereas *C. carraui* was placed in the synonymy of *C. warreni* (Powell & Henderson 2003).

Schwartz *et al.* (1979) speculated that the isolated populations of *Caribicus anelpistus* and *C. warreni*, in addition to previously discovered fossils of a large forest lizard in a cave at Cerro de San Francisco (Etheridge 1965), suggested that the large diploglossids on Hispaniola were the relicts of an ancient, widespread population and that additional isolated populations likely existed. *Caribicus anelpistus* is not included in our genetic dataset and future studies should be conducted using genetic or genomic data from this species to confirm its taxonomic status.

Caribicus darlingtoni (Cochran 1939)

Hispaniolan Striped Forest Lizard
(Fig. 7–8)

Celestus darlingtoni Cochran, 1939:2. Holotype: MCZ R-44374, collected by Philip J. Darlington, Jr. from Valle Nuevo, La Vega Province, Dominican Republic, in August 1938 (18.809, -70.682; 2,290 m).
Celestus darlingtoni—Cochran, 1941:253.
Celestus darlingtoni—Schwartz & Henderson, 1991:372.
Celestus darlingtoni—Powell *et al.*, 1999:105.
Celestus darlingtoni—Hedges *et al.*, 2019:17.
Caribicus darlingtoni—Schools & Hedges, 2021:218.
Caribicus darlingtoni—Landestoy *et al.*, 2022:204.

Material examined (n=17). DOMINICAN REPUBLIC. **La Vega**. MALT 00988–91, 00997, Miguel A. Landestoy T., 16.9 km SSE of Constanza; MCZ R-44374–76, Philip J. Darlington, Jr., Valle Nuevo, 1–31 August 1938; USNM 107563–4, Valle Nuevo, SE of Constanza, Cordillera Central, August 1938; USNM 328801–4, S. Blair Hedges and Richard Thomas, 36.7 km SE of Constanza, via old road to San Jose de Ocoa, 6 August 1983; USNM 328805–7, S. Blair Hedges and Richard Thomas, ca. 37 km SE of Constanza, via new road to San Jose de Ocoa, 13 July 1986.

Diagnosis. *Caribicus darlingtoni* has (1) a lineate dorsal pattern, (2) head markings absent/present, (3) markings in the longitudinal paramedian area absent/present, (4) dots arranged in bars in the lateral band absent/present, (5) an adult SVL of 61.1–74.9 mm, (6) ventral scale rows, 69–92, (7) midbody scale rows, 33–39, (8) total lamellae on one hand, 33–39, (9) total strigae on ten scales, 90–120, (10) relative length of all digits on one hindlimb, 26.1–31.9 %, (11) relative distance between the angled subocular and mouth, 0.768–1.13 %, (12) relative eye length, 3.45–3.92 %, (13) relative forelimb length, 20.2–23.3 %, (14) relative ear width, 1.17–1.85 %, (15) relative rostral height, 1.76–2.22 %, (16) relative head length, 17.4–20.0 %, (17) relative mental width, 2.05–2.52 %, (18) relative postmental width, 2.70–3.21 %, (19) relative cloacal width, 7.08–8.48 %, (20) relative prefrontal width, 4.51–7.09 %, (21) relative largest supraocular width, 2.70–3.12 %, (22) relative longest finger length, 4.86–6.14 %, (23) relative distance between the ear and eye, 6.83–8.58 %, (24) relative head width, 72.5–93.4 %, (25) relative frontal width, 74.3–80.7 %, (26) relative nasal height, 1.14–1.45 %, (27) relative angled subocular height, 0.810–1.05 %, (28) relative distance between the eye and naris, 4.38–5.61 %, (29) relative canthal iii length, 1.68–2.03 %, (30) relative angled subocular width, 2.24–2.81 %, and (31) relative nasal length, 1.63–1.92 %. The species stem time is 6.83 Ma and the species crown time is 0.47 Ma (Fig. 4).

Caribicus darlingtoni differs from all other species of the genus in having a lineate dorsal pattern. This species has the lowest counts in the genus of total lamellae on one hand (33–39) and total strigae on ten scales (90–120). *Caribicus darlingtoni* has the smallest SVL (61.1–74.9), relative distance between the angled subocular and mouth (0.768–1.13), relative cloacal width (7.08–8.48), and the relative frontal width (74.3–80.7) of the genus. This species also has the largest relative mental width (2.05–2.52) and relative nasal height (1.14–1.45) of any species of *Caribicus*. Notably, *Caribicus darlingtoni* has a smaller SVL than other observed members of the genus by at least 152 mm.

FIGURE 7. (A–F) *Caribicus darlingtoni* (MCZ R-44374, holotype), SVL 66.0 mm.

From *Caribicus anelpistus*, we distinguish *C. darlingtoni* by the dorsal pattern (lineate versus bands), the adult SVL (61.1–74.9 versus 279), the total lamellae on one hand (33–39 versus 43–48), the total strigae on ten scales (90–120 versus 471), the relative length of digits on one hindlimb (26.1–31.9 versus 24.6), the relative distance between angled subocular and mouth (0.768–1.13 versus 1.24), the relative ear width (1.17–1.85 versus 1.15), the relative head length (17.4–20.0 versus 23.8), the relative mental width (2.05–2.52 versus 1.82), the relative postmental width (2.70–3.21 versus 3.87), the relative cloacal width (7.08–8.48 versus 10.8), the relative largest supraocular width (2.70–3.12 versus 2.31), the relative distance between the ear and eye (6.83–8.58 versus 10.6), the relative frontal width (74.3–80.7 versus 89.3), the relative nasal height (1.14–1.45 versus 1.11), the relative angled

subocular height (0.810–1.05 versus 1.89), and the relative width of canthal iii (1.68–2.03 versus 1.64). From *C. warreni*, we distinguish *C. darlingtoni* by the dorsal pattern (lineate versus absent/bands), the adult SVL (61.1–74.9 versus 227–300), the total lamellae on one hand (33–39 versus 41–47), the total strigae on ten scales (90–120 versus 458–500), the relative distance between angled subocular and mouth (0.768–1.13 versus 1.51–1.57), the relative mental width (2.05–2.52 versus 1.46–1.87), the relative cloacal width (7.08–8.48 versus 9.33–10.3), the relative longest finger length (4.86–6.14 versus 3.41–4.71), the relative frontal width (74.3–80.7 versus 82.3), the relative nasal height (1.14–1.45 versus 1.06), and the relative nasal width (1.63–1.92 versus 1.49).

Description of holotype. MCZ R-44374. An adult; SVL 66.0 mm; tail nearly cylindrical, broken in life near tip, regenerated, 56.7 mm (85.9% SVL); axilla-to-groin distance 32.7 mm (49.5% SVL); forelimb length 15.4 mm (23.3% SVL); hindlimb length 21.7 mm (32.9% SVL); head length 12.7 mm (19.2% SVL); head width 9.80 mm (14.8% SVL); head width 77.2% head length; diameter of orbit 2.43 mm (3.68% SVL); horizontal diameter of ear opening 0.83 mm (1.26% SVL); vertical diameter of ear opening 0.66 mm (1.00% SVL); length of all toes on one foot 19.0 mm (28.8% SVL); shortest distance between angled subocular and lip 0.66 mm (1.00% SVL); shortest distance between the ocular and auricular openings 5.66 mm (8.58% SVL); longest finger length 4.05 mm (6.14% SVL); largest supraocular width 1.78 mm (2.70% SVL); cloacal width 5.08 mm (7.70% SVL); mental width 1.35 mm (2.05% SVL); postmental width 1.99 mm (3.02% SVL); prefrontal width 4.68 mm (7.09% SVL); frontal width 80.7% frontal length; nasal height 0.84 mm (1.27% SVL); angled subocular height 0.57 mm (0.864% SVL); shortest distance between the eye and naris 2.99 mm (4.53% SVL); canthal iii width 1.11 mm (1.68% SVL); angled subocular width 1.84 mm (2.79% SVL); nasal length 1.26 mm (1.91% SVL); rostral width 2.22X as wide as high, visible from above (missing), not in contact with nasals, in contact with 1st supralabial (missing), and anterior internasal (missing) (left)/(right); anterior internasals are narrower than posterior ones; a pair of prefrontals, slightly smaller than the frontonasal; frontonasal quadrilateral, bordered by posterior internasals, prefrontal, and the frontal; frontal longer than wide; a pair of frontoparietals, separated by the posterior prolongation of the frontal and the interparietal plate; interparietal plate approximately the size of parietals and separating them, posteriorly touching the interoccipital, which is wider than long; parietal separated from supraoculars by 1st temporals and frontoparietal (left)/(right); nasal single; nostril just posterior to suture between 1st and 2nd supralabials (left)/above suture between 1st and 2nd supralabials (right); 1 postnasal (left)/(right); 2 loreals (left)/(right); 1st loreal higher than wide (left)/(right), in contact with postnasal, posterior internasal, frontonasal, 1st median ocular, canthal iii, 2nd loreal, and 3rd and 4th supralabials (left)/(right); 2nd loreal shorter than 1st, approximately as high as wide (left)/(right), excluded from contact with supraocular by canthal iii (left)/(right); final loreal posteriorly bordering the upper and lower preoculars (left)/(right); canthal iii wider than high (left)/(right), contacting 1st median ocular, anterior supraciliary, upper preocular, and 1st and 2nd loreals (left)/(right); 8 (left)/9 (right) median oculars, 1st contacting the prefrontal (left)/(right); 1 upper preocular (left)/(right); an irregular anterior supraciliary (left)/(right); 5 lateral oculars (left)/(right); 5 temporals (left)/(right); 2 suboculars (left)/(right); posterior subocular large and elongate (left)/(right); anterior subocular small (left)/(right); 10 supralabials (left)/(right), 6 (left)/6–7 (right) to level below center of eye; 9 infralabials (left)/(right), 5 (left)/6–7 (right) to level below center of eye; mental small, followed by a single, slightly larger postmental; 4 pairs of enlarged chin shields; 1st pair in contact with one another; 2nd–4th pairs separated by 1–3 scales; 84 transverse rows of dorsal scales from interoccipital to base of tail; 92 transverse rows of ventral scales from mental to vent; 37 scales around midbody; 5 digits; finger lengths 3>4>2>5>1; 10 lamellae under longest finger (left)/(right); 38 total lamellae on one hand; toe lengths 4>3>5>2>1; 14 (left)/15 (right) lamellae under longest toe; keelless and striate dorsal body and caudal scales; smooth ventral scales; 111 total strigae counted on ten scales.

Color (in alcohol): dorsal surface of head medium brown with darker brown areas on scale borders; lateral surfaces of head grading from medium brown to gray-tan ventrally with irregular brown spots and darker brown eye masks; dorsal surfaces of the body are pale brown with approximately 10 dark brown dorsal stripes, the central two of which are not continuous; dorsal surface of tail same as body with a continuation of the stripes; lateral areas are the same dark brown of the dorsal stripes, heavily interspersed with cream spots grading to gray-tan; dorsal surfaces of the limbs are dark brown with pale dots; lateral and ventral areas of the limbs fade to muted brown with the same pattern as the dorsal areas; ventral surfaces of the head, body, and tail are pearl gray with pale brown markings that fade closer to the tail.

Variation. The examined material resembles the pattern of the holotype closely with dark lines extending down their dorsums. USNM 107564 is unique in lacking both a black outline on the head scales and longitudinal

paramedian lines. The lateral areas of the examined material range from being patternless to mottled to having paler dots. Measurements and other morphological data for the holotype and other examined material are presented in Table 1.

Distribution. *Caribicus darlingtoni* is distributed in the Cordillera Central, Dominican Republic at elevations of 1360–2500 m (Fig. 5).

FIGURE 8. *Caribicus darlingtoni* (USNM 328807, SBH 161688), in life. From ca. 37 km SE Constanza on road to San Jose de Ocoa, La Vega Province, Dominican Republic. Photo by SBH.

Ecology and conservation. This species is often found in high, moist, well-drained areas of pine forests, often near bogs (Schwartz & Henderson 1991). These lizards have reportedly been collected from under rocks, under bark, from the ruins of buildings, and from piles of boards and lumbering slash in sawdust at sawmill sites (Schwartz & Incháustegui 1976; Schwartz & Henderson 1991). S. Blair Hedges (SBH) and Richard Thomas collected animals under rocks and logs 37 km (by road) SE of Constanza (18.7465, -70.6114) in 1983 and 1986. The species *Panolopus marcanoi* is found in similar situations and localities, with the type series of *P. marcanoi* originally assumed to be *Caribicus darlingtoni* (Schwartz & Incháustegui 1976). Schwartz & Incháustegui (1976) reported that individuals of this species occurred in more open areas than *P. marcanoi* and that they would burrow in the grass and leaf litter to escape capture. Schwartz & Incháustegui (1976) also commented that even in the cooler months of December and January, this species was active by midmorning.

The IUCN Redlist (IUCN 2023) considers the conservation status of *Caribicus darlingtoni* to be Endangered B1ab(iii) due to its "limited distribution (with an extent of occurrence of 2,782 km^2), a severely fragmented population, and ongoing threats from agriculture expansion, wildfires due to anthropogenic causes and wood extraction." The introduced mongoose and black rats are probably additional threats. Studies are needed to determine the health of remaining populations and more thoroughly assess threats to the survival of the species.

Reproduction. Ovoviviparous. Litter size, two, based on two females, one female weighing 1.9 g (SBH, field data).

Etymology. Named after Dr. Philip Jackson Darlington, Jr., the collector of the type specimen.

Remarks. Whereas the original description of this species (Cochran 1939) is not detailed, Cochran (1941)

gave a more expanded description. Underwood (1959) speculated that *Caribicus darlingtoni* represented the most "isolated" form of many of the Antillean species (not including *Celestus microblepharis*, *Diploglossus delasagra*, and *Diploglossus pleii*, which he placed in their own group). Prior to Schools & Hedges (2021), this species was never placed in a phylogenetic group with the large diploglossids (*C. anelpistus* and *C. warreni*), although Hass *et al.* (2001) found it to be close to *C. warreni* in immunological distance.

Caribicus darlingtoni is included in our genetic dataset and has significant support in both Bayesian and ML likelihood analyses at the crown node of the species and the stem node that identifies it as the closest relative of *C. warreni*. Based on our timetree (Fig. 4), *C. darlingtoni* diverged from its closest relative 6.83 Ma, consistent with typical species of vertebrates (> 0.7 Ma; Hedges *et al.* 2015). *Caribicus darlingtoni* was recognized as a distinct species by our ASAP analysis.

Caribicus warreni (Schwartz 1970)

Hispaniolan Giant Forest Lizard
(Fig. 9–10)

Diploglossus warreni Schwartz, 1970:780. Holotype: AMNH 103215, collected by C. R. Warren at Palmiste, Tortue Island, Département du Nord Ouest, Haiti on 27 January 1968 (20.0179, -72.7246; 320 m).
Diploglossus carraui—Incháustegui *et al.*, 1985:196. Holotype: USNM 197369, collected by Niño Gómez and presented by José Antonio Carrau from Comedero in May 1978 (19.8183, -71.0617; 76 m).
Diploglossus carraui—Schwartz & Henderson, 1991:403.
Diploglossus warreni—Schwartz & Henderson, 1991:406.
Celestus warreni—Powell *et al.*, 1996:66.
Celestus carraui—Powell *et al.*, 1996:65.
Celestus warreni carraui—Hallermann & Böhme, 2002:169.
Celestus warreni warreni—Hallermann & Böhme, 2002:169.
Celestus warreni—Hedges *et al.*, 2019:17.
Celestus warreni—Langer, 2019:16.
Caribicus warreni—Schools & Hedges, 2021:218.
Caribicus warreni—Landestoy *et al.*, 2022:204.

Material examined (n=14). DOMINICAN REPUBLIC. ANSP 38502, Dominican Republic, locality not available (pet trade), 1 August 1990. MALT (one unnumbered specimen), data received from Miguel Landestoy. **Puerto Plata**. USNM 197369, Niño Gómez, Comedero, La Isabela, May 1978. **HAITI**. ANSP 38501, locality not available (pet trade), 1 June 1989; **Nord-Ouest**. AMNH 103215, C. R. Warren, Tortue Island, Palmiste, 27 January 1968; MNHNSD 723–5, 727–9, 731; KU 227530, Tortue Island, Palmiste, November 1968; USNM 59435, Riviere des Barres, 21 February 1917.

Diagnosis. *Caribicus warreni* has (1) a dorsal pattern of absent/bands, (2) head markings absent/present, (3) markings in the longitudinal paramedian area present, (4) dots arranged in bars in the lateral band absent/present, (5) a maximum SVL of 227–300 mm, (6) ventral scale rows, 78–98, (7) midbody scale rows, 33–43, (8) total lamellae on one hand, 41–47, (9) total strigae on ten scales, 458–500, (10) relative length of all digits on one hindlimb, 27.0–27.3 %, (11) relative distance between the angled subocular and mouth, 1.51–1.57 %, (12) relative eye length, 3.43–3.54 %, (13) relative forelimb length, 19.8–22.0 %, (14) relative ear width, 1.20–1.88 %, (15) relative rostral height, 1.55–1.99 %, (16) relative head length, 19.1–22.1 %, (17) relative mental width, 1.46–1.87 %, (18) relative postmental width, 2.73–3.32 %, (19) relative cloacal width, 9.33–10.3 %, (20) relative prefrontal width, 4.65–7.41 %, (21) relative largest supraocular width, 1.95–2.79 %, (22) relative longest finger length, 3.41–4.71 %, (23) relative distance between the ear and eye, 5.96–9.08 %, (24) relative head width, 71.4–83.7 %, (25) relative frontal width, 82.3 %, (26) relative nasal height, 1.06 %, (27) relative angled subocular height, 0.652–1.34 %, (28) relative distance between the eye and naris, 5.42–6.27 %, (29) relative canthal iii length, 1.90–2.17 %, (30) relative angled subocular width, 2.13–2.91 %, and (31) relative nasal length, 1.49 %. The species stem time is 6.83 Ma and the species crown time is 0.63 Ma (Fig. 4).

Caribicus warreni has the smallest relative longest finger length (3.41–4.71) and relative nasal height (1.06) of the genus. This species also has the largest relative distance between the angled subocular and mouth (1.51–1.57) of the genus.

FIGURE 9. (A–F) *Caribicus warreni* (AMNH 103215, holotype), SVL 218 mm.

FIGURE 10. *Caribicus warreni* (SBH 194521), in life. From Puerto Plata Province, Dominican Republic. Photo by SBH.

From *Caribicus anelpistus*, we distinguish *C. warreni* by the relative length of digits on one hindlimb (27.0–27.3 versus 24.6), the relative ear width (1.20–1.88 versus 1.15), and the relative rostral height (1.55–1.99 versus 2.03). From *C. darlingtoni*, we distinguish *C. warreni* by the dorsal pattern (absent/bands versus lineate), the SVL (227–300 versus 61.1–74.9), the total lamellae on one hand (41–47 versus 33–39), the total strigae on ten scales (458–500 versus 90–120), the relative distance between angled subocular and mouth (1.51–1.57 versus 0.768–1.13), the relative mental width (1.46–1.87 versus 2.05–2.52), the relative cloacal width (9.33–10.3 versus 7.08–8.48), the relative longest finger length (3.41–4.71 versus 4.86–6.14), the relative frontal width (82.3 versus 74.3–80.7), the relative nasal height (1.06 versus 1.14–1.45), and the relative nasal width (1.49 versus 1.63–1.92).

Description of holotype. AMNH 103215. An adult female; SVL 218 mm; tail nearly cylindrical, broken in life midway, regenerated, 111 mm (50.9% SVL); axilla-to-groin distance 134 mm (61.5% SVL); forelimb length 39.3 mm (18.0% SVL); hindlimb length 52.1 mm (23.9% SVL); head length 34.8 mm (16.0% SVL); head width 24.0 mm (11.0% SVL); head width 69.0% head length; diameter of orbit 6.47 mm (2.97% SVL); horizontal diameter of ear opening 1.69 mm (0.775% SVL); vertical diameter of ear opening 1.97 mm (0.904% SVL); length of all toes on one foot 46.6 mm (21.4% SVL); shortest distance between angled subocular and lip 2.18 mm (1.00% SVL); shortest distance between the ocular and auricular openings 15.7 mm (7.20% SVL); longest finger length 9.50 mm (4.36% SVL); largest supraocular width 4.47 mm (2.05% SVL); prefrontal width 10.4 mm (4.77% SVL); frontal width 79.4% frontal length; nasal height 1.95 mm (0.894% SVL); angled subocular height 2.03 mm (0.931% SVL); shortest distance between the eye and naris 9.92 mm (4.55% SVL); canthal iii width 2.17 mm (0.995% SVL); angled subocular width 4.55 mm (2.09% SVL); nasal width 2.49 mm (1.14% SVL); rostral 1.64X as wide as high, barely visible from above, not in contact with nasals, in contact with 1st supralabial and anterior internasal (left)/(right); anterior internasals are narrower than posterior ones; frontonasals and prefrontal fused into a single large plate with a slightly concave posterior margin, much wider than long, bordered by posterior internasals, 1st

loreals, canthal iii, 1st median oculars, and the frontal; frontal longer than wide; a pair of frontoparietals, separated by the posterior prolongation of the frontal and the interparietal plate; interparietal plate smaller than parietals and separating them, posteriorly touching the interoccipital (fused to both parietals), which is longer than wide; parietal separated from supraoculars by 1st and 2nd temporals and frontoparietal (left)/(right); nasal single; nostril above suture between 1st and 2nd supralabials (left)/(right); 1 postnasal (left)/(right); 2 loreals (left)/(right); 1st loreal higher than wide (left)/(right), in contact with postnasal, posterior internasal, prefrontal/frontonasal complex, canthal iii, 2nd loreal, and 3rd–4th supralabials (left)/(right); 2nd loreal shorter than 1st, approximately as high as wide (left)/(right), excluded from contact with supraocular by canthal iii (left)/(right); 2nd loreal posteriorly bordering the upper and lower preoculars (left)/(right); canthal iii wider than high (left)/(right), contacting 1st median ocular, anterior supraciliary, upper preocular, and 1st and 2nd loreals (left)/(right); 10 median oculars (left)/(right), 1st contacting the prefrontal (left)/(right); 1 (left)/2 (right) upper preoculars; an irregular anterior supraciliary (left)/(right); 7 lateral oculars (left)/(right); 5 temporals (left)/(right); 2 suboculars (left)/(right); posterior subocular large and elongate (left)/(right); anterior subocular small (left)/(right); 9 supralabials (left)/(right), 6 to level below center of eye (left)/(right); 9 infralabials (left)/(right), 5 (left)/6 (right) to level below center of eye; mental small, followed by a single, larger post mental; 5 pairs of enlarged chin shields, followed by 1 pair of reduced chin shields; 1st pair in contact with one another, 2nd pair in contact with one another anteriorly, posteriorly separated by one scale; 90 transverse rows of dorsal scales from interoccipital to base of tail; 92 transverse rows of ventral scales from mental to vent; 37 scales around midbody; 5 digits; finger lengths 3>4>2>5>1; 11 lamellae under longest finger (left)/(right); 44 total lamellae on one hand; toe lengths 4>3>5>2>1; 15 lamellae under longest toe (left)/(right); striate and slightly keeled dorsal body and caudal scales; smooth ventral scales; 436 total strigae counted on ten scales.

Color (in alcohol): dorsal surface of head golden gray-brown, patternless; lateral surfaces of head grading from golden gray-brown to dark yellow-cream; dorsal surfaces of the body are gray-brown with faded brown longitudinal paramedian markings and chevrons; dorsal surface of tail the same as the body; lateral areas grade from gray-brown to dark yellow-cream with continuations of the chevrons from the body; dorsal surfaces of the limbs are gray-brown with darker brown mottling; lateral and ventral areas of the limbs grading from gray-brown to dark yellow-cream; ventral surfaces of the head, body, and tail are dark yellow-cream and patternless.

Variation. Although faded in most cases, the examined material resembles the pattern of the holotype closely with darker bands extending laterally along the dorsum. In the type, these bands most closely resemble chevrons. All examined specimens have faded markings in the longitudinal paramedian area, in most specimens these markings are thick, short longitudinal paramedian lines, whereas in KU 227530 the longitudinal paramedian area is mottled. KU 227530 is unique in having black outlines on its head scales. Dots in the lateral area are either absent or very reduced. Measurements and other morphological data for the holotype and other examined material are presented in Table 1.

Distribution. *Caribicus warreni* is distributed in southeastern Haiti and the northern regions of the Dominican Republic and Haiti, including Tortue Island, at elevations of 30–690 m (Fig. 5).

Ecology and conservation. *Caribicus warreni* has been collected in a variety of habitats. Populations were reportedly found in lowland, pine, and cloud forests (Incháustegui *et al.* 1985; Franz & Cordier 1986). In these habitats, individuals were found associated with root systems of trees, under rocks, outside of burrows (during the day), and on asphalt roads at night (Incháustegui *et al.* 1985). On Tortue Island, individuals were collected in banana groves (Schwartz & Henderson 1991). Studies of the stomach contents of *C. warreni* show that the vast majority of prey species are associated with leaf litter (Incháustegui *et al.* 1985). Additional studies found that juvenile *C. warreni* showed preference to cricket stimuli over lettuce, cologne, and water (Cooper & Bradley 2009).

The IUCN Redlist (IUCN 2023) considers the conservation status of *Caribicus warreni* to be Vulnerable B1ab(iii) "due to its limited distribution (with an extent of occurrence of 14,646 km^2), fragmented subpopulations and ongoing threats include expanding agricultural activities, charcoal production, predation by cats, dogs and mongooses. It is killed by local people who mistakenly consider these lizards to be venomous, and it is on the illegal pet trade that continues to decline its extent of occurrence, and quality of habitat, and it is only found in a small protected area." This species has been successfully bred in captivity (McGinnity 2002). Unfortunately, eradication of introduced mammalian predators, including black rats, which are also a threat, is currently not possible on large islands such as Hispaniola. Analyses of satellite imagery of forest cover for the countries of Haiti (Hedges *et al.* 2018) and the neighboring Dominican Republic (Sangermano *et al.* 2015) have shown that protected areas and reserves are often ineffective conservation actions unless accompanied by effective management.

Reproduction. Ovoviviparous. Ten gravid females in August had 8–27 young (SVL 32–47 mm), litter size positively correlated with female SVL (Incháustegui *et al.* 1985). The maximum recorded litter size of this species is 34 (Lawler & Norris 1979).

Etymology. The species name refers to Mr. C. Rhea Warren, the collector of the original material used to describe the species.

Remarks. The original description of *Caribicus warreni* suggested a close relationship between *Caribicus warreni* and *Comptus stenurus*, in part because the paratype of *Caribicus warreni* was at one point identified as *Comptus stenurus* (Schwartz 1970). This assignment placed *Caribicus warreni* in a group with *Panolopus costatus*, in addition to *Comptus stenurus* (Schwartz 1970). Schwartz (1970) also suggested that the fossils of a large diploglossid in a cave at Cerro de San Francisco (Etheridge 1965) could be *C. warreni*, which would indicate that *C. warreni* was previously more widespread.

Caribicus carraui was described as its own species based on morphological characters (Incháustegui *et al.* 1985), before it was later designated a subspecies of *C. warreni* (Hallermann & Böhme 2002), along with *C. anelpistus*. *Caribicus anelpistus* was later elevated to a full species again (Powell & Henderson 2003), whereas *C. carraui* was placed in the synonymy of *C. warreni* (Powell & Henderson 2003). In the type description of *C. carraui*, the authors speculated that it was an intermediate form between *C. anelpistus* and *C. warreni*, but still designated *C. carraui* as a full species, primarily based on ventral differences in both coloration (cream) and pattern ("randomly placed dark brown blotches or smudges") (Incháustegui *et al.* 1985). Although we identified several diagnostic characters separating *C. warreni* from *C. anelpistus*, more data are needed from the latter, especially DNA sequences, to confirm its taxonomic status.

Strahm & Schwartz (1977) speculated that this species appeared early in the geologic history of Hispaniola and that its currently restricted range was a result of the arrival of subsequent species that out-competed them. The other theory proposed to explain the small range of *Caribicus warreni* was that they had always had a small range, and species that arrived later were more successful because they never had to compete with *C. warreni* (Strahm & Schwartz 1977). Schwartz *et al.* (1979) speculated that this species was not rare, even though the first specimen was collected in 1917 and not reported again until the collection of the holotype in 1968.

Sexual dimorphism has been reported in this species, with males having larger heads (Lawler & Norris 1979; Incháustegui *et al.* 1985). Antagonistic behavior between captive males has also been reported and was speculated to be related to the sexual dimorphism in head size (Lawler & Norris 1979).

Caribicus warreni is included in our genetic dataset and has significant support in both Bayesian and ML likelihood analyses at the crown node of the species and the stem node that places it as the closest relative to *C. darlingtoni*. Based on our timetree (Fig. 4), *C. darlingtoni* diverged from its closest relative 6.83 Ma, consistent with typical species of vertebrates (> 0.7 Ma; Hedges *et al.* 2015). *Caribicus warreni* was recognized as a distinct species by our ASAP analysis.

Genus *Celestus* Gray, 1839

Jamaican Forest Lizards

Celestus Gray, 1839:288. Type species: *Celestus striatus* Gray, 1839:288, by original designation.
Macrogongylus Werner, 1901:299. Type species *Macrogongylus brauni* Werner, 1901:299, by original designation.

Diagnosis. Species of *Celestus* have (1) a dorsal pattern of absent/flecks in series/irregular dots/dots in chevrons/mottled/chevrons/bands/bicolored, (2) head markings absent/present, (3) markings in the longitudinal paramedian area absent/present, (4) dots arranged in bars in the lateral band absent/present, (5) an adult SVL of 54.0–367 mm, (6) ventral scale rows, 87–151, (7) midbody scale rows, 35–59, (8) total lamellae on one hand, 25–66, (9) total strigae on ten scales, 64–398, (10) relative length of all digits on one hindlimb, 16.6–37.8 %, (11) relative distance between the angled subocular and mouth, 0.339–1.66 %, (12) relative eye length, 1.83–5.17 %, (13) relative forelimb length, 12.8–26.7 %, (14) relative ear width, 0.446–2.45 %, (15) relative rostral height, 1.41–2.35 %, (16) relative head length, 14.6–22.9 %, (17) relative mental width, 1.28–2.35 %, (18) relative postmental width, 2.47–3.81 %, (19) relative cloacal width, 6.59–11.2 %, (20) relative prefrontal width, 3.93–5.68 %, (21) relative largest supraocular width, 1.69–4.03 %, (22) relative longest finger length, 2.92–7.48 %, (23) relative distance between the ear

and eye, 6.07–10.9 %, (24) relative head width, 64.6–82.1 %, (25) relative frontal width, 57.3–95.5 %, (26) relative nasal height, 0.726–1.62 %, (27) relative angled subocular height, 0.553–1.61 %, (28) relative distance between the eye and naris, 4.25–6.51 %, (29) relative canthal iii length, 1.54–2.16 %, (30) relative angled subocular width, 1.63–2.90 %, and (31) relative nasal length, 1.11–2.33 %.

Content. Fourteen species (Table 3); *Celestus barbouri*, *C. capitulatus* **sp. nov.**, *C. crusculus*, *C. duquesneyi*, *C. hesperius* **sp. nov.**, *C. hewardi*, *C. jamesbondi* **sp. nov.**, *C. macrolepis*, *C. macrotus*, *C. microblepharis*, *C. molesworthi*, *C. occiduus*, *C. oligolepis* **sp. nov.**, and *C. striatus.*

Distribution: *Celestus* occurs almost entirely on Jamaica, with a single species (*C. macrotus*) on Hispaniola (Figs. 11–12).

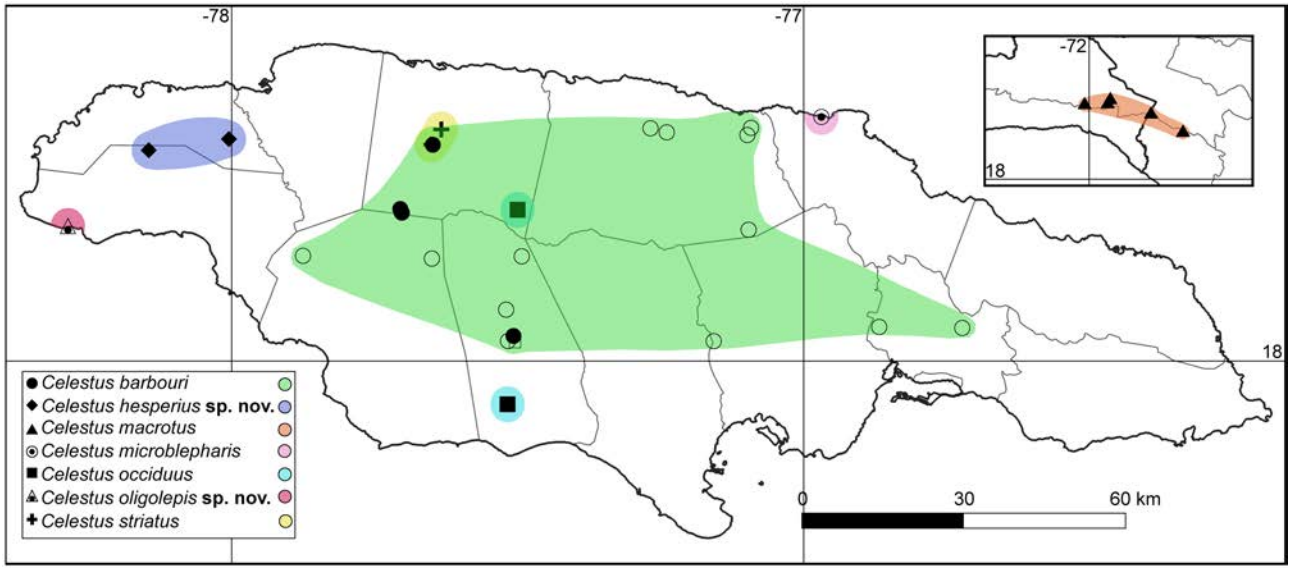

FIGURE 11. Map showing the distribution of seven species of *Celestus* in Jamaica (main map) and *C. macrotus* in Hispaniola (inset, showing the border region between Haiti and the Dominican Republic). Hollow symbols indicate unexamined records. See figure 12 for additional species of *Celestus*.

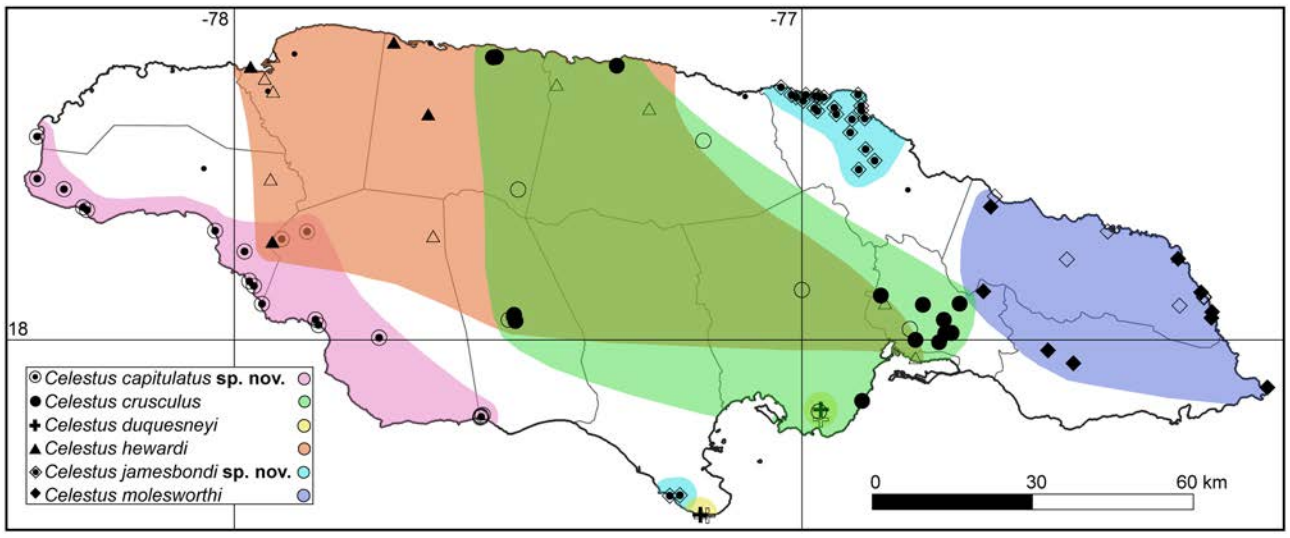

FIGURE 12. Map showing the distribution of six species of *Celestus* in Jamaica. Hollow symbols indicate unexamined records assignable to species. Small black dots indicate unexamined museum records not assignable to species. See figure 11 for additional species of Celestus.

***Celestus barbouri* Grant, 1940a**
Jamaican Chevronate Forest Lizard
(Fig. 13–14)

Celestus barbouri Grant, 1940a:101. Holotype: MCZ R-45169, collected by Chapman Grant from Mandeville between 13–15 April 1937 (18.04, -77.51).
Celestus barbouri—Cousens, 1956:2.
Celestus barbouri—Schwartz & Henderson, 1991:367.
Celestus barbouri—Hedges *et al.*, 2019:16.
Celestus barbouri—Schools & Hedges, 2021:220.
Celestus barbouri—Landestoy *et al.*, 2022:204.

Material examined (n=14). JAMAICA. **Manchester**. MCZ R-45169, Chapman Grant, Mandeville, 13–15 April 1937; USNM 38949–50, Mandeville. **Saint Elizabeth**. BMNH 1936.12.1.110, Mr. J. Armitage, Springfield, 1936. **Trelawny**. ANSP 38503, S. Blair Hedges, Carla Ann Hass, Kimberlyn Nelson, and Stephen Schaeffer, 0.5 km N of Windsor, 28 February 1990; USNM 328145–47, Minocal Stephenson, ca. 0.8 km N of Quick Step, 13 January 1984; USNM 328148, Walton and Wayne Stephenson, vicinity of Quick Step, 29 September 1984; USNM 328149, USNM 328151–3, Minocal Stephenson and family, vicinity of Quick Step, 18–22 September 1985. **Unknown.** One of two untagged specimens in one jar: BMNH 1965.234 or 1965.235 (Spur Tree, Manchester; or Mt. Diablo, Saint Ann, 1965).

Diagnosis. *Celestus barbouri* has (1) a dorsal pattern of chevrons, (2) head markings absent/present, (3) markings in the longitudinal paramedian area absent, (4) dots arranged in bars in the lateral band absent, (5) an adult SVL of 78.4–93.6 mm, (6) ventral scale rows, 118–151, (7) midbody scale rows, 47–56, (8) total lamellae on one hand, 36–49, (9) total strigae on ten scales, 105–136, (10) relative length of all digits on one hindlimb, 18.2–23.5 %, (11) relative distance between the angled subocular and mouth, 0.437–0.556 %, (12) relative eye length, 2.87–3.63 %, (13) relative forelimb length, 15.4–19.0 %, (14) relative ear width, 0.810–1.86 %, (15) relative rostral height, 1.41–1.66 %, (16) relative head length, 14.6–16.6 %, (17) relative mental width, 1.51–1.85 %, (18) relative postmental width, 2.51–3.29 %, (19) relative cloacal width, 7.64–8.26 %, (20) relative prefrontal width, 3.97–4.33 %, (21) relative largest supraocular width, 1.92–2.74 %, (22) relative longest finger length, 2.92–3.81 %, (23) relative distance between the ear and eye, 6.23–7.15 %, (24) relative head width, 73.8–81.7 %, (25) relative frontal width, 65.6–82.1 %, (26) relative nasal height, 0.930–1.12 %, (27) relative angled subocular height, 0.553–1.16 %, (28) relative distance between the eye and naris, 4.68–4.83 %, (29) relative canthal iii length, 1.54–1.93 %, (30) relative angled subocular width, 1.97–2.52 %, and (31) relative nasal length, 1.38–1.65 %. The species stem time is 4.2 Ma and the species crown time is 0.26 Ma (Fig. 4).

We distinguish *Celestus barbouri* from the other species of *Celestus* based on a complex of traits. From *Celestus capitulatus* **sp. nov.**, we distinguish *C. barbouri* by the dorsal pattern (chevrons versus irregular dots/dots in chevrons). From *C. crusculus*, we distinguish *C. barbouri* by the dorsal pattern (chevrons versus absent/flecks in series/dots in chevrons), the longitudinal paramedian lines (absent versus present), the adult SVL (78.4–93.6 versus 59.6–77.6), the ventral scale rows (118–151 versus 98–114), the midbody scale rows (47–56 versus 37–44), and the relative frontal width (65.6–82.1 versus 82.6–91.1). From *C. duquesneyi*, we distinguish *C. barbouri* by the dorsal pattern (chevrons versus bands), the adult SVL (78.4–93.6 versus 62.1), the total lamellae on one hand (36–49 versus 64), the relative length of digits on one hindlimb (18.2–23.5 versus 31.4), the relative distance between angled subocular and mouth (0.437–0.556 versus 0.644), the relative eye length (2.87–3.63 versus 4.36), the relative forelimb length (15.4–19.0 versus 24.4), the relative ear width (0.810–1.86 versus 2.45), the relative rostral height (1.41–1.66 versus 2.14), the relative head length (14.6–16.6 versus 21.6), the relative mental width (1.51–1.85 versus 2.35), the relative cloacal width (7.64–8.26 versus 9.98), the relative prefrontal width (3.97–4.33 versus 5.41), the relative longest finger length (2.92–3.81 versus 6.52), the relative distance between the ear and eye (6.23–7.15 versus 7.68), the relative head width (73.8–81.7 versus 64.6), the relative angled subocular height (0.553–1.16 versus 1.61), the relative distance between the eye and naris (4.68–4.83 versus 5.46), the relative angled subocular width (1.97–2.52 versus 2.90), and the relative nasal width (1.38–1.65 versus 2.01). From *C. hesperius* **sp. nov.**, we distinguish *C. barbouri* by the dorsal pattern (chevrons versus dots in chevrons), the adult SVL (78.4–93.6 versus 54.0–62.3), the ventral scale rows (118–151 versus 111–114), the midbody scale rows (47–56 versus 39–44), the total lamellae on one hand (36–49 versus 29–34), the relative distance between angled subocular and

mouth (0.437–0.556 versus 0.594–0.648), and the relative prefrontal width (3.97–4.33 versus 4.65–5.02). From *C. hewardi*, we distinguish *C. barbouri* by the dorsal pattern (chevrons versus mottled/bands), the adult SVL (78.4–93.6 versus 129–171), the total lamellae on one hand (36–49 versus 50–61), the total strigae on ten scales (105–136 versus 164–315), the relative length of digits on one hindlimb (18.2–23.5 versus 24.1–30.6), the relative distance between angled subocular and mouth (0.437–0.556 versus 0.744–1.40), the relative forelimb length (15.4–19.0 versus 22.2–24.6), the relative head length (14.6–16.6 versus 16.8–21.5), the relative cloacal width (7.64–8.26 versus 8.81–9.89), the relative longest finger length (2.92–3.81 versus 5.03–5.66), the relative nasal height (0.930–1.12 versus 1.21–1.24), and the relative distance between the eye and naris (4.68–4.83 versus 5.00–5.60). From *C. jamesbondi* **sp. nov.**, we distinguish *C. barbouri* by the dorsal pattern (chevrons versus absent/irregular dots/dots in chevrons), the adult SVL (78.4–93.6 versus 54.7–72.0), the ventral scale rows (118–151 versus 91–112), and the midbody scale rows (47–56 versus 35–44). From *C. macrolepis*, we distinguish *C. barbouri* by the dorsal pattern (chevrons versus bicolored), the adult SVL (78.4–93.6 versus 254–316), the ventral scale rows (118–151 versus 112–116), the total lamellae on one hand (36–49 versus 52–54), the total strigae on ten scales (105–136 versus 398), the relative length of digits on one hindlimb (18.2–23.5 versus 27.5–28.0), the relative distance between angled subocular and mouth (0.437–0.556 versus 1.39–1.66), the relative forelimb length (15.4–19.0 versus 26.1–26.7), the relative head length (14.6–16.6 versus 19.2–22.9), the relative mental width (1.51–1.85 versus 1.87), the relative postmental width (2.51–3.29 versus 3.81), the relative cloacal width (7.64–8.26 versus 11.2), the relative prefrontal width (3.97–4.33 versus 3.94), the relative longest finger length (2.92–3.81 versus 5.47–5.51), the relative distance between the ear and eye (6.23–7.15 versus 8.02–10.9), the relative nasal height (0.930–1.12 versus 1.18), the relative angled subocular height (0.553–1.16 versus 1.17), the relative distance between the eye and naris (4.68–4.83 versus 6.02), the relative width of canthal iii (1.54–1.93 versus 1.99), the relative angled subocular width (1.97–2.52 versus 2.57), and the relative nasal width (1.38–1.65 versus 1.75). From *C. macrotus*, we distinguish *C. barbouri* by the longitudinal paramedian lines (absent versus present), the dots arranged in bars in the lateral areas (absent versus present), the ventral scale rows (118–151 versus 87–93), the midbody scale rows (47–56 versus 41–45), the relative length of digits on one hindlimb (18.2–23.5 versus 30.2–31.2), the relative distance between angled subocular and mouth (0.437–0.556 versus 0.640–0.983), the relative eye length (2.87–3.63 versus 3.79–5.17), the relative forelimb length (15.4–19.0 versus 22.4–25.0), the relative head length (14.6–16.6 versus 18.2–20.5), the relative prefrontal width (3.97–4.33 versus 4.87–5.55), the relative largest supraocular width (1.92–2.74 versus 2.96–4.03), the relative longest finger length (2.92–3.81 versus 6.43–6.67), the relative distance between the ear and eye (6.23–7.15 versus 7.58–8.02), the relative nasal height (0.930–1.12 versus 1.15–1.62), the relative distance between the eye and naris (4.68–4.83 versus 5.48–5.60), the relative angled subocular width (1.97–2.52 versus 2.77–2.83), and the relative nasal width (1.38–1.65 versus 2.08–2.33). From *C. microblepharis*, we distinguish *C. barbouri* by the adult SVL (78.4–93.6 versus 96.4), the ventral scale rows (118–151 versus 109), the midbody scale rows (47–56 versus 43), the total lamellae on one hand (36–49 versus 30), the total strigae on ten scales (105–136 versus 165), the relative length of digits on one hindlimb (18.2–23.5 versus 16.6), the relative distance between angled subocular and mouth (0.437–0.556 versus 0.820), the relative eye length (2.87–3.63 versus 1.83), the relative forelimb length (15.4–19.0 versus 14.2), the relative ear width (0.810–1.86 versus 0.446), the relative rostral height (1.41–1.66 versus 1.71), the relative mental width (1.51–1.85 versus 1.44), the relative postmental width (2.51–3.29 versus 2.47), the relative prefrontal width (3.97–4.33 versus 4.37), the relative nasal height (0.930–1.12 versus 0.726), the relative angled subocular width (1.97–2.52 versus 2.90), and the relative nasal width (1.38–1.65 versus 1.11). From *C. molesworthi*, we distinguish *C. barbouri* by the dorsal pattern (chevrons versus dots in chevrons), the total strigae on ten scales (105–136 versus 138–159), the relative distance between angled subocular and mouth (0.437–0.556 versus 0.653–0.845), the relative rostral height (1.41–1.66 versus 1.72–1.81), the relative head length (14.6–16.6 versus 17.2–20.0), the relative cloacal width (7.64–8.26 versus 8.73–9.35), the relative prefrontal width (3.97–4.33 versus 4.44–4.90), the relative longest finger length (2.92–3.81 versus 4.28–5.19), the relative distance between the ear and eye (6.23–7.15 versus 7.97–8.83), the relative nasal height (0.930–1.12 versus 1.17–1.26), the relative distance between the eye and naris (4.68–4.83 versus 5.32–5.50), and the relative width of canthal iii (1.54–1.93 versus 1.99–2.09). From *C. occiduus*, we distinguish *C. barbouri* by the dorsal pattern (chevrons versus absent), the adult SVL (78.4–93.6 versus 269–367), the total lamellae on one hand (36–49 versus 50–66), the total strigae on ten scales (105–136 versus 374), the relative length of digits on one hindlimb (18.2–23.5 versus 24.4–29.7), the relative distance between angled subocular and mouth (0.437–0.556 versus 1.26–1.27), the relative forelimb length (15.4–19.0 versus 23.5–23.9), the relative head length (14.6–16.6 versus 20.4–20.6), the relative mental width (1.51–1.85 versus 1.86), the

relative postmental width (2.51–3.29 versus 3.57), the relative cloacal width (7.64–8.26 versus 9.00), the relative prefrontal width (3.97–4.33 versus 4.76), the relative longest finger length (2.92–3.81 versus 4.77–5.46), the relative distance between the ear and eye (6.23–7.15 versus 8.98–10.9), the relative frontal width (65.6–82.1 versus 63.8), the relative nasal height (0.930–1.12 versus 1.16), the relative angled subocular height (0.553–1.16 versus 1.3), the relative distance between the eye and naris (4.68–4.83 versus 6.51), and the relative nasal width (1.38–1.65 versus 1.83). From *C. oligolepis* **sp. nov.**, we distinguish *C. barbouri* by the dorsal pattern (chevrons versus dots in chevrons), the longitudinal paramedian lines (absent versus present), the ventral scale rows (118–151 versus 98), the midbody scale rows (47–56 versus 35), and the total lamellae on one hand (36–49 versus 30). From *C. striatus*, we distinguish *C. barbouri* by the adult SVL (78.4–93.6 versus 145), the ventral scale rows (118–151 versus 101–109), the midbody scale rows (47–56 versus 41–43), the total lamellae on one hand (36–49 versus 59–66), the total strigae on ten scales (105–136 versus 279), the relative length of digits on one hindlimb (18.2–23.5 versus 37.8), the relative distance between angled subocular and mouth (0.437–0.556 versus 0.710), the relative eye length (2.87–3.63 versus 3.85), the relative forelimb length (15.4–19.0 versus 26.1), the relative rostral height (1.41–1.66 versus 1.94), the relative head length (14.6–16.6 versus 18.9), the relative prefrontal width (3.97–4.33 versus 5.68), the relative longest finger length (2.92–3.81 versus 7.48), the relative distance between the ear and eye (6.23–7.15 versus 9.00), the relative head width (73.8–81.7 versus 82.1), the relative distance between the eye and naris (4.68–4.83 versus 6.16), and the relative width of canthal iii (1.54–1.93 versus 2.12).

Description of holotype. MCZ R-45169. An adult; SVL 66.6 mm; tail nearly cylindrical, broken, 12.9 mm (19.4% SVL); axilla-to-groin distance 36.4 mm (54.7% SVL); forelimb length 13.3 mm (20.0% SVL); hindlimb length 20.6 mm (30.9% SVL); head length 11.8 mm (17.7% SVL); head width 9.56 mm (14.4% SVL); head width 81.0% head length; diameter of orbit 2.14 mm (3.21% SVL); horizontal diameter of ear opening 1.11 mm (1.67% SVL); vertical diameter of ear opening 1.24 mm (1.86% SVL); length of all toes on one foot 15.6 mm (23.4% SVL); shortest distance between angled subocular and lip 0.61 mm (0.916% SVL); shortest distance between the ocular and auricular openings 5.00 mm (7.51% SVL); longest finger length 2.95 mm (4.43% SVL); largest supraocular width 3.96 mm (5.95% SVL); cloacal width 6.00 mm (9.01% SVL); mental width 1.28 mm (1.92% SVL); postmental width 2.35 mm (3.53% SVL); prefrontal width 5.99 mm (8.99% SVL); frontal width 83.9% frontal length; nasal height 1.76 mm (2.64% SVL); angled subocular height 0.66 mm (0.991% SVL); shortest distance between the eye and naris 4.47 mm (6.71% SVL); canthal iii width 1.25 mm (1.88% SVL); angled subocular width 1.43 mm (2.15% SVL); nasal width 1.11 mm (1.67% SVL); rostral 1.65X as wide as high, barely visible from above, not in contact with nasals, in contact with 1st supralabial and anterior internasal (left)/(right); anterior internasals are narrower than posterior ones; frontonasals and prefrontal fused into a single large plate with a concave posterior margin, much wider than long, bordered by posterior internasals, 1st loreals, 1st median oculars, and the frontal; frontal longer than wide; a pair of frontoparietals, separated by the posterior prolongation of the frontal and the interparietal plate; interparietal plate approximately the size of parietals and separating them, posteriorly touching the interoccipital, which is much wider than long; parietal separated from supraoculars by 1st and 2nd temporals and frontoparietal (left)/(right); nasal single; nostril above suture between 1st and 2nd supralabials (left)/(right); 1 postnasal (left)/(right); 2 loreals (left)/(right); 1st loreal higher than wide (left)/(right), in contact with postnasal, posterior internasal, prefrontal/frontonasal complex, 1st median ocular, canthal iii, 2nd loreal, and 3rd–4th supralabials (left)/(right); 2nd loreal shorter than 1st approximately as high as wide (left)/(right), excluded from contact with supraocular by canthal iii (left)/(right); final loreal posteriorly bordering the lower preocular (left)/(right); canthal iii wider than high (left)/(right), contacting 1st median ocular, anterior supraciliary, upper and lower preoculars, and 1st and 2nd loreals (left)/(right); 9 median oculars (left)/(right), 1st contacting the prefrontal (left)/(right); 1 upper preocular (left)/(right); an irregular anterior supraciliary (left)/(right); 6 lateral oculars (left)/(right); 5 temporals (left)/(right); 3 suboculars (left)/(right); posterior subocular large and elongate (left)/(right); anterior suboculars small (left)/(right); 9 supralabials (left)/(right), 6 to level below center of eye (left)/(right); 8 (left)/9 (right) infralabials, 6 to level below center of eye (left)/(right); mental small, followed by a single, larger postmental; 4 pairs of enlarged chin shields; 1st pair in contact with one another; 2nd–4th pairs separated by 1–4 scales; 136 transverse rows of dorsal scales from interoccipital to base of tail; 131 transverse rows of ventral scales from mental to vent; 50 scales around midbody; 5 digits; finger lengths 3>4>2>5>1; 9 lamellae under longest finger (left)/(right); 36 total lamellae on one hand; toe lengths 4>3>5>2>1; 14 (left)/15 (right) lamellae under longest toe; strigae and a faint median keel dorsal body and caudal scales; smooth to faintly striated ventral scales; 82 total strigae counted on ten scales.

FIGURE 13. (A–F) *Celestus barbouri* (MCZ R-45169, holotype), SVL 66.6 mm.

Color (in alcohol): dorsal surface of head medium tan and patternless; lateral surfaces of head grading from medium tan to orange-cream with some faded brown areas around the eyes and on the labial scales; dorsal surfaces of the body are medium brown with darker brown chevrons; dorsal surface of tail is golden brown with the chevrons of the body disappearing after the base; lateral areas are medium brown with white spots vaguely arranged in vertical lines; dorsal surfaces of the limbs are medium brown with a few paler gold spots; lateral and ventral areas of the limbs fade to dark cream; ventral surfaces of the head, body, and tail are dark cream and patternless other than a few faded brown areas on the chin shields.

Variation. The examined material resembles the pattern of the holotype closely with chevrons extending down the dorsum. In ANSP 38503, the chevrons become reduced posteriorly. ANSP 38503 also exhibits very faint black outlines on the head scales and lacks longitudinal paramedian markings. Measurements and other morphological data for the holotype and other examined material are presented in Table 1.

Distribution. *Celestus barbouri* is distributed in the north central region of Jamaica at elevations of 100–610 m (Fig. 11).

FIGURE 14. *Celestus barbouri* (USNM 328151, SBH 161120), SVL 78.4 mm, in life. From Quick Step, Trelawny Parish, Jamaica. Photo by SBH.

Ecology and conservation. Little information is available on the ecology of this species. Individuals have been seen in "trash" (rotting vegetation) piles (Grant 1940a), in rotting coconut debris in a dry scrub forest (Underwood 1959), and in open areas around a cultivated sinkhole (Schwartz & Henderson 1991). The natural habitat of the species is assumed to be the primary forest (limestone forest) adjacent to these disturbed areas where collections were made (see Materials and Methods). This species is rarely encountered (SBH), possibly because of habitat destruction or introduced predators or both. Two large adults weighed 7.0 and 10.8 g (SBH).

The IUCN Redlist (IUCN 2023) considers the conservation status of *Celestus barbouri* to be Endangered B1ab(i,iii,v) because "the species has an extent of occurrence of 3,125 km^2, and occurs in a single location defined by a widespread threat from the invasive Small Asian Mongoose, within which the extent and quality of habitat—and it is suspected the number of mature individuals—is declining." Studies are needed to determine the health and extent of remaining populations and threats to the survival of the species. Captive-breeding programs should be undertaken, because eradication of introduced mammalian predators is not yet possible on Jamaica.

Reproduction. No data on reproduction are available for this species.

Etymology. The species name refers to Thomas Barbour, herpetologist and director of the Museum of Comparative Zoology at Harvard at the time of description in 1940.

Remarks. *Celestus barbouri* has been confused with *C. impressus* (Grant 1940a), which we consider a synonym of *C. hewardi* (see below). *Celestus barbouri* was included in our genetic dataset and has significant support in both Bayesian and ML likelihood analyses at the crown node (two samples from the Cockpits in Trelawny). *Celestus barbouri* was identified as the closest relative to *C. oligolepis* **sp. nov.** in both our ML and Bayesian analyses; however, this relationship was not significant in either analysis (support values of 57% and 54%, respectively). Using genetic data, Schools *et al.* (2022) considered *C. barbouri* the closest relative of *C. oligolepis* **sp. nov.** with a support value of 83% in ML analyses and 89% analyses. Based on our timetree (Fig. 4), *C. barbouri* diverged from its closest relative 4.20 Ma, consistent with typical species of vertebrates (> 0.7 Ma; Hedges *et al.* 2015). Remarkably, *C. barbouri* is separated from *C. capitulatus* **sp. nov.** in our morphological data set only by dorsal pattern, yet the two are deeply divergent genetically (Figs. 3–4) and are not closest relatives. This is remarkable

because the two have not been confused previously, in that the material of *C. capitulatus* **sp. nov.** was identified as *C. crusculus*, not *C. barbouri*, in the past. It probably reflects the fact that morphological data sets in taxonomy, even large ones, never encompass the entire phenotype. *Celestus barbouri* was recognized as a distinct species by our ASAP analysis.

***Celestus capitulatus* sp. nov.**
Southwestern Jamaican Forest Lizard
(Fig. 15)

Celestus crusculus crusculus—Grant, 1940a:102.
Celestus crusculus—Schwartz & Henderson, 1991:369 (part).
Celestus crusculus crusculus—Hedges *et al.*, 2019:17 (part).
Celestus crusculus—Schools & Hedges, 2021:220 (part).
Celestus crusculus—Landestoy *et al.*, 2022:204 (part).

Holotype. USNM 328168, an adult male from Knoxwood, Saint Elizabeth Parish, Jamaica, collected by Carla Ann Hass, S. Blair Hedges, Minocal Stephenson, and Walton Stephenson on 2 October 1984 (18.00363, -77.74489; 8 m).

Paratypes (n=35). JAMAICA. **Hanover**. BMNH 1970.1713, Garth Underwood, Booby Cay, 1970. **Manchester**. BMNH 1938.4.13.8, Chapman Grant, Alligator Pond, southern coast, 1938; BMNH 1970.1721–1724 (one of several untagged specimens in the same jar), Garth Underwood, Alligator Pond, 1970. **Saint Elizabeth**. USNM 328169, Carla Ann Hass, S. Blair Hedges, Minocal Stephenson, and Walton Stephenson, Knoxwood, 2 October 1984; KU 229277, KU 229279–82, 3 mi SE Whitehouse, 10 July 1967; BMNH 1970.1719, Garth Underwood, Black River, 1970; AMNH 72365, 139138–9, Koopman, Hecht, and Williams, 1 mi S of Black River, 13 August 1950. **Westmoreland**. BMNH 1970.1717, Garth Underwood, Negril Hill, Holmes Bay, 1970; BMNH 1970.1718, Garth Underwood, north of Springfield, 1970; BMNH 1970.1715–1716, Garth Underwood, Negril, 1970; KU 229232–3, 2 mi SW Old Hope, 1 July 1967; KU 229244, 0.3 mi NW Whitehouse; KU 229250–1, 0.5 mi SE Whitehouse, 14 July 1967; KU 229252–8, 229260, 0.7 mi NW Bluefields, 17 July 1967; KU 229273–4, 0.1 mi N Beeston Spring, 18 July 1967; KU 229275–6, 3 mi N Kilmarnoch, 18 July 1967; USNM 328157, S. Blair Hedges and Carla Ann Hass, 4.5 km W of Old Hope (at Little Bay), 29 May 1988.

Diagnosis. *Celestus capitulatus* **sp. nov.** has (1) a dorsal pattern of irregular dots/dots in chevrons, (2) head markings absent/present, (3) markings in the longitudinal paramedian area absent/present, (4) dots arranged in bars in the lateral band absent/present, (5) an adult SVL of 62.1–81.8 mm, (6) ventral scale rows, 97–121, (7) midbody scale rows, 37–47, (8) total lamellae on one hand, 25–38, (9) total strigae on ten scales, 105–192, (10) relative length of all digits on one hindlimb, 17.6–22.3 %, (11) relative distance between the angled subocular and mouth, 0.525–1.17 %, (12) relative eye length, 2.75–3.80 %, (13) relative forelimb length, 14.3–18.1 %, (14) relative ear width, 0.671–2.04 %, (15) relative rostral height, 1.51–2.03 %, (16) relative head length, 15.1–17.7 %, (17) relative mental width, 1.28–1.84 %, (18) relative postmental width, 2.62–2.97 %, (19) relative cloacal width, 7.84–8.67 %, (20) relative prefrontal width, 4.30–4.72 %, (21) relative largest supraocular width, 2.03–2.61 %, (22) relative longest finger length, 3.45–3.75 %, (23) relative distance between the ear and eye, 6.45–7.84 %, (24) relative head width, 71.6–78.6 %, (25) relative frontal width, 78.1–81.6 %, (26) relative nasal height, 0.953–1.42 %, (27) relative angled subocular height, 0.586–1.01 %, (28) relative distance between the eye and naris, 4.57–5.03 %, (29) relative canthal iii length, 1.61–1.70 %, (30) relative angled subocular width, 1.93–2.32 %, and (31) relative nasal length, 1.40–1.84 %. The species stem time is 4.85 Ma and the species crown time is 1.27 Ma (Fig. 4).

We distinguish *Celestus capitulatus* **sp. nov.** from congeners based on a complex of traits. From *Celestus barbouri*, we distinguish *C. capitulatus* **sp. nov.** by the dorsal pattern (irregular dots/dots in chevrons versus chevrons). From *C. crusculus*, we distinguish *C. capitulatus* **sp. nov.** by the relative frontal width (78.1–81.6 versus 82.6–91.1). From *C. duquesneyi*, we distinguish *C. capitulatus* **sp. nov.** by the dorsal pattern (irregular dots/dots in chevrons versus bands), the midbody scale rows (37–47 versus 48), the total lamellae on one hand (25–38 versus 64), the relative length of digits on one hindlimb (17.6–22.3 versus 31.4), the relative eye length (2.75–3.80 versus 4.36), the relative forelimb length (14.3–18.1 versus 24.4), the relative ear width (0.671–2.04 versus 2.45), the relative rostral height (1.51–2.03 versus 2.14), the relative head length (15.1–17.7 versus 21.6), the relative mental

width (1.28–1.84 versus 2.35), the relative postmental width (2.62–2.97 versus 3.19), the relative cloacal width (7.84–8.67 versus 9.98), the relative prefrontal width (4.30–4.72 versus 5.41), the relative largest supraocular width (2.03–2.61 versus 2.66), the relative longest finger length (3.45–3.75 versus 6.52), the relative head width (71.6–78.6 versus 64.6), the relative frontal width (78.1–81.6 versus 75.2), the relative angled subocular height (0.586–1.01 versus 1.61), the relative distance between the eye and naris (4.57–5.03 versus 5.46), the relative angled subocular width (1.93–2.32 versus 2.90), and the relative nasal width (1.40–1.84 versus 2.01). From *C. hesperius* **sp. nov.**, we distinguish *C. capitulatus* **sp. nov.** by the relative forelimb length (14.3–18.1 versus 18.6–21.3) and the relative width of canthal iii (1.61–1.70 versus 1.77–1.93). From *C. hewardi*, we distinguish *C. capitulatus* **sp. nov.** by the dorsal pattern (irregular dots/dots in chevrons versus mottled/bands), the adult SVL (62.1–81.8 versus 129–171), the total lamellae on one hand (25–38 versus 50–61), the relative length of digits on one hindlimb (17.6–22.3 versus 24.1–30.6), the relative forelimb length (14.3–18.1 versus 22.2–24.6), the relative cloacal width (7.84–8.67 versus 8.81–9.89), the relative longest finger length (3.45–3.75 versus 5.03–5.66), and the relative frontal width (78.1–81.6 versus 57.3–75.3). From *C. jamesbondi* **sp. nov.**, we distinguish *C. capitulatus* **sp. nov.** by the relative frontal width (78.1–81.6 versus 70.5–77.6) and the relative width of canthal iii (1.61–1.70 versus 1.75–2.16). From *C. macrolepis*, we distinguish *C. capitulatus* **sp. nov.** by the dorsal pattern (irregular dots/dots in chevrons versus bicolored), the adult SVL (62.1–81.8 versus 254–316), the total lamellae on one hand (25–38 versus 52–54), the total strigae on ten scales (105–192 versus 398), the relative length of digits on one hindlimb (17.6–22.3 versus 27.5–28.0), the relative distance between angled subocular and mouth (0.525–1.17 versus 1.39–1.66), the relative forelimb length (14.3–18.1 versus 26.1–26.7), the relative head length (15.1–17.7 versus 19.2–22.9), the relative mental width (1.28–1.84 versus 1.87), the relative postmental width (2.62–2.97 versus 3.81), the relative cloacal width (7.84–8.67 versus 11.2), the relative prefrontal width (4.30–4.72 versus 3.94), the relative largest supraocular width (2.03–2.61 versus 2.64–3.01), the relative longest finger length (3.45–3.75 versus 5.47–5.51), the relative distance between the ear and eye (6.45–7.84 versus 8.02–10.9), the relative head width (71.6–78.6 versus 80.5), the relative angled subocular height (0.586–1.01 versus 1.17), the relative distance between the eye and naris (4.57–5.03 versus 6.02), and the relative angled subocular width (1.93–2.32 versus 2.57). From *C. macrotus*, we distinguish *C. capitulatus* **sp. nov.** by the dorsal pattern (irregular dots/dots in chevrons versus chevrons/bands), the ventral scale rows (97–121 versus 87–93), the total lamellae on one hand (25–38 versus 39–40), the relative length of digits on one hindlimb (17.6–22.3 versus 30.2–31.2), the relative forelimb length (14.3–18.1 versus 22.4–25.0), the relative head length (15.1–17.7 versus 18.2–20.5), the relative postmental width (2.62–2.97 versus 3.00), the relative prefrontal width (4.30–4.72 versus 4.87–5.55), the relative largest supraocular width (2.03–2.61 versus 2.96–4.03), the relative longest finger length (3.45–3.75 versus 6.43–6.67), the relative frontal width (78.1–81.6 versus 57.6–66.1), the relative distance between the eye and naris (4.57–5.03 versus 5.48–5.60), the relative angled subocular width (1.93–2.32 versus 2.77–2.83), and the relative nasal width (1.40–1.84 versus 2.08–2.33). From *C. microblepharis*, we distinguish *C. capitulatus* **sp. nov.** by the dorsal pattern (irregular dots/dots in chevrons versus chevrons), the adult SVL (62.1–81.8 versus 96.4), the relative length of digits on one hindlimb (17.6–22.3 versus 16.6), the relative eye length (2.75–3.80 versus 1.83), the relative forelimb length (14.3–18.1 versus 14.2), the relative ear width (0.671–2.04 versus 0.446), the relative head length (15.1–17.7 versus 14.7), the relative postmental width (2.62–2.97 versus 2.47), the relative longest finger length (3.45–3.75 versus 3.11), the relative nasal height (0.953–1.42 versus 0.726), the relative angled subocular width (1.93–2.32 versus 2.90), and the relative nasal width (1.40–1.84 versus 1.11). From *C. molesworthi*, we distinguish *C. capitulatus* **sp. nov.** by the relative length of digits on one hindlimb (17.6–22.3 versus 22.4–29.4), the relative cloacal width (7.84–8.67 versus 8.73–9.35), the relative longest finger length (3.45–3.75 versus 4.28–5.19), the relative distance between the ear and eye (6.45–7.84 versus 7.97–8.83), the relative angled subocular height (0.586–1.01 versus 1.11), the relative distance between the eye and naris (4.57–5.03 versus 5.32–5.50), and the relative width of canthal iii (1.61–1.70 versus 1.99–2.09). From *C. occiduus*, we distinguish *C. capitulatus* **sp. nov.** by the dorsal pattern (irregular dots/dots in chevrons versus absent), the adult SVL (62.1–81.8 versus 269–367), the total lamellae on one hand (25–38 versus 50–66), the total strigae on ten scales (105–192 versus 374), the relative length of digits on one hindlimb (17.6–22.3 versus 24.4–29.7), the relative distance between angled subocular and mouth (0.525–1.17 versus 1.26–1.27), the relative forelimb length (14.3–18.1 versus 23.5–23.9), the relative head length (15.1–17.7 versus 20.4–20.6), the relative mental width (1.28–1.84 versus 1.86), the relative postmental width (2.62–2.97 versus 3.57), the relative cloacal width (7.84–8.67 versus 9.00), the relative prefrontal width (4.30–4.72 versus 4.76), the relative longest finger length (3.45–3.75 versus 4.77–5.46), the relative distance between the ear and eye (6.45–7.84 versus 8.98–10.9), the relative frontal

width (78.1–81.6 versus 63.8), the relative angled subocular height (0.586–1.01 versus 1.30), the relative distance between the eye and naris (4.57–5.03 versus 6.51), and the relative angled subocular width (1.93–2.32 versus 2.52). From *C. oligolepis* **sp. nov.**, we distinguish *C. capitulatus* **sp. nov.** by the midbody scale rows (37–47 versus 35). From *C. striatus*, we distinguish *C. capitulatus* **sp. nov.** by the dorsal pattern (irregular dots/dots in chevrons versus absent/chevrons), the adult SVL (62.1–81.8 versus 145), the total lamellae on one hand (25–38 versus 59–66), the total strigae on ten scales (105–192 versus 279), the relative length of digits on one hindlimb (17.6–22.3 versus 37.8), the relative eye length (2.75–3.80 versus 3.85), the relative forelimb length (14.3–18.1 versus 26.1), the relative head length (15.1–17.7 versus 18.9), the relative prefrontal width (4.30–4.72 versus 5.68), the relative largest supraocular width (2.03–2.61 versus 2.63), the relative longest finger length (3.45–3.75 versus 7.48), the relative distance between the ear and eye (6.45–7.84 versus 9.00), the relative head width (71.6–78.6 versus 82.1), the relative frontal width (78.1–81.6 versus 76.5), the relative angled subocular height (0.586–1.01 versus 1.12), and the relative distance between the eye and naris (4.57–5.03 versus 6.16).

Description of holotype. USNM 328168. An adult male; SVL 71.7 mm; tail nearly cylindrical, 6.97 mm (9.72% SVL); axilla-to-groin distance 40.3 mm (56.2% SVL); forelimb length 12.9 mm (18.0% SVL); hindlimb length 18.3 mm (25.5% SVL); head length 12.7 mm (17.7% SVL); head width 9.98 mm (13.9% SVL); head width 78.6% head length; diameter of orbit 2.44 mm (3.40% SVL); horizontal diameter of ear opening 1.46 mm (2.04% SVL); vertical diameter of ear opening 2.10 mm (2.93% SVL); length of all toes on one foot 15.7 mm (21.9% SVL); shortest distance between angled subocular and lip 0.42 mm (0.586% SVL); shortest distance between the ocular and auricular openings 5.62 mm (7.84% SVL); longest finger length 2.66 mm (3.71% SVL); largest supraocular width 1.87 mm (2.61% SVL); cloacal width 5.62 mm (7.84% SVL); mental width 0.92 mm (1.28% SVL); postmental width 1.88 mm (2.62% SVL); prefrontal width 3.29 mm (4.59% SVL); frontal width 78.1% frontal length; nasal height 1.02 mm (1.42% SVL); angled subocular height 0.42 mm (0.586% SVL); shortest distance between the eye and naris 3.32 mm (4.63% SVL); canthal iii width 1.22 mm (1.70% SVL); angled subocular width 1.66 mm (2.32% SVL); nasal width 1.21 mm (1.69% SVL); rostral 1.62X as wide as high, barely visible from above, not in contact with nasals, in contact with 1st supralabial and anterior internasal (left)/(right); anterior internasals are narrower than posterior ones; frontonasals and prefrontal fused into a single large plate with a straight posterior margin, wider than long, bordered by posterior internasals, 1st loreals, canthal iii, 1st median oculars, and the frontal; frontal much longer than wide; a pair of frontoparietals, separated by the posterior prolongation of the frontal and the interparietal plate; interparietal plate smaller than parietals and separating them, posteriorly touching the interoccipital, which is wider than long; parietal separated from supraoculars by 1st and 2nd temporals (missing the 1st on the left) and frontoparietal (left)/(right); nasal single; nostril above suture between 1st and 2nd supralabials (left)/(right); 1 postnasal (left)/(right); 2 loreals (left)/(right); 1st loreal higher than wide (left)/(right), in contact with postnasal, posterior internasal, prefrontal/frontonasal complex, canthal iii, 2nd loreal, and 3rd–4th supralabials (left)/(right); 2nd loreal shorter than 1st, approximately as high as wide (left)/(right), excluded from contact with supraocular by canthal iii (left)/(right); 2nd loreal posteriorly bordering the lower preocular (left)/(right); canthal iii wider than high (left)/(right), contacting 1st median ocular, anterior supraciliary, upper and lower preoculars, prefrontal/frontonasal complex, and 1st and 2nd loreals (left)/(right); 10 (left)/9 (right) median oculars, 1st contacting the prefrontal (left)/(right); 1 upper preocular (left)/(right); an irregular anterior supraciliary (left)/(right); 5 (left)/6 (right) lateral oculars; 5 temporals (left)/(right); 2 suboculars (left)/(right); posterior subocular large and elongate (left)/(right); anterior subocular small (left)/(right); 9 supralabials (left)/(right), 6 to level below center of eye (left)/(right); 9 infralabials (left)/(right), 6 to level below center of eye (left)/(right); mental small, followed by a single, larger postmental; 4 pairs of enlarged chin shields; 1st pair in contact with one another; 2nd–4th pairs separated by 1–3 scales; 118 transverse rows of dorsal scales from interoccipital to base of tail; 113 transverse rows of ventral scales from mental to vent; 44 scales around midbody; 5 digits; finger lengths 3>4>2>5>1; 8 lamellae under longest finger (left)/(right); 32 total lamellae on one hand; toe lengths 4>3>5>2>1; 13 lamellae under longest toe (left)/(right); striate and slightly keeled dorsal body and caudal scales; smooth ventral scales; 105 total strigae counted on ten scales.

Color (in alcohol): dorsal surface of head pale brown, patternless; lateral surfaces of head grading from pale brown to yellow-cream with darker brown eye masks and markings on the labial scales; dorsal surfaces of the body are pale brown with two darker broken longitudinal paramedian lines and dotted chevrons; dorsal surface of tail the same as the body; lateral areas grade from pale brown to cream with the chevrons from the dorsum continuing; dorsal surfaces of the limbs are medium brown, patternless; lateral and ventral areas of the limbs fade to cream, patternless; ventral surfaces of the head, body, and tail are cream with some darker markings on the chin shields.

FIGURE 15. (A–F) *Celestus capitulatus* **sp. nov.** (USNM 328168, holotype), SVL 71.7 mm.

Variation. The dorsal ground color of all examined specimens is pale to medium brown with darker brown dots that form broken chevrons that stretch across the dorsums. All have cream, virtually patternless venter. The throats of both paratypes have a darker gray tone than the rest of their cream-colored venter. Markings in the longitudinal paramedian area range from absent to mottled to bearing small lines with the holotype having the most pronounced longitudinal paramedian lines. The majority of specimens do not exhibit dots arranged in bars in the lateral bands, many of those that do show mottling as opposed to clear dots. Measurements and other morphological data for the holotype and other examined material are presented in Table 1.

Distribution. *Celestus capitulatus* **sp. nov.** is distributed on the southwestern coast of Jamaica in Westmoreland and St. Elizabeth at elevations of 0–530 m (Fig. 12). It has a range size of 1,130 km^2.

Ecology and conservation. Little is known of the ecology of this species other than the holotype and one other animal collected at the same time were both collected in rotting vegetation. A different specimen (USNM 328157) was collected at dusk in sea grape leaf litter. Given the large number of locations (Fig. 12) and occurrence in coastal dry areas as well as inland mesic areas, this species is likely common and tolerant of human disturbance.

We consider the conservation status of *Celestus capitulatus* **sp. nov.** to be Least Concern, based on IUCN Redlist criteria (IUCN 2023). However, its relatively small range is of concern, and therefore studies are needed to determine the health and extent of the populations, and any threats to the survival of the species.

Reproduction. No data on reproduction are available for this species.

Etymology. The species name (*capitulatus*) is a masculine nominative singular adjective (Latin) meaning "small head," in reference to the relatively small average head length of adults in this species.

Remarks. Specimens of this species were observed in the majority of the museum collections examined (AMNH, BMNH, KU, and USNM), having been collected as recently as the 1980s. *Celestus capitulatus* **sp. nov.** is included in our genetic dataset and has significant support in both Bayesian and ML likelihood analyses at the crown node. The stem node that places it outside of the group including *Celestus duquesneyi*, *Celestus hesperius* **sp. nov.**, *Celestus hewardi*, *Celestus jamesbondi* **sp. nov.**, *Celestus macrolepis*, *Celestus molesworthi*, *Celestus occiduus*, and *Celestus striatus* had significant support in our ML analysis and 81% in our Bayesian analyses. Based on our timetree (Fig. 4), *C. capitulatus* **sp. nov.** diverged from its closest relative 4.85 Ma, consistent with typical species of vertebrates (> 0.7 Ma; Hedges *et al.* 2015). *Celestus capitulatus* **sp. nov.** was recognized as a distinct species by our ASAP analysis.

Celestus crusculus (Garman 1887)

Common Jamaican Forest Lizard
(Fig. 16–17)

Diploglossus crusculus Garman, 1887:22. Holotype: MCZ R-6051, collected by Samuel Walton Garman at Kingston, Saint Andrew Parish, Jamaica, on 22 December 1878 (17.97, -76.78).
Diploglossus bakeri—Boulenger, 1900:13. Holotype: BMNH 1946.8.29.38, presented by Mr. C. H. Baker to the Corporation Museum of Leicester from Jamaica.
Celestus impressus—Barbour, 1922:669.
Celestus impressus—Barbour, 1935:123.
Celestus impressus—Barbour, 1937:139.
Celestus crusculus cundalli Grant, 1940a:157. Holotype: MCZ R-45163, collected by Chapman Grant in Mandeville between 13–15 February 1937 (18.04, -77.51).
Celestus crusculus crusculus—Grant, 1940a:102.
Celestus crusculus cundalli—Grant, 1940a:103.
Diploglossus crusculus crusculus—Greer, 1967:94.
Celestus crusculus—Schwartz & Henderson, 1991:369.
Celestus crusculus cundalli—Schwartz & Henderson, 1991:370.
Celestus crusculus crusculus—Hedges *et al.*, 2019:17.
Celestus crusculus cundalli—Hedges *et al.*, 2019:17.
Celestus crusculus—Schools & Hedges, 2021:220.
Celestus crusculus cundalli—Schools & Hedges, 2021:220.
Celestus crusculus—Landestoy *et al.*, 2022:204.

Material examined (n=26). JAMAICA. **Manchester.** MCZ R-45163, MCZ R-45166–7, Chapman Grant, Mandeville, 13–15 February 1937; USNM 108220–2, Mandeville, 22 March 1938. **Saint Andrew.** BMNH 1940.3.11.69, Ivan Sanderson, Constant Spring; BMNH 1954.1.2.37, Garth Underwood, "St. Andrews" (no specific locality); BMNH 1965.129, 1965.135, 1965.139, Mona; BMNH 1970.1726, J. Rankin, Red Hills; BMNH 1970.1727, Garth Underwood, Papine; MCZ R-6051, Samuel Walton Garman, Kingston, 22 December 1878. **Saint Ann.** BMNH 1970.1714, Garth Underwood, St. Ann, Runaway Bay (0 m). **Saint Catherine.** USNM 328186, S. Blair Hedges and Carla Ann Hass, 5.6 km SW of Braeton (in Hellshire Hills, at Hellshire Beach), 15 August 1987 (17.897835, -76.894068; 7 m). **Trelawny.** ANSP 38504, Carla Ann Hass, S. Blair Hedges, Kimberlyn Nelson, and Stephen Schaeffer, 0.3 km W Duncans (jct with Silver Sands access road), 3 March 1990 (18.47105, -77.53887; 101 m); USNM 328159–60, 328161–7, Carla Ann Hass, S. Blair Hedges, Kimberlyn Nelson, and Stephen Schaeffer, 0.3 km W Duncans (jct with Silver Sands access road).

FIGURE 16. (A–F) *Celestus crusculus* (MCZ R-6051, holotype), SVL 75.4 mm.

Diagnosis. *Celestus crusculus* has (1) a dorsal pattern of absent/flecks in series/dots in chevrons, (2) head markings absent/present, (3) markings in the longitudinal paramedian area present, (4) dots arranged in bars in the lateral band absent, (5) an adult SVL of 59.6–77.6 mm, (6) ventral scale rows, 98–114, (7) midbody scale rows, 37–44, (8) total lamellae on one hand, 30–39, (9) total strigae on ten scales, 106–194, (10) relative length of all digits on one hindlimb, 18.7–24.7 %, (11) relative distance between the angled subocular and mouth, 0.339–0.884 %, (12) relative eye length, 2.93–3.61 %, (13) relative forelimb length, 12.8–20.7 %, (14) relative ear width, 0.716–

2.00 %, (15) relative rostral height, 1.62–2.04 %, (16) relative head length, 15.5–20.3 %, (17) relative mental width, 1.37–2.31 %, (18) relative postmental width, 2.73–3.37 %, (19) relative cloacal width, 6.89–8.77 %, (20) relative prefrontal width, 3.93–4.67 %, (21) relative largest supraocular width, 1.97–2.65 %, (22) relative longest finger length, 2.94–4.10 %, (23) relative distance between the ear and eye, 6.07–8.61 %, (24) relative head width, 72.1–76.4 %, (25) relative frontal width, 82.6–91.1 %, (26) relative nasal height, 0.925–1.37 %, (27) relative angled subocular height, 0.953–1.21 %, (28) relative distance between the eye and naris, 4.31–4.86 %, (29) relative canthal iii length, 1.59–2.07 %, (30) relative angled subocular width, 2.03–2.43 %, and (31) relative nasal length, 1.27–1.60 %. The species stem time is 4.73 Ma and the species crown time is 1.75 Ma (Fig. 4).

We distinguish *Celestus crusculus* from the other species of *Celestus* based on a complex of traits. From *Celestus barbouri*, we distinguish *C. crusculus* by the dorsal pattern (absent/flecks in series/dots in chevrons versus chevrons), the longitudinal paramedian lines (present versus absent), the adult SVL (59.6–77.6 versus 78.4–93.6), the ventral scale rows (98–114 versus 118–151), the midbody scale rows (37–44 versus 47–56), and the relative frontal width (82.6–91.1 versus 65.6–82.1). From *C. capitulatus* **sp. nov.**, we distinguish *C. crusculus* by the relative frontal width (82.6–91.1 versus 78.1–81.6). From *C. duquesneyi*, we distinguish *C. crusculus* by the dorsal pattern (absent/flecks in series/dots in chevrons versus bands), the longitudinal paramedian lines (present versus absent), the midbody scale rows (37–44 versus 48), the total lamellae on one hand (30–39 versus 64), the relative length of digits on one hindlimb (18.7–24.7 versus 31.4), the relative eye length (2.93–3.61 versus 4.36), the relative forelimb length (12.8–20.7 versus 24.4), the relative ear width (0.716–2.00 versus 2.45), the relative rostral height (1.62–2.04 versus 2.14), the relative head length (15.5–20.3 versus 21.6), the relative mental width (1.37–2.31 versus 2.35), the relative cloacal width (6.89–8.77 versus 9.98), the relative prefrontal width (3.93–4.67 versus 5.41), the relative largest supraocular width (1.97–2.65 versus 2.66), the relative longest finger length (2.94–4.10 versus 6.52), the relative frontal width (82.6–91.1 versus 75.2), the relative angled subocular height (0.953–1.21 versus 1.61), the relative distance between the eye and naris (4.31–4.86 versus 5.46), the relative angled subocular width (2.03–2.43 versus 2.90), and the relative nasal width (1.27–1.60 versus 2.01). From *C. hesperius* **sp. nov.**, we distinguish *C. crusculus* by the relative head width (72.1–76.4 versus 76.5–79.8). From *C. hewardi*, we distinguish *C. crusculus* by the dorsal pattern (absent/flecks in series/dots in chevrons versus mottled/bands), the adult SVL (59.6–77.6 versus 129–171), the total lamellae on one hand (30–39 versus 50–61), the relative forelimb length (12.8–20.7 versus 22.2–24.6), the relative cloacal width (6.89–8.77 versus 8.81–9.89), the relative longest finger length (2.94–4.10 versus 5.03–5.66), the relative frontal width (82.6–91.1 versus 57.3–75.3), and the relative distance between the eye and naris (4.31–4.86 versus 5.00–5.60). From *C. jamesbondi* **sp. nov.**, we distinguish *C. crusculus* by the relative frontal width (82.6–91.1 versus 70.5–77.6). From *C. macrolepis*, we distinguish *C. crusculus* by the dorsal pattern (absent/flecks in series/dots in chevrons versus bicolored), the longitudinal paramedian lines (present versus absent), the adult SVL (59.6–77.6 versus 254–316), the midbody scale rows (37–44 versus 46–48), the total lamellae on one hand (30–39 versus 52–54), the total strigae on ten scales (106–194 versus 398), the relative length of digits on one hindlimb (18.7–24.7 versus 27.5–28.0), the relative distance between angled subocular and mouth (0.339–0.884 versus 1.39–1.66), the relative eye length (2.93–3.61 versus 3.63–3.70), the relative forelimb length (12.8–20.7 versus 26.1–26.7), the relative postmental width (2.73–3.37 versus 3.81), the relative cloacal width (6.89–8.77 versus 11.2), the relative longest finger length (2.94–4.10 versus 5.47–5.51), the relative frontal width (82.6–91.1 versus 78.4), the relative distance between the eye and naris (4.31–4.86 versus 6.02), the relative angled subocular width (2.03–2.43 versus 2.57), and the relative nasal width (1.27–1.60 versus 1.75). From *C. macrotus*, we distinguish *C. crusculus* by the dorsal pattern (absent/flecks in series/dots in chevrons versus chevrons/bands), the dots arranged in bars in the lateral areas (absent versus present), the ventral scale rows (98–114 versus 87–93), the relative length of digits on one hindlimb (18.7–24.7 versus 30.2–31.2), the relative eye length (2.93–3.61 versus 3.79–5.17), the relative forelimb length (12.8–20.7 versus 22.4–25.0), the relative prefrontal width (3.93–4.67 versus 4.87–5.55), the relative largest supraocular width (1.97–2.65 versus 2.96–4.03), the relative longest finger length (2.94–4.10 versus 6.43–6.67), the relative frontal width (82.6–91.1 versus 57.6–66.1), the relative distance between the eye and naris (4.31–4.86 versus 5.48–5.60), the relative angled subocular width (2.03–2.43 versus 2.77–2.83), and the relative nasal width (1.27–1.60 versus 2.08–2.33). From *C. microblepharis*, we distinguish *C. crusculus* by the dorsal pattern (absent/flecks in series/dots in chevrons versus chevrons), the longitudinal paramedian lines (present versus absent), the adult SVL (59.6–77.6 versus 96.4), the relative length of digits on one hindlimb (18.7–24.7 versus 16.6), the relative eye length (2.93–3.61 versus 1.83), the relative ear width (0.716–2.00 versus 0.446), the relative head length (15.5–20.3 versus 14.7), the relative postmental width (2.73–3.37 versus 2.47), the relative

nasal height (0.925–1.37 versus 0.726), the relative angled subocular height (0.953–1.21 versus 0.778), the relative angled subocular width (2.03–2.43 versus 2.90), and the relative nasal width (1.27–1.60 versus 1.11). From *C. molesworthi*, we distinguish *C. crusculus* by the adult SVL (59.6–77.6 versus 78.1–103), the relative longest finger length (2.94–4.10 versus 4.28–5.19), and the relative distance between the eye and naris (4.31–4.86 versus 5.32–5.50). From *C. occiduus*, we distinguish *C. crusculus* by the longitudinal paramedian lines (present versus absent), the adult SVL (59.6–77.6 versus 269–367), the midbody scale rows (37–44 versus 46–56), the total lamellae on one hand (30–39 versus 50–66), the total strigae on ten scales (106–194 versus 374), the relative distance between angled subocular and mouth (0.339–0.884 versus 1.26–1.27), the relative forelimb length (12.8–20.7 versus 23.5–23.9), the relative head length (15.5–20.3 versus 20.4–20.6), the relative postmental width (2.73–3.37 versus 3.57), the relative cloacal width (6.89–8.77 versus 9.00), the relative prefrontal width (3.93–4.67 versus 4.76), the relative longest finger length (2.94–4.10 versus 4.77–5.46), the relative distance between the ear and eye (6.07–8.61 versus 8.98–10.9), the relative frontal width (82.6–91.1 versus 63.8), the relative angled subocular height (0.953–1.21 versus 1.30), the relative distance between the eye and naris (4.31–4.86 versus 6.51), the relative angled subocular width (2.03–2.43 versus 2.52), and the relative nasal width (1.27–1.60 versus 1.83). From *C. oligolepis* **sp. nov.**, we distinguish *C. crusculus* by the midbody scale rows (37–44 versus 35). From *C. striatus*, we distinguish *C. crusculus* by the adult SVL (59.6–77.6 versus 145), the total lamellae on one hand (30–39 versus 59–66), the total strigae on ten scales (106–194 versus 279), the relative length of digits on one hindlimb (18.7–24.7 versus 37.8), the relative eye length (2.93–3.61 versus 3.85), the relative forelimb length (12.8–20.7 versus 26.1), the relative prefrontal width (3.93–4.67 versus 5.68), the relative longest finger length (2.94–4.10 versus 7.48), the relative distance between the ear and eye (6.07–8.61 versus 9.00), the relative frontal width (82.6–91.1 versus 76.5), the relative distance between the eye and naris (4.31–4.86 versus 6.16), and the relative width of canthal iii (1.59–2.07 versus 2.12).

Description of holotype. MCZ R-6051. An adult; SVL 75.4 mm; tail nearly cylindrical, broken off at base and tip, tip regenerated, 71.5 mm (94.8% SVL); axilla-to-groin distance 44.9 mm (59.5% SVL); forelimb length 13.8 mm (18.3% SVL); hindlimb length 21.1 mm (28.0% SVL); head length 14.0 mm (18.6% SVL); head width 10.7 mm (14.2% SVL); head width 76.4% head length; diameter of orbit 2.67 mm (3.54% SVL); horizontal diameter of ear opening 0.54 mm (0.716% SVL); vertical diameter of ear opening 1.37 mm (1.82% SVL); length of all toes on one foot 14.1 mm (18.7% SVL); shortest distance between angled subocular and lip 0.39 mm (0.517% SVL); shortest distance between the ocular and auricular openings 6.49 mm (8.61% SVL); longest finger length 2.99 mm (3.97% SVL); largest supraocular width 1.83 mm (2.43% SVL); cloacal width 6.49 mm (8.61% SVL); mental width 1.03 mm (1.37% SVL); postmental width 2.21 mm (2.93% SVL); prefrontal width 3.52 mm (4.67% SVL); frontal width 91.1% frontal length; nasal height 0.92 mm (1.22% SVL); angled subocular height 0.87 mm (1.15% SVL); shortest distance between the eye and naris 3.43 mm (4.55% SVL); canthal iii width 1.21 mm (1.60% SVL); angled subocular width 1.61 mm (2.14% SVL); nasal width 0.97 mm (1.29% SVL); rostral 1.70X as wide as high, visible from above, not in contact with nasals, in contact with 1st supralabial and anterior internasal (left)/(right); anterior internasals are narrower than posterior ones; frontonasals and prefrontal fused into a single large plate with a slightly concave posterior margin, much wider than long, bordered by posterior internasals, 1st loreals, canthal iii, 1st median oculars, and the frontal; frontal longer than wide; a pair of frontoparietals, separated by the posterior prolongation of the frontal and the interparietal plate; interparietal plate smaller than parietals and separating them, posteriorly touching the interoccipital, which is wider than long; parietal separated from supraoculars by 1st and 2nd temporals and frontoparietal (left)/(right); nasal single; nostril above suture between 1st and 2nd supralabials (left)/(right); 1 postnasal (left)/(right); 2 loreals (left)/(right); 1st loreal higher than wide (left)/(right), in contact with postnasal, posterior internasal, prefrontal/frontonasal complex, canthal iii, 2nd loreal, and 3rd–4th supralabial (left)/(right); 2nd loreal shorter than 1st, approximately as high as wide (left)/(right), excluded from contact with supraocular by canthal iii (left)/(right); final loreal posteriorly bordering the lower preocular (left)/(right); canthal iii wider than high (left)/(right), contacting 1st median ocular, anterior supraciliary, upper and lower preoculars, and 1st and 2nd loreals (left)/(right); 10 (left)/9 (right) median oculars, 1st contacting the prefrontal (left)/(right); 1 upper preocular (left)/(right); an irregular anterior supraciliary (left)/(right); 6 lateral oculars (left)/(right); 5 temporals (left)/(right); 2 suboculars (left)/(right); posterior subocular large and elongate (left)/(right); anterior subocular small (left)/(right); 9 (left)/8 (right) supralabials, 6 (left)/5 (right) to level below center of eye; 10 (left)/9 (right) infralabials, 6 (left)/5–6 (right) to level below center of eye; mental small, followed by a single, larger postmental; 4 pairs of enlarged chin shields; 1st pair in contact with one another; 2nd–4th pairs separated by 1–3 scales; 96 transverse rows of dorsal scales from interoccipital to base of tail; 100 transverse rows of ventral scales from mental to vent; 42 scales around

midbody; 5 digits; finger lengths 3>4>2>5>1; 8 (left)/7 (right) lamellae under longest finger; 30 total lamellae on one hand; toe lengths 4>3>5>2>1; 14 lamellae under longest toe on the right side; many missing, striate with a small median keel towards trunk dorsal body and caudal scales; smooth ventral scales.

Color (in alcohol): mid shed, dorsal surface of head dark gold, patternless; lateral surfaces of head grading from dark brown to gray-tan with irregular brown mottling and darker brown eye masks; dorsal surfaces of the body are pale brown with two darker longitudinal paramedian lines that end before the forearms and brown dots arranged into almost complete chevrons; dorsal surface of tail the same as body with more complete chevrons; lateral areas grade from medium brown to cream; dorsal surfaces of the limbs are medium brown with some irregular brown mottling; lateral and ventral areas of the limbs fade to gray-tan, patternless; ventral surfaces of the head, body, and tail are cream, darker brown mottling begins under the head and ends near the forelimbs.

Variation. The majority of the specimens are similar to the holotype in scalation and pattern with specimens ranging in dorsal pattern from obscure mottling to chevrons. All specimens other than the holotype exhibit markings on their head scales. The longitudinal paramedian markings are most pronounced in the holotype whereas they range from being completely absent to very thin in the other specimens. Measurements and other morphological data for the holotype and other examined material are presented in Table 1.

Ecology and conservation. No ecological information is associated with the type specimen. The specimens used in our genetic analysis were found under rocks along the road. Past literature accounts of ecological data for this species conflate multiple species and therefore cannot be used. However, this species is considered to be common (SBH), has a relatively wide distribution, and is tolerant of human disturbance.

We consider the conservation status of *C. crusculus* **sp. nov.** to be Least Concern, based on IUCN Redlist criteria (IUCN 2023). However, studies are needed to determine the health and extent of the populations and any threats to the survival of the species.

Reproduction. Past literature accounts of reproductive data (Greer 1967) for this species conflate multiple species and therefore cannot be used.

Distribution. *Celestus crusculus* is distributed in and around Kingston, Jamaica, and extending through the central areas of the country to the north coast at elevations of 0–860 m (Fig. 12).

FIGURE 17. *Celestus crusculus* (voucher not available), in life. From 0.3 km W Duncans, Trelawny Parish, Jamaica. Photo by SBH.

Etymology. The species name *crusculus* is derived from the Latin "*crusculum*" meaning "little leg", likely in reference to the species' shorter legs.

Remarks. The description of this species lists the type locality as "Kingston, Jamaica." Cochran (1941) speculated that *Celestus crusculus* could possibly be young *C. occiduus*, which was incorrect because adult male and female *C. crusculus* exist and the two species differ in habitus and scalation. This species was confused with *C. impressus* by Thomas Barbour (1922, 1935, 1937), a taxon that we consider here to be a synonym of *C. hewardi*.

Diploglossus bakeri (locality unknown other that "Jamaica") was designated as a synonym for *C. crusculus* by Barbour (1910), who described *Diploglossus bakeri* as "identical" to *C. crusculus*. We were unable to examine the holotype of *D. bakeri* and therefore additional studies should examine it for the morphological characters presented herein to confirm this placement.

Both Grant (1940a) and Barbour (1922, 1935, & 1937) considered this species to be common but poorly-known. When Grant (1940a) introduced *Celestus crusculus cundalli* as a subspecies of *C. crusculus*, he noted that scale counts between the two subspecies blended together on an elevational gradient. We agree with Cousens (1956) that *C. crusculus cundalli* is not supported as a valid taxon with available morphological data, although a thorough genetic analysis of *C. crusculus* is warranted (i.e., with additional samples from throughout the distribution of that taxon).

Celestus crusculus is included in our genetic dataset and has significant support values at the crown node in our Bayesian and ML analyses. The stem node that identifies it as the closest relative of *C. oligolepis* **sp. nov.** and *C. barbouri* has significant support in our ML analysis and 93% in our Bayesian analysis. Based on our timetree (Fig. 4), *C. crusculus* diverged from its closest relative 4.73 Ma, consistent with typical species of vertebrates (> 0.7 Ma; Hedges *et al.* 2015). *Celestus crusculus* was recovered as conspecific with *Celestus jamesbondi* **sp. nov.** in our ASAP analysis.

Celestus duquesneyi (Grant 1940b)

Jamaican Blue-tailed Forest Lizard
(Fig. 18–19)

Celestus duquesneyi Grant, 1940b:157. Holotype: MCZ R-45194, collected by Chapman Grant at Portland Point, Clarendon Parish, Jamaica, on 18 April 1937 (17.72, -77.16).
Celestus duquesneyi—Grant, 1940a:105.
Celestus duquesneyi—Schwartz & Henderson, 1991:372.
Celestus duquesneyi—Wilson & Vogel, 2000:244.
Celestus duquesneyi—Hedges *et al.*, 2019:17.
Celestus duquesneyi—Schools & Hedges, 2021:220.
Celestus duquesneyi—Landestoy *et al.*, 2022:204.

Material examined (n=1). JAMAICA. **Clarendon**. MCZ R-45194, Chapman Grant, Portland Point, 18 April 1937.

Diagnosis. *Celestus duquesneyi* has (1) a dorsal pattern of bands, (2) head markings absent, (3) markings in the longitudinal paramedian area absent, (4) dots arranged in bars in the lateral band absent, (5) an adult SVL of 62.1 mm, (6) ventral scale rows, unavailable, (7) midbody scale rows, 48, (8) total lamellae on one hand, 64, (9) total strigae on ten scales, 130, (10) relative length of all digits on one hindlimb, 31.4 %, (11) relative distance between the angled subocular and mouth, 0.644 %, (12) relative eye length, 4.36 %, (13) relative forelimb length, 24.4 %, (14) relative ear width, 2.45 %, (15) relative rostral height, 2.14 %, (16) relative head length, 21.6 %, (17) relative mental width, 2.35 %, (18) relative postmental width, 3.19 %, (19) relative cloacal width, 9.98 %, (20) relative prefrontal width, 5.41 %, (21) relative largest supraocular width, 2.66 %, (22) relative longest finger length, 6.52 %, (23) relative distance between the ear and eye, 7.68 %, (24) relative head width, 64.6 %, (25) relative frontal width, 75.2 %, (26) relative nasal height, unavailable, (27) relative angled subocular height, 1.61 %, (28) relative distance between the eye and naris, 5.46 %, (29) relative canthal iii length, 1.59 %, (30) relative angled subocular width, 2.90 %, and (31) relative nasal length, 2.01 %. The species stem time is 3.59 Ma and the species crown time is not available (Fig. 4).

Celestus duquesneyi differs from most other species of the genus in having a dorsal pattern of bands. This species also has a smaller relative head width (64.6) than all other species of the genus. *Celestus duquesneyi* also has a larger total lamellae count on one hand (64), relative length of digits on one hindlimb (31.4), relative eye length (4.36), relative ear width (2.45), relative rostral height (2.14), relative head length (21.6), relative mental width (2.35), relative cloacal width (9.98), relative longest finger length (6.52), relative angled subocular height (1.61), and relative angled subocular width (2.90) than most other species of the genus.

From *Celestus barbouri*, we distinguish *C. duquesneyi* by the dorsal pattern (bands versus chevrons), the adult SVL (62.1 versus 78.4–93.6), the total lamellae on one hand (64 versus 36–49), the relative length of digits on one

hindlimb (31.4 versus 18.2–23.5), the relative distance between angled subocular and mouth (0.644 versus 0.437–0.556), the relative eye length (4.36 versus 2.87–3.63), the relative forelimb length (24.4 versus 15.4–19.0), the relative ear width (2.45 versus 0.810–1.86), the relative rostral height (2.14 versus 1.41–1.66), the relative head length (21.6 versus 14.6–16.6), the relative mental width (2.35 versus 1.51–1.85), the relative cloacal width (9.98 versus 7.64–8.26), the relative prefrontal width (5.41 versus 3.97–4.33), the relative longest finger length (6.52 versus 2.92–3.81), the relative distance between the ear and eye (7.68 versus 6.23–7.15), the relative head width (64.6 versus 73.8–81.7), the relative angled subocular height (1.61 versus 0.553–1.16), the relative distance between the eye and naris (5.46 versus 4.68–4.83), the relative angled subocular width (2.90 versus 1.97–2.52), and the relative nasal width (2.01 versus 1.38–1.65). From *C. capitulatus* **sp. nov.**, we distinguish *C. duquesneyi* by the dorsal pattern (bands versus irregular dots/dots in chevrons), the midbody scale rows (48 versus 37–47), the total lamellae on one hand (64 versus 25–38), the relative length of digits on one hindlimb (31.4 versus 17.6–22.3), the relative eye length (4.36 versus 2.75–3.80), the relative forelimb length (24.4 versus 14.3–18.1), the relative ear width (2.45 versus 0.671–2.04), the relative rostral height (2.14 versus 1.51–2.03), the relative head length (21.6 versus 15.1–17.7), the relative mental width (2.35 versus 1.28–1.84), the relative postmental width (3.19 versus 2.62–2.97), the relative cloacal width (9.98 versus 7.84–8.67), the relative prefrontal width (5.41 versus 4.30–4.72), the relative largest supraocular width (2.66 versus 2.03–2.61), the relative longest finger length (6.52 versus 3.45–3.75), the relative head width (64.6 versus 71.6–78.6), the relative frontal width (75.2 versus 78.1–81.6), the relative angled subocular height (1.61 versus 0.586–1.01), the relative distance between the eye and naris (5.46 versus 4.57–5.03), the relative angled subocular width (2.90 versus 1.93–2.32), and the relative nasal width (2.01 versus 1.40–1.84). From *C. crusculus*, we distinguish *C. duquesneyi* by the dorsal pattern (bands versus absent/flecks in series/dots in chevrons), the longitudinal paramedian lines (absent versus present), the midbody scale rows (48 versus 37–44), the total lamellae on one hand (64 versus 30–39), the relative length of digits on one hindlimb (31.4 versus 18.7–24.7), the relative eye length (4.36 versus 2.93–3.61), the relative forelimb length (24.4 versus 12.8–20.7), the relative ear width (2.45 versus 0.716–2.00), the relative rostral height (2.14 versus 1.62–2.04), the relative head length (21.6 versus 15.5–20.3), the relative mental width (2.35 versus 1.37–2.31), the relative cloacal width (9.98 versus 6.89–8.77), the relative prefrontal width (5.41 versus 3.93–4.67), the relative largest supraocular width (2.66 versus 1.97–2.65), the relative longest finger length (6.52 versus 2.94–4.10), the relative frontal width (75.2 versus 82.6–91.1), the relative angled subocular height (1.61 versus 0.953–1.21), the relative distance between the eye and naris (5.46 versus 4.31–4.86), the relative angled subocular width (2.9 versus 2.03–2.43), and the relative nasal width (2.01 versus 1.27–1.60). From *C. hesperius* **sp. nov.**, we distinguish *C. duquesneyi* by the dorsal pattern (bands versus dots in chevrons), the midbody scale rows (48 versus 39–44), the total lamellae on one hand (64 versus 29–34), and the relative ear width (2.45 versus 1.52–1.59). From *C. hewardi*, we distinguish *C. duquesneyi* by the adult SVL (62.1 versus 129–171), the total lamellae on one hand (64 versus 50–61), the total strigae on ten scales (130 versus 164–315), the relative length of digits on one hindlimb (31.4 versus 24.1–30.6), the relative distance between angled subocular and mouth (0.644 versus 0.744–1.40), the relative eye length (4.36 versus 2.98–4.05), the relative ear width (2.45 versus 1.40–1.82), the relative rostral height (2.14 versus 1.50–1.76), the relative mental width (2.35 versus 1.75–1.81), the relative cloacal width (9.98 versus 8.81–9.89), the relative prefrontal width (5.41 versus 4.18–4.80), the relative longest finger length (6.52 versus 5.03–5.66), the relative head width (64.6 versus 68.4–77.1), the relative angled subocular height (1.61 versus 0.918–1.30), the relative width of canthal iii (1.59 versus 1.70–2.12), the relative angled subocular width (2.90 versus 1.63–2.23), and the relative nasal width (2.01 versus 1.56–1.88). From *C. jamesbondi* **sp. nov.**, we distinguish *C. duquesneyi* by the dorsal pattern (bands versus absent/irregular dots/dots in chevrons), the midbody scale rows (48 versus 35–44), the total lamellae on one hand (64 versus 30–36), the relative length of digits on one hindlimb (31.4 versus 19.8–26.3), the relative eye length (4.36 versus 2.94–4.06), the relative forelimb length (24.4 versus 14.4–19.9), the relative ear width (2.45 versus 0.917–2.18), the relative head length (21.6 versus 15.1–20.4), the relative mental width (2.35 versus 1.59–2.01), the relative postmental width (3.19 versus 2.61–2.92), the relative cloacal width (9.98 versus 6.59–9.08), the relative prefrontal width (5.41 versus 4.29–5.09), the relative longest finger length (6.52 versus 3.66–4.33), the relative head width (64.6 versus 76.0–80.8), the relative angled subocular height (1.61 versus 0.893–1.18), the relative width of canthal iii (1.59 versus 1.75–2.16), the relative angled subocular width (2.90 versus 2.09–2.76), and the relative nasal width (2.01 versus 1.42–1.75). From *C. macrolepis*, we distinguish *C. duquesneyi* by the dorsal pattern (bands versus bicolored), the adult SVL (62.1 versus 254–316), the total strigae on ten scales (130 versus 398), the relative distance between angled subocular and mouth (0.644 versus 1.39–1.66), and the relative ear width (2.45 versus

0.760–1.43). From *C. macrotus*, we distinguish *C. duquesneyi* by the longitudinal paramedian lines (absent versus present), the dots arranged in bars in the lateral areas (absent versus present), the midbody scale rows (48 versus 41–45), the total lamellae on one hand (64 versus 39–40), the relative ear width (2.45 versus 1.75–2.08), and the relative rostral height (2.14 versus 1.61–1.95). From *C. microblepharis*, we distinguish *C. duquesneyi* by the dorsal pattern (bands versus chevrons), the total lamellae on one hand (64 versus 30), the relative length of digits on one hindlimb (31.4 versus 16.6), the relative eye length (4.36 versus 1.83), the relative forelimb length (24.4 versus 14.2), the relative ear width (2.45 versus 0.446), the relative mental width (2.35 versus 1.44), the relative longest finger length (6.52 versus 3.11), and the relative angled subocular height (1.61 versus 0.778), and the relative nasal width (2.01 versus 1.11). From *C. molesworthi*, we distinguish *C. duquesneyi* by the dorsal pattern (bands versus dots in chevrons), the adult SVL (62.1 versus 78.1–103), the total lamellae on one hand (64 versus 32–44), the total strigae on ten scales (130 versus 138–159), the relative length of digits on one hindlimb (31.4 versus 22.4–29.4), the relative distance between angled subocular and mouth (0.644 versus 0.653–0.845), the relative eye length (4.36 versus 3.28–3.70), the relative forelimb length (24.4 versus 17.5–24.2), the relative ear width (2.45 versus 1.37–1.50), the relative rostral height (2.14 versus 1.72–1.81), and the relative head length (21.6 versus 17.2–20.0). From *C. occiduus*, we distinguish *C. duquesneyi* by the dorsal pattern (bands versus absent), the adult SVL (62.1 versus 269–367), the total strigae on ten scales (130 versus 374), and the relative ear width (2.45 versus 0.948–1.39). From *C. oligolepis* **sp. nov.**, we distinguish *C. duquesneyi* by the dorsal pattern (bands versus dots in chevrons), the head markings (absent versus present), the longitudinal paramedian lines (absent versus present), and the total lamellae on one hand (64 versus 30). From *C. striatus*, we distinguish *C. duquesneyi* by the dorsal pattern (bands versus absent/chevrons), the adult SVL (62.1 versus 145), the total strigae on ten scales (130 versus 279), and the relative ear width (2.45 versus 1.30).

Description of holotype. MCZ R-45194. An adult; SVL 62.1 mm; tail nearly cylindrical, broken, 121 mm (195% SVL); axilla-to-groin distance 33.2 mm (53.5% SVL); forelimb length 15.2 mm (24.5% SVL); hindlimb length 23.2 mm (37.4% SVL); head length 13.4 mm (21.6% SVL); head width 8.63 mm (13.9% SVL); head width 64.4% head length; diameter of orbit 2.71 mm (4.36% SVL); horizontal diameter of ear opening 1.52 mm (2.45% SVL); vertical diameter of ear opening 1.77 mm (2.85% SVL); length of all toes on one foot 19.5 mm (31.4% SVL); shortest distance between angled subocular and lip 0.40 mm (0.644% SVL); shortest distance between the ocular and auricular openings 4.77 mm (7.68% SVL); longest finger length 4.05 mm (6.52% SVL); largest supraocular width 1.65 mm (2.66% SVL); cloacal width 6.20 mm (9.98% SVL); mental width 1.46 mm (2.35% SVL); postmental width 1.98 mm (3.19% SVL); prefrontal width 3.36 mm (5.41% SVL); frontal width 75.2% frontal length; angled subocular height 1.00 mm (1.61% SVL); shortest distance between the eye and naris 3.39 mm (5.46% SVL); canthal iii width 0.99 mm (1.59% SVL); angled subocular width 1.80 mm (2.90% SVL); nasal width 1.25 mm (2.01% SVL); rostral 2.14X as wide as high, visible from above, not in contact with nasals, in contact with 1st supralabial and anterior internasal (left)/(right); anterior internasals are narrower than posterior ones; frontonasals and prefrontal fused into a single large plate with a concave posterior margin, much wider than long, bordered by posterior internasals, 1st loreals, 1st and 2nd median oculars, and the frontal; frontal longer than wide; a pair of frontoparietals (left damaged), separated by the posterior prolongation of the frontal; interparietal plate smaller than parietals and separating them, posteriorly touching the interoccipital, which is wider than long; parietal separated from supraoculars by 1st temporal and frontoparietal (right)/damaged (left); nasal single; nostril above suture between 1st and 2nd supralabials (left)/(right); 1 postnasal (left)/(right); 2 (left)/(right) loreals; 1st loreal higher than wide (left)/(right), in contact with postnasal, posterior internasal, prefrontal/frontonasal complex, 1st median ocular, canthal iii, 2nd loreal, and 3rd–5th supralabials (left)/(right); 2nd loreal shorter than 1st, approximately as high as wide (left)/(right), excluded from contact with supraocular by canthal iii (left)/(right); final loreal posteriorly bordering the upper and lower preoculars (left)/(right); canthal iii wider than high (left)/(right), contacting 1st median ocular, anterior supraciliary, upper preocular, and 1st and 2nd loreals (left)/(right); 10 median oculars (left)/(right), 1st and 2nd contacting the prefrontal (left)/(right); 1 upper preocular (left)/(right); an irregular anterior supraciliary (left)/(right); 6 lateral oculars (left)/(right); 6 (right)/damaged (left) temporals; 3 (left)/4 (right) suboculars; posterior subocular large and elongate (left)/(right); anterior subocular small (left)/(right); 10 supralabials (left)/(right), 7 to level below center of eye (left)/(right); 11 infralabials (left)/(right), 7 to level below center of eye (left)/(right); mental small, followed by a single, larger postmental; 6 pairs of enlarged chin shields; 1st pair in contact with one another; 2nd–6th pairs separated by 1–7 scales; 114 transverse rows of dorsal scales from interoccipital to base of tail; 48 scales around midbody; 5 digits; finger lengths 3>4>52>5>1; 15 (right)/damaged (left) lamellae under longest finger; 64

total lamellae on one hand; toe lengths 4>3>5>2>1; 23 (left)/24 (right) lamellae under longest toe; striate with a median keel dorsal body and caudal scales; faintly striated ventral scales; 130 total strigae counted on ten scales.

FIGURE 18. (A–F) *Celestus duquesneyi* (MCZ R-45194, holotype), SVL 62.1 mm.

Color (in alcohol): dorsal surface of head golden tan and patternless; lateral surfaces of head grading from golden tan to cream with darker brown eye masks; dorsal surfaces of the body are medium brown and covered in darker brown and cream bands; dorsal surface of tail paler cream with spots that fade to stripes of dark and pale brown; lateral areas are the same color as the dorsum with the dots from the dorsum aligning on the sides, which fade to cream; dorsal surfaces of the limbs are golden tan with paler mottling; lateral and ventral areas of the limbs fade to pale cream, patternless; ventral surfaces of the head, body, and tail are pale cream and patternless (blue in life, especially in young and young adult specimens).

FIGURE 19. *Celestus duquesneyi* (vouchers not available), in life. From Hellshire Hills, St. Catherine Parish, Jamaica. Photo by Byron S. Wilson.

Variation. No other specimens were available for examination. Measurements and other morphological data for the holotype are presented in Table 1.

Distribution. *Celestus duquesneyi* is found on the Portland Ridge peninsula and in the Hellshire Hills region of southern Jamaica at elevations of 10–160 m (Fig. 12).

Ecology and conservation. Little information is available on the ecology of *Celestus duquesneyi*. This species has been observed in dry leaf litter of a dry forest (Grant 1940a, b; Wilson & Vogel 2000).

The IUCN Redlist (IUCN 2023) considers the conservation status of *Celestus duquesneyi* to be Critically Endangered B1ab(iii,v) because "following this species' presumed extinction at Portland Ridge it is restricted to a single location, the Hillshire Hills, with an extent of occurrence (and consequently a maximum area of occupancy) estimated to be no more than 13 km^2. It is undergoing continuing declines in the extent, area, and quality of habitat, and number of mature individuals, and has lost one of its two subpopulations within the past 80 years." Arboreal habits might have allowed this species to persist after the introduction of the mongoose in Jamaica (Schools & Hedges 2022). Studies are needed to determine the health and extent of remaining populations and threats to the survival of the species. Captive-breeding programs should be undertaken because eradication of introduced mammalian predators is not yet possible on Jamaica.

Reproduction. No data on reproduction are available for this species.

Etymology. The species name refers to Douglas DuQuesnay, the collector of the type specimen.

Remarks. In the original description, this species was identified as unique based on its banded blue and black tail and was placed in the "long-legged" group of Jamaican celestines (Grant 1940a). At the time, Grant (1940a) suspected that it was most closely related to *Celestus occiduus*. Upon collection, the nearby lighthouse custodian noted that he had seen others of the species (Grant 1940a). Later, an individual *C. hewardi*, collected far from the type locality of *C. duquesneyi*, had blue and brown bands on its tail (Schwartz 1971a). This led to speculation that a close relationship existed between *C. duquesneyi*, *C. fowleri* (another member of the "long-legged" Jamaican celestines; determined to be a synonym of *C. striatus* in this work), and *C. hewardi* (Schwartz 1971a).

Celestus duquesneyi is included in our genetic dataset and is identified as the closest relative of *C. hewardi* in our ML analysis with a significant support value and in our Bayesian analysis with a support value of 71%. Genomic data from Schools *et al.* (2022) identified *C. duquesneyi* as the closest relative of *C. molesworthi* with a support value of 52% in ML analyses and a significant support value in Bayesian analyses. Based on our timetree (Fig. 4), *C. duquesneyi* diverged from its closest relative 3.59 Ma, consistent with typical species of vertebrates (> 0.7 Ma; Hedges *et al.* 2015). *Celestus duquesneyi* was recognized as a distinct species by our ASAP analysis.

***Celestus hesperius* sp. nov.**
Western Jamaican Forest Lizard
(Fig. 20–21)

Celestus crusculus crusculus—Grant, 1940:102 (part).
Celestus crusculus—Schwartz & Henderson, 1991:369 (part).
Celestus crusculus crusculus—Hedges *et al.*, 2019:17 (part).
Celestus crusculus—Schools & Hedges, 2021:220 (part).
Celestus crusculus—Landestoy *et al.*, 2022:204 (part).

Holotype. USNM 328154, an adult female from 3.2 km SE of Content, Hanover Parish, Jamaica, collected by S. Blair Hedges and David Powars on 8 January 1984 (18.351, -77.991, 201 m).

Paratypes (n=2). Hanover. USNM 328155, S. Blair Hedges and David Powars, 3.2 km SE of Content (18.351, -77.991, 201 m), 8 January 1984. **Westmoreland.** USNM 328156, S. Blair Hedges and David Powars, 5.3 km N of Town Head, 16 January 1984.

Diagnosis. *Celestus hesperius* **sp. nov.** has (1) a dorsal pattern of dots in chevrons, (2) head markings absent, (3) markings in the longitudinal paramedian area absent/present, (4) dots arranged in bars in the lateral band absent, (5) an adult SVL of 54.0–62.3 mm, (6) ventral scale rows, 111–114, (7) midbody scale rows, 39–44, (8) total lamellae on one hand, 29–34, (9) total strigae on ten scales, 95–122, (10) relative length of all digits on one hindlimb, 21.7–26.2 %, (11) relative distance between the angled subocular and mouth, 0.594–0.648 %, (12) relative eye length, 3.61–3.74 %, (13) relative forelimb length, 18.6–21.3 %, (14) relative ear width, 1.52–1.59 %, (15) relative rostral height, 1.60–1.77 %, (16) relative head length, 15.7–17.7 %, (17) relative mental width, 1.51–1.78 %, (18) relative postmental width, 2.87–2.92 %, (19) relative cloacal width, 7.99–8.55 %, (20) relative prefrontal width, 4.65–5.02 %, (21) relative largest supraocular width, 1.91–2.22 %, (22) relative longest finger length, 3.50–4.04 %, (23) relative distance between the ear and eye, 6.74–7.53 %, (24) relative head width, 76.5–79.8 %, (25) relative frontal width, 80.5–86.1 %, (26) relative nasal height, 1.09–1.44 %, (27) relative angled subocular height, 0.963–1.24 %, (28) relative distance between the eye and naris, 4.70–5.28 %, (29) relative canthal iii length, 1.77–1.93 %, (30) relative angled subocular width, 2.01–2.48 %, and (31) relative nasal length, 1.52–1.78 %. The species stem time is 2.33 Ma and the species crown time is 0.41 Ma (Fig. 4).

We distinguish *Celestus hesperius* **sp. nov.** from the other species of *Celestus* based on a complex of traits. From *Celestus barbouri*, we distinguish *C. hesperius* **sp. nov.** by the dorsal pattern (dots in chevrons versus chevrons), the adult SVL (54.0–62.3 versus 78.4–93.6), the ventral scale rows (111–114 versus 118–151), the midbody scale rows (39–44 versus 47–56), the total lamellae on one hand (29–34 versus 36–49), the relative distance between angled subocular and mouth (0.594–0.648 versus 0.437–0.556), and the relative prefrontal width (4.65–5.02 versus 3.97–4.33). From *C. capitulatus* **sp. nov.**, we distinguish *C. hesperius* **sp. nov.** by relative forelimb length (18.6–21.3 versus 14.3–18.1) and the relative width of canthal iii (1.77–1.93 versus 1.61–1.70). From *C. crusculus*, we distinguish *C. hesperius* **sp. nov.** by the relative head width (76.5–79.8 versus 72.1–76.4). From *C. duquesneyi*, we distinguish *C. hesperius* **sp. nov.** by the dorsal pattern (dots in chevrons versus bands), the midbody scale rows (39–44 versus 48), the total lamellae on one hand (29–34 versus 64), and the relative ear width (1.52–1.59 versus 2.45). From *C. hewardi*, we distinguish *C. hesperius* **sp. nov.** by the dorsal pattern (dots in chevrons versus mottled/bands), the adult SVL (54.0–62.3 versus 129–171), the total lamellae on one hand (29–34 versus 50–61), the total strigae on ten scales (95–122 versus 164–315), the relative distance between angled subocular and mouth (0.594–0.648 versus 0.744–1.40), the relative forelimb length (18.6–21.3 versus 22.2–24.6), the relative cloacal width (7.99–8.55 versus 8.81–9.89), the relative largest supraocular width (1.91–2.22 versus 2.43–2.96), the relative longest finger length (3.50–4.04 versus 5.03–5.66), and the relative frontal width (80.5–86.1 versus 57.3–75.3).

From *C. jamesbondi* **sp. nov.**, we distinguish *C. hesperius* **sp. nov.** by the relative frontal width (80.5–86.1 versus 70.5–77.6). From *C. macrolepis*, we distinguish *C. hesperius* **sp. nov.** by the dorsal pattern (dots in chevrons versus bicolored), the adult SVL (54.0–62.3 versus 254–316), the midbody scale rows (39–44 versus 46–48), the total lamellae on one hand (29–34 versus 52–54), the total strigae on ten scales (95–122 versus 398), the relative length of digits on one hindlimb (21.7–26.2 versus 27.5–28.0), the relative distance between angled subocular and mouth (0.594–0.648 versus 1.39–1.66), the relative forelimb length (18.6–21.3 versus 26.1–26.7), the relative ear width (1.52–1.59 versus 0.760–1.43), the relative head length (15.7–17.7 versus 19.2–22.9), the relative largest supraocular width (1.91–2.22 versus 2.64–3.01), the relative longest finger length (3.50–4.04 versus 5.47–5.51), and the relative distance between the ear and eye (6.74–7.53 versus 8.02–10.9). From *C. macrotus*, we distinguish *C. hesperius* **sp. nov.** by the dorsal pattern (dots in chevrons versus chevrons/bands), the dots arranged in bars in the lateral areas (absent versus present), the ventral scale rows (111–114 versus 87–93), the total lamellae on one hand (29–34 versus 39–40), the relative length of digits on one hindlimb (21.7–26.2 versus 30.2–31.2), the relative eye length (3.61–3.74 versus 3.79–5.17), the relative forelimb length (18.6–21.3 versus 22.4–25.0), the relative ear width (1.52–1.59 versus 1.75–2.08), the relative head length (15.7–17.7 versus 18.2–20.5), the relative largest supraocular width (1.91–2.22 versus 2.96–4.03), the relative longest finger length (3.50–4.04 versus 6.43–6.67), the relative distance between the ear and eye (6.74–7.53 versus 7.58–8.02), the relative frontal width (80.5–86.1 versus 57.6–66.1), the relative distance between the eye and naris (4.70–5.28 versus 5.48–5.60), the relative angled subocular width (2.01–2.48 versus 2.77–2.83), and the relative nasal width (1.52–1.78 versus 2.08–2.33). From *C. microblepharis*, we distinguish *C. hesperius* **sp. nov.** by the dorsal pattern (dots in chevrons versus chevrons), the adult SVL (54.0–62.3 versus 96.4), the ventral scale rows (111–114 versus 109), the relative eye length (3.61–3.74 versus 1.83), and the relative ear width (1.52–1.59 versus 0.446). From *C. molesworthi*, we distinguish *C. hesperius* **sp. nov.** by the adult SVL (54.0–62.3 versus 78.1–103), the total strigae on ten scales (95–122 versus 138–159), the relative distance between angled subocular and mouth (0.594–0.648 versus 0.653–0.845), the relative ear width (1.52–1.59 versus 1.37–1.50), the relative mental width (1.51–1.78 versus 1.81–2.00), the relative postmental width (2.87–2.92 versus 2.97–3.08), the relative cloacal width (7.99–8.55 versus 8.73–9.35), the relative longest finger length (3.50–4.04 versus 4.28–5.19), the relative distance between the ear and eye (6.74–7.53 versus 7.97–8.83), the relative distance between the eye and naris (4.70–5.28 versus 5.32–5.50), and the relative width of canthal iii (1.77–1.93 versus 1.99–2.09). From *C. occiduus*, we distinguish *C. hesperius* **sp. nov.** by the dorsal pattern (dots in chevrons versus absent), the adult SVL (54.0–62.3 versus 269–367), the midbody scale rows (39–44 versus 46–56), the total lamellae on one hand (29–34 versus 50–66), the total strigae on ten scales (95–122 versus 374), the relative distance between angled subocular and mouth (0.594–0.648 versus 1.26–1.27), the relative eye length (3.61–3.74 versus 2.87–3.33), the relative forelimb length (18.6–21.3 versus 23.5–23.9), the relative ear width (1.52–1.59 versus 0.948–1.39), the relative head length (15.7–17.7 versus 20.4–20.6), the relative largest supraocular width (1.91–2.22 versus 2.27–3.02), the relative longest finger length (3.50–4.04 versus 4.77–5.46), and the relative distance between the ear and eye (6.74–7.53 versus 8.98–10.9). From *C. oligolepis* **sp. nov.**, we distinguish *C. hesperius* **sp. nov.** by the head markings (absent versus present), the ventral scale rows (111–114 versus 98), and the midbody scale rows (39–44 versus 35). From *C. striatus*, we distinguish *C. hesperius* **sp. nov.** by the dorsal pattern (dots in chevrons versus absent/chevrons), the adult SVL (54.0–62.3 versus 145), the ventral scale rows (111–114 versus 101–109), the total lamellae on one hand (29–34 versus 59–66), and the total strigae on ten scales (95–122 versus 279).

Description of holotype. USNM 328154. An adult; SVL 62.3 mm; tail nearly cylindrical, broken near base, 10.8 mm (17.3% SVL); axilla-to-groin distance 35.2 mm (56.5% SVL); forelimb length 11.6 mm (18.6% SVL); hindlimb length 15.3 mm (24.6% SVL); head length 9.79 mm (15.7% SVL); head width 7.81 mm (12.5% SVL); head width 79.8% head length; diameter of orbit 2.25 mm (3.61% SVL); horizontal diameter of ear opening 0.95 mm (1.52% SVL); length of all toes on one foot 13.5 mm (21.7% SVL); shortest distance between angled subocular and lip 0.37 mm (0.594% SVL); shortest distance between the ocular and auricular openings 4.20 mm (6.74% SVL); longest finger length 2.18 mm (3.50% SVL); largest supraocular width 1.19 mm (1.91% SVL); cloacal width 4.98 mm (7.99% SVL); mental width 0.94 mm (1.51% SVL); postmental width 1.79 mm (2.87% SVL); prefrontal width 2.90 mm (4.65% SVL); frontal width 86.1% frontal length; nasal height 0.68 mm (1.09% SVL); angled subocular height 0.60 mm (0.963% SVL); shortest distance between the eye and naris 2.93 mm (4.70% SVL); canthal iii width 1.10 mm (1.77% SVL); angled subocular width 1.25 mm (2.01% SVL); nasal width 0.95 mm (1.52% SVL); rostral 1.77X as wide as high, barely visible from above, not in contact with nasals, in contact with 1st supralabial and anterior internasal (left)/(right); anterior internasals are narrower than posterior ones; frontonasals and prefrontal

fused into a single large plate with a convex posterior margin, wider than long, bordered by posterior internasals, 1st loreals, canthal iii, 1st median oculars, and the frontal; frontal longer than wide; a pair of frontoparietals, separated by the posterior prolongation of the frontal and the interparietal plate; interparietal plate approximately the size of parietals and separating them, posteriorly touching the interoccipital, which is wider than long; parietal separated from supraoculars by 1st and 2nd temporals and frontoparietal (left)/(right); nasal single; nostril above suture between 1st and 2nd supralabials (left)/(right); 1 postnasal (left)/(right); 2 loreals (left)/(right); 1st loreal higher than wide (left)/(right), in contact with postnasal, posterior internasal, prefrontal/frontonasal complex, canthal iii, 2nd loreal, and 3rd–4th supralabial (left)/(right); 2nd loreal shorter than 1st, slightly wider than high (left)/(right), excluded from contact with supraocular by canthal iii (left)/(right); final loreal posteriorly bordering the lower and upper preoculars (left)/(right); canthal iii wider than high (left)/(right), contacting 1st median ocular, anterior superciliary, upper preocular, frontonasal plate, and 1st and 2nd loreals (left)/(right); 11 (left)/10 (right) median oculars, 1st contacting the prefrontal (left)/(right); 1 upper preoculars (left)/(right); an irregular anterior superciliary (left)/(right); 6 (left)/6 (right) lateral oculars; 5 temporals (left)/(right); 2 (left)/(right) suboculars; posterior subocular large and elongate (left)/(right); anterior suboculars small (left)/(right); 9 supralabials (left)/(right), 6 to level below center of eye (left)/(right); 8 infralabials (left)/(right), 5 to level below center of eye (left)/(right); mental small, followed by a single, larger postmental; 4 with one additional shield bordering the postmental on the left pairs of enlarged chin shields; 1st pair in contact with one another; 2nd–4th pairs separated by 1–3 scales; 111 transverse rows of dorsal scales from interoccipital to base of tail; 113 transverse rows of ventral scales from mental to vent; 44 scales around midbody; 4 digits; finger lengths 3>4>2>5>1; 8 (left)/missing (right) lamellae under longest finger; 32 total lamellae on one hand; toe lengths 4>3>5>2>1; 14 (left)/(right) lamellae under longest toe; striate with a faint median keel dorsal body and caudal scales; smooth ventral scales; 95 total strigae counted on ten scales.

Color (in alcohol): dorsal surface of head light brown, patternless; lateral surfaces of head grading from light brown to faded yellow with darker brown areas around the eyes and on the labial scales; dorsum same as the head with darker brown markings forming small longitudinal paramedian lines and darker brown dots forming herringbones; dorsal surface of tail the same color as the body with several darker brown irregular dots; lateral areas grade from light brown to faded yellow with some lighter brown dots in the lateral band; dorsal surfaces of the limbs are medium brown with some lighter brown dots; lateral and ventral areas of the limbs fading from medium brown to faded yellow; ventral surfaces of the head, body, and tail are faded yellow with some darker brown dots on the chin shields and under the throat.

Variation. See Remarks.

Distribution. *Celestus hesperius* **sp. nov.** is known only from inland areas in northwestern of Jamaica at elevations of 140–280 m in Hanover and Westmoreland (Fig. 12). It has an extent of occurrence ~160 km^2.

Ecology and conservation. Little is known of the ecology of this species other than the specimens of the type series were collected during the day under rocks along a road.

We consider the conservation status of *Celestus hesperius* **sp. nov.** to be Endangered B1ab(iii), based on IUCN Redlist criteria (IUCN 2023). It faces a primary threat from habitat destruction from agriculture and urbanization and has an extent of occupancy of 160 km^2. Secondary threats include predation from introduced mammals, including the mongoose and black rats. Studies are needed to determine the health and extent of remaining populations and threats to the survival of the species. Captive-breeding programs should be undertaken, because eradication of introduced mammalian predators is not yet possible on Jamaica.

Reproduction. No data on reproduction are available for this species.

Etymology. The species name (*hesperius*) is a masculine nominative singular adjective meaning "western," in reference to the distribution of this species in western Jamaica.

Remarks. The only known specimens of this species were collected by one of us (SBH) in January of 1984. *Celestus hesperius* **sp. nov.** was included in our genetic dataset and has significant support in our ML and Bayesian analyses at the crown node and the stem node that identifies it as the closest relative to *C. jamesbondi* **sp. nov.** That result is surprising because the two species are separated by 110–140 km, an area mainly occupied by another species, *C. crusculus* (*sensu stricto*), which is not closely related to *C. hesperius* **sp. nov.** and *C. jamesbondi* **sp. nov.**, even though the two new species were considered to be *C. crusculus* (*sensu lato*) until this study. Based on our timetree (Fig. 4), *C. hesperius* **sp. nov.** diverged from its closest relative 2.33 Ma, consistent with typical species of vertebrates (> 0.7 Ma; Hedges *et al.* 2015). *Celestus hesperius* **sp. nov.** was recognized as a distinct species by our ASAP analysis.

FIGURE 20. (A–F) *Celestus hesperius* **sp. nov.** (USNM 328154, holotype), SVL 62.3 mm.

FIGURE 21. *Celestus hesperius* **sp. nov.** (USNM 328156, SBH 101554), in life. From 5.3 km N Town Head, Westmoreland Parish, Jamaica. Photo by SBH.

***Celestus hewardi* (Gray 1845)**
Red-spotted Forest Lizard
(Fig. 22)

Celestus hewardii—Gray, 1845:118. Replacement name for *Tiliqua striata* Gray (1839:293), a junior homonym of *Celestus striatus* Gray (1839:288). Holotype: BMNH 1946.8.7.99.
Diploglossus (*Celestus*) *variegatus*—Peters, 1874:370. Holotype: ZMB 8029, "unbestimmter Herkunft, gekauft" (of unknown origin, bought).
Celestus impressus—Cope, 1868:127. Lectotype: ANSP 9225.
Diploglossus hewardii—Boulenger, 1885:291.
Celestus occiduus hewardii—Grant, 1940:106.
Celestus hewardi—Schwartz & Henderson, 1991:374.
Celestus hewardii—Hedges *et al.*, 2019:17.
Celestus hewardii—Schools & Hedges, 2021:220.
Celestus hewardii—Landestoy *et al.*, 2022:204.

Material examined (n=23). JAMAICA. **Manchester**. BMNH 1938.4.13.6, C. Grant, Mandeville; BMNH 1946.8.7.99 (holotype, collected by R. Heward in Jamaica with no precise locality); BMNH 1845.12.27.6–8 (one of the series, specimen number unmarked); USNM 108234, 108238, Mandeville, 5 May 1939; MCZ R-45173, R-45177, Chapman Grant, Mandeville, 11 May 1937; MCZ R-127906–7, Thomas A. Jenssen, Mandeville, 16 June 1970; USNM 102651, Kensworth, February 1937; USNM 108231, Mandeville, 13 April 1937. **Saint Ann**. USNM 251919, 1.5 mi NE of Orange Valley, 4 September 1976. **Saint James**. USNM 108329, 108330–5, 5 mi W of Montego Bay, 25 March 1938. **Trelawny**. KU 226546, Duncans, 13 July 1961; USNM 251918, 1.1 mi NW of Windsor, 4 July 1971. **Westmoreland**. KU 226549–50, 6.9 mi SSE Darliston, 11 July 1967.

Diagnosis. *Celestus hewardi* has (1) a dorsal pattern of mottled/bands, (2) head markings absent, (3) markings in the longitudinal paramedian area absent/present, (4) dots arranged in bars in the lateral band absent/present, (5) an adult SVL of 129–171 mm, (6) ventral scale rows, 113–137, (7) midbody scale rows, 43–59, (8) total lamellae on one hand, 50–61, (9) total strigae on ten scales, 164–315, (10) relative length of all digits on one hindlimb, 24.1–30.6 %, (11) relative distance between the angled subocular and mouth, 0.744–1.40 %, (12) relative eye length, 2.98–4.05 %, (13) relative forelimb length, 22.2–24.6 %, (14) relative ear width, 1.40–1.82 %, (15) relative rostral height, 1.50–1.76 %, (16) relative head length, 16.8–21.5 %, (17) relative mental width, 1.75–1.81 %, (18) relative postmental width, 2.84–3.44 %, (19) relative cloacal width, 8.81–9.89 %, (20) relative prefrontal width, 4.18–4.80 %, (21) relative largest supraocular width, 2.43–2.96 %, (22) relative longest finger length, 5.03–5.66 %, (23) relative distance between the ear and eye, 6.72–8.73 %, (24) relative head width, 68.4–77.1 %, (25) relative frontal width, 57.3–75.3 %, (26) relative nasal height, 1.21–1.24 %, (27) relative angled subocular height, 0.918–1.30 %, (28) relative distance between the eye and naris, 5.00–5.60 %, (29) relative canthal iii length, 1.70–2.12 %, (30) relative angled subocular width, 1.63–2.23 %, and (31) relative nasal length, 1.56–1.88 %. The species stem time is 3.59 Ma and the species crown time is unavailable (Fig. 4).

Celestus hewardi differs from most (except two) species in the genus *Celestus* in having a dorsal pattern of mottled/bands. From *Celestus barbouri*, we distinguish *C. hewardi* by the dorsal pattern (mottled/bands versus chevrons), the adult SVL (129–171 versus 78.4–93.6), the total lamellae on one hand (50–61 versus 36–49), the total strigae on ten scales (164–315 versus 105–136), the relative length of digits on one hindlimb (24.1–30.6 versus 18.2–23.5), the relative distance between angled subocular and mouth (0.744–1.40 versus 0.437–0.556), the relative forelimb length (22.2–24.6 versus 15.4–19.0), the relative head length (16.8–21.5 versus 14.6–16.6), the relative cloacal width (8.81–9.89 versus 7.64–8.26), the relative longest finger length (5.03–5.66 versus 2.92–3.81), the relative nasal height (1.21–1.24 versus 0.930–1.12), and the relative distance between the eye and naris (5.00–5.60 versus 4.68–4.83). From *C. capitulatus* **sp. nov.**, we distinguish *C. hewardi* by the dorsal pattern (mottled/bands versus irregular dots/dots in chevrons), the adult SVL (129–171 versus 62.1–81.8), the total lamellae on one hand (50–61 versus 25–38), the relative length of digits on one hindlimb (24.1–30.6 versus 17.6–22.3), the relative forelimb length (22.2–24.6 versus 14.3–18.1), the relative cloacal width (8.81–9.89 versus 7.84–8.67), the relative longest finger length (5.03–5.66 versus 3.45–3.75), and the relative frontal width (57.3–75.3 versus 78.1–81.6). From *C. crusculus*, we distinguish *C. hewardi* by the dorsal pattern (mottled/bands versus absent/flecks in series/dots in chevrons), the adult SVL (129–171 versus 59.6–77.6), the total lamellae on one hand (50–61 versus 30–39), the relative forelimb length (22.2–24.6 versus 12.8–20.7), the relative cloacal width (8.81–9.89 versus 6.89–8.77), the relative longest finger length (5.03–5.66 versus 2.94–4.10), the relative frontal width (57.3–75.3 versus 82.6–91.1), and the relative distance between the eye and naris (5.00–5.60 versus 4.31–4.86). From *C. duquesneyi*, we distinguish *C. hewardi* by the adult SVL (129–171 versus 62.1), the total lamellae on one hand (50–61 versus 64), the total strigae on ten scales (164–315 versus 130), the relative length of digits on one hindlimb (24.1–30.6 versus 31.4), the relative distance between angled subocular and mouth (0.744–1.40 versus 0.644), the relative eye length (2.98–4.05 versus 4.36), the relative ear width (1.40–1.82 versus 2.45), the relative rostral height (1.50–1.76 versus 2.14), the relative mental width (1.75–1.81 versus 2.35), the relative cloacal width (8.81–9.89 versus 9.98), the relative prefrontal width (4.18–4.80 versus 5.41), the relative longest finger length (5.03–5.66 versus 6.52), the relative head width (68.4–77.1 versus 64.6), the relative angled subocular height (0.918–1.30 versus 1.61), the relative width of canthal iii (1.70–2.12 versus 1.59), the relative angled subocular width (1.63–2.23 versus 2.90), and the relative nasal width (1.56–1.88 versus 2.01). From *C. hesperius* **sp. nov.**, we distinguish *C. hewardi* by the dorsal pattern (mottled/bands versus dots in chevrons), the adult SVL (129–171 versus 54.0–62.3), the total lamellae on one hand (50–61 versus 29–34), the total strigae on ten scales (164–315 versus 95–122), the relative distance between angled subocular and mouth (0.744–1.40 versus 0.594–0.648), the relative forelimb length (22.2–24.6 versus 18.6–21.3), the relative cloacal width (8.81–9.89 versus 7.99–8.55), the relative largest supraocular width (2.43–2.96 versus 1.91–2.22), the relative longest finger length (5.03–5.66 versus 3.50–4.04), and the relative frontal width (57.3–75.3 versus 80.5–86.1). From *C. jamesbondi* **sp. nov.**, we distinguish *C. hewardi* by the dorsal pattern (mottled/bands versus absent/irregular dots/dots in chevrons), the adult SVL (129–171 versus 54.7–72.0), the ventral scale rows (113–137 versus 91–112), the total lamellae on one hand (50–61 versus 30–36), the relative forelimb length (22.2–24.6 versus 14.4–19.9), and the relative longest finger length (5.03–5.66 versus 3.66–4.33). From *C. macrolepis*, we distinguish *C. hewardi* by the dorsal pattern (mottled/bands versus bicolored), the adult SVL (129–171 versus 254–316), the total strigae on ten scales (164–315 versus 398), the relative forelimb length (22.2–24.6

versus 26.1–26.7), the relative mental width (1.75–1.81 versus 1.87), the relative postmental width (2.84–3.44 versus 3.81), the relative cloacal width (8.81–9.89 versus 11.2), the relative prefrontal width (4.18–4.80 versus 3.94), the relative head width (68.4–77.1 versus 80.5), the relative frontal width (57.3–75.3 versus 78.4), the relative nasal height (1.21–1.24 versus 1.18), the relative distance between the eye and naris (5.00–5.60 versus 6.02), and the relative angled subocular width (1.63–2.23 versus 2.57). From *C. macrotus*, we distinguish *C. hewardi* by the adult SVL (129–171 versus 60.0–86.1), the ventral scale rows (113–137 versus 87–93), the total lamellae on one hand (50–61 versus 39–40), the total strigae on ten scales (164–315 versus 64–115), the relative prefrontal width (4.18–4.80 versus 4.87–5.55), the relative longest finger length (5.03–5.66 versus 6.43–6.67), the relative angled subocular width (1.63–2.23 versus 2.77–2.83), and the relative nasal width (1.56–1.88 versus 2.08–2.33). From *C. microblepharis*, we distinguish *C. hewardi* by the dorsal pattern (mottled/bands versus chevrons), the adult SVL (129–171 versus 96.4), the ventral scale rows (113–137 versus 109), the total lamellae on one hand (50–61 versus 30), the relative length of digits on one hindlimb (24.1–30.6 versus 16.6), the relative eye length (2.98–4.05 versus 1.83), the relative forelimb length (22.2–24.6 versus 14.2), the relative ear width (1.40–1.82 versus 0.446), the relative head length (16.8–21.5 versus 14.7), the relative mental width (1.75–1.81 versus 1.44), the relative postmental width (2.84–3.44 versus 2.47), the relative cloacal width (8.81–9.89 versus 8.02), the relative largest supraocular width (2.43–2.96 versus 2.06), the relative longest finger length (5.03–5.66 versus 3.11), the relative nasal height (1.21–1.24 versus 0.726), the relative angled subocular height (0.918–1.30 versus 0.778), the relative distance between the eye and naris (5.00–5.60 versus 4.79), the relative angled subocular width (1.63–2.23 versus 2.90), and the relative nasal width (1.56–1.88 versus 1.11). From *C. molesworthi*, we distinguish *C. hewardi* by the dorsal pattern (mottled/bands versus dots in chevrons), the adult SVL (129–171 versus 78.1–103), the total lamellae on one hand (50–61 versus 32–44), the total strigae on ten scales (164–315 versus 138–159), and the relative frontal width (57.3–75.3 versus 75.9–95.5). From *C. occiduus*, we distinguish *C. hewardi* by the dorsal pattern (mottled/bands versus absent), the adult SVL (129–171 versus 269–367), the total strigae on ten scales (164–315 versus 374), the relative ear width (1.40–1.82 versus 0.948–1.39), the relative mental width (1.75–1.81 versus 1.86), the relative postmental width (2.84–3.44 versus 3.57), the relative distance between the ear and eye (6.72–8.73 versus 8.98–10.9), the relative nasal height (1.21–1.24 versus 1.16), the relative distance between the eye and naris (5.00–5.60 versus 6.51), and the relative angled subocular width (1.63–2.23 versus 2.52). From *C. oligolepis* **sp. nov.**, we distinguish *C. hewardi* by the dorsal pattern (mottled/bands versus dots in chevrons), the head markings (absent versus present), the ventral scale rows (113–137 versus 98), the midbody scale rows (43–59 versus 35), and the total lamellae on one hand (50–61 versus 30). From *C. striatus*, we distinguish *C. hewardi* by the dorsal pattern (mottled/bands versus absent/chevrons), the ventral scale rows (113–137 versus 101–109), the relative length of digits on one hindlimb (24.1–30.6 versus 37.8), the relative distance between angled subocular and mouth (0.744–1.40 versus 0.710), the relative forelimb length (22.2–24.6 versus 26.1), the relative ear width (1.40–1.82 versus 1.30), the relative rostral height (1.50–1.76 versus 1.94), the relative cloacal width (8.81–9.89 versus 7.93), the relative prefrontal width (4.18–4.80 versus 5.68), the relative longest finger length (5.03–5.66 versus 7.48), the relative distance between the ear and eye (6.72–8.73 versus 9.00), the relative head width (68.4–77.1 versus 82.1), the relative frontal width (57.3–75.3 versus 76.5), the relative nasal height (1.21–1.24 versus 1.08), the relative distance between the eye and naris (5.00–5.60 versus 6.16), and the relative angled subocular width (1.63–2.23 versus 2.29).

Description of syntype. BMNH 1946.8.7.99. A juvenile; SVL 117 mm; tail nearly cylindrical, broken, 78.0 mm (66.7% SVL); axilla-to-groin distance 65.5 mm (56.0% SVL); forelimb length 27.5 mm (23.5% SVL); hindlimb length 41.4 mm (35.4% SVL); head length 21.2 mm (18.1% SVL); head width 15.5 mm (13.3% SVL); head width 73.4% head length; diameter of orbit 4.66 mm (3.98% SVL); horizontal diameter of ear opening 2.72 mm (2.32% SVL); vertical diameter of ear opening 3.13 mm (2.68% SVL); length of all toes on one foot 35.8 mm (30.6% SVL); shortest distance between angled subocular and lip 0.99 mm (0.846% SVL); shortest distance between the ocular and auricular openings 8.04 mm (6.87% SVL); longest finger length 6.83 mm (5.84% SVL); largest supraocular width 3.41 mm (2.91% SVL); cloacal width 4.98 mm (4.26% SVL); mental width 0.91 mm (0.778% SVL); prefrontal width 5.65 mm (4.83% SVL); frontal width 70.1% frontal length; nasal height 1.51 mm (1.29% SVL); angled subocular height 1.47 mm (1.26% SVL); shortest distance between the eye and naris 5.99 mm (5.12% SVL); canthal iii width 2.40 mm (2.05% SVL); angled subocular width 2.12 mm (1.81% SVL); nasal width 1.48 mm (1.26% SVL); rostral 1.66X as wide as high, missing, visible from above, not in contact with nasals, in contact with 1st supralabial and anterior internasal (left)/(right); anterior internasals are narrower than posterior ones; two

frontonasals (absent divided prefrontal), concave posterior margin, bordered by posterior internasals, 1st loreals, canthal iii, 1st median oculars, and the frontal; frontal much longer than wide; a pair of frontoparietals, separated by the posterior prolongation of the frontal and the interparietal plate; interparietal plate smaller than parietals and separating them, posteriorly touching the interoccipital, which is wider than long; parietal separated from supraoculars by 1st and 2nd temporals and frontoparietal (left)/1st temporal and frontoparietal (right); nasal single; nostril above suture between 1st and 2nd supralabials (left)/(right); 1 postnasal (left)/(right); 2 loreals (left)/(right); 1st loreal higher than wide (left)/(right), in contact with postnasal, posterior internasal, frontonasal, canthal iii, 2nd loreal, and 3rd–4th supralabials (left)/postnasal, posterior internasal, frontonasal, canthal iii, 2nd loreal, and 4th–5th supralabials (right); 2nd loreal shorter than 1st,approximately as high as wide (left)/(right), excluded from contact with supraocular by canthal iii (left)/(right); final loreal posteriorly bordering the upper and lower preoculars (left)/(right); canthal iii wider than high (left)/(right), contacting 1st median ocular, anterior supraciliary, upper preocular, 1st and 2nd loreals, and the frontonasal (left)/(right); 11 median oculars (left)/(right), 1st contacting the prefrontal (left)/(right); 2 upper preoculars (left)/(right); an irregular anterior supraciliary (left)/(right); 6 lateral oculars (left)/(right); 6 temporals (left)/(right); 2 suboculars (left)/(right); posterior subocular large and elongate (left)/(right); anterior subocular small (left)/(right); 9 (left)/10 (right) supralabials, 6 (left)/7 (right) to level below center of eye; 10 (left)/11 (right) infralabials, 7 (left)/8 (right) to level below center of eye; mental small, followed by a single, larger postmental; 5 pairs of enlarged chin shields, followed by 1 pair of reduced chin shields; 1st pair in contact with one another, 2nd pair in contact with one another anteriorly, posteriorly separated by one scale; 3rd–6th pairs separated by 1–6 scales; 124 transverse rows of dorsal scales from interoccipital to base of tail; 131 transverse rows of ventral scales from mental to vent; 50 scales around midbody; 5 digits; finger lengths 3>4>2>5>1; 14 (left)/15 (right) lamellae under longest finger; 60 total lamellae on one hand; toe lengths 4>3>5>2>1; 20 (left)/(right) lamellae under longest toe; dorsal body and caudal scales striate with a median keel; smooth ventral scales; 162 total strigae counted on ten scales.

Color (in alcohol): dorsal surface of head dark tan to brown and patternless; lateral surfaces of head grading from dark tan-brown to gray; dorsal surfaces of the body are dark tan-brown with darker brown markings arranged in chevrons across the body; dorsal surface of tail paler than the body with the same pattern; lateral areas grade from dark brown to gray-tan with continuations of the dorsal pattern in the lateral band that appear mottled; dorsal surfaces of the limbs are dark brown with paler mottling and patches; lateral and ventral areas of the limbs fade to gray-tan with mottling on the forelimbs; ventral surfaces of the head, body, and tail are anteriorly gray with paler mottling, tan posteriorly.

Variation. The examined material resembles the syntype closely in pattern with most specimens exhibiting the same alternating dark and pale bands extending down the body. In some cases, these bands appear mottled (MCZ R-45173) or more closely resemble chevrons (MCZ R-127907). In MCZ R-45177, the entirety of the dorsum appears more mottled than banded. Markings in the longitudinal paramedian area range from absent to mottled to lineate, whereas dots in the lateral bands range from more closely resembling mottling (in KU 226549 and KU 226550) to well defined. Measurements and other morphological data for the syntype and other examined material are presented in Table 1.

Distribution. *Celestus hewardi* is widespread from central to northern Jamaica at elevations of 0–1000 m (Fig. 12).

Ecology and conservation. Little is known of the ecology of this species. It has been sighted in rocky areas near pastures and on stone walls and piles of rotting vegetation (Grant 1940a, Schwartz 1971a; Schwartz & Henderson 1991). The natural habitat of the species is assumed to be the primary limestone forest adjacent to the disturbed areas where collections were made (see Materials and Methods). This species is reported to bask in the sun and is assumed to be diurnal (Grant 1940a). When examined, the majority of stomach contents were "cow's tongues," a slug-like invertebrate (Grant 1940a). One of us (SBH) spent about a year (cumulative) collecting reptiles all over Jamaica and has encountered only a single individual of this species in the late 1970s. Although it has been seen alive in recent years by resident naturalists, it remains one of the rarest reptiles in Jamaica.

The IUCN Redlist (IUCN 2023) considers the conservation status of *Celestus hewardi* to be Endangered B1ab(iii,v) because "the species has an extent of occurrence of around 3,500 km^2 and occurs in one location defined by a significant widespread threat from mongoose predation. There is a continuing decline in the extent and quality of its habitat driven by multiple factors, and in the number of mature individuals inferred from both this and the continuing presence of invasive predators. The species is therefore listed as Endangered." Studies are needed to determine the health and extent of remaining populations and threats to the survival of the species. Captive-breeding programs should be undertaken, because eradication of introduced mammalian predators is not yet possible on Jamaica.

FIGURE 22. (A–F) *Celestus hewardi* (BMNH 1946.8.7.99), the same specimen formerly called BMNH 36.12.3.88 and 1836.12.3.88), SVL 117 mm.

Reproduction. No data on reproduction are available for this species.

Etymology. This species was named after Robert Heward, who obtained one individual of the type series.

Remarks. *Tiliqua striata* was first used in reference to this lizard (Gray 1838); however, this name was a junior homonym of *Celestus striatus*, which was referenced previously in the same publication. The name *C. hewardi* was later introduced (Gray 1845) to correct this oversight. The original description was based on three syntypes (BMNH 1946.8.7.88, 1946.8.7.99, and 1946.8.8.2), one of which (1946.8.7.99) is described in detail above (description of holotype section).

The type locality of *Celestus hewardi* is unknown, with only "Jamaica" being recorded in the original description. The description of *C. variegatus* (later synonymized with *C. hewardi*) recorded the type locality as "unbestimmter Herkunft" (= "undetermined origin"). Grant (1940a) listed this species as *C. occiduus hewardi* based on a correspondence with Stejneger, in which they agreed that it was possible that the "original 'galliwasp' has been exterminated. If that is true, and if the ecological niche of our *occiduus* has helped in differentiating a recognizable subspecies, my guess would be that the name should be *C. occiduus hewardi* Gray." Our genetic data show that this conclusion was incorrect because *C. occiduus* is most closely related to *C. striatus*, and all three species (*C. occiduus*, *C. hewardi*, and *C. striatus*) are valid and separated by 3.5–4.3 million years (Fig. 4). Also, these three species are sympatric in the same region of Jamaica.

Grant (1951) said that he believed that *Celestus impressus* is a synonym of *C. occiduus*. However, Schwartz (1964) reported that one syntype of *C. impressus*, which he designated as lectotype (ANSP 9225), was *C. hewardi* and the other was *C. crusculus*. We examined those specimens and agree with Schwartz, although the damage to both specimens is substantial. One specimen of *C. hewardi* was collected with a blue-and-brown-striped tail, a trait of *C. duquesneyi*, further supporting the close genetic relationship between those two species (Fig. 3) with significant support in our ML analysis and a support value of 71% in our Bayesian analysis. Schools *et al.* (2022) showed the same topology as our ML analysis with a support value of 70% at the stem node in the ML analysis and a support value less than 50% in the Bayesian analysis. Based on our timetree (Fig. 4), *C. hewardi* diverged from *C. duquesneyi* 3.59 Ma, consistent with typical species of vertebrates (> 0.7 Ma; Hedges *et al.* 2015). *Celestus hewardi* was recognized as a distinct species by our ASAP analysis.

***Celestus jamesbondi* sp. nov.**

James Bond Forest Lizard
(Fig. 23–24)

Celestus crusculus crusculus—Grant, 1940:102 (part).
Celestus crusculus—Schwartz & Henderson, 1991:369 (part).
Celestus crusculus crusculus—Hedges *et al.*, 2019:17 (part).
Celestus crusculus—Schools & Hedges, 2021:220 (part).
Celestus crusculus—Landestoy *et al.*, 2022:204 (part).

Holotype. USNM 328184, an adult female from ca. 6.4 km S of Port Maria, Saint Mary Parish, Jamaica, collected by S. Blair Hedges and Carla Ann Hass on 10 August 1987 (18.31715, -76.88786; 59 m).

Paratypes (n=40). JAMAICA. **Saint Mary**. AMNH 107325–9, Herndon G. Dowling, 2 mi W Port Maria, Dowling's house, 18 December 1970; KU 229363, 6.1 mi W Oracabessa, 16 August 1967; KU 229364–5, 0.6 mi S Spring Valley, 17 August 1967; KU 229366, 4.3 mi W, thence 1 mi S Oracabessa, 17 August 1967; KU 229368, 8.6 mi WNW Annotto Bay, 18 August 1967; KU 229369–70, 3.3 mi W, thence 1.4 mi S Oracabessa, 18 August 1967; KU 229371–2, 2.8 mi W Oracabessa, 18 August 1967; KU 229373, 4.7 mi E Ocho Rios, 19 August 1967; KU 229374, 2.5 mi N Port Maria, 20 August 1967; KU 229375–6, 3.2 mi E Oracabessa, 21 August 1967; KU 229377, KU 229379, 2.8 mi E Oracabessa, 21–22 August 1967; KU 229378, 2 mi E Oracabessa, 22 August 1967; MCZ R-45149–50, Chapman Grant, None Such, 6 mi SE of Port Maria, 19 March 1938; MCZ R-45152–3, Chapman Grant, Brimmer Hall, 4 miles S of Port Maria, 19 March 1938; MCZ R-45154–5, Chapman Grant, N of Port Maria, 19 March 1938; USNM 328170, S. Blair Hedges and Carla Ann Hass, Clarendon, Jackson's Bay (on beach at hunting club), 5 October 1984; USNM 328171, S. Blair Hedges and Carla Ann Hass, Clarendon, ca. 1.6 km ESE of Jackson's Bay (at entrance to Jackson's Bay Caves), 5 October 1984; USNM 328172, S. Blair Hedges and David Powars, vicinity of Jacks River (town of), 11 January 1984; USNM 328173, S. Blair Hedges and David Powars, ca.

1.6 km S of Oracabessa (on road to Jacks River), 11 January 1984; USNM 328174–5, S. Blair Hedges and Carla Ann Hass, 6.2 km W of Oracabessa, 25 May 1988; USNM 328176, S. Blair Hedges and Carla Ann Hass, St. Mary, Salt Gut (vicinity of Boscobel Airport, E side), 25 September 1985; USNM 328177–9, Leonard Buchnor, 2.9 km N of Port Maria, 29 May 1988; USNM 328180, 328182–328183, S. Blair Hedges and Carla Ann Hass, ca. 6.4 km S of Port Maria, 10 August 1987.

FIGURE 23. (A–F) *Celestus jamesbondi* **sp. nov.** (USNM 328184, holotype), SVL 69.7 mm.

Diagnosis. *Celestus jamesbondi* **sp. nov.** has (1) a dorsal pattern of absent/irregular dots/dots in chevrons, (2) head markings absent/present, (3) markings in the longitudinal paramedian area absent/present, (4) dots arranged in bars in the lateral band absent/present, (5) an adult SVL of 54.7–72.0 mm, (6) ventral scale rows, 91–112, (7) midbody scale rows, 35–44, (8) total lamellae on one hand, 30–36, (9) total strigae on ten scales, 101–173, (10)

relative length of all digits on one hindlimb, 19.8–26.3 %, (11) relative distance between the angled subocular and mouth, 0.363–1.01 %, (12) relative eye length, 2.94–4.06 %, (13) relative forelimb length, 14.4–19.9 %, (14) relative ear width, 0.917–2.18 %, (15) relative rostral height, 1.62–2.35 %, (16) relative head length, 15.1–20.4 %, (17) relative mental width, 1.59–2.01 %, (18) relative postmental width, 2.61–2.92 %, (19) relative cloacal width, 6.59–9.08 %, (20) relative prefrontal width, 4.29–5.09 %, (21) relative largest supraocular width, 2.16–2.79 %, (22) relative longest finger length, 3.66–4.33 %, (23) relative distance between the ear and eye, 6.92–7.80 %, (24) relative head width, 76.0–80.8 %, (25) relative frontal width, 70.5–77.6 %, (26) relative nasal height, 1.12–1.21 %, (27) relative angled subocular height, 0.893–1.18 %, (28) relative distance between the eye and naris, 4.25–5.54 %, (29) relative canthal iii length, 1.75–2.16 %, (30) relative angled subocular width, 2.09–2.76 %, and (31) relative nasal length, 1.42–1.75 %. The species stem time is 2.33 Ma and the species crown time is 0.10 Ma (Fig. 4).

We distinguish *Celestus jamesbondi* **sp. nov.** from other species of *Celestus* based on a complex of traits. From *Celestus barbouri*, we distinguish *C. jamesbondi* **sp. nov.** by the dorsal pattern (absent/irregular dots/dots in chevrons versus chevrons), the adult SVL (54.7–72.0 versus 78.4–93.6), the ventral scale rows (91–112 versus 118–151), and the midbody scale rows (35–44 versus 47–56). From *C. capitulatus* **sp. nov.**, we distinguish *C. jamesbondi* **sp. nov.** by the relative frontal width (70.5–77.6 versus 78.1–81.6) and the relative width of canthal iii (1.75–2.16 versus 1.61–1.70). From *C. crusculus*, we distinguish *C. jamesbondi* **sp. nov.** by the relative frontal width (70.5–77.6 versus 82.6–91.1). From *C. duquesneyi*, we distinguish *C. jamesbondi* **sp. nov.** by the dorsal pattern (absent/irregular dots/dots in chevrons versus bands), the midbody scale rows (35–44 versus 48), the total lamellae on one hand (30–36 versus 64), the relative length of digits on one hindlimb (19.8–26.3 versus 31.4), the relative eye length (2.94–4.06 versus 4.36), the relative forelimb length (14.4–19.9 versus 24.4), the relative ear width (0.917–2.18 versus 2.45), the relative head length (15.1–20.4 versus 21.6), the relative mental width (1.59–2.01 versus 2.35), the relative postmental width (2.61–2.92 versus 3.19), the relative cloacal width (6.59–9.08 versus 9.98), the relative prefrontal width (4.29–5.09 versus 5.41), the relative longest finger length (3.66–4.33 versus 6.52), the relative head width (76.0–80.8 versus 64.6), the relative angled subocular height (0.893–1.18 versus 1.61), the relative width of canthal iii (1.75–2.16 versus 1.59), the relative angled subocular width (2.09–2.76 versus 2.90), and the relative nasal width (1.42–1.75 versus 2.01). From *C. hesperius* **sp. nov.**, we distinguish *C. jamesbondi* **sp. nov.** by the relative frontal width (70.5–77.6 versus 80.5–86.1). From *C. hewardi*, we distinguish *C. jamesbondi* **sp. nov.** by the dorsal pattern (absent/irregular dots/dots in chevrons versus mottled/bands), the adult SVL (54.7–72.0 versus 129–171), the ventral scale rows (91–112 versus 113–137), the total lamellae on one hand (30–36 versus 50–61), the relative forelimb length (14.4–19.9 versus 22.2–24.6), and the relative longest finger length (3.66–4.33 versus 5.03–5.66). From *C. macrolepis*, we distinguish *C. jamesbondi* **sp. nov.** by the dorsal pattern (absent/irregular dots/dots in chevrons versus bicolored), the adult SVL (54.7–72.0 versus 254–316), the midbody scale rows (35–44 versus 46–48), the total lamellae on one hand (30–36 versus 52–54), the total strigae on ten scales (101–173 versus 398), the relative length of digits on one hindlimb (19.8–26.3 versus 27.5–28.0), the relative distance between angled subocular and mouth (0.363–1.01 versus 1.39–1.66), the relative forelimb length (14.4–19.9 versus 26.1–26.7), the relative postmental width (2.61–2.92 versus 3.81), the relative cloacal width (6.59–9.08 versus 11.2), the relative prefrontal width (4.29–5.09 versus 3.94), the relative longest finger length (3.66–4.33 versus 5.47–5.51), the relative distance between the ear and eye (6.92–7.80 versus 8.02–10.9), the relative frontal width (70.5–77.6 versus 78.4), and the relative distance between the eye and naris (4.25–5.54 versus 6.02). From *C. macrotus*, we distinguish *C. jamesbondi* **sp. nov.** by the dorsal pattern (absent/irregular dots/dots in chevrons versus chevrons/bands), the total lamellae on one hand (30–36 versus 39–40), the relative length of digits on one hindlimb (19.8–26.3 versus 30.2–31.2), the relative forelimb length (14.4–19.9 versus 22.4–25.0), the relative postmental width (2.61–2.92 versus 3.00), the relative largest supraocular width (2.16–2.79 versus 2.96–4.03), the relative longest finger length (3.66–4.33 versus 6.43–6.67), the relative frontal width (70.5–77.6 versus 57.6–66.1), the relative angled subocular width (2.09–2.76 versus 2.77–2.83), and the relative nasal width (1.42–1.75 versus 2.08–2.33). From *C. microblepharis*, we distinguish *C. jamesbondi* **sp. nov.** by the dorsal pattern (absent/irregular dots/dots in chevrons versus chevrons), the adult SVL (54.7–72.0 versus 96.4), the relative length of digits on one hindlimb (19.8–26.3 versus 16.6), the relative eye length (2.94–4.06 versus 1.83), the relative forelimb length (14.4–19.9 versus 14.2), the relative ear width (0.917–2.18 versus 0.446), the relative head length (15.1–20.4 versus 14.7), the relative mental width (1.59–2.01 versus 1.44), the relative postmental width (2.61–2.92 versus 2.47), the relative largest supraocular width (2.16–2.79 versus 2.06), the relative longest finger length (3.66–4.33 versus 3.11), the relative head width (76.0–80.8 versus 75.4), the relative nasal height (1.12–1.21 versus 0.726), the relative

angled subocular height (0.893–1.18 versus 0.778), the relative width of canthal iii (1.75–2.16 versus 1.74), the relative angled subocular width (2.09–2.76 versus 2.90), and the relative nasal width (1.42–1.75 versus 1.11). From *C. molesworthi*, we distinguish *C. jamesbondi* **sp. nov.** by the adult SVL (54.7–72.0 versus 78.1–103), the relative postmental width (2.61–2.92 versus 2.97–3.08), and the relative distance between the ear and eye (6.92–7.80 versus 7.97–8.83). From *C. occiduus*, we distinguish *C. jamesbondi* **sp. nov.** by the adult SVL (54.7–72.0 versus 269–367), the midbody scale rows (35–44 versus 46–56), the total lamellae on one hand (30–36 versus 50–66), the total strigae on ten scales (101–173 versus 374), the relative distance between angled subocular and mouth (0.363–1.01 versus 1.26–1.27), the relative forelimb length (14.4–19.9 versus 23.5–23.9), the relative postmental width (2.61–2.92 versus 3.57), the relative longest finger length (3.66–4.33 versus 4.77–5.46), the relative distance between the ear and eye (6.92–7.80 versus 8.98–10.9), the relative head width (76.0–80.8 versus 73.8), the relative frontal width (70.5–77.6 versus 63.8), the relative angled subocular height (0.893–1.18 versus 1.30), the relative distance between the eye and naris (4.25–5.54 versus 6.51), and the relative nasal width (1.42–1.75 versus 1.83). From *C. oligolepis* **sp. nov.**, we distinguish *C. jamesbondi* **sp. nov.** by the relative mental to vent scales (2.14–2.77 versus 2.80) (see Remarks). From *C. striatus*, we distinguish *C. jamesbondi* **sp. nov.** by the adult SVL (54.7–72.0 versus 145), the total lamellae on one hand (30–36 versus 59–66), the total strigae on ten scales (101–173 versus 279), the relative length of digits on one hindlimb (19.8–26.3 versus 37.8), the relative forelimb length (14.4–19.9 versus 26.1), the relative prefrontal width (4.29–5.09 versus 5.68), the relative longest finger length (3.66–4.33 versus 7.48), the relative distance between the ear and eye (6.92–7.80 versus 9.00), the relative head width (76.0–80.8 versus 82.1), the relative nasal height (1.12–1.21 versus 1.08), and the relative distance between the eye and naris (4.25–5.54 versus 6.16).

Description of holotype. USNM 328184. An adult female; SVL 69.7 mm; tail nearly cylindrical, broken, 8.94 mm (12.8% SVL); axilla-to-groin distance 39.1 mm (56.1% SVL); forelimb length 12.2 mm (17.5% SVL); hindlimb length 17.8 mm (25.5% SVL); head length 11.1 mm (15.9% SVL); head width 8.93 mm (12.8% SVL); head width 80.5% head length; diameter of orbit 2.34 mm (3.36% SVL); horizontal diameter of ear opening 1.28 mm (1.84% SVL); vertical diameter of ear opening 1.18 mm (1.69% SVL); length of all toes on one foot 15.1 mm (21.7% SVL); shortest distance between angled subocular and lip 0.44 mm (0.631% SVL); shortest distance between the ocular and auricular openings 4.89 mm (7.02% SVL); longest finger length 2.72 mm (3.90% SVL); largest supraocular width 1.60 mm (2.30% SVL); cloacal width 4.59 mm (6.59% SVL); mental width 1.40 mm (2.01% SVL); postmental width 1.91 mm (2.74% SVL); prefrontal width 3.01 mm (4.32% SVL); frontal width 2.95 mm (4.23% SVL); nasal height 0.79 mm (1.13% SVL); angled subocular height 0.82 mm (1.18% SVL); shortest distance between the eye and naris 2.96 mm (4.25% SVL); angled subocular width 1.46 mm (2.09% SVL); nasal width 0.99 mm (1.42% SVL); rostral 1.89X as wide as high, visible from above, not in contact with nasals, in contact with 1st supralabial and anterior internasal (left)/(right); anterior internasals are narrower than posterior ones; frontonasals and prefrontal fused into a single large plate with an irregular posterior margin, wider than long, bordered by posterior internasals, the loreal 1 (left), additional scale over right loreal 1 (right), median ocular 1, canthal iii (left), and the frontal; frontal mostly missing, longer than wide; a pair of frontoparietals, separated by the posterior prolongation of the frontal and the interparietal plate; interparietal plate smaller than parietals and separating them, posteriorly touching the interoccipital, which is wider than long; parietal separated from supraoculars by 1st and 2nd temporals and frontoparietal (left)/(right); nasal single; nostril above suture between 1st and 2nd supralabials (left)/(right); 1 postnasal (left)/(right); 2 loreals (left)/(right); 1st loreal higher than wide (left)/(right), in contact with postnasal, posterior internasal, prefrontal/frontonasal complex, canthal iii, 2nd loreal, and supralabials 3–4 (left)/postnasal, posterior internasal, additional scale above 1st loreal (separating it from the prefrontal/frontonasal complex), canthal iii, 2nd loreal, and 3rd–4th supralabials (right); 2nd loreal shorter than 1st, approximately as high as wide (left)/(right), excluded from contact with supraocular by canthal iii (left)/(right); final loreal posteriorly bordering the upper and lower preoculars (left)/(right); canthal iii missing, wider than high (left)/(right), contacting 1st median ocular (missing on left), anterior supraciliary, upper preocular, prefrontal/frontonasal complex, and 1st and 2nd loreals (left)/(right); 9 median oculars (left)/(right), 1st contacting the prefrontal (left)/damaged (right); 1 upper preocular (left)/(right); an irregular anterior supraciliary (left)/(right); 6 lateral oculars (left)/(right); 5 temporals (left)/(right); 2 suboculars (left)/(right); posterior subocular large and elongate (left)/(right); anterior subocular small (left)/(right); 9 supralabials (left)/(right), 6 to level below center of eye (left)/(right); 9 infralabials (left)/(right), 6 to level below center of eye (left)/(right); mental small, followed by a single, larger postmental; 4 pairs of enlarged chin shields; 1st pair in contact with one another; 2nd–4th pairs separated by 1–3 scales; 95 transverse rows of dorsal

scales from interoccipital to base of tail; 104 transverse rows of ventral scales from mental to vent; 42 scales around midbody; 5 digits; finger lengths 3>4>2>5>1; 8 (left)/missing limb (right) lamellae under longest finger; 32 total lamellae on one hand; toe lengths 4>3>5>2>1; 13 (left)/14 (right) lamellae under longest toe; striate and keeled dorsal body and caudal scales; smooth ventral scales; 120 total strigae counted on ten scales.

Color (in alcohol): dorsal surface of head medium brown with darker brown markings around scale borders; lateral surfaces of head grading from medium brown to dark yellow with darker brown eye masks; dorsal surfaces of the body are medium brown with darker markings in longitudinal paramedian series and others that continue down the body as chevrons; dorsal surface of tail the same as the body with less pronounced chevrons; lateral areas grade from dark brown to dark yellow; dorsal surfaces of the limbs are dark brown with some medium brown flecks; lateral and ventral areas of the limbs fade to deep yellow; ventral surfaces of the head, body, and tail are dark yellow and patternless.

Variation. The majority of the specimens are similar to the holotype in scalation and pattern. USNM 328170 has a pale tan dorsal color and is the lightest of the specimens. This specimen has none of the pattern around the neck or dotting down the dorsum seen in the majority of the other specimens. The other paratypes have a medium to dark brown dorsum. All specimens have markings on the neck that range from mottling to small longitudinal paramedian lines. The majority of the specimens have dots that begin on their necks and are arranged in a herring bone pattern that becomes sparser posteriorly. USNM 328180 has few spots arranged as chevrons. All paratypes have dark lateral bands, some of which bear paler spots (USNM 328174, USNM 328182). All have cream colored, patternless venters. The underside of the throats of all the adult specimens appears as a darker gray-cream in comparison to the rest of their venters. No specimens show dots in bars in the lateral bands. Measurements and other morphological data for the holotype and other examined material are presented in Table 1.

Distribution. *Celestus jamesbondi* **sp. nov.** has a disjunct distribution, known primarily from the north-central coast of Jamaica at elevations of 0–60 m in St. Mary Parish, and from the southern coast near Jackson's Bay in Clarendon Parish (Fig. 12). It has an extent of occurrence of ~650 km^2.

Ecology and conservation. Little is known of the ecology of this species, although it appears to be rather common and tolerant of disturbance (SBH). The majority of animals were collected during the day under boards, rocks, logs, and in rotting palm vegetation. One specimen (SBH 103460) was collected at night on rocks next to a sinkhole near the entrances of large caves.

We consider the conservation status of *Celestus jamesbondi* **sp. nov.** to be Least Concern, based on IUCN Redlist criteria (IUCN 2023). However, its relatively small range is of concern and therefore studies are needed to determine the health and extent of the populations and any threats to the survival of the species.

Reproduction. Ovoviviparous. Litter sizes of 1–3 have been recorded. Two enlarging eggs (0.55 g) were in one female (6.3 g, live) (SBH, field data).

Etymology. The species name (*jamesbondi*) is a Latinized version of the name "James Bond," curator of ornithology and expert on Caribbean birds at the Philadelphia Academy of Natural Sciences in the 20th Century. Ian Fleming borrowed his name in 1953 for the fictional character in a series of books, starting with *Casino Royale*. The writer's house, Goldeneye (near Oracabessa), where Fleming created the character, is in the range of this species, which is why we give it this name.

Remarks. Specimens of *Celestus jamesbondi* **sp. nov.** were observed in the majority of the museum collections examined (AMNH, KU, MCZ, and USNM), having been collected as recently as the 1980s. Although *C. jamesbondi* and *C. oligolepis* cannot be morphologically separated based on our standard suite of characters, the one known specimen of *C. oligolepis* is a juvenile, meaning that only traits pertaining to pattern and scale counts could be applied to this comparison (also the two species are separated genetically by 5.0 million years; Fig. 4). However, *C. jamesbondi* and *C. oligolepis* are morphologically separated based on the ratio of mental to vent scales divided by midbody scales (2.14–2.77 [n=35] versus 2.80 [n=1]). Also, the two species are separated by 110–140 km straight line distance.

Celestus jamesbondi **sp. nov.** is included in our genetic dataset and has significant support in both Bayesian and ML likelihood analyses at the crown node of the species and the stem node that places it as the closest relative to *C. hesperius*. Based on our timetree (Fig. 4), *C. jamesbondi* **sp. nov.** diverged from its closest relative 2.33 Ma, consistent with typical species of vertebrates (> 0.7 Ma; Hedges *et al.* 2015). *Celestus jamesbondi* **sp. nov.** was recovered as conspecific with *Celestus crusculus* in our ASAP analysis.

FIGURE 24. *Celestus jamesbondi* **sp. nov.** (USNM 328173, SBH 101615), in life. From ca. 1.6 km S Oracabessa on road to Jack's River, Saint Mary Parish, Jamaica. Photo by SBH.

***Celestus macrolepis* (Gray 1845)**
Black Giant Forest Lizard
(Fig. 25)

Celestus macrolepis Gray, 1845:118. Holotype: BMNH 1946.8.3.82 (locality unknown).
Celestus occiduus—Boulenger, 1885:290 (part).
Celestus occiduus—Schwartz & Henderson, 1988:99 (part).
Celestus macrolepis—Schools & Hedges, 2021:220.
Celestus macrolepis—Landestoy *et al.*, 2022:204.

Material examined (n=2). JAMAICA. Localities unknown. BMNH 1946.8.3.82; BMNH 1961.1851.

Diagnosis. *Celestus macrolepis* has (1) a dorsal pattern bicolored (dark anteriorly, pale posteriorly), (2) head markings absent, (3) markings in the longitudinal paramedian area absent, (4) dots arranged in bars in the lateral band absent, (5) an adult SVL of 254–316 mm, (6) ventral scale rows, 112–116, (7) midbody scale rows, 46–48, (8) total lamellae on one hand, 52–54, (9) total strigae on ten scales, 398, (10) relative length of all digits on one hindlimb, 27.5–28.0 %, (11) relative distance between the angled subocular and mouth, 1.39–1.66 %, (12) relative eye length, 3.63–3.70 %, (13) relative forelimb length, 26.1–26.7 %, (14) relative ear width, 0.760–1.43 %, (15) relative rostral height, 1.53–1.75 %, (16) relative head length, 19.2–22.9 %, (17) relative mental width, 1.87 %, (18) relative postmental width, 3.81 %, (19) relative cloacal width, 11.2 %, (20) relative prefrontal width, 3.94 %, (21) relative largest supraocular width, 2.64–3.01 %, (22) relative longest finger length, 5.47–5.51 %, (23) relative distance between the ear and eye, 8.02–10.9 %, (24) relative head width, 80.5 %, (25) relative frontal width, 78.4 %, (26) relative nasal height, 1.18 %, (27) relative angled subocular height, 1.17 %, (28) relative distance between the eye and naris, 6.02 %, (29) relative canthal iii length, 1.99 %, (30) relative angled subocular width, 2.57 %, and (31) relative nasal length, 1.75 %. The species stem time is 4.64 Ma and the species crown time is unavailable (Fig. 4).

Celestus macrolepis differs from all other species of the genus in having a bicolored dorsal pattern (dark anteriorly, pale posteriorly). This species also has a smaller relative prefrontal width (3.94) than most other species of the genus. *Celestus macrolepis* has a larger SVL (254–316), total strigae on ten scales count (398), relative distance between the angled subocular and mouth (1.39–1.66), relative forelimb length (26.1–26.7), relative postmental

width (3.81), relative cloacal width (11.2), and relative distance between the eye and naris (6.02) than most other species of the genus.

From *Celestus barbouri*, we distinguish *C. macrolepis* by the dorsal pattern (bicolored versus chevrons), the adult SVL (254–316 versus 78.4–93.6), the ventral scale rows (112–116 versus 118–151), the total lamellae on one hand (52–54 versus 36–49), the total strigae on ten scales (398 versus 105–136), the relative length of digits on one hindlimb (27.5–28.0 versus 18.2–23.5), the relative distance between angled subocular and mouth (1.39–1.66 versus 0.437–0.556), the relative forelimb length (26.1–26.7 versus 15.4–19.0), the relative head length (19.2–22.9 versus 14.6–16.6), the relative mental width (1.87 versus 1.51–1.85), the relative postmental width (3.81 versus 2.51–3.29), the relative cloacal width (11.2 versus 7.64–8.26), the relative prefrontal width (3.94 versus 3.97–4.33), the relative longest finger length (5.47–5.51 versus 2.92–3.81), the relative distance between the ear and eye (8.02–10.9 versus 6.23–7.15), the relative nasal height (1.18 versus 0.930–1.12), the relative angled subocular height (1.17 versus 0.553–1.16), the relative distance between the eye and naris (6.02 versus 4.68–4.83), the relative width of canthal iii (1.99 versus 1.54–1.93), the relative angled subocular width (2.57 versus 1.97–2.52), and the relative nasal width (1.75 versus 1.38–1.65). From *C. capitulatus* **sp. nov.**, we distinguish *C. macrolepis* by the dorsal pattern (bicolored versus irregular dots/dots in chevrons), the adult SVL (254–316 versus 62.1–81.8), the total lamellae on one hand (52–54 versus 25–38), the total strigae on ten scales (398 versus 105–192), the relative length of digits on one hindlimb (27.5–28.0 versus 17.6–22.3), the relative distance between angled subocular and mouth (1.39–1.66 versus 0.525–1.17), the relative forelimb length (26.1–26.7 versus 14.3–18.1), the relative head length (19.2–22.9 versus 15.1–17.7), the relative mental width (1.87 versus 1.28–1.84), the relative postmental width (3.81 versus 2.62–2.97), the relative cloacal width (11.2 versus 7.84–8.67), the relative prefrontal width (3.94 versus 4.30–4.72), the relative largest supraocular width (2.64–3.01 versus 2.03–2.61), the relative longest finger length (5.47–5.51 versus 3.45–3.75), the relative distance between the ear and eye (8.02–10.9 versus 6.45–7.84), the relative head width (80.5 versus 71.6–78.6), the relative angled subocular height (1.17 versus 0.586–1.01), the relative distance between the eye and naris (6.02 versus 4.57–5.03), and the relative angled subocular width (2.57 versus 1.93–2.32). From *C. crusculus*, we distinguish *C. macrolepis* by the dorsal pattern (bicolored versus absent/flecks in series/dots in chevrons), the longitudinal paramedian lines (absent versus present), the adult SVL (254–316 versus 59.6–77.6), the midbody scale rows (46–48 versus 37–44), the total lamellae on one hand (52–54 versus 30–39), the total strigae on ten scales (398 versus 106–194), the relative length of digits on one hindlimb (27.5–28.0 versus 18.7–24.7), the relative distance between angled subocular and mouth (1.39–1.66 versus 0.339–0.884), the relative eye length (3.63–3.70 versus 2.93–3.61), the relative forelimb length (26.1–26.7 versus 12.8–20.7), the relative postmental width (3.81 versus 2.73–3.37), the relative cloacal width (11.2 versus 6.89–8.77), the relative longest finger length (5.47–5.51 versus 2.94–4.10), the relative frontal width (78.4 versus 82.6–91.1), the relative distance between the eye and naris (6.02 versus 4.31–4.86), the relative angled subocular width (2.57 versus 2.03–2.43), and the relative nasal width (1.75 versus 1.27–1.60). From *C. duquesneyi*, we distinguish *C. macrolepis* by the dorsal pattern (bicolored versus bands), the adult SVL (254–316 versus 62.1), the total strigae on ten scales (398 versus 130), the relative distance between angled subocular and mouth (1.39–1.66 versus 0.644), and the relative ear width (0.760–1.43 versus 2.45). From *C. hesperius* **sp. nov.**, we distinguish *C. macrolepis* by the dorsal pattern (bicolored versus dots in chevrons), the adult SVL (254–316 versus 54.0–62.3), the midbody scale rows (46–48 versus 39–44), the total lamellae on one hand (52–54 versus 29–34), the total strigae on ten scales (398 versus 95–122), the relative length of digits on one hindlimb (27.5–28.0 versus 21.7–26.2), the relative distance between angled subocular and mouth (1.39–1.66 versus 0.594–0.648), the relative forelimb length (26.1–26.7 versus 18.6–21.3), the relative ear width (0.760–1.43 versus 1.52–1.59), the relative head length (19.2–22.9 versus 15.7–17.7), the relative largest supraocular width (2.64–3.01 versus 1.91–2.22), the relative longest finger length (5.47–5.51 versus 3.50–4.04), and the relative distance between the ear and eye (8.02–10.9 versus 6.74–7.53). From *C. hewardi*, we distinguish *C. macrolepis* by the dorsal pattern (bicolored versus mottled/bands), the adult SVL (254–316 versus 129–171), the total strigae on ten scales (398 versus 164–315), the relative forelimb length (26.1–26.7 versus 22.2–24.6), the relative mental width (1.87 versus 1.75–1.81), the relative postmental width (3.81 versus 2.84–3.44), the relative cloacal width (11.2 versus 8.81–9.89), the relative prefrontal width (3.94 versus 4.18–4.80), the relative head width (80.5 versus 68.4–77.1), the relative frontal width (78.4 versus 57.3–75.3), the relative nasal height (1.18 versus 1.21–1.24), the relative distance between the eye and naris (6.02 versus 5.00–5.60), and the relative angled subocular width (2.57 versus 1.63–2.23). From *C. jamesbondi* **sp. nov.**, we distinguish *C. macrolepis* by the dorsal pattern (bicolored versus absent/irregular dots/dots in chevrons), the adult SVL (254–316 versus 54.7–72.0), the midbody

scale rows (46–48 versus 35–44), the total lamellae on one hand (52–54 versus 30–36), the total strigae on ten scales (398 versus 101–173), the relative length of digits on one hindlimb (27.5–28.0 versus 19.8–26.3), the relative distance between angled subocular and mouth (1.39–1.66 versus 0.363–1.01), the relative forelimb length (26.1–26.7 versus 14.4–19.9), the relative postmental width (3.81 versus 2.61–2.92), the relative cloacal width (11.2 versus 6.59–9.08), the relative prefrontal width (3.94 versus 4.29–5.09), the relative longest finger length (5.47–5.51 versus 3.66–4.33), the relative distance between the ear and eye (8.02–10.9 versus 6.92–7.80), the relative frontal width (78.4 versus 70.5–77.6), and the relative distance between the eye and naris (6.02 versus 4.25–5.54). From *C. macrotus*, we distinguish *C. macrolepis* by the dorsal pattern (bicolored versus chevrons/bands), the longitudinal paramedian lines (absent versus present), the dots arranged in bars in the lateral areas (absent versus present), the adult SVL (254–316 versus 60.0–86.1), the ventral scale rows (112–116 versus 87–93), the midbody scale rows (46–48 versus 41–45), the total lamellae on one hand (52–54 versus 39–40), the total strigae on ten scales (398 versus 64–115), the relative length of digits on one hindlimb (27.5–28.0 versus 30.2–31.2), the relative distance between angled subocular and mouth (1.39–1.66 versus 0.640–0.983), the relative eye length (3.63–3.70 versus 3.79–5.17), the relative forelimb length (26.1–26.7 versus 22.4–25.0), the relative ear width (0.760–1.43 versus 1.75–2.08), and the relative longest finger length (5.47–5.51 versus 6.43–6.67). From *C. microblepharis*, we distinguish *C. macrolepis* by the dorsal pattern (bicolored versus chevrons), the adult SVL (254–316 versus 96.4), the total lamellae on one hand (52–54 versus 30), the total strigae on ten scales (398 versus 165), the relative length of digits on one hindlimb (27.5–28.0 versus 16.6), the relative distance between angled subocular and mouth (1.39–1.66 versus 0.820), the relative eye length (3.63–3.70 versus 1.83), the relative forelimb length (26.1–26.7 versus 14.2), the relative ear width (0.760–1.43 versus 0.446), the relative longest finger length (5.47–5.51 versus 3.11), and the relative nasal height (1.18 versus 0.726). From *C. molesworthi*, we distinguish *C. macrolepis* by the dorsal pattern (bicolored versus dots in chevrons), the adult SVL (254–316 versus 78.1–103), the total lamellae on one hand (52–54 versus 32–44), the total strigae on ten scales (398 versus 138–159), the relative distance between angled subocular and mouth (1.39–1.66 versus 0.653–0.845), the relative forelimb length (26.1–26.7 versus 17.5–24.2), and the relative longest finger length (5.47–5.51 versus 4.28–5.19). From *C. occiduus*, we distinguish *C. macrolepis* by the dorsal pattern (bicolored versus absent), the relative distance between angled subocular and mouth (1.39–1.66 versus 1.26–1.27), the relative eye length (3.63–3.70 versus 2.87–3.33), the relative forelimb length (26.1–26.7 versus 23.5–23.9), and the relative longest finger length (5.47–5.51 vs 4.77–5.46). From *C. oligolepis* **sp. nov.**, we distinguish *C. macrolepis* by the dorsal pattern (bicolored versus dots in chevrons), the head markings (absent versus present), the longitudinal paramedian lines (absent versus present), the ventral scale rows (112–116 versus 98), the midbody scale rows (46–48 versus 35), and the total lamellae on one hand (52–54 versus 30). From *C. striatus*, we distinguish *C. macrolepis* by the dorsal pattern (bicolored versus absent/chevrons), the adult SVL (254–316 versus 145), the ventral scale rows (112–116 versus 101–109), the midbody scale rows (46–48 versus 41–43), the total lamellae on one hand (52–54 versus 59–66), and the relative distance between angled subocular and mouth (1.39–1.66 versus 0.710).

Description of holotype. BMNH 1946.8.3.82. An adult; SVL 254 mm; tail laterally compressed, 150 mm (59.1% SVL); axilla-to-groin distance 141 mm (55.5% SVL); forelimb length 67.9 mm (26.7% SVL); hindlimb length 88.2 mm (34.7% SVL); head length 48.6 mm (19.1% SVL); head width 39.1 mm (15.4% SVL); head width 80.5% head length; diameter of orbit 9.41 mm (3.70% SVL); horizontal diameter of ear opening 3.64 mm (1.43% SVL); vertical diameter of ear opening 6.46 mm (2.54% SVL); length of all toes on one foot 71.0 mm (28.0% SVL); shortest distance between angled subocular and lip 3.52 mm (1.39% SVL); shortest distance between the ocular and auricular openings 20.4 mm (8.03% SVL); longest finger length 13.9 mm (5.47% SVL); largest supraocular width 6.70 mm (2.64% SVL); cloacal width 28.4 mm (11.2% SVL); mental width 4.75 mm (1.87% SVL); postmental width 9.68 mm (3.81% SVL); prefrontal width 10.0 mm (3.94% SVL); frontal width 78.4% frontal length; nasal height 3.00 mm (1.18% SVL); angled subocular height 2.98 mm (1.17% SVL); shortest distance between the eye and naris 15.3 mm (6.02% SVL); canthal iii width 5.05 mm (1.99% SVL); angled subocular width 6.53 mm (2.57% SVL); nasal width 4.44 mm (1.75% SVL); rostral 1.53X as wide as high, visible from above, not in contact with nasals, in contact with 1st supralabial and anterior internasal (left)/(right); anterior internasals are narrower than posterior ones; frontonasals and prefrontal fused into a single large plate with a concave posterior margin, much wider than long, bordered by posterior internasals, 1st loreals, 1st and 2nd median oculars, and the frontal; frontal much longer than wide; a pair of frontoparietals, separated by the posterior prolongation of the frontal and the interparietal plate; interparietal plate smaller than parietals and fused to them, posteriorly touching the fused to interoccipital, which is

wider than long; parietal separated from supraoculars by 1st temporal and frontoparietal (left)/1st and 2nd temporals and frontoparietal (right); nasal single; nostril above suture between 1st and 2nd supralabials (left)/(right); 1 postnasal (left)/(right); 3 loreals (left)/(right); 1st loreal small, higher than wide (left)/(right); 2nd loreal large, irregular, fused with 3rd loreal at the very bottom (left), higher than long, in contact with posterior internasals, prefrontal/frontonasal complex, anterior most ocular, canthal iii, 1st loreal, 3rd loreal, and supralabials 3–4 (left)/large, irregular, higher than wide, in contact with posterior internasals, prefrontal/frontonasal complex, median ocular 1, canthal iii, subcanthal (Savage and Lips 2008), 1st and 3rd loreals, and supralabials 3–5 (right); 3rd loreal irregular, excluded from contact with supraocular by canthal iii (left)/rectangular, excluded from contact with canthal iii by subcanthal (right); final loreal posteriorly bordering the upper and lower preoculars (left)/(right); canthal iii wider than high (left)/(right), contacting 1st median ocular, anterior supraciliary, upper preocular, and 2nd and 3rd loreals (left)/1st median ocular, anterior supraciliary, upper preocular, subcanthal, and the loreals 2–3 (right); 11 (left)/10 (right) median oculars, 1st and 2nd contacting the prefrontal (left)/(right); 2 upper preoculars (left)/(right); an irregular anterior supraciliary (left)/(right); 6 lateral oculars (left)/(right); 5 temporals (left)/(right); 2 suboculars (left)/(right); posterior subocular large and elongate (left)/(right); anterior subocular small (left)/(right); 10 supralabials (left)/(right), 7 to level below center of eye (left)/(right); 9 (left)/10 (right) infralabials, 7 to level below center of eye (left)/(right); mental small, followed by a single, slightly larger postmental; 4 pairs of enlarged chin shields; 1st pair in contact with one another anteriorly, posteriorly separated by one scale; 2nd–4th pairs separated by 1–5 scales; 109 transverse rows of dorsal scales from interoccipital to base of tail; 116 transverse rows of ventral scales from mental to vent; 48 scales around midbody; 5 digits; finger lengths 3>4>2>5>1; 13 (3 are fused) (left)/13 (2 are fused) (right) lamellae under longest finger; 54 total lamellae on one hand; toe lengths 4>3>5>2>1; 24 lamellae under longest toe (left)/(right); dorsal body and caudal scales striate, some with a faint median keel; smooth ventral scales; 398 total strigae counted on ten scales.

Color (in alcohol): dorsal surface of head very dark brown, patternless; lateral surfaces of head grading from dark brown to medium brown, patternless; dorsal surfaces of the body are dark brown, interspersed with large, gray-tan patches that have several dark brown scales in them; dorsal surface of tail the same as the body, interspersed with large, gray-tan patches that have several dark brown scales in them; lateral areas have the same coloration and pattern as the dorsal areas; dorsal surfaces of the limbs are dark brown with gray-tan patches; lateral and ventral areas of the limbs same as the body; ventral surfaces of the head, body, and tail are the same as the dorsal body scales with slightly reduced colors.

Variation. The other examined specimen closely resembles the holotype in pattern and scalation. Measurements and other morphological data for the holotype and other examined material are presented in Table 1.

Distribution. No information is known on the distribution of *Celestus macrolepis* as the most specific location recorded for any of the specimens is "Jamaica" (BMNH 1961.1851).

Ecology and conservation. Based on literature reports, *Celestus macrolepis* is a swamp-dwelling lizard. Although confusion has persisted throughout the literature regarding the identification of *C. macrolepis*, ecological reports of a dark brown diploglossid (presumably *C. macrolepis*) living in the Jamaican swamps confirm its placement in the Swamp Ecomorph. Browne (1789) described *C. occiduus* as normally being a dirty brown color, but often changing to a fine golden color. Diploglossids are not known for such dramatic color change, and he more likely was referring to both the dark brown *C. macrolepis* and the yellow *C. occiduus*. Sloane (1725) described a giant Jamaican diploglossid that lived "both in water and on land," He also noted that upon dissection, the specimen had crabs in its stomach. Based on the brown color of the specimen that he dissected, Sloane was probably referring to a member of the species *C. macrolepis*, not *C. occiduus*. As reported in Ahrenfeldt (1954), Duméril & Bibron (1839) had also doubted that the species described by Sloane was *C. occiduus. Celestus macrolepis* also has a strongly laterally compressed tail, a common adaptation for swimming in vertebrates (Gray 1845). A laterally compressed tail was also reported for *C. occiduus* by Boulenger (1885); however, his description included the holotype of *C. macrolepis*, in addition to other specimens that are identified as *C. occiduus*.

The IUCN Redlist (IUCN 2023) considers the conservation status of *Celestus macrolepis* to be Critically Endangered (Possibly Extinct) C2a(i,ii); D. It faces a primary threat from habitat destruction from agriculture and urbanization. Secondary threats include predation from introduced mammals, including the mongoose and black rats. Studies are needed to determine the health and extent of remaining populations and threats to the survival of the species. Captive-breeding programs should be undertaken, because eradication of introduced mammalian predators is not possible on Jamaica.

FIGURE 25. (A–F) *Celestus macrolepis* (BMNH 1946.8.3.82, holotype), SVL 254 mm.

Reproduction. No data on reproduction are available for this species.

Etymology. The species name is derived from the prefix *macro-* (large) and *lepis* (scale). Gray (1845), who described the species, named it the "Large-scaled Galliwasp."

Remarks. The species *Celestus macrolepis* was recently recognized as a valid species (Schools & Hedges 2021) long after it had been synonymized with *C. occiduus* (Boulenger 1885). Although both species share a laterally compressed tail (Schools & Hedges 2022), several key differences exist between *C. macrolepis* and *C. occiduus*. In addition to its darker coloration, *C. macrolepis* also has scale differences and a more robust head than *C. occiduus* (Schools & Hedges 2021). We recognize BMNH 1961.1851 as a member of *C. macrolepis* largely because it shares the distinct bicolored pattern as the holotype (Fig. 25).

Celestus macrolepis is included in our genetic dataset and is placed outside the group containing *C. duquesneyi*, *C. hesperius* **sp. nov.**, *C. hewardi*, *C. jamesbondi* **sp. nov.**, *C. molesworthi*, *C. occiduus*, and *C. striatus* with significant support in our ML analysis and a support value of 80% in out Bayesian analysis. Based on our timetree (Fig. 4), *C. macrolepis* diverged from its closest relative 4.64 Ma, consistent with typical species of vertebrates (> 0.7 Ma; Hedges *et al.* 2015). *Celestus macrolepis* **sp. nov.** was recognized as a distinct species in our ASAP analysis.

Celestus macrotus Thomas & Hedges, 1989

Laselle-Baoruco Forest Lizard

(Fig. 26–27)

Celestus macrotus Thomas & Hedges, 1989:886. Holotype: USNM 286917 collected by S. Blair Hedges and Richard Thomas from ca. 15 km W of Gros Cheval by logging roads, on the northeastern slope of Morne La Selle, Département de l'Ouest, Haiti, on 18 November 1984 (18.3509, -71.9020; 2020 m).
Celestus macrotus—Schwartz & Henderson, 1991:375.
Celestus macrotus—Powell *et al.*, 1999:105.
Celestus macrotus—Schools & Hedges, 2021:220.
Celestus macrolepis—Schools *et al.* 2022.
Celestus macrotus—Landestoy *et al.*, 2022:204.

Material examined (n=7). DOMINICAN REPUBLIC. Pedernales. MALT 00796–99, 7 km NNE of Los Arroyos, helipad at Loma del Toro. **HAITI. Ouest.** ANSP 38506, S. Blair Hedges, southeast of Pic La Selle, 20 November 2011; USNM 286917, S. Blair Hedges and Richard Thomas, ca. 15 km W of Gros Cheval by logging roads, northeastern slope of Morne La Selle in the Massif de la Selle, 18 November 1984. **Sud-Est.** ANSP 38505, S. Blair Hedges, Tiffany Cloud, Miguel Landestoy, and Marcos Rodriguez, Southeast of Pic La Selle, 20 November 2011.

Diagnosis. *Celestus macrotus* has (1) a dorsal pattern of chevrons/bands, (2) head markings absent/present, (3) markings in the longitudinal paramedian area present, (4) dots arranged in bars in the lateral band present, (5) a maximum SVL of 60.0–86.1 mm, (6) ventral scale rows, 87–93, (7) midbody scale rows, 41–45, (8) total lamellae on one hand, 39–40, (9) total strigae on ten scales, 64–115, (10) relative length of all digits on one hindlimb, 30.2–31.2 %, (11) relative distance between the angled subocular and mouth, 0.640–0.983 %, (12) relative eye length, 3.79–5.17 %, (13) relative forelimb length, 22.4–25.0 %, (14) relative ear width, 1.75–2.08 %, (15) relative rostral height, 1.61–1.95 %, (16) relative head length, 18.2–20.5 %, (17) relative mental width, 1.77 %, (18) relative postmental width, 3.00 %, (19) relative cloacal width, 7.80–9.48 %, (20) relative prefrontal width, 4.87–5.55 %, (21) relative largest supraocular width, 2.96–4.03 %, (22) relative longest finger length, 6.43–6.67 %, (23) relative distance between the ear and eye, 7.58–8.02 %, (24) relative head width, 67.6–80.6 %, (25) relative frontal width, 57.6–66.1 %, (26) relative nasal height, 1.15–1.62 %, (27) relative angled subocular height, 1.00–1.07 %, (28) relative distance between the eye and naris, 5.48–5.60 %, (29) relative canthal iii length, 1.85 %, (30) relative angled subocular width, 2.77–2.83 %, and (31) relative nasal length, 2.08–2.33 %. The species stem time is 5.58 Ma and the species crown time is 1.22 Ma (Fig. 4).

Celestus macrotus has a lower number of ventral scale rows (87–93) than most other species of the genus. This species also has a larger relative longest finger length (6.43–6.67) than most other species of the genus.

From *Celestus barbouri*, we distinguish *C. macrotus* by the longitudinal paramedian lines (present versus absent), the dots arranged in bars in the lateral areas (present versus absent), the ventral scale rows (87–93 versus 118–151), the midbody scale rows (41–45 versus 47–56), the relative length of digits on one hindlimb (30.2–31.2

versus 18.2–23.5), the relative distance between angled subocular and mouth (0.640–0.983 versus 0.437–0.556), the relative eye length (3.79–5.17 versus 2.87–3.63), the relative forelimb length (22.4–25.0 versus 15.4–19.0), the relative head length (18.2–20.5 versus 14.6–16.6), the relative prefrontal width (4.87–5.55 versus 3.97–4.33), the relative largest supraocular width (2.96–4.03 versus 1.92–2.74), the relative longest finger length (6.43–6.67 versus 2.92–3.81), the relative distance between the ear and eye (7.58–8.02 versus 6.23–7.15), the relative nasal height (1.15–1.62 versus 0.930–1.12), the relative distance between the eye and naris (5.48–5.60 versus 4.68–4.83), the relative angled subocular width (2.77–2.83 versus 1.97–2.52), and the relative nasal width (2.08–2.33 versus 1.38–1.65). From *C. capitulatus* **sp. nov.**, we distinguish *C. macrotus* by the dorsal pattern (chevrons/bands versus irregular dots/dots in chevrons), the ventral scale rows (87–93 versus 97–121), the total lamellae on one hand (39–40 versus 25–38), the relative length of digits on one hindlimb (30.2–31.2 versus 17.6–22.3), the relative forelimb length (22.4–25.0 versus 14.3–18.1), the relative head length (18.2–20.5 versus 15.1–17.7), the relative postmental width (3.00 versus 2.62–2.97), the relative prefrontal width (4.87–5.55 versus 4.30–4.72), the relative largest supraocular width (2.96–4.03 versus 2.03–2.61), the relative longest finger length (6.43–6.67 versus 3.45–3.75), the relative frontal width (57.6–66.1 versus 78.1–81.6), the relative distance between the eye and naris (5.48–5.60 versus 4.57–5.03), the relative angled subocular width (2.77–2.83 versus 1.93–2.32), and the relative nasal width (2.08–2.33 versus 1.40–1.84). From *C. crusculus*, we distinguish *C. macrotus* by the dorsal pattern (chevrons/bands versus absent/flecks in series/dots in chevrons), the dots arranged in bars in the lateral areas (present versus absent), the ventral scale rows (87–93 versus 98–114), the relative length of digits on one hindlimb (30.2–31.2 versus 18.7–24.7), the relative eye length (3.79–5.17 versus 2.93–3.61), the relative forelimb length (22.4–25.0 versus 12.8–20.7), the relative prefrontal width (4.87–5.55 versus 3.93–4.67), the relative largest supraocular width (2.96–4.03 versus 1.97–2.65), the relative longest finger length (6.43–6.67 versus 2.94–4.10), the relative frontal width (57.6–66.1 versus 82.6–91.1), the relative distance between the eye and naris (5.48–5.60 versus 4.31–4.86), the relative angled subocular width (2.77–2.83 versus 2.03–2.43), and the relative nasal width (2.08–2.33 versus 1.27–1.60). From *C. duquesneyi*, we distinguish *C. macrotus* by the longitudinal paramedian lines (present versus absent), the dots arranged in bars in the lateral areas (present versus absent), the midbody scale rows (41–45 versus 48), the total lamellae on one hand (39–40 versus 64), the relative ear width (1.75–2.08 versus 2.45), and the relative rostral height (1.61–1.95 versus 2.14). From *C. hesperius* **sp. nov.**, we distinguish *C. macrotus* by the dorsal pattern (chevrons/bands versus dots in chevrons), the dots arranged in bars in the lateral areas (present versus absent), the ventral scale rows (87–93 versus 111–114), the total lamellae on one hand (39–40 versus 29–34), the relative length of digits on one hindlimb (30.2–31.2 versus 21.7–26.2), the relative eye length (3.79–5.17 versus 3.61–3.74), the relative forelimb length (22.4–25.0 versus 18.6–21.3), the relative ear width (1.75–2.08 versus 1.52–1.59), the relative head length (18.2–20.5 versus 15.7–17.7), the relative largest supraocular width (2.96–4.03 versus 1.91–2.22), the relative longest finger length (6.43–6.67 versus 3.50–4.04), the relative distance between the ear and eye (7.58–8.02 versus 6.74–7.53), the relative frontal width (57.6–66.1 versus 80.5–86.1), the relative distance between the eye and naris (5.48–5.60 versus 4.70–5.28), the relative angled subocular width (2.77–2.83 versus 2.01–2.48), and the relative nasal width (2.08–2.33 versus 1.52–1.78). From *C. hewardi*, we distinguish *C. macrotus* by the adult SVL (60.0–86.1 versus 129–171), the ventral scale rows (87–93 versus 113–137), the total lamellae on one hand (39–40 versus 50–61), the total strigae on ten scales (64–115 versus 164–315), the relative prefrontal width (4.87–5.55 versus 4.18–4.80), the relative longest finger length (6.43–6.67 versus 5.03–5.66), the relative angled subocular width (2.77–2.83 versus 1.63–2.23), and the relative nasal width (2.08–2.33 versus 1.56–1.88). From *C. jamesbondi* **sp. nov.**, we distinguish *C. macrotus* by the dorsal pattern (chevrons/bands versus absent/irregular dots/dots in chevrons), the total lamellae on one hand (39–40 versus 30–36), the relative length of digits on one hindlimb (30.2–31.2 versus 19.8–26.3), the relative forelimb length (22.4–25.0 versus 14.4–19.9), the relative postmental width (3.00 versus 2.61–2.92), the relative largest supraocular width (2.96–4.03 versus 2.16–2.79), the relative longest finger length (6.43–6.67 versus 3.66–4.33), the relative frontal width (57.6–66.1 versus 70.5–77.6), the relative angled subocular width (2.77–2.83 versus 2.09–2.76), and the relative nasal width (2.08–2.33 versus 1.42–1.75). From *C. macrolepis*, we distinguish *C. macrotus* by the dorsal pattern (chevrons/bands versus bicolored), the longitudinal paramedian lines (present versus absent), the dots arranged in bars in the lateral areas (present versus absent), the adult SVL (60.0–86.1 versus 254–316), the ventral scale rows (87–93 versus 112–116), the midbody scale rows (41–45 versus 46–48), the total lamellae on one hand (39–40 versus 52–54), the total strigae on ten scales (64–115 versus 398), the relative length of digits on one hindlimb (30.2–31.2 versus 27.5–28.0), the relative distance between angled subocular and mouth (0.640–0.983 versus 1.39–1.66), the relative eye length (3.79–5.17 versus

3.63–3.70), the relative forelimb length (22.4–25.0 versus 26.1–26.7), the relative ear width (1.75–2.08 versus 0.760–1.43), and the relative longest finger length (6.43–6.67 versus 5.47–5.51). From *C. microblepharis*, we distinguish *C. macrotus* by the longitudinal paramedian lines (present versus absent), the dots arranged in bars in the lateral areas (present versus absent), the adult SVL (60.0–86.1 versus 96.4), the ventral scale rows (87–93 versus 109), the total lamellae on one hand (39–40 versus 30), the relative length of digits on one hindlimb (30.2–31.2 versus 16.6), the relative eye length (3.79–5.17 versus 1.83), the relative forelimb length (22.4–25.0 versus 14.2), the relative ear width (1.75–2.08 versus 0.446), the relative longest finger length (6.43–6.67 versus 3.11), the relative nasal height (1.15–1.62 versus 0.726), and the relative nasal width (2.08–2.33 versus 1.11). From *C. molesworthi*, we distinguish *C. macrotus* by the dorsal pattern (chevrons/bands versus dots in chevrons), the ventral scale rows (87–93 versus 102–125), the total strigae on ten scales (64–115 versus 138–159), the relative length of digits on one hindlimb (30.2–31.2 versus 22.4–29.4), the relative eye length (3.79–5.17 versus 3.28–3.70), the relative ear width (1.75–2.08 versus 1.37–1.50), the relative largest supraocular width (2.96–4.03 versus 1.69–2.80), the relative longest finger length (6.43–6.67 versus 4.28–5.19), the relative frontal width (57.6–66.1 versus 75.9–95.5), the relative angled subocular height (1.00–1.07 versus 1.11), the relative angled subocular width (2.77–2.83 versus 2.09–2.48), and the relative nasal width (2.08–2.33 versus 1.55–1.72). From *C. occiduus*, we distinguish *C. macrotus* by the dorsal pattern (chevrons/bands versus absent), the longitudinal paramedian lines (present versus absent), the dots arranged in bars in the lateral areas (present versus absent), the adult SVL (60.0–86.1 versus 269–367), the ventral scale rows (87–93 versus 109–134), the midbody scale rows (41–45 versus 46–56), the total lamellae on one hand (39–40 versus 50–66), the total strigae on ten scales (64–115 versus 374), the relative length of digits on one hindlimb (30.2–31.2 versus 24.4–29.7), the relative distance between angled subocular and mouth (0.640–0.983 versus 1.26–1.27), the relative eye length (3.79–5.17 versus 2.87–3.33), the relative ear width (1.75–2.08 versus 0.948–1.39), the relative longest finger length (6.43–6.67 versus 4.77–5.46), and the relative distance between the ear and eye (7.58–8.02 versus 8.98–10.9). From *C. oligolepis* **sp. nov.**, we distinguish *C. macrotus* by the dorsal pattern (chevrons/bands versus dots in chevrons), the dots arranged in bars in the lateral areas (present versus absent), the ventral scale rows (87–93 versus 98), the midbody scale rows (41–45 versus 35), and the total lamellae on one hand (39–40 versus 30). From *C. striatus*, we distinguish *C. macrotus* by the dots arranged in bars in the lateral areas (present versus absent), the adult SVL (60.0–86.1 versus 145), the ventral scale rows (87–93 versus 101–109), the total lamellae on one hand (39–40 versus 59–66), and the total strigae on ten scales (64–115 versus 279).

Description of holotype. USNM 286917. An adult; SVL 60.0 mm; tail nearly cylindrical, broken, 8.05 mm (13.4% SVL); axilla-to-groin distance 32.0 mm (53.3% SVL); forelimb length 13.4 mm (22.3% SVL); hindlimb length 16.9 mm (28.2% SVL); head length 12.3 mm (20.5% SVL); head width 8.31 mm (13.9% SVL); head width 67.6% head length; diameter of orbit 3.10 mm (5.17% SVL); horizontal diameter of ear opening 1.25 mm (2.08% SVL); vertical diameter of ear opening 1.28 mm (2.13% SVL); length of all toes on one foot 18.1 mm (30.2% SVL); shortest distance between angled subocular and lip 0.59 mm (0.983% SVL); shortest distance between the ocular and auricular openings 4.94 mm (8.23% SVL); longest finger length 4.00 mm (6.67% SVL); largest supraocular width 2.42 mm (4.03% SVL); cloacal width 4.68 mm (7.80% SVL); prefrontal width 3.33 mm (5.55% SVL); frontal width 57.6% frontal length; nasal height 0.97 mm (1.62% SVL); angled subocular height 0.60 mm (1.00% SVL); shortest distance between the eye and naris 3.36 mm (5.60% SVL); canthal iii width 1.11 mm (1.85% SVL); angled subocular width 1.66 mm (2.77% SVL); nasal width 1.25 mm (2.08% SVL); rostral 1.76X as wide as high, visible from above, not in contact with nasals, in contact with 1st supralabial and anterior internasal (left)/(right); anterior internasals are narrower than posterior ones; frontonasals and prefrontal fused into a single large plate with a concave posterior margin, much wider than long, bordered by posterior internasals, 1st loreals, 1st and 2nd median oculars, and the frontal; frontal much longer than wide; a pair of frontoparietals, separated by the posterior prolongation of the frontal and the interparietal plate; interparietal plate smaller than parietals and separating them, posteriorly touching the interoccipital, which is much wider than long; parietal separated from supraoculars by 1st and 2nd temporals and frontoparietal (left)/1st temporals and frontoparietal (right); nasal single; nostril above suture between 1st and 2nd supralabials (left)/(right); 1 postnasal (left)/(right); 2 loreals (left)/(right); 1st loreal higher than wide (left)/(right), in contact with postnasal, posterior internasal, prefrontal/frontonasal complex, 1st median ocular, canthal iii, 2nd loreal, and 3rd and 4th supralabials (left)/(right); 2nd loreal shorter than 1st, approximately as high as wide (left)/(right), excluded from contact with supraocular by canthal iii (left)/(right); 2nd loreal posteriorly bordering the lower preocular (left)/(right); canthal iii wider than high (left)/(right), contacting 1st median ocular,

anterior supraciliary, lower preocular, and 1st and 2nd loreals (left)/(right); 9 (left)/10 (right) median oculars, 1st and 2nd contacting the prefrontal (left)/(right); 1 upper preocular (left)/(right); an irregular anterior supraciliary (left)/(right); 6 lateral oculars (left)/(right); 5 temporals (left)/(right); 3 (left)/2 (right) suboculars; posterior subocular large and elongate (left)/(right); anterior subocular small (left)/(right); 10 supralabials (left)/(right), 6 to level below center of eye (left)/(right); 10 infralabials (left)/(right), 6 (left)/6–7(right) to level below center of eye; mental small, followed by a single, larger postmental; 4 pairs of enlarged chin shields; 1st pair in contact with one another anteriorly, posteriorly separated by one scale; 2nd–4th pairs separated by 1–3 scales; 89 transverse rows of dorsal scales from interoccipital to base of tail; 93 transverse rows of ventral scales from mental to vent; 41 scales around midbody; 5 digits; finger lengths 3>4>2>5>1; 10 lamellae under longest finger (left)/(right); 39 total lamellae on one hand; toe lengths 4>3>5>2>1; 17 (left)/15 (right) lamellae under longest toe; striate, angled to give impression of a faint median keel dorsal body and caudal scales; smooth ventral scales; 64 total strigae counted on ten scales.

FIGURE 26. (A–F) *Celestus macrotus* (USNM 286917, holotype), SVL 60.0 mm.

FIGURE 27. *Celestus macrotus* (ANSP 38506, SBH 269931), SVL 42.1 mm (juvenile), in life. From southeast of Pic La Selle, Sud-Est Department, Haiti. Photo by SBH.

Color (in alcohol): dorsal surface of head dark brown, patternless; lateral surfaces of head grading from dark brown to gray with darker brown eye masks; dorsal surfaces of the body are dark brown with darker brown longitudinal paramedian lines and irregular spotting; dorsal surface of tail the same as the body; lateral areas grade from dark brown to gray with darker spots in rows; dorsal surfaces of the limbs are dark brown with gray mottling; lateral and ventral areas of the limbs fade to gray with darker brown mottling; ventral surfaces of the head, body, and tail are gray with brown mottling over the entire surface.

Variation. The examined material resembles the pattern of the holotype with darker spots ranging from occurring irregularly down the extent of the dorsum in a heavy pattern (ANSP 38505) to being arranged in chevrons (ANSP 38506). Unlike the holotype, both ANSP 38505 and ANSP 38506 have head scale borders with darker outlines whereas ANSP 38505 also has irregular darker markings on its head. All specimens exhibit longitudinal paramedian lines. Measurements and other morphological data for the holotype and other examined material are presented in Table 1.

Distribution. *Celestus macrotus* is found in the Massif de la Selle of Haiti and the Sierra de Bahoruco of the Dominican Republic at elevations of 1930–2320 m (Fig. 11).

Ecology and conservation. The holotype was collected under rocks and logs in mature stands of pine forest, *Pinus occidentalis*, alongside *Wetmorena surda* (Thomas & Hedges 1989). The other Haitian specimens, south of Pic La Selle, were collected in the same habitat, alongside *W. surda* and *Panolopus aporus*. In both localities, *Celestus macrotus* was considerably rarer than other species.

The IUCN Redlist (IUCN 2023) considers the conservation status of *Celestus macrotus* to be Endangered B1ab(i,iii) "due to its limited distribution (with an extent of occurrence of about 128 km^2), occurrence in a single location, and ongoing threats from agriculture expansion, wildfires due to anthropogenic causes and wood extraction." Studies are needed to determine the health of remaining populations and threats to the survival of the species.

Reproduction. No data on reproduction are available for this species.

Etymology. From the Greek, *macro*, long (large in common usage), and *otos*, ear, in reference to the large external auditory meatus.

Remarks. Thomas & Hedges (1989) discussed the scales surrounding the eyes of diploglossid lizards, particularly as that applies to *Celestus macrotus*. However, this scale terminology was not used in later works (Savage & Lips 1993; Savage *et al.* 2008). Thomas & Hedges (1989) also noted that, with preliminary protein electrophoretic data, *Celestus macrotus* was considerably divergent, falling outside of a cluster containing *Celestus barbouri*, *Panolopus costatus*, *Celestus crusculus*, *Panolopus curtissi*, *Caribicus darlingtoni*, and *Comptus stenurus*.

Celestus macrotus is included in our genetic dataset and has significant support in both Bayesian and ML likelihood analyses at the crown node of the species and the stem node that places it as the closest relative of a group containing all other species of *Celestus*. Based on our timetree (Fig. 4), *C. macrotus* diverged from its closest relative 5.58 Ma, consistent with typical species of vertebrates (> 0.7 Ma; Hedges *et al.* 2015). *Celestus macrotus* was recognized as a distinct species in our ASAP analysis.

Celestus microblepharis (Underwood 1959)

Small-eyed Forest Lizard
(Fig. 28)

Diploglossus microblepharis Underwood, 1959:2. Holotype: MCZ R-55764, collected by R. P. Bengry and G. R. Proctor at Boscobel, Saint Mary Parish, Jamaica, on 8 July 1953 (18.40, -76.97).
Celestus microblepharis—Schwartz & Henderson, 1991:377.
Celestus microblepharis—Hedges *et al.*, 2019:17
Celestus microblepharis—Schools & Hedges, 2021:220.
Celestus microblepharis—Landestoy *et al.*, 2022:204.

Material examined (n=1). JAMAICA. Saint Mary. MCZ R-55764, R. P. Bengry and G. R. Proctor, Boscobel, 8 July 1953.

Diagnosis. *Celestus microblepharis* has (1) a dorsal pattern of chevrons, (2) head markings absent, (3) markings in the longitudinal paramedian area absent, (4) dots arranged in bars in the lateral band absent, (5) an adult SVL of 96.4 mm, (6) ventral scale rows, 109, (7) midbody scale rows, 43, (8) total lamellae on one hand, 30, (9) total strigae on ten scales, 165, (10) relative length of all digits on one hindlimb, 16.6 %, (11) relative distance between the angled subocular and mouth, 0.820 %, (12) relative eye length, 1.83 %, (13) relative forelimb length, 14.2 %, (14) relative ear width, 0.446 %, (15) relative rostral height, 1.71 %, (16) relative head length, 14.7 %, (17) relative mental width, 1.44 %, (18) relative postmental width, 2.47 %, (19) relative cloacal width, 8.02 %, (20) relative prefrontal width, 4.37 %, (21) relative largest supraocular width, 2.06 %, (22) relative longest finger length, 3.11 %, (23) relative distance between the ear and eye, 7.05 %, (24) relative head width, 75.4 %, (25) relative frontal width, unavailable, (26) relative nasal height, 0.726 %, (27) relative angled subocular height, 0.778 %, (28) relative distance between the eye and naris, 4.79 %, (29) relative canthal iii length, 1.74 %, (30) relative angled subocular width, 2.90 %, and (31) relative nasal length, 1.11 %. No genetic data are available for estimating the species stem time or crown time.

Celestus microblepharis has a smaller relative length of all digits on one hindlimb (16.6), a smaller relative eye length (1.83), a smaller relative forelimb length (14.2), a smaller relative auricular length (0.446), relative head length (14.7), relative postmental width (2.47), relative longest finger length (3.11), relative nasal height (0.726), and relative angled subocular height (0.778) than most other species of the genus. This species also has a larger relative angled subocular width (2.90) than most other species of the genus.

From *Celestus barbouri*, we distinguish *C. microblepharis* by the adult SVL (96.4 versus 78.4–93.6), the ventral scale rows (109 versus 118–151), the midbody scale rows (43 versus 47–56), the total lamellae on one hand (30 versus 36–49), the total strigae on ten scales (165 versus 105–136), the relative length of digits on one hindlimb (16.6 versus 18.2–23.5), the relative distance between angled subocular and mouth (0.820 versus 0.437–0.556), the relative eye length (1.83 versus 2.87–3.63), the relative forelimb length (14.2 versus 15.4–19.0), the relative ear width (0.446 versus 0.810–1.86), the relative rostral height (1.71 versus 1.41–1.66), the relative mental width (1.44 versus 1.51–1.85), the relative postmental width (2.47 versus 2.51–3.29), the relative prefrontal width (4.37 versus 3.97–4.33), the relative nasal height (0.726 versus 0.930–1.12), the relative angled subocular width (2.90 versus 1.97–2.52), and the relative nasal width (1.11 versus 1.38–1.65). From *C. capitulatus* **sp. nov.**, we distinguish *C. microblepharis* by the dorsal pattern (chevrons versus irregular dots/dots in chevrons), the adult SVL (96.4 versus

62.1–81.8), the relative length of digits on one hindlimb (16.6 versus 17.6–22.3), the relative eye length (1.83 versus 2.75–3.80), the relative forelimb length (14.2 versus 14.3–18.1), the relative ear width (0.446 versus 0.671–2.04), the relative head length (14.7 versus 15.1–17.7), the relative postmental width (2.47 versus 2.62–2.97), the relative longest finger length (3.11 versus 3.45–3.75), the relative nasal height (0.726 versus 0.953–1.42), the relative angled subocular width (2.90 versus 1.93–2.32), and the relative nasal width (1.11 versus 1.40–1.84). From *C. crusculus*, we distinguish *C. microblepharis* by the dorsal pattern (chevrons versus absent/flecks in series/dots in chevrons), the longitudinal paramedian lines (absent versus present), the adult SVL (96.4 versus 59.6–77.6), the relative length of digits on one hindlimb (16.6 versus 18.7–24.7), the relative eye length (1.83 versus 2.93–3.61), the relative ear width (0.446 versus 0.716–2.00), the relative head length (14.7 versus 15.5–20.3), the relative postmental width (2.47 versus 2.73–3.37), the relative nasal height (0.726 versus 0.925–1.37), the relative angled subocular height (0.778 versus 0.953–1.21), the relative angled subocular width (2.90 versus 2.03–2.43), and the relative nasal width (1.11 versus 1.27–1.60). From *C. duquesneyi*, we distinguish *C. microblepharis* by the dorsal pattern (chevrons versus bands), the total lamellae on one hand (30 versus 64), the relative length of digits on one hindlimb (16.6 versus 31.4), the relative eye length (1.83 versus 4.36), the relative forelimb length (14.2 versus 24.4), the relative ear width (0.446 versus 2.45), the relative mental width (1.44 versus 2.35), the relative longest finger length (3.11 versus 6.52), the relative angled subocular height (0.778 versus 1.61), and the relative nasal width (1.11 versus 2.01). From *C. hesperius* **sp. nov.**, we distinguish *C. microblepharis* by the dorsal pattern (chevrons versus dots in chevrons), the adult SVL (96.4 versus 54.0–62.3), the ventral scale rows (109 versus 111–114), the relative eye length (1.83 versus 3.61–3.74), and the relative ear width (0.446 versus 1.52–1.59). From *C. hewardi*, we distinguish *C. microblepharis* by the dorsal pattern (chevrons versus mottled/bands), the adult SVL (96.4 versus 129–171), the ventral scale rows (109 versus 113–137), the total lamellae on one hand (30 versus 50–61), the relative length of digits on one hindlimb (16.6 versus 24.1–30.6), the relative eye length (1.83 versus 2.98–4.05), the relative forelimb length (14.2 versus 22.2–24.6), the relative ear width (0.446 versus 1.40–1.82), the relative head length (14.7 versus 16.8–21.5), the relative mental width (1.44 versus 1.75–1.81), the relative postmental width (2.47 versus 2.84–3.44), the relative cloacal width (8.02 versus 8.81–9.89), the relative largest supraocular width (2.06 versus 2.43–2.96), the relative longest finger length (3.11 versus 5.03–5.66), the relative nasal height (0.726 versus 1.21–1.24), the relative angled subocular height (0.778 versus 0.918–1.30), the relative distance between the eye and naris (4.79 versus 5.00–5.60), the relative angled subocular width (2.9 versus 1.63–2.23), and the relative nasal width (1.11 versus 1.56–1.88). From *C. jamesbondi* **sp. nov.**, we distinguish *C. microblepharis* by the dorsal pattern (chevrons versus absent/irregular dots/dots in chevrons), the adult SVL (96.4 versus 54.7–72.0), the relative length of digits on one hindlimb (16.6 versus 19.8–26.3), the relative eye length (1.83 versus 2.94–4.06), the relative forelimb length (14.2 versus 14.4–19.9), the relative ear width (0.446 versus 0.917–2.18), the relative head length (14.7 versus 15.1–20.4), the relative mental width (1.44 versus 1.59–2.01), the relative postmental width (2.47 versus 2.61–2.92), the relative largest supraocular width (2.06 versus 2.16–2.79), the relative longest finger length (3.11 versus 3.66–4.33), the relative head width (75.4 versus 76.0–80.8), the relative nasal height (0.726 versus 1.12–1.21), the relative angled subocular height (0.778 versus 0.893–1.18), the relative width of canthal iii (1.74 versus 1.75–2.16), the relative angled subocular width (2.90 versus 2.09–2.76), and the relative nasal width (1.11 versus 1.42–1.75). From *C. macrolepis*, we distinguish *C. microblepharis* by the dorsal pattern (chevrons versus bicolored), the adult SVL (96.4 versus 254–316), the total lamellae on one hand (30 versus 52–54), the total strigae on ten scales (165 versus 398), the relative length of digits on one hindlimb (16.6 versus 27.5–28.0), the relative distance between angled subocular and mouth (0.820 versus 1.39–1.66), the relative eye length (1.83 versus 3.63–3.70), the relative forelimb length (14.2 versus 26.1–26.7), the relative ear width (0.446 versus 0.760–1.43), the relative longest finger length (3.11 versus 5.47–5.51), and the relative nasal height (0.726 versus 1.18). From *C. macrotus*, we distinguish *C. microblepharis* by the longitudinal paramedian lines (absent versus present), the dots arranged in bars in the lateral areas (absent versus present), the adult SVL (96.4 versus 60.0–86.1), the ventral scale rows (109 versus 87–93), the total lamellae on one hand (30 versus 39–40), the relative length of digits on one hindlimb (16.6 versus 30.2–31.2), the relative eye length (1.83 versus 3.79–5.17), the relative forelimb length (14.2 versus 22.4–25.0), the relative ear width (0.446 versus 1.75–2.08), the relative longest finger length (3.11 versus 6.43–6.67), the relative nasal height (0.726 versus 1.15–1.62), and the relative nasal width (1.11 versus 2.08–2.33). From *C. molesworthi*, we distinguish *C. microblepharis* by the dorsal pattern (chevrons versus dots in chevrons), the total lamellae on one hand (30 versus 32–44), the total strigae on ten scales (165 versus 138–159), the relative length of digits on one hindlimb (16.6 versus 22.4–29.4), the relative eye length (1.83 versus 3.28–3.70), the relative forelimb length (14.2 versus 17.5–

24.2), the relative ear width (0.446 versus 1.37–1.50), the relative rostral height (1.71 versus 1.72–1.81), the relative head length (14.7 versus 17.2–20.0), and the relative nasal height (0.726 versus 1.17–1.26). From *C. occiduus*, we distinguish *C. microblepharis* by the dorsal pattern (chevrons versus absent), the adult SVL (96.4 versus 269–367), the midbody scale rows (43 versus 46–56), the total lamellae on one hand (30 versus 50–66), the total strigae on ten scales (165 versus 374), the relative distance between angled subocular and mouth (0.820 versus 1.26–1.27), the relative eye length (1.83 versus 2.87–3.33), the relative forelimb length (14.2 versus 23.5–23.9), the relative ear width (0.446 versus 0.948–1.39), the relative nasal height (0.726 versus 1.16), and the relative angled subocular height (0.778 versus 1.30). From *C. oligolepis* **sp. nov.**, we distinguish *C. microblepharis* by the dorsal pattern (chevrons versus dots in chevrons), the head markings (absent versus present), the longitudinal paramedian lines (absent versus present), the ventral scale rows (109 versus 98), the midbody scale rows (43 versus 35). From *C. striatus*, we distinguish *C. microblepharis* the total lamellae on one hand (30 versus 59–66), the total strigae on ten scales (165 versus 279), the relative length of digits on one hindlimb (16.6 versus 37.8), the relative eye length (1.83 versus 3.85), the relative forelimb length (14.2 versus 26.1), the relative ear width (0.446 versus 1.30), the relative longest finger length (3.11 versus 7.48).

Description of holotype. MCZ R-55764. An adult; SVL 96.4 mm; tail nearly cylindrical, broken in life near tip, regenerated, 87.3 mm (90.6% SVL); axilla-to-groin distance 58.2 mm (60.4% SVL); forelimb length 13.7 mm (14.2% SVL); hindlimb length 21.3 mm (22.1% SVL); head length 14.2 mm (14.7% SVL); head width 10.7 mm (11.1% SVL); head width 75.4% head length; diameter of orbit 1.76 mm (1.83% SVL); horizontal diameter of ear opening 0.43 mm (0.446% SVL); vertical diameter of ear opening 0.48 mm (0.498% SVL); length of all toes on one foot 16.0 mm (16.6% SVL); shortest distance between angled subocular and lip 0.79 mm (0.820% SVL); shortest distance between the ocular and auricular openings 6.80 mm (7.05% SVL); longest finger length 3.00 mm (3.11% SVL); largest supraocular width 1.99 mm (2.06% SVL); cloacal width 7.73 mm (8.02% SVL); postmental width 2.38 mm (2.47% SVL); mental width 1.39 mm (1.44% SVL); prefrontal width 4.21 mm (4.37% SVL); nasal height 0.70 mm (0.726% SVL); angled subocular height 0.75 mm (0.778% SVL); shortest distance between the eye and naris 4.62 mm (4.79% SVL); canthal iii width 1.68 mm (1.74% SVL); angled subocular width 2.80 mm (2.90% SVL); nasal width 1.07 mm (1.11% SVL); rostral 1.71X as wide as high, visible from above, not in contact with nasals, in contact with 1st supralabial and anterior internasal (left)/(right); anterior internasals are narrower than posterior ones (left divided); frontonasals and prefrontal fused into a single large plate with an irregular posterior margin, much wider than long, bordered by posterior internasals, 1st and 2nd loreals, 1st median oculars, and the frontal; frontal and frontoparietals fused into a single plate, wider than long; interparietal plate slightly smaller than parietals and separating them, posteriorly touching the interoccipital, which is wider than long; parietal separated from supraoculars by 1st temporals and frontoparietal/frontal plate (left)/(right); nasal single; nostril above suture between 1st and 2nd supralabials (left)/(right); 1 postnasal (left)/(right); 2 loreals (left)/(right); 1st loreal approximately as high as wide (left)/(right), in contact with postnasal, posterior internasal, prefrontal/frontonasal complex, 2nd loreal, and 3rd–4th supralabials (left)/postnasal, posterior internasal, prefrontal/frontonasal complex, 2nd loreal, and 3rd–5th supralabials (right); 2nd loreal shorter than 1st, approximately as high as wide (left)/(right), in contact with supraocular (left)/(right); final loreal posteriorly bordering the lower preocular (left)/(right); 7 (left)/6 (right) median oculars, 1st contacting the prefrontal (left)/(right); 0 upper preoculars (left)/(right); an irregular anterior supraciliary (left)/(right); 4 lateral oculars (left)/(right); 4 temporals (left)/(right); 1 subocular (left)/(right); posterior subocular large and elongate (left)/(right); 8 supralabials (left)/(right), 5 to level below center of eye (left)/(right); 8 infralabials (left)/(right), 5 to level below center of eye (left)/(right); mental small, followed by a single, slightly larger postmental; 4 pairs of enlarged chin shields; 1st pair in contact with one another anteriorly, posteriorly separated by one scale; 2nd–4th pairs separated by 1–5 scales; 105 transverse rows of dorsal scales from interoccipital to base of tail; 109 transverse rows of ventral scales from mental to vent; 43 scales around midbody; 5 digits; finger lengths 3>4>2>5>1; 7 (left)/8 (right) lamellae under longest finger; 30 total lamellae on one hand; toe lengths 4>3>5>2>1; 11 (left)/12 (right) lamellae under longest toe; striate with a median keel dorsal body and caudal scales; smooth ventral scales; 165 total strigae counted on ten scales.

Color (in alcohol): dorsal surface of head yellow-tan, patternless; lateral surfaces of head grading from yellow-tan to pale yellow ventrally with darker faded eye masks; dorsal surfaces of the body are yellow-tan with remains of a faded dotted chevron pattern; dorsal surface of tail the same yellow-tan to pale yellow as noted on the head, remains of a faded dotted chevron pattern appear as very pale brown; lateral areas are pale yellow with no pattern to indicate the presence of a lateral band; dorsal surfaces of the limbs are pale yellow with some pale brown spots;

lateral and ventral areas of the limbs fade to pale yellow-tan; ventral surfaces of the head, body, and tail are yellow-tan, patternless.

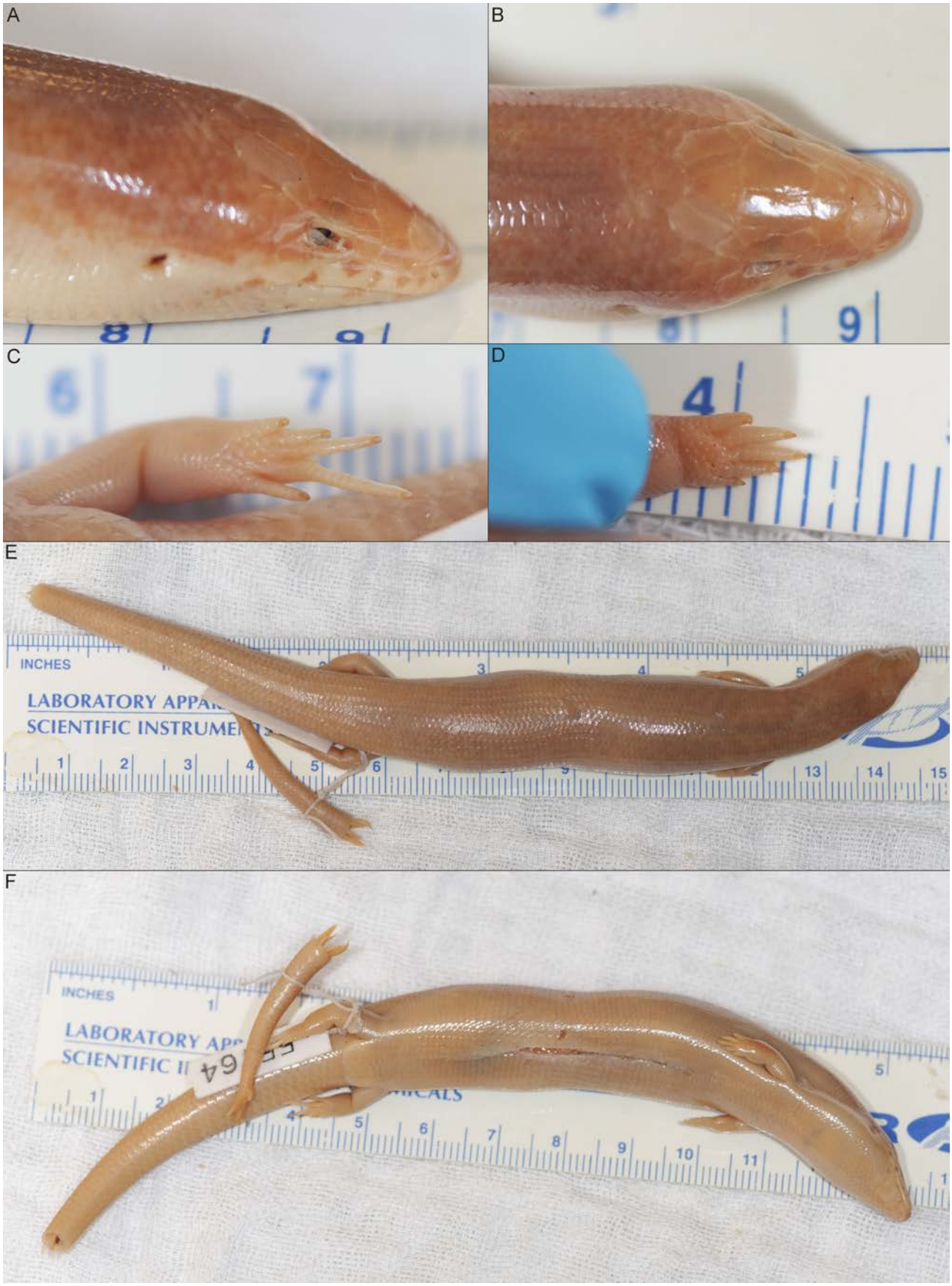

FIGURE 28. (A–F) *Celestus microblepharis* (MCZ R-55764, holotype), SVL 96.4 mm.

Variation. No other specimens are known. Measurements and other morphological data for the holotype are presented in Table 1.

Distribution. *Celestus microblepharis* is known only from the holotype, collected at Boscobel, on the north-central coast of Jamaica where it was collected at 20 m elevation (Fig. 11).

Ecology and conservation. The holotype of this species was collected under rotting coconut husks with *Celestus jamesbondi* **sp. nov.** near a coastal area that backed up to limestone hills covered with dry scrub forest.

The IUCN Redlist (IUCN 2023) considers the conservation status of *Celestus microblepharis* to be Critically Endangered B1ab(iii,v) because "the species' has a tiny known extent of occurrence and has not been found within or beyond the type locality despite extensive surveys over the last 40 years; it occurs (or occurred) at one locality, within which the extent and quality of its habitat (although poorly-known) is assumed to be declining based on inference given the extent of conversion of remnant forest, scrub, and coconut plantations for tourism and residential development." Studies are needed to determine the health and extent of remaining populations and threats to the survival of the species. Captive-breeding programs should be undertaken, because eradication of introduced mammalian predators is not yet possible on Jamaica.

Reproduction. No data on reproduction are available for this species.

Etymology. The species name is an adjective from the prefix *micro-* (small), the Greek word *blepharon* (eyelid), and the prefix *-aris* (pertaining to), referring to the small eyes of this species.

Remarks. The original description of *Celestus microblepharis* placed it in a group with *Diploglossus delasagra* and *Diploglossus pleii*, presumably based on morphological similarities (Underwood 1959). This grouping was retained in later works (Schwartz 1971a) but is contradicted by our placement in *Celestus*. *Celestus microblepharis* was not included in our genetic dataset. Future studies using genetic or genomic data are needed to determine the relationships of *C. microblepharis* within *Celestus.*

***Celestus molesworthi* Grant, 1940b**

Eastern Jamaican Forest Lizard
(Fig. 29–30)

Celestus crusculus molesworthi Grant, 1940b:157. Holotype: MCZ R-45184, collected by Chapman Grant near Buff Bay, Portland Parish, Jamaica, on 2 May 1937 (18.233, -76.658).
Celestus crusculus molesworthi—Grant, 1940b:104.
Diploglossus crusculus molesworthi—Greer, 1967:96.
Celestus molesworthi—Hedges *et al.*, 2019:17.
Celestus molesworthi—Schools & Hedges, 2021:220.
Celestus molesworthi—Landestoy *et al.*, 2022:205.

Material examined (n=11). JAMAICA. Kingston. MCZ R-45184, Chapman Grant, 2 May 1937. **Portland.** BMNH 1970.1741, Garth Underwood, Priestman's River; MCZ R-45185, Chapman Grant, Buff Bay, 2 May 1937; USNM 108158–9, 1 mi S of Buff Bay, 2 May 1939. **Saint Andrew.** USNM 117672, Clydesdale, 6 July 1941. **Saint Thomas.** BMNH 1970.1747, W G. Lynn, Trinityville, Half a Bottle Trail; BMNH 1965.194, Morant Point; One of six untagged specimens in one jar: BMNH 1970.1731–6, BMNH 1970.1737, Garth Underwood, Morant Point; USNM 326600, 4.8 mi N of Hordley, 24 July 1981.

Diagnosis. *Celestus molesworthi* has (1) a dorsal pattern of dots in chevrons, (2) head markings absent/present, (3) markings in the longitudinal paramedian area absent/present, (4) dots arranged in bars in the lateral band absent/present, (5) an adult SVL of 78.1–103 mm, (6) ventral scale rows, 102–125, (7) midbody scale rows, 41–49, (8) total lamellae on one hand, 32–44, (9) total strigae on ten scales, 138–159, (10) relative length of all digits on one hindlimb, 22.4–29.4 %, (11) relative distance between the angled subocular and mouth, 0.653–0.845 %, (12) relative eye length, 3.28–3.70 %, (13) relative forelimb length, 17.5–24.2 %, (14) relative ear width, 1.37–1.50 %, (15) relative rostral height, 1.72–1.81 %, (16) relative head length, 17.2–20.0 %, (17) relative mental width, 1.81–2.00 %, (18) relative postmental width, 2.97–3.08 %, (19) relative cloacal width, 8.73–9.35 %, (20) relative prefrontal width, 4.44–4.90 %, (21) relative largest supraocular width, 1.69–2.80 %, (22) relative longest finger length, 4.28–5.19 %, (23) relative distance between the ear and eye, 7.97–8.83 %, (24) relative head width, 69.1–76.5 %, (25) relative frontal width, 75.9–95.5 %, (26) relative nasal height, 1.17–1.26 %, (27) relative angled subocular height,

1.11 %, (28) relative distance between the eye and naris, 5.32–5.50 %, (29) relative canthal iii length, 1.99–2.09 %, (30) relative angled subocular width, 2.09–2.48 %, and (31) relative nasal length, 1.55–1.72 %. The species stem time is 4.17 Ma and the species crown time is 0.39 Ma (Fig. 4).

We distinguish *Celestus molesworthi* from all other species of *Celestus* based on a complex of traits. From *Celestus barbouri*, we distinguish *C. molesworthi* by the dorsal pattern (dots in chevrons versus chevrons), the total strigae on ten scales (138–159 versus 105–136), the relative distance between angled subocular and mouth (0.653–0.845 versus 0.437–0.556), the relative rostral height (1.72–1.81 versus 1.41–1.66), the relative head length (17.2–20.0 versus 14.6–16.6), the relative cloacal width (8.73–9.35 versus 7.64–8.26), the relative prefrontal width (4.44–4.90 versus 3.97–4.33), the relative longest finger length (4.28–5.19 versus 2.92–3.81), the relative distance between the ear and eye (7.97–8.83 versus 6.23–7.15), the relative nasal height (1.17–1.26 versus 0.930–1.12), the relative distance between the eye and naris (5.32–5.50 versus 4.68–4.83), and the relative width of canthal iii (1.99–2.09 versus 1.54–1.93). From *C. capitulatus* **sp. nov.**, we distinguish *C.* molesworthi by the relative length of digits on one hindlimb (22.4–29.4 versus 17.6–22.3), the relative cloacal width (8.73–9.35 versus 7.84–8.67), the relative longest finger length (4.28–5.19 versus 3.45–3.75), the relative distance between the ear and eye (7.97–8.83 versus 6.45–7.84), the relative angled subocular height (1.11 versus 0.586–1.01), the relative distance between the eye and naris (5.32–5.50 versus 4.57–5.03), and the relative width of canthal iii (1.99–2.09 versus 1.61–1.70). From *C. crusculus*, we distinguish *C. molesworthi* by the adult SVL (78.1–103 versus 59.6–77.6), the relative longest finger length (4.28–5.19 versus 2.94–4.10), and the relative distance between the eye and naris (5.32–5.50 versus 4.31–4.86). From *C. duquesneyi*, we distinguish *C. molesworthi* by the dorsal pattern (dots in chevrons versus bands), the adult SVL (78.1–103 versus 62.1), the total lamellae on one hand (32–44 versus 64), the total strigae on ten scales (138–159 versus 130), the relative length of digits on one hindlimb (22.4–29.4 versus 31.4), the relative distance between angled subocular and mouth (0.653–0.845 versus 0.644), the relative eye length (3.28–3.70 versus 4.36), the relative forelimb length (17.5–24.2 versus 24.4), the relative ear width (1.37–1.50 versus 2.45), the relative rostral height (1.72–1.81 versus 2.14), and the relative head length (17.2–20.0 versus 21.6). From *C. hesperius* **sp. nov.**, we distinguish *C. molesworthi* by the adult SVL (78.1–103 versus 54.0–62.3), the total strigae on ten scales (138–159 versus 95–122), the relative distance between angled subocular and mouth (0.653–0.845 versus 0.594–0.648), the relative ear width (1.37–1.50 versus 1.52–1.59), the relative mental width (1.81–2.00 versus 1.51–1.78), the relative postmental width (2.97–3.08 versus 2.87–2.92), the relative cloacal width (8.73–9.35 versus 7.99–8.55), the relative longest finger length (4.28–5.19 versus 3.50–4.04), the relative distance between the ear and eye (7.97–8.83 versus 6.74–7.53), the relative distance between the eye and naris (5.32–5.50 versus 4.70–5.28), and the relative width of canthal iii (1.99–2.09 versus 1.77–1.93). From *C. hewardi*, we distinguish *C. molesworthi* by the dorsal pattern (dots in chevrons versus mottled/bands), the adult SVL (78.1–103 versus 129–171), the total lamellae on one hand (32–44 versus 50–61), the total strigae on ten scales (138–159 versus 164–315), and the relative frontal width (75.9–95.5 versus 57.3–75.3). From *C. jamesbondi* **sp. nov.**, we distinguish *C. molesworthi* by the adult SVL (78.1–103 versus 54.7–72.0), the relative postmental width (2.97–3.08 versus 2.61–2.92), and the relative distance between the ear and eye (7.97–8.83 versus 6.92–7.80). From *C. macrolepis*, we distinguish *C. molesworthi* by the dorsal pattern (dots in chevrons versus bicolored), the adult SVL (78.1–103 versus 254–316), the total lamellae on one hand (32–44 versus 52–54), the total strigae on ten scales (138–159 versus 398), the relative distance between angled subocular and mouth (0.653–0.845 versus 1.39–1.66), the relative forelimb length (17.5–24.2 versus 26.1–26.7), and the relative longest finger length (4.28–5.19 versus 5.47–5.51). From *C. macrotus*, we distinguish *C. molesworthi* by the dorsal pattern (dots in chevrons versus chevrons/bands), the ventral scale rows (102–125 versus 87–93), the total strigae on ten scales (138–159 versus 64–115), the relative length of digits on one hindlimb (22.4–29.4 versus 30.2–31.2), the relative eye length (3.28–3.70 versus 3.79–5.17), the relative ear width (1.37–1.50 versus 1.75–2.08), the relative largest supraocular width (1.69–2.80 versus 2.96–4.03), the relative longest finger length (4.28–5.19 versus 6.43–6.67), the relative frontal width (75.9–95.5 versus 57.6–66.1), the relative angled subocular height (1.11 versus 1.00–1.07), the relative angled subocular width (2.09–2.48 versus 2.77–2.83), and the relative nasal width (1.55–1.72 versus 2.08–2.33). From *C. microblepharis*, we distinguish *C. molesworthi* by the dorsal pattern (dots in chevrons versus chevrons), the total lamellae on one hand (32–44 versus 30), the total strigae on ten scales (138–159 versus 165), the relative length of digits on one hindlimb (22.4–29.4 versus 16.6), the relative eye length (3.28–3.70 versus 1.83), the relative forelimb length (17.5–24.2 versus 14.2), the relative ear width (1.37–1.50 versus 0.446), the relative rostral height (1.72–1.81 versus 1.71), the relative head length (17.2–20.0 versus 14.7), and the relative nasal height (1.17–1.26 versus 0.726). From *C. occiduus*, we distinguish *C. molesworthi* by

the dorsal pattern (dots in chevrons versus absent), the adult SVL (78.1–103 versus 269–367), the total lamellae on one hand (32–44 versus 50–66), the total strigae on ten scales (138–159 versus 374), the relative distance between angled subocular and mouth (0.653–0.845 versus 1.26–1.27), the relative head length (17.2–20.0 versus 20.4–20.6), and the relative distance between the ear and eye (7.97–8.83 versus 8.98–10.9). From *C. oligolepis* **sp. nov.**, we distinguish *C. molesworthi* by the ventral scale rows (102–125 versus 98), the midbody scale rows (41–49 versus 35), and the total lamellae on one hand (32–44 versus 30). From *C. striatus*, we distinguish *C. molesworthi* by the dorsal pattern (dots in chevrons versus absent/chevrons), the adult SVL (78.1–103 versus 145), the total lamellae on one hand (32–44 versus 59–66), the total strigae on ten scales (138–159 versus 279), the relative length of digits on one hindlimb (22.4–29.4 versus 37.8), the relative eye length (3.28–3.70 versus 3.85), the relative forelimb length (17.5–24.2 versus 26.1), the relative ear width (1.37–1.50 versus 1.30), the relative rostral height (1.72–1.81 versus 1.94).

Description of holotype. MCZ R-45184. An adult; SVL 85.6 mm; tail nearly cylindrical, 82.0 mm (95.8% SVL); axilla-to-groin distance 47.5 mm (55.5% SVL); forelimb length 15.0 mm (17.5% SVL); hindlimb length 25.9 mm (30.3% SVL); head length 15.8 mm (18.5% SVL); head width 12.1 mm (14.1% SVL); head width 76.6% head length; diameter of orbit 2.82 mm (3.29% SVL); horizontal diameter of ear opening 1.28 mm (1.50% SVL); vertical diameter of ear opening 1.49 mm (1.74% SVL); length of all toes on one foot 20.3 mm (23.7% SVL); shortest distance between angled subocular and lip 0.87 mm (1.02% SVL); shortest distance between the ocular and auricular openings 6.82 mm (7.97% SVL); longest finger length 3.66 mm (4.28% SVL); largest supraocular width 1.45 mm (1.69% SVL); cloacal width 8.00 mm (9.35% SVL); mental width 1.71 mm (2.00% SVL); postmental width 2.54 mm (2.97% SVL); prefrontal width 3.80 mm (4.44% SVL); frontal width 95.5% frontal length; nasal height 1.00 mm (1.17% SVL); angled subocular height 0.95 mm (1.11% SVL); shortest distance between the eye and naris 4.55 mm (5.32% SVL); canthal iii width 1.79 mm (2.09% SVL); angled subocular width 1.79 mm (2.09% SVL); nasal width 1.33 mm (1.55% SVL); rostral 1.72X as wide as high, barely visible from above, not in contact with nasals, in contact with 1st supralabial and anterior internasal (left)/(right); anterior internasals are narrower than posterior ones; frontonasals and prefrontal fused into a single large plate with a straight posterior margin, much wider than long, bordered by posterior internasals, 1st loreals, canthal iii, 1st median oculars, and the frontal; frontal longer than wide; a pair of frontoparietals, separated by the posterior prolongation of the frontal and the interparietal plate; interparietal plate approximately the size of parietals and separating them, posteriorly touching the interoccipital, which is wider than long; parietal separated from supraoculars by 1st temporals and frontoparietal (left)/(right); nasal single; nostril above suture between 1st and 2nd supralabials (left)/(right); 1 postnasal (left)/(right); 2 loreals (left)/(right); 1st loreal higher than wide (left)/(right), in contact with postnasal, posterior internasal, prefrontal/frontonasal complex, canthal iii, 2nd loreal, and 3rd–4th supralabials (left)/(right); 2nd loreal shorter than 1st, approximately as high as wide (left)/(right), excluded from contact with supraocular by canthal iii (left)/(right); final loreal posteriorly bordering the upper and lower preoculars (left)/(right); canthal iii wider than high (left)/(right), contacting 1st median ocular, anterior supraciliary, upper preocular, prefrontal/frontonasal complex, and 1st and 2nd loreals (left)/(right); 10 median oculars (left)/(right), 1st contacting the prefrontal (left)/(right); 1 upper preocular (left)/(right); an irregular anterior supraciliary (left)/(right); 7 (left)/6 (right) lateral oculars; 5 temporals (left)/(right); 2 suboculars (left)/(right); posterior subocular large and elongate (left)/(right); anterior subocular small (left)/(right); 10 (left)/9 (right) supralabials, 6 to level below center of eye (left)/(right); 10 (left)/9 (right) infralabials, 6 to level below center of eye (left)/(right); mental small, followed by a single, slightly larger postmental; 4 pairs of enlarged chin shields; 1st pair in contact with one another; 2nd to 4th pair separated by 1–3 scales; 115 transverse rows of dorsal scales from interoccipital to base of tail; 119 transverse rows of ventral scales from mental to vent; 46 scales around midbody; 5 digits; finger lengths 3>4>2>5>1; 8 (right) lamellae under longest finger; 34 total lamellae on one hand; toe lengths 4>3>5>2>1; 15 (left)/14 (right) lamellae under longest toe; striate with a faint median keel dorsal body and caudal scales; smooth to faintly striated ventral scales; 138 total strigae counted on ten scales.

Color (in alcohol): dorsal surface of head a golden tan, patternless; lateral surfaces of head grading from golden tan to dark cream with darker brown eye masks and areas on the labial scales; dorsal surfaces of the body are a pale tan with medium brown chevrons; dorsal surface of tail same as the body with the chevrons of the body disappearing after the base; lateral areas grade from dark brown around the forelimb to pale tan down the rest of the side that is interspersed with regular medium brown and white dots that are continuations of the chevrons from the back that appear as vertical or diagonal lines down the sides; dorsal surfaces of the limbs are medium brown with paler gold spots; lateral and ventral areas of the limbs fade to cream; ventral surfaces of the head, body, and tail are pale cream, patternless.

FIGURE 29. (A–F) *Celestus molesworthi* (MCZ R-45184, holotype), SVL 85.6 mm.

FIGURE 30. *Celestus molesworthi* (USNM 328144, SBH 172465), in life. From 1.3 km WSW Section, Portland Parish, Jamaica. Photo by SBH.

Variation. The examined material resembles the dorsal pattern of the holotype with dots arranged in broken chevrons. Specimens have both patternless heads or exhibit head scales with darker outlines. Markings in the longitudinal paramedian series range from absent, to mottling, to broken longitudinal paramedian lines, to present longitudinal paramedian lines. Measurements and other morphological data for the holotype and other examined material are presented in Table 1.

Distribution. *Celestus molesworthi* is distributed on the coast and in inland areas of northeastern Jamaica at elevations of 0–960 m (Fig. 12).

Ecology and conservation. The original description of this species reported that individuals were recovered from under rotting piles of coconut husks (Grant 1940b). Grant (1940a) also noted that as an escape mechanism, this species will "wriggle with astonishing speed," but will not use its legs.

We consider the conservation status of *Celestus molesworthi* to be Endangered B1ab(iii,v) because "the species has a small extent of occurrence (around 1330 km^2), and is inferred to occur in only a single location and to be undergoing continuing decline in the extent and quality of its habitat and the number of mature individuals (based on the prevalence of conversion of moist forest habitat to residential and tourism developments, and the depredations of mongoose and cats, throughout its small range)," based on IUCN Redlist criteria (IUCN 2023). Studies are needed to determine the health and extent of remaining populations and threats to the survival of the species. Captive-breeding programs should be undertaken, because eradication of introduced mammalian predators is not yet possible on Jamaica.

Reproduction. Little data exist on the reproduction of this species. One neonate SVL 26 mm, tail 30 mm was recorded (Grant 1940a).

Etymology. The species was named for Mr. Delves Molesworth, who served as the Secretary of the Institute of Jamaica from 1936–1938.

Remarks. *Celestus molesworthi* was originally described as a subspecies of *C. crusculus* (*C. crusculus molesworthi*) (Grant 1940b) but was referred to as a full species in later works (Hedges *et al.* 2019; Hedges 2023). Sexual dimorphism was reported in this species with males recorded as having "thicker, heavier heads," in addition to being "apparently somewhat larger" than females (Grant 1940a).

Celestus molesworthi is included in our genetic dataset and has significant support in both Bayesian and ML likelihood analyses at the crown node for the species. The stem node that places it as the closest relative to *C.*

duquesneyi and *C. hewardi* has a support value of 84% in ML analyses and 83% in Bayesian analyses. Genomic data in Schools *et al.* (2022) placed *C. molesworthi* (referred to as *C. cundalli*) as the closest relative to *C. duquesneyi* with a support value of 52% in ML analyses and a significant value in Bayesian analyses. Based on our timetree (Fig. 4), *C. molesworthi* diverged from its closest relative 4.17 Ma, consistent with typical species of vertebrates (> 0.7 Ma; Hedges *et al.* 2015). *Celestus molesworthi* was recognized as a distinct species in our ASAP analysis.

***Celestus occiduus* (Shaw 1802)**
Yellow Giant Forest Lizard
(Fig. 31)

Lacerta Occidua Shaw, 1802:288. Holotype: BMNH XV.115A.
Scincus gallivasp—Daudin, 1802:239. Syntypes: MNHN-RA-0.1227, from Jamaica.
Diploglossus Shawii—Duméril & Bibron, 1839:590. Syntypes: MNHN-RA-0.1227, from Jamaica.
Diploglossus occiduus—Boulenger, 1885:290.
Diploglossus impressus—Boulenger, 1885:291.
Macrogongylus brauni—Werner, 1901:299. Holotype: unknown, from Jamaica.
Celestus impressus—Barbour, 1910:298.
Celestus occiduus—Barbour, 1930:100.
Celestus occiduus—Barbour, 1935:123.
Celestus occiduus—Barbour, 1937:139.
Celestus occiduus occiduus—Grant, 1940a:108.
Celestus occiduus—Schwartz & Henderson, 1991:378.
Celestus occiduus—Hedges *et al.*, 2019:17.
Celestus occiduus—Schools & Hedges, 2021:220.
Celestus occiduus—Landestoy *et al.*, 2022:205.

Material examined (n=6). JAMAICA. ANSP 9776; BMNH 1970.1816; BMNH XV.115.A; MCZ R-131774, Ex. Army Medical College, 28 December 1938. **Manchester.** USNM 102652, Kensworth, near Newport, 23 February 1937. **Saint Elizabeth.** USNM 73272, Balaclava, 1914.

Diagnosis. *Celestus occiduus* has (1) a dorsal pattern of absent, (2) head markings absent, (3) markings in the longitudinal paramedian area absent, (4) dots arranged in bars in the lateral band absent, (5) an adult SVL of 269–367 mm, (6) ventral scale rows, 109–134, (7) midbody scale rows, 46–56, (8) total lamellae on one hand, 50–66, (9) total strigae on ten scales, 374, (10) relative length of all digits on one hindlimb, 24.4–29.7 %, (11) relative distance between the angled subocular and mouth, 1.26–1.27 %, (12) relative eye length, 2.87–3.33 %, (13) relative forelimb length, 23.5–23.9 %, (14) relative ear width, 0.948–1.39 %, (15) relative rostral height, 1.60–1.83 %, (16) relative head length, 20.4–20.6 %, (17) relative mental width, 1.86 %, (18) relative postmental width, 3.57 %, (19) relative cloacal width, 9.00 %, (20) relative prefrontal width, 4.76 %, (21) relative largest supraocular width, 2.27–3.02 %, (22) relative longest finger length, 4.77–5.46 %, (23) relative distance between the ear and eye, 8.98–10.9 %, (24) relative head width, 73.8 %, (25) relative frontal width, 63.8 %, (26) relative nasal height, 1.16 %, (27) relative angled subocular height, 1.30 %, (28) relative distance between the eye and naris, 6.51 %, (29) relative canthal iii length, unavailable, (30) relative angled subocular width, 2.52 %, and (31) relative nasal length, 1.83 %. The species stem time is 3.49 Ma and the species crown time is 0.41 Ma (Fig. 4).

Celestus occiduus differs from all but one other member of the genus (*C. striatus*) in lacking a dorsal pattern. This species also has a larger SVL (269–367), number of total strigae on ten scales (374), relative distance between the angled subocular and mouth (1.26–1.27), and relative distance between the eye and naris (6.51) than most other species of the genus.

From *Celestus barbouri*, we distinguish *C. occiduus* by the dorsal pattern (absent versus chevrons), the adult SVL (269–367 versus 78.4–93.6), the total lamellae on one hand (50–66 versus 36–49), the total strigae on ten scales (374 versus 105–136), the relative length of digits on one hindlimb (24.4–29.7 versus 18.2–23.5), the relative distance between angled subocular and mouth (1.26–1.27 versus 0.437–0.556), the relative forelimb length (23.5–23.9 versus 15.4–19.0), the relative head length (20.4–20.6 versus 14.6–16.6), the relative mental width (1.86 versus 1.51–1.85), the relative postmental width (3.57 versus 2.51–3.29), the relative cloacal width (9.00 versus 7.64–8.26), the relative prefrontal width (4.76 versus 3.97–4.33), the relative longest finger length (4.77–5.46 versus 2.92–3.81), the relative distance between the ear and eye (8.98–10.9 versus 6.23–7.15), the relative frontal width

(63.8 versus 65.6–82.1), the relative nasal height (1.16 versus 0.930–1.12), the relative angled subocular height (1.30 versus 0.553–1.16), the relative distance between the eye and naris (6.51 versus 4.68–4.83), and the relative nasal width (1.83 versus 1.38–1.65). From *C. capitulatus* **sp. nov.**, we distinguish *C. occiduus* by the dorsal pattern (absent versus irregular dots/dots in chevrons), the adult SVL (269–367 versus 62.1–81.8), the total lamellae on one hand (50–66 versus 25–38), the total strigae on ten scales (374 versus 105–192), the relative length of digits on one hindlimb (24.4–29.7 versus 17.6–22.3), the relative distance between angled subocular and mouth (1.26–1.27 versus 0.525–1.17), the relative forelimb length (23.5–23.9 versus 14.3–18.1), the relative head length (20.4–20.6 versus 15.1–17.7), the relative mental width (1.86 versus 1.28–1.84), the relative postmental width (3.57 versus 2.62–2.97), the relative cloacal width (9.00 versus 7.84–8.67), the relative prefrontal width (4.76 versus 4.30–4.72), the relative longest finger length (4.77–5.46 versus 3.45–3.75), the relative distance between the ear and eye (8.98–10.9 versus 6.45–7.84), the relative frontal width (63.8 versus 78.1–81.6), the relative angled subocular height (1.30 versus 0.586–1.01), the relative distance between the eye and naris (6.51 versus 4.57–5.03), and the relative angled subocular width (2.52 versus 1.93–2.32). From *C. crusculus*, we distinguish *C. occiduus* by the longitudinal paramedian lines (absent versus present), the adult SVL (269–367 versus 59.6–77.6), the midbody scale rows (46–56 versus 37–44), the total lamellae on one hand (50–66 versus 30–39), the total strigae on ten scales (374 versus 106–194), the relative distance between angled subocular and mouth (1.26–1.27 versus 0.339–0.884), the relative forelimb length (23.5–23.9 versus 12.8–20.7), the relative head length (20.4–20.6 versus 15.5–20.3), the relative postmental width (3.57 versus 2.73–3.37), the relative cloacal width (9.00 versus 6.89–8.77), the relative prefrontal width (4.76 versus 3.93–4.67), the relative longest finger length (4.77–5.46 versus 2.94–4.10), the relative distance between the ear and eye (8.98–10.9 versus 6.07–8.61), the relative frontal width (63.8 versus 82.6–91.1), the relative angled subocular height (1.30 versus 0.953–1.21), the relative distance between the eye and naris (6.51 versus 4.31–4.86), the relative angled subocular width (2.52 versus 2.03–2.43), and the relative nasal width (1.83 versus 1.27–1.60). From *C. duquesneyi*, we distinguish *C. occiduus* by the dorsal pattern (absent versus bands), the adult SVL (269–367 versus 62.1), the total strigae on ten scales (374 versus 130), and the relative ear width (0.948–1.39 versus 2.45). From *C. hesperius* **sp. nov.**, we distinguish *C. occiduus* by the dorsal pattern (absent versus dots in chevrons), the adult SVL (269–367 versus 54.0–62.3), the midbody scale rows (46–56 versus 39–44), the total lamellae on one hand (50–66 versus 29–34), the total strigae on ten scales (374 versus 95–122), the relative distance between angled subocular and mouth (1.26–1.27 versus 0.594–0.648), the relative eye length (2.87–3.33 versus 3.61–3.74), the relative forelimb length (23.5–23.9 versus 18.6–21.3), the relative ear width (0.948–1.39 versus 1.52–1.59), the relative head length (20.4–20.6 versus 15.7–17.7), the relative largest supraocular width (2.27–3.02 versus 1.91–2.22), the relative longest finger length (4.77–5.46 versus 3.50–4.04), and the relative distance between the ear and eye (8.98–10.9 versus 6.74–7.53). From *C. hewardi*, we distinguish *C. occiduus* by the dorsal pattern (absent versus mottled/bands), the adult SVL (269–367 versus 129–171), the total strigae on ten scales (374 versus 164–315), the relative ear width (0.948–1.39 versus 1.40–1.82), the relative mental width (1.86 versus 1.75–1.81), the relative postmental width (3.57 versus 2.84–3.44), the relative distance between the ear and eye (8.98–10.9 versus 6.72–8.73), the relative nasal height (1.16 versus 1.21–1.24), the relative distance between the eye and naris (6.51 versus 5.00–5.60), and the relative angled subocular width (2.52 versus 1.63–2.23). From *C. jamesbondi* **sp. nov.**, we distinguish *C. occiduus* by the adult SVL (269–367 versus 54.7–72.0), the midbody scale rows (46–56 versus 35–44), the total lamellae on one hand (50–66 versus 30–36), the total strigae on ten scales (374 versus 101–173), the relative distance between angled subocular and mouth (1.26–1.27 versus 0.363–1.01), the relative forelimb length (23.5–23.9 versus 14.4–19.9), the relative postmental width (3.57 versus 2.61–2.92), the relative longest finger length (4.77–5.46 versus 3.66–4.33), the relative distance between the ear and eye (8.98–10.9 versus 6.92–7.80), the relative head width (73.8 versus 76.0–80.8), the relative frontal width (63.8 versus 70.5–77.6), the relative angled subocular height (1.30 versus 0.893–1.18), the relative distance between the eye and naris (6.51 versus 4.25–5.54), and the relative nasal width (1.83 versus 1.42–1.75). From *C. macrolepis*, we distinguish *C. occiduus* by the dorsal pattern (absent versus bicolored), the relative distance between angled subocular and mouth (1.26–1.27 versus 1.39–1.66), the relative eye length (2.87–3.33 versus 3.63–3.70), the relative forelimb length (23.5–23.9 versus 26.1–26.7), and the relative longest finger length (4.77–5.46 vs 5.47–5.51). From *C. macrotus*, we distinguish *C. occiduus* by the dorsal pattern (absent versus chevrons/bands), the longitudinal paramedian lines (absent versus present), the dots arranged in bars in the lateral areas (absent versus present), the adult SVL (269–367 versus 60.0–86.1), the ventral scale rows (109–134 versus 87–93), the midbody scale rows (46–56 versus 41–45), the total lamellae on one hand (50–66 versus 39–40), the total strigae on ten scales (374 versus 64–115), the relative

length of digits on one hindlimb (24.4–29.7 versus 30.2–31.2), the relative distance between angled subocular and mouth (1.26–1.27 versus 0.640–0.983), the relative eye length (2.87–3.33 versus 3.79–5.17), the relative ear width (0.948–1.39 versus 1.75–2.08), the relative longest finger length (4.77–5.46 versus 6.43–6.67), the relative distance between the ear and eye (8.98–10.9 versus 7.58–8.02). From *C. microblepharis*, we distinguish *C. occiduus* by the dorsal pattern (absent versus chevrons), the adult SVL (269–367 versus 96.4), the midbody scale rows (46–56 versus 43), the total lamellae on one hand (50–66 versus 30), the total strigae on ten scales (374 versus 165), the relative distance between angled subocular and mouth (1.26–1.27 versus 0.820), the relative eye length (2.87–3.33 versus 1.83), the relative forelimb length (23.5–23.9 versus 14.2), the relative ear width (0.948–1.39 versus 0.446), the relative nasal height (1.16 versus 0.726), and the relative angled subocular height (1.30 versus 0.778). From *C. molesworthi*, we distinguish *C. occiduus* by the dorsal pattern (absent versus dots in chevrons), the adult SVL (269–367 versus 78.1–103), the total lamellae on one hand (50–66 versus 32–44), the total strigae on ten scales (374 versus 138–159), the relative distance between angled subocular and mouth (1.26–1.27 versus 0.653–0.845), the relative head length (20.4–20.6 versus 17.2–20.0), the relative distance between the ear and eye (8.98–10.9 versus 7.97–8.83). From *C. oligolepis* **sp. nov.**, we distinguish *C. occiduus* by the dorsal pattern (absent versus dots in chevrons), the head markings (absent versus present), the longitudinal paramedian lines (absent versus present), the ventral scale rows (109–134 versus 98), the midbody scale rows (46–56 versus 35), and the total lamellae on one hand (50–66 versus 30). From *C. striatus*, we distinguish *C. occiduus* by the adult SVL (269–367 versus 145), the midbody scale rows (46–56 versus 41–43), and the relative distance between angled subocular and mouth (1.26–1.27 versus 0.710).

Description of holotype. BMNH XV.115A. An adult; SVL 269 mm; tail laterally compressed, broken, 172 mm (63.9% SVL); axilla-to-groin distance 138 mm (51.3% SVL); forelimb length 63.3 mm (23.5% SVL); hindlimb length 91.8 mm (34.1% SVL); head length 54.9 mm (20.4% SVL); head width 40.5 mm (15.1% SVL); head width 73.8% head length; diameter of orbit 8.95 mm (3.33% SVL); horizontal diameter of ear opening 2.55 mm (0.948% SVL); vertical diameter of ear opening 5.16 mm (1.92% SVL); length of all toes on one foot 80.0 mm (29.7% SVL); shortest distance between angled subocular and lip 3.40 mm (1.26% SVL); shortest distance between the ocular and auricular openings 24.2 mm (9.00% SVL); longest finger length 14.7 mm (5.46% SVL); largest supraocular width 8.12 mm (3.02% SVL); cloacal width 24.2 mm (9.00% SVL); mental width 5.01 mm (1.86% SVL); postmental width 9.60 mm (3.57% SVL); prefrontal width 12.8 mm (4.76% SVL); frontal width 63.8% frontal length; shortest distance between eye and naris 17.5 mm (6.51% SVL); angled subocular width 6.78 mm (2.52% SVL); nasal width 4.92 mm (1.83% SVL); rostral 1.60X as wide as high, visible from above, not in contact with nasals, in contact with 1st supralabial and anterior internasal (left)/(right); anterior internasals are narrower than posterior ones; frontonasals and prefrontal fused into a single large plate with a concave posterior margin, wider than long, bordered by posterior internasals, 1st loreals, 1st and 2nd median oculars, and the frontal; frontal much longer than wide; a pair of frontoparietals (left fused with frontal), separated by the interparietal plate; interparietal plate much smaller than parietals and separating them (missing), posteriorly touching the interoccipital, which is approximately as wide as long; parietal separated from supraoculars by fused frontal/frontoparietal/uppermost temporal complex (left)/ 1st and 2nd temporals and frontoparietal (right); nasal single; nostril above suture between 1st and 2nd supralabials (left)/(right); 1 postnasal (left)/(right); 2 loreals (left)/(right); 1st loreal higher than wide (left)/(right), in contact with postnasal, posterior internasal, prefrontal/frontonasal complex, 1st median ocular, canthal iii, 2nd loreal, and 3rd–5th supralabials (left)/(right); 2nd loreal shorter than 1st, higher than wide (left)/(right), excluded from contact with supraocular by canthal iii (left)/(right); final loreal posteriorly bordering the lower preocular (left)/(right); canthal iii wider than high (left)/divided into two scales, together are wider than high (right), contacting 1st median ocular, anterior supraciliary, lower preocular, and 1st and 2nd loreals (left)/(right); 8 (left)/9 (right) median oculars, 1st and 2nd contacting the prefrontal (left)/(right); 0 upper preoculars (left)/(right); an irregular anterior supraciliary (left)/(right); 6 lateral oculars (left)/(right); 5 (several are fused) (left)/5 (right) temporals; 2 suboculars (left)/(right); posterior subocular large and elongate (left)/(right); anterior subocular small (left)/(right); 11 supralabials (left)/ (right), 7 (left)/8 (right) to level below center of eye; mental small, followed by a single, larger postmental; 5 pairs of enlarged chin shields; 1st pair in contact with one another; 2nd–5th pairs separated by 1–5 scales; 128 transverse rows of dorsal scales from interoccipital to base of tail; 124 transverse rows of ventral scales from mental to vent; 48 scales around midbody; 5 digits; finger lengths 3>4>2>5>1; 17 lamellae under longest finger (left)/(right); 66 total lamellae on one hand; toe lengths 4>3>5>2>1; 23(right) lamellae under longest toe; dorsal body and caudal scales striate with a faint median keel; smooth ventral scales; 374 total strigae counted on ten scales.

Color (in alcohol): dorsal surface of head dark gold with some darker brown areas; lateral surfaces of head grading from dark gold to creamy yellow, patternless; dorsal surfaces of the body are dark gold, patternless; dorsal surface of tail the same dark gold as the head; lateral areas grade from the same dark gold as the head to creamy yellow; dorsal surfaces of the limbs are dark gold; lateral and ventral areas of the limbs fade to creamy yellow; ventral surfaces of the head, body, and tail are yellow-cream, patternless.

Variation. The examined material closely resembles the holotype in a lack of pattern. Measurements and other morphological data for the holotype and other examined material are presented in Table 1.

Distribution. Little data are available on the distribution of *Celestus occiduus* as most specimen accounts give either no information or refer to "West Indies" or "Jamaica" as the area from which the specimens were collected. Gosse (1851) has previously referred to this species as the "Morass Galliwasp," indicating that it was from the area of the Black River on the southwestern coast of Jamaica (Fig. 11).

Ecology and conservation. Based on literature reports, *Celestus occiduus* is a swamp-dwelling lizard. Although confusion has persisted throughout the literature regarding the identification of *C. occiduus*, ecological reports of a yellow diploglossid (presumably *C. occiduus*) living in the Jamaican swamps confirm its placement in the Swamp Ecomorph. Gosse (1851: 77) described the "Yellow Galliwasp" as occurring in the "swamps and morasses of Westmoreland Parish," where it "might be observed sitting idly in the mouth of its burrow, or feeding on the wild fruits and marshy plants that constitute its food." Later in the book (Gosse 1851: 214), he mentioned that *C. occiduus* eats fruit from the Alligator Apple tree (*Annona paulustris*), which occurs in and around the same morasses. This descriptive yellow color of *C. occiduus* agrees more closely with the holotype, a pale specimen in preservative, than with the holotype of *C. macrolepis*, a specimen that is predominantly dark brown, with pale blotches (Schools & Hedges 2021: fig. 12). As reported by the naturalist Anthony Robinson during the 1760s (in Cockerell 1894), the species "*Celestus occiduus*" was observed to hunt for fish from riverbanks, from which they would jump into the water to catch fish and return with them to the riverbanks. When discussing *C. occiduus*, Shaw (1802) commented that the back teeth of the species resemble the molars of mammals. This might be an adaptation for eating hard invertebrates, such as the crabs found in the stomach of *C. macrolepis*, an association noted in other species of lizards (Renesto & Dalla Vecchia 2000).

The IUCN Redlist (IUCN 2023) considers the conservation status of *Celestus occiduus* to be Critically Endangered (Possibly Extinct) C2a(i,ii); D because it was "last recorded in the mid-nineteenth century, it is thought that the introduction of predatory species (primarily mongoose) to Jamaica, and the extensive conversion of woody swamp habitat, resulted in the extinction of *C. occiduus*. Recent surveys, although extensive, have not yet been exhaustive, given the difficulties of access into and around the Black River Morass, leaving room for some hope that the species may persist, albeit with a tiny population. Any remnant population is thought likely to number fewer than 50 mature individuals of this large species and is likely to be restricted to a very small area likely at risk from habitat degradation and continued impacts of mongoose predation." Studies are needed to determine the health and extent of any remaining populations and threats to the survival of the species.

Reproduction. No data on reproduction are available for this species.

Etymology. The species name is Latin meaning western, presumably for its distribution in western Jamaica (or at least west of the major population area of Jamaica, Kingston).

Remarks. *Celestus occiduus*, first described in 1802, has had a long and confusing taxonomic history, especially because of its confusion with *C. macrolepis*. Cochran (1941) also suggested that *C. crusculus* may in fact be juvenile *C. occiduus*, a hypothesis that can be discounted because many adult specimens (including gravid females) of *C. crusculus*, a much smaller species, exist.

Grant (1951) said that he believed that *Celestus impressus* is a synonym of *C. occiduus*. However, Schwartz (1964) reported that one syntype of *C. impressus*, which he designated as lectotype (ANSP 9225), was *C. hewardi* and the other was *C. crusculus*. We examined those specimens and agree with Schwartz, although the damage to both specimens is substantial.

Cousens (1956) reported that a giant Galliwasp had not been seen in over 100 years; however, Grant (1940a) suspected that *Celestus occiduus* could still exist. Later, Schwartz (1970) said that he found it highly unlikely that the species could still exist, and speculated that *C. barbouri*, *C. crusculus*, *C. hewardi*, and *C. occiduus* might form a group. Since the introduction of the mongoose, many species, including *C. occiduus*, likely were more widespread, but are now found only in the highlands (Barbour 1910). If this is the case, *C. occiduus*, a swamp dweller, might not have been able to find refuge in the highlands, in contrast to the other species.

FIGURE 31. (A–F) *Celestus occiduus* (BMNH XV.115A, holotype), SVL 269 mm.

The holotype number of *Celestus occiduus* was incorrectly reported as BMNH XV.118A by Schwartz & Henderson (1991) and Schools & Hedges (2021). This presumably was a result of the confusion of *C. macrolepis* with *C. occiduus*, and, because the holotype number for *C. macrolepis* is BMNH XV.118.A or 1946.8.3.82. The correct holotype number for *C. occiduus* is BMNH XV.115.A and the Natural History Museum has made that correction on the specimen tag as well.

Celestus occiduus (two individuals) is included in our genetic dataset and has significant support in both Bayesian and ML likelihood analyses at the crown node of the species and the stem node that places it as the closest relative to *C. striatus*. Based on our timetree (Fig. 4), *C. occiduus* diverged from its closest relative 3.49 Ma, consistent with typical species of vertebrates (> 0.7 Ma; Hedges *et al.* 2015). *Celestus occiduus* was recognized as a distinct species in our ASAP analysis.

***Celestus oligolepis* sp. nov.**
Jamaican Few-scaled Forest Lizard
(Fig. 32)

Celestus crusculus—Schwartz & Henderson, 1991:369 (part).
Celestus crusculus crusculus—Hedges *et al.*, 2019:17 (part).
Celestus crusculus—Schools & Hedges, 2021:220 (part).
Celestus crusculus—Landestoy *et al.*, 2022:204 (part).

Holotype. USNM 328158, a juvenile from 7.0 km WSW of Old Hope, Westmoreland Parish, Jamaica, collected by S. Blair Hedges and Carla Ann Hass on 29 May 1988 (18.2232, -78.2861; 0 m).

Diagnosis. *Celestus oligolepis* **sp. nov.** has (1) a dorsal pattern of dots in chevrons, (2) head markings present, (3) markings in the longitudinal paramedian area present, (4) dots arranged in bars in the lateral band absent, (5) a SVL of 30.7 mm (juvenile, only specimen), (6) ventral scale rows, 98, (7) midbody scale rows, 35, (8) total lamellae on one hand, 30, (9) total strigae on ten scales, 83, (10) relative length of all digits on one hindlimb, 34.6 %, (11) relative distance between the angled subocular and mouth, 0.651 %, (12) relative eye length, 4.85 %, (13) relative forelimb length, 21.4 %, (14) relative ear width, 2.28 %, (15) relative rostral height, 2.11 %, (16) relative head length, 19.5 %, (17) relative mental width, 2.28 %, (18) relative postmental width, 4.20 %, (19) relative cloacal width, 8.95 %, (20) relative prefrontal width, 6.41 %, (21) relative largest supraocular width, 4.03 %, (22) relative longest finger length, 5.14 %, (23) relative distance between the ear and eye, 9.14 %, (24) relative head width, 78.3 %, (25) relative frontal width, 74.3 %, (26) relative nasal height, 2.34 %, (27) relative angled subocular height, 1.89 %, (28) relative distance between the eye and naris, 5.63 %, (29) relative canthal iii length, 2.77 %, (30) relative angled subocular width, 3.12 %, and (31) relative nasal length, 2.44 %. The species stem time is 4.20 Ma and the species crown time is unavailable (Fig. 4).

Because the only known specimen of *Celestus oligolepis* **sp. nov.** is a juvenile, we only differentiate it from other species of *Celestus* based on pattern and scale count characters. Although pattern can have ontogenetic differences, the number of scales usually does not change with age. *Celestus oligolepis* **sp. nov.** has a smaller number of midbody scale rows than most other species of the genus.

From *Celestus barbouri*, we distinguish *C. oligolepis* **sp. nov.** by the dorsal pattern (dots in chevrons versus chevrons), the longitudinal paramedian lines (present versus absent), the ventral scale rows (98 versus 118–151), the midbody scale rows (35 versus 47–56), and the total lamellae on one hand (30 versus 36–49). From *C. capitulatus* **sp. nov.**, we distinguish *C. oligolepis* **sp. nov.** by the midbody scale rows (35 versus 37–47). From *C. crusculus*, we distinguish *C. oligolepis* **sp. nov.** by the midbody scale rows (35 versus 37–44). From *C. duquesneyi*, we distinguish *C. oligolepis* **sp. nov.** by the dorsal pattern (dots in chevrons versus bands), the head markings (present versus absent), the longitudinal paramedian lines (present versus absent), and the total lamellae on one hand (30 versus 64). From *C. hesperius* **sp. nov.**, we distinguish *C. oligolepis* **sp. nov.** by the head markings (present versus absent), the ventral scale rows (98 versus 111–114), and the midbody scale rows (35 versus 39–44). From *C. hewardi*, we distinguish *C. oligolepis* **sp. nov.** by the dorsal pattern (dots in chevrons versus mottled/bands), the head markings (present versus absent), the ventral scale rows (98 versus 113–137), the midbody scale rows (35 versus 43–59), and the total lamellae on one hand (30 versus 50–61). From *C. jamesbondi* **sp. nov.**, we distinguish *C. oligolepis* **sp. nov.** by the relative mental to vent scales (2.80 versus 2.14–2.77) (see Remarks). From *C. macrolepis*, we distinguish

C. oligolepis **sp. nov.** by the dorsal pattern (dots in chevrons versus bicolored), the head markings (present versus absent), the longitudinal paramedian lines (present versus absent), the ventral scale rows (98 versus 112–116), the midbody scale rows (35 versus 46–48), and the total lamellae on one hand (30 versus 52–54). From *C. macrotus*, we distinguish *C. oligolepis* **sp. nov.** by the dorsal pattern (dots in chevrons versus chevrons/bands), the dots arranged in bars in the lateral areas (absent versus present), the ventral scale rows (98 versus 87–93), the midbody scale rows (35 versus 41–45), and the total lamellae on one hand (30 versus 39–40). From *C. microblepharis*, we distinguish *C. oligolepis* **sp. nov.** by the dorsal pattern (dots in chevrons versus chevrons), the head markings (present versus absent), and the longitudinal paramedian lines (present versus absent). From *C. molesworthi*, we distinguish *C. oligolepis* **sp. nov.** by the ventral scale rows (98 versus 102–125), the midbody scale rows (35 versus 41–49), and the total lamellae on one hand (30 versus 32–44). From *C. occiduus*, we distinguish *C. oligolepis* **sp. nov.** by the dorsal pattern (dots in chevrons versus absent), the head markings (present versus absent), the longitudinal paramedian lines (present versus absent), the ventral scale rows (98 versus 109–134), the midbody scale rows (35 versus 46–56), the total lamellae on one hand (30 versus 50–66). From *C. striatus*, we distinguish *C. oligolepis* **sp. nov.** by the dorsal pattern (dots in chevrons versus absent/chevrons), the ventral scale rows (98 versus 101–109), the midbody scale rows (35 versus 41–43), and the total lamellae on one hand (30 versus 59–66).

Description of holotype. USNM 328158. A juvenile, based on the small SVL 30.7 mm (smaller than 25% of the largest SVL of the closest relative [*Celestus barbouri*]); tail nearly cylindrical, broken, 2.74 mm (8.93% SVL); axilla-to-groin distance 15.6 mm (50.8% SVL); forelimb length 6.58 mm (21.4% SVL); hindlimb length 9.20 mm (30.0% SVL); head length 5.99 mm (19.5% SVL); head width 4.69 mm (15.3% SVL); head width 78.3% head length; diameter of orbit 1.49 mm (4.85% SVL); horizontal diameter of ear opening 0.70 mm (2.28% SVL); vertical diameter of ear opening 0.55 mm (1.79% SVL); length of all toes on one foot 10.6 mm (34.5% SVL); shortest distance between angled subocular and lip 0.20 mm (0.651% SVL); shortest distance between the ocular and auricular openings 2.81 mm (9.15% SVL); longest finger length 1.58 mm (5.15% SVL); largest supraocular width 1.24 mm (4.04% SVL); cloacal width 2.75 mm (8.96% SVL); mental width 0.70 mm (2.28% SVL); postmental width 1.29 mm (4.20% SVL); prefrontal width 1.97 mm (6.42% SVL); frontal width 74.3% frontal length; nasal height 0.72 mm (2.35% SVL); angled subocular height 0.58 mm (1.89% SVL); shortest distance between the eye and naris 1.73 mm (5.64% SVL); canthal iii width 0.85 mm (2.77% SVL); angled subocular width 0.96 mm (3.13% SVL); nasal width 0.75 mm (2.44% SVL); rostral 2.11X as wide as high, visible from above, not in contact with nasals, in contact with 1st supralabial and anterior internasal (left)/(right); anterior internasals are narrower than posterior ones; frontonasals and prefrontal fused into a single large plate with a slightly concave posterior margin, wider than long, bordered by posterior internasals, 1st loreals, canthal iii, 1st median oculars, and the frontal; frontal longer than wide; a pair of frontoparietals, separated by the posterior prolongation of the frontal and the interparietal plate; interparietal plate smaller than parietals and separating them, posteriorly touching the interoccipital, which is much wider than long; parietal separated from supraoculars by 1st and 2nd temporals and frontoparietal (left)/(right); nasal single; nostril above suture between 1st and 2nd supralabials (left)/(right); 1 postnasal (left)/(right); 2 loreals (left)/(right); 1st loreal higher than wide (left)/(right), in contact with postnasal, posterior internasal, prefrontal/frontonasal complex, canthal iii, 2nd loreal, and the 3rd–4th supralabials (left)/(right); 2nd loreal shorter than 1st, approximately as high as wide (left)/(right), excluded from contact with supraocular by canthal iii (left)/(right); 2nd loreal posteriorly bordering the lower preocular (left)/upper and lower preoculars (right); canthal iii wider than high (left)/(right), contacting 1st median ocular, anterior supraciliary, upper and lower preoculars, prefrontal/frontonasal complex, and 1st and 2nd loreals (left)/(right); 9 median oculars (left)/(right), 1st contacting the prefrontal (left)/(right); 1 upper preocular (left)/(right); an irregular anterior supraciliary (left)/(right); 5 (left)/6 (right) lateral oculars; 5 temporals (left)/(right); 2 suboculars (left)/(right); posterior subocular large and elongate (left)/(right); anterior subocular small (left)/(right); 9 (left)/8 (right) supralabials, 6 to level below center of eye (left)/(right); 8 infralabials (left)/(right), 6 (left)/(right) to level below center of eye; mental small, followed by a single, larger postmental; 4 pairs of enlarged chin shields; 1st pair in contact with one another; 2nd to 4th pair separated by 1–2 scales; 100 transverse rows of dorsal scales from interoccipital to base of tail; 98 transverse rows of ventral scales from mental to vent; 35 scales around midbody; 5 digits; finger lengths 3>4>2>5>1; 7 lamellae under longest finger (left)/(right); 30 total lamellae on one hand; toe lengths 4>3>5>2>1; 12 (left)/11 (right) lamellae under longest toe; dorsal body and caudal scales striate with a small median keel; smooth ventral scales; 83 total strigae counted on ten scales.

Color (in alcohol): dorsal surface of head tan with the median supraorbital series outlined in darker brown; lateral surfaces of head grading from tan to cream with darker brown eye masks and markings on the labial scales; dorsal surfaces of the body are tan with longitudinal paramedian lines and darker flecks vaguely arranged into

herring bones; dorsal surface of tail the same as the body; lateral areas grade from medium brown to cream; dorsal surfaces of the limbs are medium brown; lateral and ventral areas of the limbs fade from medium brown to cream; ventral surfaces of the head, body, and tail are cream with some lineate markings under the throat and chest.

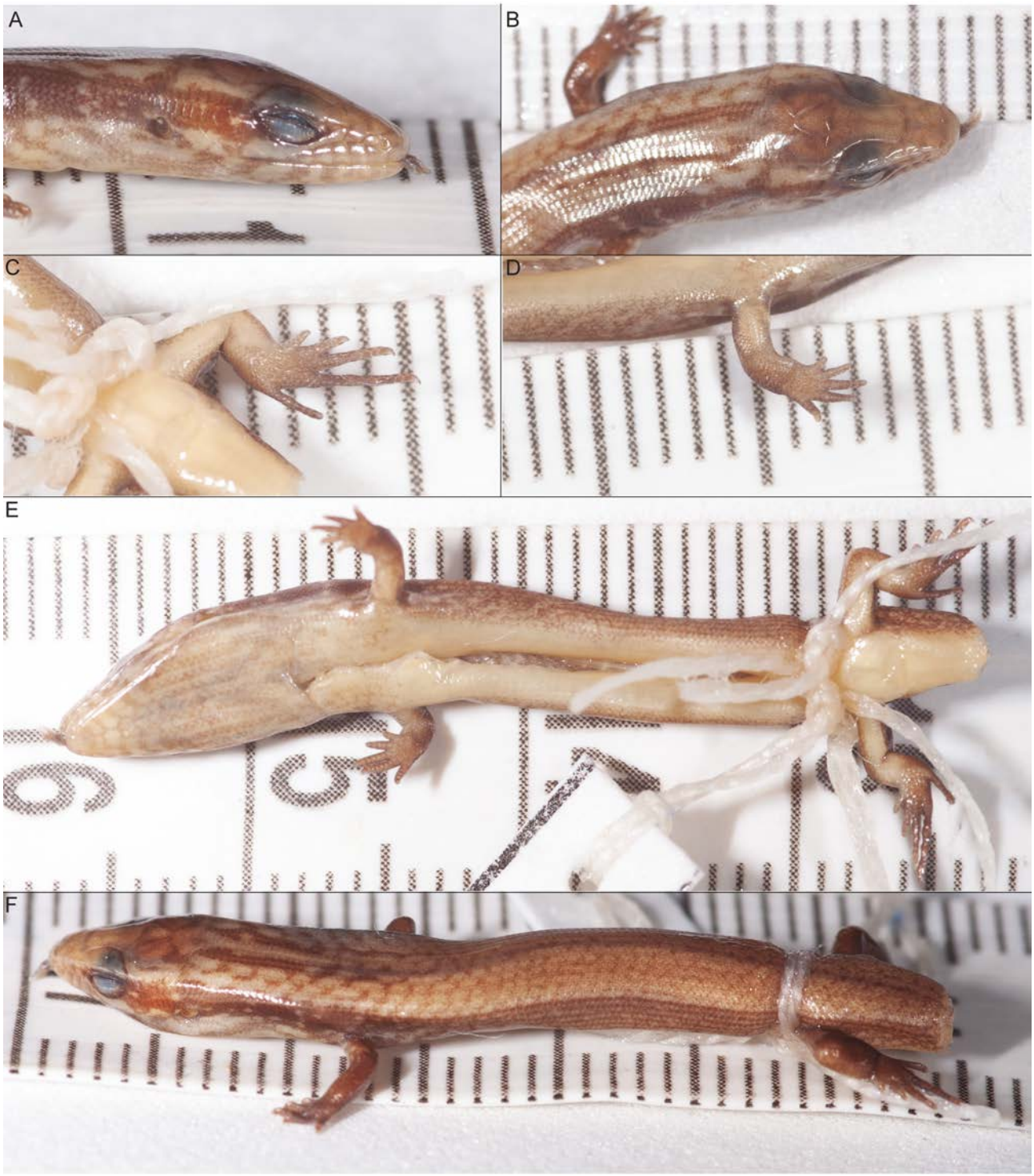

FIGURE 32. (A–F) *Celestus oligolepis* **sp. nov.** (USNM 328158, holotype), SVL 30.7 mm.

Variation. No other specimens are known. Measurements and other morphological data for the holotype are presented in Table 1.

Distribution. *Celestus oligolepis* **sp. nov.** is known only from the holotype, which was collected on the southern coast of the western tip of Jamaica at "0 m" elevation in Westmoreland Parish (Fig. 11).

Ecology and conservation. Little is known of the ecology of this species other than the holotype was collected at dusk in sea grape leaf litter. The specimen was assumed to be a *C. crusculus* at the time it was collected and the

habitat is unremarkable and disturbed as one might expect along the busy coastal road. Given the abundance of sympatric *C. capitulatus* **sp. nov.** (N = 36 examined), to the east and west along the coast, compared with this single specimen of *C. oligolepis* **sp. nov.**, suggests that it is localized and rare.

We consider the conservation status of *Celestus oligolepis* **sp. nov.** to be Critically Endangered B1ab(iii), based on IUCN Redlist criteria (IUCN 2023). It faces a primary threat from habitat destruction from agriculture and urbanization. Secondary threats include predation from introduced mammals, including the mongoose and black rats. Studies are needed to determine the health and extent of remaining populations and threats to the survival of the species. Captive-breeding programs should be undertaken, because eradication of introduced mammalian predators is not yet possible on Jamaica.

Reproduction. No data on reproduction are available for this species.

Etymology. The species name (*oligolepis*) is a Latin adjective meaning "few scales," in reference to the low scale counts of this species.

Remarks. Because the only known representative is a juvenile, we only use morphological characters that are based on pattern and scale counts in our morphological diagnoses. Whereas *C. jamesbondi* and *C. oligolepis* cannot be morphologically separated based on our standard suite of characters, they can be morphologically separated based on the ratio of mental to vent scales by midbody scales (2.80 [n=1] versus 2.14–2.77 [n=35]).

Despite having only a single specimen, we are confident that it represents a distinct species because of its combination of morphological differences and large genetic divergence from other species. *Celestus oligolepis* **sp. nov.** is included in our genetic dataset and has support values of 57% and 54% at the node that places it as the closest relative of *C. barbouri* in our ML and Bayesian analyses, respectively. Based on our timetree (Fig. 4), *Celestus oligolepis* **sp. nov.** diverged from its closest relative 4.20 Ma, consistent with typical species of vertebrates (> 0.7 Ma; Hedges *et al*. 2015). *Celestus oligolepis* **sp. nov.** was recognized as a distinct species by our ASAP analysis.

Celestus striatus Gray, 1839

Golden Forest Lizard
(Fig. 33–34)

Celestus striatus—Gray, 1839:288. Holotype: BMNH 1946.8.8.3 (locality unknown).
Diploglossus Cliftii—Duméril & Bibron, 1839:595.
Celestus striatus—Gray, 1845:117.
Celestus striatus—Bocourt, 1879:377
Diploglossus striatus—Boulenger, 1885:289.
Diploglossus striatus—Fischer, 1888:29.
Celestus occiduus—Barbour, 1910:297 (part).
Diploglossus fowleri—Schwartz, 1971a:3. Holotype: MCZ R-125601, collected by Danny C. Fowler at Windsor (near Windsor Cave, "153 m"), Trelawny Parish, Jamaica, on 15 August 1970 (18.35, -77.65).
Celestus fowleri—Schwartz & Henderson, 1991:373.
Celestus fowleri—Hedges *et al.*, 2019:17.
Celestus fowleri—Schools & Hedges, 2021:220.
Celestus striatus—Schools & Hedges, 2021:220.
Celestus fowleri—Landestoy *et al.*, 2022: 204.
Celestus striatus—Landestoy *et al.*, 2022: 205.

Material examined (n=3). JAMAICA. BMNH 1946.8.8.3. **Trelawny**. KU 226528, Windsor, 12 July 1961; MCZ R-125601, Danny C. Fowler, Windsor, 15 August 1970.

Diagnosis. *Celestus striatus* has (1) a dorsal pattern of absent/chevrons, (2) head markings absent/present, (3) markings in the longitudinal paramedian area absent/present, (4) dots arranged in bars in the lateral band absent, (5) an adult SVL of 145 mm, (6) ventral scale rows, 101–109, (7) midbody scale rows, 41–43, (8) total lamellae on one hand, 59–66, (9) total strigae on ten scales, 279, (10) relative length of all digits on one hindlimb, 37.8 %, (11) relative distance between the angled subocular and mouth, 0.710 %, (12) relative eye length, 3.85 %, (13) relative forelimb length, 26.1 %, (14) relative ear width, 1.30 %, (15) relative rostral height, 1.94 %, (16) relative head length, 18.9 %, (17) relative mental width, unavailable, (18) relative postmental width, unavailable, (19) relative cloacal width, 7.93 %, (20) relative prefrontal width, 5.68 %, (21) relative largest supraocular width, 2.63 %, (22) relative longest finger length, 7.48 %, (23) relative distance between the ear and eye, 9.00 %, (24) relative head

width, 82.1 %, (25) relative frontal width, 76.5 %, (26) relative nasal height, 1.08 %, (27) relative angled subocular height, 1.12 %, (28) relative distance between the eye and naris, 6.16 %, (29) relative canthal iii length, 2.12 %, (30) relative angled subocular width, 2.29 %, and (31) relative nasal length, 1.59 %. The species stem time is 3.49 Ma and the species crown time is 0.30 Ma (Fig. 4).

Celestus striatus has a larger relative length of all digits on one hindlimb (37.8), relative forelimb length (26.1), relative prefrontal width (5.68), relative longest finger length (7.48), larger relative head width (82.1), and relative distance between the eye and naris (6.16) than most other species of the genus.

From *C. barbouri*, we distinguish *C. striatus* by the adult SVL (145 versus 78.4–93.6), the ventral scale rows (101–109 versus 118–151), the midbody scale rows (41–43 versus 47–56), the total lamellae on one hand (59–66 versus 36–49), the total strigae on ten scales (279 versus 105–136), the relative length of digits on one hindlimb (37.8 versus 18.2–23.5), the relative distance between angled subocular and mouth (0.710 versus 0.437–0.556), the relative eye length (3.85 versus 2.87–3.63), the relative forelimb length (26.1 versus 15.4–19.0), the relative rostral height (1.94 versus 1.41–1.66), the relative head length (18.9 versus 14.6–16.6), the relative prefrontal width (5.68 versus 3.97–4.33), the relative longest finger length (7.48 versus 2.92–3.81), the relative distance between the ear and eye (9.00 versus 6.23–7.15), the relative head width (82.1 versus 73.8–81.7), the relative distance between the eye and naris (6.16 versus 4.68–4.83), and the relative width of canthal iii (2.12 versus 1.54–1.93). From *C. capitulatus* **sp. nov.**, we distinguish *C. striatus* by the dorsal pattern (absent/chevrons versus irregular dots/dots in chevrons), the adult SVL (145 versus 62.1–81.8), the total lamellae on one hand (59–66 versus 25–38), the total strigae on ten scales (279 versus 105–192), the relative length of digits on one hindlimb (37.8 versus 17.6–22.3), the relative eye length (3.85 versus 2.75–3.80), the relative forelimb length (26.1 versus 14.3–18.1), the relative head length (18.9 versus 15.1–17.7), the relative prefrontal width (5.68 versus 4.30–4.72), the relative largest supraocular width (2.63 versus 2.03–2.61), the relative longest finger length (7.48 versus 3.45–3.75), the relative distance between the ear and eye (9.00 versus 6.45–7.84), the relative head width (82.1 versus 71.6–78.6), the relative frontal width (76.5 versus 78.1–81.6), the relative angled subocular height (1.12 versus 0.586–1.01), and the relative distance between the eye and naris (6.16 versus 4.57–5.03). From *C. crusculus*, we distinguish *C. striatus* by the adult SVL (145 versus 59.6–77.6), the total lamellae on one hand (59–66 versus 30–39), the total strigae on ten scales (279 versus 106–194), the relative length of digits on one hindlimb (37.8 versus 18.7–24.7), the relative eye length (3.85 versus 2.93–3.61), the relative forelimb length (26.1 versus 12.8–20.7), the relative prefrontal width (5.68 versus 3.93–4.67), the relative longest finger length (7.48 versus 2.94–4.10), the relative distance between the ear and eye (9.00 versus 6.07–8.61), the relative frontal width (76.5 versus 82.6–91.1), the relative distance between the eye and naris (6.16 versus 4.31–4.86), and the relative width of canthal iii (2.12 versus 1.59–2.07). From *C. duquesneyi*, we distinguish *C. striatus* by the dorsal pattern (absent/chevrons versus bands), the adult SVL (145 versus 62.1), the total strigae on ten scales (279 versus 130), and the relative ear width (1.30 versus 2.45). From *C. hesperius* **sp. nov.**, we distinguish *C. striatus* by the dorsal pattern (absent/chevrons versus dots in chevrons), the adult SVL (145 versus 54.0–62.3), the ventral scale rows (101–109 versus 111–114), the total lamellae on one hand (59–66 versus 29–34), and the total strigae on ten scales (279 versus 95–122). From *C. hewardi*, we distinguish *C. striatus* by the dorsal pattern (absent/chevrons versus mottled/bands), the ventral scale rows (101–109 versus 113–137), the relative length of digits on one hindlimb (37.8 versus 24.1–30.6), the relative distance between angled subocular and mouth (0.710 versus 0.744–1.40), the relative forelimb length (26.1 versus 22.2–24.6), the relative ear width (1.30 versus 1.40–1.82), the relative rostral height (1.94 versus 1.50–1.76), the relative cloacal width (7.93 versus 8.81–9.89), the relative prefrontal width (5.68 versus 4.18–4.80), the relative longest finger length (7.48 versus 5.03–5.66), the relative distance between the ear and eye (9.00 versus 6.72–8.73), the relative head width (82.1 versus 68.4–77.1), the relative frontal width (76.5 versus 57.3–75.3), the relative nasal height (1.08 versus 1.21–1.24), the relative distance between the eye and naris (6.16 versus 5.00–5.60), and the relative angled subocular width (2.29 versus 1.63–2.23). From *C. jamesbondi* **sp. nov.**, we distinguish *C. striatus* by the adult SVL (145 versus 54.7–72.0), the total lamellae on one hand (59–66 versus 30–36), the total strigae on ten scales (279 versus 101–173), the relative length of digits on one hindlimb (37.8 versus 19.8–26.3), the relative forelimb length (26.1 versus 14.4–19.9), the relative prefrontal width (5.68 versus 4.29–5.09), the relative longest finger length (7.48 versus 3.66–4.33), the relative distance between the ear and eye (9.00 versus 6.92–7.80), the relative head width (82.1 versus 76.0–80.8), the relative nasal height (1.08 versus 1.12–1.21), and the relative distance between the eye and naris (6.16 versus 4.25–5.54). From *C. macrolepis*, we distinguish *C. striatus* by the dorsal pattern (absent/chevrons versus bicolored), adult SVL (145 versus 254–316), the ventral scale rows (101–109 versus 112–116), the midbody scale rows (41–43

versus 46–48), the total lamellae on one hand (59–66 versus 52–54), and the relative distance between angled subocular and mouth (0.710 versus 1.39–1.66). From *C. macrotus*, we distinguish *C. striatus* by the dots arranged in bars in the lateral areas (absent versus present), the adult SVL (145 versus 60.0–86.1), the ventral scale rows (101–109 versus 87–93), the total lamellae on one hand (59–66 versus 39–40), the total strigae on ten scales (279 versus 64–115). From *C. microblepharis*, we distinguish *C. striatus* by the total lamellae on one hand (59–66 versus 30), the total strigae on ten scales (279 versus 165), the relative length of digits on one hindlimb (37.8 versus 16.6), the relative eye length (3.85 versus 1.83), the relative forelimb length (26.1 versus 14.2), the relative ear width (1.30 versus 0.446), and the relative longest finger length (7.48 versus 3.11). From *C. molesworthi*, we distinguish *C. striatus* by the dorsal pattern (absent/chevrons versus dots in chevrons), the adult SVL (145 versus 78.1–103), the total lamellae on one hand (59–66 versus 32–44), the total strigae on ten scales (279 versus 138–159), the relative length of digits on one hindlimb (37.8 versus 22.4–29.4), the relative eye length (3.85 versus 3.28–3.70), the relative forelimb length (26.1 versus 17.5–24.2), the relative ear width (1.30 versus 1.37–1.50), and the relative rostral height (1.94 versus 1.72–1.81). From *C. occiduus*, we distinguish *C. striatus* by the adult SVL (145 versus 269–367), the midbody scale rows (41–43 versus 46–56), the relative distance between angled subocular and mouth (0.710 versus 1.26–1.27). From *C. oligolepis* **sp. nov.**, we distinguish *C. striatus* by the dorsal pattern (absent/chevrons versus dots in chevrons), the ventral scale rows (101–109 versus 98), the midbody scale rows (41–43 versus 35), and the total lamellae on one hand (59–66 versus 30).

Description of holotype. BMNH 1946.8.8.3. An adult; SVL 145 mm; tail slightly compressed, 138 mm (95.2% SVL); axilla-to-groin distance 68.5 mm (47.2% SVL); forelimb length 37.8 mm (26.1% SVL); hindlimb length 53.9 mm (37.2% SVL); head length 27.3 mm (18.8% SVL); head width 22.4 mm (15.4% SVL); head width 82.1% head length; diameter of orbit 5.58 mm (3.85% SVL); horizontal diameter of ear opening 1.88 mm (1.30% SVL); vertical diameter of ear opening 1.59 mm (1.10% SVL); length of all toes on one foot 54.8 mm (37.8% SVL); shortest distance between angled subocular and lip 1.03 mm (0.710% SVL); shortest distance between the ocular and auricular openings 13.1 mm (9.03% SVL); longest finger length 10.9 mm (7.52% SVL); largest supraocular width 3.81 mm (2.63% SVL); cloacal width 11.5 mm (7.93% SVL); prefrontal width 8.23 mm (5.68% SVL); frontal width 76.5% SVL; nasal height 1.56 mm (1.08% SVL); angled subocular height 1.62 mm (1.12% SVL); shortest distance between the eye and naris 8.93 mm (6.16% SVL); canthal iii width 3.08 mm (2.12% SVL); angled subocular width 3.32 mm (2.29% SVL); nasal width 2.30 mm (1.59% SVL); rostral 1.94X as wide as high, barely visible from above, not in contact with nasals, in contact with 1st supralabial and anterior internasal (left)/(right); anterior internasals are narrower than posterior ones; frontonasals and prefrontal fused into a single large plate with a concave posterior margin, wider than long, bordered by posterior internasals, 1st loreals, canthal iii, 1st median oculars, and the frontal; frontal much longer than wide; a pair of frontoparietals, separated by the posterior prolongation of the frontal and the interparietal plate; interparietal plate smaller than parietals and separating them, posteriorly touching the interoccipital, which is wider than long; parietal separated from supraoculars by 1st and 2nd temporals and frontoparietal (left)/(right); nasal single; nostril just posterior to suture between 1st and 2nd supralabials (left)/(right); 1 postnasal (left)/(right); 2 loreals (left)/(right); 1st loreal higher than wide (left)/(right), in contact with postnasal, posterior internasal, prefrontal/frontonasal complex, canthal iii, 2nd loreal, and 3rd–5th supralabials (left)/(right); 2nd loreal shorter than 1st, approximately as high as wide (left)/(right), excluded from contact with supraocular by canthal iii (left)/(right); final loreal posteriorly bordering the upper and lower preoculars (left)/(right); canthal iii wider than high (left)/(right), contacting 1st median ocular, anterior supraciliary, upper preocular, prefrontal/frontonasal complex, and 1st and 2nd loreals (left)/(right); 11 (left)/10 (right) median oculars, 1st contacting the prefrontal (left)/(right); 1 upper preocular (left)/(right); an irregular anterior supraciliary (left)/(right); 6 lateral oculars (left)/(right); 5 temporals (left)/(right); 2 suboculars (left)/(right); posterior subocular large and elongate (left)/(right); anterior subocular small (left)/(right); 11 supralabials (left)/(right), 7 to level below center of eye (left)/(right); 8 (left)/9 (right) infralabials, 6 (left)/7 (right) to level below center of eye; mental small, followed by a single, much larger postmental; 5 pairs of enlarged chin shields, followed by 1 pair of reduced chin shields; 1st pair in contact with one another; 2nd–5th pairs separated by 1–7 scales; 97 transverse rows of dorsal scales from interoccipital to base of tail; 109 transverse rows of ventral scales from mental to vent; 43 scales around midbody; 5 digits; finger lengths 3>4>2>5>1; 16 lamellae under longest finger (left)/(right); 66 total lamellae on one hand; toe lengths 4>3>5>2>1; 23 (left)/22 (right) lamellae under longest toe; faintly striated and keeled dorsal body and caudal scales; smooth ventral scales; 279 total strigae counted on ten scales.

Color (in alcohol): dorsal surface of head dark gold, patternless; lateral surfaces of head grading from dark gold to slightly paler gold, patternless; dorsal surfaces of the body are dark gold, patternless; dorsal surface of tail the

same dark gold as the head, patternless; lateral areas are the same dark gold as the head, patternless; dorsal surfaces of the limbs are dark gold, patternless; lateral and ventral areas of the limbs fade to pale gold, patternless; ventral surfaces of the head, body, and tail are pale gold, patternless.

Color (in life): From the photograph by Rudi Diesel that he provided to SBH in the 1990s, and has since been on the Caribherp website (Hedges 2024), it can be seen that the ground color is golden tan with dark brown markings and pale tan accenting of the dorsal crossbands/chevrons. The iris is orange-red.

Variation. Both KU 226528 and MCZ R-125601 have a much more pronounced dorsal pattern of chevrons than the holotype, which is patternless (probably faded in preservative). MCZ R-125601 and KU 226528 have darker outlines on the borders of their head scales. KU 226528 also has large dots in a longitudinal paramedian series and no dots in the lateral band. Measurements and other morphological data for the holotype and other examined material are presented in Table 1.

Distribution. *Celestus striatus* is only known from three specimens, two of which were found at Windsor in North-central Jamaica in the Cockpit country, 160 m (Fig. 11). The type locality is simply reported as "West Indies" (Gray 1845; Boulenger 1885).

Ecology and conservation. Little data exist on the ecology of this species. Both the holotype and paratype of *Celestus fowleri* (synonymized herein with *C. striatus*) were collected from bromeliads in the Cockpit region of Jamaica (near Windsor Cave) up to 2.5 m off the ground (Schwartz 1971a), suggesting that it is an arboreal species. *Celestus fowleri* was the first Antillean diploglossid to be found in bromeliads, a niche "virtually unoccupied by Antillean reptiles" (Schwartz 1971a). At the time of collection, Schwartz (1971a) had little doubt that the bromeliad was a diurnal retreat for the species and mentioned that it was possible that this species was in fact terrestrial, only using the bromeliads as a refuge during the day. This was followed by the caveat that there was in fact no evidence to support this hypothesis. Like Crombie (1999), one of us (SBH) has never seen this species despite examining hundreds of bromeliads during repeated visits to the type locality and many other places in the Cockpits. In the 1990s, researchers studying the bromeliad crab at Windsor encountered and photographed *C. striatus* in a bromeliad at Windsor (R. Diesel, pers. comm. to SBH) and sent photographs to one of us (SBH), reproduced here (Fig. 34). The species is likely extant but very rare.

We consider the conservation status of *Celestus striatus* to be Critically Endangered B1ab(iii) because of its extreme rarity and greatly restricted distribution, probably related to some aspect of human impact (habitat alteration, introduced predators, etc.), based on IUCN Redlist criteria (IUCN 2023). Currently, IUCN 2023 considers this species to be Vulnerable D2 because "this species is endemic to Jamaica, known only from around the type locality, Windsor Cave, in the Cockpit Country, Trelawny Parish; at an elevation near 160 m asl (Schwartz 1970; Henderson & Powell 2009). The species may occur at other localities in the Cockpits; however, exhaustive searches in bromeliads by herpetologists through the region have not yet yielded any records (S.B. Hedges pers. comm. 2015)." Studies are needed to determine the health and extent of remaining populations and threats to the survival of the species.

Reproduction. No data on reproduction are available for this species.

Etymology. The species name (*striatus*) is a masculine Latin adjective meaning "striate," in reference to the scales of this species, which were noted by Gray (1839) as striate but not keeled.

Remarks. As we summarized elsewhere (Schools & Hedges 2021), the taxonomic history of this species is confusing because it has been synonymized with other species including *Celestus occiduus* (as was *C. hewardi*) and *Comptus stenurus*. It differs morphologically from other species in multiple characters (see Diagnosis section) and we retain its classification as an independent species, clearly part of the Jamaican radiation of *Celestus*. It is also the type species of the genus *Celestus*.

Remarkable is the fact that this important taxon, which carries the generic and subfamilial names and was known from a single specimen for most of the last two centuries, has gone from essential obscurity to being extant. Several factors have contributed to this delay or solved the mystery. First, the species was probably limited in distribution or rarely encountered even before introduction of the mongoose. An arboreal species would have been more difficult to collect than terrestrial species like *C. occiduus* or *C. crusculus*. Secondly, Straham & Schwartz (1977) considered *C. striatus* to be Central American based on its unusual scalation, which was an error stemming from a misinterpretation of a photograph of the type specimen (see Schools & Hedges 2021). The third factor, and the one that definitively solved this mystery, was the collection of DNA sequences from these old specimens (holotypes of *C. striatus* and *C. fowleri*), which was made possible by forward-thinking museums and curators, who permitted this research to take place.

FIGURE 33. (A–F) *Celestus striatus* (BMNH 1946.8.8.3, holotype), SVL 145 mm.

FIGURE 34. (A–B) *Celestus striatus* (vouchers not available), in life. From near Windsor Cave, Trelawny Parish, Jamaica. Photos by Rudolf Diesel.

The type specimen now has no discernable pattern, possibly because it has been in preservative for nearly two centuries. Gray (1839, 1845) described it as "silvery" and "bleached," and named it "The Golden Galliwasp." However, he also noted that it was "brown-varied" and "sides brown-spotted." Boulenger's (1885) illustration shows distinct side barring and thin cross-bands across the back, consistent with Gray's description. Because Boulenger listed synonyms and additional specimens of *C. striatus* (unsupported by us), the pattern shown in his illustration might be a composite of multiple specimens of different species. However, the habitus of the lizard in the illustration resembles the type specimen and the simplest explanation is that in life the animal originally had a pale ground color (tan or golden) with the markings exactly as shown by Boulenger (1885), and that all remnants of pattern have since

faded with time. The photograph in life of *Celestus striatus* (Fig. 34) is clear only at the anterior end of the lizard, but it shows a golden tan ground color with dark brown marks on the side of the head and thin dark brown crossbands or chevrons not unlike those illustrated by Boulenger.

Herein, we synonymize *Celestus fowleri* with *Celestus striatus* based on genetic and morphological data. The original specimen of *Celestus fowleri* collected was a juvenile in 1961, prior to the collection of the holotype in 1970 (Schwartz 1971a). This extended time between collection dates led Schwartz (1971a) to speculate that *C. fowleri* was, "extremely uncommon, remarkably elusive, or ecologically or altitudinally restricted." As members of the "long-legged" group of Jamaican lizards, Schwartz (1971a) suspected that a close relationship existed between *Celestus duquesneyi*, *C. fowleri*, and *C. hewardi*, suggesting that *C. duquesneyi* and *C. fowleri* were either ecological or geographic isolates of *C. hewardi*.

The holotypes of *Celestus striatus* (BMNH 1946.8.8.3) and *Celestus fowleri* (MCZ R-125601) are included in our genetic dataset and their sequences are similar, indicating that they belong to a single species, *C. striatus*. This is not surprising because of their similar morphology, including scale counts, showing adaptations (long limbs and long digits) for climbing trees. The species has significant support in both Bayesian and ML likelihood analyses at the crown node of the species and the stem node that places it as the closest relative of the much larger *C. occiduus*. Based on our timetree (Fig. 4), *C. striatus* diverged from its closest relative 3.49 Ma, consistent with typical species of vertebrates (> 0.7 Ma; Hedges *et al.* 2015). *Celestus striatus* was recognized as a distinct species by our ASAP analysis.

Genus *Comptus* Schools & Hedges, 2021

Caribbean Rough-scaled Forest Lizards
(Fig. 35)

Type species. *Diploglossus stenurus* Cope, 1862:188.

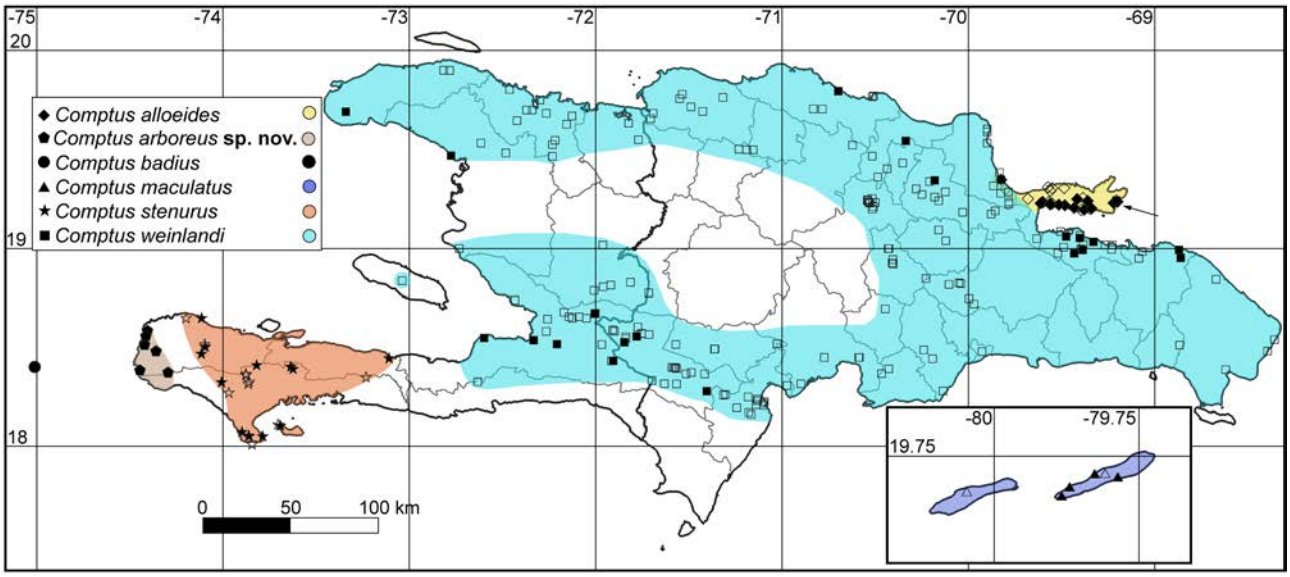

FIGURE 35. Map showing the distribution of *Comptus*. The black arrow indicates an instance of sympatry between *C. alloeides* and *C. weinlandi*. Hollow symbols indicate unexamined records assignable to species.

Diagnosis. Species of *Comptus* have (1) a dorsal pattern of absent/irregular dots/dots in series/dots in chevrons/mottled/chevrons, (2) head markings absent/present, (3) markings in the longitudinal paramedian area absent/present, (4) dots arranged in bars in the lateral band absent/present, (5) a maximum SVL of 60.1–161 mm, (6) ventral scale rows, 81–110, (7) midbody scale rows, 36–45, (8) total lamellae on one hand, 32–58, (9) total strigae on ten scales, 143–323, (10) relative length of all digits on one hindlimb, 23.4–39.7 %, (11) relative distance between the angled subocular and mouth, 0.403–1.12 %, (12) relative eye length, 2.83–4.43 %, (13) relative forelimb length, 19.3–27.9 %, (14) relative ear width, 0.451–2.18 %, (15) relative rostral height, 1.46–2.42 %, (16) relative head

length, 14.7–20.0 %, (17) relative mental width, 0.840–1.95 %, (18) relative postmental width, 2.32–3.05 %, (19) relative cloacal width, 8.29–10.3 %, (20) relative prefrontal width, 3.95–5.47 %, (21) relative largest supraocular width, 2.23–3.49 %, (22) relative longest finger length, 4.14–7.19 %, (23) relative distance between the ear and eye, 6.03–9.51 %, (24) relative head width, 62.8–82.2 %, (25) relative frontal width, 58.8–86.5 %, (26) relative nasal height, 0.863–1.32 %, (27) relative angled subocular height, 0.568–1.33 %, (28) relative distance between the eye and naris, 4.38–6.77 %, (29) relative canthal iii length, 1.37–2.42 %, (30) relative angled subocular width, 1.64–3.36 %, and (31) relative nasal length, 1.39–2.03 %.

Content. Six species (Table 3): *Comptus alloeides*, *C. arboreus* **sp. nov.**, *C. badius*, *C. maculatus*, *C. stenurus*, and *C. weinlandi*.

Distribution. *Comptus* occurs in the Cayman Islands, Navassa Island, and throughout most of Hispaniola, including the associated islets of Ile-a-Vache, Île à Cabrit, and Ile Grande Cayemite.

Comptus alloeides (Schwartz 1964)

Samana Keeled Forest Lizard
(Fig. 36)

Diploglossus stenurus alloeides Schwartz, 1964:18. Holotype: MCZ R-77152, collected by Richard Thomas 6 km E. Sanchez, Samana, Dominican Republic, on 10 October 1963 (19.227, -69.558; 40 m).
Celestus stenurus alloeides—Schwartz & Henderson, 1988:100.
Celestus stenurus alloeides—Schwartz & Henderson, 1991:378.
Celestus stenurus alloeides—Hedges *et al.*, 2019.
Celestus stenurus alloeides—Schools & Hedges, 2021:226.

Material examined (n=44). DOMINICAN REPUBLIC. Samaná. AMNH 27748, John King, nr Samaná, 1924; AMNH 38376–7, William G. Hassler, Samaná, 1929; AMNH 39877–80, William G. Hassler, Samaná, November–December 1929; AMNH 40232, William G. Hassler, Laguna, November 1929; AMNH 40261–2, 40264, 40267–8, William G. Hassler, Samaná, October–December 1929; AMNH 40396, 40402, 40404, William G. Hassler, Samaná, October 1929; AMNH 40980, 40982–3, John King, Samaná, May 1923; KU 226555, 13 km W Samaná, 30 October 1963; KU 226556, 6 km W Samaná, 1 November 1963; KU 226557–60, 8 km W Samaná, 2 November 1963; KU 226561, 13 km W Samaná, 2 November 1963; KU 226562, 6 km E Sanchez, 30 October 1963; KU 226563, 11 km E Sanchez, 30 October 1963; KU 226564–9, 14 km E Sanchez, 2 November 1963; MCZ R-44398, Philip J. Darlington, Jr., Sanchez, 1–31 July 1938; MCZ R-77152, Richard Thomas, 6 km E. Sanchez, 10 October 1963; USNM 61931, near Laguna, 10 March 1919; USMN 61932, near Laguna, 7 March 1919; USNM 62363–4, Sanchez, 12 August 1919; USNM 66760–1; USNM 66975–6, Laguna, 6 mi NE of Samaná, Samaná Peninsula, February 1924.
Diagnosis. *Comptus alloeides* has (1) a dorsal pattern of irregular dots/dots in series/dots in chevrons, (2) head markings absent/present, (3) markings in the longitudinal paramedian area present, (4) dots arranged in bars in the lateral band absent/present, (5) an adult SVL of 124–161 mm, (6) ventral scale rows, 84–109, (7) midbody scale rows, 36–44, (8) total lamellae on one hand, 43–58, (9) total strigae on ten scales, 237–323, (10) relative length of all digits on one hindlimb, 23.8–35.2 mm, (11) relative distance between the angled subocular and mouth, 0.587–1.03 mm, (12) relative eye length, 3.16–3.90 mm, (13) relative forelimb length, 21.4–25.3 mm, (14) relative ear width, 0.710–1.83 mm, (15) relative rostral height, 1.52–1.99 mm, (16) relative head length, 15.5–20.0 mm, (17) relative mental width, 0.840–1.95 mm, (18) relative postmental width, 2.54–2.97 mm, (19) relative cloacal width, 8.86–10.3 mm, (20) relative prefrontal width, 4.25–5.07 mm, (21) relative largest supraocular width, 2.66–2.95 mm, (22) relative longest finger length, 5.32–5.95 mm, (23) relative distance between the ear and eye, 6.43–8.53 mm, (24) relative head width, 70.0–74.2 mm, (25) relative frontal width, 64.9–75.1 mm, (26) relative nasal height, 0.863–1.30 mm, (27) relative angled subocular height, 0.733–1.23 mm, (28) relative distance between the eye and naris, 4.82–6.77 mm, (29) relative canthal iii length, 1.60–2.20 mm, (30) relative angled subocular width, 2.26–3.01 mm, and (31) relative nasal length, 1.46–2.03 mm. The species stem time is 1.46 Ma and no genetic data are available to estimate the species crown time (Fig. 4).

We distinguish *Comptus alloeides* from the other species of *Comptus* based on a complex of traits. From *Comptus arboreus* **sp. nov.**, we distinguish *C. alloeides* by the adult SVL (124–161 versus 93.2–123), the total strigae on ten scales (237–323 versus 143–207), the relative length of digits on one hindlimb (23.8–35.2 versus 37.4–39.7), and

the relative longest finger length (5.32–5.95 versus 6.01–6.37). From *C. badius*, we distinguish *C. alloeides* by the adult SVL (124–161 versus 78.2–99.1), the relative postmental width (2.54–2.97 versus 2.39), the relative longest finger length (5.32–5.95 versus 4.38–5.04), and the relative head width (70.0–74.2 versus 62.8–69.3). From *C. maculatus*, we distinguish *C. alloeides* by the dorsal pattern (irregular dots/dots in series/dots in chevrons versus absent/chevrons), the adult SVL (124–161 versus 60.1–81.3), the total lamellae on one hand (43–58 versus 32–37), the total strigae on ten scales (237–323 versus 149–201), and the relative longest finger length (5.32–5.95 versus 4.14–5.01). From *C. stenurus*, we distinguish *C. alloeides* by the total strigae on ten scales (237–323 versus 176–234). From *C. weinlandi*, we distinguish *C. alloeides* by the total strigae on ten scales (237–323 versus 167–236).

Description of holotype. MCZ R-77152. An adult male; SVL 115 mm; tail nearly cylindrical, broken in life midway, regenerated, 113 mm (98.3% SVL); axilla-to-groin distance 63.6 mm (55.3% SVL); forelimb length 25.7 mm (22.3% SVL); hindlimb length 38.2 mm (33.2% SVL); head length 18.9 mm (16.4% SVL); head width 13.8 mm (12.0% SVL); head width 73.0% head length; diameter of orbit 4.34 mm (3.77% SVL); horizontal diameter of ear opening 1.58 mm (1.37% SVL); vertical diameter of ear opening 1.39 mm (1.21% SVL); length of all toes on one foot 34.0 mm (29.6% SVL); shortest distance between angled subocular and lip 0.96 mm (0.835% SVL); shortest distance between the ocular and auricular openings 7.82 mm (6.80% SVL); longest finger length 7.48 mm (6.50% SVL); largest supraocular width 2.89 mm (2.51% SVL); cloacal width 11.4 mm (9.91% SVL); mental width 2.17 mm (1.89% SVL); postmental width 3.21 mm (2.79% SVL); prefrontal width 5.00 mm (4.35% SVL); frontal width 74.9% frontal length; nasal height 1.51 mm (1.31% SVL); angled subocular height 1.07 mm (0.930% SVL); shortest distance between the eye and naris 5.05 mm (4.39% SVL); canthal iii width 2.02 mm (1.76% SVL); angled subocular width 2.00 mm (1.74% SVL); nasal width 2.06 mm (1.79% SVL); rostral 1.53X as wide as high, visible from above, not in contact with nasals, in contact with 1st supralabial and anterior internasal (left)/(right); anterior internasals are narrower than posterior ones; frontonasals and prefrontal fused into a single large plate with a slightly concave posterior margin, wider than long, bordered by posterior internasals, 1st loreals, canthal iii (left), 1st and 2nd median oculars, and the frontal; frontal longer than wide; a pair of frontoparietals, separated by the posterior prolongation of the frontal and the interparietal plate; interparietal plate much smaller than parietals and separating them, posteriorly touching the interoccipital, which is approximately as wide as long; parietal separated from supraoculars by 1st and 2nd temporals and frontoparietal (left)/1st and 2nd temporals and frontoparietal (1st fused with FP) (right); nasal single; nostril above suture between 1st and 2nd supralabials (left)/(right); 1 postnasal (left)/(right); 2 loreals (left)/(right); 1st loreal higher than wide (left)/(right), in contact with postnasal, posterior internasal, prefrontal/frontonasal complex, canthal iii, 2nd loreal, and 3rd–4th supralabials (left)/postnasal, posterior internasal, prefrontal/frontonasal complex, median ocular 1, canthal iii, 2nd loreal, and 3rd–4th supralabials(right); 2nd loreal shorter than 1st, approximately as high as wide (left)/(right), excluded from contact with supraocular by canthal iii (left)/(right); final loreal posteriorly bordering the upper and lower preoculars (left)/(right); canthal iii wider than high (left)/(right), contacting 1st median ocular, anterior supraciliary, upper preocular, prefrontal/frontonasal complex, and 1st and 2nd loreals (left)/1st median ocular, anterior supraciliary, upper preocular, and 1st and 2nd loreals (right); 10 median oculars (left)/(right), 1st and 2nd contacting the prefrontal (left)/(right); 1 upper preocular (left)/(right); an irregular anterior supraciliary (left)/(right); 6 lateral oculars (left)/(right); 5 (left)/4 (1st fused with FP) (right) temporals; 2 suboculars (left)/(right); posterior subocular large and elongate (left)/(right); anterior subocular small (left)/(right); 9 supralabials (left)/(right), 6 to level below center of eye (left)/(right); 9 infralabials (left)/(right), 6 to level below center of eye (left)/(right); mental small, followed by a single, slightly larger postmental; 4 pairs of enlarged chin shields, followed by 1 pair of reduced chin shields; 1st pair in contact with one another anteriorly, posteriorly separated by one scale; 2nd–5th pairs separated by 1–5 scales; 92 transverse rows of dorsal scales from interoccipital to base of tail; 92 transverse rows of ventral scales from mental to vent; 39 scales around midbody; 5 digits; finger lengths 3>4>2>5>1; 12 lamellae under longest finger (left)/(right); 38 total lamellae on one hand; toe lengths 4>3>5>2>1; 17 (left)/18 (right) lamellae under longest toe; strigae and median keel dorsal body and caudal scales; faint striations ventral scales; 195 total strigae counted on ten scales.

Color (in alcohol): dorsal surface of head golden tan with some slightly darker brown spots and darker brown areas on scale borders; lateral surfaces of head grading from golden tan to cream with some darker brown areas, especially on the labials and a darker lateral band beginning anterior to the eye; dorsal surfaces of the body are gray-brown with two darker longitudinal paramedian lines that extend halfway down the back, other areas of the back have a regular spotted pattern arranged into chevrons; dorsal surface of tail gray-brown to yellow (on regenerated section); lateral areas grade from gray-brown to white with dark brown and off-white spots arranged in bars; dorsal

surfaces of the limbs are bronze with paler spots on them; lateral and ventral areas of the limbs fade to cream; ventral surfaces of the head, body, and tail are pale cream, patternless.

FIGURE 36. (A–F) *Comptus alloeides* (MCZ R-77152, holotype), SVL 115 mm.

Variation. The examined material overall resembles the holotype in dorsal pattern with all specimens having a pattern of enlarged dots, many of which are continuations of the longitudinal paramedian lines or arranged in broken chevrons. All specimens show longitudinal paramedian lines with the most reduced form occurring in AMNH 40232. The majority of specimens show patternless heads with the holotype, KU 226562, and KU 226555 showing some darker outlines on head scale borders and KU 226563, MCZ R-44398, and USNM 66975 showing irregular, darker markings on their head. The majority of specimens show dots arranged in bars in the lateral band whereas this trait is absent or only present anteriorly in a minority of specimens. Measurements and other morphological data for the holotype and other examined material are presented in Table 1.

Distribution. *Comptus alloeides* is known from Peninsula de Samaná and associated islets in the Bahía de Samaná, where it has been collected at elevations of 0–330 m (Fig. 35). It has an extent of occurrence of ~790 km^2.

Ecology and conservation. SBH and Richard Thomas collected this species under rocks and among rotting coconut husks and fronds under palm trees (6 km SSW Las Galeras). As with other species confused in the past with *Comptus stenurus*, this species appears to be tolerant of some habitat disturbance.

We consider the conservation status of *Comptus alloeides* **sp. nov.** to be Least Concern, primarily because it has been encountered frequently in the past, based on IUCN Redlist criteria (IUCN 2023). However, it has a relatively small range, which is of concern. Conversion of forests to agricultural and urban areas will reduce available habitat. Also, introduced predators, including the mongoose and black rats, likely prey upon it. Therefore, studies are needed to determine the health and extent of the populations, and threats to the survival of the species.

Reproduction. No data on reproduction are available for this species.

Etymology. The species name *alloeides* is derived from the Greek words *alloe-* (meaning "of a different kind") and *eidos* (meaning "form or resemblance"). As noted in the original description (Schwartz 1964), the name likely alludes to the prominent longitudinal paramedian lines of this species distinguishing this taxon from its close relatives.

Remarks. Large numbers of specimens of this species exist in museum collections. *Comptus alloeides* is included in our genetic dataset and is placed as the closest relative to *C. weinlandi* with significant support in ML and Bayesian analyses at the stem node. Based on our timetree (Fig. 4), *C. alloeides* diverged from its closest relative 1.46 Ma, consistent with typical species of vertebrates (> 0.7 Ma; Hedges *et al.* 2015). We further recognize it as a distinct species because of the diagnostic trait that separates it from *C. weinlandi* (the total strigae on ten scales). This species is also sympatric with *C. weinlandi* at one locality on the Samana Peninsula. Although not diagnostic, the prominent longitudinal paramedian lines that were used to originally identify this species are apparent in all specimens. *Comptus alloeides* was recovered as conspecific with *Comptus weinlandi* in our ASAP analysis.

***Comptus arboreus* sp. nov.**
Tiburon Keeled Forest Lizard
(Fig. 37–38)

Celestus stenurus—Schwartz & Henderson, 1991:378 (part, from ca. 5 km S Dame Marie).

Holotype. ANSP 38540, an adult from Belandier (5.0 km N Dame Marie), collected by S. Blair Hedges and Richard Thomas on 26 July 2010 (18.58568, -74.40762; 24 m).

Paratypes (n=8). HAITI. Grand'Anse. ANSP 38538–39, an adult, S. Blair Hedges and Richard Thomas, Belandier (5.0 km N Dame Marie [turn back locality]), 26 July 2010; ANSP 38543, S. Blair Hedges and Richard Thomas, 1.5 km N Carcasse, 26 July 2010; KU 227117–8, ca 5 km (airline) S Dame Marie, 13 March 1966; SBH 191945–6, 0.8 km E of Dame Marie, 29 May 1991; SBH 269065, juvenile, Bourdon (9.2 km E Ause D'Hainalt).

Diagnosis. *Comptus arboreus* **sp. nov.** has (1) a dorsal pattern of dots in series/dots in chevrons, (2) head markings absent/present, (3) markings in the longitudinal paramedian area present, (4) dots arranged in bars in the lateral band present, (5) an adult SVL of 93.2–123 mm, (6) ventral scale rows, 102–110, (7) midbody scale rows, 41–44, (8) total lamellae on one hand, 48–54, (9) total strigae on ten scales, 143–207, (10) relative length of all digits on one hindlimb, 37.4–39.7 %, (11) relative distance between the angled subocular and mouth, 0.723–0.923 %, (12) relative eye length, 3.46–4.18 %, (13) relative forelimb length, 24.1–25.3 %, (14) relative ear width,

1.22–1.60 %, (15) relative rostral height, 1.53–1.85 %, (16) relative head length, 15.5–18.0 %, (17) relative mental width, 1.54–1.74 %, (18) relative postmental width, 2.95–3.01 %, (19) relative cloacal width, 9.05–9.51 %, (20) relative prefrontal width, 4.50–4.82 %, (21) relative largest supraocular width, 2.61–3.05 %, (22) relative longest finger length, 6.01–6.37 %, (23) relative distance between the ear and eye, 6.45–7.03 %, (24) relative head width, 71.7–80.3 %, (25) relative frontal width, 62.6–71.4 %, (26) relative nasal height, 1.03–1.20 %, (27) relative angled subocular height, 0.929–0.992 %, (28) relative distance between the eye and naris, 5.11–5.52 %, (29) relative canthal iii length, 1.86–1.94 %, (30) relative angled subocular width, 2.82–3.28 %, and (31) relative nasal length, 1.47–1.99 %. The species stem time is 2.38 Ma and the species crown time is 0.02 Ma (Fig. 4).

FIGURE 37. (A–F) *Comptus arboreus* **sp. nov.** (ANSP 38540, holotype), SVL 116 mm.

FIGURE 38. *Comptus arboreus* **sp. nov.** (ANSP 38538, SBH 269043), SVL 123 mm, in life. From Belandier, Grand'Anse Department, Haiti. Photo by SBH.

Comptus arboreus differs from all other species of the genus in having the largest relative length of digits on one hindlimb (37.4–39.7).

From *Comptus alloeides*, we distinguish *C. arboreus* **sp. nov.** by the adult SVL (93.2–123 versus 124–161), the total strigae on ten scales (143–207 versus 237–323), the relative length of digits on one hindlimb (37.4–39.7 versus 23.8–35.2), and the relative longest finger length (6.01–6.37 versus 5.32–5.95). From *C. badius*, we distinguish *C. arboreus* **sp. nov.** by the dorsal pattern (dots in series/dots in chevrons versus irregular dots/mottled), the total lamellae on one hand (48–54 versus 40–45), the relative length of digits on one hindlimb (37.4–39.7 versus 23.4–33.9), the relative forelimb length (24.1–25.3 versus 19.6–23.0), the relative mental width (1.54–1.74 versus 1.38), the relative postmental width (2.95–3.01 versus 2.39), the relative longest finger length (6.01–6.37 versus 4.38–5.04), the relative head width (71.7–80.3 versus 62.8–69.3), and the relative angled subocular width (2.82–3.28 versus 1.91–2.31). From *C. maculatus*, we distinguish *C. arboreus* **sp. nov.** by the dorsal pattern (dots in series/dots in chevrons versus absent/chevrons), the adult SVL (93.2–123 versus 60.1–81.3), the total lamellae on one hand (48–54 versus 32–37), the relative length of digits on one hindlimb (37.4–39.7 versus 24.8–27.0), the relative forelimb length (24.1–25.3 versus 19.3–21.6), the relative postmental width (2.95–3.01 versus 2.32–2.86), the relative longest finger length (6.01–6.37 versus 4.14–5.01), the relative width of canthal iii (1.86–1.94 versus 1.73–1.85), and the relative angled subocular width (2.82–3.28 versus 2.25–2.52). From *C. stenurus*, we distinguish *C. arboreus* **sp. nov.** by the relative length of digits on one hindlimb (37.4–39.7 versus 29.2–37.1) and the relative angled subocular height (0.929–0.992 versus 0.697–0.893). From *C. weinlandi*, we distinguish *C. arboreus* **sp. nov.** by the relative length of digits on one hindlimb (37.4–39.7 versus 24.5–36.5) and the relative postmental width (2.95–3.01 versus 2.57–2.91).

Description of holotype. ANSP 38540. An adult; SVL 116 mm; tail nearly cylindrical, tip regenerated, 54.4 mm (46.9% SVL); axilla-to-groin distance 65.0 mm (56.0% SVL); forelimb length 28.0 mm (24.1% SVL); hindlimb length 38.6 mm (33.3% SVL); head length 19.9 mm (17.2% SVL); head width 14.5 mm (12.5% SVL); head width 72.9% head length; diameter of orbit 4.37 mm (3.77% SVL); horizontal diameter of ear opening 1.78 mm (1.53% SVL); vertical diameter of ear opening 1.33 mm (1.15% SVL); length of all toes on one foot 46.0 mm (39.7% SVL); shortest distance between angled subocular and lip 0.90 mm (0.776% SVL); shortest distance between the ocular and auricular openings 7.48 mm (6.45% SVL); longest finger length 6.97 mm (6.01% SVL); largest supraocular width 3.03 mm (2.61% SVL); cloacal width 10.5 mm (9.05% SVL); mental width 1.89 mm (1.63% SVL); postmental

width 3.49 mm (3.01% SVL); prefrontal width 5.22 mm (4.50% SVL); frontal width 66.5% SVL; nasal height 1.20 mm (1.03% SVL); angled subocular height 1.09 mm (0.940% SVL); shortest distance between the eye and naris 6.29 mm (5.42% SVL); canthal iii width 2.18 mm (1.88% SVL); angled subocular width 3.38 mm (2.91% SVL); nasal width 1.71 mm (1.47% SVL); rostral 1.74X as wide as high, visible from above, not in contact with nasals, in contact with 1st supralabial and anterior internasal (left)/(right); anterior internasals are narrower than posterior ones; frontonasals and prefrontal fused into a single large plate with a concave posterior margin, wider than long, bordered by posterior internasals, 1st loreals, 1st median oculars, and the frontal; frontal longer than wide; a pair of frontoparietals, separated by the posterior prolongation of the frontal and the interparietal plate; interparietal plate smaller than parietals and separating them, posteriorly touching the interoccipital, which is wider than long; parietal separated from supraoculars by 1st and 2nd temporals and frontoparietal (left)/(right); nasal single; nostril above suture between 1st and 2nd supralabials (left)/(right); 1 postnasal (left)/(right); 2 loreals (left)/(right); 1st loreal higher than wide (left)/(right), in contact with postnasal, posterior internasal, prefrontal/frontonasal complex, 1st median ocular, canthal iii, 2nd loreal, and 3rd–4th supralabials (left)/(right); 2nd loreal shorter than 1st, approximately as high as wide (left)/(right), excluded from contact with supraocular by canthal iii (left)/(right); 2nd loreal posteriorly bordering the upper and lower preoculars (left)/(right); canthal iii wider than high (left)/(right), contacting 1st median ocular, anterior supraciliary, upper preocular, and 1st and 2nd loreals (left)/(right); 10 (left)/9 (right) median oculars, 1st contacting the prefrontal (left)/(right); 2 upper preoculars (left)/(right); an irregular anterior supraciliary (left)/(right); 8 (left)/7 (right) lateral oculars; 5 temporals (left)/(right); 2 (left)/(right) suboculars (left)/(right); posterior subocular large and elongate (left)/(right); anterior subocular small (left)/(right); 9 supralabials (left)/(right), 6 to level below center of eye (left)/(right); mental small, followed by a single, larger postmental; 4 pairs of enlarged chin shields, followed by 1 pair of reduced chin shields; 1st pair in contact with one another anteriorly, posteriorly separated by one scale; 2nd–5th pairs separated by 1–5 scales; 103 transverse rows of dorsal scales from interoccipital to base of tail; 105 transverse rows of ventral scales from mental to vent; 42 scales around midbody; 5 digits; finger lengths 3>4>5>2>1; 12 lamellae under longest finger (left)/(right); 49 total lamellae on one hand; toe lengths 4>3>5>2>1; 19 (left)/20 (right) lamellae under longest toe; dorsal body and caudal scales striate with a median keel; 207 total strigae counted on ten scales.

Color (in alcohol): dorsal surface of head dark tan, patternless; lateral surfaces of head grading from dark tan to yellow-cream, some darker spotting behind the eye and on the supralabial scales; dorsal surfaces of the body are medium brown with six lines of broken spots that extend down the length of the body, the median two lines made of large dark brown spots, outside of those are lines of small dark brown spots, outside of those are two lines of small gray spots; dorsal surface of tail the same as the body, with outer lines of dark brown dots joining to form thin, dark brown lines across the width of the tail; lateral areas grade from medium brown to yellow-cream with lines of dark brown and gray-white dots that extend down the sides and fade before the venter; dorsal surfaces of the limbs are dark brown with small off-white spots; lateral and ventral areas of the limbs fade to yellow-cream, patternless; ventral surfaces of the head, body, and tail are yellow-white with gray mottling on the chin shields.

Variation. The examined material resembles the dorsal pattern of the holotype with most specimens showing large dots that are continuations of the longitudinal paramedian series. In some specimens, the large dorsal dots are arranged in broken chevrons. Most specimens have patternless heads except for ANSP 38543, which has several irregular, darker areas on the head scales. The dorsal color of all is pale tan with markings in a longitudinal paramedian series that extend down the body. No darker lateral band is present; however, rows of dark brown and pale cream dots extend down the sides. In the majority of specimens, the dots in the lateral band are arranged in bars. Measurements and other morphological data for the holotype and other examined material are presented in Table 1.

Distribution. *Comptus arboreus* **sp. nov.** is known only from the western tip of the Tiburon Peninsula of Haiti, where it has been collected at elevations of 20–1100 m in the Grand'Anse and Sud departments (Fig. 35).

Ecology and conservation. Little is known of the ecology of this species except that two individuals were found in a cacao grove among rotting cacao and palm husks and fronds. As with other species confused in the past with *Comptus stenurus*, this species appears to be tolerant of some habitat disturbance.

We consider the conservation status of *Comptus arboreus* **sp. nov.** to be Least Concern, primarily because it has been encountered frequently in the past, based on IUCN Redlist criteria (IUCN 2023). However, it has a relatively small range, which is of concern. Conversion of forests to agricultural and urban areas will reduce available habitat, and forests in general are under severe threat in Haiti (Hedges *et al*. 2018). Also, introduced predators, including the

mongoose and black rats, likely prey on it. Therefore, studies are needed to determine the health and extent of the populations, and threats to the survival of the species.

Reproduction. No data on reproduction are available for this species.

Etymology. The species name (*arboreus*) is a masculine adjective meaning "of trees," in reference to the speculative arboreal habits of this species, given its long digits.

Remarks. *Comptus arboreus* **sp. nov.** is included in our genetic dataset and has significant support in both Bayesian and ML likelihood analyses at the crown node of the species and the stem node that places it as the closest relative to *C. stenurus*. Based on our timetree (Fig. 4), *C. arboreus* **sp. nov.** diverged from its closest relative 2.38 Ma, consistent with typical species of vertebrates (> 0.7 Ma; Hedges *et al.* 2015). *Comptus arboreus* **sp. nov.** was recognized as a distinct species by our ASAP analysis.

Comptus badius (Cope 1868)

Navassa Forest Lizard
(Fig. 39–40)

Celestus badius Cope, 1868:126. Syntypes: USNM 25817–8, collected by W. J. Rasin on Navassa Island (18.4, -75.0).
Celestus badius—Barbour, 1930:99.
Celestus badius—Barbour, 1935:123.
Celestus badius—Barbour, 1937:139.
Diploglossus badius—Schwartz, 1964:38.
Celestus costatus badius—Schwartz & Henderson, 1988:94.
Celestus badius—Powell, 1999:4.
Celestus badius—Hedges *et al.*, 2019:16.
Comptus badius—Schools & Hedges, 2021:226.
Comptus badius—Landestoy *et al.*, 2022: 205.

Material examined (n=6). NAVASSA ISLAND. AMNH 17079, Rollo H. Beck, 1917; AMNH 120486, Craig Ferris, July 1981; AMNH 120487, Craig Ferris, 20 July 1981; USNM 25817–8, W. J. Rasin; USNM 157378.

Diagnosis. *Comptus badius* has (1) a dorsal pattern of irregular dots/mottled, (2) head markings absent/present, (3) markings in the longitudinal paramedian area present, (4) dots arranged in bars in the lateral band absent/present, (5) an adult SVL of 78.2–99.1 mm, (6) ventral scale rows, 94–109, (7) midbody scale rows, 39–44, (8) total lamellae on one hand, 40–45, (9) total strigae on ten scales, 203–241, (10) relative length of all digits on one hindlimb, 23.4–33.9 %, (11) relative distance between the angled subocular and mouth, 0.403–0.866 %, (12) relative eye length, 2.83–3.53 %, (13) relative forelimb length, 19.6–23.0 %, (14) relative ear width, 1.34–1.75 %, (15) relative rostral height, 1.83–2.42 %, (16) relative head length, 14.7–18.3 %, (17) relative mental width, 1.38 %, (18) relative postmental width, 2.39 %, (19) relative cloacal width, 7.92–9.30 %, (20) relative prefrontal width, 4.59–5.47 %, (21) relative largest supraocular width, 2.57–2.74 %, (22) relative longest finger length, 4.38–5.04 %, (23) relative distance between the ear and eye, 6.99–9.51 %, (24) relative head width, 62.8–69.3 %, (25) relative frontal width, 71.3–86.5 %, (26) relative nasal height, 0.999–1.06 %, (27) relative angled subocular height, 0.691–1.33 %, (28) relative distance between the eye and naris, 4.96–5.24 %, (29) relative canthal iii length, 1.45–2.42 %, (30) relative angled subocular width, 1.91–2.31 %, and (31) relative nasal length, 1.54–1.82 %. The species stem time is 3.52 Ma and the species crown time is 0.0 Ma (Fig. 4).

Comptus badius has a smaller relative head width than all other species of the genus (62.8–69.3). Notably, this species also has the most reduced keels (to the point of complete absence) of the genus.

From *Comptus alloeides*, we distinguish *C. badius* by the adult SVL (78.2–99.1 versus 124–161), the relative postmental width (2.39 versus 2.54–2.97), the relative longest finger length (4.38–5.04 versus 5.32–5.95), and the relative head width (62.8–69.3 versus 70.0–74.2). From *C. arboreus* **sp. nov.**, we distinguish *C. badius* by the dorsal pattern (irregular dots/mottled versus dots in series/dots in chevrons), the total lamellae on one hand (40–45 versus 48–54), the relative length of digits on one hindlimb (23.4–33.9 versus 37.4–39.7), the relative forelimb length (19.6–23.0 versus 24.1–25.3), the relative mental width (1.38 versus 1.54–1.74), the relative postmental width (2.39 versus 2.95–3.01), the relative longest finger length (4.38–5.04 versus 6.01–6.37), the relative head width (62.8–69.3 versus 71.7–80.3), and the relative angled subocular width (1.91–2.31 versus 2.82–3.28). From *C. maculatus*, we distinguish *C. badius* by the dorsal pattern (irregular dots/mottled versus absent/chevrons), the total lamellae on

one hand (40–45 versus 32–37), the total strigae on ten scales (203–241 versus 149–201), the relative mental width (1.38 versus 1.69–1.85), and the relative head width (62.8–69.3 versus 69.6–80.0). From *C. stenurus*, we distinguish *C. badius* by the dorsal pattern (irregular dots/mottled versus dots in series/dots in chevrons), the adult SVL (78.2–99.1 versus 121–146), the total lamellae on one hand (40–45 versus 47–57), the relative mental width (1.38 versus 1.52–1.78), the relative postmental width (2.39 versus 2.61–3.05), the relative longest finger length (4.38–5.04 versus 5.89–7.19), and the relative head width (62.8–69.3 versus 70.2–74.2). From *C. weinlandi*, we distinguish *C. badius* by the adult SVL (78.2–99.1 versus 101–133), the relative mental width (1.38 versus 1.41–1.90), the relative postmental width (2.39 versus 2.57–2.91), the relative longest finger length (4.38–5.04 versus 5.08–6.31), and the relative head width (62.8–69.3 versus 73.6–82.2).

Description of syntype. USNM 25818. An adult; SVL 99.1 mm; tail nearly cylindrical, broken, 9.15 mm (9.23% SVL); axilla-to-groin distance 55.7 mm (56.2% SVL); forelimb length 19.7 mm (19.9% SVL); hindlimb length 29.4 mm (29.7% SVL); head length 18.0 mm (18.2% SVL); head width 11.3 mm (11.4% SVL); head width 62.8% head length; diameter of orbit 3.40 mm (3.43% SVL); horizontal diameter of ear opening 1.67 mm (1.69% SVL); vertical diameter of ear opening 1.57 mm (1.58% SVL); length of all toes on one foot 27.1 mm (27.3% SVL); shortest distance between angled subocular and lip 0.61 mm (0.616% SVL); shortest distance between the ocular and auricular openings 7.84 mm (7.91% SVL); longest finger length 4.99 mm (5.04% SVL); largest supraocular width 2.72 mm (2.74% SVL); cloacal width 9.22 mm (9.30% SVL); prefrontal width 4.93 mm (4.97% SVL); frontal width 77.3% frontal length; nasal height 0.99 mm (1.00% SVL); angled subocular height 1.32 mm (1.33% SVL); shortest distance between the eye and naris 5.19 mm (5.24% SVL); canthal iii width 1.44 mm (1.45% SVL); angled subocular width 2.29 mm (2.31% SVL); nasal width 1.53 mm (1.54% SVL); rostral 2.42X as wide as high, visible from above, not in contact with nasals, in contact with 1st supralabial and anterior internasal (left)/(right); anterior internasals are narrower than posterior ones; frontonasals and prefrontal fused into a single large plate with a concave posterior margin, much wider than long, bordered by posterior internasals, 1st loreals, canthal iii, 1st median ocular (and 2nd on the right), and the frontal; frontal longer than wide; a pair of frontoparietals, separated by the posterior prolongation of the frontal and the interparietal plate; interparietal plate smaller than parietals and separating them, posteriorly touching the interoccipital, which is much wider than long; parietal separated from supraoculars by 1st and 2nd temporals and frontoparietal (left)/(right); nasal single; nostril above suture between 1st and 2nd supralabials (left)/(right); 1 postnasal (left)/(right); 2 loreals (left)/(right); 1st loreal higher than wide (left)/(right), in contact with postnasal, posterior internasal, prefrontal/frontonasal complex, canthal iii, 2nd loreal, and 3rd–4th supralabials (left)/(right); 2nd loreal shorter than 1st, approximately as high as wide (left)/(right), excluded from contact with supraocular by canthal iii (left)/(right); final loreal posteriorly bordering the upper and lower preoculars (left)/(right); canthal iii wider than high (left)/(right), contacting 1st median ocular, anterior supraciliary, upper and lower preoculars, prefrontal/frontonasal complex, and 1st and 2nd loreals (left)/(right); 9 (left)/10 (right) median oculars, 1st contacting the prefrontal (left)/1st and 2nd (right); 1 upper preocular (left)/(right); an irregular anterior supraciliary (left)/(right); 6 (left)/5 (right) lateral oculars; 5 temporals (left)/(right); 2 suboculars (left)/(right); posterior subocular large and elongate (left)/(right); anterior subocular small (left)/(right); 8 supralabials (left)/(right), 5 to level below center of eye (left)/(right); 9 infralabials (left)/(right), 5 (left)/5–6(right) to level below center of eye; mental small, followed by a single, larger post mental; 4 pairs of enlarged chin shields; 1st pair in contact with one another; 2nd–4th pairs separated by 1–3 scales; 100 transverse rows of dorsal scales from interoccipital to base of tail; 97 transverse rows of ventral scales from mental to vent; 42 scales around midbody; 5 digits; finger lengths 4>3>2>5>1; 12 (left)/11 (right) lamellae under longest finger; 43 total lamellae on one hand; toe lengths 4>3>5>2>1; 20 lamellae under longest toe (left)/(right); keelless and striate dorsal body and caudal scales; smooth ventral scales; 227 total strigae counted on ten scales.

Color (in alcohol): dorsal surface of head pale tan, patternless; lateral surfaces of head grading from pale tan to creamy yellow with pale brown eye masks; dorsal surfaces of the body are pale tan with faded darker brown markings near the hindlimbs; dorsal surface of tail the same as the body; lateral areas grade from medium brown to creamy yellow with faded, paler mottling; dorsal surfaces of the limbs are medium brown with some paler mottling; lateral and ventral areas of the limbs fade to creamy yellow, patternless; ventral surfaces of the head, body, and tail are creamy yellow, patternless.

Variation. The other material examined was less faded than the syntypes. In all other specimens examined a similar pattern was expressed of dots or mottling down the dorsum and present longitudinal paramedian lines. In AMNH 17079 the dots in the lateral band appeared as bars whereas in the other specimens examined this trait was

expressed as mottling. Measurements and other morphological data for the holotype and other examined material are presented in Table 1.

FIGURE 39. (A–F) *Comptus badius* (USNM 25818, syntype), SVL 99.1 mm.

FIGURE 40. *Comptus badius* (SBH 194991), in life. From Navassa Island, United States. Photo by SBH.

Distribution. *Comptus badius* is distributed on Navassa Island where it has been collected at elevations from near sea level to 70 m (Fig. 35).

Ecology and conservation. No ecological information is associated with the types. However, authors have commented that this species was common on Navassa Island (Thomas 1966; Powell 1999). Thomas (1966) noted that this species was often observed "scurrying" in dead leaves, although he thought this behavior might have been because of the end of the dry season. Powell (1999) also noticed this species abundantly in leaf litter. Powell (1999) noted that he observed *Comptus badius* as early as sunrise but that they became most abundant at 0930–1000 h and stayed active until twilight. Thomas (1966) noted abundant juveniles and gravid females in April. Powell (1999) also noted that juveniles were common when he visited the island in late summer (with several small individuals collected in pitfall traps), leading him to believe that the species had an extended breeding season on Navassa Island, or potentially a bimodal breeding season, peaking both in April and late summer.

Comptus badius has been seen in grassy savannahs, near former human settlements, and climbing rock walls, likely to bask (Powell 1999). A large male was recovered with a partially swallowed earthworm, suggesting that the diet of these lizards consists largely of leaf litter-dwelling invertebrates (Powell 1999). Powell (1999) also studied the differences between the cloacal temperatures of *C. badius* and the corresponding surface temperatures. The cloacal temperatures of two adult lizards were 31.4°C and 32.3°C when taken at 1130 and 1500 h. Cloacal temperatures and the surface temperatures differed little, suggesting that the lizards could thermoconform (Powell 1999). As surface temperatures and deep ground litter temperatures differed, Powell (1999) speculated that the lizards could regulate their body temperatures by moving to different litter depths.

The IUCN Redlist (IUCN 2023) considers the conservation status of *Comptus badius* to be Least Concern because "although the distribution is limited (with an extent of occurrence of 5.28 km^2), the population appears to be stable, there are no current threats, and Navassa is a protected area."

Reproduction. Ovoviviparous. Many gravid females and juveniles were recorded in August (Thomas 1966); Additional juveniles were described as being abundant in late July–early August (Powell 1999).

Etymology. The species name is Latin and translates to "brown" or "chestnut-colored," presumably in reference to the dorsal color of this species.

Remarks. Because of a lack of fresh material, morphological similarities, and relationships between the fauna of Hispaniola and Navassa Island, Schwartz (1964) said "it seems not inappropriate" to consider *Comptus badius* as a subspecies of *Panolopus costatus* (*Celestus costatus badius*). *Comptus badius* was reelevated to a full species by Powell (1999) based on morphological differences and geographic isolation.

Comptus badius is included in our genetic dataset and we show that it is a member of *Comptus*, not *Panolopus* as was once thought when it was treated as a subspecies of "*Celestus*" (=*Panolopus*) *costatus* (Schwartz 1964). It has significant support in both Bayesian and ML likelihood analyses at the crown node and the stem node places it outside of *C. alloeides*, *C. maculatus*, and *C. weinlandi*. Based on our timetree (Fig. 4), *C. badius* diverged from its closest relative 3.52 Ma, consistent with typical species of vertebrates (> 0.7 Ma; Hedges *et al.* 2015). *Comptus badius* was recognized as a distinct species by our ASAP analysis.

Comptus maculatus **(Garman 1888)**

Lesser Cayman Forest Lizard
(Fig. 41–42)

Diploglossus maculatus Garman, 1888:105. Holotype: MCZ R-6231, collected by Charles J. Maynard on Cayman Brac, on 16 May 1845 (19.7, -79.8).
Celestus maculatus—Barbour, 1930:100.
Celestus maculatus—Barbour, 1935:123.
Celestus maculatus—Barbour, 1937:139.
Celestus maculatus—Grant, 1941:41.
Celestus crusculus maculatus—Cousens, 1956:2.
Celestus crusculus maculatus—Schwartz & Henderson, 1991:370.
Celestus maculatus—Hedges *et al.*, 2019.
Comptus maculatus—Schools & Hedges, 2021:226.
Comptus maculatus—Landestoy *et al.*, 2022: 205.

Material examined (n=9). CAYMAN BRAC. ANSP 38507, S. Blair Hedges and Carla Hass, 0.7 km E Hawkesbill Bay on A7 (~10km E West End), 1.7 km E Ashton Reid Drive, 14 April 2003; ANSP 38508–11, S. Blair Hedges and Carla Hass, West End, Tiara Beach Hotel and surrounding area, 15 April 2003; ANSP 38512, S. Blair Hedges and Carla Hass, 1.2 km E of West End, 15 April 2003; MCZ R-6231, Charles J. Maynard, 16 May 1845; SBH 266554, S. Blair Hedges and Carla Hass, West End, Tiara Beach Hotel and surrounding area, 15 April 2003, USNM 107973, 31 March–25 April 1938.

Diagnosis. *Comptus maculatus* has (1) a dorsal pattern of absent/chevrons, (2) head markings absent/present, (3) markings in the longitudinal paramedian area absent/present, (4) dots arranged in bars in the lateral band absent/present, (5) an adult SVL of 60.1–81.3 mm, (6) ventral scale rows, 94–108, (7) midbody scale rows, 37–41, (8) total lamellae on one hand, 32–37, (9) total strigae on ten scales, 149–201, (10) relative length of all digits on one hindlimb, 24.8–27.0 %, (11) relative distance between the angled subocular and mouth, 0.556–0.849 %, (12) relative eye length, 3.51–3.91 %, (13) relative forelimb length, 19.3–21.6 %, (14) relative ear width, 0.993–1.70 %, (15) relative rostral height, 1.67–1.88 %, (16) relative head length, 16.6–18.3 %, (17) relative mental width, 1.69–1.85 %, (18) relative postmental width, 2.32–2.86 %, (19) relative cloacal width, 8.29–9.23 %, (20) relative prefrontal width, 3.95–4.73 %, (21) relative largest supraocular width, 2.23–2.74 %, (22) relative longest finger length, 4.14–5.01 %, (23) relative distance between the ear and eye, 6.93–7.60 %, (24) relative head width, 69.6–80.0 %, (25) relative frontal width, 66.6–81.9 %, (26) relative nasal height, 0.873–1.11 %, (27) relative angled subocular height, 0.815–1.05 %, (28) relative distance between the eye and naris, 4.81–5.20 %, (29) relative canthal iii length, 1.73–1.85 %, (30) relative angled subocular width, 2.25–2.52 %, and (31) relative nasal length, 1.50–1.77 %. The species stem time is 2.43 Ma and the species crown time is 0.01 Ma (Fig. 4).

Comptus maculatus differs in having a dorsal pattern of absent/chevrons from all other species of the genus and in having a smaller total lamellae count on one hand (32–37) than all other species of the genus.

From *Comptus alloeides*, we distinguish *C. maculatus* by the dorsal pattern (absent/chevrons versus irregular dots/dots in series/dots in chevrons), the adult SVL (60.1–81.3 versus 124–161), the total lamellae on one hand (32–37 versus 43–58), the total strigae on ten scales (149–201 versus 237–323), and the relative longest finger length (4.14–5.01 versus 5.32–5.95). From *C. arboreus* **sp. nov.**, we distinguish *C. maculatus* by the dorsal pattern (absent/chevrons versus dots in series/dots in chevrons), the adult SVL (60.1–81.3 versus 93.2–123), the total lamellae on one hand (32–37 versus 48–54), the relative length of digits on one hindlimb (24.8–27.0 versus 37.4–39.7), the relative forelimb length (19.3–21.6 versus 24.1–25.3), the relative postmental width (2.32–2.86 versus 2.95–3.01), the relative longest finger length (4.14–5.01 versus 6.01–6.37), the relative width of canthal iii (1.73–1.85 versus

1.86–1.94), and the relative angled subocular width (2.25–2.52 versus 2.82–3.28). From *C. badius*, we distinguish *C. maculatus* by the dorsal pattern (absent/chevrons versus irregular dots/mottled), the total lamellae on one hand (32–37 versus 40–45), the total strigae on ten scales (149–201 versus 203–241), the relative mental width (1.69–1.85 versus 1.38), and the relative head width (69.6–80.0 versus 62.8–69.3). From *C. stenurus*, we distinguish *C. maculatus* by the dorsal pattern (absent/chevrons versus dots in series/dots in chevrons), the adult SVL (60.1–81.3 versus 121–146), the total lamellae on one hand (32–37 versus 47–57), the relative length of digits on one hindlimb (24.8–27.0 versus 29.2–37.1), the relative forelimb length (19.3–21.6 versus 22.3–27.5), and the relative longest finger length (4.14–5.01 versus 5.89–7.19). From *C. weinlandi*, we distinguish *C. maculatus* by the dorsal pattern (absent/chevrons versus irregular dots/dots in series/dots in chevrons), the adult SVL (60.1–81.3 versus 101–133), the total lamellae on one hand (32–37 versus 43–55), and the relative longest finger length (4.14–5.01 versus 5.08–6.31).

Description of holotype. MCZ R-6231. An adult; SVL 54.0 mm; tail nearly cylindrical, broken in life near tip, regenerated, 62.7 mm (116% SVL); axilla-to-groin distance 34.1 mm (63.1% SVL); forelimb length 10.7 mm (19.8% SVL); hindlimb length 16.1 mm (29.8% SVL); head length 8.74 mm (16.2% SVL); head width 6.64 mm (12.3% SVL); head width 76.0% head length; diameter of orbit 2.11 mm (3.91% SVL); horizontal diameter of ear opening 0.41 mm (0.759% SVL); vertical diameter of ear opening 0.47 mm (0.870% SVL); length of all toes on one foot 13.9 mm (25.7% SVL); shortest distance between angled subocular and lip 0.30 mm (0.556% SVL); shortest distance between the ocular and auricular openings 3.80 mm (7.04% SVL); longest finger length 2.83 mm (5.24% SVL); largest supraocular width 1.31 mm (2.43% SVL); cloacal width 4.35 mm (8.06% SVL); prefrontal width 2.47 mm (4.57% SVL); frontal width 81.7% frontal length; nasal height 0.68 mm (1.26% SVL); angled subocular height 0.67 mm (1.24% SVL); shortest distance between the eye and naris 2.39 mm (4.43% SVL); canthal iii width 0.91 mm (1.69% SVL); angled subocular width 1.77 mm (3.28% SVL); nasal width 0.92 mm (1.70% SVL); rostral 1.91X as wide as high, barely visible from above, not in contact with nasals, in contact with 1st supralabial and anterior internasal (left)/(right); anterior internasals are narrower than posterior ones; frontonasals and prefrontal fused into a single large plate with a slightly concave posterior margin, much wider than long, bordered by posterior internasals, 1st loreals, 1st median oculars, and the frontal; frontal longer than wide; a pair of frontoparietals, separated by the posterior prolongation of the frontal and the interparietal plate; interparietal plate smaller than parietals and separating them, posteriorly touching the interoccipital, which is wider than long; nasal single; nostril just posterior to suture between 1st and 2nd supralabials (left)/(right); 1 postnasal (left)/(right); 2 loreals (left)/(right); 1st loreal higher than wide (left)/(right), in contact with postnasal, posterior internasal, prefrontal/frontonasal complex, 1st median ocular, canthal iii, 2nd loreal, and 3rd–4th supralabials (left)/(right); 2nd loreal shorter than 1st, approximately as high as wide (left)/shorter than 1st, wider than high (right), excluded from contact with supraocular by canthal iii (left)/(right); final loreal posteriorly bordering the lower preocular (left)/upper and lower preoculars (right); canthal iii wider than high (left)/(right), contacting 1st median ocular, anterior supraciliary, upper and lower preocular, and 1st and 2nd loreals (left)/(right); 9 median oculars (left)/(right), 1st contacting the prefrontal (left)/(right); 1 upper preocular (left)/(right); an irregular anterior supraciliary (left)/(right); 6 lateral oculars (left)/(right); 4 (left)/5 (right) temporals; 2 suboculars (left)/(right); posterior subocular large and elongate (left)/(right); anterior subocular small (left)/(right); 9 supralabials (left)/(right), 6 to level below center of eye (left)/(right); 8 infralabials (left)/(right), 5 to level below center of eye (left)/(right); mental small, followed by a single, small postmental; 4 pairs of enlarged chin shields; 1st pair in contact with one another; 2nd–4th pairs separated by 1–3 scales; 99 transverse rows of dorsal scales from interoccipital to base of tail; 97 transverse rows of ventral scales from mental to vent; 38 scales around midbody; 5 digits; finger lengths 3>4>2>5>1; 9 lamellae under longest finger (left)/(right); 35 total lamellae on one hand; toe lengths 4>3>5>2>1; 13 (14th divided) (left)/14 (15th divided) (right) lamellae under longest toe; dorsal body and caudal scales striate with a faint median keel; smooth to faintly striated ventral scales; 122 total strigae counted on ten scales.

Color (in alcohol): dorsal surface of head pale tan, patternless; lateral surfaces of head grading from pale tan to pale cream with some medium brown mottling on the supralabials and darker brown eye masks; dorsal surfaces of the body are pale tan, patternless; dorsal surface of tail same as body; lateral areas fade from pale medium brown to yellow-cream; dorsal surfaces of the limbs are medium brown; lateral and ventral areas of the limbs fade to yellow-cream; ventral surfaces of the head, body, and tail are yellow-cream, patternless.

Variation. All of the material examined display a dorsal pattern of faded chevrons that is more prominent than that of the holotype. ANSP 38510 is the only specimen that displays any markings in the longitudinal paramedian area. Most specimens examined are patternless, however, ANSP 38511 and ANSP 38508 both show darker outlines

on the head scale borders. Dots are arranged in bars in the lateral band most clearly in ANSP 38512, whereas SBH 266554 and ANSP 38507 display this pattern anteriorly. Measurements and other morphological data for the holotype and other examined material are presented in Table 1.

FIGURE 41. (A–E) *Comptus maculatus* (MCZ R-6231, holotype), SVL 54.0 mm.

Distribution. *Comptus maculatus* is distributed on Cayman Brac and Little Cayman Island, where it has been collected at elevations of 0–20 m (Fig. 35).

Ecology and conservation. Little is known of the ecology of this species other than that the holotype was taken from under a pile of coconut husks (Garman 1888). On March 15–16, 2003, SBH found this species at three locations on Cayman Brac, among coconut husks under palm trees, after searching a much larger number of similarly ideal locations. Considerable search effort for this species was made throughout the length of Little Cayman without success.

The IUCN Redlist (IUCN 2023) considers the conservation status of *Comptus maculatus* to be Endangered B1ab(iii)+2ab(iii) "due to its limited distribution (with an extent of occurrence of 163 km^2), known occurrence in at most five locations that are subject to ongoing threats from development (current and planned). However, because this species is secretive, research is needed to better clarify the current distribution, population status, and life history." Studies are needed to determine the health of remaining populations and threats to the survival of the species. Captive-breeding programs should be undertaken, if possible.

Reproduction. On Cayman Brac, one female (58 mm SVL) was captured with two large yolked follicles in January (Seidel & Franz 1994); litter size three (SBH, field data).

Etymology. The species name is a Latin singular masculine adjective meaning spotted, in reference to the lizard's spotted pattern.

Remarks. The type description speculated that this species was closely related to *Celestus crusculus* and *Celestus occiduus*. Cousens (1956) felt that the morphological differences between *Comptus maculatus* and *Celestus crusculus* were insufficient, so she designated *Comptus maculatus* as a subspecies of *Celestus crusculus* (*Celestus crusculus maculatus*), keeping it as a subspecies because of a different colored tail. *Comptus maculatus* was referred to as a full species in later works (Hedges 2008; Henderson & Powell 2009; Hedges *et al.* 2019; Hedges 2024).

Interestingly, *Comptus maculatus* was likely treated as a subspecies of *Celestus crusculus* because of the smaller distance between Jamaica and the Cayman Islands, in comparison to that between Hispaniola and the Cayman Islands. Initial genetic data showing that it was closer to *Comptus stenurus*, reported later by Dennison (2010), an honors student working in the laboratory of SBH, led SBH to raise it to full species status in Caribherp (Hedges 2008). The phylogeny built by Schools & Hedges (2021) with expanded genetic data had a topology that placed *C. maculatus* within the genus *Comptus*, the remainder of which is found on Hispaniola. Schools *et al.* (2022) confirmed this placement with genomic data and indicated that an overwater dispersal event between Hispaniola and the Cayman Islands led to the current distribution of *Comptus maculatus*.

Comptus maculatus is included in our genetic dataset and has significant support in both Bayesian and ML likelihood analyses at the crown node of the species and the stem node that places it as the closest relative to *C. alloeides* and *C. weinlandi*. Based on our timetree (Fig. 4), *C. maculatus* diverged from its closest relative 2.43 Ma, consistent with typical species of vertebrates (> 0.7 Ma; Hedges *et al.* 2015). *Comptus maculatus* was recognized as a distinct species by our ASAP analysis.

FIGURE 42. *Comptus maculatus* (ANSP 38511), in life. From West End, Cayman Brac, Cayman Islands. Photo by SBH.

***Comptus stenurus* (Cope 1862a)**
Macaya Keeled Forest Lizard
(Fig. 43–44)

Diploglossus stenurus Cope, 1862:188. Holotype: MCZ R-3612, collected by David Friedrich Weinland from "near Jeremie," Grand'Anse department, Haiti. Date of collection inferred to be 1857–1858 (Weinland 1858). (18.64, -74.11).
Celestus stenurus—Cope, 1879:272.
Diploglossus stenurus stenurus—Schwartz, 1964:8.
Celestus stenurus—Schwartz & Henderson, 1988:100.
Celestus stenurus—Schwartz & Henderson, 1991:378.
Comptus stenurus—Schools & Hedges, 2021:226.
Comptus stenurus—Landestoy *et al.* 2022 2022:205.

Material examined (n=14). HAITI. Sud. ANSP 38544–5, Richard Thomas and Manuel Leal, 8.6 km SW of Carretour Joute on the Presquille de Port Salut, near Riviere la Source, 6 June 1991; ANSP 38546, S. Blair Hedges, Caye Madeline, 3 October 2010; ANSP 38550, S. Blair Hedges and Richard Thomas, Port Salut, Gumbwa, near Ça Vilason, 24 July 2010; BMNH 1964.309–10, Camp Perrin; KU 227167, 4.5 mi N Camp Perrin, 27 June 1979; MCZ R-133108–9, George Whiteman, St Croix, 7–8 mi NE Paillant, 1–31 July 1972; SBH 269020, S. Blair Hedges and Richard Thomas, Port Salut, Gumbwa, near Ça Vilason, 24 July 2010; SBH 267494, Eladio Fernandez, Île-à-Vache. **Grand'Anse.** MCZ R-3612, David Friedrich Weinland, Jeremie, 1857–8; MCZ R-119419–20, Thomas Preston Webster III, Alan Ross Kiester, and Haitians, Castillon, 31 August 1969.

Diagnosis. *Comptus stenurus* has (1) a dorsal pattern of dots in series/dots in chevrons, (2) head markings absent/present, (3) markings in the longitudinal paramedian area present, (4) dots arranged in bars in the lateral band absent/present, (5) an adult SVL of 121–146 mm, (6) ventral scale rows, 87–110, (7) midbody scale rows, 38–45, (8) total lamellae on one hand, 47–57, (9) total strigae on ten scales, 176–234, (10) relative length of all digits on one hindlimb, 29.2–37.1 %, (11) relative distance between the angled subocular and mouth, 0.676–1.12 %, (12) relative eye length, 2.99–3.92 %, (13) relative forelimb length, 22.3–27.5 %, (14) relative ear width, 0.451–1.87 %, (15) relative rostral height, 1.68–2.03 %, (16) relative head length, 15.8–18.9 %, (17) relative mental width, 1.52–1.78 %, (18) relative postmental width, 2.61–3.05 %, (19) relative cloacal width, 8.73–10.3 %, (20) relative prefrontal width, 4.32–4.71 %, (21) relative largest supraocular width, 2.53–3.11 %, (22) relative longest finger length, 5.89–7.19 %, (23) relative distance between the ear and eye, 6.18–7.42 %, (24) relative head width, 70.2–74.2 %, (25) relative frontal width, 68.0–79.2 %, (26) relative nasal height, 0.992–1.17 %, (27) relative angled subocular height, 0.697–0.893 %, (28) relative distance between the eye and naris, 4.38–5.53 %, (29) relative canthal iii length, 1.37–1.97 %, (30) relative angled subocular width, 2.31–2.85 %, and (31) relative nasal length, 1.39–1.82 %. The species stem time is 2.38 Ma and the species crown time is 0.08 Ma (Fig. 4).

We distinguish *Comptus stenurus* from the other species of *Comptus* based on a complex of traits. From *Comptus alloeides*, we distinguish *C. stenurus* by the total strigae on ten scales (176–234 versus 237–323). From *C. arboreus* **sp. nov.**, we distinguish *C. stenurus* by the relative length of digits on one hindlimb (29.2–37.1 versus 37.4–39.7) and the relative angled subocular height (0.697–0.893 versus 0.929–0.992). From *C. badius*, we distinguish *C. stenurus* by the dorsal pattern (dots in series/dots in chevrons versus irregular dots/mottled), the adult SVL (121–146 versus 78.2–99.1), the total lamellae on one hand (47–57 versus 40–45), the relative mental width (1.52–1.78 versus 1.38), the relative postmental width (2.61–3.05 versus 2.39), the relative longest finger length (5.89–7.19 versus 4.38–5.04), and the relative head width (70.2–74.2 versus 62.8–69.3). From *C. maculatus*, we distinguish *C. stenurus* by the dorsal pattern (dots in series/dots in chevrons versus absent/chevrons), the adult SVL (121–146 versus 60.1–81.3), the total lamellae on one hand (47–57 versus 32–37), the relative length of digits on one hindlimb (29.2–37.1 versus 24.8–27.0), the relative forelimb length (22.3–27.5 versus 19.3–21.6), and the relative longest finger length (5.89–7.19 versus 4.14–5.01). From *C. weinlandi*, we cannot distinguish *C. stenurus* based on our standard suite of characters (see Remarks).

Description of holotype. MCZ R-3612. An adult male; SVL 146 mm; tail nearly cylindrical, broken at tip, regenerated, 241 mm (165% SVL); axilla-to-groin distance 79.6 mm (54.5% SVL); forelimb length 40.2 mm (27.5% SVL); hindlimb length 52.0 mm (35.6% SVL); head length 25.9 mm (17.7% SVL); head width 18.3 mm (12.5% SVL); head width 70.7% head length; diameter of orbit 5.55 mm (3.80% SVL); horizontal diameter of ear opening 2.04 mm (1.40% SVL); vertical diameter of ear opening 1.76 mm (1.21% SVL); length of all toes on one foot 56.4 mm (38.6% SVL); shortest distance between angled subocular and lip 1.42 mm (0.973% SVL);

shortest distance between the ocular and auricular openings 10.8 mm (7.40% SVL); longest finger length 10.5 mm (7.19% SVL); largest supraocular width 3.70 mm (2.53% SVL); cloacal width 15.0 mm (10.3% SVL); mental width 2.60 mm (1.78% SVL); postmental width 4.46 mm (3.05% SVL); prefrontal width 6.48 mm (4.44% SVL); frontal width 79.2% frontal length; nasal height 1.59 mm (1.09% SVL); angled subocular height 1.19 mm (0.815% SVL); shortest distance between the eye and naris 7.29 mm (4.99% SVL); canthal iii width 2.00 mm (1.37% SVL); angled subocular width 4.16 mm (2.85% SVL); nasal width 2.66 mm (1.82% SVL); rostral 2.03X as wide as high, visible from above, not in contact with nasals, in contact with 1st supralabial and anterior internasal (left)/(right); anterior internasals are narrower than posterior ones; frontonasals and prefrontal fused into a single large plate with a concave posterior margin, wider than long, bordered by posterior internasals, 1st loreals, 1st and 2nd median oculars, and the frontal; frontal longer than wide; a pair of frontoparietals, separated by the posterior prolongation of the frontal and the interparietal plate; interparietal plate slightly smaller than parietals and separating them, posteriorly touching the interoccipital, which is wider than long; parietal separated from supraoculars by 1st and 2nd temporals and frontoparietal (left)/(right); nasal single; nostril above suture between 1st and 2nd supralabials (left)/(right); 1 postnasal (left)/(right); 2 (left)/3 (right) loreals; 1st loreal higher than wide (left)/(right), in contact with postnasal, posterior internasal, prefrontal/frontonasal complex, 1st median ocular, canthal iii, 2nd loreal, and 3rd–4th supralabials (left)/(right); 2nd loreal shorter than 1st, approximately as high as wide (left)/shorter than 1st, irregular (right), excluded from contact with supraocular by canthal iii (left)/(right); 3rd loreal shorter than 1st, approximately as high as wide, excluded from contact with supraocular by canthal iii (right); final loreal posteriorly bordering the lower and upper preocular (left)/(right); canthal iii wider than high (left)/(right), contacting 1st median ocular, anterior supraciliary, upper preocular, and 1st and 2nd loreals (left)/1st median ocular, anterior supraciliary, upper preocular, and 1st–3rd loreals (right); 10 (left)/(right) median oculars, 1st and 2nd contacting the prefrontal (left)/(right); 1 upper preocular (left)/(right); an irregular anterior supraciliary (left)/(right); 6 lateral oculars (left)/(right); 5 temporals (left)/(right); 2 suboculars (left)/(right); posterior subocular large and elongate (left)/(right); anterior subocular small (left)/(right); 9 supralabials (left)/(right), 6 to level below center of eye (left)/(right); 9 (left)/10 (right) infralabials, 5 (left)/6 (right) to level below center of eye; mental small, followed by a single, larger postmental; 4 pairs of enlarged chin shields; 1st pair in contact with one another anteriorly, posteriorly separated by one scale; 2nd–4th pairs separated by 1–5 scales; 97 transverse rows of dorsal scales from interoccipital to base of tail; 98 transverse rows of ventral scales from mental to vent; 42 scales around midbody; 5 digits; finger lengths 3>4>2>5>1; 13 lamellae under longest finger (left)/(right); 52 total lamellae on one hand; toe lengths 4>3>5>2>1; 19 (left)/20 (right) lamellae under longest toe; dorsal body and caudal scales striate with a median keel; ventral scales lightly striated; 210 total strigae counted on ten scales.

Color (in alcohol): dorsal surface of head golden tan, patternless; lateral surfaces of head grading from golden tan to cream; dorsal surfaces of the body are golden tan with some darker brown scales, most scales are missing; dorsal surfaces of tail are golden tan with some darker brown scales, most scales are missing; almost all scales missing on the lateral areas; dorsal surfaces of the limbs are golden tan with darker spots; lateral and ventral areas of the limbs fade to cream, patternless; ventral surfaces of the head, body, and tail are pale cream, patternless.

Variation. The other specimens examined have more scales intact than the holotype. All specimens show large dots that are continuations of the longitudinal paramedian series whereas the large dots in ANSP 38550 appear in multiple series and the large dots in KU 227167 appear as almost stripes across the back. The longitudinal paramedian lines appear as either complete lines or large dots in series. Dots arranged in bars in the lateral band are split almost evenly as being present and absent. Measurements and other morphological data for the holotype and other examined material are presented in Table 1.

Distribution. *Comptus stenurus* is distributed in the western portion of the Tiburon peninsula of Haiti, including Île-à-Vache and the Macaya mountains, but not at the tip of the peninsula (region of Tiburon), at elevations of 0–1070 m (Fig. 35).

Ecology and conservation. Past literature accounts of ecological data for this species conflate multiple species and therefore cannot be used. SBH found individuals under rocks and logs in areas recently cleared of forest. Six males 110–123 mm SVL weighed 18.5–31 g, whereas two females, 140 and 143 mm SVL, weighed 44 and 58 g (SBH field data from Grand'Anse, Haiti, between Marche Leon and Castillon). This species appears to be tolerant of some habitat disturbance and can be abundant in places.

FIGURE 43. (A–F) *Comptus stenurus* (MCZ R-3612, holotype), SVL 146 mm.

FIGURE 44. *Comptus stenurus* (SBH 269019), in life. From Gumbwa, Port Salut, Sud Department, Haiti. Photo by SBH.

We consider the conservation status of *Comptus stenurus* **sp. nov.** to be Least Concern, primarily because it has been encountered frequently in the past, based on IUCN Redlist criteria (IUCN 2023). However, clearing of forests for agriculture in Haiti is a severe environmental pressure on biodiversity (Hedges *et al.* 2018). Also, introduced predators, including the mongoose and black rats, likely prey upon this species. Therefore, studies are needed to determine the health and extent of the populations, and threats to the survival of the species.

Reproduction. Past literature accounts of ecological data for this species conflate multiple species and therefore cannot be used.

Etymology. The species name *stenurus* is derived from the Greek words *stenos* meaning "narrow" and *oura* meaning "tail," referring to the tail of the species.

Remarks. Cochran (1941) synonymized *Comptus stenurus* with *Panolopus costatus*, along with numerous other species; however, this taxonomic action was not retained in later works (Schwartz 1970). When *Caribicus warreni* was described, Schwartz (1970) speculated that its closest relative was *Comptus stenurus* because of the presence of median keels on the dorsal and caudal scales, a suggestion not supported by our molecular phylogeny, which places them in different generic clades. Previously, both *Comptus stenurus rugosus* and *C. weinlandi* were regarded as subspecies of *C. stenurus*. However, we synonymize *C. stenurus rugosus* with *C. weinlandi* (see accounts below).

Comptus stenurus and *C. weinlandi* cannot be distinguished based on our suite of morphological characters; however, both of these species are morphologically distinct from their closest relatives (*C. arboreus* and *C. alloeides*, respectively). Additionally, *C. stenurus* and *C. weinlandi* are genetically distinct (Fig. 3) and diverged 4.22 Ma (Fig. 4). Future studies should examine additional characters to morphologically distinguish *C. stenurus* from *C. weinlandi*.

Comptus stenurus is included in our genetic dataset and has significant support in both Bayesian and ML likelihood analyses at the crown node of the species and the stem node that places it as the closest relative to *C.*

arboreus **sp. nov.** Based on our timetree (Fig. 4), *C. stenurus* diverged from its closest relative 2.38 Ma, consistent with typical species of vertebrates (> 0.7 Ma; Hedges *et al.* 2015). *Comptus stenurus* was recognized as a distinct species by our ASAP analysis.

***Comptus weinlandi* (Cope 1868)**
Hispaniolan Keeled Forest Lizard
(Fig. 45–46)

Celestus stenurus weinlandii Cope, 1868:125. Holotype: USNM 12145, received from T. Younglove from within 25 mi of Port-au-Prince, Haiti, between January and June 1866.
Celestus rugosus—Cope, 1879:272. Holotype: ANSP 10260, from Puerto Plata, Dominican Republic.
Diploglossus rugosus—Boulenger, 1885:288.
Celestus rugosus—Barbour, 1930:99.
Celestus rugosus—Barbour, 1935:123.
Celestus rugosus—Barbour, 1937:138.
Diploglossus stenurus weinlandi—Schwartz, 1964:10.
Diploglossus stenurus rugosus—Schwartz, 1964:14.
Celestus stenurus rugosus—Schwartz & Henderson, 1988:100.
Celestus stenurus weinlandi—Schwartz & Henderson, 1988:101.
Celestus stenurus rugosus—Schwartz & Henderson, 1991:379.
Celestus stenurus weinlandi—Schwartz & Henderson, 1991:379.
Celestus stenurus rugosus—Hedges *et al.*, 2019:17.
Celestus stenurus weinlandi—Hedges *et al.*, 2019:17.
Comptus stenurus rugosus—Schools & Hedges, 2021:226.
Comptus stenurus weinlandi—Schools & Hedges, 2021:226.

Material examined (n=53). DOMINICAN REPUBLIC. Duarte. ANSP 38529–31, Richard Thomas, Manuel Leal, and Herman Dominicia, 10.1 km NE of San Francisco de Macoris, 15 July 1993. **El Seibo.** ANSP 38523, S. Blair Hedges, Richard Thomas, and Nicholas Plummer, 4.2 km N, 8.4 km W (airline), Nisibon, Playa Cucharera (= beach W Punta Limon), 14 July 1991; ANSP 38528, Richard Thomas, 5 km airline W Sabana de Nisibon, 6 August 2001. **Hato Mayor.** ANSP 38513–4, Richard Thomas, 5.6 km airline W El Valle, 2 August 2001; ANSP 38515–22, Andres Perez, Dan Rabosky, and Richard Thomas, Loma del Fresca, 5.7 km airline SW Sabana de la Mar, 3 August 2001; ANSP 38524–7, Andres Perez, Dan Rabosky, and Richard Thomas, 7.8 km S of Sabana de la Mar, 2 August 2001; SBH 267001, Andres Perez, Dan Rabosky, and Richard Thomas, Loma del Fresca, 5.7 km airline SW Sabana de la Mar, 3 August 2001; SBH 267017, SBH 267031, Andres Perez, Dan Rabosky, and Richard Thomas, 7.8 km S Sabana de la Mar, 2 August 2001. **Independencia.** ANSP 38547–8, S. Blair Hedges, Kristin Nastase, Renee Sharp, and Patrick Parker, 5.1 km NW of La Descubierta, 30 May 1996; SBH 194492–3, S. Blair Hedges, Kristin Nastase, Renee Sharp, and Patrick Parker, 5.1 km NW of La Descubierta, 30 May 1996. **Los Tabucos.** ANSP 38534–7, Richard Thomas, 8.8 km N, thence 0.5 km W Tenares, Salcedo, 21 July 1993. **Maria Trinidad Sanchez.** MCZ R-126742, Alan Ross Kiester, 15 km S of Nagua, 14 September 1944–29 January 1971. **Puerto Plata.** USNM 10260, Puerto Plato (= San Felipe de Puerto Plata), 1878. **Salcedo.** ANSP 38532–3, Richard Thomas, 23.2 km N of thence 4.5 km W Tenares, = 0.2 km E Jaiba, 21 July 1993; SBH 193218, Richard Thomas, 23.2 km N of thence 4.5 km W Tenares, = 0.2 km E Jaiba, 21 July 1993. **HAITI. Artibonite.** ANSP 38542, S. Blair Hedges, Richard Thomas, Nicholas Plummer, and Manuel Leal, 11.8 km W of Ça Soleil, 11 June 1991; SBH 192406, 192408, S. Blair Hedges, Richard Thomas, Nicholas Plummer, and Manuel Leal, 11.8 km W of Ça Soleil, 11 June 1991. **Nord'Ouest.** ANSP 38541, S. Blair Hedges and Richard Thomas, Bombardopolis, 28 April 1997. **Ouest.** ANSP 38549, S. Blair Hedges, Richard Thomas, Manuel Leal, and Nicholas Plummer, 10.1 km ENE of Petionville, 9 June 1991; ANSP 38551–4, S. Blair Hedges, Richard Thomas, Nicholas Plummer, and Manuel Leal, 18.7 km E of Thomaseau, 19 May 1991; MCZ R-163165, E. Wade Davis, Mariani (on Port-au-Prince to Leogane road), 1–31 July; SBH 191620, 191649–50, S. Blair Hedges, Richard Thomas, Manuel Leal, and Nicholas Plummer, 18.1 km E of Thomaseau, 19 May 1991; SBH 191622–4, S. Blair Hedges, Richard Thomas, Nicholas Plummer, and Manuel Leal, 18.7 km E of Thomaseau, 19 May 1991; SBH 192424, S. Blair Hedges Richard Thomas Manuel Leal, and Nicholas Plummer, 10.1 km ENE of Petionville, 9 June 1991; USNM 12145, within 25 mi of Port-au-Prince, January–June 1866.

FIGURE 45. (A–F) *Comptus weinlandi* (USNM 12145, holotype), SVL 94.0 mm.

Diagnosis. *Comptus weinlandi* has (1) a dorsal pattern of irregular dots/dots in series/dots in chevrons, (2) head markings absent/present, (3) markings in the longitudinal paramedian area absent/present, (4) dots arranged in bars in the lateral band absent/present, (5) an adult SVL of 101–133 mm, (6) ventral scale rows, 81–105, (7) midbody scale rows, 37–44, (8) total lamellae on one hand, 43–55, (9) total strigae on ten scales, 167–236, (10) relative length of all digits on one hindlimb, 24.5–36.5 %, (11) relative distance between the angled subocular and mouth, 0.449–0.901 %, (12) relative eye length, 3.33–4.43 %, (13) relative forelimb length, 20.1–27.9 %, (14) relative ear width, 0.802–2.18 %, (15) relative rostral height, 1.46–1.86 %, (16) relative head length, 15.8–18.5 %, (17) relative mental width, 1.41–1.90 %, (18) relative postmental width, 2.57–2.91 %, (19) relative cloacal width, 8.76–10.1 %, (20) relative prefrontal width, 4.29–4.88 %, (21) relative largest supraocular width, 2.31–3.49 %, (22) relative

longest finger length, 5.08–6.31 %, (23) relative distance between the ear and eye, 6.03–7.95 %, (24) relative head width, 73.6–82.2 %, (25) relative frontal width, 58.8–84.6 %, (26) relative nasal height, 0.965–1.32 %, (27) relative angled subocular height, 0.568–1.23 %, (28) relative distance between the eye and naris, 4.67–5.72 %, (29) relative canthal iii length, 1.65–2.08 %, (30) relative angled subocular width, 1.64–3.36 %, and (31) relative nasal length, 1.48–1.95 %. The species stem time is 1.46 Ma and the species crown time is 0.68 Ma (Fig. 4).

We distinguish *Comptus weinlandi* from the other species of *Comptus* based on a complex of traits. From *Comptus alloeides*, we distinguish *C. weinlandi* by the total strigae on ten scales (167–236 versus 237–323). From *C. arboreus* **sp. nov.**, we distinguish *C. weinlandi* by the relative length of digits on one hindlimb (24.5–36.5 versus 37.4–39.7) and the relative postmental width (2.57–2.91 versus 2.95–3.01). From *C. badius*, we distinguish *C. weinlandi* by the adult SVL (101–133 versus 78.2–99.1), the relative mental width (1.41–1.90 versus 1.38), the relative postmental width (2.57–2.91 versus 2.39), the relative longest finger length (5.08–6.31 versus 4.38–5.04), and the relative head width (73.6–82.2 versus 62.8–69.3). From *C. maculatus*, we distinguish *C. weinlandi* by the dorsal pattern (irregular dots/dots in series/dots in chevrons versus absent/chevrons), the adult SVL (101–133 versus 60.1–81.3), the total lamellae on one hand (43–55 versus 32–37), and the relative longest finger length (5.08–6.31 versus 4.14–5.01). From *C. stenurus*, we cannot distinguish *C. weinlandi* based on our standard suite of characters (see Remarks).

Description of holotype. USNM 12145. An adult; SVL 94.0 mm; tail nearly cylindrical, broken, 15.5 mm (16.5% SVL); axilla-to-groin distance 44.7 mm (47.6% SVL); forelimb length 22.0 mm (23.4% SVL); hindlimb length 35.3 mm (37.6% SVL); head length 16.5 mm (17.6% SVL); head width 11.3 mm (12.0% SVL); head width 68.5% head length; diameter of orbit 3.93 mm (4.18% SVL); horizontal diameter of ear opening 1.05 mm (1.12% SVL); vertical diameter of ear opening 1.44 mm (1.53% SVL); length of all toes on one foot 31.9 mm (33.9% SVL); shortest distance between angled subocular and lip 0.61 mm (0.649% SVL); shortest distance between the ocular and auricular openings 6.38 mm (6.79% SVL); longest finger length 5.75 mm (6.12% SVL); largest supraocular width 2.46 mm (2.62% SVL); cloacal width 8.66 mm (9.21% SVL); mental width 1.70 mm (1.81% SVL); postmental width 2.52 mm (2.68% SVL); prefrontal width 4.79 mm (5.10% SVL); frontal width 78.0% frontal length; nasal height 1.19 mm (1.27% SVL); angled subocular height 0.88 mm (0.936% SVL); shortest distance between the eye and naris 4.49 mm (4.78% SVL); canthal iii width 1.79 mm (1.90% SVL); angled subocular width 2.35 mm (0.250% SVL); nasal width 1.66 mm (1.77% SVL); rostral 1.86X as wide as high, visible from above, not in contact with nasals, in contact with 1st supralabial and anterior internasal (left)/(right); anterior internasals are narrower than posterior ones; frontonasals and prefrontal fused into a single large plate with a concave posterior margin, much wider than long, bordered by posterior internasals, 1st loreals, 1st and 2nd median oculars, and the frontal; frontal longer than wide; a pair of frontoparietals, separated by the posterior prolongation of the frontal and the interparietal plate; interparietal plate smaller than parietals and separating them, posteriorly touching the interoccipital, which is wider than long; parietal separated from supraoculars by 1st temporals and frontoparietal (left)/(right); nasal single; nostril above suture between 1st and 2nd supralabials (left)/(right); 1 postnasal (left)/(right); 2 (left)/3 (right) loreals; 1st loreal higher than wide (left)/small (right), in contact with postnasal, posterior internasal, prefrontal/frontonasal complex, 1st median ocular, canthal iii, 2nd loreal (fused with canthal iii), and 3rd–4th supralabials (left); 2nd loreal shorter than 1st, approximately as high as wide, fused with canthal iii (left)/higher than wide, in contact with posterior internasal, prefrontal/frontonasal complex, median ocular 1, canthal iii, supralabials 3–4, and the 1st–3rd labials (right), excluded from contact with supraocular by canthal iii (fused with loreal 2) (left); 3rd loreal shorter than 1st, approximately as high as wide (left); final loreal posteriorly bordering the lower preocular (left)/(right); canthal iii wider than high, fused with loreal 2 (left)/wider than high (right), contacting 1st median ocular (fused with), anterior supraciliary, upper and lower preoculars, 1st and 2nd loreals, and the additional scale (left)/1st median ocular, anterior supraciliary, upper and lower preoculars, and 1st and 2nd loreals (right); 10 median oculars (left)/(right), 1st and 2nd contacting the prefrontal (left)/(right); 1 upper preocular (left)/(right); an irregular anterior supraciliary (left)/(right); 6 lateral oculars (left)/(right); 5 temporals (left)/(right); 2 suboculars (left)/(right); posterior subocular large and elongate (left)/(right); anterior subocular small (left)/(right); 9 (left)/10 (right) supralabials, 6 to level below center of eye (left)/(right); 9 (left)/10 (right) infralabials, 6 to level below center of eye (left)/(right); mental small, followed by a single, larger post mental; 4 pairs of enlarged chin shields, followed by 1 pair of reduced chin shields; 1st pair in contact with one another anteriorly, posteriorly separated by one scale; 2nd pair in contact with one another anteriorly, posteriorly separated by one scale; 3rd–5th pairs separated by 1–4 scales; 93 transverse rows of ventral scales from mental to vent; 39 scales around midbody; 5 digits; finger lengths 3>4>5>2>1; 12 lamellae under longest finger

(left)/(right); 50 total lamellae on one hand; toe lengths 4>3>5>2>1; 21 (left)/19 (right) lamellae under longest toe; strigae and median keel (more so on anterior scales, posterior have little to no keel) dorsal body and caudal scales; smooth ventral scales; 185 total strigae counted on ten scales.

Color (in alcohol): dorsal surface of head gray-brown, patternless; lateral surfaces of head grading from gray-brown to yellow-orange; dorsal surfaces of the body are gray-brown with faded brown markings in longitudinal paramedian series that continue down the body; dorsal surface of tail the same as the body; lateral areas grade from gray-brown to orange-yellow; dorsal surfaces of the limbs are gray-brown with some orange mottling; lateral and ventral areas of the limbs grade to yellow-orange, patternless; ventral surfaces of the head, body, and tail are yellow-orange, patternless.

Variation. The majority of the examined material examined have a similar pattern of large dots that are continuations of the longitudinal paramedian series. Several specimens exhibit more irregular dots in dots also arranged in chevrons. All specimens except for ANSP 38525 show marking in the longitudinal paramedian series that range from dots in series to complete longitudinal paramedian lines. Most specimens show a pattern on their head scales in the form of these scales either having darker outlines or irregular, darker dots. A minority of the specimens have a completely patternless head. All specimens that are not faded show dots arranged in bars in the lateral area except for USNM 10260, in which this trait is absent. Measurements and other morphological data for the holotype and other examined material are presented in Table 1.

Distribution. *Comptus weinlandi*, with the largest range in the genus *Comptus*, is distributed throughout most of the island and in both countries at elevations of 0–1060 m. However, it is missing from nearly all the Tiburon Peninsula, Barahona Peninsula, Central Haiti, West-Central Dominican Republic, and offshore islets (Fig. 35). It has an extent of occurrence of ~41,680 km^2.

Ecology and conservation. No ecological data are available for this species. We consider the conservation status of *Comptus weinlandi* to be Least Concern, based on IUCN Redlist criteria (IUCN 2023). It is a common species tolerant of some habitat disturbance. However, it faces a primary threat of habitat destruction resulting from agriculture and urbanization. A secondary threat is predation from introduced mammals, including the mongoose and black rats. We need studies to determine the health and extent of remaining populations and better understand the threats to the survival of the species.

Reproduction. Ovoviviparous. Embryos observed in ANSP 38535.

Etymology. This species was named after David Friedrich Weinland for his contributions to the study of reptiles in Haiti. Weinland made a six-month visit to Jérémie, Haiti, in 1857–1858 (Weinland 1858).

Remarks. The type locality of *Comptus weinlandi* was given incorrectly as Gonave island in the type description (Cope 1868); however, this error was later noted and corrected (Schwartz 1964). The correct type locality is from within 25 miles of Port-au-Prince, Haiti. Both *C. rugosus* and *C. weinlandi* were previously considered to be subspecies of "*Celestus*" (= *Comptus*) *stenurus* (Schwartz 1964). Because of a lack of genetic and morphological differentiation, we synonymize *C. stenurus rugosus* under the name *C. weinlandi*. Schwartz (1964) also was unable to find a diagnostic character to separate the two taxa, although he found some non-diagnostic trends in pattern.

Comptus weinlandi and *C. stenurus* cannot be distinguished based on our suite of morphological characters; however, both species are morphologically distinct from their respective closest relatives (*C. alloeides* and *C. arboreus*, respectively). Additionally, *C. weinlandi* and *C. stenurus* are genetically distinct (Fig. 3) and diverged 4.22 Ma (Fig. 4). Future studies should examine additional characters to morphologically distinguish *C. weinlandi* and *C. stenurus*.

Comptus weinlandi is included in our genetic dataset and has a significant support value in our ML analysis and a support value of 92% in our Bayesian analysis at the node that defines it as a species. The stem node that places *C. weinlandi* as the closest relative to *C. alloeides* has a significant support value in both our ML and Bayesian analyses. Based on our timetree (Fig. 4), *C. weinlandi* diverged from its closest relative 1.46 Ma, consistent with typical species of vertebrates (> 0.7 Ma; Hedges *et al.* 2015). We further recognize it as a distinct species because of the diagnostic trait that separates it from *C. alloeides* (the total strigae on ten scales). This species is also sympatric with *C. alloeides* at one locality on the Samana Peninsula. *Comptus weinlandi* was recovered as conspecific with *Comptus alloeides* in our ASAP analysis.

FIGURE 46. *Comptus weinlandi* (SBH 267796), in life. From an unnamed beach near Cueva Infierno and Cueva del Angel, Hato Mayor Province, Dominican Republic. Photo by SBH.

Genus *Guarocuyus* (Landestoy *et al.* 2022)
Jaragua Forest Lizards

Type species. *Guarocuyus jaraguanus* Landestoy *et al.*, 2022: 201.
Diagnosis. See *Guarocuyus jaraguanus* Diagnosis section.
Content. One species (Table 3): *Guarocuyus jaraguanus.*
Distribution. See *Guarocuyus jaraguanus* Distribution section.

***Guarocuyus jaraguanus* (Landestoy *et al.* 2022)**
Jaragua Forest Lizard
(Fig. 47)

Guarocuyus jaraguanus—Landestoy *et al.*, 2022: 201. Holotype: MNHNSD 23.3937, collected by Miguel A. Landestoy from Cayo de las Iguanas, Pedernales Province, Dominican Republic on 22 September 2021 (17.73205, -71.37126; near sea level).

Material examined (n=19). DOMINICAN REPUBLIC. Pedernales. IIBZ-HER00001–00004, MNHNSD 23.3912–3916, Miguel A. Landestoy, Gerson Féliz, and Juan Pérez-Vidal, Parque Nacional Jaragua, Laguna de Oviedo Cayo de las Iguanas, 29 April 2021; IIBZ-HER00005–00008, MNHNSD 23.3934–3936, Miguel A. Landestoy, Parque Nacional Jaragua, Laguna de Oviedo Cayo de las Iguanas, 29 April 2021; MNHNSD 23.3937, Miguel A. Landestoy, Parque Nacional Jaragua, Laguna de Oviedo, Cayo de las Iguanas, 22 September 2021; MNHNSD 23.3948–3949, Miguel A. Landestoy and Gerson Féliz, Laguna de Oviedo, Cayo Pei, 4 June 2022.

Diagnosis. Landestoy *et al.* (2022) discussed several unique morphological traits observed in *Guarocuyus jaraguanus.* These include the number of scales in contact with the nasal scale (ranging from 4–5), the number of postnasal scales (1–2), the semi-prehensile tail, and the presence of scaleless webbing between toes II to IV.

Guarocuyus jaraguanus has (1) a dorsal pattern of mottled/chevrons/bands, (2) head markings present, (3) markings in the longitudinal paramedian area present, (4) dots arranged in bars in the lateral band absent, (5) a maximum SVL of 84.6–110 mm, (6) ventral scale rows, 100–114, (7) midbody scale rows, 40, (8) total lamellae on one hand, unavailable, (9) total strigae on ten scales, unavailable, (10) relative length of all digits on one hindlimb, unavailable, (11) relative distance between the angled subocular and mouth, unavailable, (12) relative eye length, unavailable, (13) relative forelimb length, unavailable, (14) relative ear width, 2.33–2.90 %,

(15) relative rostral height, 1.55–1.85 %, (16) relative head length, 18.6 %, (17) relative mental width, unavailable, (18) relative postmental width, unavailable, (19) relative cloacal width, unavailable, (20) relative prefrontal width, unavailable, (21) relative largest supraocular width, unavailable, (22) relative longest finger length, unavailable, (23) relative distance between the ear and eye, unavailable, (24) relative head width, 74.5 %, (25) relative frontal width, unavailable, (26) relative nasal height, unavailable, (27) relative angled subocular height, unavailable, (28) relative distance between the eye and naris, unavailable, (29) relative canthal iii length, unavailable, (30) relative angled subocular width, unavailable, and (31) relative nasal length, unavailable. The species stem time is 8.59 Ma and the species crown time is 0.01 Ma (Fig. 4).

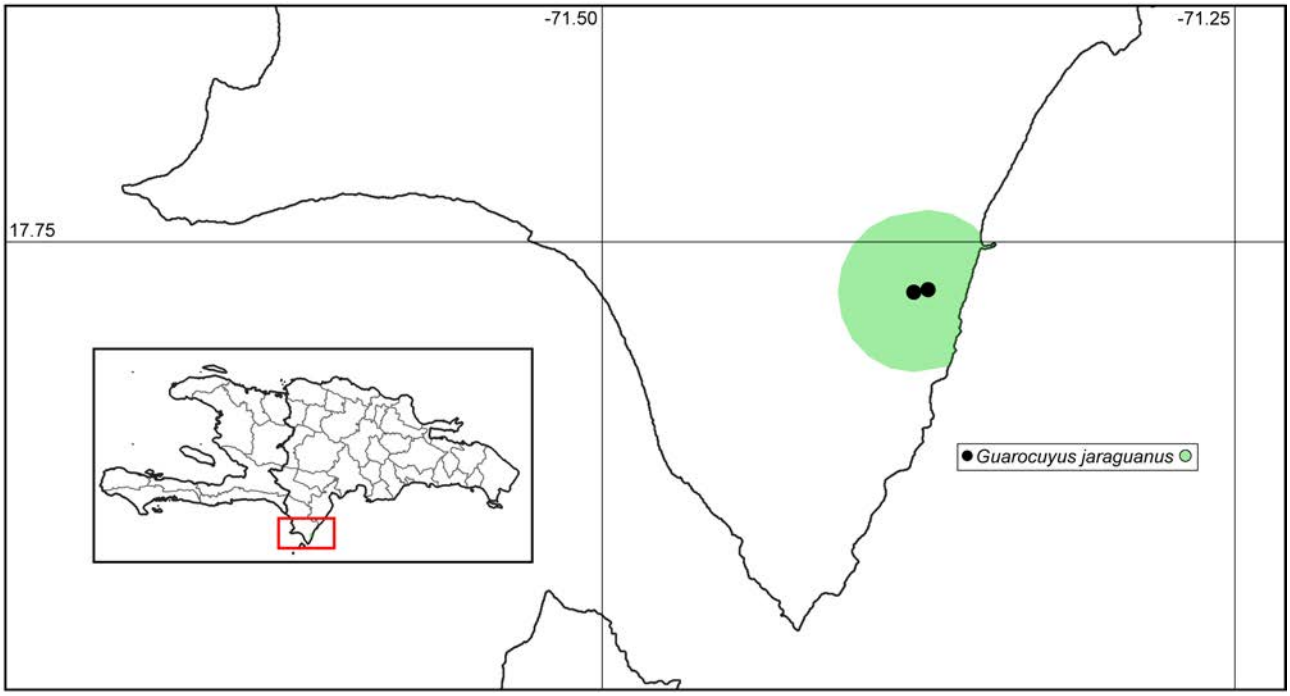

FIGURE 47. Map showing known locality for *Guarocuyus jaraguanus*. Inset shows all of Hispaniola, with a red box indicating the mapped area.

Description of holotype. MNHNSD 23.3937. An adult male; SVL 96.0 mm; tail cylindrical, partially regenerated; axilla-to-groin distance 51.8 mm (54.0% SVL); head length 17.9 mm (18.6% SVL); head width 13.3 mm (13.9% SVL); head width 74.3% head length; horizontal diameter of ear opening 2.60 mm (2.71% SVL); rostral 58.3X as wide as high, barely visible from above, not in contact with nasals, in contact with 1st supralabial and anterior internasal (left); anterior internasals are narrower than posterior ones; frontonasals and prefrontal fused into a single large plate with a straight posterior margin, much wider than long; frontal longer than wide; a pair of frontoparietals, separated by the posterior prolongation of the frontal and the interparietal plate; interparietal plate smaller than parietals and separating them; parietal separated from supraoculars by 1st temporals and frontoparietal (left)/(right); nasal single; nostril above suture between 1st and 2nd supralabials (left); 1 (left)/(right) postnasal; 2 (left)/(right) loreals; 1st loreal higher than wide (left)/; 2nd loreal shorter than 1st, approximately as high as wide (left) excluded from contact with supraocular by canthal iii (left); canthal iii wider than high (left); 10 (left) median oculars; 6 (left) lateral oculars; 6 (left) temporals; 10 (left)/(right) supralabials, 7 (left)/(right) to level below center of eye; mental small, followed by a single, larger postmental; 4 pairs of enlarged chin shields, followed by 1 pairs of reduced chin shields; 1st pair in contact with one another anteriorly, posteriorly separated by one scale; 2nd–5th pairs separated by 1–5 scales; 91 transverse rows of dorsal scales from interoccipital to base of tail; 106 transverse rows of ventral scales from mental to vent; 40 scales around midbody; 5 (left)/4 (one missing) (right) digits; finger lengths 3>4>2>5>1; toe lengths 4>3>5>2>1; 24 lamellae under longest toe (left)/(right); dorsal body and caudal scales striate with a median keel.

Color (in alcohol): dorsal surface of head covered with mottling of various shades of brown and cream; lateral surfaces of head grading from mottled brown to cream; dorsal surfaces of the body are mottled brown with mottling arranged into bands across the body; dorsal surface of tail the same as the body; lateral areas grade from mottled

brown to cream with continuations of the dorsal pattern; dorsal surfaces of the limbs are the same as the body; lateral and ventral areas of the limbs fade to light cream; ventral surfaces of the head, body, and tail are light cream, patternless.

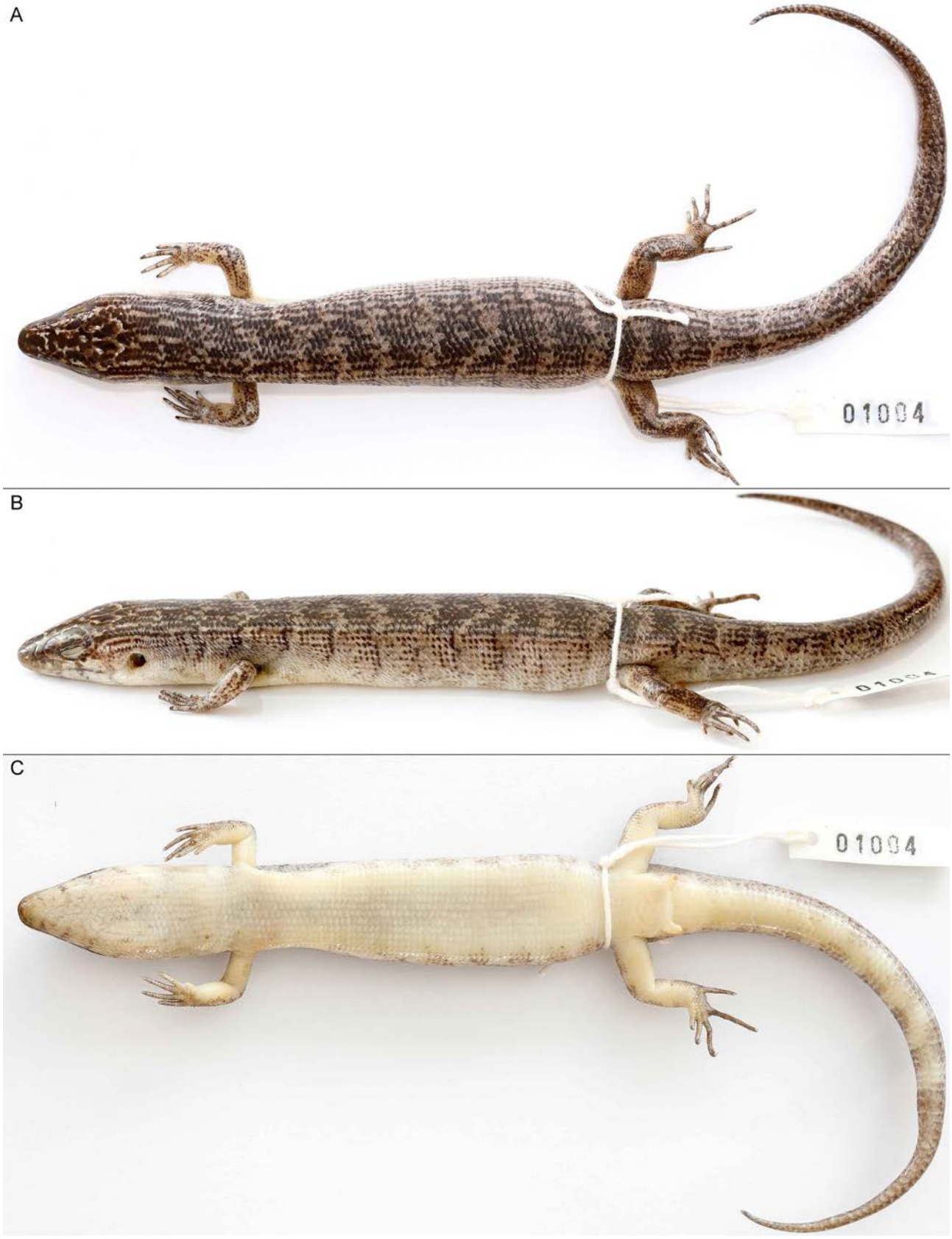

FIGURE 48. (A–C) *Guarocuyus jaraguanus* (MNHNSD 23.3937, holotype), SVL 96.0 mm.

Variation. Measurements and other morphological data for the holotype and other examined material are presented in Table 1.

Distribution. *Guarocuyus jaraguanus* is distributed on Cayo de las Iguanas and adjacent Cayo Pei, Laguna de Oviedo, on the Barahona Peninsula of the Dominican Republic (Fig. 48).

Ecology and conservation. Members of this species have been collected exposed on the ground (rocks, leaf litter, and black mangrove roots) and under large bromeliads and agaves at and after dusk. Several were collected while foraging on dry mud within the root system of black mangroves (*Avicennia germinans*). One animal was observed 1.5 m high in epiphytic bromeliads (*Tillandsia utriculata*). All individuals were collected from 1900–2130 h, suggesting that this is a nocturnal species. Individuals with complete, non-regenerated tails exhibited semi-prehensile ability. This, coupled with the animal observed in a bromeliad indicates that this is an arboreal species (Landestoy *et al.* 2022).

Guarocuyus jaraguanus was assessed as Critically Endangered (CR B2a), based on its very small distribution and threats from habitat alteration and introduced predators (Landestoy *et al.* 2022), based on IUCN Redlist criteria (IUCN 2022). Studies are needed to determine the health and extent of remaining populations and threats to the survival of the species.

Reproduction. All collected females were gravid, of which only the second smallest (IIBZ-HER00004, SVL 77.5 mm) was dissected and contained a single, well-developed fetus (IIBZ-HER00012, SVL 27.8 mm).

Etymology. The species name (*jaraguanus*) is a masculine nominative singular adjective meaning "pertaining to Jaragua," the name of the national park that encompasses the type locality.

Remarks. This species could represent an ecological equivalent of *Comptus stenurus* and *Panolopus costatus* (Landestoy *et al.* 2022). Another hypothesis proposed was that *Guarocuyus jaraguanus* could also represent a relic of a formerly widespread lineage. *Guarocuyus jaraguanus* diverged from its closest relative 8.59 Ma (Fig. 4), consistent with typical species of vertebrates (> 0.7 Ma; Hedges *et al.* 2015), and was recognized as a distinct species by our ASAP analysis.

Genus *Panolopus* Cope, 1862b

Caribbean Smooth-scaled Forest Lizards
(Figs. 49–50)

Panolopus Cope, 1862:494. Type species: *Panolopus costatus* Cope, 1862:494, by original designation.

Diagnosis. *Panolopus* has (1) a dorsal pattern of absent/irregular flecks/irregular dots/dots in series/dots in chevrons, (2) head markings absent/present, (3) markings in the longitudinal paramedian area absent/present, (4) dots arranged in bars in the lateral band absent/present, (5) a maximum SVL of 59.3–113 mm, (6) ventral scale rows, 77–114, (7) midbody scale rows, 32–45, (8) total lamellae on one hand, 32–59, (9) total strigae on ten scales, 141–413, (10) relative length of all digits on one hindlimb, 20.8–41.3 %, (11) relative distance between the angled subocular and mouth, 0.00–1.17 %, (12) relative eye length, 2.36–4.01 %, (13) relative forelimb length, 15.1–27.6 %, (14) relative ear width, 0.558–2.39 %, (15) relative rostral height, 1.40–2.88 %, (16) relative head length, 10.2–22.5 %, (17) relative mental width, 1.33–2.91 %, (18) relative postmental width, 2.07–3.58 %, (19) relative cloacal width, 7.13–9.65 %, (20) relative prefrontal width, 3.74–5.49 %, (21) relative largest supraocular width, 1.88–3.62 %, (22) relative longest finger length, 3.48–7.23 %, (23) relative distance between the ear and eye, 5.36–10.0 %, (24) relative head width, 58.8–85.0 %, (25) relative frontal width, 56.2–88.2 %, (26) relative nasal height, 0.854–1.55 %, (27) relative angled subocular height, 0.484–1.33 %, (28) relative distance between the eye and naris, 4.00–6.43 %, (29) relative canthal iii length, 1.16–2.70 %, (30) relative angled subocular width, 1.61–3.14 %, and (31) relative nasal length, 1.23–2.09 %.

Content. Twenty species (Table 3): *Panolopus aenetergum*, *P. aporus*, *P. chalcorhabdus*, *P. costatus*, *P. curtissi*, *P. diastatus*, *P. emys*, *P. hylonomus*, *P. lanceolatus* **sp. nov.**, *P. lapierrae* **sp. nov.**, *P. leionotus*, *P. marcanoi*, *P. melanchrous*, *P. neiba*, *P. nesobous*, *P. oreistes*, *P. psychonothes*, *P. saonae*, *P. semitaeniatus* **sp. nov.**, and *P. unicolor* **sp. nov.**

Distribution: *Panolopus* occurs on Hispaniola and some surrounding islets.

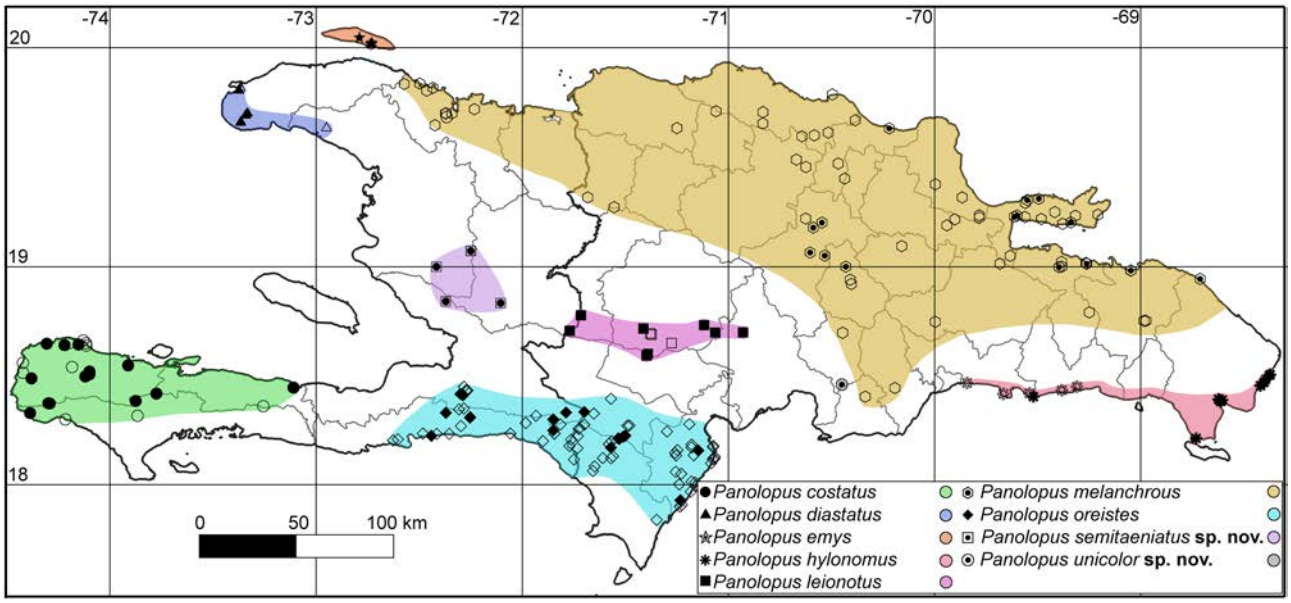

FIGURE 49. Map showing the distribution of nine species of *Panolopus* in Hispaniola. Hollow symbols indicate unexamined records.

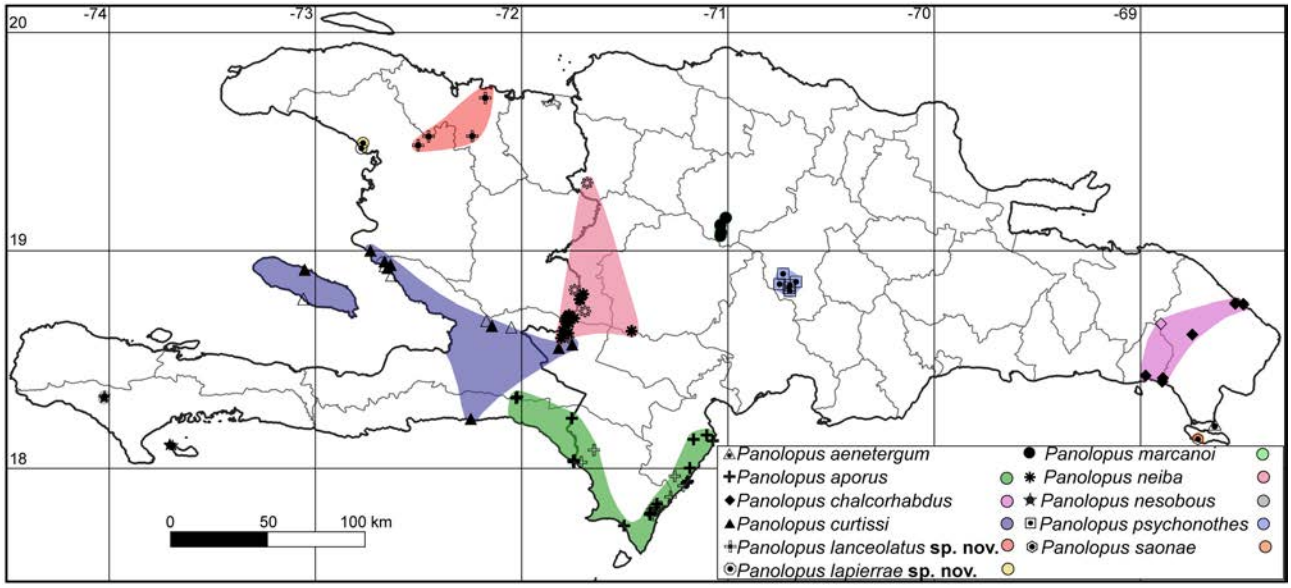

FIGURE 50. Map showing the distribution of eleven species of *Panolopus* in Hispaniola. Hollow symbols indicate unexamined records assignable to species.

***Panolopus aenetergum* (Schwartz & Jacobs 1989)**

Isla Catalinita Forest Lizard
(Fig. 51)

Celestus costatus aenetergum Schwartz & Jacobs, 1989:193. Holotype: USNM 197323, an adult male, collected by Jeremy F. Jacobs and Ronald I. Crombie on Isla Catalinita, La Altagracia, Dominican Republic, on 27 July 1975 (18.195, -68.638; 0 m).
Celestus costatus aenetergum—Schwartz & Henderson, 1991:368.
Celestus costatus aenetergum—Schools & Hedges, 2021:231.

Material examined (n=1). LA ALTAGRACIA. Isla Catalinita. USNM 197323, Jeremy F. Jacobs and Ronald I. Crombie, just south of central part of island, inland, 27 July 1975.

Diagnosis. *Panolopus aenetergum* has (1) a dorsal pattern of irregular dots, (2) head markings absent, (3) markings in the longitudinal paramedian area absent, (4) dots arranged in bars in the lateral band present, (5) an adult SVL of 83.0–92.0 mm, (6) ventral scale rows, 80–86, (7) midbody scale rows, 35–36, (8) total lamellae on one hand, 40, (9) total strigae on ten scales, 267, (10) relative length of all digits on one hindlimb, 26.8 %, (11) relative distance between the angled subocular and mouth, 0.717 %, (12) relative eye length, 3.34 %, (13) relative forelimb length, 20.6 %, (14) relative ear width, 1.29 %, (15) relative rostral height, 2.09 %, (16) relative head length, 17.5 %, (17) relative mental width, 1.63 %, (18) relative postmental width, 2.62 %, (19) relative cloacal width, 7.60 %, (20) relative prefrontal width, 4.15 %, (21) relative largest supraocular width, 2.49 %, (22) relative longest finger length, 4.83 %, (23) relative distance between the ear and eye, 8.40 %, (24) relative head width, 76.4 %, (25) relative frontal width, 88.2 %, (26) relative nasal height, 1.15 %, (27) relative angled subocular height, 1.08 %, (28) relative distance between the eye and naris, 4.35 %, (29) relative canthal iii length, 1.86 %, (30) relative angled subocular width, 2.07 %, and (31) relative nasal length, 1.92 %. No genetic data are available to estimate the species stem or crown time.

Panolopus aenetergum has a smaller relative angled subocular width (2.07) and a larger relative frontal width (88.2) than most other species of the genus.

From *Panolopus aporus*, we distinguish *P. aenetergum* by the midbody scale rows (35–36 versus 37–42), the total strigae on ten scales (267 versus 150–235), the relative length of digits on one hindlimb (26.8 versus 27.7–33.7), the relative distance between angled subocular and mouth (0.717 versus 0.441–0.669), the relative mental width (1.63 versus 1.72–2.08), the relative cloacal width (7.60 versus 7.92–8.86), the relative prefrontal width (4.15 versus 4.18–4.53), the relative largest supraocular width (2.49 versus 2.74–3.62), the relative frontal width (88.2 versus 61.7–75.1), the relative angled subocular height (1.08 versus 0.638–1.02), the relative distance between the eye and naris (4.35 versus 4.69–5.44), the relative angled subocular width (2.07 versus 2.32–2.73), and the relative nasal width (1.92 versus 1.56–1.78). From *P. chalcorhabdus*, we distinguish *P. aenetergum* by the ventral scale rows (80–86 versus 88–97), the total strigae on ten scales (267 versus 184–233), the relative length of digits on one hindlimb (26.8 versus 31.3–36.0), the relative cloacal width (7.60 versus 7.74–9.08), the relative prefrontal width (4.15 versus 4.37–4.93), the relative largest supraocular width (2.49 versus 2.52–2.86), the relative longest finger length (4.83 versus 5.29–6.97), the relative head width (76.4 versus 65.0–76.3), the relative frontal width (88.2 versus 62.5–80.8), the relative angled subocular height (1.08 versus 0.739–0.854), the relative distance between the eye and naris (4.35 versus 4.93–5.62), the relative width of canthal iii (1.86 versus 1.98–2.05), and the relative angled subocular width (2.07 versus 2.36–2.71). From *P. costatus*, we distinguish *P. aenetergum* the ventral scale rows (80–86 versus 89–106), the midbody scale rows (35–36 versus 39–43), the total lamellae on one hand (40 versus 49–58), the total strigae on ten scales (267 versus 158–217), the relative length of digits on one hindlimb (26.8 versus 31.5–37.8), the relative mental width (1.63 versus 1.66–2.00), the relative longest finger length (4.83 versus 5.53–6.66), the relative frontal width (88.2 versus 56.2–67.4), the relative angled subocular height (1.08 versus 0.562–0.886), the relative distance between the eye and naris (4.35 versus 5.08–5.50), the relative angled subocular width (2.07 versus 2.36–2.81), and the relative nasal width (1.92 versus 1.58–1.74). From *P. curtissi*, we distinguish *P. aenetergum* by the dorsal pattern (irregular dots versus absent/irregular flecks), the dots arranged in bars in the lateral areas (present versus absent), the ventral scale rows (80–86 versus 90–103), the total lamellae on one hand (40 versus 32–39), the total strigae on ten scales (267 versus 165–260), the relative distance between angled subocular and mouth (0.717 versus 0.393–0.587), the relative forelimb length (20.6 versus 15.1–20.5), the relative longest finger length (4.83 versus 3.59–4.54), the relative distance between the ear and eye (8.40 versus 5.36–7.71), the relative frontal width (88.2 versus 65.4–83.1), the relative angled subocular width (2.07 versus 2.26–2.76), and the relative nasal width (1.92 versus 1.44–1.82). From *P. diastatus*, we distinguish *P. aenetergum* by the dorsal pattern (irregular dots versus absent/irregular flecks), the total strigae on ten scales (267 versus 169–234), the relative distance between angled subocular and mouth (0.717 versus 0.00–0.614), the relative eye length (3.34 versus 2.71–3.32), the relative forelimb length (20.6 versus 16.2–20.1), the relative head width (76.4 versus 69.4–74.8), the relative frontal width (88.2 versus 57.4–86.2), and the relative nasal width (1.92 versus 1.41–1.77). From *P. emys*, we distinguish *P. aenetergum* by the dorsal pattern (irregular dots versus absent/irregular flecks), the adult SVL (83.0–92.0 versus 99.0–113), the ventral scale rows (80–86 versus 89–104), the relative length of digits on one hindlimb (26.8 versus 28.9–35.2), the relative rostral height (2.09 versus 2.10–2.37), the relative cloacal width (7.60 versus 8.24–8.96), the relative longest finger length (4.83 versus 5.15–5.83), the relative frontal width (88.2 versus 67.7–74.5), the relative nasal height (1.15 versus 0.963–1.10), the relative angled subocular height

(1.08 versus 0.696–0.981), and the relative distance between the eye and naris (4.35 versus 4.37–5.19). From *P. hylonomus*, we distinguish *P. aenetergum* by the dorsal pattern (irregular dots versus absent/irregular flecks), the dots arranged in bars in the lateral areas (present versus absent), the adult SVL (83.0–92.0 versus 59.3–76.5), the total strigae on ten scales (267 versus 169–222), the relative postmental width (2.62 versus 2.67–2.89), the relative cloacal width (7.6 versus 7.98–8.57), the relative prefrontal width (4.15 versus 4.23–4.87), the relative largest supraocular width (2.49 versus 2.65–2.90), the relative distance between the ear and eye (8.40 versus 6.78–8.05), the relative frontal width (88.2 versus 64.0–74.5), and the relative width of canthal iii (1.86 versus 1.95–2.03). From *P. lanceolatus* **sp. nov.**, we distinguish *P. aenetergum* by the longitudinal paramedian lines (absent versus present), the ventral scale rows (80–86 versus 93–102), the midbody scale rows (35–36 versus 37–43), the total lamellae on one hand (40 versus 41–52), the total strigae on ten scales (267 versus 186–234), the relative length of digits on one hindlimb (26.8 versus 28.4–35.9), the relative distance between angled subocular and mouth (0.717 versus 0.567–0.704), the relative cloacal width (7.60 versus 8.01–8.76), the relative distance between the ear and eye (8.4 versus 6.45–7.70), the relative frontal width (88.2 versus 63.1–72.1), the relative nasal height (1.15 versus 0.904–1.06), the relative angled subocular height (1.08 versus 0.484–0.854), the relative distance between the eye and naris (4.35 versus 4.58–5.05), and the relative angled subocular width (2.07 versus 2.38–3.09). From *P. lapierrae* **sp. nov.**, we distinguish *P. aenetergum* by the dorsal pattern (irregular dots versus absent/dots in chevrons) and the ventral scale rows (80–86 versus 90–98). From *P. leionotus*, we distinguish *P. aenetergum* by the total lamellae on one hand (40 versus 43–48), the total strigae on ten scales (267 versus 191–266), the relative mental width (1.63 versus 1.67–2.02), the relative cloacal width (7.60 versus 8.03–8.69), the relative frontal width (88.2 versus 68.7–81.2), the relative distance between the eye and naris (4.35 versus 4.46–5.61), and the relative angled subocular width (2.07 versus 2.48–2.95). From *P. marcanoi*, we distinguish *P. aenetergum* by the head markings (absent versus present), the longitudinal paramedian lines (absent versus present), the ventral scale rows (80–86 versus 89–102), the midbody scale rows (35–36 versus 38–45), the total strigae on ten scales (267 versus 141–254), the relative mental width (1.63 versus 1.75–2.33), the relative prefrontal width (4.15 versus 4.19–5.19), the relative frontal width (88.2 versus 59.0–73.0), the relative angled subocular height (1.08 versus 0.505–0.793), the relative distance between the eye and naris (4.35 versus 4.68–5.82), and the relative angled subocular width (2.07 versus 2.19–3.14). From *P. melanchrous*, we distinguish *P. aenetergum* by the longitudinal paramedian lines (absent versus present), the adult SVL (83.0–92.0 versus 93.2–124), the ventral scale rows (80–86 versus 89–113), the total lamellae on one hand (40 versus 47–58), the relative length of digits on one hindlimb (26.8 versus 30.7–41.3), the relative postmental width (2.62 versus 2.71–3.38), the relative cloacal width (7.60 versus 7.61–9.20), the relative prefrontal width (4.15 versus 4.21–5.06), the relative longest finger length (4.83 versus 5.76–7.09), the relative frontal width (88.2 versus 61.3–71.4), the relative nasal height (1.15 versus 0.897–0.952), the relative angled subocular height (1.08 versus 0.680–0.856), the relative distance between the eye and naris (4.35 versus 4.89–5.59), and the relative angled subocular width (2.07 versus 2.28–2.82). From *P. neiba*, we distinguish *P. aenetergum* by the dorsal pattern (irregular dots versus irregular flecks/dots in chevrons), the total lamellae on one hand (40 versus 45–49), the total strigae on ten scales (267 versus 179–239), the relative length of digits on one hindlimb (26.8 versus 29.5–36.6), the relative mental width (1.63 versus 1.66–2.36), the relative prefrontal width (4.15 versus 4.41–5.49), the relative longest finger length (4.83 versus 5.61–6.66), the relative frontal width (88.2 versus 63.3–74.0), the relative nasal height (1.15 versus 0.963–1.08), the relative angled subocular height (1.08 versus 0.713–0.885), the relative distance between the eye and naris (4.35 versus 4.51–5.01), and the relative angled subocular width (2.07 versus 2.34–2.83). From *P. nesobous*, we distinguish *P. aenetergum* by the longitudinal paramedian lines (absent versus present), the midbody scale rows (35–36 versus 38–43), and the total lamellae on one hand (40 versus 50–59). From *P. oreistes*, we distinguish *P. aenetergum* by the longitudinal paramedian lines (absent versus present), the relative length of digits on one hindlimb (26.8 versus 31.2–40.1), the relative prefrontal width (4.15 versus 4.18–4.96), the relative longest finger length (4.83 versus 5.27–7.23), the relative frontal width (88.2 versus 61.6–76.9), the relative nasal height (1.15 versus 0.878–1.06), the relative angled subocular height (1.08 versus 0.737–0.978), the relative distance between the eye and naris (4.35 versus 5.01–5.63), the relative angled subocular width (2.07 versus 2.13–3.04), and the relative nasal width (1.92 versus 1.37–1.65). From *P. psychonothes*, we distinguish *P. aenetergum* by the ventral scale rows (80–86 versus 88–109), the total strigae on ten scales (267 versus 172–244), the relative longest finger length (4.83 versus 4.89–5.81), the relative distance between the ear and eye (8.4 versus 6.79–8.29), the relative frontal width (88.2 versus 66.5–81.0), and the relative angled subocular height (1.08 versus 0.803–0.952). From *P. saonae*, we distinguish *P. aenetergum* by the dorsal pattern (irregular dots versus absent), the ventral scale rows

(80–86 versus 92–95), the relative distance between angled subocular and mouth (0.717 versus 0.517–0.630), and the relative eye length (3.34 versus 3.06–3.20). From *P. semitaeniatus* **sp. nov.**, we distinguish *P. aenetergum* by the total strigae on ten scales (267 versus 174–204), the relative length of digits on one hindlimb (26.8 versus 30.4–34.6), the relative forelimb length (20.6 versus 21.3–23.8), the relative ear width (1.29 versus 1.90–2.30), the relative mental width (1.63 versus 1.69–2.09), the relative cloacal width (7.60 versus 8.08–8.23), the relative prefrontal width (4.15 versus 4.38–4.94), the relative largest supraocular width (2.49 versus 2.59–3.32), the relative longest finger length (4.83 versus 5.17–6.05), the relative distance between the ear and eye (8.40 versus 6.64–7.90), the relative head width (76.4 versus 58.8–63.8), the relative frontal width (88.2 versus 63.6–76.5), and the relative angled subocular height (1.08 versus 0.654).From *P. unicolor* **sp. nov.**, we distinguish *P. aenetergum* by the dorsal pattern (irregular dots versus absent), the longitudinal paramedian lines (absent versus present), the total strigae on ten scales (267 versus 144), and the relative frontal width (88.2 versus 58.2).

Description of holotype. USNM 197323. An adult; SVL 92.0 mm; tail nearly cylindrical, broken in life midway, regenerated, 115 mm (125% SVL); axilla-to-groin distance 54.7 mm (59.5% SVL); forelimb length 19.0 mm (20.7% SVL); hindlimb length 25.7 mm (27.9% SVL); head length 16.1 mm (17.5% SVL); head width 12.3 mm (13.4% SVL); head width 76.4% head length; diameter of orbit 3.07 mm (3.34% SVL); horizontal diameter of ear opening 1.19 mm (1.29% SVL); vertical diameter of ear opening 1.44 mm (1.57% SVL); length of all toes on one foot 24.7 mm (26.8% SVL); shortest distance between angled subocular and lip 0.66 mm (0.717% SVL); shortest distance between the ocular and auricular openings 7.73 mm (8.40 SVL); longest finger length 4.44 mm (4.83% SVL); largest supraocular width 2.29 mm (2.49% SVL); cloacal width 6.99 mm (7.60% SVL); mental width 1.50 mm (1.63% SVL); postmental width 2.41 mm (2.62% SVL); prefrontal width 3.82 mm (4.15% SVL); frontal width 88.2% frontal length; nasal height 1.06 mm (1.15% SVL); angled subocular height 0.99 mm (1.08% SVL); shortest distance between the eye and naris 4.00 mm (4.35% SVL); canthal iii width 1.71 mm (1.86% SVL); angled subocular width 1.90 mm (2.07% SVL); nasal width 1.77 mm (1.92% SVL); rostral 2.09X as wide as high, visible from above, not in contact with nasals, in contact with 1st supralabial and anterior internasal (left)/(right); anterior internasals are narrower than posterior ones; frontonasals and prefrontal fused into a single large plate with an irregular posterior margin, much wider than long, bordered by posterior internasals, 1st loreals, 1st and 2nd median oculars, and the frontal; frontal longer than wide; a pair of frontoparietals, separated by the posterior prolongation of the frontal and the interparietal plate (fused with parietals); interparietal plate smaller than parietals and fused with them, posteriorly touching the interoccipital, which is wider than long; parietal separated from supraoculars by 1st and 2nd temporals and frontoparietal (1st fused with the frontoparietal) (left)/1st–3rd temporals and frontoparietal (1st temporal divided) (right); nasal single; nostril above suture between 1st and 2nd supralabials (left)/(right); postnasal 1 (left)/(right); loreals 2 (left)/(right); 1st loreal higher than wide (left)/(right), in contact with postnasal, posterior internasal, prefrontal/frontonasal complex, 1st median ocular, canthal iii (fused with 1st median ocular), additional scale above 2nd loreal, 2nd loreal, and 3rd–4th supralabials (left)/in contact with postnasal, posterior internasal, prefrontal/frontonasal complex, 1st median ocular, canthal iii, 2nd loreal, and 3rd–4th supralabials (right); 2nd loreal shorter than 1st, approximately as high as wide (left)/(right), excluded from contact with supraocular by canthal iii (fused with median ocular 1), additional scale above 2nd loreal (left)/canthal iii (right); 2nd loreal posteriorly bordering the lower preocular (left)/(right); canthal iii fused with 1st median ocular (left)/wider than high (right), contacting 1st median ocular (fused), anterior supraciliary, upper and lower preoculars, 1st and 2nd loreals, and the additional scale (left)/1st median ocular, anterior supraciliary, upper preocular, and 1st and 2nd loreals (right); 10 median oculars (left)/(right), 1st and 2nd contacting the prefrontal (left)/(right); 1 upper preocular (left)/(right); an irregular anterior supraciliary (left)/(right); 6 lateral oculars (left)/(right); 5 (left)/6 (right) temporals; 1 (left)/2 (right) suboculars; posterior subocular large and elongate (left)/(right); anterior subocular small (right); 10 (left)/9 (right) supralabials, 6 to level below center of eye (left)/(right); 10 (left)/9 (right) infralabials, 5 to level below center of eye (left)/(right); mental small, followed by a single, larger postmental; 4 pairs of enlarged chin shields, 1st pair in contact with one another; 2nd–4th pairs separated by 1–2 scales; 97 transverse rows of dorsal scales from interoccipital to base of tail; 86 transverse rows of ventral scales from mental to vent; 36 scales around midbody; 5 digits; finger lengths 3>4>2>5>1; 10 (left) lamellae under longest finger; 40 total lamellae on one hand; toe lengths 4>3>5>2>1; 17 (left) lamellae under longest toe; dorsal body and caudal scales keelless and striate; ventral scales with faint striations; 267 total strigae counted on ten scales.

FIGURE 51. (A–F) *Panolopus aenetergum* (USNM 197323, holotype), SVL 92.0 mm.

Color (in alcohol): dorsal surface of head brown-gray, patternless; lateral surfaces of head grading from brown-gray to cream with darker brown eye masks and other darker brown areas on the labial scales; dorsal surfaces of the body are brown-gray with many darker brown flecks; dorsal surface of tail the same as the body; lateral areas grade from dark brown to cream with cream and dark brown dots in rows; dorsal surfaces of the limbs are dark brown with paler gray mottling; lateral and ventral areas of the limbs grade to cream with some darker brown mottling; ventral surfaces of the head, body, and tail are cream with several flecks under the throat.

Variation. No other specimens were examined for this species. Measurements and other morphological data for the holotype are presented in Table 1.

Distribution. *Panolopus aenetergum* is distributed on Isla Catalinita at 0–5 m (Fig. 50).

Ecology and conservation. Both the holotype and paratype of this species were collected as they actively foraged in leaf litter during the day (0900–1130 h) in a way that the collectors believed them to be *Ameiva* (Schwartz & Jacobs 1989).

We consider the conservation status of *Panolopus aenetergum* to be Least Concern, based on IUCN Redlist criteria (IUCN 2023). It is likely a common species tolerant of some habitat disturbance, based on what is known of most species of *Panolopus*. However, its range appears to be very small, which is a concern. Studies are needed to determine the health and extent of remaining populations and better understand the threats to the survival of the species.

Reproduction. No data on reproduction are available for this species.

Etymology. The species name (*aenetergum*) is an appositional noun derived from the Latin *aene* (bronze) and *tergum* (back) in reference to the metallic dorsal color of this species.

Remarks. Schwartz & Jacobs (1989) noted that the fauna of Isla Catalinita, including *Panolopus aenetergum*, could have been derived from either the mainland or nearby Isla Saona. *Panolopus aenetergum* is not included in our genetic dataset and future studies should be conducted using genetic or genomic data from this species.

***Panolopus aporus* (Schwartz 1964)**

Barahona Smooth-scaled Forest Lizard
(Fig. 52–53)

Diploglossus curtissi aporus Schwartz, 1964:45. Holotype: MCZ R-77159, collected by David C. Leber and Richard Thomas from 13.1 mi SW Enriquillo, Pedernales Prov., Dominican Republic, on 30 July 1963 (17.7939, -71.3753; 8 m).
Diploglossus curtissi aporus—Greer, 1967:96.
Diploglossus curtissi aporus—Ober, 1970:275.
Celestus curtissi aporus—Schwartz & Henderson, 1988:98.
Celestus curtissi aporus—Schwartz & Henderson, 1991:371.
Celestus curtissi aporus—Hedges *et al.*, 2019.
Panolopus curtissi aporus—Schools & Hedges, 2022:230.

Material examined (n=41). DOMINICAN REPUBLIC. Barahona. KU 79827, 5 km NE Enriquillo, 7 August 1963; KU 226024, 226027–8, 0.5 mi NE Caleton, 8 December 1971; USNM 328742, Richard Thomas and S. Blair Hedges, ca. 4–5 km S Barahona, 2.7 km W of, via coast road and road to Filipinas, 20 August 1984; USNM 328743, S. Blair Hedges and Richard Thomas, ca. 4.5 km S, 4.0 km W of Barahona, via coast road and road to Filipinas, 20 August 1984; USNM 328744, S. Blair Hedges, 15 km SSW of La Guazara, 21 June 1985; USNM 328793, S. Blair Hedges and Richard Thomas, 11.3 km S of Barahona, 20 August 1984. **Pedernales.** Hispaniola. AMNH 92798, D. C. Leber, 5 mi NE Oviedo, 30 July 1963; ANSP 38623–7, S. Blair Hedges, Richard Thomas, and locals, Bucan Detwi, 6 January 1998; ANSP 38628–9, S. Blair Hedges, Matthew Heinicke, N. Coro, Pedernales town, in palm grove, 20 August 2005; KU 226021–3, 13.1 mi SW Enriquillo, 30 July 1963; KU 226041–2, 13.1 mi SW Enriquillo; MCZ R-77159, David C. Leber and Richard Thomas, 13.1 mi SW Enriquillo, 30 July 1963; USNM 328766–8, S. Blair Hedges and Richard Thomas, Juancho, 17 August 1984; USNM 328769–72, Richard Thomas and S. Blair Hedges, Los Arroyos, 27 August 1984; USNM 328794–800, S. Blair Hedges and Richard Thomas, 6.4 km SW, 0.7 km SE (road) of Juancho, 16 August 1984. **HAITI. Sud-Est.** ANSP 38630–1, S. Blair Hedges, Tiffany Cloud, Miguel Landestoy, Marcos Rodriguez, Southeast of Pic La Selle, 20 November 2011; SBH 269908, 269910–1, S. Blair Hedges, Tiffany Cloud, Miguel Landestoy, Marcos Rodriguez, Southeast of Pic La Selle, 20 November 2011.

Diagnosis. *Panolopus aporus* has (1) a dorsal pattern of absent/irregular flecks/irregular dots/dots in chevrons, (2) head markings absent, (3) markings in the longitudinal paramedian area absent/present, (4) dots arranged in bars in the lateral band present, (5) an adult SVL of 77.8–100 mm, (6) ventral scale rows, 85–102, (7) midbody scale rows, 37–42, (8) total lamellae on one hand, 36–48, (9) total strigae on ten scales, 150–235, (10) relative length of all digits on one hindlimb, 27.7–33.7 %, (11) relative distance between the angled subocular and mouth, 0.441–0.669 %, (12) relative eye length, 2.91–3.76 %, (13) relative forelimb length, 19.3–26.4 %, (14) relative ear width, 1.06–1.88 %, (15) relative rostral height, 2.01–2.40 %, (16) relative head length, 10.2–18.6 %, (17) relative mental

width, 1.72–2.08 %, (18) relative postmental width, 2.42–2.92 %, (19) relative cloacal width, 7.92–8.86 %, (20) relative prefrontal width, 4.18–4.53 %, (21) relative largest supraocular width, 2.74–3.62 %, (22) relative longest finger length, 4.57–5.72 %, (23) relative distance between the ear and eye, 6.73–8.49 %, (24) relative head width, 71.4–83.2 %, (25) relative frontal width, 61.7–75.1 %, (26) relative nasal height, 1.08–1.23 %, (27) relative angled subocular height, 0.638–1.02 %, (28) relative distance between the eye and naris, 4.69–5.44 %, (29) relative canthal iii length, 1.85–1.96 %, (30) relative angled subocular width, 2.32–2.73 %, and (31) relative nasal length, 1.56–1.78 %. The species stem time is 2.04 Ma and the species crown time is 0.27 Ma (Fig. 4).

We distinguish *Panolopus aporus* from the other species of *Panolopus* based on a complex of traits. From *Panolopus aenetergum*, we distinguish *P. aporus* by the midbody scale rows (37–42 versus 35–36), the total strigae on ten scales (150–235 versus 267), the relative length of digits on one hindlimb (27.7–33.7 versus 26.8), the relative distance between angled subocular and mouth (0.441–0.669 versus 0.717), the relative mental width (1.72–2.08 versus 1.63), the relative cloacal width (7.92–8.86 versus 7.60), the relative prefrontal width (4.18–4.53 versus 4.15), the relative largest supraocular width (2.74–3.62 versus 2.49), the relative frontal width (61.7–75.1 versus 88.2), the relative angled subocular height (0.638–1.02 versus 1.08), the relative distance between the eye and naris (4.69–5.44 versus 4.35), the relative angled subocular width (2.32–2.73 versus 2.07), and the relative nasal width (1.56–1.78 versus 1.92). From *P. chalcorhabdus*, we distinguish *P. aporus* by the relative width of canthal iii (1.85–1.96 versus 1.98–2.05). From *P. costatus*, we distinguish *P. aporus* by the total lamellae on one hand (36–48 versus 49–58). From *P. curtissi*, we distinguish *P. aporus* by the dots arranged in bars in the lateral areas (present versus absent) and the relative longest finger length (4.57–5.72 versus 3.59–4.54). From *P. diastatus*, we distinguish *P. aporus* by the relative length of digits on one hindlimb (27.7–33.7 versus 21.5–27.4) and the relative largest supraocular width (2.74–3.62 versus 1.88–2.57). From *P. emys*, we distinguish *P. aporus* by the total strigae on ten scales (150–235 versus 238–311) and the relative angled subocular width (2.32–2.73 versus 2.12–2.20). From *P. hylonomus*, we distinguish *P. aporus* by the dots arranged in bars in the lateral areas (present versus absent) and the adult SVL (77.8–100 versus 59.3–76.5). From *P. lanceolatus* **sp. nov.**, we distinguish *P. aporus* by the relative largest supraocular width (2.74–3.62 versus 2.20–2.71) and the relative nasal height (1.08–1.23 versus 0.904–1.06). From *P. lapierrae* **sp. nov.**, we distinguish *P. aporus* the relative prefrontal width (4.18–4.53 versus 4.73–4.75), the relative longest finger length (4.57–5.72 versus 4.49–4.55), the relative frontal width (61.7–75.1 versus 77.6–79.0), and the relative nasal width (1.56–1.78 versus 1.81). From *P. leionotus*, we distinguish *P. aporus* by the relative largest supraocular width (2.74–3.62 versus 1.94–2.50). From *P. marcanoi*, we distinguish *P. aporus* by the head markings (absent versus present). From *P. melanchrous*, we distinguish *P. aporus* by the relative longest finger length (4.57–5.72 versus 5.76–7.09) and the relative nasal height (1.08–1.23 versus 0.897–0.952). From *P. neiba*, we distinguish *P. aporus* by the relative distance between angled subocular and mouth (0.441–0.669 versus 0.670–0.747). From *P. nesobous*, we distinguish *P. aporus* by the total lamellae on one hand (36–48 versus 50–59), the relative length of digits on one hindlimb (27.7–33.7 versus 35.1), the relative prefrontal width (4.18–4.53 versus 4.74–4.81), the relative longest finger length (4.57–5.72 versus 6.19–6.33), the relative distance between the eye and naris (4.69–5.44 versus 5.62–5.73), and the relative width of canthal iii (1.85–1.96 versus 2.01–2.12). From *P. oreistes*, we distinguish *P. aporus* by the relative nasal height (1.08–1.23 versus 0.878–1.06). From *P. psychonothes*, we distinguish *P. aporus* by the relative largest supraocular width (2.74–3.62 versus 1.92–2.68). From *P. saonae*, we distinguish *P. aporus* by the relative mental width (1.72–2.08 versus 1.52), the relative prefrontal width (4.18–4.53 versus 4.14), the relative nasal height (1.08–1.23 versus 1.01), the relative distance between the eye and naris (4.69–5.44 versus 6.43), the relative width of canthal iii (1.85–1.96 versus 1.99), and the relative angled subocular width (2.32–2.73 versus 2.31). From *P. semitaeniatus* **sp. nov.**, we distinguish *P. aporus* by the relative ear width (1.06–1.88 versus 1.90–2.30), the relative rostral height (2.01–2.40 versus 2.41–2.63), the relative head width (71.4–83.2 versus 58.8–63.8), the relative distance between the eye and naris (4.69–5.44 versus 4.61), the relative width of canthal iii (1.85–1.96 versus 1.80), and the relative nasal width (1.56–1.78 versus 1.51). From *P. unicolor* **sp. nov.**, we distinguish *P. aporus* by the adult SVL (77.8–100 versus 67.6), the total strigae on ten scales (150–235 versus 144), the relative length of digits on one hindlimb (27.7–33.7 versus 36.8), the relative cloacal width (7.92–8.86 versus 7.61), the relative prefrontal width (4.18–4.53 versus 4.69), the relative longest finger length (4.57–5.72 versus 6.65), the relative head width (71.4–83.2 versus 70.8), the relative frontal width (61.7–75.1 versus 58.2), the relative distance between the eye and naris (4.69–5.44 versus 5.52), the relative width of canthal iii (1.85–1.96 versus 1.79), the relative angled subocular width (2.32–2.73 versus 2.90), and the relative nasal width (1.56–1.78 versus 2.00).

FIGURE 52. (A–F) *Panolopus aporus* (MCZ R-77159, holotype), SVL 78.4 mm.

Description of holotype. MCZ R-77159. An adult female; SVL 78.4 mm; tail nearly cylindrical, broken, 28.7 mm (36.6% SVL); axilla-to-groin distance 46.9 mm (59.8% SVL); forelimb length 15.1 mm (19.3% SVL); hindlimb length 23.7 mm (30.2% SVL); head length 13.1 mm (16.7% SVL); head width 9.35 mm (11.9% SVL); head width 71.4% head length; diameter of orbit 2.44 mm (3.11% SVL); horizontal diameter of ear opening 0.83

mm (1.06% SVL); vertical diameter of ear opening 0.68 mm (0.867% SVL); length of all toes on one foot 21.7 mm (27.7% SVL); shortest distance between angled subocular and lip 0.48 mm (0.612% SVL); shortest distance between the ocular and auricular openings 5.85 mm (7.46% SVL); longest finger length 3.69 mm (4.71% SVL); largest supraocular width 2.15 mm (2.74% SVL); cloacal width 6.67 mm (8.51% SVL); mental width 1.63 mm (2.08% SVL); postmental width 1.90 mm (2.42% SVL); prefrontal width 3.28 mm (4.18% SVL); frontal width 61.7% frontal length; nasal height 0.92 mm (1.17% SVL); angled subocular height 0.80 mm (1.02% SVL); shortest distance between the eye and naris 3.68 mm (4.69% SVL); canthal iii width 1.54 mm (1.96% SVL); angled subocular width 1.82 mm (2.32% SVL); nasal width 1.22 mm (1.56% SVL); rostral 2.32 X as wide as high, visible from above, not in contact with nasals, in contact with 1st supralabial and anterior internasal (left)/(right); anterior internasals are narrower than posterior ones; frontonasals and prefrontal fused into a single large plate with a slightly concave posterior margin, much wider than long, bordered by posterior internasals, 1st loreals, canthal iii, 1st and 2nd median oculars, and the frontal; frontal longer than wide; a pair of frontoparietals (fused with frontal on the left), separated by the posterior prolongation of the frontal and the interparietal plate; interparietal plate slightly smaller than parietals and separating them, posteriorly touching the interoccipital, which is wider than long; parietal separated from supraoculars by temporals 1–2 and frontoparietal (left)/(right); nasal single; nostril just posterior to suture between 1st and 2nd supralabials (left)/(right); 1 postnasal (left)/(right); 2 loreals (left)/(right); 1st loreal higher than wide (left)/(right), in contact with postnasal, posterior internasal, prefrontal/frontonasal complex, canthal iii, 2nd loreal, and 3rd–4th supralabials (left)/(right); 2nd loreal shorter than 1st, approximately as high as wide (left)/(right), excluded from contact with supraocular by canthal iii (left)/(right); final loreal posteriorly bordering the lower preocular (left)/(right); canthal iii wider than high (left)/(right), contacting 1st median ocular, anterior supraciliary, the upper and lower preoculars, prefrontal/frontonasal complex, and 1st and 2nd loreals (left)/(right); 10 median oculars (left)/(right), 1st and 2nd contacting the prefrontal (left)/(right); 1 upper preocular (left)/(right); an irregular anterior supraciliary (left)/(right); 5 lateral oculars (left)/(right); 5 temporals (left)/(right); 2 suboculars (left)/(right); posterior subocular large and elongate (left)/(right); anterior subocular small (left)/(right); 9 (left)/10 (right) supralabials, 6 (left)/7 (right) to level below center of eye; 9 (left)/10 (right) infralabials, 6 to level below center of eye (left)/(right); mental small, followed by a single, larger postmental; 4 pairs of enlarged chin shields; 1st pair in contact with one another anteriorly, posteriorly separated by one scale; 2nd–4th pairs separated by 1–3 scales; 91 transverse rows of dorsal scales from interoccipital to base of tail; 97 transverse rows of ventral scales from mental to vent; 38 scales around midbody; 5 digits; finger lengths 3>4>2>5>1; 11 (left)/12 (right) lamellae under longest finger; 44 total lamellae on one hand; toe lengths 4>3>5>2>1; 17 (left)/18 (right) lamellae under longest toe; dorsal body and caudal scales keelless and striate; smooth ventral scales; 189 total strigae counted on ten scales.

Color (in alcohol): dorsal surface of head gray-tan, patternless; lateral surfaces of head grading from pale tan to cream with darker brown eye masks and other darker brown areas on the supralabial scales; dorsal surfaces of the body are red-gray with faint longitudinal paramedian lines that end before the forearms; dorsal surface of tail red-gray; lateral areas grading from dark red-brown to cream with darker brown and off-white dots arranged in bars; dorsal surfaces of the limbs are golden tan with darker brown mottling; lateral and ventral areas of the limbs fade to pale cream, patternless; ventral surfaces of the head, body, and tail are pale cream with some brown mottling under the throat.

Variation. Dorsal pattern in this species ranges from completely absent to irregular flecks or dots to dots arranged in chevrons. The dorsal color ranges from medium brown to gray-brown. In all specimens the head scales are patternless. Markings in the longitudinal paramedian series range from completely absent (ANSP 38629) to dots in series to broken or complete longitudinal paramedian lines. Dots in the lateral band are arranged in bars in all specimens. Measurements and other morphological data for the holotype and other examined material are presented in Table 1.

Distribution. *Panolopus aporus* is distributed primarily on the Barahona Peninsula of the Dominican Republic at coastal and near-coastal locations (0–1928 m). It also is found in the Massif de la Selle, southeast of Pic La Selle.

Ecology and conservation. Specimens of this species were commonly collected during the day from under logs, rocks, leaf litter, and rotting coconut husks and fronds.

We consider the conservation status of *Panolopus aporus* to be Least Concern, based on IUCN Redlist criteria (IUCN 2023). It is likely a common species tolerant of some habitat disturbance, based on what is known of most species of *Panolopus*. However, it faces a primary threat of habitat destruction resulting from agriculture and

charcoaling. A secondary threat is predation from introduced mammals, including the mongoose and black rats. Studies are needed to determine the health and extent of remaining populations and better understand the threats to the survival of the species.

FIGURE 53. *Panolopus aporus* (USNM 328744, SBH 160291), SVL 97.8 mm, in life. From 15 km SSW of La Guazara, Barahona Province, Dominican Republic. Photo by SBH.

Reproduction. Litter sizes of 3–6 have been recorded in this species (SBH, field data).

Etymology. According to Schwartz (1964), the name (*aporus*) is derived from the Greek word for "puzzled," in reference to the lack of understanding of the affinities of the taxon.

Remarks. Previously considered a subspecies of *Panolopus curtissi*, herein we elevate *P. aporus* to species level based on morphological and genetic distinction. Museum collections commonly include this species; however, additional sampling to determine the current state of present-day populations would benefit future assessments.

Panolopus aporus is included in our genetic dataset and has significant support in both Bayesian and ML likelihood analyses at the crown node that defines it as a species. The stem node placing *P. aporus* as the closest relative to *P. curtissi* had a support value of 58% in our ML analysis and was not supported in our Bayesian analysis. Schools *et al.* (2022) used genomic data to place *P. aporus* as the closest relative to *P. curtissi* with a significant support value in the ML analysis and a support value of 80% in the Bayesian analysis. Based on our timetree (Fig. 4), *P. aporus* diverged from its closest relative 2.04 Ma, consistent with typical species of vertebrates (> 0.7 Ma; Hedges *et al.* 2015). *Panolopus aporus* was recovered as conspecific with *Panolopus oreistes* in our ASAP analysis.

***Panolopus chalcorhabdus* (Schwartz 1964)**
Big-nosed Smooth-scaled Forest Lizard
(Fig. 54)

Diploglossus costatus chalcorhabdus Schwartz, 1964:37. Holotype: MCZ R-77158, collected by Richard Thomas from 0.9 mi. SE El Macas, La Romana Province, Dominican Republic, on 31 August 1963 (18.4278, -68.9743; 31 m).

Celestus costatus chalcorhabdus—Schwartz & Henderson, 1988:94.
Celestus costatus chalcorhabdus—Schwartz & Henderson, 1991:368.
Celestus costatus chalcorhabdus—Hedges *et al.*, 2019:16.
Celestus costatus chalcorhabdus—Schools & Hedges, 2021:231.

Material examined (n=8). DOMINICAN REPUBLIC. La Altagracia. KU 225001, 0.9 mi SE El Macao, 31 August 1963; KU 225003, 3.2 mi W Higuey, 28 August 1963; KU 225076–7, mouth Rio Chavon, W side, 15 July 1972; KU 225078–9, 3.3 mi SE El Macao, 20 July 1972. **La Romana.** KU 225002, 8 km E La Romana, 19 July 1963; MCZ R-77158, Richard Thomas, 0.9 mi. SE El Macas, 31 August 1963.

Diagnosis. *Panolopus chalcorhabdus* has (1) a dorsal pattern of absent/irregular flecks/irregular dots, (2) head markings absent/present, (3) markings in the longitudinal paramedian area absent/present, (4) dots arranged in bars in the lateral band present, (5) an adult SVL of 71.9–95.4 mm, (6) ventral scale rows, 88–97, (7) midbody scale rows, 36–41, (8) total lamellae on one hand, 40–52, (9) total strigae on ten scales, 184–233, (10) relative length of all digits on one hindlimb, 31.3–36.0 %, (11) relative distance between the angled subocular and mouth, 0.481–0.818 %, (12) relative eye length, 3.07–3.71 %, (13) relative forelimb length, 20.4–23.7 %, (14) relative ear width, 1.26–1.65 %, (15) relative rostral height, 1.85–2.24 %, (16) relative head length, 16.6–18.8 %, (17) relative mental width, 1.47–2.00 %, (18) relative postmental width, 2.38–3.31 %, (19) relative cloacal width, 7.74–9.08 %, (20) relative prefrontal width, 4.37–4.93 %, (21) relative largest supraocular width, 2.52–2.86 %, (22) relative longest finger length, 5.29–6.97 %, (23) relative distance between the ear and eye, 6.82–8.58 %, (24) relative head width, 65.0–76.3 %, (25) relative frontal width, 62.5–80.8 %, (26) relative nasal height, 0.854–1.55 %, (27) relative angled subocular height, 0.739–0.854 %, (28) relative distance between the eye and naris, 4.93–5.62 %, (29) relative canthal iii length, 1.98–2.05 %, (30) relative angled subocular width, 2.36–2.71 %, and (31) relative nasal length, 1.70–2.01 %. No genetic data are available to estimate the species stem of crown time.

We distinguish *Panolopus chalcorhabdus* from the other species of *Panolopus* based on a complex of traits. From *Panolopus aenetergum*, we distinguish *P. chalcorhabdus* by the ventral scale rows (88–97 versus 80–86), the total strigae on ten scales (184–233 versus 267), the relative length of digits on one hindlimb (31.3–36.0 versus 26.8), the relative cloacal width (7.74–9.08 versus 7.60), the relative prefrontal width (4.37–4.93 versus 4.15), the relative largest supraocular width (2.52–2.86 versus 2.49), the relative longest finger length (5.29–6.97 versus 4.83), the relative head width (65.0–76.3 versus 76.4), the relative frontal width (62.5–80.8 versus 88.2), the relative angled subocular height (0.739–0.854 versus 1.08), the relative distance between the eye and naris (4.93–5.62 versus 4.35), the relative width of canthal iii (1.98–2.05 versus 1.86), and the relative angled subocular width (2.36–2.71 versus 2.07). From *P. aporus*, we distinguish *P. chalcorhabdus* by the relative width of canthal iii (1.98–2.05 versus 1.85–1.96). From *P. costatus*, we distinguish *P. chalcorhabdus* by the relative width of canthal iii (1.98–2.05 versus 1.82–1.90). From *P. curtissi*, we distinguish *P. chalcorhabdus* by the dots arranged in bars in the lateral areas (present versus absent), the total lamellae on one hand (40–52 versus 32–39), the relative length of digits on one hindlimb (31.3–36.0 versus 20.8–28.1), the relative longest finger length (5.29–6.97 versus 3.59–4.54), and the relative width of canthal iii (1.98–2.05 versus 1.75–1.93). From *P. diastatus*, we distinguish *P. chalcorhabdus* by the relative length of digits on one hindlimb (31.3–36.0 versus 21.5–27.4), the relative forelimb length (20.4–23.7 versus 16.2–20.1), and the relative longest finger length (5.29–6.97 versus 3.48–4.87). From *P. emys*, we distinguish *P. chalcorhabdus* by the adult SVL (71.9–95.4 versus 99.0–113), the total strigae on ten scales (184–233 versus 238–311), the relative prefrontal width (4.37–4.93 versus 3.99–4.36), the relative angled subocular width (2.36–2.71 versus 2.12–2.20), and the relative nasal width (1.70–2.01 versus 1.23–1.58). From *P. hylonomus*, we distinguish *P. chalcorhabdus* by the dots arranged in bars in the lateral areas (present versus absent), the relative length of digits on one hindlimb (31.3–36.0 versus 22.8–28.2), and the relative longest finger length (5.29–6.97 versus 4.47–5.27). From *P. lanceolatus* **sp. nov.**, we distinguish *P. chalcorhabdus* by the angled subocular width by the angled subocular height (2.77–3.28 versus 3.29–5.91) (see Remarks). From *P. lapierrae* **sp. nov.**, we distinguish *P. chalcorhabdus* by the relative length of digits on one hindlimb (31.3–36.0 versus 24.3–30.9), the relative longest finger length (5.29–6.97 versus 4.49–4.55), the relative head width (65.0–76.3 versus 77.7–78.1), and the relative width of canthal iii (1.98–2.05 versus 1.54–1.86). From *P. leionotus*, we distinguish *P. chalcorhabdus* by the relative largest supraocular width (2.52–2.86 versus 1.94–2.50) and the relative width of canthal iii (1.98–2.05 versus 1.55–1.89). From *P. marcanoi*, we distinguish *P. chalcorhabdus* by the angled subocular width by the angled subocular height (2.77–3.28 versus 3.37–5.36) (see Remarks). From *P. melanchrous*, we distinguish *P. chalcorhabdus* by the relative width of canthal iii (1.98–2.05 versus 1.67–1.94). From *P. neiba*, we distinguish *P. chalcorhabdus* by

the relative width of canthal iii (1.98–2.05 versus 1.51–1.95). From *P. nesobous*, we distinguish *P. chalcorhabdus* by the relative rostral height (1.85–2.24 versus 2.26–2.38). From *P. oreistes*, we distinguish *P. chalcorhabdus* by the relative nasal width (1.70–2.01 versus 1.37–1.65). From *P. psychonothes*, we distinguish *P. chalcorhabdus* the angled subocular width by the angled subocular height (2.77–3.28 versus 2.37–2.72) (see Remarks). From *P. saonae*, we distinguish *P. chalcorhabdus* by the relative length of digits on one hindlimb (31.3–36.0 versus 26.5–29.8), the relative forelimb length (20.4–23.7 versus 19.0–20.2), the relative prefrontal width (4.37–4.93 versus 4.14), the relative longest finger length (5.29–6.97 versus 5.01), the relative distance between the eye and naris (4.93–5.62 versus 6.43), and the relative angled subocular width (2.36–2.71 versus 2.31). From *P. semitaeniatus* **sp. nov.**, we distinguish *P. chalcorhabdus* the relative ear width (1.26–1.65 versus 1.90–2.30), the relative rostral height (1.85–2.24 versus 2.41–2.63), the relative head width (65.0–76.3 versus 58.8–63.8), the relative angled subocular height (0.739–0.854 versus 0.654), the relative distance between the eye and naris (4.93–5.62 versus 4.61), the relative width of canthal iii (1.98–2.05 versus 1.80), the relative nasal width (1.70–2.01 versus 1.51). From *P. unicolor* **sp. nov.**, we distinguish *P. chalcorhabdus* by the adult SVL (71.9–95.4 versus 67.6), the total strigae on ten scales (184–233 versus 144), the relative length of digits on one hindlimb (31.3–36.0 versus 36.8), the relative cloacal width (7.74–9.08 versus 7.61), the relative largest supraocular width (2.52–2.86 versus 3.12), the relative frontal width (62.5–80.8 versus 58.2), the relative width of canthal iii (1.98–2.05 versus 1.79), and the relative angled subocular width (2.36–2.71 versus 2.90).

Description of holotype. MCZ R-77158. An adult male; SVL 95.1 mm; tail nearly cylindrical, 129 mm (136% SVL); axilla-to-groin distance 55.0 mm (57.8% SVL); forelimb length 22.6 mm (23.8% SVL); hindlimb length 30.5 mm (32.1% SVL); head length 17.5 mm (18.4% SVL); head width 13.2 mm (13.9% SVL); head width 75.4% head length; diameter of orbit 2.97 mm (3.12% SVL); horizontal diameter of ear opening 1.50 mm (1.58% SVL); vertical diameter of ear opening 1.30 mm (1.37% SVL); length of all toes on one foot 29.9 mm (31.4% SVL); shortest distance between angled subocular and lip 0.78 mm (0.820% SVL); shortest distance between the ocular and auricular openings 8.19 mm (8.61% SVL); longest finger length 5.07 mm (5.33% SVL); largest supraocular width 2.40 mm (2.52% SVL); cloacal width 8.66 mm (9.11% SVL); mental width 1.70 mm (1.79% SVL); prefrontal width 4.42 mm (4.65% SVL); frontal width 80.8% frontal length; nasal height 1.48 mm (1.56% SVL); angled subocular height 0.78 mm (0.820% SVL); shortest distance between the eye and naris 4.76 mm (5.01% SVL); canthal iii width 1.89 mm (1.99% SVL); angled subocular width 2.56 mm (2.69% SVL); nasal width 1.92 mm (2.02% SVL); rostral 2.23X as wide as high, visible from above, not in contact with nasals, in contact with 1st supralabial and anterior internasal (left)/(right); anterior internasals are narrower than posterior ones; frontonasals and prefrontal fused into a single large plate with an almost straight posterior margin, much wider than long, bordered by posterior internasals, 1st loreals, 1st and 2nd median oculars, and the frontal; frontal longer than wide; a pair of frontoparietals, separated by the posterior prolongation of the frontal and the interparietal plate; interparietal plate much smaller than parietals and separating them, posteriorly touching the interoccipital, which is approximately as wide as long; parietal separated from supraoculars by 1st and 2nd temporals and frontoparietal (left)/(right); nasal single; nostril above suture between 1st and 2nd supralabials (left)/(right); 1 postnasal (left)/(right); 2 loreals (left)/(right); 1st loreal higher than wide (left)/(right), in contact with postnasal, posterior internasal, prefrontal/frontonasal complex, 1st median ocular, canthal iii, 2nd loreal, and 3rd–4th supralabials (left)/(right); 2nd loreal shorter than 1st, approximately as high as wide (left)/(right), excluded from contact with supraocular by canthal iii (left)/(right); final loreal posteriorly bordering the upper and lower preoculars (left)/(right); canthal iii wider than high (left)/(right), contacting 1st median ocular, anterior supraciliary, upper preocular, and 1st and 2nd loreals (left)/(right); 9 median oculars (left)/(right), 1st and 2nd contacting the prefrontal (left)/(right); 1 upper preocular (left)/(right); an irregular anterior supraciliary (left)/(right); 6 lateral oculars (left)/(right); 5 temporals (left)/(right); 2 suboculars (left)/(right); posterior subocular large and elongate (left)/(right); anterior subocular small (left)/(right); 9 supralabials (left)/(right), 6 to level below center of eye (left)/(right); 9 (left)/8 (right) infralabials, 6 (left)/5 (right) to level below center of eye; mental small, followed by a single, larger postmental; 4 pairs of enlarged chin shields; 1st pair in contact with one another anteriorly, posteriorly separated by one scale; 2nd–4th pairs separated by 1–4 scales; 88 transverse rows of dorsal scales from interoccipital to base of tail; 89 transverse rows of ventral scales from mental to vent; 40 scales around midbody; 5 digits; finger lengths 3>4>2>5>1; 11 (left)/12 (right) lamellae under longest finger; 45 total lamellae on one hand; toe lengths 4>3>5>2>1; 18 (left)/17 (right) lamellae under longest toe; dorsal body and caudal scales keelless and striate; faintly striated ventral scales; 238 total strigae counted on ten scales.

FIGURE 54. (A–F) *Panolopus chalcorhabdus* (MCZ R-77158, holotype), SVL 95.1 mm.

Color (in alcohol): dorsal surface of head golden tan; lateral surfaces of head grading from golden tan to cream with darker brown eye masks; dorsal surfaces of the body are red-gray with small, irregular, darker brown flecks; dorsal surface of tail red-gray with irregular, darker brown spots; lateral areas grade from dark brown to cream with darker brown and off-white dots in bars; dorsal surfaces of the limbs are golden tan with darker brown mottling; lateral and ventral areas of the limbs fade to pale cream, patternless; ventral surfaces of the head, body, and tail are pale cream color with some brown mottling under the chest and tail.

Variation. The examined material has dorsal patterns that range from completely absent to irregular flecks or dots. In KU 225002 the pattern vaguely resembles chevrons. All specimens have patternless heads except for KU 225001, which has a few dark, irregular markings on the head scales. The majority of specimens have a few flecks in the longitudinal paramedian series; however, KU 225078 has no markings and KU 225002 has small longitudinal paramedian lines. All specimens have dots arranged in bars in the lateral band. Measurements and other morphological data for the holotype and other examined material are presented in Table 1.

Distribution. *Panolopus chalcorhabdus* is distributed in the extreme east of the Dominican Republic at elevations of 0–110 m (Fig. 50).

Ecology and conservation. No ecological data are associated with this species. We consider the conservation status of *Panolopus chalcorhabdus* to be Least Concern, based on IUCN Redlist criteria (IUCN 2023). It is likely a common species tolerant of some habitat disturbance, based on what is known of most species of *Panolopus*. However, it faces a primary threat of habitat destruction resulting from deforestation. A secondary threat is predation from introduced mammals, including the mongoose and black rats. Studies are needed to determine the health and extent of remaining populations and better understand the threats to the survival of the species.

Reproduction. No data on reproduction are available for this species.

Etymology. The species name is derived from the Greek *chalcos* (copper or bronze) and *rhabdos* (line or stripe) in reference to the distinctive dorsal pattern of this species.

Remarks. Originally a subspecies of *Panolopus costatus*, we elevate this taxon to species level. *Panolopus chalcorhabdus* and *P. lanceolatus* **sp. nov.** cannot be morphologically separated based on our standard suite of characters, however, they can be separated by the angled subocular width divided by the angled subocular height (2.77–3.28 [n=5] versus 3.29–5.91 [n=7]). *Panolopus chalcorhabdus* and *P. marcanoi* cannot be morphologically separated based on our standard suite of characters, however, they can be separated by the angled subocular width divided by the angled subocular height (2.77–3.28 [n=5] versus 3.37–5.36 [n=18]). *Panolopus chalcorhabdus* and *P. psychonothes* cannot be morphologically separated based on our standard suite of characters, however, they can be separated by the angled subocular width divided by the angled subocular height (2.77–3.28 [n=5] versus 2.37–2.72 [n=5]).

Additional museum specimens identified as *P. costatus* from the region should be examined to determine if they are members of *P. chalcorhabdus*. *Panolopus chalcorhabdus* was not included in our genetic dataset and future studies using genetic or genomic data should be made to determine the relationships of *P. chalcorhabdus*.

Panolopus costatus Cope, 1862b

Tiburon Smooth-scaled Forest Lizard
(Fig. 55–56)

Panolopus costatus Cope 1862:494. Holotype: MCZ R-3606, collected by Dr. David Friedrich Weinland from “near Jeremie,” Grand’Anse department, Haiti. Date of collection inferred to be 1857–1858 (Weinland 1858). (18.64, -74.11).
Celestus phoxinus—Cope, 1868:125. Holotype: R-12457, collected by Dr. David Friedrich Weinland from “near Jeremie,” Grand’Anse department, Haiti. Date of collection inferred to be 1857–1858 (Weinland 1858). (18.64, -74.11).
Diploglossus phoxinus—Boulenger, 1885:289.
Panolopus costatus—Boulenger, 1885:295.
Diploglossus ohlendorffi—Fischer, 1886:3. Holotype: HZM, destroyed in WWII.
Diploglossus nuchalis—Boulenger, 1898:920. Holotype: BMNH 1897.3.16.1, from Dr. F. Werner of unknown origin.
Celestus costatus—Barbour, 1930:99.
Celestus costatus—Barbour, 1935:123.
Celestus costatus—Barbour, 1937:139.
Celestus costatus—Mertens, 1939:70.
Celestus costatus—Cochran, 1941:243.

Diploglossus costatus costatus—Schwartz, 1964:21.
Celestus costatus—Schwartz & Henderson, 1991:368.
Celestus costatus—Powell *et al.*, 1999:104.
Celestus costatus—Hedges *et al.*, 2019:16.
Panolopus costatus—Schools & Hedges, 2021:230.
Panolopus costatus—Landestoy *et al.*, 2022: 205.

Material examined (n=24). HAITI. Grand'Anse. ANSP 38558, S. Blair Hedges, Richard Thomas, Manuel Leal, and Nicholas Plummer, Abricots (outskirts), 31 May 1991; ANSP 38559, S. Blair Hedges, 17.0 km S of Beaumont, 1 June 1991; KU 225088, 7 mi W Jeremie, 19 June 1971; KU 225089, 225091, btw La Foret and Jeremie, 16 March 1966; KU 225116–7, ca 3 km (airline) SW Corail, 20 March 1966; KU 225171, 225173, Castillon to ca 2 km S Castillon, 26 June 1971; MCZ R-3606, David Friedrich Weinland, Jeremie, 1857–1858; SBH 269064, 6.2 km E Anse d'Hainault at source cacao; USNM 328773, locals, vic. of Castillon (8.0 km S, 0.3 km E Marche Leon [airline]), 2 November 1984; USNM 328775–9, locals, Castillion, 2 November 1984; USNM 328780, S. Blair Hedges and Richard Thomas, 3 km SW of Castillion, 31 October 1984. **Nippes**. MCZ R-134262–4, George Whiteman, 7–8 mi NE Paillant, 1–31 July 1972. **Sud.** ANSP 38560, S. Blair Hedges, 11.6 km NW Les Anglais, on Morne Grand Bois, 26 July 2011; ANSP 38561, S. Blair Hedges and Richard Thomas, ca. 1 km NE of Tiburon, 21 July 2010; SBH 268974, S. Blair Hedges and Richard Thomas, ca. 1 km NE Tiburon.

Diagnosis. *Panolopus costatus* has (1) a dorsal pattern of absent/irregular dots/dots in series/dots in chevrons, (2) head markings absent/present, (3) markings in the longitudinal paramedian area absent/present, (4) dots arranged in bars in the lateral band present, (5) an adult SVL of 83.6–107 mm, (6) ventral scale rows, 89–106, (7) midbody scale rows, 39–43, (8) total lamellae on one hand, 49–58, (9) total strigae on ten scales, 158–217, (10) relative length of all digits on one hindlimb, 31.5–37.8 %, (11) relative distance between the angled subocular and mouth, 0.582–0.916 %, (12) relative eye length, 2.52–3.73 %, (13) relative forelimb length, 19.9–24.2 %, (14) relative ear width, 0.590–2.07 %, (15) relative rostral height, 1.78–2.26 %, (16) relative head length, 16.3–20.0 %, (17) relative mental width, 1.66–2.00 %, (18) relative postmental width, 2.29–2.92 %, (19) relative cloacal width, 7.27–8.51 %, (20) relative prefrontal width, 3.97–4.67 %, (21) relative largest supraocular width, 1.93–3.01 %, (22) relative longest finger length, 5.53–6.66 %, (23) relative distance between the ear and eye, 7.32–8.89 %, (24) relative head width, 68.3–76.8 %, (25) relative frontal width, 56.2–67.4 %, (26) relative nasal height, 1.02–1.28 %, (27) relative angled subocular height, 0.562–0.886 %, (28) relative distance between the eye and naris, 5.08–5.50 %, (29) relative canthal iii length, 1.82–1.90 %, (30) relative angled subocular width, 2.36–2.81 %, and (31) relative nasal length, 1.58–1.74 %. The species stem time is 2.43 Ma and the species crown time is 0.73 Ma (Fig. 4).

We distinguish *Panolopus costatus* from the other species of *Panolopus* based on a complex of traits. From *Panolopus aenetergum*, we distinguish *P. costatus* by the ventral scale rows (89–106 versus 80–86), the midbody scale rows (39–43 versus 35–36), the total lamellae on one hand (49–58 versus 40), the total strigae on ten scales (158–217 versus 267), the relative length of digits on one hindlimb (31.5–37.8 versus 26.8), the relative mental width (1.66–2.00 versus 1.63), the relative longest finger length (5.53–6.66 versus 4.83), the relative frontal width (56.2–67.4 versus 88.2), the relative angled subocular height (0.562–0.886 versus 1.08), the relative distance between the eye and naris (5.08–5.50 versus 4.35), the relative angled subocular width (2.36–2.81 versus 2.07), and the relative nasal width (1.58–1.74 versus 1.92). From *P. aporus*, we distinguish *P. costatus* by the total lamellae on one hand (49–58 versus 36–48). From *P. chalcorhabdus*, we distinguish *P. costatus* by the relative width of canthal iii (1.82–1.90 versus 1.98–2.05). From *P. curtissi*, we distinguish *P. costatus* by the dots arranged in bars in the lateral areas (present versus absent), the midbody scale rows (39–43 versus 32–38), the total lamellae on one hand (49–58 versus 32–39), the relative length of digits on one hindlimb (31.5–37.8 versus 20.8–28.1), the relative longest finger length (5.53–6.66 versus 3.59–4.54), and the relative distance between the eye and naris (5.08–5.50 versus 4.02–5.03). From *P. diastatus*, we distinguish *P. costatus* by the total lamellae on one hand (49–58 versus 35–41), the relative length of digits on one hindlimb (31.5–37.8 versus 21.5–27.4), the relative longest finger length (5.53–6.66 versus 3.48–4.87), and the relative distance between the eye and naris (5.08–5.50 versus 4.06–4.94). From *P. emys*, we distinguish *P. costatus* by the total strigae on ten scales (158–217 versus 238–311), the relative frontal width (56.2–67.4 versus 67.7–74.5), and the relative angled subocular width (2.36–2.81 versus 2.12–2.20). From *P. hylonomus*, we distinguish *P. costatus* by the dots arranged in bars in the lateral areas (present versus absent), the adult SVL (83.6–107 versus 59.3–76.5), the total lamellae on one hand (49–58 versus 34–47), the relative length of digits on one hindlimb (31.5–37.8 versus 22.8–28.2), the relative longest finger length (5.53–6.66 versus 4.47–5.27), the

relative distance between the eye and naris (5.08–5.50 versus 4.03–4.98), and the relative width of canthal iii (1.82–1.90 versus 1.95–2.03). From *P. lanceolatus* **sp. nov.**, we distinguish *P. costatus* by the relative distance between the eye and naris (5.08–5.50 versus 4.58–5.05). From *P. lapierrae* **sp. nov.**, we distinguish *P. costatus* by the midbody scale rows (39–43 versus 33–38), the total lamellae on one hand (49–58 versus 38–47), the total strigae on ten scales (158–217 versus 228–231), the relative length of digits on one hindlimb (31.5–37.8 versus 24.3–30.9), the relative cloacal width (7.27–8.51 versus 8.55–8.81), the relative prefrontal width (3.97–4.67 versus 4.73–4.75), the relative longest finger length (5.53–6.66 versus 4.49–4.55), the relative head width (68.3–76.8 versus 77.7–78.1), the relative frontal width (56.2–67.4 versus 77.6–79.0), and the relative nasal width (1.58–1.74 versus 1.81). From *P. leionotus*, we distinguish *P. costatus* by the total lamellae on one hand (49–58 versus 43–48) and the relative frontal width (56.2–67.4 versus 68.7–81.2). From *P. marcanoi*, we distinguish *P. costatus* by the total lamellae on one hand (49–58 versus 36–44). From *P. melanchrous*, we distinguish *P. costatus* by the relative nasal height (1.02–1.28 versus 0.897–0.952). From *P. neiba*, we distinguish *P. costatus* by the relative distance between the eye and naris (5.08–5.50 versus 4.51–5.01). From *P. nesobous*, we distinguish *P. costatus* by the relative prefrontal width (3.97–4.67 versus 4.74–4.81), the relative distance between the eye and naris (5.08–5.50 versus 5.62–5.73), and the relative width of canthal iii (1.82–1.90 versus 2.01–2.12). From *P. oreistes*, we distinguish *P. costatus* by the area of the nasal scale by the SVL (1.59–2.03 versus 1.06–1.57) (see Remarks). From *P. psychonothes*, we distinguish *P. costatus* by the total lamellae on one hand (49–58 versus 37–44). From *P. saonae*, we distinguish *P. costatus* by the total lamellae on one hand (49–58 versus 40–42), the relative length of digits on one hindlimb (31.5–37.8 versus 26.5–29.8), the relative mental width (1.66–2.00 versus 1.52), the relative longest finger length (5.53–6.66 versus 5.01), the relative frontal width (56.2–67.4 versus 72.5), the relative nasal height (1.02–1.28 versus 1.01), the relative distance between the eye and naris (5.08–5.50 versus 6.43), the relative width of canthal iii (1.82–1.90 versus 1.99), and the relative angled subocular width (2.36–2.81 versus 2.31). From *P. semitaeniatus* **sp. nov.**, we distinguish *P. costatus* by the total lamellae on one hand (49–58 versus 34–46), the relative rostral height (1.78–2.26 versus 2.41–2.63), the relative head width (68.3–76.8 versus 58.8–63.8), the relative distance between the eye and naris (5.08–5.50 versus 4.61), the relative width of canthal iii (1.82–1.90 versus 1.80), and the relative nasal width (1.58–1.74 versus 1.51). From *P. unicolor* **sp. nov.**, we distinguish *P. costatus* by the adult SVL (83.6–107 versus 67.6), the total lamellae on one hand (49–58 versus 48), the total strigae on ten scales (158–217 versus 144), the relative distance between angled subocular and mouth (0.582–0.916 versus 0.533), the relative prefrontal width (3.97–4.67 versus 4.69), the relative largest supraocular width (1.93–3.01 versus 3.12), the relative distance between the eye and naris (5.08–5.50 versus 5.52), the relative width of canthal iii (1.82–1.90 versus 1.79), the relative angled subocular width (2.36–2.81 versus 2.90), and the relative nasal width (1.58–1.74 versus 2.00).

Description of holotype. MCZ R-3606. An adult male; SVL 94.4 mm; tail slightly laterally compressed, broken, 16.3 mm (17.3% SVL); axilla-to-groin distance 51.3 mm (54.3% SVL); head length 18.9 mm (20.0% SVL); head width 12.9 mm (13.7% SVL); head width 68.3% head length; diameter of orbit 3.23 mm (3.42% SVL); horizontal diameter of ear opening 1.02 mm (1.08% SVL); vertical diameter of ear opening 0.88 mm (0.932% SVL); shortest distance between angled subocular and lip 0.70 mm (0.742% SVL); shortest distance between the ocular and auricular openings 8.34 mm (8.83% SVL); largest supraocular width 1.88 mm (1.99% SVL); cloacal width 7.56 mm (8.01% SVL); prefrontal width 4.41 mm (4.67% SVL); postmental width 2.62 mm (2.78% SVL); frontal width 67.4% frontal length; angled subocular height 0.65 mm (0.689% SVL); shortest distance between the eye and naris 4.98 mm (5.28% SVL); canthal iii width 1.73 mm (1.83% SVL); angled subocular width 2.53 mm (2.68% SVL); frontonasals and prefrontal fused into a single large plate with an irregular posterior margin, much wider than long, bordered by rostral complex plate, 1st loreals, 1st median oculars, and the frontal; frontal longer than wide; a pair of frontoparietals, separated by the posterior prolongation of the frontal and the interparietal plate; interparietal plate smaller than parietals and separating them, posteriorly touching the interoccipital, which is much wider than long; parietal separated from supraoculars by 1st and 2nd temporals and frontoparietal (left)/(right); 2 loreals (left)/(right); 1st loreal wider than high (left)/higher than wide (right), in contact with postnasal, rostral complex, prefrontal/frontonasal complex, 1st median ocular, canthal iii, 2nd loreal, additional 2 scales preventing contact from 3rd supralabial, and supralabial 2 (left)/postnasal, rostral complex, prefrontal/frontonasal complex, 1st median ocular, canthal iii, 2nd loreal, and supralabial 2 (right); 2nd loreal shorter than 1st, wider than high (left)/shorter than 1st, approximately as high as wide (right), excluded from contact with supraocular by canthal iii (left)/(right); final loreal posteriorly bordering the upper and lower preoculars and 1 additional scale (left)/upper and lower preoculars (right); canthal iii wider than high (left)/(right), contacting 1st median ocular, anterior supraciliary,

upper preocular, and 1st and 2nd loreals (left)/(right); 9 (left)/10 (right) median oculars, 1st contacting the prefrontal (left)/(right); 1 upper preocular (left)/(right); an irregular anterior supraciliary (left)/(right); 5 (left)/6 (right) lateral oculars; 5 temporals (left)/(right); 2 suboculars (left)/(right); posterior subocular large and elongate (left)/(right); anterior subocular small (left)/(right); mental fused with postmental; 4 pairs of enlarged chin shields, followed by 1 pair of reduced chin shields; 1st pair in contact with one another; 2nd (damaged) to 5th pair separated by 1–5 scales; 94 transverse rows of dorsal scales from interoccipital to base of tail; 89 transverse rows of ventral scales from mental to vent; 43 scales around midbody; keelless and striate dorsal body and caudal scales; striate ventral scales; 201 total strigae counted on ten scales.

Color (in alcohol): faded, dorsal surface of head tan, patternless; lateral surfaces of head grading from tan to yellow-cream with darker brown eye masks; dorsal surfaces of the body are medium brown with irregular, small, darker brown flecks; dorsal surface of tail the same as the body; lateral areas medium brown grading to yellow-cream with darker brown and off-white spots arranged in bars; dorsal surfaces of the limbs are golden tan with darker brown mottling; lateral and ventral areas of the limbs fade to yellow-cream, patternless; ventral surfaces of the head, body, and tail are yellow-cream, patternless.

Variation. The majority of the examined material has a dorsal pattern of irregular flecks or dots with only ANSP 38559 showing no pattern and MCZ R-134264 having the dots on its dorsum arranged in vague chevrons. MCZ R-134264 also has irregular, darker areas on its head scales, whereas the other specimens have patternless heads. All specimens other than the holotype have either dots in the longitudinal paramedian series or complete or broken longitudinal paramedian lines. Dots in the lateral band are arranged into bars on all specimens. Measurements and other morphological data for the holotype and other examined material are presented in Table 1.

Distribution. *Panolopus costatus* is distributed in the western Tiburon Peninsula of Haiti at elevations of 0–1210 m (Fig. 49). It has an extent of occurrence of ~3,900 km^2.

Ecology and conservation. Past literature accounts of ecological data for this species conflate multiple species and therefore cannot be used. Most individuals were found under objects on the ground, but one juvenile individual (ANSP 38559) was found in a bromeliad in a tree (SBH, field notes).

We consider the conservation status of *Panolopus costatus* to be Least Concern, based on IUCN Redlist criteria (IUCN 2023). It is likely a common species tolerant of some habitat disturbance, based on what is known of most species of *Panolopus*. However, it faces a primary threat of habitat destruction resulting from deforestation. A secondary threat is predation from introduced mammals, including the mongoose and black rats. Studies are needed to determine the health and extent of remaining populations and better understand the threats to the survival of the species.

Reproduction. Past literature accounts of ecological data for this species conflate multiple species and therefore cannot be used. A litter size of 2–6 has been recorded in *Panolopus costatus sensu stricto* (SBH, field data).

Etymology. The species name is derived from the Latin adjective meaning "ribbed," in apparent allusion to the series of "numerous blackish brown vertical bars" on the sides of the body as described by Cope for the type specimen.

Remarks. Schwartz (1964) discussed the 19th Century synonyms: *Celestus phoxinus, Diploglossus ohlendorffi, and Diploglossus nuchalis*. The first was collected by Weinland at the same place and about the same time as the type of *C. costatus*. Schwartz examined the type of *C. phoxinus* and concurred with Garman (1887) that it is *C. costatus* (here, *Panolopus costatus sensu stricto*). Descriptions of the other two were clear enough to assign them as synonyms of *C. costatus* (sensu lato) as well, but they lacked specific localities and sufficient details to assign them to the subspecies of Schwartz (1964) or to our species. Schwartz (1964) concluded (and we agree) that these three names should be direct synonyms of "*Celestus c. costatus*" (here, *P. costatus sensu stricto*) "until additional information becomes available."

Prior to this work, *Panolopus costatus* was reported to have 11 subspecies: *P. c. aenetergum, P. c. chalcorhabdus, P. c. costatus, P. c. emys, P. c. leionotus, P. c. melanchrous, P. c. neiba, P. c. nesobous, P. c. oreistes, P. c. psychonothes,* and *P. c. saonae*. All of these subspecies are elevated to the species level herein. Further analyses of museum specimens that have been recorded as *P. costatus* should be undertaken to assign all individuals to the correct species.

Panolopus costatus and *P. oreistes* cannot be morphologically separated based on our standard suite of characters, however, they can be separated by the area of the nasal scale by the SVL (1.59–2.03 [n=4] versus 1.06–1.57 [n=14]).

FIGURE 55. (A–F) *Panolopus costatus* (MCZ R-3606, holotype), SVL 94.4 mm.

Panolopus costatus was included in our genetic dataset and has significant support in both Bayesian and ML likelihood analyses at the crown node of the species and the stem node that places it as the closest relative to *P. oreistes*. Based on our timetree (Fig. 4), *P. costatus* diverged from its closest relative 2.43 Ma, consistent with typical species of vertebrates (> 0.7 Ma; Hedges *et al.* 2015). *Panolopus costatus* was recognized as a distinct species by our ASAP analysis.

FIGURE 56. *Panolopus costatus* (ANSP 38561, SBH 268996), in life. From ca. 1 km NE Tiburon, Sud Department, Haiti. Photo by SBH.

Panolopus curtissi **(Grant 1951)**
Hispaniolan Khaki Forest Lizard
(Fig. 57–58)

Celestus curtissi Grant, 1951:68. Holotype: USNM 11733, a juvenile female, collected by Anthony Curtiss from Trou Forban on 19 April 1943 (18.921, -72.654).
Diploglossus curtissi curtissi—Schwartz, 1964:40.
Celestus curtissi curtissi—Schwartz & Henderson, 1988:97.
Celestus curtissi curtissi—Schwartz & Henderson, 1991:371.
Celestus curtissi curtissi—Hedges *et al.*, 2019:16.
Panolopus curtissi—Schools & Hedges, 2021:230 (part).
Panolopus curtissi—Landestoy *et al.*, 2022: 205 (part).

Material examined (n=18). DOMINICAN REPUBLIC. Independencia. ANSP 38632, S. Blair Hedges, Kristin Nastase, Renee Sharp, and Patrick Parker, La Descubierta, 5.1 km NW of, 30 May 1996; KU 226253, 2 km E Boca de Cachon, 5 August 1974; SBH 194494, S. Blair Hedges, Kristin Nastase, Renee Sharp, and Patrick Parker, 5.1 km NW of La Descubierta, 30 May 1996. **HAITI. Artibonite.** ANSP 38633–5, S. Blair Hedges and Miguel Landestoy, La Gonave, near Richard, along coast road, 2 April 2011; KU 226192, Pierre Payen, 9 mi S St Marc, 13 July 1974. **Ouest.** KU 226242–3, 10.1 km SE Montrouis, 13 July 1974; KU 226248, 0.3 mi S Terre Rouge, 26 May 1974; USNM 117265, Trou Caiman, 16 February 1943; USNM 117266, Trou Forban, 12 December 1942; USNM 117267–8, Trou Forban, 31 August 1942; USNM 117337–8, Trou Forban, 19 April 1943; USNM 129399, Trou Forban. **Gonave Island.** MCZ R-80800, George Whiteman, Pointe-a-Roquettes, 1 January 1964–31 December 1964.

Diagnosis. *Panolopus curtissi* has (1) a dorsal pattern of absent/irregular flecks, (2) head markings absent, (3) markings in the longitudinal paramedian area absent/present, (4) dots arranged in bars in the lateral band absent, (5) an adult SVL of 64.1–85.5 mm, (6) ventral scale rows, 90–103, (7) midbody scale rows, 32–38, (8) total lamellae on one hand, 32–39, (9) total strigae on ten scales, 165–260, (10) relative length of all digits on one hindlimb, 20.8–

28.1 %, (11) relative distance between the angled subocular and mouth, 0.393–0.587 %, (12) relative eye length, 2.66–4.01 %, (13) relative forelimb length, 15.1–20.5 %, (14) relative ear width, 0.827–2.09 %, (15) relative rostral height, 1.77–2.66 %, (16) relative head length, 13.6–17.9 %, (17) relative mental width, 1.60–2.09 %, (18) relative postmental width, 2.07–2.72 %, (19) relative cloacal width, 7.49–8.61 %, (20) relative prefrontal width, 3.96–4.68 %, (21) relative largest supraocular width, 1.88–2.98 %, (22) relative longest finger length, 3.59–4.54 %, (23) relative distance between the ear and eye, 5.36–7.71 %, (24) relative head width, 68.3–78.1 %, (25) relative frontal width, 65.4–83.1 %, (26) relative nasal height, 1.04–1.25 %, (27) relative angled subocular height, 0.708–1.19 %, (28) relative distance between the eye and naris, 4.02–5.03 %, (29) relative canthal iii length, 1.75–1.93 %, (30) relative angled subocular width, 2.26–2.76 %, and (31) relative nasal length, 1.44–1.82 %. The species stem time is 2.04 Ma and the species crown time is 0.64 Ma (Fig. 4).

Panolopus curtissi has a smaller relative longest finger length (3.59–4.54) than most species of the genus. From *Panolopus aenetergum*, we distinguish *P. curtissi* by the dorsal pattern (absent/irregular flecks versus irregular dots), the dots arranged in bars in the lateral areas (absent versus present), the ventral scale rows (90–103 versus 80–86), the total lamellae on one hand (32–39 versus 40), the total strigae on ten scales (165–260 versus 267), the relative distance between angled subocular and mouth (0.393–0.587 versus 0.717), the relative forelimb length (15.1–20.5 versus 20.6), the relative longest finger length (3.59–4.54 versus 4.83), the relative distance between the ear and eye (5.36–7.71 versus 8.40), the relative frontal width (65.4–83.1 versus 88.2), the relative angled subocular width (2.26–2.76 versus 2.07), and the relative nasal width (1.44–1.82 versus 1.92). From *P. aporus*, we distinguish *P. curtissi* by the dots arranged in bars in the lateral areas (absent versus present) and the relative longest finger length (3.59–4.54 versus 4.57–5.72). From *P. chalcorhabdus*, we distinguish *P. curtissi* by the dots arranged in bars in the lateral areas (absent versus present), the total lamellae on one hand (32–39 versus 40–52), the relative length of digits on one hindlimb (20.8–28.1 versus 31.3–36.0), the relative longest finger length (3.59–4.54 versus 5.29–6.97), and the relative width of canthal iii (1.75–1.93 versus 1.98–2.05). From *P. costatus*, we distinguish *P. curtissi* by the dots arranged in bars in the lateral areas (absent versus present), the midbody scale rows (32–38 versus 39–43), the total lamellae on one hand (32–39 versus 49–58), the relative length of digits on one hindlimb (20.8–28.1 versus 31.5–37.8), the relative longest finger length (3.59–4.54 versus 5.53–6.66), and the relative distance between the eye and naris (4.02–5.03 versus 5.08–5.50). From *P. diastatus*, we distinguish *P. curtissi* by the nasal length by the nasal height (1.21–1.46 versus 1.47–1.73) (see Remarks). From *P. emys*, we distinguish *P. curtissi* by the dots arranged in bars in the lateral areas (absent versus present), the adult SVL (64.1–85.5 versus 99.0–113), the relative length of digits on one hindlimb (20.8–28.1 versus 28.9–35.2), the relative longest finger length (3.59–4.54 versus 5.15–5.83), and the relative angled subocular width (2.26–2.76 versus 2.12–2.20). From *P. hylonomus*, we distinguish *P. curtissi* by the relative width of canthal iii (1.75–1.93 versus 1.95–2.03). From *P. lanceolatus* **sp. nov.**, we distinguish *P. curtissi* by the dots arranged in bars in the lateral areas (absent versus present), the total lamellae on one hand (32–39 versus 41–52), the relative length of digits on one hindlimb (20.8–28.1 versus 28.4–35.9), and the relative longest finger length (3.59–4.54 versus 4.76–6.36). From *P. lapierrae* **sp. nov.**, we distinguish *P. curtissi* by the relative distance between angled subocular and mouth (0.393–0.587 versus 0.620–0.725), the relative prefrontal width (3.96–4.68 versus 4.73–4.75), the relative distance between the ear and eye (5.36–7.71 versus 7.78–8.43), and the relative distance between the eye and naris (4.02–5.03 versus 5.21). From *P. leionotus*, we distinguish *P. curtissi* by the dots arranged in bars in the lateral areas (absent versus present), the adult SVL (64.1–85.5 versus 86.3–105), the total lamellae on one hand (32–39 versus 43–48), and the relative longest finger length (3.59–4.54 versus 4.58–6.10). From *P. marcanoi*, we distinguish *P. curtissi* by the dorsal pattern (absent/irregular flecks versus irregular dots/dots in chevrons), the head markings (absent versus present), the dots arranged in bars in the lateral areas (absent versus present), and the relative longest finger length (3.59–4.54 versus 4.75–6.68). From *P. melanchrous*, we distinguish *P. curtissi* by the dots arranged in bars in the lateral areas (absent versus present), the adult SVL (64.1–85.5 versus 93.2–124), the total lamellae on one hand (32–39 versus 47–58), the relative length of digits on one hindlimb (20.8–28.1 versus 30.7–41.3), the relative longest finger length (3.59–4.54 versus 5.76–7.09), and the relative nasal height (1.04–1.25 versus 0.897–0.952). From *P. neiba*, we distinguish *P. curtissi* by the dots arranged in bars in the lateral areas (absent versus present), the total lamellae on one hand (32–39 versus 45–49), the relative length of digits on one hindlimb (20.8–28.1 versus 29.5–36.6), the relative distance between angled subocular and mouth (0.393–0.587 versus 0.670–0.747), and the relative longest finger length (3.59–4.54 versus 5.61–6.66). From *P. nesobous*, we distinguish *P. curtissi* by the dorsal pattern (absent/irregular flecks versus irregular dots/dots in series), the dots arranged in bars in the lateral areas (absent versus present), the

total lamellae on one hand (32–39 versus 50–59), the relative length of digits on one hindlimb (20.8–28.1 versus 35.1), the relative forelimb length (15.1–20.5 versus 23.3–25.1), the relative postmental width (2.07–2.72 versus 2.82–3.02), the relative prefrontal width (3.96–4.68 versus 4.74–4.81), the relative longest finger length (3.59–4.54 versus 6.19–6.33), the relative distance between the ear and eye (5.36–7.71 versus 7.91–10.0), the relative frontal width (65.4–83.1 versus 60.8–63.5), the relative distance between the eye and naris (4.02–5.03 versus 5.62–5.73), and the relative width of canthal iii (1.75–1.93 versus 2.01–2.12). From *P. oreistes*, we distinguish *P. curtissi* by the dorsal pattern (absent/irregular flecks versus irregular dots/dots in series/dots in chevrons), the dots arranged in bars in the lateral areas (absent versus present), the relative length of digits on one hindlimb (20.8–28.1 versus 31.2–40.1), and the relative longest finger length (3.59–4.54 versus 5.27–7.23). From *P. psychonothes*, we distinguish *P. curtissi* by the dorsal pattern (absent/irregular flecks versus irregular dots/dots in series/dots in chevrons) and the relative longest finger length (3.59–4.54 versus 4.89–5.81). From *P. saonae*, we distinguish *P. curtissi* by the adult SVL (64.1–85.5 versus 90.9–98.3), the total lamellae on one hand (32–39 versus 40–42), the relative mental width (1.60–2.09 versus 1.52), the relative longest finger length (3.59–4.54 versus 5.01), the relative nasal height (1.04–1.25 versus 1.01), the relative distance between the eye and naris (4.02–5.03 versus 6.43), and the relative width of canthal iii (1.75–1.93 versus 1.99). From *P. semitaeniatus* **sp. nov.**, we distinguish *P. curtissi* by the relative length of digits on one hindlimb (20.8–28.1 versus 30.4–34.6), the relative distance between angled subocular and mouth (0.393–0.587 versus 0.666–0.808), the relative forelimb length (15.1–20.5 versus 21.3–23.8), the relative longest finger length (3.59–4.54 versus 5.17–6.05), the relative head width (68.3–78.1 versus 58.8–63.8), and the relative angled subocular height (0.708–1.19 versus 0.654). From *P. unicolor* **sp. nov.**, we distinguish *P. curtissi* by the dots arranged in bars in the lateral areas (absent versus present), the midbody scale rows (32–38 versus 40), the total lamellae on one hand (32–39 versus 48), the total strigae on ten scales (165–260 versus 144), the relative length of digits on one hindlimb (20.8–28.1 versus 36.8), the relative forelimb length (15.1–20.5 versus 23.5), the relative postmental width (2.07–2.72 versus 2.80), the relative prefrontal width (3.96–4.68 versus 4.69), the relative largest supraocular width (1.88–2.98 versus 3.12), the relative longest finger length (3.59–4.54 versus 6.65), the relative frontal width (65.4–83.1 versus 58.2), the relative distance between the eye and naris (4.02–5.03 versus 5.52), the relative angled subocular width (2.26–2.76 versus 2.90), and the relative nasal width (1.44–1.82 versus 2.00).

Description of holotype. USNM 11733. A juvenile female; SVL 75.0 mm; tail nearly cylindrical, broken in life near tip, regenerated, 96.2 mm (128% SVL); axilla-to-groin distance 44.7 mm (59.6% SVL); forelimb length 14.1 mm (18.8% SVL); hindlimb length 22.3 mm (29.7% SVL); head length 13.0 mm (17.3% SVL); head width 8.88 mm (11.8% SVL); head width 68.3% head length; diameter of orbit 3.01 mm (4.01% SVL); horizontal diameter of ear opening 1.33 mm (1.77% SVL); vertical diameter of ear opening 1.30 mm (1.73% SVL); length of all toes on one foot 20.3 mm (27.1% SVL); shortest distance between angled subocular and lip 0.44 mm (0.587% SVL); shortest distance between the ocular and auricular openings 5.78 mm (7.71% SVL); longest finger length 3.02 mm (4.03% SVL); largest supraocular width 1.95 mm (2.60% SVL); cloacal width 5.94 mm (7.92% SVL); mental width 1.57 mm (2.09% SVL); postmental width 2.04 mm (2.72% SVL); prefrontal width 3.38 mm (4.51% SVL); frontal width 70.4% frontal length; nasal height 0.91 mm (1.21% SVL); angled subocular height 0.89 mm (1.19% SVL); shortest distance between the eye and naris 3.50 mm (4.67% SVL); canthal iii width 1.44 mm (1.92% SVL); angled subocular width 2.03 mm (2.71% SVL); nasal width 1.10 mm (1.47% SVL); rostral 2.15X as wide as high, visible from above, not in contact with nasals, in contact with 1st supralabial and anterior internasal (left)/(right); anterior internasals are narrower than posterior ones; frontonasals and prefrontal fused into a single large plate with a straight posterior margin, much wider than long, bordered by posterior internasals, 1st loreals, 1st (and 2nd on the right) median ocular(s), and the frontal; frontal longer than wide; a pair of frontoparietals, separated by the posterior prolongation of the frontal and the interparietal plate; interparietal plate much smaller than parietals and separating them, posteriorly touching the interoccipital, which is much wider than long; parietal separated from supraoculars by 1st and 2nd temporals and frontoparietal (left)/(right); nasal single; nostril above suture between 1st and 2nd supralabials (left)/just posterior to suture between 1st and 2nd supralabials (right); 1 postnasal (left)/(right); 2 loreals (left)/(right); 1st loreal higher than wide (left)/(right), in contact with postnasal, posterior internasal, prefrontal/frontonasal complex, 1st median ocular, canthal iii, 2nd loreal, and 3rd–4th supralabials (left)/(right); 2nd loreal shorter than 1st, approximately as high as wide (left)/(right), excluded from contact with supraocular by canthal iii (left)/(right); final loreal posteriorly bordering the upper and lower preoculars (left)/lower preocular (right); canthal iii wider than high (left)/(right), contacting 1st median ocular, anterior supraciliary, upper and lower preoculars, and 1st and 2nd loreals (left)/(right); 10 median oculars (left)/(right), 1st (left)/1st and 2nd (right) contacting the prefrontal; 1 upper preocular

(left)/(right); an irregular (left)/fused to first lateral ocular (right) anterior supraciliary; 6 lateral oculars (left)/(right); 5 temporals (left)/(right); 2 suboculars (left)/(right); posterior subocular large and elongate (left)/(right); anterior subocular small (left)/(right); 9 supralabials (left)/(right), 6 to level below center of eye (left)/(right); 8 infralabials (left)/(right), 5 to level below center of eye (left)/(right); mental small, followed by a single, larger postmental; 4 pairs of enlarged chin shields; 1st pair in contact with one another; 2nd–4th pairs separated by 1–2 scales; 99 transverse rows of dorsal scales from interoccipital to base of tail; 94 transverse rows of ventral scales from mental to vent; 37 scales around midbody; 5 digits; finger lengths 3>4>2>5>1; 10 (left)/9 (right) lamellae under longest finger; 36 total lamellae on one hand; toe lengths 4>3>5>2>1; 16 lamellae under longest toe (left)/(right); keelless and striate dorsal body and caudal scales; smooth ventral scales; 188 total strigae counted on ten scales.

Color (in alcohol): dorsal surface of head gray-brown, patternless; lateral surfaces of head grading from gray-brown to cream with darker brown eye masks and other darker brown areas on the labial scales; dorsal surfaces of the body are gray-brown, patternless; dorsal surface of tail gray-brown, patternless, faded yellow on regenerated portion of tail; lateral areas grade from dark brown to cream; dorsal surfaces of the limbs are dark red-brown; lateral and ventral areas of the limbs fade to cream; ventral surfaces of the head, body, and tail are yellow-cream that is darker under the tail.

Variation. The examined material resembles the holotype in dorsal pattern. All specimens examined lack a patterned head, longitudinal paramedian lines, and dots arranged in bars in the lateral band. Measurements and other morphological data for the holotype and other examined material are presented in Table 1.

Distribution. *Panolopus curtissi* is distributed in south-central Haiti and adjacent Dominican Republic at elevations of 20–910 m (Fig. 50). It mostly occupies the trough separating the north and south paleo islands of Hispaniola, called the Plaine du Cul de Sac in Haiti and the Valle de Neiba in the Dominican Republic, including areas below sea level. The range also extends along the dry coast west of the Chaine des Matheux of Haiti, Gonave, and south to Jacmel. It has an extent of occurrence of ~3,710 km^2.

Ecology and conservation. Past literature accounts of ecological data for this species conflate multiple species and therefore cannot be used. We consider the conservation status of *Panolopus curtissi* to be Least Concern, based on IUCN Redlist criteria (IUCN 2023). It is likely a common species tolerant of some habitat disturbance, based on what is known of most species of *Panolopus*. However, it faces a primary threat of habitat destruction resulting from deforestation. A secondary threat is predation from introduced mammals, including the mongoose and black rats. Studies are needed to determine the health and extent of remaining populations and better understand the threats to the survival of the species.

Reproduction. Past literature accounts of ecological data for this species conflate multiple species and therefore cannot be used.

Etymology. The species name refers to Mr. Anthony Curtiss, the collector of the type specimen.

Remarks. Prior to this work, *Panolopus curtissi* was reported to have four subspecies: *P. c. curtissi*, *P. c. aporus*, *P. c. diastatus*, and *P. c. hylonomus*. We elevate all of them to species level. Further analyses of museum specimens that have been recorded as *P. curtissi* should be undertaken to assign all individuals to the correct species.

Panolopus curtissi and *P. diastatus* cannot be morphologically separated based on our standard suite of characters, however, they can be separated by the nasal length by the nasal height (1.21–1.46 [n=5] versus 1.47–1.73 [n=10]).

Panolopus curtissi was included in our genetic dataset and has significant support in both Bayesian and ML likelihood analyses at the crown node. The stem node that places *P. curtissi* as the closest relative to *P. aporus* had a support value of 58% in our ML analysis and was not supported in our Bayesian analysis. Schools *et al.* (2021) places *P. curtissi* and *P. aporus* as closest relatives with significant support in the ML analysis and a support value of 80% in the Bayesian analysis. Based on our timetree (Fig. 4), *P. curtissi* diverged from its closest relative 2.04 Ma, consistent with typical species of vertebrates (> 0.7 Ma; Hedges *et al.* 2015). *Panolopus curtissi* was recognized as a distinct species by our ASAP analysis.

FIGURE 57. (A–F) *Panolopus curtissi* (USNM 11733, holotype), SVL 75.0 mm.

FIGURE 58. *Panolopus curtissi* (ANSP 38634, SBH 269347), SVL 77.5 mm, in life. From near Richard, Gonave Island, Ouest Department, Haiti. Photo by SBH.

***Panolopus diastatus* (Schwartz 1964)**
Northwestern Smooth-scaled Forest Lizard
(Fig. 59)

Diploglossus curtissi diastatus Schwartz, 1964:42. Holotype: MCZ R-63402, collected by Austin Stanley Rand and James Draper Lazell, Jr. from Bombardopolis, Nord-Ouest department, Haiti, on 22 July 1960 (19.695, -73.341).
Celestus curtissi diastatus—Schwartz & Henderson, 1988:98.
Celestus curtissi diastatus—Schwartz & Henderson, 1991:371.
Celestus curtissi diastatus—Hedges *et al.*, 2019:17.

Material examined (n=16). HAITI. AMNH 49816, William G. Hassler, N part of Haiti, near intersection of Jean Rabel and Port a l'Ecu Road, 2 April 1935. **Nord'Ouest.** ANSP 38636–40, S. Blair Hedges and Richard Thomas, Bombardopolis, 28 April 1997; ANSP 38641–2, S. Blair Hedges and Richard Thomas, about 3.5 mi SW Bombardopolis (on S facing slope of Morne Tony), 29 April 1997; ANSP 38643–6, S. Blair Hedges, Richard Thomas, and Felix Charles, Mole St. Nicolas, 25 April 1997. **Port-de-Paix.** MCZ R-63395, R-63400, R-63402, Austin Stanley Rand, James Draper Lazell, Jr., Bombardopolis, 22 July 1960; MCZ R-63412, Austin Stanley Rand, James Draper Lazell, Jr., Mole St. Nicolas, 26 July 1960.

Diagnosis. *Panolopus diastatus* has (1) a dorsal pattern of absent/irregular flecks, (2) head markings absent, (3) markings in the longitudinal paramedian area absent, (4) dots arranged in bars in the lateral band absent/present, (5) an adult SVL of 66.1–83.7 mm, (6) ventral scale rows, 86–114, (7) midbody scale rows, 33–39, (8) total lamellae on one hand, 35–41, (9) total strigae on ten scales, 169–234, (10) relative length of all digits on one hindlimb, 21.5–27.4 %, (11) relative distance between the angled subocular and mouth, 0.00–0.614 %, (12) relative eye length, 2.71–3.32 %, (13) relative forelimb length, 16.2–20.1 %, (14) relative ear width, 0.667–1.43 %, (15) relative rostral height, 1.89–2.45 %, (16) relative head length, 14.2–18.8 %, (17) relative mental width, 1.51–2.00 %, (18) relative postmental width, 2.43–3.17 %, (19) relative cloacal width, 7.15–8.06 %, (20) relative prefrontal width, 3.74–4.61 %, (21) relative largest supraocular width, 1.88–2.57 %, (22) relative longest finger length, 3.48–4.87 %, (23) relative distance between the ear and eye, 6.32–8.58 %, (24) relative head width, 69.4–74.8 %, (25) relative frontal width, 57.4–86.2 %, (26) relative nasal height, 0.913–1.19 %, (27) relative angled subocular height, 0.564–1.08 %, (28) relative distance between the eye and naris, 4.06–4.94 %, (29) relative canthal iii length, 1.21–2.70 %, (30)

relative angled subocular width, 1.93–2.86 %, and (31) relative nasal length, 1.41–1.77 %. The species stem time is 1.81 Ma and the species crown time is 0.23 Ma (Fig. 4).

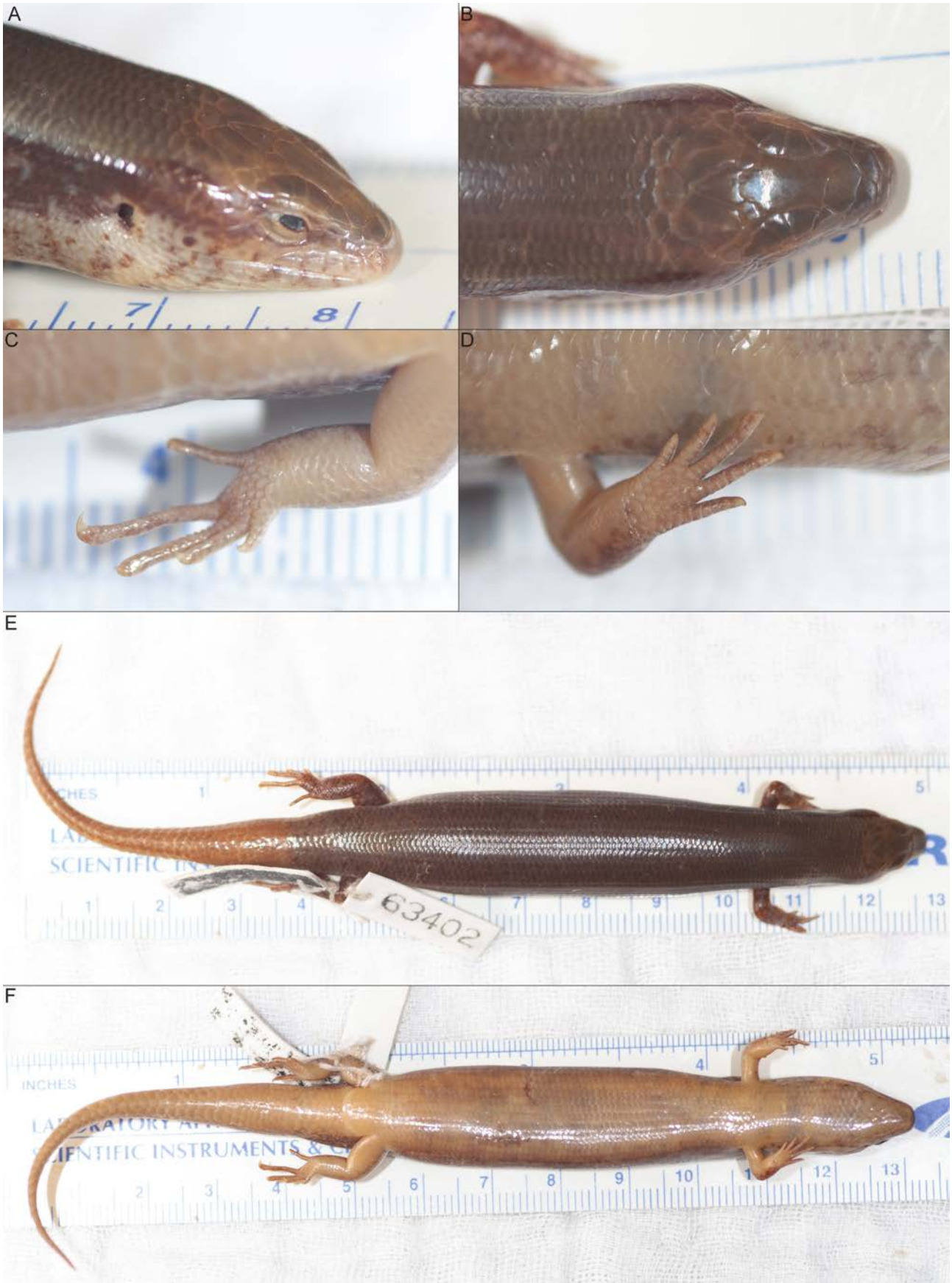

FIGURE 59. (A–F) *Panolopus diastatus* (MCZ R-63402, holotype), SVL 83.7 mm.

We distinguish *Panolopus diastatus* from the other species of *Panolopus* based on a complex of traits. From *Panolopus aenetergum*, we distinguish *P. diastatus* by the dorsal pattern (absent/irregular flecks versus irregular dots), the total strigae on ten scales (169–234 versus 267), the relative distance between angled subocular and mouth (0.00–0.614 versus 0.717), the relative eye length (2.71–3.32 versus 3.34), the relative forelimb length (16.2–20.1 versus 20.6), the relative head width (69.4–74.8 versus 76.4), the relative frontal width (57.4–86.2 versus 88.2), and the relative nasal width (1.41–1.77 versus 1.92). From *P. aporus*, we distinguish *P. diastatus* by the relative length of digits on one hindlimb (21.5–27.4 versus 27.7–33.7) and the relative largest supraocular width (1.88–2.57 versus 2.74–3.62). From *P. chalcorhabdus*, we distinguish *P. diastatus* by the relative length of digits on one hindlimb (21.5–27.4 versus 31.3–36.0), the relative forelimb length (16.2–20.1 versus 20.4–23.7), and the relative longest finger length (3.48–4.87 versus 5.29–6.97). From *P. costatus*, we distinguish *P. diastatus* by the total lamellae on one hand (35–41 versus 49–58), the relative length of digits on one hindlimb (21.5–27.4 versus 31.5–37.8), the relative longest finger length (3.48–4.87 versus 5.53–6.66), and the relative distance between the eye and naris (4.06–4.94 versus 5.08–5.50). From *P. curtissi*, we distinguish *P. diastatus* by the nasal height by the nasal length by the nasal height (1.47–1.73 versus 1.21–1.46) (see Remarks). From *P. emys*, we distinguish *P. diastatus* by the adult SVL (66.1–83.7 versus 99.0–113), the total strigae on ten scales (169–234 versus 238–311), the relative length of digits on one hindlimb (21.5–27.4 versus 28.9–35.2), the relative cloacal width (7.15–8.06 versus 8.24–8.96), and the relative longest finger length (3.48–4.87 versus 5.15–5.83). From *P. hylonomus*, we distinguish *P. diastatus* by the relative largest supraocular width (1.88–2.57 versus 2.65–2.90). From *P. lanceolatus* **sp. nov.**, we distinguish *P. diastatus* by the longitudinal paramedian lines (absent versus present) and the relative length of digits on one hindlimb (21.5–27.4 versus 28.4–35.9). From *P. lapierrae* sp. nov., we distinguish *P. diastatus* by the relative distance between angled subocular and mouth (0.00–0.614 versus 0.620–0.725), the relative cloacal width (7.15–8.06 versus 8.55–8.81), the relative prefrontal width (3.74–4.61 versus 4.73–4.75), the relative head width (69.4–74.8 versus 77.7–78.1), the relative distance between the eye and naris (4.06–4.94 versus 5.21), and the relative nasal width (1.41–1.77 versus 1.81). From *P. leionotus*, we distinguish *P. diastatus* by the adult SVL (66.1–83.7 versus 86.3–105) and the total lamellae on one hand (35–41 versus 43–48). From *P. marcanoi*, we distinguish *P. diastatus* by the dorsal pattern (absent/irregular flecks versus irregular dots/dots in chevrons), the head markings (absent versus present), and the longitudinal paramedian lines (absent versus present). From *P. melanchrous*, we distinguish *P. diastatus* by the longitudinal paramedian lines (absent versus present), the adult SVL (66.1–83.7 versus 93.2–124), the total lamellae on one hand (35–41 versus 47–58), the relative length of digits on one hindlimb (21.5–27.4 versus 30.7–41.3), and the relative longest finger length (3.48–4.87 versus 5.76–7.09). From *P. neiba*, we distinguish *P. diastatus* by the total lamellae on one hand (35–41 versus 45–49), the relative length of digits on one hindlimb (21.5–27.4 versus 29.5–36.6), the relative distance between angled subocular and mouth (0.00–0.614 versus 0.670–0.747), and the relative longest finger length (3.48–4.87 versus 5.61–6.66). From *P. nesobous*, we distinguish *P. diastatus* by the dorsal pattern (absent/irregular flecks versus irregular dots/dots in series), the longitudinal paramedian lines (absent versus present), the total lamellae on one hand (35–41 versus 50–59), the relative length of digits on one hindlimb (21.5–27.4 versus 35.1), the relative eye length (2.71–3.32 versus 3.41–3.63), the relative forelimb length (16.2–20.1 versus 23.3–25.1), the relative cloacal width (7.15–8.06 versus 8.11–8.21), the relative prefrontal width (3.74–4.61 versus 4.74–4.81), the relative largest supraocular width (1.88–2.57 versus 2.85–3.11), the relative longest finger length (3.48–4.87 versus 6.19–6.33), and the relative distance between the eye and naris (4.06–4.94 versus 5.62–5.73). From *P. oreistes*, we distinguish *P. diastatus* by the dorsal pattern (absent/irregular flecks versus irregular dots/dots in series/dots in chevrons), the longitudinal paramedian lines (absent versus present), the relative length of digits on one hindlimb (21.5–27.4 versus 31.2–40.1), the relative longest finger length (3.48–4.87 versus 5.27–7.23), and the relative distance between the eye and naris (4.06–4.94 versus 5.01–5.63). From *P. psychonothes*, we distinguish *P. diastatus* by the dorsal pattern (absent/irregular flecks versus irregular dots/dots in series/dots in chevrons) and the relative longest finger length (3.48–4.87 versus 4.89–5.81). From *P. saonae*, we distinguish *P. diastatus* by the adult SVL (66.1–83.7 versus 90.9–98.3), the relative cloacal width (7.15–8.06 versus 8.20), the relative largest supraocular width (1.88–2.57 versus 2.77), the relative longest finger length (3.48–4.87 versus 5.01), and the relative distance between the eye and naris (4.06–4.94 versus 6.43). From *P. semitaeniatus* **sp. nov.**, we distinguish *P. diastatus* by the relative length of digits on one hindlimb (21.5–27.4 versus 30.4–34.6), the relative distance between angled subocular and mouth (0.00–0.614 versus 0.666–0.808), the relative forelimb length (16.2–20.1 versus 21.3–23.8), the relative ear width (0.667–1.43 versus 1.90–2.30), the relative cloacal width (7.15–8.06 versus 8.08–8.23), the relative largest supraocular width (1.88–2.57 versus 2.59–3.32), the relative longest finger

length (3.48–4.87 versus 5.17–6.05), and the relative head width (69.4–74.8 versus 58.8–63.8). From *P. unicolor* **sp. nov.**, we distinguish *P. diastatus* by the longitudinal paramedian lines (absent versus present), the midbody scale rows (33–39 versus 40), the total lamellae on one hand (35–41 versus 48), the total strigae on ten scales (169–234 versus 144), the relative length of digits on one hindlimb (21.5–27.4 versus 36.8), the relative eye length (2.71–3.32 versus 3.38), the relative forelimb length (16.2–20.1 versus 23.5), the relative ear width (0.667–1.43 versus 1.60), the relative prefrontal width (3.74–4.61 versus 4.69), the relative largest supraocular width (1.88–2.57 versus 3.12), the relative longest finger length (3.48–4.87 versus 6.65), the relative distance between the eye and naris (4.06–4.94 versus 5.52), the relative angled subocular width (1.93–2.86 versus 2.90), and the relative nasal width (1.41–1.77 versus 2.00).

Description of holotype. MCZ R-63402. An adult male; SVL 83.7 mm; tail nearly cylindrical, broken in life midway, regenerated, 67.7 mm (80.9% SVL); axilla-to-groin distance 50.8 mm (60.7% SVL); forelimb length 16.7 mm (20.0% SVL); hindlimb length 21.8 mm (26.0% SVL); head length 14.7 mm (17.6% SVL); head width 10.7 mm (12.8% SVL); head width 72.8% head length; diameter of orbit 2.35 mm (2.81% SVL); horizontal diameter of ear opening 0.91 mm (1.09% SVL); vertical diameter of ear opening 1.25 mm (1.49% SVL); length of all toes on one foot 21.7 mm (25.9% SVL); shortest distance between angled subocular and lip 0.40 mm (0.478% SVL); shortest distance between the ocular and auricular openings 7.18 mm (8.58% SVL); longest finger length 3.69 mm (4.41% SVL); largest supraocular width 1.57 mm (1.88% SVL); cloacal width 6.68 mm (7.98% SVL); mental width 1.54 mm (1.84% SVL); postmental width 2.28 mm (2.72% SVL); prefrontal width 3.33 mm (3.98% SVL); frontal width 86.2% frontal length; nasal height 0.98 mm (1.17% SVL); angled subocular height 0.90 mm (1.08% SVL); shortest distance between the eye and naris 3.59 mm (4.29% SVL); canthal iii width 1.49 mm (1.78% SVL); angled subocular width 2.39 mm (2.86% SVL); nasal width 1.45 mm (1.73% SVL); rostral 1.89X as wide as high, visible from above, not in contact with nasals, in contact with 1st supralabial and anterior internasal (left)/(right); anterior internasals are narrower than posterior ones; frontonasals and prefrontal fused into a single large plate with a slightly concave posterior margin, much wider than long also fused with frontal, bordered by posterior internasals, 1st loreals, 1st median oculars, and the frontal; frontal longer than wide; a pair of frontoparietals, separated by the posterior prolongation of the frontal and the interparietal plate; interparietal plate smaller than parietals and separating them, posteriorly touching the interoccipital, which is wider than long; parietal separated from supraoculars by 1st and 2nd temporals and frontoparietal (left)/(right); nasal single; nostril above suture between 1st and 2nd supralabials (left)/(right); 1 postnasal (left)/(right); 2 loreals (left)/(right); 1st loreal higher than wide (left)/(right), in contact with postnasal, posterior internasal, prefrontal/frontonasal complex, 1st median ocular, canthal iii, 2nd loreal, and 3rd–4th supralabials (left)/(right); 2nd loreal shorter than 1st, approximately as high as wide (left)/(right), excluded from contact with supraocular by canthal iii (left)/(right); final loreal posteriorly bordering the lower preocular (left)/upper and lower preoculars (right); canthal iii wider than high (left)/(right), contacting 1st median ocular, anterior supraciliary, upper and lower preoculars, and 1st and 2nd loreals (left)/1st median ocular, anterior supraciliary, upper preocular, and 1st and 2nd loreals (right); 10 (left)/9 (right) median oculars, 1st contacting the prefrontal (left)/(right); 1 upper preocular (left)/(right); an irregular anterior supraciliary (left)/(right); 6 lateral oculars (left)/(right); 5 temporals (left)/(right); 2 suboculars (left)/(right); posterior subocular large and elongate (left)/(right); anterior subocular small (left)/(right); 9 supralabials (left)/(right), 6 to level below center of eye (left)/(right); 9 infralabials (left)/(right), 6 (left)/5 (right) to level below center of eye; mental small, followed by a single, larger postmental; 4 pairs of enlarged chin shields; 1st pair in contact with one another; 2nd–4th pairs separated by 1–2 scales; 95 transverse rows of dorsal scales from interoccipital to base of tail; 86 transverse rows of ventral scales from mental to vent; 35 scales around midbody; 5 digits; finger lengths 3>4>2>5>1; 10 lamellae under longest finger (left)/(right); 39 total lamellae on one hand; toe lengths 4>3>5>2>1; 16 lamellae under longest toe (left)/(right); keelless and striate dorsal body and caudal scales; smooth ventral scales; 211 total strigae counted on ten scales.

Color (in alcohol): dorsal surface of head gray-brown, patternless; lateral surfaces of head grading from gray-brown to cream with darker brown eye masks and other darker brown areas on the supralabial scales; dorsal surfaces of the body are gray-brown with irregular darker brown spots towards the posterior; dorsal surface of tail red-gray to yellow (on regenerated section) with irregular darker brown spots; lateral areas fading from dark red-brown to yellow-cream with some irregular off-white dots; dorsal surfaces of the limbs are golden tan with darker brown mottling; lateral and ventral areas of the limbs fade to pale cream, patternless; ventral surfaces of the head, body, and tail are cream, patternless except for a few darker brown flecks under the chin.

Variation. The majority of examined specimens lack a dorsal pattern with a few specimens displaying several

irregular flecks posteriorly. No specimens show a patterned head, longitudinal paramedian markings, or dots arranged in bars in the lateral band. Measurements and other morphological data for the holotype and other examined material are presented in Table 1.

Distribution. *Panolopus diastatus* is distributed in northwestern Haiti at elevations of 10–500 m (Fig. 49).

Ecology and conservation. No ecological data are available for this species. We consider the conservation status of *Panolopus diastatus* to be Least Concern, based on IUCN Redlist criteria (IUCN 2023). It is likely a common species tolerant of some habitat disturbance, based on what is known of most species of *Panolopus*. However, it faces a primary threat of habitat destruction resulting from deforestation. A secondary threat is predation from introduced mammals, including the mongoose and black rats. Studies are needed to determine the health and extent of remaining populations and better understand the threats to the survival of the species.

Reproduction. No data on reproduction are available for this species.

Etymology. The name is from the Greek noun *diastatus*, meaning divided, in allusion to the large distributional hiatus between *Panolopus diastatus* and *P. curtissi*, discussed in the original description (Schwartz 1964).

Remarks. Previously regarded as a subspecies of *Panolopus curtissi*, this species appears in multiple museum collections. Addition museum specimens catalogued as *P. curtissi* should be examined for diagnostic characters to potentially assign them to *P. diastatus.*

Panolopus diastatus and *P. curtissi* cannot be morphologically separated based on our standard suite of characters, however, they can be separated by the nasal length by the nasal height (1.21–1.46 [n=5] versus 1.47–1.73 [n=10]).

Panolopus diastatus was included in our genetic dataset and has significant support in both Bayesian and ML likelihood analyses at the crown node. The placement of *P. diastatus* within *Panolopus* had a support value of 63% in our ML analysis and was not supported in our Bayesian analysis. Schools *et al.* (2022) used genomic data to place *P. diastatus* outside of *P. unicolor* **sp. nov.**, *P. leionotus*, *P. marcanoi*, *P. neiba*, and *P. semitaeniatus* **sp. nov.** with significant support in ML and Bayesian analyses. Based on our timetree (Fig. 4), *P. diastatus* diverged from its closest relative 1.81 Ma, consistent with typical species of vertebrates (> 0.7 Ma; Hedges *et al.* 2015). *Panolopus diastatus* was recognized as a distinct species by our ASAP analysis.

Panolopus emys **(Schwartz 1971b)**

Tortue Smooth-scaled Forest Lizard
(Fig. 60)

Diploglossus costatus emys Schwartz, 1971b:163. Holotype: USNM 167300, collected from Palmiste, Tortue Island, Nord-Ouest department, Haiti on 4–5 September 1968 (20.018, -72.725; 320 m).
Celestus costatus emys—Schwartz & Henderson, 1988:95.
Celestus costatus emys—Schwartz & Henderson, 1991:267.
Celestus costatus emys—Hedges *et al.*, 2019:16.
Celestus costatus emys—Schools & Hedges, 2021:231.

Material examined (n=20). HAITI. Nord-Ouest. Tortue Island. KU 225005–6, November 1968; KU 225008–17, ca Palmiste, 1970; MCZ R-119382, Cecil R. Warren, Palmiste, 4–5 September 1970; MCZ, R-119396–8, Cecil R. Warren, Palmiste, 15–17 August 1970; USNM 167300, Palmiste, 4–5 September 1968; USNM 167316–18, Palmiste, 15–17 August 1970.

Diagnosis. *Panolopus emys* has (1) a dorsal pattern of absent/irregular flecks, (2) head markings absent, (3) markings in the longitudinal paramedian area absent/present, (4) dots arranged in bars in the lateral band present, (5) an adult SVL of 99.0–113 mm, (6) ventral scale rows, 89–104, (7) midbody scale rows, 34–40, (8) total lamellae on one hand, 39–54, (9) total strigae on ten scales, 238–311, (10) relative length of all digits on one hindlimb, 28.9–35.2 %, (11) relative distance between the angled subocular and mouth, 0.533–0.826 %, (12) relative eye length, 2.87–3.40 %, (13) relative forelimb length, 18.5–23.4 %, (14) relative ear width, 0.756–1.75 %, (15) relative rostral height, 2.10–2.37 %, (16) relative head length, 14.5–18.6 %, (17) relative mental width, 1.49–2.01 %, (18) relative postmental width, 2.20–2.87 %, (19) relative cloacal width, 8.24–8.96 %, (20) relative prefrontal width, 3.99–4.36 %, (21) relative largest supraocular width, 2.01–2.89 %, (22) relative longest finger length, 5.15–5.83 %, (23) relative distance between the ear and eye, 7.03–8.44 %, (24) relative head width, 71.1–78.7 %, (25) relative frontal

width, 67.7–74.5 %, (26) relative nasal height, 0.963–1.10 %, (27) relative angled subocular height, 0.696–0.981 %, (28) relative distance between the eye and naris, 4.37–5.19 %, (29) relative canthal iii length, 1.54–2.01 %, (30) relative angled subocular width, 2.12–2.20 %, and (31) relative nasal length, 1.23–1.58 %. No data are available to estimate the species stem or crown time.

We distinguish *Panolopus emys* from the other species of *Panolopus* based on a complex of traits. From *Panolopus aenetergum*, we distinguish *P. emys* by the dorsal pattern (absent/irregular flecks versus irregular dots), the adult SVL (99.0–113 versus 83.0–92.0), the ventral scale rows (89–104 versus 80–86), the relative length of digits on one hindlimb (28.9–35.2 versus 26.8), the relative rostral height (2.10–2.37 versus 2.09), the relative cloacal width (8.24–8.96 versus 7.60), the relative longest finger length (5.15–5.83 versus 4.83), the relative frontal width (67.7–74.5 versus 88.2), the relative nasal height (0.963–1.10 versus 1.15), the relative angled subocular height (0.696–0.981 versus 1.08), and the relative distance between the eye and naris (4.37–5.19 versus 4.35). From *P. aporus*, we distinguish *P. emys* by the total strigae on ten scales (238–311 versus 150–235) and the relative angled subocular width (2.12–2.20 versus 2.32–2.73). From *P. chalcorhabdus*, we distinguish *P. emys* by the adult SVL (99.0–113 versus 71.9–95.4), the total strigae on ten scales (238–311 versus 184–233), the relative prefrontal width (3.99–4.36 versus 4.37–4.93), the relative angled subocular width (2.12–2.20 versus 2.36–2.71), and the relative nasal width (1.23–1.58 versus 1.70–2.01). From *P. costatus*, we distinguish *P. emys* by the total strigae on ten scales (238–311 versus 158–217), the relative frontal width (67.7–74.5 versus 56.2–67.4), and the relative angled subocular width (2.12–2.20 versus 2.36–2.81). From *P. curtissi*, we distinguish *P. emys* by the dots arranged in bars in the lateral areas (present versus absent), the adult SVL (99.0–113 versus 64.1–85.5), the relative length of digits on one hindlimb (28.9–35.2 versus 20.8–28.1), the relative longest finger length (5.15–5.83 versus 3.59–4.54), and the relative angled subocular width (2.12–2.20 versus 2.26–2.76). From *P. diastatus*, we distinguish *P. emys* by the adult SVL (99.0–113 versus 66.1–83.7), the total strigae on ten scales (238–311 versus 169–234), the relative length of digits on one hindlimb (28.9–35.2 versus 21.5–27.4), the relative cloacal width (8.24–8.96 versus 7.15–8.06), and the relative longest finger length (5.15–5.83 versus 3.48–4.87). From *P. hylonomus*, we distinguish *P. emys* by the dots arranged in bars in the lateral areas (present versus absent), the adult SVL (99.0–113 versus 59.3–76.5), the total strigae on ten scales (238–311 versus 169–222), and the relative length of digits on one hindlimb (28.9–35.2 versus 22.8–28.2). From *P. lanceolatus* **sp. nov.**, we distinguish *P. emys* by the total strigae on ten scales (238–311 versus 186–234) and the relative angled subocular width (2.12–2.20 versus 2.38–3.09). From *P. lapierrae* **sp. nov.**, we distinguish *P. emys* by the adult SVL (99.0–113 versus 72.6–88.3), the total strigae on ten scales (238–311 versus 228–231), the relative rostral height (2.10–2.37 versus 1.86–2.06), the relative prefrontal width (3.99–4.36 versus 4.73–4.75), the relative longest finger length (5.15–5.83 versus 4.49–4.55), the relative frontal width (67.7–74.5 versus 77.6–79.0), and the relative distance between the eye and naris (4.37–5.19 versus 5.21). From *P. leionotus*, we distinguish *P. emys* by the relative angled subocular width (2.12–2.20 versus 2.48–2.95) and the relative nasal width (1.23–1.58 versus 1.59–2.01). From *P. marcanoi*, we distinguish *P. emys* by the dorsal pattern (absent/irregular flecks versus irregular dots/dots in chevrons), the head markings (absent versus present), the adult SVL (99.0–113 versus 64.6–85.8), and the relative nasal width (1.23–1.58 versus 1.64–1.96). From *P. melanchrous*, we distinguish *P. emys* by the relative nasal height (0.963–1.10 versus 0.897–0.952) and the relative angled subocular width (2.12–2.20 versus 2.28–2.82). From *P. neiba*, we distinguish *P. emys* by the relative prefrontal width (3.99–4.36 versus 4.41–5.49), the relative angled subocular width (2.12–2.20 versus 2.34–2.83), and the relative nasal width (1.23–1.58 versus 1.67–1.92). From *P. nesobous*, we distinguish *P. emys* by the dorsal pattern (absent/irregular flecks versus irregular dots/dots in series), the total strigae on ten scales (238–311 versus 155–222), the relative eye length (2.87–3.40 versus 3.41–3.63), the relative cloacal width (8.24–8.96 versus 8.11–8.21), the relative prefrontal width (3.99–4.36 versus 4.74–4.81), the relative longest finger length (5.15–5.83 versus 6.19–6.33), the relative frontal width (67.7–74.5 versus 60.8–63.5), the relative nasal height (0.963–1.10 versus 1.12–1.14), the relative distance between the eye and naris (4.37–5.19 versus 5.62–5.73), the relative angled subocular width (2.12–2.20 versus 2.61–2.82), and the relative nasal width (1.23–1.58 versus 1.69–1.71). From *P. oreistes*, we distinguish *P. emys* by the dorsal pattern (absent/irregular flecks versus irregular dots/dots in series/dots in chevrons). From *P. psychonothes*, we distinguish *P. emys* by the dorsal pattern (absent/irregular flecks versus irregular dots/dots in series/dots in chevrons), the adult SVL (99.0–113 versus 70.9–97.2), the relative nasal height (0.963–1.10 versus 1.12–1.32), and the relative nasal width (1.23–1.58 versus 1.68–1.94). From *P. saonae*, we distinguish *P. emys* by the adult SVL (99.0–113 versus 90.9–98.3), the relative cloacal width (8.24–8.96 versus 8.2), the relative longest finger length (5.15–5.83 versus 5.01), and the relative distance between the eye and naris (4.37–5.19 versus 6.43).

From *P. semitaeniatus* **sp. nov.**, we distinguish *Panolopus emys* by the SVL (99.0–113 versus 77.4–84.1), the total strigae on ten scales (238–311 versus 174–204), the relative ear width (0.756–1.75 versus 1.90–2.30), the relative rostral height (2.10–2.37 versus 2.41–2.63), the relative cloacal width (8.24–8.96 versus 8.08–8.23), the relative prefrontal width (3.99–4.36 versus 4.38–4.94), the relative head width (71.1–78.7 versus 58.8–63.8), and the relative angled subocular height (0.696–0.981 versus 0.654). From *P. unicolor* **sp. nov.**, we distinguish *P. emys* by the adult SVL (99.0–113 versus 67.6), the total strigae on ten scales (238–311 versus 144), the relative length of digits on one hindlimb (28.9–35.2 versus 36.8), the relative forelimb length (18.5–23.4 versus 23.5), the relative cloacal width (8.24–8.96 versus 7.61), the relative prefrontal width (3.99–4.36 versus 4.69), the relative largest supraocular width (2.01–2.89 versus 3.12), the relative longest finger length (5.15–5.83 versus 6.65), the relative head width (71.1–78.7 versus 70.8), the relative frontal width (67.7–74.5 versus 58.2), the relative nasal height (0.963–1.10 versus 1.15), and the relative distance between the eye and naris (4.37–5.19 versus 5.52).

Description of holotype. USNM 167300. An adult female; SVL 107 mm; tail nearly cylindrical, 80.6 mm (75.3% SVL); axilla-to-groin distance 61.7 mm (57.7% SVL); forelimb length 21.3 mm (19.9% SVL); hindlimb length 33.5 mm (31.3% SVL); head length 16.4 mm (15.3% SVL); head width 12.9 mm (12.1% SVL); head width 78.7% head length; diameter of orbit 3.57 mm (3.34% SVL); horizontal diameter of ear opening 1.46 mm (1.36% SVL); vertical diameter of ear opening 1.43 mm (1.34% SVL); length of all toes on one foot 32.3 mm (30.2% SVL); shortest distance between angled subocular and lip 0.57 mm (0.533% SVL); shortest distance between the ocular and auricular openings 7.83 mm (7.32% SVL); longest finger length 5.91 mm (5.52% SVL); largest supraocular width 2.15 mm (2.01% SVL); postmental width 2.35 mm (2.20% SVL); postmental width 2.35 mm (2.20% SVL); prefrontal width 4.27 mm (3.99% SVL); frontal width 73.0% frontal length; nasal height 1.12 mm (1.05% SVL); angled subocular height 1.05 mm (0.981% SVL); shortest distance between the eye and naris 4.82 mm (4.50% SVL); canthal iii width 1.65 mm (1.54% SVL); angled subocular width 2.35 mm (2.20% SVL); nasal width 1.32 mm (1.23% SVL); rostral 2.35X as wide as high, visible from above, not in contact with nasals, in contact with 1st supralabial and anterior internasal (left)/(right); anterior internasals are narrower than posterior ones; frontonasals and prefrontal fused into a single large plate with a concave posterior margin, wider than long, bordered by posterior internasals, 1st loreals, canthal iii (left), 1st median oculars, and the frontal; frontal longer than wide; a pair of frontoparietals, separated by the posterior prolongation of the frontal and the interparietal plate; interparietal plate much smaller than parietals and separating them, posteriorly touching the interoccipital, which is wider than long; parietal separated from supraoculars by 1st and 2nd temporals and frontoparietal (left)/(right); nasal single; nostril above suture between 1st and 2nd supralabials (left)/(right); 1 postnasal (left)/(right); 2 loreals (left)/(right); 1st loreal higher than wide (left)/(right), in contact with postnasal, posterior internasal, prefrontal/frontonasal complex, canthal iii, 2nd loreal, and 3rd–4th supralabials (left)/postnasal, posterior internasal, prefrontal/frontonasal complex, 1st median ocular, canthal iii, 2nd loreal, and 3rd–4th supralabials (right); 2nd loreal shorter than 1st, approximately as high as wide (left)/(right), excluded from contact with supraocular by canthal iii (left)/(right); final loreal posteriorly bordering the lower preocular (left)/(right); canthal iii wider than high (left)/(right), contacting 1st median ocular, anterior supraciliary, upper preocular, prefrontal/frontonasal complex, and 1st and 2nd loreals (left)/1st median ocular, anterior supraciliary, upper preocular, and 1st and 2nd loreals (right); 10 median oculars (left)/(right), 1st contacting the prefrontal (left)/(right); 2 upper preoculars (left)/(right); an irregular anterior supraciliary (left)/(right); 7 (left)/6 (right) lateral oculars; 5 temporals (left)/(right); 2 suboculars (left)/(right); posterior subocular large and elongate (left)/(right); anterior subocular small (left)/(right); 10 (left)/9 (right) supralabials, 6 to level below center of eye (left)/(right); 10 infralabials (left)/(right), 6 to level below center of eye (left)/(right); mental small, followed by a single, larger postmental; 4 pairs of enlarged chin shields; 1st pair in contact with one another; 2nd–4th pairs separated by 1–3 scales; 94 transverse rows of dorsal scales from interoccipital to base of tail; 96 transverse rows of ventral scales from mental to vent; 37 scales around midbody; 5 digits; finger lengths 4>3>2>5>1; 11 lamellae under longest finger (left)/(right); 44 total lamellae on one hand; toe lengths 4>3>5>2>1; 17 (left)/18 (right) lamellae under longest toe; keelless and striate dorsal body and caudal scales; smooth ventral scales; 272 total strigae counted on ten scales.

Color (in alcohol): dorsal surface of head golden brown, patternless; lateral surfaces of head grading from golden brown to cream with darker brown eye masks and other darker brown areas on the supralabial, infralabial, and throat scales; dorsal surfaces of the body are golden brown, patternless; dorsal surface of tail golden brown, patternless; lateral areas grade from dark brown to cream with dots in the longitudinal paramedian area extending in series; dorsal surfaces of the limbs are medium brown with darker brown mottling; lateral and ventral areas of the

limbs fade to yellow-cream; ventral surfaces of the head, body, and tail are yellow-cream with some darker flecks under the head.

FIGURE 60. (A–F) *Panolopus emys* (USNM 167300, holotype), SVL 107 mm.

Variation. The majority of the examined material lacks a dorsal pattern with several specimens exhibiting several irregular flecks or dots. All specimens have patternless heads with several specimens showing tiny longitudinal paramedian lines or flecks in the longitudinal paramedian series. Dots in the lateral band arranged in bars appear on all specimens. Measurements and other morphological data for the holotype and other examined material are presented in Table 1.

Distribution. *Panolopus emys* is known only from Palmiste on Tortue Island at an elevation of 320 m (Fig. 49).

Ecology and conservation. No ecological information is associated with the type series; however, the original description noted that the area around Palmiste on Tortue Island is mesic (Schwartz 1971b).

We consider the conservation status of *Panolopus emys* to be Least Concern, based on IUCN Redlist criteria (IUCN 2023). It is likely a common species tolerant of some habitat disturbance, based on what is known of most species of *Panolopus*. However, it faces a primary threat of habitat destruction resulting from deforestation. A secondary threat is predation from introduced mammals, including the mongoose and black rats. Considering that it was last seen by scientists more than five decades ago, studies are needed to determine the health and extent of remaining populations and better understand the threats to the survival of the species.

Reproduction. No data on reproduction are available for this species.

Etymology. The species name (*emys*) is Greek for "turtle" in reference to its distribution on Tortue Island (Tortuga in Spanish). Columbus named the island for its shape that resembles a turtle shell viewed from the side.

Remarks. Schwartz (1971b) noted that endemism of subspecies on Tortue Island was low, with *Panolopus emys* (*Celestus costatus emys* at the time of collection) being one of the few endemic taxa, although he later described an endemic frog (*Eleutherodactylus warreni*) from the island. *Panolopus emys* is not included in our genetic dataset and future studies should be conducted using genetic or genomic data from this species.

***Panolopus hylonomus* (Schwartz 1964)**

Southeastern Smooth-scaled Forest Lizard
(Fig. 61–62)

Diploglossus curtissi hylonomus Schwartz, 1964:49. Holotype: MCZ R-77160, collected by Albert Schwartz, Jr. and Richard Thomas from 0.5 mi. N. Boca de Yuma on 30 August 1963 (18.383, -68.609; 28 m).
Celestus curtissi hylonomus—Schwartz & Henderson, 1988:98.
Celestus curtissi hylonomus—Schwartz & Henderson, 1991:371.
Celestus curtissi hylonomus—Hedges *et al.*, 2019:17.
Celestus curtissi hylonomus—Schools & Hedges, 2021:214.

Material examined (n=12). DOMINICAN REPUBLIC. AMNH 49771, William G. Hassler, at caves near Rio Chavon, E of La Romana, 30 July 1935. **Distrito Nacional.** AMNH 92799, D. C. Leber, 7 mi E Boca Chica, 14 June 1963. **La Altagracia.** KU 226274, 0.5 mi NW Boca de Yuma, 30 August 1963; KU 226275–6, 4 mi SE San Rafael del Yuma, 30 August 1963; KU 226281–2, Juanillo, 18 August 1969; KU 226387, 1.2 km SSW Punta Cana, 25 November 1971; MCZ R-75028–9, Clayton E. Ray, Robert Ross Allen, Juanillo, 29 March 1963; USNM 259954, "Caldera" Pigeon shooting camp on Lagoon E of Punta Palmillas, 18 February 1965. **La Romana.** MCZ R-77160, Albert Schwartz, Jr., Richard Thomas, 0.5 mi. N. Boca de Yuma, 30 August 1963.

Diagnosis. *Panolopus hylonomus* has (1) a dorsal pattern of absent/irregular flecks, (2) head markings absent, (3) markings in the longitudinal paramedian area absent/present, (4) dots arranged in bars in the lateral band absent, (5) an adult SVL of 59.3–76.5 mm, (6) ventral scale rows, 80–97, (7) midbody scale rows, 33–39, (8) total lamellae on one hand, 34–47, (9) total strigae on ten scales, 169–222, (10) relative length of all digits on one hindlimb, 22.8–28.2 %, (11) relative distance between the angled subocular and mouth, 0.424–0.873 %, (12) relative eye length, 2.78–3.72 %, (13) relative forelimb length, 17.1–20.7 %, (14) relative ear width, 0.902–2.08 %, (15) relative rostral height, 1.72–2.28 %, (16) relative head length, 15.1–18.5 %, (17) relative mental width, 1.63–2.11 %, (18) relative postmental width, 2.67–2.89 %, (19) relative cloacal width, 7.98–8.57 %, (20) relative prefrontal width, 4.23–4.87 %, (21) relative largest supraocular width, 2.65–2.90 %, (22) relative longest finger length, 4.47–5.27 %, (23) relative distance between the ear and eye, 6.78–8.05 %, (24) relative head width, 73.8–76.4 %, (25) relative frontal width, 64.0–74.5 %, (26) relative nasal height, 0.961–1.37 %, (27) relative angled subocular height, 0.690–1.13 %,

(28) relative distance between the eye and naris, 4.03–4.98 %, (29) relative canthal iii length, 1.95–2.03 %, (30) relative angled subocular width, 1.61–2.75 %, and (31) relative nasal length, 1.48–2.01 %. The species stem time is 0.85 Ma and no data are available to estimate the species crown time (Fig. 4).

We distinguish *Panolopus hylonomus* from the other species of *Panolopus* based on a complex of traits. From *Panolopus aenetergum*, we distinguish *P. hylonomus* by the dorsal pattern (absent/irregular flecks versus irregular dots), the dots arranged in bars in the lateral areas (absent versus present), the adult SVL (59.3–76.5 versus 83.0–92.0), the total strigae on ten scales (169–222 versus 267), the relative postmental width (2.67–2.89 versus 2.62), the relative cloacal width (7.98–8.57 versus 7.60), the relative prefrontal width (4.23–4.87 versus 4.15), the relative largest supraocular width (2.65–2.90 versus 2.49), the relative distance between the ear and eye (6.78–8.05 versus 8.40), the relative frontal width (64.0–74.5 versus 88.2), and the relative width of canthal iii (1.95–2.03 versus 1.86). From *P. aporus*, we distinguish *P. hylonomus* by the dots arranged in bars in the lateral areas (absent versus present) and the adult SVL (59.3–76.5 versus 77.8–100). From *P. chalcorhabdus*, we distinguish *P. hylonomus* by the dots arranged in bars in the lateral areas (absent versus present), the relative length of digits on one hindlimb (22.8–28.2 versus 31.3–36.0), and the relative longest finger length (4.47–5.27 versus 5.29–6.97). From *P. costatus*, we distinguish *P. hylonomus* the dots arranged in bars in the lateral areas (absent versus present), the adult SVL (59.3–76.5 versus 83.6–107), the total lamellae on one hand (34–47 versus 49–58), the relative length of digits on one hindlimb (22.8–28.2 versus 31.5–37.8), the relative longest finger length (4.47–5.27 versus 5.53–6.66), the relative distance between the eye and naris (4.03–4.98 versus 5.08–5.50), and the relative width of canthal iii (1.95–2.03 versus 1.82–1.90). From *P. curtissi*, we distinguish *P. hylonomus* by the relative width of canthal iii (1.95–2.03 versus 1.75–1.93). From *P. diastatus*, we distinguish *P. hylonomus* by the relative largest supraocular width (2.65–2.90 versus 1.88–2.57). From *P. emys*, we distinguish *P. hylonomus* by the dots arranged in bars in the lateral areas (absent versus present), the adult SVL (59.3–76.5 versus 99.0–113), the total strigae on ten scales (169–222 versus 238–311), and the relative length of digits on one hindlimb (22.8–28.2 versus 28.9–35.2). From *P. lanceolatus* **sp. nov.**, we distinguish *P. hylonomus* by the dots arranged in bars in the lateral areas (absent versus present), the adult SVL (59.3–76.5 versus 78.5–104), the relative length of digits on one hindlimb (22.8–28.2 versus 28.4–35.9), and the relative postmental width (2.67–2.89 versus 2.36–2.66). From *P. lapierrae* **sp. nov.**, we distinguish *P. hylonomus* by the total strigae on ten scales (169–222 versus 228–231), the relative head width (73.8–76.4 versus 77.7–78.1), the relative frontal width (64.0–74.5 versus 77.6–79.0), the relative distance between the eye and naris (4.03–4.98 versus 5.21), and the relative width of canthal iii (1.95–2.03 versus 1.54–1.86). From *P. leionotus*, we distinguish *P. hylonomus* by the dots arranged in bars in the lateral areas (absent versus present), the adult SVL (59.3–76.5 versus 86.3–105), the relative largest supraocular width (2.65–2.90 versus 1.94–2.50), and the relative width of canthal iii (1.95–2.03 versus 1.55–1.89). From *P. marcanoi*, we distinguish *P. hylonomus* by the dorsal pattern (absent/irregular flecks versus irregular dots/dots in chevrons), the head markings (absent versus present), and the dots arranged in bars in the lateral areas (absent versus present). From *P. melanchrous*, we distinguish *P. hylonomus* by the dots arranged in bars in the lateral areas (absent versus present), the adult SVL (59.3–76.5 versus 93.2–124), the relative length of digits on one hindlimb (22.8–28.2 versus 30.7–41.3), the relative longest finger length (4.47–5.27 versus 5.76–7.09), the relative nasal height (0.961–1.37 versus 0.897–0.952), and the relative width of canthal iii (1.95–2.03 versus 1.67–1.94). From *P. neiba*, we distinguish *P. hylonomus* by the dots arranged in bars in the lateral areas (absent versus present), the adult SVL (59.3–76.5 versus 77.9–102), the relative length of digits on one hindlimb (22.8–28.2 versus 29.5–36.6), and the relative longest finger length (4.47–5.27 versus 5.61–6.66). From *P. nesobous*, we distinguish *P. hylonomus* by the dorsal pattern (absent/irregular flecks versus irregular dots/dots in series), the dots arranged in bars in the lateral areas (absent versus present), the adult SVL (59.3–76.5 versus 82.3–108), the total lamellae on one hand (34–47 versus 50–59), the relative length of digits on one hindlimb (22.8–28.2 versus 35.1), the relative forelimb length (17.1–20.7 versus 23.3–25.1), the relative longest finger length (4.47–5.27 versus 6.19–6.33), the relative frontal width (64.0–74.5 versus 60.8–63.5), and the relative distance between the eye and naris (4.03–4.98 versus 5.62–5.73). From *P. oreistes*, we distinguish *P. hylonomus* by the dorsal pattern (absent/irregular flecks versus irregular dots/dots in series/dots in chevrons), the dots arranged in bars in the lateral areas (absent versus present), the adult SVL (59.3–76.5 versus 77.3–103), the relative length of digits on one hindlimb (22.8–28.2 versus 31.2–40.1), and the relative distance between the eye and naris (4.03–4.98 versus 5.01–5.63). From *P. psychonothes*, we distinguish *P. hylonomus* by the dorsal pattern (absent/irregular flecks versus irregular dots/dots in series/dots in chevrons). From *P. saonae*, we distinguish *P. hylonomus* by the adult SVL (59.3–76.5 versus 90.9–98.3), the relative mental width (1.63–2.11 versus 1.52), the

relative postmental width (2.67–2.89 versus 2.43), the relative prefrontal width (4.23–4.87 versus 4.14), the relative head width (73.8–76.4 versus 73.5), and the relative distance between the eye and naris (4.03–4.98 versus 6.43). From *P. semitaeniatus* **sp. nov.**, we distinguish *P. hylonomus* by the SVL (59.3–76.5 versus 77.4–84.1), the relative length of digits on one hindlimb (22.8–28.2 versus 30.4–34.6), the relative forelimb length (17.1–20.7 versus 21.3–23.8), the relative rostral height (1.72–2.28 versus 2.41–2.63), the relative head width (73.8–76.4 versus 58.8–63.8), the relative angled subocular height (0.690–1.13 versus 0.654), and the relative width of canthal iii (1.95–2.03 versus 1.80). From *P. unicolor* **sp. nov.**, we distinguish *P. hylonomus* by the dots arranged in bars in the lateral areas (absent versus present), the midbody scale rows (33–39 versus 40), the total lamellae on one hand (34–47 versus 48), the total strigae on ten scales (169–222 versus 144), the relative length of digits on one hindlimb (22.8–28.2 versus 36.8), the relative forelimb length (17.1–20.7 versus 23.5), the relative cloacal width (7.98–8.57 versus 7.61), the relative largest supraocular width (2.65–2.90 versus 3.12), the relative longest finger length (4.47–5.27 versus 6.65), the relative head width (73.8–76.4 versus 70.8), the relative frontal width (64.0–74.5 versus 58.2), the relative distance between the eye and naris (4.03–4.98 versus 5.52), the relative width of canthal iii (1.95–2.03 versus 1.79), and the relative angled subocular width (1.61–2.75 versus 2.90).

Description of holotype. MCZ R-77160. An adult male; SVL 72.3 mm; tail nearly cylindrical, broken in life midway, regenerated, 67.0 mm (92.7% SVL); axilla-to-groin distance 40.6 mm (56.2% SVL); forelimb length 14.1 mm (19.5% SVL); hindlimb length 20.5 mm (28.4% SVL); head length 13.2 mm (18.3% SVL); head width 9.96 mm (13.8% SVL); head width 75.5% head length; diameter of orbit 2.69 mm (3.72% SVL); horizontal diameter of ear opening 1.02 mm (1.41% SVL); vertical diameter of ear opening 1.18 mm (1.63% SVL); length of all toes on one foot 19.8 mm (27.4% SVL); shortest distance between angled subocular and lip 0.41 mm (0.567% SVL); shortest distance between the ocular and auricular openings 5.59 mm (7.73% SVL); longest finger length 3.81 mm (5.27% SVL); largest supraocular width 2.00 mm (2.77% SVL); cloacal width 6.00 mm (8.30% SVL); mental width 1.35 mm (1.87% SVL); postmental width 1.96 mm (2.71% SVL); prefrontal width 3.52 mm (4.87% SVL); frontal width 74.5% frontal length; nasal height 0.99 mm (1.37% SVL); angled subocular height 0.82 mm (1.13% SVL); shortest distance between the eye and naris 3.52 mm (4.87% SVL); canthal iii width 1.45 mm (2.01% SVL); angled subocular width 1.99 mm (2.75% SVL); nasal width 1.45 mm (2.01% SVL); rostral 1.75X as wide as high, visible from above, not in contact with nasals, in contact with 1st supralabial and anterior internasal (left)/(right); anterior internasals are narrower than posterior ones; frontonasals and prefrontal fused into a single large plate with a concave posterior margin, wider than long, bordered by posterior internasals, 1st loreals, 1st median oculars, and the frontal; frontal much longer than wide; a pair of frontoparietals, separated by the posterior prolongation of the frontal and the interparietal plate; interparietal plate smaller than parietals and separating them, posteriorly touching the interoccipital, which is wider than long; parietal separated from supraoculars by 1st and 2nd temporals and frontoparietal (left)/(right); nasal single; nostril above suture between 1st and 2nd supralabials (left)/(right); 1 postnasal (left)/(right); 2 loreals (left)/(right); 1st loreal higher than wide (left)/(right), in contact with postnasal, posterior internasal, prefrontal/frontonasal complex, 1st median ocular, canthal iii, 2nd loreal, and 3rd–4th supralabials (left)/(right); 2nd loreal shorter than 1st, approximately as high as wide (left)/(right), excluded from contact with supraocular by canthal iii (left)/(right); final loreal posteriorly bordering the lower preocular (left)/upper and lower preoculars (right); canthal iii wider than high (left)/(right), contacting 1st median ocular, anterior supraciliary, upper and lower preoculars, and 1st and 2nd loreals (left)/1st median ocular, anterior supraciliary, upper preocular, and 1st and 2nd loreals (right); 9 (left)/10 (right) median oculars, 1st contacting the prefrontal (left)/(right); 2 (left)/1 (right) upper preoculars; an irregular anterior supraciliary (left)/(right); 5 lateral oculars (left)/(right); 5 temporals (left)/(right); 3 suboculars (left)/(right); posterior subocular large and elongate (left)/(right); anterior suboculars small (left)/(right); 9 supralabials (left)/(right), 6 to level below center of eye (left)/(right); 10 (left)/9 (right) infralabials, 5–7 (left)/5 (right) to level below center of eye; mental small, followed by a single, larger postmental; 4 pairs of enlarged chin shields, followed by 1 pair of reduced chin shields; 1st pair in contact with one another; 2nd–4th pairs separated by 1–3 scales; 90 transverse rows of dorsal scales from interoccipital to base of tail; 97 transverse rows of ventral scales from mental to vent; 38 scales around midbody; 5 digits; finger lengths 3>4>2>5>1; 10 (right) lamellae under longest finger; 41 total lamellae on one hand; toe lengths 4>3>5>2>1; 17 (right) lamellae under longest toe; keelless and striate dorsal body and caudal scales; ventral scales smooth to faintly striated; 195 total strigae counted on ten scales.

FIGURE 61. (A–F) *Panolopus hylonomus* (MCZ R-77160, holotype), SVL 72.3 mm.

FIGURE 62. *Panolopus hylonomus* (SBH 267793), in life. From ca. 2 km S Juanillo, Altagracia Province, Dominican Republic. Photo by SBH.

Color (in alcohol): dorsal surface of head gray-tan, patternless; lateral surfaces of head grading from pale tan to cream with darker brown eye masks and other darker brown areas on the supralabial, infralabial, and throat scales; dorsal surfaces of the body are red-gray with a few paler brown flecks; dorsal surface of tail red-gray to yellow-gray (on regenerated section) with a few pale brown spots; lateral areas fading from dark gray-brown to cream with darker brown spots arranged in vertical lines; dorsal surfaces of the limbs are pale brown with darker brown mottling; lateral and ventral areas of the limbs fade to pale cream, patternless; ventral surfaces of the head, body, and tail are pale cream with some brown mottling under the throat and nearer to the sides.

Variation. No specimen has a patterned head and only AMNH 92799 shows markings in the longitudinal paramedian area (small dots in series). The lateral band is reduced in this species with no specimen showing dots arranged in bars in the lateral band before it ends. Measurements and other morphological data for the holotype and other examined material are presented in Table 1.

Distribution. *Panolopus hylonomus* is distributed along the extreme southeastern coast of the Dominican Republic at elevations of 0–80 m (Fig. 49).

Ecology and conservation. No ecological data are associated with this species. We consider the conservation status of *Panolopus hylonomus* to be Least Concern, based on IUCN Redlist criteria (IUCN 2023). It is likely a common species tolerant of some habitat disturbance, based on what is known of most species of *Panolopus*. However, it faces a primary threat of habitat destruction resulting from deforestation. A secondary threat is predation from introduced mammals, including the mongoose and black rats. Studies are needed to determine the health and extent of remaining populations and better understand the threats to the survival of the species.

Reproduction. No data on reproduction are available for this species.

Etymology. The species name is from the Greek *hylo-* (forest) and *nomus* (wanderer), in likely allusion to the relatively isolated range of this mesic, forest-dwelling species in eastern Hispaniola (Schwartz 1964).

Remarks. Previously considered a subspecies of *Panolopus curtissi*, herein we elevate *P. hylonomus* to the species level based on genetic and morphological differences. Additional specimens categorized as *P. costatus* and *P. curtissi* in museum collections should be examined for the diagnostic characters reported herein to potentially assign them to this species.

Panolopus hylonomus was included in our genetic dataset and has significant support in both Bayesian and ML likelihood analyses at the stem node that places it as the closest relative of *P. unicolor* **sp. nov.** Based on our timetree (Fig. 4), *P. hylonomus* diverged from its closest relative 0.85 Ma, consistent with typical species of vertebrates (> 0.7

Ma; Hedges *et al.* 2015). We also recognize *P. hylonomus* as a distinct species because of the multiple morphological traits that separate it from *P. unicolor* **sp. nov.**, its closest relative. *Panolopus hylonomus* was recognized as a distinct species by our ASAP analysis.

***Panolopus lanceolatus* sp. nov.**
Westcentral Smooth-scaled Forest Lizard
(Fig. 63)

Celestus costatus—Schwartz & Henderson, 1991:368 (part).
Celestus costatus—Powell *et al.*, 1999:104 (part).
Celestus costatus—Hedges et al., 2019:16 (part).
Panolopus costatus—Schools & Hedges, 2021:230 (part).
Panolopus costatus—Landestoy *et al.*, 2022:205 (part).

Holotype. MCZ R-190692, an adult female from first and only major intersection between Ennery and Plaisance, a couple hundred meters E on intersecting road, collected by D. Luke Mahler and Richard E. Glor on 6 August 2009 (19.52387, -72.45154; 925 m).

Paratypes (n=8). HAITI. Artibonite. KU 226436–9, 1.2 mi W Ennery, 1977. **Nord.** MCZ R-63383–4, Austin Stanley Rand and James Draper Lazell, Dondon, 16 July 1960; MCZ R-63386, Austin Stanley Rand, James Draper Lazell, Jr., Jean Bernard between Cap Haitien and Grande Riviere du Nord, 16 July 1960; MCZ R-190691, D. Luke Mahler, Richard E. Glor, first and only major intersection between Ennery and Plaisance, couple hundred meters E on intersecting road, 6 August 2009.

Diagnosis. *Panolopus lanceolatus* **sp. nov.** has (1) a dorsal pattern of absent/irregular dots/dots in series/dots in chevrons, (2) head markings absent/present, (3) markings in the longitudinal paramedian area present, (4) dots arranged in bars in the lateral band present, (5) an adult SVL of 78.5–104 mm, (6) ventral scale rows, 93–102, (7) midbody scale rows, 37–43, (8) total lamellae on one hand, 41–52, (9) total strigae on ten scales, 186–234, (10) relative length of all digits on one hindlimb, 28.4–35.9 %, (11) relative distance between the angled subocular and mouth, 0.567–0.704 %, (12) relative eye length, 3.01–3.51 %, (13) relative forelimb length, 17.4–23.9 %, (14) relative ear width, 0.770–1.35 %, (15) relative rostral height, 1.78–2.28 %, (16) relative head length, 15.2–18.2 %, (17) relative mental width, 1.45–1.96 %, (18) relative postmental width, 2.36–2.66 %, (19) relative cloacal width, 8.01–8.76 %, (20) relative prefrontal width, 3.97–4.55 %, (21) relative largest supraocular width, 2.20–2.71 %, (22) relative longest finger length, 4.76–6.36 %, (23) relative distance between the ear and eye, 6.45–7.70 %, (24) relative head width, 68.0–77.6 %, (25) relative frontal width, 63.1–72.1 %, (26) relative nasal height, 0.904–1.06 %, (27) relative angled subocular height, 0.484–0.854 %, (28) relative distance between the eye and naris, 4.58–5.05 %, (29) relative canthal iii length, 1.73–2.00 %, (30) relative angled subocular width, 2.38–3.09 %, and (31) relative nasal length, 1.48–1.95 %. No genetic data are available for estimating the species stem time or crown time.

We distinguish *Panolopus lanceolatus* **sp. nov.** from the other species of *Panolopus* based on a complex of traits. From *Panolopus aenetergum*, we distinguish *P. lanceolatus* **sp. nov.** by the longitudinal paramedian lines (present versus absent), the ventral scale rows (93–102 versus 80–86), the midbody scale rows (37–43 versus 35–36), the total lamellae on one hand (41–52 versus 40), the total strigae on ten scales (186–234 versus 267), the relative length of digits on one hindlimb (28.4–35.9 versus 26.8), the relative distance between angled subocular and mouth (0.567–0.704 versus 0.717), the relative cloacal width (8.01–8.76 versus 7.60), the relative distance between the ear and eye (6.45–7.70 versus 8.40), the relative frontal width (63.1–72.1 versus 88.2), the relative nasal height (0.904–1.06 versus 1.15), the relative angled subocular height (0.484–0.854 versus 1.08), the relative distance between the eye and naris (4.58–5.05 versus 4.35), and the relative angled subocular width (2.38–3.09 versus 2.07). From *P. aporus*, we distinguish *P. lanceolatus* **sp. nov.** by the relative largest supraocular width (2.20–2.71 versus 2.74–3.62) and the relative nasal height (0.904–1.06 versus 1.08–1.23). From *P. chalcorhabdus*, we distinguish *P. lanceolatus* **sp. nov.** by the angled subocular height (3.29–5.91 versus 2.77–3.28) (see Remarks). From *P. costatus*, we distinguish *P. lanceolatus* **sp. nov.** by the relative distance between the eye and naris (4.58–5.05 versus 5.08–5.50). From *P. curtissi*, we distinguish *P. lanceolatus* **sp. nov.** by the dots arranged in bars in the lateral areas (present versus absent), the total lamellae on one hand (41–52 versus 32–39), the relative length of digits on one hindlimb (28.4–35.9 versus 20.8–28.1), and the relative longest finger length (4.76–6.36 versus 3.59–4.54). From *P. diastatus*, we distinguish *P.*

lanceolatus **sp. nov.** by the longitudinal paramedian lines (present versus absent) and the relative length of digits on one hindlimb (28.4–35.9 versus 21.5–27.4). From *P. emys*, we distinguish *P. lanceolatus* **sp. nov.** by the total strigae on ten scales (186–234 versus 238–311) and the relative angled subocular width (2.38–3.09 versus 2.12–2.20). From *P. hylonomus*, we distinguish *P. lanceolatus* **sp. nov.** by the dots arranged in bars in the lateral areas (present versus absent), the adult SVL (78.5–104 versus 59.3–76.5), the relative length of digits on one hindlimb (28.4–35.9 versus 22.8–28.2), and the relative postmental width (2.36–2.66 versus 2.67–2.89). From *P. lapierrae* **sp. nov.**, we distinguish *P. lanceolatus* **sp. nov.** by the relative postmental width (2.36–2.66 versus 2.68–3.58), the relative prefrontal width (3.97–4.55 versus 4.73–4.75), the relative longest finger length (4.76–6.36 versus 4.49–4.55), the relative distance between the ear and eye (6.45–7.70 versus 7.78–8.43), the relative head width (68.0–77.6 versus 77.7–78.1), the relative frontal width (63.1–72.1 versus 77.6–79.0), and the relative distance between the eye and naris (4.58–5.05 versus 5.21). From *P. leionotus*, we distinguish *P. lanceolatus* **sp. nov.** by the frontal width by the SVL (3.48–3.84 versus 3.89–5.00) (see Remarks). From *P. marcanoi*, we distinguish *P. lanceolatus* **sp. nov.** by the relative nasal height (0.904–1.06 versus 1.07–1.28). From *P. melanchrous*, we distinguish *P. lanceolatus* **sp. nov.** by the relative postmental width (2.36–2.66 versus 2.71–3.38). From *P. neiba*, we distinguish *P. lanceolatus* **sp. nov.** by the frontal width by the SVL (3.48–3.84 versus 3.86–4.52) (see Remarks). From *P. nesobous*, we distinguish *P. lanceolatus* **sp. nov.** by the relative ear width (0.770–1.35 versus 1.39–1.60), the relative postmental width (2.36–2.66 versus 2.82–3.02), the relative prefrontal width (3.97–4.55 versus 4.74–4.81), the relative largest supraocular width (2.20–2.71 versus 2.85–3.11), the relative distance between the ear and eye (6.45–7.70 versus 7.91–10.0), the relative nasal height (0.904–1.06 versus 1.12–1.14), the relative distance between the eye and naris (4.58–5.05 versus 5.62–5.73), and the relative width of canthal iii (1.73–2.00 versus 2.01–2.12). From *P. oreistes*, we distinguish *P. lanceolatus* **sp. nov.** by the relative distance between the eye and naris (4.58–4.98 versus 5.01–5.63). From *P. psychonothes*, we distinguish *P. lanceolatus* **sp. nov.** by the relative nasal height (0.904–1.06 versus 1.12–1.32). From *P. saonae*, we distinguish *P. lanceolatus* **sp. nov.** by the longitudinal paramedian lines (present versus absent), the relative largest supraocular width (2.20–2.71 versus 2.77), the relative frontal width (63.1–72.1 versus 72.5), the relative distance between the eye and naris (4.58–5.05 versus 6.43), and the relative angled subocular width (2.38–3.09 versus 2.31). From *P. semitaeniatus* **sp. nov.**, we distinguish *P. lanceolatus* **sp. nov.** the relative ear width (0.770–1.35 versus 1.90–2.30), the relative rostral height (1.78–2.28 versus 2.41–2.63), the relative head width (68.0–77.6 versus 58.8–63.8), and the relative nasal height (0.904–1.06 versus 1.08). From *P. unicolor* **sp. nov.**, we distinguish *P. lanceolatus* **sp. nov.** by the adult SVL (78.5–104 versus 67.6), the total strigae on ten scales (186–234 versus 144), the relative length of digits on one hindlimb (28.4–35.9 versus 36.8), the relative distance between angled subocular and mouth (0.567–0.704 versus 0.533), the relative ear width (0.770–1.35 versus 1.60), the relative postmental width (2.36–2.66 versus 2.80), the relative cloacal width (8.01–8.76 versus 7.61), the relative prefrontal width (3.97–4.55 versus 4.69), the relative largest supraocular width (2.20–2.71 versus 3.12), the relative longest finger length (4.76–6.36 versus 6.65), the relative frontal width (63.1–72.1 versus 58.2), the relative nasal height (0.904–1.06 versus 1.15), the relative distance between the eye and naris (4.58–5.05 versus 5.52), and the relative nasal width (1.48–1.95 versus 2.00).

Description of holotype. MCZ R-190692. An adult female; SVL 95.1 mm; tail nearly cylindrical, 106 mm (111% SVL); axilla-to-groin distance 56.3 mm (59.2% SVL); forelimb length 20.6 mm (21.7% SVL); hindlimb length 31.0 mm (32.6% SVL); head length 16.3 mm (17.1% SVL); head width 11.2 mm (11.8% SVL); head width 68.7% head length; diameter of orbit 3.29 mm (3.46% SVL); horizontal diameter of ear opening 1.03 mm (1.08% SVL); vertical diameter of ear opening 1.18 mm (1.24% SVL); length of all toes on one foot 31.8 mm (33.4% SVL); shortest distance between angled subocular and lip 0.67 mm (0.705% SVL); shortest distance between the ocular and auricular openings 6.67 mm (7.01% SVL); longest finger length 5.66 mm (5.95% SVL); largest supraocular width 2.34 mm (2.46% SVL); cloacal width 7.62 mm (8.01% SVL); mental width 1.63 mm (1.71% SVL); postmental width 2.24 mm (2.36% SVL); prefrontal width 3.78 mm (3.97% SVL); frontal width 70.8% frontal length; nasal height 0.92 mm (0.967% SVL); angled subocular height 0.46 mm (0.484% SVL); shortest distance between the eye and naris 4.74 mm (4.98% SVL); canthal iii width 1.72 mm (1.81% SVL); angled subocular width 2.72 mm (2.86% SVL); nasal width 1.46 mm (1.54% SVL); rostral 2.28X as wide as high, visible from above, not in contact with nasals, in contact with 1st supralabial and anterior internasal (left)/(right); anterior internasals are narrower than posterior ones; frontonasals and prefrontal fused into a single large plate with a slightly concave posterior margin, wider than long, bordered by posterior internasals, 1st loreals, 1st median oculars, 2nd median ocular on the left, and the frontal; frontal longer than wide; a pair of frontoparietals, separated by the posterior prolongation

of the frontal and the interparietal plate; interparietal plate smaller than parietals and separating them, posteriorly touching the interoccipital, which is wider than long; parietal separated from supraoculars by 1st and 2nd temporals and frontoparietal (left)/(right); nasal single; nostril above suture between 1st and 2nd supralabials (left)/(right); 1 postnasal (left)/(right); 2 loreals (left)/(right); 1st loreal higher than wide (left)/(right), in contact with postnasal, posterior internasal, prefrontal/frontonasal complex, 1st median ocular, canthal iii, 2nd loreal, and 3rd–4th supralabial (left)/(right); 2nd loreal shorter than 1st, approximately as high as wide (left)/(right), excluded from contact with supraocular by canthal iii (left)/(right); final loreal posteriorly bordering the upper and lower preoculars (left)/(right); canthal iii wider than high (left)/(right), contacting 1st median ocular, anterior supraciliary, upper preocular, and 1st and 2nd loreals (left)/(right); 10 (left)/9 (right) median oculars, 1st and 2nd contacting the prefrontal (left)/1st (right); 1 (left)/2 (right) upper preoculars; an irregular anterior supraciliary (left)/(right); 6 (left)/5 (right) lateral oculars; 5 temporals (left)/(right); 1 subocular (left)/(right); posterior subocular large and elongate (left)/(right); 9 supralabials (left)/(right), 6 to level below center of eye (left)/(right); 9 (left)/10 (right) infralabials, 6 (left)/7 (right) to level below center of eye; mental small, followed by a single, larger postmental; 4 pairs of enlarged chin shields; 1st pair in contact with one another; 2nd–4th pairs separated by 1–3 scales; 94 transverse rows of dorsal scales from interoccipital to base of tail; 98 transverse rows of ventral scales from mental to vent; 37 scales around midbody; 5 digits; finger lengths 3>4>2>5>1; 13 (left)/14 (right) lamellae under longest finger; 52 total lamellae on one hand; toe lengths 4>3>2>5>1; 17 (left)/18 (right) lamellae under longest toe; keelless and striate dorsal body and caudal scales; striate ventral scales; 234 total strigae counted on ten scales.

Color (in alcohol): dorsal surface of head medium brown, patternless; lateral surfaces of head grading from medium brown to pale gray with darker brown eye masks and markings on the labial scales; dorsal surfaces of the body are the same medium brown as the head with several darker brown spots in the longitudinal paramedian area; dorsal surface of tail the same as the head and body; lateral areas grading from medium brown to gray-cream with darker and paler dots arranged in bars in the lateral area; dorsal surfaces of the limbs are dark brown with some paler mottling; lateral and ventral areas of the limbs fading from dark brown to pale cream with some darker brown flecks; ventral surfaces of the head, body, and tail are gray-cream with a few darker spots on the chest.

Variation. Members of this species resemble the holotype in pattern with specimens possessing irregular dots or dots occurring in and extension of the longitudinal paramedian markings or arranged in chevrons. Only KU 226436 lacks a dorsal pattern outside of longitudinal paramedian markings. Only MCZ R-63383 has head scales with dark outlines, all others have patternless heads. All specimens possess dots arranged in series in the longitudinal paramedian area or broken longitudinal paramedian lines. All specimens have dots arranged in bars in the lateral area (this trait is reduced in KU 226436 and KU 226438). Measurements and other morphological data for the holotype and other examined material are presented in Table 1.

Distribution. *Panolopus lanceolatus* **sp. nov.** is distributed in northcentral Haiti to the northern coast at elevations of 20–900 m (Fig. 50).

Ecology and conservation. Little ecological information is available for this species other than that the individuals collected at 900 m are accompanied with the field notes "rock wall."

We consider the conservation status of *Panolopus lanceolatus* to be Least Concern, based on IUCN Redlist criteria (IUCN 2023). It is likely a common species tolerant of some habitat disturbance, based on what is known of most species of *Panolopus*. However, it faces a primary threat of habitat destruction resulting from deforestation. A secondary threat is predation from introduced mammals, including the mongoose and black rats. Studies are needed to determine the health and extent of remaining populations and better understand the threats to the survival of the species.

Reproduction. Ovoviviparous. MCZ R-63383 has developed embryos whereas MCZ R-63384 has follicles.

Etymology. The species name (*lanceolatus*) is a feminine Latin adjective, meaning spear-like, referring to the flat and pointed head of this species.

Remarks. When several animals were collected in 1960, they were identified as *Panolopus diastatus* in museum collections because they were captured near the range of that species. Given the morphological differences between this species and *P. diastatus* (the longitudinal paramedian lines present versus absent) and the relative length of digits on one hindlimb (28.4–35.9 versus 21.5–27.4) we are confident that these specimens are not that species. Schwartz (1964) plotted several locations for "*Celestus*" (*Panolopus*) *costatus* in that general vicinity, with question marks, but did not discuss them. Later, Schwartz & Henderson (1988) mentioned in the remarks section for that species that "specimens of *C. costatus* from northern Haiti (Dondon; Jean Bernard between Cap-Haitien and Grande

Rivière du Nord)…remain unassigned subspecifically." We believe that they are referring to the specimens that we describe herein as *P. lanceolatus* **sp. nov.**

FIGURE 63. (A–F) *Panolopus lanceolatus* **sp. nov.** (MCZ R-190692, holotype), SVL 95.1 mm.

Panolopus lanceolatus and *P. chalcorhabdus* cannot be morphologically separated based on our standard suite of characters; however, they can be separated by the angled subocular width divided by the angled subocular

height (3.29–5.91 [n=7] versus 2.77–3.28 [n=5]). *Panolopus lanceolatus* **sp. nov.** and *P. leionotus* cannot be morphologically separated based on our standard suite of characters; however, they can be separated by the frontal width divided by the SVL (3.48–3.84 [n=8] versus 3.89–5.00 [n=5]). *Panolopus lanceolatus* **sp. nov.** and *P. neiba* cannot be morphologically separated based on our standard suite of characters; however, they can be separated by the frontal width divided by the SVL (3.48–3.84 [n=8] versus 3.86–4.52 [n=5]).

Panolopus lanceolatus **sp. nov.** is not included in our genetic dataset and future studies should be conducted to obtain additional specimens for better definition of the range of the species, and to obtain genetic or genomic data from this species to clarify its relationship with other species.

***Panolopus lapierrae* sp. nov.**
Lapierre Forest Lizard
(Fig. 64)

Diploglossus curtissi diastatus—Schwartz, 1964:42 (part).
Celestus curtissi diastatus—Schwartz & Henderson, 1988:98 (part).
Celestus curtissi diastatus—Schwartz & Henderson, 1991:371 (part).
Celestus curtissi diastatus—Hedges *et al.*, 2019:17 (part).
Celestus curtissi—Schools & Hedges, 2021:230 (part).

Holotype. ANSP 38578, an adult male from 11.8 km W of Ça Soleil, collected by S. Blair Hedges, Richard Thomas, Nicholas Plummer, and Manuel Leal on 11 June 1991 (19.46955, -72.77713; ca. 100 m).

Paratypes (n=4). HAITI. Artibonite. KU 226257–8, 7.6 mi W Ça Soleil, 14 July 1978; KU 226261, 7.6 mi W Ça Soleil, 17 July 1978; SBH 192407, 11.8 km W of Ça Soleil, 6 November 1991.

Diagnosis. *Panolopus lapierrae* **sp. nov.** has (1) a dorsal pattern of absent/dots in chevrons, (2) head markings absent/present, (3) markings in the longitudinal paramedian area absent/present, (4) dots arranged in bars in the lateral band absent/present, (5) an adult SVL of 72.6–88.3 mm, (6) ventral scale rows, 90–98, (7) midbody scale rows, 33–38, (8) total lamellae on one hand, 38–47, (9) total strigae on ten scales, 228–231, (10) relative length of all digits on one hindlimb, 24.3–30.9 %, (11) relative distance between the angled subocular and mouth, 0.620–0.725 %, (12) relative eye length, 2.88–3.67 %, (13) relative forelimb length, 18.5–20.6 %, (14) relative ear width, 0.929–1.58 %, (15) relative rostral height, 1.86–2.06 %, (16) relative head length, 17.0–18.7 %, (17) relative mental width, 1.92–1.94 %, (18) relative postmental width, 2.68–3.58 %, (19) relative cloacal width, 8.55–8.81 %, (20) relative prefrontal width, 4.73–4.75 %, (21) relative largest supraocular width, 1.91–2.77 %, (22) relative longest finger length, 4.49–4.55 %, (23) relative distance between the ear and eye, 7.78–8.43 %, (24) relative head width, 77.7–78.1 %, (25) relative frontal width, 77.6–79.0 %, (26) relative nasal height, 1.06–1.09 %, (27) relative angled subocular height, 0.838–0.978 %, (28) relative distance between the eye and naris, 5.21 %, (29) relative canthal iii length, 1.54–1.86 %, (30) relative angled subocular width, 2.71 %, and (31) relative nasal length, 1.81 %. The species stem time is 1.53 Ma and no data are available to estimate the species crown time (Fig. 4).

Panolopus lapierrae **sp. nov.** has a smaller relative longest finger length (4.49–4.55) than most other species of the genus. From *Panolopus aenetergum*, we distinguish *P. lapierrae* **sp. nov.** by the dorsal pattern (absent/dots in chevrons versus irregular dots) and the ventral scale rows (90–98 versus 80–86). From *P. aporus*, we distinguish *P. lapierrae* **sp. nov.** by the relative prefrontal width (4.73–4.75 versus 4.18–4.53), the relative longest finger length (4.49–4.55 versus 4.57–5.72), the relative frontal width (77.6–79.0 versus 61.7–75.1), and the relative nasal width (1.81 versus 1.56–1.78). From *P. chalcorhabdus*, we distinguish *P. lapierrae* **sp. nov.** by the relative length of digits on one hindlimb (24.3–30.9 versus 31.3–36.0), the relative longest finger length (4.49–4.55 versus 5.29–6.97), the relative head width (77.7–78.1 versus 65.0–76.3), and the relative width of canthal iii (1.54–1.86 versus 1.98–2.05). From *P. costatus*, we distinguish *P. lapierrae* **sp. nov.** by the midbody scale rows (33–38 versus 39–43), the total lamellae on one hand (38–47 versus 49–58), the total strigae on ten scales (228–231 versus 158–217), the relative length of digits on one hindlimb (24.3–30.9 versus 31.5–37.8), the relative cloacal width (8.55–8.81 versus 7.27–8.51), the relative prefrontal width (4.73–4.75 versus 3.97–4.67), the relative longest finger length (4.49–4.55 versus 5.53–6.66), the relative head width (77.7–78.1 versus 68.3–76.8), the relative frontal width (77.6–79.0 versus 56.2–67.4), and the relative nasal width (1.81 versus 1.58–1.74). From *P. curtissi*, we distinguish *P. lapierrae* **sp. nov.** the relative distance between angled subocular and mouth (0.620–0.725 versus 0.393–0.587), the relative prefrontal

width (4.73–4.75 versus 3.96–4.68), the relative distance between the ear and eye (7.78–8.43 versus 5.36–7.71), and the relative distance between the eye and naris (5.21 versus 4.02–5.03). From *P. diastatus*, we distinguish *P. lapierrae* **sp. nov.** by the relative distance between angled subocular and mouth (0.620–0.725 versus 0.00–0.614), the relative cloacal width (8.55–8.81 versus 7.15–8.06), the relative prefrontal width (4.73–4.75 versus 3.74–4.61), the relative head width (77.7–78.1 versus 69.4–74.8), the relative distance between the eye and naris (5.21 versus 4.06–4.94), and the relative nasal width (1.81 versus 1.41–1.77). From *P. emys*, we distinguish *P. lapierrae* **sp. nov.** by the adult SVL (72.6–88.3 versus 99.0–113), the total strigae on ten scales (228–231 versus 238–311), the relative rostral height (1.86–2.06 versus 2.10–2.37), the relative prefrontal width (4.73–4.75 versus 3.99–4.36), the relative longest finger length (4.49–4.55 versus 5.15–5.83), the relative frontal width (77.6–79.0 versus 67.7–74.5), and the relative distance between the eye and naris (5.21 versus 4.37–5.19). From *P. hylonomus*, we distinguish *P. lapierrae* **sp. nov.** by the total strigae on ten scales (228–231 versus 169–222), the relative head width (77.7–78.1 versus 73.8–76.4), the relative frontal width (77.6–79.0 versus 64.0–74.5), the relative distance between the eye and naris (5.21 versus 4.03–4.98), and the relative width of canthal iii (1.54–1.86 versus 1.95–2.03). From *P. lanceolatus* **sp. nov.**, we distinguish *P. lapierrae* **sp. nov.** by the relative postmental width (2.68–3.58 versus 2.36–2.66), the relative prefrontal width (4.73–4.75 versus 3.97–4.55), the relative longest finger length (4.49–4.55 versus 4.76–6.36), the relative distance between the ear and eye (7.78–8.43 versus 6.45–7.70), the relative head width (77.7–78.1 versus 68.0–77.6), the relative frontal width (77.6–79.0 versus 63.1–72.1), and the relative distance between the eye and naris (5.21 versus 4.58–5.05). From *P. leionotus*, we distinguish *P. lapierrae* **sp. nov.** by the relative longest finger length (4.49–4.55 versus 4.58–6.10). From *P. marcanoi*, we distinguish *P. lapierrae* **sp. nov.** by the relative longest finger length (4.49–4.55 versus 4.75–6.68), the relative frontal width (77.6–79.0 versus 59.0–73.0), and the relative angled subocular height (0.838–0.978 versus 0.505–0.793). From *P. melanchrous*, we distinguish *P. lapierrae* **sp. nov.** by the adult SVL (72.6–88.3 versus 93.2–124), the relative longest finger length (4.49–4.55 versus 5.76–7.09), the relative frontal width (77.6–79.0 versus 61.3–71.4), and the relative nasal height (1.06–1.09 versus 0.897–0.952). From *P. neiba*, we distinguish *P. lapierrae* **sp. nov.** by the relative longest finger length (4.49–4.55 versus 5.61–6.66), the relative frontal width (77.6–79.0 versus 63.3–74.0), and the relative distance between the eye and naris (5.21 versus 4.51–5.01). From *P. nesobous*, we distinguish *P. lapierrae* **sp. nov.** by the dorsal pattern (absent/dots in chevrons versus irregular dots/dots in series), the total lamellae on one hand (38–47 versus 50–59), the total strigae on ten scales (228–231 versus 155–222), the relative length of digits on one hindlimb (24.3–30.9 versus 35.1), the relative forelimb length (18.5–20.6 versus 23.3–25.1), the relative rostral height (1.86–2.06 versus 2.26–2.38), the relative mental width (1.92–1.94 versus 1.96–2.18), the relative cloacal width (8.55–8.81 versus 8.11–8.21), the relative largest supraocular width (1.91–2.77 versus 2.85–3.11), the relative longest finger length (4.49–4.55 versus 6.19–6.33), the relative head width (77.7–78.1 versus 71.2–76.4), the relative frontal width (77.6–79.0 versus 60.8–63.5), the relative nasal height (1.06–1.09 versus 1.12–1.14), the relative angled subocular height (0.838–0.978 versus 0.669–0.750), and the relative width of canthal iii (1.54–1.86 versus 2.01–2.12). From *P. oreistes*, we distinguish *P. lapierrae* **sp. nov.** by the relative length of digits on one hindlimb (24.3–30.9 versus 31.2–40.1), the relative mental width (1.92–1.94 versus 1.54–1.90), the relative longest finger length (4.49–4.55 versus 5.27–7.23), the relative frontal width (77.6–79.0 versus 61.6–76.9), and the relative nasal width (1.81 versus 1.37–1.65). From *P. psychonothes*, we distinguish *P. lapierrae* **sp. nov.** by the relative cloacal width (8.55–8.81 versus 7.56–8.53), the relative longest finger length (4.49–4.55 versus 4.89–5.81), the relative nasal height (1.06–1.09 versus 1.12–1.32), and the relative angled subocular width (2.71 versus 2.01–2.44). From *P. saonae*, we distinguish *P. lapierrae* **sp. nov.** by the adult SVL (72.6–88.3 versus 90.9–98.3) and the relative rostral height (1.86–2.06 versus 2.15–2.46). From *P. semitaeniatus* **sp. nov.**, we distinguish *P. lapierrae* **sp. nov.** by the total strigae on ten scales (228–231 versus 174–204), the relative forelimb length (18.5–20.6 versus 21.3–23.8), the relative ear width (0.929–1.58 versus 1.90–2.30), the relative rostral height (1.86–2.06 versus 2.41–2.63), the relative cloacal width (8.55–8.81 versus 8.08–8.23), the relative longest finger length (4.49–4.55 versus 5.17–6.05), the relative head width (77.7–78.1 versus 58.8–63.8), and the relative frontal width (77.6–79.0 versus 63.6–76.5). From *P. unicolor* **sp. nov.**, we distinguish *P. lapierrae* **sp. nov.** by the midbody scale rows (33–38 versus 40), the total lamellae on one hand (38–47 versus 48), and the total strigae on ten scales (228–231 versus 144).

Description of holotype. ANSP 38578. An adult male; SVL 72.6 mm; tail nearly cylindrical, broken in life midway, regenerated, 66.3 mm (91.3% SVL); axilla-to-groin distance 40.4 mm (55.6% SVL); forelimb length 14.9 mm (20.5% SVL); hindlimb length 21.9 mm (30.2% SVL); head length 13.6 mm (18.7% SVL); head width 10.6 mm (14.6% SVL); head width 77.9% head length; diameter of orbit 2.66 mm (3.66% SVL); horizontal diameter

FIGURE 64. (A–F) *Panolopus lapierrae* **sp. nov.** (ANSP 38578, holotype), SVL 72.6 mm.

of ear opening 1.15 mm (1.58% SVL); vertical diameter of ear opening 1.49 mm (2.05% SVL); length of all toes on one foot 22.5 mm (31.0% SVL); shortest distance between angled subocular and lip 0.45 mm (0.620% SVL); shortest distance between the ocular and auricular openings 6.12 mm (8.43% SVL); longest finger length 3.30 mm (4.55% SVL); largest supraocular width 2.01 mm (2.77% SVL); cloacal width 6.39 mm (8.80% SVL); mental width 1.39 mm (1.91% SVL); postmental width 2.60 mm (3.58% SVL); prefrontal width 3.43 mm (4.72% SVL); frontal width 77.6% frontal length; nasal height 0.77 mm (1.06% SVL); angled subocular height 0.71 mm (0.978% SVL); shortest distance between the eye and naris 3.78 mm (5.21% SVL); canthal iii width 1.35 mm (1.86% SVL); angled subocular width 1.97 mm (2.71% SVL); nasal width 1.31 mm (1.80% SVL); rostral 1.94X as wide as high, visible from above, not in contact with nasals, in contact with 1st supralabial and anterior internasal (left)/(right); anterior internasals are narrower than posterior ones; frontonasals and prefrontal fused into a single large plate with a straight posterior margin, wider than long, bordered by posterior internasals, 1st loreals, 1st median oculars, and the frontal; frontal much longer than wide; a pair of frontoparietals, separated by the posterior prolongation of the frontal and the interparietal plate; interparietal plate smaller than parietals and separating them, posteriorly touching the interoccipital, which is wider than long; parietal separated from supraoculars by 1st and 2nd temporals and frontoparietal (left)/(right); nasal single; nostril above suture between 1st and 2nd supralabials (left)/(right); 1 postnasal (left)/(right); 2 loreals (left)/(right); 1st loreal higher than wide (left)/(right), in contact with postnasal, posterior internasal, prefrontal/frontonasal complex, 1st median ocular, canthal iii, 2nd loreal, and 3rd–4th supralabials (left)/(right); 2nd loreal shorter than 1st, approximately as high as wide (left)/(right), excluded from contact with supraocular by canthal iii (left)/(right); final loreal posteriorly bordering the upper and lower preoculars (left)/(right); canthal iii wider than high (left)/(right), contacting 1st median ocular, anterior supraciliary, upper preocular, and 1st and 2nd loreals (left)/(right); 10 (left)/9 (right) median oculars, 1st contacting the prefrontal (left)/(right); 2 (left)/(right) upper preoculars; an irregular anterior supraciliary (left)/(right); 6 lateral oculars (left)/(right); 5 temporals (left)/(right); 1 (left)/2 (right) suboculars; posterior subocular large and elongate (left)/(right); 9 supralabials (left)/(right), 6 to level below center of eye (left)/(right); 8 (left)/9 (right) infralabials, 5 (left)/6(right) to level below center of eye; mental small, followed by a single, larger postmental; 3 pairs of enlarged chin shields, followed by one extra bordering postmental (left), one extra after final pair (right) pair of reduced chin shields; 1st pair in contact anteriorly, posteriorly separated by 1 scale; 2nd–3rd pairs separated by 1–3 scales; 90 transverse rows of dorsal scales from interoccipital to base of tail; 96 transverse rows of ventral scales from mental to vent; 37 scales around midbody; 5 digits; finger lengths 3>4>2>5>1; 9 (left)/10 (right) lamellae under longest finger; 41 total lamellae on one hand; toe lengths 4>3>5>2>1; 16 (left) lamellae under longest toe; keelless and striate dorsal body and caudal scales; smooth to faintly striate ventral scales; 228 total strigae counted on ten scales.

Color (in alcohol): dorsal surface of head gray-tan, patternless; lateral surfaces of head grading from gray-tan to off-white with some darker brown spots and darker brown eye masks; dorsal surfaces of the body are gray-tan, patternless; dorsal surface of tail yellow-gray to dark yellow (on regenerated section) with a few pale brown spots; lateral areas grade from dark brown to cream with white spots arranged in vertical lines anteriorly; dorsal surfaces of the limbs are golden tan with darker brown mottling and cream spots; lateral and ventral areas of the limbs fade to yellow-cream, patternless; ventral surfaces of the head, body, and tail are yellow-cream with darker brown lines under the throat.

Variation. The majority of the material examined resembles the holotype in having patternless dorsums except for SBH 192407, which has dots arranged in chevrons. Similarly, SBH 192407 possesses darker outlines on its head scale borders and dots in series in the longitudinal paramedian area whereas the other material examined lack patterned heads and longitudinal paramedian markings. In the majority of specimens, the dots that occur in lateral bands are reduced or only occur anteriorly. Measurements and other morphological data for the holotype and other examined material are presented in Table 1.

Distribution. *Panolopus lapierrae* **sp. nov.** is known only from the region of Lapierre in northwestern Haiti at elevations of 100–250 m (Fig. 50). It has an extent of occurrence of ~70 km^2.

Ecology and conservation. No ecological data are associated with this species. SBH has visited this general area of Lapierre twice (July 1985 and June 1991) but only encountered two animals of this species, both on the second trip in 1991. No specific notation was made on exactly where these two individuals were collected, but all lizards at that site were taken under rocks and therefore these were as well. Besides these two specimens of *Panolopus lapierrae* **sp. nov.,** approximately 100 other lizards were collected in this area on those two visits, including *Ameiva lineolata*, *Anolis olssoni*, *Anolis websteri*, *Anolis saxatilis*, *Leiocephalus schreibersi*, *Phyllodactylus sommeri*,

Sphaerodactylus asterulus, *S. sommeri*, *Spondylurus lineolatus*, and *Comptus weinlandi*. *Panolopus lapierrae* **sp. nov.** ranks among the rarest of those species. SBH returned to that region of northwestern Haiti for a third time in April 1997, and collected extensively, although not in the area of Lapierre. Members of *P. diastatus* were found near Bombardopolis and Mole St. Nicolas, but no additional material of *P. lapierrae* **sp. nov.** was found, suggesting that it may be restricted to Lapierre.

Lapierre probably has the largest number of lizard species of any site in northern Haiti. Besides those mentioned above, it is the type locality of *Leiocephalus rhutidira*. Three species are only known from Lapierre: *Panolopus lapierrae* **sp. nov.**, *Leiocephalus rhutidira*, and *Phyllodactylus sommeri*. A fourth species, *Sphaerodactylus sommeri*, is only known from there and another nearby location. The ecological or evolutionary significance of Lapierre is unclear. It is a mostly barren, rocky strip of land at the base of a mountain, Morne Lapierre, adjacent to the coast. The mountain is a source of freshwater in this otherwise dry area, and that may explain the unusual abundance of species. Unfortunately, Morne Lapierre is essentially completely deforested, which may be why some of these species are rare or have not been seen in decades. *Panolopus lapierrae* **sp. nov.** has not been encountered since 1991, *Leiocephalus rhutidira* since 1979, and *Spondylurus lineolatus* since 1985.

We consider the conservation status of *Panolopus lapierrae* **sp. nov.** to be Critically Endangered B1ab(iii), based on IUCN Redlist criteria (IUCN 2023). It faces a primary threat from habitat destruction (deforestation). Secondary threats to this species include predation from introduced predators, including the mongoose and black rats. Studies are needed to determine the health of any remaining populations and threats to the survival of the species. Captive-breeding programs should be undertaken, because eradication of introduced mammalian predators is currently not possible on large islands.

Reproduction. No data on reproduction are available for this species.

Etymology. The species name (*lapierrae*) is a feminine genitive singular noun referring to the distribution of the species in the region of Lapierre, Artibonite Department, Haiti.

Remarks. Members of this species in museum collections were previously classified as *Panolopus curtissi diastatus*. Additional museum specimens catalogued as *P. curtissi diastatus* from this region should be examined for diagnostic traits to determine if they are additional representatives of *P. lapierrae* **sp. nov.**

Panolopus lapierrae **sp. nov.** was included in our genetic dataset; however, its placement within *Panolopus* has support values of 83% and 72% in our ML and Bayesian analyses, respectively. Based on our timetree (Fig. 4), *P. lapierrae* **sp. nov.** diverged from its closest relative 1.53 Ma, consistent with typical species of vertebrates (> 0.7 Ma; Hedges *et al*. 2015). *Panolopus lapierrae* **sp. nov.** was recognized as a distinct species by our ASAP analysis.

***Panolopus leionotus* (Schwartz 1964)**

Pale Neiba Forest Lizard
(Fig. 65–66)

Diploglossus costatus leionotus Schwartz, 1964:28. Holotype: MCZ R-77154, collected by Richard Thomas 15 km E. San Juan, San Juan province, Dominican Republic, on 14 August 1963 (18.732, -71.112; 345).
Celestus costatus leionotus—Schwartz & Henderson, 1988:95.
Celestus costatus leionotus—Schwartz & Henderson, 1991:367.
Celestus costatus leionotus—Hedges *et al.*, 2019:16.
Panolopus costatus leionotus—Schools & Hedges, 2021:230.

Material examined (n=20). DOMINICAN REPUBLIC. Azua. Hispaniola. AMNH 92796, D. C. Leber, 5 km S Padre las Casas, 13 August 1967. **Baoruco.** ANSP 38562–5, S. Blair Hedges, ca. 5 km N of Apolinar Perdomo, 25 May 1996; ANSP 38567–8, S. Blair Hedges, Patrick Parker, Kristin Nastase, and Renee Sharp, Loma Monte Bonito, 24 May 1996. **San Juan.** ANSP 38566, Richard Thomas, 1.6 mi NNE of El Azul, 2 August 1999; KU 225018–9, 15 km SE San Juan, 14 August 1963; MCZ R-77154, Richard Thomas, 15 km E. San Juan, 14 August 1963; SBH 266286, Richard Thomas, 1.6 mi. NNE El Azul, 2 August 1999. **Elias Piña.** ANSP 38573–7, Jennifer B. Pramuk, Richard Thomas, and S. Blair Hedges, 0.6 km NE of Rosa de la Piedra, 2 August 1999; SBH 266313, Jennifer B. Pramuk, Richard Thomas, S. Blair Hedges, 0.6 km NE Rosa de la Piedra, 3 August 1999; USNM 328752–3, Richard Thomas, S. Blair Hedges, and locals, 17 km N Cacique Enriquillo (31 km N of Los Pinos), 3 July 1986.

FIGURE 65. (A–F) *Panolopus leionotus* (MCZ R-77154, holotype), SVL 100 mm.

FIGURE 66. *Panolopus leionotus* (USNM 328752, SBH 161498), in life. From 17 km N Cacique Enriquillo (31 km N of Los Pinos), Elias Pina Province, Dominican Republic. Photo by SBH.

Diagnosis. *Panolopus leionotus* has (1) a dorsal pattern of absent/irregular dots/dots in series/dots in chevrons, (2) head markings absent, (3) markings in the longitudinal paramedian area absent/present, (4) dots arranged in bars in the lateral band present, (5) an adult SVL of 86.3–105 mm, (6) ventral scale rows, 84–101, (7) midbody scale rows, 35–40, (8) total lamellae on one hand, 43–48, (9) total strigae on ten scales, 191–266, (10) relative length of all digits on one hindlimb, 25.4–34.1 %, (11) relative distance between the angled subocular and mouth, 0.524–1.17 %, (12) relative eye length, 2.36–3.75 %, (13) relative forelimb length, 18.6–23.5 %, (14) relative ear width, 1.06–2.24 %, (15) relative rostral height, 1.79–2.36 %, (16) relative head length, 14.6–19.7 %, (17) relative mental width, 1.67–2.02 %, (18) relative postmental width, 2.43–3.18 %, (19) relative cloacal width, 8.03–8.69 %, (20) relative prefrontal width, 4.06–5.21 %, (21) relative largest supraocular width, 1.94–2.50 %, (22) relative longest finger length, 4.58–6.10 %, (23) relative distance between the ear and eye, 6.78–8.80 %, (24) relative head width, 67.3–82.9 %, (25) relative frontal width, 68.7–81.2 %, (26) relative nasal height, 0.971–1.18 %, (27) relative angled subocular height, 0.750–1.33 %, (28) relative distance between the eye and naris, 4.46–5.61 %, (29) relative canthal iii length, 1.55–1.89 %, (30) relative angled subocular width, 2.48–2.95 %, and (31) relative nasal length, 1.59–2.01 %. The species stem time is 0.74 Ma and the species crown time is 0.07 Ma (Fig. 4).

We distinguish *Panolopus leionotus* from the other species of *Panolopus* based on a complex of traits. From *Panolopus aenetergum*, we distinguish *P. leionotus* by the total lamellae on one hand (43–48 versus 40), the total strigae on ten scales (191–266 versus 267), the relative mental width (1.67–2.02 versus 1.63), the relative cloacal width (8.03–8.69 versus 7.60), the relative frontal width (68.7–81.2 versus 88.2), the relative distance between the eye and naris (4.46–5.61 versus 4.35), and the relative angled subocular width (2.48–2.95 versus 2.07). From *P. aporus*, we distinguish *P. leionotus* by the relative largest supraocular width (1.94–2.50 versus 2.74–3.62). From *P. chalcorhabdus*, we distinguish *P. leionotus* by the relative largest supraocular width (1.94–2.50 versus 2.52–2.86) and the relative width of canthal iii (1.55–1.89 versus 1.98–2.05). From *P. costatus*, we distinguish *P. leionotus* by the total lamellae on one hand (43–48 versus 49–58) and the relative frontal width (68.7–81.2 versus 56.2–67.4). From *P. curtissi*, we distinguish *P. leionotus* by the dots arranged in bars in the lateral areas (present versus absent), the adult SVL (86.3–105 versus 64.1–85.5), the total lamellae on one hand (43–48 versus 32–39), and the relative longest finger length (4.58–6.10 versus 3.59–4.54). From *P. diastatus*, we distinguish *P. leionotus* by the adult SVL (86.3–105 versus 66.1–83.7) and the total lamellae on one hand (43–48 versus 35–41). From *P. emys*, we distinguish *P. leionotus* by the relative angled subocular width (2.48–2.95 versus 2.12–2.20) and the relative nasal

width (1.59–2.01 versus 1.23–1.58). From *P. hylonomus*, we distinguish *P. leionotus* by the dots arranged in bars in the lateral areas (present versus absent), the adult SVL (86.3–105 versus 59.3–76.5), the relative largest supraocular width (1.94–2.50 versus 2.65–2.90), and the relative width of canthal iii (1.55–1.89 versus 1.95–2.03). From *P. lanceolatus* **sp. nov.**, we distinguish *P. leionotus* by the frontal width by the SVL (3.89–5.00 versus 3.48–3.84) (see Remarks). From *P. lapierrae* **sp. nov.**, we distinguish *P. leionotus* by the relative longest finger length (4.58–6.10 versus 4.49–4.55). From *P. marcanoi*, we distinguish *P. leionotus* by the head markings (absent versus present) and the adult SVL (86.3–105 versus 64.6–85.8). From *P. melanchrous*, we distinguish *P. leionotus* by the relative nasal height (0.971–1.18 versus 0.897–0.952). From *P. neiba*, we distinguish *P. leionotus* by the nasal height by the nasal width (1.47–1.80 versus 1.82–2.18) (see Remarks). From *P. nesobous*, we distinguish *P. leionotus* by the total lamellae on one hand (43–48 versus 50–59), the relative length of digits on one hindlimb (25.4–34.1 versus 35.1), the relative largest supraocular width (1.94–2.50 versus 2.85–3.11), the relative longest finger length (4.58–6.10 versus 6.19–6.33), the relative frontal width (68.7–81.2 versus 60.8–63.5), the relative distance between the eye and naris (4.46–5.61 versus 5.62–5.73), and the relative width of canthal iii (1.55–1.89 versus 2.01–2.12). From *P. oreistes*, we cannot distinguish *P. leionotus* based on our standard suite of characters (see Remarks). From *P. psychonothes*, we distinguish *P. leionotus* by the relative angled subocular width (2.48–2.95 versus 2.01–2.44). From *P. saonae*, we distinguish *P. leionotus* by the total lamellae on one hand (43–48 versus 40–42), the relative mental width (1.67–2.02 versus 1.52), the relative largest supraocular width (1.94–2.50 versus 2.77), the relative distance between the eye and naris (4.46–5.61 versus 6.43), the relative width of canthal iii (1.55–1.89 versus 1.99), and the relative angled subocular width (2.48–2.95 versus 2.31). From *P. semitaeniatus* **sp. nov.**, we distinguish *P. leionotus* by the SVL (86.3–105 versus 77.4–84.1), the relative rostral height (1.79–2.36 versus 2.41–2.63), the relative largest supraocular width (1.94–2.50 versus 2.59–3.32), the relative head width (67.3–82.9 versus 58.8–63.8), the relative angled subocular height (0.750–1.33 versus 0.654), and the relative nasal width (1.59–2.01 versus 1.51). From *P. unicolor* **sp. nov.**, we distinguish *P. leionotus* by the adult SVL (86.3–105 versus 67.6), the total strigae on ten scales (191–266 versus 144), the relative length of digits on one hindlimb (25.4–34.1 versus 36.8), the relative cloacal width (8.03–8.69 versus 7.61), the relative largest supraocular width (1.94–2.50 versus 3.12), the relative longest finger length (4.58–6.10 versus 6.65), and the relative frontal width (68.7–81.2 versus 58.2).

Description of holotype. MCZ R-77154. An adult male; SVL 100 mm; tail nearly cylindrical, broken in life midway, regenerated, 80.8 mm (80.8% SVL); axilla-to-groin distance 62.6 mm (62.6% SVL); forelimb length 17.9 mm (17.9% SVL); hindlimb length 27.1 mm (27.1% SVL); head length 16.3 mm (16.3% SVL); head width 12.0 mm (12.0% SVL); head width 73.6% head length; diameter of orbit 3.11 mm (3.11% SVL); horizontal diameter of ear opening 1.06 mm (1.06% SVL); vertical diameter of ear opening 1.48 mm (1.48% SVL); length of all toes on one foot 25.5 mm (25.5% SVL); shortest distance between angled subocular and lip 0.56 mm (0.560% SVL); shortest distance between the ocular and auricular openings 7.96 mm (7.96% SVL); longest finger length 5.00 mm (5.00% SVL); largest supraocular width 1.95 mm (1.95% SVL); cloacal width 8.45 mm (8.45% SVL); mental width 1.69 mm (1.69% SVL); postmental width 2.76 mm (2.76% SVL); prefrontal width 4.65 mm (4.65% SVL); frontal width 72.8% frontal length; nasal height 1.10 mm (1.10% SVL); angled subocular height 0.99 mm (0.990% SVL); shortest distance between the eye and naris 4.46 mm (4.46% SVL); canthal iii width 1.79 mm (1.79% SVL); angled subocular width 2.77 mm (2.77% SVL); nasal width 1.81 mm (1.81% SVL); rostral 1.79X as wide as high, barely visible from above, not in contact with nasals, in contact with 1st supralabial and anterior internasal (left)/(right); anterior internasals are narrower than posterior ones; frontonasals and prefrontal fused into a single large plate with an irregular posterior margin, much wider than long, bordered by posterior internasals, 1st loreals, canthal iii, 1st median oculars, and the frontal; frontal longer than wide; a pair of frontoparietals, separated by the posterior prolongation of the frontal and the interparietal plate; interparietal plate smaller than parietals and separating them, posteriorly touching the interoccipital, which is wider than long; parietal separated from supraoculars by 1st and 2nd temporals and frontoparietal (left)/(right); nasal single; nostril above suture between 1st and 2nd supralabials (left)/just posterior to suture between 1st and 2nd supralabials (right); 1 postnasal (left)/(right); 2 loreals (left)/(right); 1st loreal higher than wide (left)/(right), in contact with postnasal, posterior internasal, prefrontal/frontonasal complex, canthal iii, 2nd loreal, and 3rd–4th supralabials (left)/(right); 2nd loreal shorter than 1st, wider than high (left)/(right), excluded from contact with supraocular by canthal iii (left)/(right); final loreal posteriorly bordering the upper and lower preoculars (left)/(right); canthal iii wider than high (left)/(right), contacting 1st median ocular, anterior supraciliary, upper preocular, prefrontal/frontonasal complex, and 1st and 2nd loreals (left)/(right); 8 (left)/9 (right) median oculars, 1st contacting the prefrontal (left)/(right); 1 upper preocular (left)/(right); an irregular anterior supraciliary (left)/(right); 6 (left)/5 (right) lateral oculars; 5 temporals (left)/(right); 2 suboculars (left)/(right); posterior subocular large and

elongate (left)/(right); anterior subocular small (left)/(right); 9 supralabials (left)/(right), 6 to level below center of eye (left)/(right); 9 infralabials (left)/(right), 5 to level below center of eye (left)/(right); mental small, followed by a single, larger postmental; 4 pairs of enlarged chin shields; 1st pair in contact with one another; 2nd–4th pairs separated by 1–2 scales; 86 transverse rows of dorsal scales from interoccipital to base of tail; 91 transverse rows of ventral scales from mental to vent; 36 scales around midbody; 5 digits; finger lengths 3>4>2>5>1; 11 (left)/12 (right) lamellae under longest finger; 45 total lamellae on one hand; toe lengths 4>3>5>2>1; 17 (left)/16 (right) lamellae under longest toe; striate and keelless dorsal body and caudal scales; smooth to faintly striated ventral scales; 204 total strigae counted on ten scales.

Color (in alcohol): dorsal surface of head pale tan, patternless; lateral surfaces of head grading from pale tan to cream with darker brown eye masks; dorsal surfaces of the body are red-brown, patternless; dorsal surface of tail red-brown to yellow (on regenerated section), patternless; lateral areas slightly darker than body with some darker brown lines near the forelimb grading to yellow-cream; dorsal surfaces of the limbs are golden tan with darker brown mottling; lateral and ventral areas of the limbs fade to yellow-cream, patternless; ventral surfaces of the head, body, and tail are pale cream, patternless.

Variation. Several other specimens resemble the holotype in lacking a dorsal pattern. The majority of other specimens have irregular flecks or dots, dots arranged in chevrons, or dots occurring in series. All specimens have patternless head scales. The majority of specimens have markings in the longitudinal paramedian series, with only AMNH 92796 completely lacking any pattern in the longitudinal paramedian area. All specimens possess dots arranged in bars in the lateral band. Measurements and other morphological data for the holotype and other examined material are presented in Table 1.

Distribution. *Panolopus leionotus* occurs primarily in the Sierra de Neiba of central Hispaniola and adjacent areas at elevations of 320–1700 m (Fig. 49). Currently, it is known only from the Dominican Republic, but is found next to the border with Haiti and therefore is expected to occur in adjacent areas of that country.

Ecology and conservation. Many animals of this species were collected from under rocks during the day.

We consider the conservation status of *Panolopus leionotus* to be Least Concern, based on IUCN Redlist criteria (IUCN 2023). It is likely a common species tolerant of some habitat disturbance, based on what is known of most species of *Panolopus*. However, it faces a primary threat of habitat destruction resulting from deforestation. A secondary threat is predation from introduced mammals, including the mongoose and black rats. Studies are needed to determine the health and extent of remaining populations and better understand the threats to the survival of the species.

Reproduction. No data on reproduction are available for this species.

Etymology. The species name *leionotus* is derived from the Greek words *leios*, meaning "bald", and *notos*, meaning "back," referring to the distinctive patternless dorsum of this species.

Remarks. Previously a subspecies of *Panolopus costatus*, herein we elevate *P. leionotus* to a full species based on genetic and morphological differences. Additional museum specimens identified as *P. costatus* and *P. curtissi*, from this region of the island, should be examined to determine if they are additional members of *P. leionotus*.

Panolopus leionotus and *P. lanceolatus* **sp. nov.** cannot be morphologically separated based on our standard suite of characters; however, they can be separated by the frontal width divided by the SVL (3.89–5.00 [n=5] versus 3.48–3.84 [n=8]). *Panolopus leionotus* and *P. neiba* cannot be morphologically separated based on our standard suite of characters; however, they can be separated by the nasal height by the nasal width (1.47–1.80 [n=7] versus 1.82–2.18 [n=5]). *Panolopus leionotus* and *P. oreistes* cannot be distinguished based on our suite of morphological characters; however, both of these species are morphologically distinct from their respective closest relative (*P. semitaeniatus* **sp. nov.** and *P. costatus*, respectively). Additionally, *P. leionotus* and *P. oreistes* are genetically distinct (Fig. 3) and diverged 3.81 Ma (Fig. 4). Future studies should examine additional characters to morphologically diagnose *P. leionotus* and *P. oreistes*.

Panolopus leionotus is included in our genetic dataset and has significant support in both Bayesian and ML likelihood analyses at the crown node of the species and the stem node that places it as the closest relative to *P. semitaeniatus* **sp. nov.** Based on our timetree (Fig. 4), *P. leionotus* is separated from that species by 0.74 Ma, consistent with typical species of vertebrates (> 0.7 Ma; Hedges *et al*. 2015). We recognize *P. leionotus* as a distinct species based on the multiple morphological characters that separate it from *P. semitaeniatus* **sp. nov**. *Panolopus leionotus* also occurs in sympatry with *P. neiba*, with the two species being separated by 1.23 Ma. *Panolopus leionotus* was recovered as conspecific with *Panolopus neiba* and *Panolopus semitaeniatus* **sp. nov.** in our ASAP analysis.

***Panolopus marcanoi* (Schwartz & Incháustegui 1976)**
Pico Duarte Forest Lizard
(Fig. 67–68)

FIGURE 67. (A–F) *Panolopus marcanoi* (USNM 197299, holotype), SVL 73.0 mm.

Diploglossus marcanoi Schwartz & Incháustegui, 1976:242. Holotype: USNM 197299, collected by Sixto J. Incháustegui from Valle de Bao, Santiago Province, Dominican Republic, on 29 December 1972 (19.0833, -71.0333; 1800 m).
Celestus marcanoi—Schwartz & Henderson, 1988:99.
Celestus marcanoi—Schwartz & Henderson, 1991:376.

Celestus marcanoi—Powell *et al.*, 1999:105.
Panolopus marcanoi—Schools & Hedges, 2021:230,
Panolopus marcanoi—Landestoy *et al.*, 2022: 205.

Material examined (n=23). DOMINICAN REPUBLIC. Santiago. ANSP 38648, Richard Thomas, Herman Dominicia, and S. Blair Hedges, La Lagus, 3 August 1993; ANSP 38649, Richard Thomas, Herman Dominicia, and S. Blair Hedges, Loma los Baderos, east slope, 2 August 1993; ANSP 38650–62, Richard Thomas, Herman Dominicia, and S. Blair Hedges, Valle de Bao, 31 July 1993; KU 226551–4, Valle de Bao, Cordillera Central (road to Pico Duarte), 29 December 1971; SBH 193288–9, S. Blair Hedges, Richard Thomas, and Herman Dominicia, Valle de Bao, 31 July 1993; SBH 193293, S. Blair Hedges, Richard Thomas, and Herman Dominicia, Valle de Bao, 31 July 1993; USNM 197299, Sixto J. Incháustegui, Valle de Bao, Cordillera Central, 29 December 1972.

Diagnosis. *Panolopus marcanoi* has (1) a dorsal pattern of irregular dots/dots in chevrons, (2) head markings present, (3) markings in the longitudinal paramedian area present, (4) dots arranged in bars in the lateral band present, (5) an adult SVL of 64.6–85.8 mm, (6) ventral scale rows, 89–102, (7) midbody scale rows, 38–45, (8) total lamellae on one hand, 36–44, (9) total strigae on ten scales, 141–254, (10) relative length of all digits on one hindlimb, 26.3–31.9 %, (11) relative distance between the angled subocular and mouth, 0.451–0.755 %, (12) relative eye length, 3.03–3.93 %, (13) relative forelimb length, 19.9–23.6 %, (14) relative ear width, 0.936–2.25 %, (15) relative rostral height, 1.96–2.38 %, (16) relative head length, 15.7–19.9 %, (17) relative mental width, 1.75–2.33 %, (18) relative postmental width, 2.46–3.24 %, (19) relative cloacal width, 7.18–9.56 %, (20) relative prefrontal width, 4.19–5.19 %, (21) relative largest supraocular width, 2.47–3.33 %, (22) relative longest finger length, 4.75–6.68 %, (23) relative distance between the ear and eye, 7.02–8.81 %, (24) relative head width, 68.4–77.9 %, (25) relative frontal width, 59.0–73.0 %, (26) relative nasal height, 1.07–1.28 %, (27) relative angled subocular height, 0.505–0.793 %, (28) relative distance between the eye and naris, 4.68–5.82 %, (29) relative canthal iii length, 1.60–2.23 %, (30) relative angled subocular width, 2.19–3.14 %, and (31) relative nasal length, 1.64–1.96 %. The species stem time is 1.87 Ma and the species crown time is 0.07 Ma (Fig. 4).

We distinguish *Panolopus marcanoi* from the other species of *Panolopus* based on a complex of traits. From *Panolopus aenetergum*, we distinguish *P. marcanoi* by the head markings (present versus absent), the longitudinal paramedian lines (present versus absent), the ventral scale rows (89–102 versus 80–86), the midbody scale rows (38–45 versus 35–36), the total strigae on ten scales (141–254 versus 267), the relative mental width (1.75–2.33 versus 1.63), the relative prefrontal width (4.19–5.19 versus 4.15), the relative frontal width (59.0–73.0 versus 88.2), the relative angled subocular height (0.505–0.793 versus 1.08), the relative distance between the eye and naris (4.68–5.82 versus 4.35), and the relative angled subocular width (2.19–3.14 versus 2.07). From *P. aporus*, we distinguish *P. marcanoi* by the head markings (present versus absent). From *P. chalcorhabdus*, we distinguish *P. marcanoi* by the angled subocular width by the angled subocular height (3.37–5.36 versus 2.77–3.28) (see Remarks). From *P. costatus*, we distinguish *P. marcanoi* by the total lamellae on one hand (36–44 versus 49–58). From *P. curtissi*, we distinguish *P. marcanoi* by the dorsal pattern (irregular dots/dots in chevrons versus absent/irregular flecks), the head markings (present versus absent), the dots arranged in bars in the lateral areas (present versus absent), and the relative longest finger length (4.75–6.68 versus 3.59–4.54). From *P. diastatus*, we distinguish *P. marcanoi* by the dorsal pattern (irregular dots/dots in chevrons versus absent/irregular flecks), the head markings (present versus absent), and the longitudinal paramedian lines (present versus absent). From *P. emys*, we distinguish *P. marcanoi* by the dorsal pattern (irregular dots/dots in chevrons versus absent/irregular flecks), the head markings (present versus absent), the adult SVL (64.6–85.8 versus 99.0–113), and the relative nasal width (1.64–1.96 versus 1.23–1.58). From *P. hylonomus*, we distinguish *P. marcanoi* by the dorsal pattern (irregular dots/dots in chevrons versus absent/irregular flecks), the head markings (present versus absent), and the dots arranged in bars in the lateral areas (present versus absent). From *P. lanceolatus* **sp. nov.**, we distinguish *P. marcanoi* by the relative nasal height (1.07–1.28 versus 0.904–1.06). From *P. lapierrae* **sp. nov.**, we distinguish *P. marcanoi* by the relative longest finger length (4.75–6.68 versus 4.49–4.55), the relative frontal width (59.0–73.0 versus 77.6–79.0), and the relative angled subocular height (0.505–0.793 versus 0.838–0.978). From *P. leionotus*, we distinguish *P. marcanoi* by the head markings (present versus absent), and the adult SVL (64.6–85.8 versus 86.3–105). From *P. melanchrous*, we distinguish *P. marcanoi* by the adult SVL (64.6–85.8 versus 93.2–124), the total lamellae on one hand (36–44 versus 47–58), and the relative nasal height (1.07–1.28 versus 0.897–0.952). From *P. neiba*, we distinguish *P. marcanoi* by the head markings (present versus absent) and the total lamellae on one hand (36–44 versus 45–49). From *P. nesobous*, we distinguish *P. marcanoi* by the head markings (present versus absent), the total lamellae on one hand

(36–44 versus 50–59), and the relative length of digits on one hindlimb (26.3–31.9 versus 35.1). From *P. oreistes*, we distinguish *P. marcanoi* by the relative nasal height (1.07–1.28 versus 0.878–1.06). From *P. psychonothes*, we distinguish *P. marcanoi* by the relative angled subocular height (0.505–0.793 versus 0.803–0.952). From *P. saonae*, we distinguish *P. marcanoi* by the dorsal pattern (irregular dots/dots in chevrons versus absent), the head markings (present versus absent), the longitudinal paramedian lines (present versus absent), the adult SVL (64.6–85.8 versus 90.9–98.3), the relative mental width (1.75–2.33 versus 1.52), the relative postmental width (2.46–3.24 versus 2.43), the relative prefrontal width (4.19–5.19 versus 4.14), the relative nasal height (1.07–1.28 versus 1.01), the relative angled subocular height (0.505–0.793 versus 0.847), and the relative distance between the eye and naris (4.68–5.82 versus 6.43). From *P. semitaeniatus* **sp. nov.**, we distinguish *P. marcanoi* by the relative rostral height (1.96–2.38 versus 2.41–2.63), the relative head width (68.4–77.9 versus 58.8–63.8), the relative distance between the eye and naris (4.68–5.82 versus 4.61), and the relative nasal width (1.64–1.96 versus 1.51). From *P. unicolor* **sp. nov.**, we distinguish *P. marcanoi* by the dorsal pattern (irregular dots/dots in chevrons versus absent), the head markings (present versus absent), the total lamellae on one hand (36–44 versus 48), the relative length of digits on one hindlimb (26.3–31.9 versus 36.8), the relative mental width (1.75–2.33 versus 1.73), the relative frontal width (59.0–73.0 versus 58.2), the relative angled subocular height (0.505–0.793 versus 0.814), and the relative nasal width (1.64–1.96 versus 2.00).

Description of holotype. USNM 197299. An adult male; SVL 73.0 mm; tail nearly cylindrical, broken in life midway, regenerated, 77.8 mm (107% SVL); axilla-to-groin distance 42.2 mm (57.8% SVL); forelimb length 16.9 mm (23.2% SVL); hindlimb length 24.7 mm (33.8% SVL); head length 13.9 mm (19.0% SVL); head width 10.4 mm (14.2% SVL); head width 74.8% head length; diameter of orbit 2.87 mm (3.93% SVL); horizontal diameter of ear opening 1.64 mm (2.25% SVL); vertical diameter of ear opening 1.52 mm (2.08% SVL); length of all toes on one foot 23.3 mm (31.9% SVL); shortest distance between angled subocular and lip 0.48 mm (0.658% SVL); shortest distance between the ocular and auricular openings 6.43 mm (8.81% SVL); longest finger length 4.88 mm (6.68% SVL); largest supraocular width 2.32 mm (3.18% SVL); cloacal width 6.98 mm (9.56% SVL); postmental width 2.05 mm (2.81% SVL); prefrontal width 3.79 mm (5.19% SVL); frontal width 72.5% frontal length; nasal height 0.84 mm (1.15% SVL); angled subocular height 0.56 mm (0.767% SVL); shortest distance between the eye and naris 3.79 mm (5.19% SVL); canthal iii width 1.54 mm (2.11% SVL); angled subocular width 2.29 mm (3.14% SVL); nasal width 1.23 mm (1.68% SVL); rostral 2.30X as wide as high, visible from above, not in contact with nasals, in contact with 1st supralabial and anterior internasal (left)/(right); anterior internasals are narrower than posterior ones; frontonasals and prefrontal fused into a single large plate with an irregular posterior margin, much wider than long, bordered by posterior internasals, 1st loreals, 1st and 2nd median oculars, and the frontal; frontal longer than wide; a pair of frontoparietals, separated by the posterior prolongation of the frontal and the interparietal plate; interparietal plate smaller than parietals and separating them, posteriorly touching the interoccipital, which is wider than long; parietal separated from supraoculars by 1st and 2nd temporals and frontoparietal (left)/(right); nasal single; nostril above suture between 1st and 2nd supralabials (left)/(right); 1 postnasal (left)/(right); 2 loreals (left)/(right); 1st loreal higher than wide (left)/(right), in contact with postnasal, posterior internasal, prefrontal/frontonasal complex, 1st median ocular, canthal iii, 2nd loreal, and 3rd–4th supralabials (left)/(right); 2nd loreal shorter than 1st, approximately as high as wide (left)/(right), excluded from contact with supraocular by canthal iii (left)/(right); 2nd loreal posteriorly bordering the lower preocular (left)/(right); canthal iii wider than high (left)/(right), contacting 1st median ocular, anterior supraciliary, lower preocular, and 1st and 2nd loreals (left)/(right); 10 median oculars (left)/(right), 1st and 2nd contacting the prefrontal (left)/(right); an irregular anterior supraciliary (left)/(right); 6 lateral oculars (left)/(right); 5 temporals (left)/(right); 2 suboculars (left)/(right); posterior subocular large and elongate (left)/(right); anterior subocular small (left)/(right); 10 (left)/9 (right) supralabials, 6 to level below center of eye (left)/(right); 9 infralabials (left)/(right), 6 to level below center of eye (left)/(right); mental small, followed by a single, larger postmental; 4 pairs of enlarged chin shields; 1st pair in contact with one another anteriorly, posteriorly separated by one scale; 2nd–4th pairs separated by 1–3 scales; 96 transverse rows of dorsal scales from interoccipital to base of tail; 96 transverse rows of ventral scales from mental to vent; 40 scales around midbody; 5 digits; finger lengths 3>4>2>5>1; 11 lamellae under longest finger (left)/(right); 44 total lamellae on one hand; toe lengths 4>3>5>2>1; 16 (right) lamellae under longest toe; keelless and striate dorsal body and caudal scales; smooth ventral scales; 173 total strigae counted on ten scales.

Color (in alcohol): dorsal surface of head brown-gray with irregular dark brown spots; lateral surfaces of head grading from brown-gray to muted brown-gray with darker brown eye masks and other darker brown areas on

the labial scales and sides of neck; dorsal surfaces of the body are brown-gray with many markings vaguely in longitudinal paramedian series that become more random posteriorly; dorsal surface of tail brown-gray with many markings vaguely continuing the longitudinal paramedian series; lateral areas grade from brown-gray to muted brown-gray with dots in vertical lines; dorsal surfaces of the limbs are dark brown with paler gray mottling; lateral and ventral areas of the limbs fade to muted gray-brown; ventral surfaces of the head, body, and tail are muted gray-brown with a few darker flecks under the chest and tail.

Variation. The material examined resembled the holotype in dorsal pattern. All specimens examined have a heavy pattern of either irregular dots or dots arranged into broken chevrons. All specimens examined have large, irregular dark markings on their head whereas several specimens also possess darker outlines on their head scale borders. All examined material possess markings in the longitudinal paramedian area in the form of complete or broken longitudinal paramedian lines. Of the specimens examined, all have dots arranged in bars in the lateral band. Measurements and other morphological data for the holotype and other examined material are presented in Table 1.

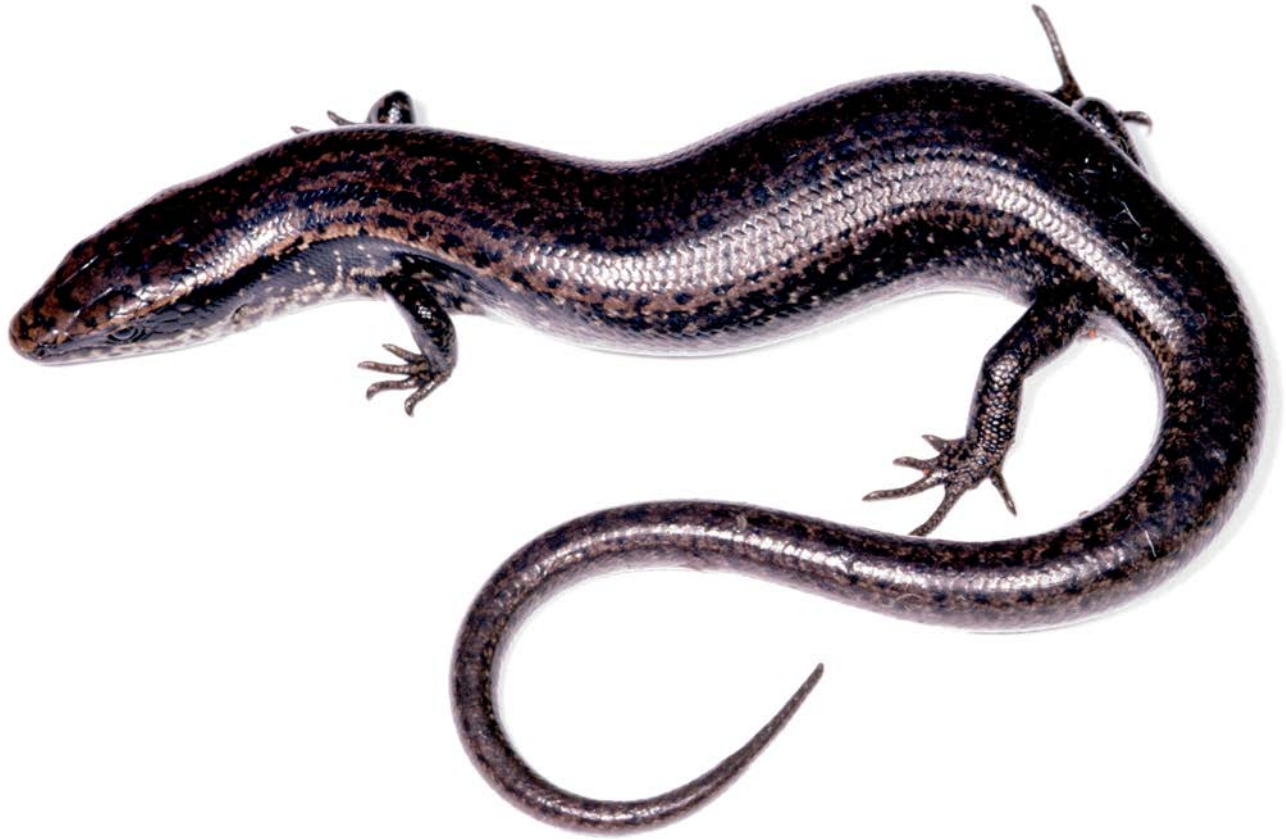

FIGURE 68. *Panolopus marcanoi* (ANSP 38662, SBH 193346), SVL 73.5 mm, in life. From Valle de Bao, Santiago Province, Dominican Republic. Photograph by SBH.

Distribution. *Panolopus marcanoi* is distributed in the Cordillera Central of the Dominican Republic where it is found at 1500–1800 m (Fig. 50).

Ecology and conservation. The type series of this species was collected in a high-elevation river valley where two creeks were present and the soil was relatively dry. They were collected from under rocks in the early morning, when they were close to immobile, presumably because of the cool temperatures (frost present on the ground). Schwartz & Incháustegui (1976) noted that Valle de Bao (the type locality of *Panolopus marcanoi*) is less favorable for diurnal activity than other areas of the Cordillera Central. These lizards were relatively common (approximately one lizard collected every ten rocks).

The IUCN Redlist (IUCN 2023) considers the conservation status of *Panolopus marcanoi* to be of Least Concern, because "although the distribution is limited (with an extent of occurrence of 120 km^2), there are no current major threats, and its distribution occurs in one protected area." Studies are needed to determine the health of remaining populations and threats to the survival of the species.

Reproduction. No data on reproduction are available for this species.

Etymology. The species name refers to Dr. Eugenio de Jesús Marcano F., the organizer of the two expeditions that led to the discovery of the species.

Remarks. *Panolopus marcanoi* and *P. chalcorhabdus* cannot be morphologically separated based on our standard suite of characters; however, they can be separated by the angled subocular width divided by the angled subocular height (3.37–5.36 [n=18] versus 2.77–3.28 [n=5]).

Panolopus marcanoi was included in our genetic dataset and has significant support in our ML and Bayesian analyses at the crown node. However, the stem node placing *P. marcanoi* within *Panolopus* has support values of 76% and 57% in our ML and Bayesian analyses, respectively. Schools *et al.* (2022) used genomic data to place *P. marcanoi* outside of *P. unicolor* **sp. nov.**, *P. diastatus*, *P. leionotus*, *P. marcanoi*, *P. neiba*, and *P. semitaeniatus* **sp. nov.** with support values of 94% and 92% in their ML and Bayesian analyses, respectively, at the stem node. Based on our timetree (Fig. 4), *P. marcanoi* diverged from its closest relative 1.87 Ma, consistent with typical species of vertebrates (> 0.7 Ma; Hedges *et al.* 2015). *Panolopus marcanoi* was recognized as a distinct species by our ASAP analysis.

***Panolopus melanchrous* (Schwartz 1964)**
Hispaniolan Chevronate Forest Lizard
(Fig. 69)

Diploglossus costatus melanchrous Schwartz, 1964:34. Holotype: MCZ R-77157, collected by Richard Thomas from 8 km E. Gaspar Hernandez, Espaillat province, Dominican Republic, on 18 June 1963 (19.631, -70.220; 17 m).
Celestus costatus melanchrous—Schwartz & Henderson, 1991:367.
Celestus costatus melanchrous—Hedges *et al.*, 2019:16.
Celestus costatus melanchrous—Schools & Hedges, 2021:230.

Material examined (n=80). DOMINICAN REPUBLIC. AMNH 40945, 40947–8, 40950–4, 40956–8, 40960–1, Gladwyn K. Noble, La Bracita [=Los Bracitos], 20 August 1922; AMNH 40967, 40969–72, Gladwyn K. Noble, La Bracita [=Los Bracitos], August 1922. **El Seibo.** USNM 66678, Guarabo, 24 November 1923; USNM 66679, Jovero (= Miches), 30 November 1923**. Espaillat.** KU 225232, 10 mi N San Victor, 1971; MCZ R-77157, Richard Thomas, 8 km E. Gaspar Hernandez, 18 June 1963. **Hato Mayor.** KU 225255, 2.3 mi N El Valle, 1971; USNM 65780, Las Canitas, 23 February 1923. **La Altagracia.** KU 225261, 225263, 225266, Playa El Coco, 46 km N Higuey, 1969. **La Vega.** AMNH 40975, Gladwyn K. Noble, Paso Bajito, 3 September 1922; KU 225028, 7 km E Paso Bajito, 10 July 1963; KU 225313–4, 12 km NE Jarabacoa, 1964; KU 225315, 4 km S La Vega, 1968; KU 225318, 1.5 km W Jayaco, 1973. **Puerto Plata.** KU 225021, 3 km NE Sosua, 15 October 1963; KU 225298–300, 7.6 mi NE Sanchez, 1971; KU 225311, 5.1 mi NW El Limon, 1971; KU 225321, 0.25 km NW Sabaneta de Yasica, 1973. **Samaná.** AMNH 38378–85, William G. Hassler, Samaná, 1929; AMNH 39361, William G. Hassler, Roja Cabo, 18 November 1929; AMNH 39876, William G. Hassler, Samaná, November–December 1929; AMNH 40231, William G. Hassler, Laguna, November 1929; AMNH 40258, 40260, 40263, 40265–6, 40272, 44745–52, 44825, 44827–8, William G. Hassler, Samaná, October 1929–December 1929; AMNH 40393–5, 40397–01, 40403, 40405, William G. Hassler, Samaná, October 1929; AMNH 40981, Samaná, May 1923; USNM 62361, Sanchez, 11 August 1919. **Santiago.** KU 225348, 0.5 mi SE Pedro Garcia, 1971.

Diagnosis. *Panolopus melanchrous* has (1) a dorsal pattern of absent/irregular flecks/irregular dots/dots in chevrons, (2) head markings absent/present, (3) markings in the longitudinal paramedian area present, (4) dots arranged in bars in the lateral band present, (5) an adult SVL of 93.2–124 mm, (6) ventral scale rows, 89–113, (7) midbody scale rows, 35–42, (8) total lamellae on one hand, 47–58, (9) total strigae on ten scales, 168–413, (10) relative length of all digits on one hindlimb, 30.7–41.3 %, (11) relative distance between the angled subocular and mouth, 0.442–0.883 %, (12) relative eye length, 2.78–3.97 %, (13) relative forelimb length, 19.5–27.6 %, (14) relative ear width, 0.569–2.39 %, (15) relative rostral height, 1.40–2.75 %, (16) relative head length, 15.2–22.5 %, (17) relative mental width, 1.33–2.06 %, (18) relative postmental width, 2.71–3.38 %, (19) relative cloacal width, 7.61–9.20 %, (20) relative prefrontal width, 4.21–5.06 %, (21) relative largest supraocular width, 2.39–3.26 %, (22) relative longest finger length, 5.76–7.09 %, (23) relative distance between the ear and eye, 6.70–9.14 %, (24)

relative head width, 68.3–83.6 %, (25) relative frontal width, 61.3–71.4 %, (26) relative nasal height, 0.897–0.952 %, (27) relative angled subocular height, 0.680–0.856 %, (28) relative distance between the eye and naris, 4.89–5.59 %, (29) relative canthal iii length, 1.67–1.94 %, (30) relative angled subocular width, 2.28–2.82 %, and (31) relative nasal length, 1.44–2.09 %. No genetic data are available to estimate the species stem or crown time.

We distinguish *Panolopus melanchrous* from the other species of *Panolopus* based on a complex of traits. From *Panolopus aenetergum*, we distinguish *P. melanchrous* by the longitudinal paramedian lines (present versus absent), the adult SVL (93.2–124 versus 83.0–92.0), the ventral scale rows (89–113 versus 80–86), the total lamellae on one hand (47–58 versus 40), the relative length of digits on one hindlimb (30.7–41.3 versus 26.8), the relative postmental width (2.71–3.38 versus 2.62), the relative cloacal width (7.61–9.20 versus 7.60), the relative prefrontal width (4.21–5.06 versus 4.15), the relative longest finger length (5.76–7.09 versus 4.83), the relative frontal width (61.3–71.4 versus 88.2), the relative nasal height (0.897–0.952 versus 1.15), the relative angled subocular height (0.680–0.856 versus 1.08), the relative distance between the eye and naris (4.89–5.59 versus 4.35), and the relative angled subocular width (2.28–2.82 versus 2.07). From *P. aporus*, we distinguish *P. melanchrous* by the relative longest finger length (5.76–7.09 versus 4.57–5.72) and the relative nasal height (0.897–0.952 versus 1.08–1.23). From *P. chalcorhabdus*, we distinguish *P. melanchrous* by the relative width of canthal iii (1.67–1.94 versus 1.98–2.05). From *P. costatus*, we distinguish *P. melanchrous* by the relative nasal height (0.897–0.952 versus 1.02–1.28). From *P. curtissi*, we distinguish *P. melanchrous* by the dots arranged in bars in the lateral areas (present versus absent), the adult SVL (93.2–124 versus 64.1–85.5), the total lamellae on one hand (47–58 versus 32–39), the relative length of digits on one hindlimb (30.7–41.3 versus 20.8–28.1), the relative longest finger length (5.76–7.09 versus 3.59–4.54), and the relative nasal height (0.897–0.952 versus 1.04–1.25). From *P. diastatus*, we distinguish *P. melanchrous* by the longitudinal paramedian lines (present versus absent), the adult SVL (93.2–124 versus 66.1–83.7), the total lamellae on one hand (47–58 versus 35–41), the relative length of digits on one hindlimb (30.7–41.3 versus 21.5–27.4), and the relative longest finger length (5.76–7.09 versus 3.48–4.87). From *P. emys*, we distinguish *P. melanchrous* by the relative nasal height (0.897–0.952 versus 0.963–1.10) and the relative angled subocular width (2.28–2.82 versus 2.12–2.20). From *P. hylonomus*, we distinguish *P. melanchrous* by the dots arranged in bars in the lateral areas (present versus absent), the adult SVL (93.2–124 versus 59.3–76.5), the relative length of digits on one hindlimb (30.7–41.3 versus 22.8–28.2), the relative longest finger length (5.76–7.09 versus 4.47–5.27), the relative nasal height (0.897–0.952 versus 0.961–1.37), and the relative width of canthal iii (1.67–1.94 versus 1.95–2.03). From *P. lanceolatus* **sp. nov.**, we distinguish *P. melanchrous* by the relative postmental width (2.71–3.38 versus 2.36–2.66). From *P. lapierrae* **sp. nov.**, we distinguish *P. melanchrous* by the adult SVL (93.2–124 versus 72.6–88.3), the relative longest finger length (5.76–7.09 versus 4.49–4.55), the relative frontal width (61.3–71.4 versus 77.6–79.0), and the relative nasal height (0.897–0.952 versus 1.06–1.09). From *P. leionotus*, we distinguish *P. melanchrous* by the relative nasal height (0.897–0.952 versus 0.971–1.18). From *P. marcanoi*, we distinguish *P. melanchrous* by the adult SVL (93.2–124 versus 64.6–85.8), the total lamellae on one hand (47–58 versus 36–44), and the relative nasal height (0.897–0.952 versus 1.07–1.28). From *P. neiba*, we distinguish *P. melanchrous* by the relative nasal height (0.897–0.952 versus 0.963–1.08). From *P. nesobous*, we distinguish *P. melanchrous* by the relative nasal height (0.897–0.952 versus 1.12–1.14), the relative distance between the eye and naris (4.89–5.59 versus 5.62–5.73), and the relative width of canthal iii (1.67–1.94 versus 2.01–2.12). From *P. oreistes*, we cannot distinguish *P. melanchrous* based on our standard suite of characters (see Remarks). From *P. psychonothes*, we distinguish *P. melanchrous* by the total lamellae on one hand (47–58 versus 37–44) and the relative nasal height (0.897–0.952 versus 1.12–1.32). From *P. saonae*, we distinguish *P. melanchrous* the longitudinal paramedian lines (present versus absent), the total lamellae on one hand (47–58 versus 40–42), the relative length of digits on one hindlimb (30.7–41.3 versus 26.5–29.8), the relative postmental width (2.71–3.38 versus 2.43), the relative prefrontal width (4.21–5.06 versus 4.14), the relative longest finger length (5.76–7.09 versus 5.01), the relative frontal width (61.3–71.4 versus 72.5), the relative nasal height (0.897–0.952 versus 1.01), the relative distance between the eye and naris (4.89–5.59 versus 6.43), and the relative width of canthal iii (1.67–1.94 versus 1.99). From *P. semitaeniatus* **sp. nov.**, we distinguish *P. melanchrous* by the SVL (93.2–124 versus 77.4–84.1), the total lamellae on one hand (47–58 versus 34–46), the relative head width (68.3–83.6 versus 58.8–63.8), the relative nasal height (0.897–0.952 versus 1.08), the relative angled subocular height (0.680–0.856 versus 0.654), and the relative distance between the eye and naris (4.89–5.59 versus 4.61). From *P. unicolor* **sp. nov.**, we distinguish *P. melanchrous* by the adult SVL (93.2–124 versus 67.6), the total strigae on ten scales (168–413 versus 144), the relative frontal width (61.3–71.4 versus 58.2), the relative nasal height (0.897–0.952 versus 1.15), and the relative angled subocular width (2.28–2.82 versus 2.90).

FIGURE 69. (A–F) *Panolopus melanchrous* (MCZ R-77157, holotype), SVL 95.9 mm.

Description of holotype. MCZ R-77157. An adult; SVL 95.9 mm; tail slightly laterally compressed,136 mm (142% SVL); axilla-to-groin distance 53.7 mm (56.0% SVL); forelimb length 23.4 mm (24.4% SVL); hindlimb length 34.3 mm (35.8% SVL); head length 18.0 mm (18.8% SVL); head width 12.3 mm (12.8% SVL); head width 68.3% head length; diameter of orbit 3.34 mm (3.48% SVL); horizontal diameter of ear opening 1.15 mm (1.20% SVL); vertical diameter of ear opening 1.40 mm (1.46% SVL); length of all toes on one foot 35.5 mm (37.0% SVL); shortest distance between angled subocular and lip 0.69 mm (0.719% SVL); shortest distance between the ocular and auricular openings 8.41 mm (8.77% SVL); longest finger length 6.80 mm (7.09% SVL); largest supraocular width 2.44 mm (2.54% SVL); cloacal width 8.82 mm (9.20% SVL); mental width 1.90 mm (1.98% SVL); postmental width 2.68 mm (2.79% SVL); prefrontal width 4.48 mm (4.67% SVL); frontal width 64.3% frontal length; nasal height 0.90 mm (0.938% SVL); angled subocular height 0.70 mm (0.730% SVL); shortest distance between the eye and naris 5.36 mm (5.59% SVL); canthal iii width 1.77 mm (1.85% SVL); angled subocular width 2.36 mm (2.46% SVL); nasal width 2.00 mm (2.09% SVL); rostral 2.10X as wide as high, visible from above, not in contact with nasals, in contact with 1st supralabial and anterior internasal (left)/(right); anterior internasals are narrower than posterior ones; frontonasals and prefrontal fused into a single large plate with a concave posterior margin, much wider than long, bordered by posterior internasals, 1st loreals, 1st (and 2nd on the left) median oculars, and the frontal; frontal longer than wide; a pair of frontoparietals, separated by the posterior prolongation of the frontal and the interparietal plate; interparietal plate smaller than parietals and separating them, posteriorly touching the interoccipital, which is wider than long; parietal separated from supraoculars by 1st and 2nd temporals and frontoparietal (left)/(right); nasal single; nostril above suture between 1st and 2nd supralabials (left)/(right); 1 postnasal (left)/(right); 2 loreals (left)/(right); 1st loreal higher than wide (left)/(right), in contact with postnasal, posterior internasal, prefrontal/frontonasal complex, 1st median ocular, canthal iii, 2nd loreal, and 3rd–4th supralabial (left)/(right); 2nd loreal shorter than 1st, approximately as high as wide (left)/(right), excluded from contact with supraocular by canthal iii (left)/(right); final loreal posteriorly bordering the upper and lower preoculars (left)/(right); canthal iii wider than high (left)/(right), contacting 1st median ocular, anterior supraciliary, upper preocular, and 1st and 2nd loreals (left)/(right); 9 (left)/10 (right) median oculars, 1st and 2nd contacting the prefrontal (left)/1st (right); 1 upper preocular (left)/(right); an irregular anterior supraciliary (left)/(right); 6 lateral oculars (left)/(right); 5 temporals (left)/(right); 2 suboculars (left)/(right); posterior subocular large and elongate (left)/(right); anterior subocular small (left)/(right); 10 supralabials (left)/(right), 6 to level below center of eye (left)/(right); 11 (left)/10 (right) infralabials, 6 to level below center of eye (left)/(right); mental small, followed by a single, larger postmental; 4 pairs of enlarged chin shields, followed by 1 pair of reduced chin shields; 1st pair in contact with one another; 2nd–5th pairs separated by 1–5 scales; 90 transverse rows of dorsal scales from interoccipital to base of tail; 97 transverse rows of ventral scales from mental to vent; 38 scales around midbody; 5 digits; finger lengths 3>4>2>5>1; 13 lamellae under longest finger (left)/(right); 51 total lamellae on one hand; toe lengths 4>3>2>5>1; 18 lamellae under longest toe (left)/(right); dorsal body and caudal scales striate with a faint median keel; striate ventral scales; 216 total strigae counted on ten scales.

Color (in alcohol): dorsal surface of head medium brown with several darker brown spots; lateral surfaces of head grading from medium brown to cream with darker brown eye masks; dorsal surfaces of the body are medium brown with darker brown dots in longitudinal paramedian series and smalls dots continuing down the back in broken chevrons; dorsal surface of tail same as the body; lateral areas grade from dark brown to cream with rows of darker brown and off-white dots in bars; dorsal surfaces of the limbs are medium brown with darker brown mottling; lateral and ventral areas of the limbs grading from medium brown to cream, patternless; ventral surfaces of the head, body, and tail are cream, patternless.

Variation. Measurements and other morphological data for the holotype and other examined material are presented in Table 1.

Distribution. *Panolopus melanchrous* is distributed in the northeastern portion of Hispaniola at elevations of 0–690 m (Fig. 49).

Ecology and conservation. No ecological data are associated with this species. We consider the conservation status of *Panolopus melanchrous* to be Least Concern, based on IUCN Redlist criteria (IUCN 2023). It is likely a common species tolerant of some habitat disturbance, based on what is known of most species of *Panolopus*. However, it faces a primary threat of habitat destruction resulting from deforestation. A secondary threat is predation from introduced mammals, including the mongoose and black rats. Studies are needed to determine the health and extent of remaining populations and better understand the threats to the survival of the species.

Reproduction. No data on reproduction are available for this species.

Etymology. Schwartz (1964) did not give the etymology of the species name (*melanchrous*), but it likely refers to the unique dark dorsal chevron-shaped crossbands of this species.

Remarks. *Panolopus melanchrous* and *P. oreistes* cannot be distinguished based on our suite of morphological characters and future studies should examine additional characters to morphologically diagnose *P. melanchrous* and *P. oreistes*.

Prior to this work, *Panolopus melanchrous* was regarded to be a widely distributed subspecies of *P. costatus*. Several museum specimens that were identified as *P. melanchrous*, including MCZ R-126743 and MCZ R-186653 (both members of the genus *Comptus*), were misidentified. Further studies should examine additional museum material that has been identified as *P. melanchrous* to confirm its correct designation. *Panolopus melanchrous* is not included in our genetic dataset and future studies should be conducted using genetic or genomic data from this species.

Panolopus neiba **(Schwartz 1964)**

Dark Neiba Forest Lizard
(Fig. 70)

Diploglossus costatus neiba Schwartz, 1964:30. Holotype: MCZ R-77155, collected by Richard Thomas from 19 km SW Hondo Valle, Elías Piña province, Dominican Republic, on 11 August 1963 (18.682, -71.788; 1,891 m).
Celestus costatus neiba—Schwartz & Henderson, 1988:95.
Celestus costatus neiba—Schwartz & Henderson, 1991:367.
Celestus costatus neiba—Hedges *et al.*, 2019:16.
Celestus costatus neiba—Schools & Hedges, 2021:230.

Material examined (n=27). DOMINICAN REPUBLIC. San Rafael. Hispaniola. AMNH 92797, Richard Thomas, 15 km SW Elías Piña, 13 August 1963; MCZ R-77155, Richard Thomas, 19 km SW Hondo Valle, 11 August 1963. **Independencia.** ANSP 38579, S. Blair Hedges, Matthew Heinicke, Eladio Fernandez, Andreas Schubert, ca. 7 km W by road Los Pinos, 24 August 2005; KU 225353–4, Sabana Real, 0.7 mi W, 17.7 mi N La Descubierta, 6 September 1971; KU 225356–8, Sabana Real, 14 km N Los Pinos, 25 July 1975; USNM 328763, S. Blair Hedges and Richard Thomas, 9 km N of Cacique Enriquillo, 3 July 1986; USNM 328764, Richard Thomas and S. Blair Hedges, 7 km N of Cacique Enriquillo, 4 July 1986; USNM 328765, Richard Thomas and S. Blair Hedges, 6.2 km N, 4.0 km W (airline) of La Descubierta, 29 August 1984. **Elías Piña.** KU 79826, 15 km S Comendador, 17 August 1963; KU 225030–1, 14 km SW Hondo Valle, 11 August 1963; USNM 328745–8, S. Blair Hedges and Richard Thomas, ca. 24 km N of Los Pinos, 29 August 1984; USNM 328749–51, S. Blair Hedges and Richard Thomas, ca. 27 km N of Los Pinos, 29 August 1984; USNM 328754–6, Richard Thomas S. Blair Hedges, and locals, 17 km N of Cacique Enriquillo, 3 July 1986; USNM 328759, S. Blair Hedges and Richard Thomas, 13 km N of Cacique Enriquillo, 2 July 1986. **Baoruco.** MCZ R-171776–7, G. Flores and locals, Alto de la Pena, stream just off the path from El Aguacate (La Venta) to Sabana del Silencio, 17 July 1985.

Diagnosis. *Panolopus neiba* has (1) a dorsal pattern of irregular flecks/dots in chevrons, (2) head markings absent, (3) markings in the longitudinal paramedian area absent/present, (4) dots arranged in bars in the lateral band present, (5) an adult SVL of 77.9–102 mm, (6) ventral scale rows, 84–102, (7) midbody scale rows, 35–43, (8) total lamellae on one hand, 45–49, (9) total strigae on ten scales, 179–239, (10) relative length of all digits on one hindlimb, 29.5–36.6 %, (11) relative distance between the angled subocular and mouth, 0.670–0.747 %, (12) relative eye length, 2.95–3.93 %, (13) relative forelimb length, 19.8–25.7 %, (14) relative ear width, 0.966–1.97 %, (15) relative rostral height, 1.75–2.23 %, (16) relative head length, 15.4–19.8 %, (17) relative mental width, 1.66–2.36 %, (18) relative postmental width, 2.27–3.29 %, (19) relative cloacal width, 7.58–8.77 %, (20) relative prefrontal width, 4.41–5.49 %, (21) relative largest supraocular width, 2.06–3.04 %, (22) relative longest finger length, 5.61–6.66 %, (23) relative distance between the ear and eye, 6.69–8.66 %, (24) relative head width, 67.9–78.4 %, (25) relative frontal width, 63.3–74.0 %, (26) relative nasal height, 0.963–1.08 %, (27) relative angled subocular height, 0.713–0.885 %, (28) relative distance between the eye and naris, 4.51–5.01 %, (29) relative canthal iii length, 1.51–1.95 %, (30) relative angled subocular width, 2.34–2.83 %, and (31) relative nasal length, 1.67–1.92 %. The species stem time is 1.23 Ma and the species crown time is 0.40 Ma (Fig. 4).

FIGURE 70. (A–F) *Panolopus neiba* (MCZ R-77155, holotype), SVL 88.4 mm.

We distinguish *Panolopus neiba* from the other species of *Panolopus* based on a complex of traits. From *P. aenetergum*, we distinguish *P. neiba* by the dorsal pattern (irregular flecks/dots in chevrons versus irregular dots), the total lamellae on one hand (45–49 versus 40), the total strigae on ten scales (179–239 versus 267), the relative length of digits on one hindlimb (29.5–36.6 versus 26.8), the relative mental width (1.66–2.36 versus 1.63), the relative prefrontal width (4.41–5.49 versus 4.15), the relative longest finger length (5.61–6.66 versus 4.83), the relative frontal width (63.3–74.0 versus 88.2), the relative nasal height (0.963–1.08 versus 1.15), the relative angled subocular height (0.713–0.885 versus 1.08), the relative distance between the eye and naris (4.51–5.01 versus 4.35),

and the relative angled subocular width (2.34–2.83 versus 2.07). From *P. aporus*, we distinguish *P. neiba* by the relative distance between angled subocular and mouth (0.670–0.747 versus 0.441–0.669). From *P. chalcorhabdus*, we distinguish *P. neiba* by the relative width of canthal iii (1.51–1.95 versus 1.98–2.05). From *P. costatus*, we distinguish *P. neiba* by the relative distance between the eye and naris (4.51–5.01 versus 5.08–5.50). From *P. curtissi*, we distinguish *P. neiba* by the dots arranged in bars in the lateral areas (present versus absent), the total lamellae on one hand (45–49 versus 32–39), the relative length of digits on one hindlimb (29.5–36.6 versus 20.8–28.1), the relative distance between angled subocular and mouth (0.670–0.747 versus 0.393–0.587), and the relative longest finger length (5.61–6.66 versus 3.59–4.54). From *P. diastatus*, we distinguish *P. neiba* by the total lamellae on one hand (45–49 versus 35–41), the relative length of digits on one hindlimb (29.5–36.6 versus 21.5–27.4), the relative distance between angled subocular and mouth (0.670–0.747 versus 0.00–0.614), and the relative longest finger length (5.61–6.66 versus 3.48–4.87). From *P. emys*, we distinguish *P. neiba* by the relative prefrontal width (4.41–5.49 versus 3.99–4.36), the relative angled subocular width (2.34–2.83 versus 2.12–2.20), and the relative nasal width (1.67–1.92 versus 1.23–1.58). From *P. hylonomus*, we distinguish *P. neiba* by the dots arranged in bars in the lateral areas (present versus absent), the adult SVL (77.9–102 versus 59.3–76.5), the relative length of digits on one hindlimb (29.5–36.6 versus 22.8–28.2), and the relative longest finger length (5.61–6.66 versus 4.47–5.27). From *P. lanceolatus* **sp. nov.**, we distinguish *P. neiba* by the frontal width by the SVL (3.86–4.52 versus 3.48–3.84) (see Remarks). From *P. lapierrae* **sp. nov.**, we distinguish *P. neiba* by the relative longest finger length (5.61–6.66 versus 4.49–4.55), the relative frontal width (63.3–74.0 versus 77.6–79.0), and the relative distance between the eye and naris (4.51–5.01 versus 5.21). From *P. leionotus*, we distinguish *P. neiba* by the nasal height by the nasal width (1.82–2.18 versus 1.47–1.80) (see Remarks). From *P. marcanoi*, we distinguish *P. neiba* by the head markings (absent versus present) and the total lamellae on one hand (45–49 versus 36–44). From *P. melanchrous*, we distinguish *P. neiba* by the relative nasal height (0.963–1.08 versus 0.897–0.952). From *P. nesobous*, we distinguish *P. neiba* by the dorsal pattern (irregular flecks/dots in chevrons versus irregular dots/dots in series), the total lamellae on one hand (45–49 versus 50–59), the relative rostral height (1.75–2.23 versus 2.26–2.38), the relative nasal height (0.963–1.08 versus 1.12–1.14), the relative distance between the eye and naris (4.51–5.01 versus 5.62–5.73), and the relative width of canthal iii (1.51–1.95 versus 2.01–2.12). From *P. oreistes*, we distinguish *P. neiba* by the relative nasal width (1.67–1.92 versus 1.37–1.65). From *P. psychonothes*, we distinguish *P. neiba* by the total lamellae on one hand (45–49 versus 37–44) and the relative nasal height (0.963–1.08 versus 1.12–1.32). From *P. saonae*, we distinguish *P. neiba* by the dorsal pattern (irregular flecks/dots in chevrons versus absent), the total lamellae on one hand (45–49 versus 40–42), the relative distance between angled subocular and mouth (0.670–0.747 versus 0.517–0.630), the relative mental width (1.66–2.36 versus 1.52), the relative prefrontal width (4.41–5.49 versus 4.14), the relative longest finger length (5.61–6.66 versus 5.01), the relative distance between the eye and naris (4.51–5.01 versus 6.43), the relative width of canthal iii (1.51–1.95 versus 1.99), and the relative angled subocular width (2.34–2.83 versus 2.31). From *P. semitaeniatus* **sp. nov.**, we distinguish *P. neiba* by the relative rostral height (1.75–2.23 versus 2.41–2.63), the relative head width (67.9–78.4 versus 58.8–63.8), the relative angled subocular height (0.713–0.885 versus 0.654), and the relative nasal width (1.67–1.92 versus 1.51). From *P. unicolor* **sp. nov.**, we distinguish *P. neiba* by the dorsal pattern (irregular flecks/dots in chevrons versus absent), the adult SVL (77.9–102 versus 67.6), the total strigae on ten scales (179–239 versus 144), the relative length of digits on one hindlimb (29.5–36.6 versus 36.8), the relative distance between angled subocular and mouth (0.670–0.747 versus 0.533), the relative largest supraocular width (2.06–3.04 versus 3.12), the relative frontal width (63.3–74.0 versus 58.2), the relative nasal height (0.963–1.08 versus 1.15), the relative distance between the eye and naris (4.51–5.01 versus 5.52), the relative angled subocular width (2.34–2.83 versus 2.90), and the relative nasal width (1.67–1.92 versus 2.00).

Description of holotype. MCZ R-77155. An adult female; SVL 88.4 mm; tail nearly cylindrical, broken in life midway, regenerated, 58.5 mm (66.2% SVL); axilla-to-groin distance 51.3 mm (58.0% SVL); forelimb length 19.9 mm (22.5% SVL); hindlimb length 28.6 mm (32.4% SVL); head length 15.6 mm (17.6% SVL); head width 10.6 mm (12.0% SVL); head width 67.9% head length; diameter of orbit 2.99 mm (3.38% SVL); horizontal diameter of ear opening 1.39 mm (1.57% SVL); vertical diameter of ear opening 1.52 mm (1.72% SVL); length of all toes on one foot 27.8 mm (31.4% SVL); shortest distance between angled subocular and lip 0.60 mm (0.679% SVL); shortest distance between the ocular and auricular openings 7.08 mm (8.01% SVL); longest finger length 5.80 mm (6.56% SVL); largest supraocular width 1.82 mm (2.06% SVL); cloacal width 7.75 mm (8.77% SVL); mental width 1.68 mm (1.90% SVL); postmental width 2.41 mm (2.73% SVL); prefrontal width 3.90 mm (4.41% SVL); frontal width 63.3% frontal length; nasal height 0.92 mm (1.04% SVL); angled subocular height 0.63 mm (0.713% SVL);

shortest distance between the eye and naris 3.99 mm (4.51% SVL); canthal iii width 1.65 mm (1.87% SVL); angled subocular width 2.22 mm (2.51% SVL); nasal width 1.48 mm (1.67% SVL); rostral 1.95X as wide as high, visible from above, not in contact with nasals, in contact with 1st supralabial and anterior internasal (left)/(right); anterior internasals are narrower than posterior ones; frontonasals and prefrontal fused into a single large plate with a concave posterior margin, much wider than long, bordered by posterior internasals, 1st loreals, 1st median oculars, and the frontal; frontal longer than wide; a pair of frontoparietals, separated by the posterior prolongation of the frontal and the interparietal plate; interparietal plate slightly smaller than parietals and separating them, posteriorly touching the interoccipital, which is wider than long; parietal separated from supraoculars by 1st temporals and frontoparietal (left)/1st and 2nd temporals and frontoparietal (right); nasal single; nostril above suture between 1st and 2nd supralabials (left)/(right); 1 postnasal (left)/(right); 2 loreals (left)/(right); 1st loreal higher than wide (left)/(right), in contact with postnasal, posterior internasal, prefrontal/frontonasal complex, median ocular 1, canthal iii, 2nd loreal, and 3rd–4th supralabials (left)/(right); 2nd loreal shorter than 1st, approximately as high as wide (left)/(right), excluded from contact with supraocular by canthal iii (left)/(right); final loreal posteriorly bordering the upper and lower preoculars (left)/(right); canthal iii wider than high (left)/(right), contacting 1st median ocular, anterior supraciliary, upper preocular, and 1st and 2nd loreals (left)/(right); 9 median oculars (left)/(right), 1st contacting the prefrontal (left)/(right); 1 upper preocular (left)/(right); an irregular anterior supraciliary (left)/(right); 6 lateral oculars (left)/(right); 5 temporals (left)/(right); 2 suboculars (left)/(right); posterior subocular large and elongate (left)/(right); anterior subocular small (left)/(right); 10 supralabials (left)/(right), 6 to level below center of eye (left)/(right); 10 (left)/11 (right) infralabials, 6 to level below center of eye (left)/(right); mental small, followed by a single, larger postmental; 4 pairs of enlarged chin shields; 1st pair in contact with one another; 2nd–4th pairs separated by 1–3 scales; 97 transverse rows of dorsal scales from interoccipital to base of tail; 90 transverse rows of ventral scales from mental to vent; 40 scales around midbody; 5 digits; finger lengths 3>4>2>5>1; 12 lamellae under longest finger (left)/(right); 47 total lamellae on one hand; toe lengths 4>3>5>2>1; 17 lamellae under longest toe (left)/(right); keelless and striate dorsal body and caudal scales; smooth ventral scales; 190 total strigae counted on ten scales.

Color (in alcohol): dorsal surface of head medium brown, patternless; lateral surfaces of head grading from medium brown to cream with darker brown eye masks and other darker brown areas on the labial scales and sides of neck; dorsal surfaces of the body are red-gray with darker brown markings in longitudinal paramedian series and some darker brown irregular flecks on the remainder of the dorsum; dorsal surface of tail same as body, dark yellow on the regenerated section; lateral areas lateral areas grade from dark red-brown to cream with darker brown dots arranged in bars; dorsal surfaces of the limbs are medium brown with darker brown mottling; lateral and ventral areas of the limbs fade to cream with less mottling; ventral surfaces of the head, body, and tail are cream with some pale brown spotting under the throat.

Variation. The dorsal pattern of the majority of the examined material resembles the holotype of irregularly occurring dots of flecks. At times, this pattern is arranged into chevrons. KU 79826 has dots only on the back of its neck. All specimens have patternless heads except for KU 225030, which has some irregular flecks on its head scales. The holotype has the most pronounced longitudinal paramedian lines of the examined material with other specimens displaying broken longitudinal paramedian lines, dots in series, streaking, or even no markings (MCZ R-171777). All examined material shows dots arranged in bars in the lateral band. Measurements and other morphological data for the holotype and other examined material are presented in Table 1.

Distribution. *Panolopus neiba* is distributed in the Sierra de Neiba of the Dominican Republic at elevations of 390–1920 m (Fig. 50).

Ecology and conservation. Little information is available on the ecology of this species other than that many specimens were collected under rocks.

We consider the conservation status of *Panolopus neiba* to be Least Concern, based on IUCN Redlist criteria (IUCN 2023). It is likely a common species tolerant of some habitat disturbance, based on what is known of most species of *Panolopus*. However, it faces a primary threat of habitat destruction resulting from deforestation. A secondary threat is predation from introduced mammals, including the mongoose and black rats. Studies are needed to determine the health and extent of remaining populations and better understand the threats to the survival of the species.

Reproduction. A litter size of 4–8 (3.2–5.0 g) has been recorded in this species (SBH, field data).

Etymology. The species name (*neiba*) refers to the geographic distribution of this species in the Sierra de Neiba.

Remarks. Previously considered a subspecies of *Panolopus costatus*, herein we recognize *P. neiba* as a full species based on genetic and morphological differences. Additional museum specimens classified as *P. costatus* from the range of *P. neiba* should be examined to determine if they are members of this species.

Panolopus neiba and *P. lanceolatus* **sp. nov.** cannot be morphologically separated based on our standard suite of characters, however, they can be separated by the frontal width divided by the SVL (3.86–4.52 [n=5] versus 3.48–3.84 [n=8]). *Panolopus neiba* and *P. leionotus* cannot be morphologically separated based on our standard suite of characters; however, they can be separated by the nasal height by the nasal width (1.82–2.18 [n=5] versus 1.47–1.80 [n=7]).

Panolopus neiba is included in our genetic dataset and has significant support in ML and Bayesian analyses at the crown node and the stem node that places it outside of *P. leionotus* and *P. semitaeniatus* **sp. nov.** Based on our timetree (Fig. 4), *P. neiba* diverged from its closest relative 1.23 Ma, consistent with typical species of vertebrates (> 0.7 Ma; Hedges *et al.* 2015). We further recognize *P. neiba* as a distinct species because of the diagnostic traits that separate it from both *P. leionotus* and *P. semitaeniatus* **sp. nov.** *Panolopus neiba* also occurs in sympatry with *P. leionotus*. *Panolopus neiba* was recovered as conspecific with *Panolopus leionotus* and *Panolopus semitaeniatus* **sp. nov.** in our ASAP analysis.

Panolopus nesobous (Schwartz 1964)

Ile-a-Vache Forest Lizard
(Fig. 71–72)

Diploglossus costatus nesobous Schwartz, 1964:23. Holotype: MCZ R-77153, collected by Albert Schwartz, Jr. on Ile-a-Vache, Sud department, Haiti, on 6 August 1962 (18.10, -73.70).
Celestus costatus nesobous—Schwartz & Henderson, 1988:96.
Celestus costatus nesobous—Schwartz & Henderson, 1991:367.
Celestus costatus nesobous—Hedges *et al.*, 2019:16.
Celestus costatus nesobous—Schools & Hedges, 2021:230.

Material examined (n=8). HAITI. Sud. ANSP 38580–2, S. Blair Hedges, Richard Thomas, Nicholas Plummer, and Manuel Leal, Caye Michel, previously called Caye Paul (10.7 km WNW Les Platons Citadel), 1 June 1991; KU 225032–3, Île-à-Vache western end, 6 August 1962; ANSP 38583, locals, Île-à-Vache, 24 July 2011; MCZ R-77153, Albert Schwartz, Jr., Île-à-Vache, western end, 6 August 1962; SBH 269117, Plaine Formon near Caye Michel.

Diagnosis. *Panolopus nesobous* has (1) a dorsal pattern of irregular dots/dots in series, (2) head markings absent, (3) markings in the longitudinal paramedian area present, (4) dots arranged in bars in the lateral band present, (5) an adult SVL of 82.3–108 mm, (6) ventral scale rows, 77–96, (7) midbody scale rows, 38–43, (8) total lamellae on one hand, 50–59, (9) total strigae on ten scales, 155–222, (10) relative length of all digits on one hindlimb, 35.1 %, (11) relative distance between the angled subocular and mouth, 0.486–0.843 %, (12) relative eye length, 3.41–3.63 %, (13) relative forelimb length, 23.3–25.1 %, (14) relative ear width, 1.39–1.60 %, (15) relative rostral height, 2.26–2.38 %, (16) relative head length, 17.9–19.8 %, (17) relative mental width, 1.96–2.18 %, (18) relative postmental width, 2.82–3.02 %, (19) relative cloacal width, 8.11–8.21 %, (20) relative prefrontal width, 4.74–4.81 %, (21) relative largest supraocular width, 2.85–3.11 %, (22) relative longest finger length, 6.19–6.33 %, (23) relative distance between the ear and eye, 7.91–10.0 %, (24) relative head width, 71.2–76.4 %, (25) relative frontal width, 60.8–63.5 %, (26) relative nasal height, 1.12–1.14 %, (27) relative angled subocular height, 0.669–0.750 %, (28) relative distance between the eye and naris, 5.62–5.73 %, (29) relative canthal iii length, 2.01–2.12 %, (30) relative angled subocular width, 2.61–2.82 %, and (31) relative nasal length, 1.69–1.71 %. The species stem time is 3.51 Ma and the species crown time is 0.02 Ma (Fig. 4).

We distinguish *Panolopus nesobous* from the other species of *Panolopus* based on a complex of traits. From *Panolopus aenetergum*, we distinguish *P. nesobous* by the longitudinal paramedian lines (present versus absent), the midbody scale rows (38–43 versus 35–36), and the total lamellae on one hand (50–59 versus 40). From *P. aporus*, we distinguish *P. nesobous* by the total lamellae on one hand (50–59 versus 36–48), the relative length of digits on one hindlimb (35.1 versus 27.7–33.7), the relative prefrontal width (4.74–4.81 versus 4.18–4.53), the relative longest finger length (6.19–6.33 versus 4.57–5.72), the relative distance between the eye and naris (5.62–5.73 versus 4.69–5.44), and the relative width of canthal iii (2.01–2.12 versus 1.85–1.96). From *P. chalcorhabdus*, we distinguish *P. nesobous* by the relative rostral height (2.26–2.38 versus 1.85–2.24). From *P. costatus*, we distinguish *P. nesobous*

by the relative prefrontal width (4.74–4.81 versus 3.97–4.67), the relative distance between the eye and naris (5.62–5.73 versus 5.08–5.50), and the relative width of canthal iii (2.01–2.12 versus 1.82–1.90). From *P. curtissi*, we distinguish *P. nesobous* by the dorsal pattern (irregular dots/dots in series versus absent/irregular flecks), the dots arranged in bars in the lateral areas (present versus absent), the total lamellae on one hand (50–59 versus 32–39), the relative length of digits on one hindlimb (35.1 versus 20.8–28.1), the relative forelimb length (23.3–25.1 versus 15.1–20.5), the relative postmental width (2.82–3.02 versus 2.07–2.72), the relative prefrontal width (4.74–4.81 versus 3.96–4.68), the relative longest finger length (6.19–6.33 versus 3.59–4.54), the relative distance between the ear and eye (7.91–10.0 versus 5.36–7.71), the relative frontal width (60.8–63.5 versus 65.4–83.1), the relative distance between the eye and naris (5.62–5.73 versus 4.02–5.03), and the relative width of canthal iii (2.01–2.12 versus 1.75–1.93). From *P. diastatus*, we distinguish *P. nesobous* by the dorsal pattern (irregular dots/dots in series versus absent/irregular flecks), the longitudinal paramedian lines (present versus absent), the total lamellae on one hand (50–59 versus 35–41), the relative length of digits on one hindlimb (35.1 versus 21.5–27.4), the relative eye length (3.41–3.63 versus 2.71–3.32), the relative forelimb length (23.3–25.1 versus 16.2–20.1), the relative cloacal width (8.11–8.21 versus 7.15–8.06), the relative prefrontal width (4.74–4.81 versus 3.74–4.61), the relative largest supraocular width (2.85–3.11 versus 1.88–2.57), the relative longest finger length (6.19–6.33 versus 3.48–4.87), and the relative distance between the eye and naris (5.62–5.73 versus 4.06–4.94). From *P. emys*, we distinguish *P. nesobous* by the dorsal pattern (irregular dots/dots in series versus absent/irregular flecks), the total strigae on ten scales (155–222 versus 238–311), the relative eye length (3.41–3.63 versus 2.87–3.40), the relative cloacal width (8.11–8.21 versus 8.24–8.96), the relative prefrontal width (4.74–4.81 versus 3.99–4.36), the relative longest finger length (6.19–6.33 versus 5.15–5.83), the relative frontal width (60.8–63.5 versus 67.7–74.5), the relative nasal height (1.12–1.14 versus 0.963–1.10), the relative distance between the eye and naris (5.62–5.73 versus 4.37–5.19), the relative angled subocular width (2.61–2.82 versus 2.12–2.20), and the relative nasal width (1.69–1.71 versus 1.23–1.58). From *P. hylonomus*, we distinguish *P. nesobous* by the dorsal pattern (irregular dots/dots in series versus absent/irregular flecks), the dots arranged in bars in the lateral areas (present versus absent), the adult SVL (82.3–108 versus 59.3–76.5), the total lamellae on one hand (50–59 versus 34–47), the relative length of digits on one hindlimb (35.1 versus 22.8–28.2), the relative forelimb length (23.3–25.1 versus 17.1–20.7), the relative longest finger length (6.19–6.33 versus 4.47–5.27), the relative frontal width (60.8–63.5 versus 64.0–74.5), and the relative distance between the eye and naris (5.62–5.73 versus 4.03–4.98). From *P. lanceolatus* **sp. nov.**, we distinguish *P. nesobous* by the relative ear width (1.39–1.60 versus 0.770–1.35), the relative postmental width (2.82–3.02 versus 2.36–2.66), the relative prefrontal width (4.74–4.81 versus 3.97–4.55), the relative largest supraocular width (2.85–3.11 versus 2.20–2.71), the relative distance between the ear and eye (7.91–10.0 versus 6.45–7.70), the relative nasal height (1.12–1.14 versus 0.904–1.06), the relative distance between the eye and naris (5.62–5.73 versus 4.58–5.05), and the relative width of canthal iii (2.01–2.12 versus 1.73–2.00). From *P. lapierrae* **sp. nov.**, we distinguish *P. nesobous* by the dorsal pattern (irregular dots/dots in series versus absent/dots in chevrons), the total lamellae on one hand (50–59 versus 38–47), the total strigae on ten scales (155–222 versus 228–231), the relative length of digits on one hindlimb (35.1 versus 24.3–30.9), the relative forelimb length (23.3–25.1 versus 18.5–20.6), the relative rostral height (2.26–2.38 versus 1.86–2.06), the relative mental width (1.96–2.18 versus 1.92–1.94), the relative cloacal width (8.11–8.21 versus 8.55–8.81), the relative largest supraocular width (2.85–3.11 versus 1.91–2.77), the relative longest finger length (6.19–6.33 versus 4.49–4.55), the relative head width (71.2–76.4 versus 77.7–78.1), the relative frontal width (60.8–63.5 versus 77.6–79.0), the relative nasal height (1.12–1.14 versus 1.06–1.09), the relative angled subocular height (0.669–0.750 versus 0.838–0.978), and the relative width of canthal iii (2.01–2.12 versus 1.54–1.86). From *P. leionotus*, we distinguish *P. nesobous* by the total lamellae on one hand (50–59 versus 43–48), the relative length of digits on one hindlimb (35.1 versus 25.4–34.1), the relative largest supraocular width (2.85–3.11 versus 1.94–2.50), the relative longest finger length (6.19–6.33 versus 4.58–6.10), the relative frontal width (60.8–63.5 versus 68.7–81.2), the relative distance between the eye and naris (5.62–5.73 versus 4.46–5.61), and the relative width of canthal iii (2.01–2.12 versus 1.55–1.89). From *P. marcanoi*, we distinguish *P. nesobous* by the head markings (absent versus present), the total lamellae on one hand (50–59 versus 36–44), and the relative length of digits on one hindlimb (35.1 versus 26.3–31.9). From *P. melanchrous*, we distinguish *P. nesobous* by the relative nasal height (1.12–1.14 versus 0.897–0.952), the relative distance between the eye and naris (5.62–5.73 versus 4.89–5.59), and the relative width of canthal iii (2.01–2.12 versus 1.67–1.94). From *P. neiba*, we distinguish *P. nesobous* by the dorsal pattern (irregular dots/dots in series versus irregular flecks/dots in chevrons), the total lamellae on one hand (50–59 versus 45–49), the relative rostral height (2.26–2.38 versus 1.75–2.23), the relative nasal height (1.12–1.14 versus 0.963–1.08), the relative distance between the eye and naris

(5.62–5.73 versus 4.51–5.01), and the relative width of canthal iii (2.01–2.12 versus 1.51–1.95). From *P. oreistes*, we distinguish *P. nesobous* by the relative mental width (1.96–2.18 versus 1.54–1.90), the relative nasal height (1.12–1.14 versus 0.878–1.06), and the relative nasal width (1.69–1.71 versus 1.37–1.65). From *P. psychonothes*, we distinguish *P. nesobous* by the total lamellae on one hand (50–59 versus 37–44), the relative length of digits on one hindlimb (35.1 versus 26.5–33.1), the relative largest supraocular width (2.85–3.11 versus 1.92–2.68), the relative longest finger length (6.19–6.33 versus 4.89–5.81), the relative frontal width (60.8–63.5 versus 66.5–81.0), the relative angled subocular height (0.669–0.750 versus 0.803–0.952), and the relative angled subocular width (2.61–2.82 versus 2.01–2.44). From *P. saonae*, we distinguish *P. nesobous* by the dorsal pattern (irregular dots/dots in series versus absent), the longitudinal paramedian lines (present versus absent), the total lamellae on one hand (50–59 versus 40–42), the relative length of digits on one hindlimb (35.1 versus 26.5–29.8), the relative eye length (3.41–3.63 versus 3.06–3.20), the relative forelimb length (23.3–25.1 versus 19.0–20.2), the relative ear width (1.39–1.60 versus 0.880–1.35), and the relative head length (17.9–19.8 versus 15.4–17.5). From *P. semitaeniatus* **sp. nov.**, we distinguish *P. nesobous* by the total lamellae on one hand (50–59 versus 34–46), the relative length of digits on one hindlimb (35.1 versus 30.4–34.6), the relative ear width (1.39–1.60 versus 1.90–2.30), the relative rostral height (2.26–2.38 versus 2.41–2.63), the relative longest finger length (6.19–6.33 versus 5.17–6.05), the relative distance between the ear and eye (7.91–10.0 versus 6.64–7.90), the relative head width (71.2–76.4 versus 58.8–63.8), and the relative frontal width (60.8–63.5 versus 63.6–76.5). From *P. unicolor* **sp. nov.**, we distinguish *P. nesobous* by the dorsal pattern (irregular dots/dots in series versus absent) and the total lamellae on one hand (50–59 versus 48).

Description of holotype. MCZ R-77153. A young adult; SVL 78.9 mm; tail nearly cylindrical, broken at tip, 86.5 mm (110% SVL); axilla-to-groin distance 42.4 mm (53.7% SVL); forelimb length 18.9 mm (24.0% SVL); hindlimb length 29.4 mm (37.3% SVL); head length 15.6 mm (19.8% SVL); head width 10.5 mm (13.3% SVL); head width 67.3% head length; diameter of orbit 2.72 mm (3.45% SVL); horizontal diameter of ear opening 1.03 mm (1.31% SVL); vertical diameter of ear opening 1.07 mm (1.36% SVL); length of all toes on one foot 31.2 mm (39.5% SVL); shortest distance between angled subocular and lip 0.56 mm (0.710% SVL); shortest distance between the ocular and auricular openings 7.38 mm (9.35% SVL); longest finger length 5.00 mm (6.34% SVL); largest supraocular width 1.99 mm (2.52% SVL); cloacal width 6.48 mm (8.21% SVL); mental width 1.73 mm (2.19% SVL); postmental width 2.11 mm (2.67% SVL); prefrontal width 3.59 mm (4.55% SVL); frontal width 73.5% frontal length; nasal height 0.88 mm (1.12% SVL); angled subocular height 0.58 mm (0.735% SVL); shortest distance between the eye and naris 4.41 mm (5.59% SVL); canthal iii width 1.73 mm (2.19% SVL); angled subocular width 2.14 mm (2.71% SVL); nasal width 1.40 mm (1.77% SVL); rostral 2.42X as wide as high, visible from above, not in contact with nasals, in contact with 1st supralabial and anterior internasal (left)/(right); anterior internasals are narrower than posterior ones; frontonasals and prefrontal fused into a single large plate with an irregular posterior margin, much wider than long, bordered by posterior internasals, 1st loreals, 1st and 2nd median oculars, and the frontal; frontal longer than wide; a pair of frontoparietals, separated by the posterior prolongation of the frontal and the interparietal plate; interparietal plate smaller than parietals and separating them, posteriorly touching the interoccipital, which is wider than long; parietal separated from supraoculars by 1st and 2nd temporals and frontoparietal (left)/(right); nasal single; nostril just posterior to suture between 1st and 2nd supralabials (left)/(right); 1 postnasal (left)/(right); 2 loreals (left)/(right); 1st loreal higher than wide (left)/(right), in contact with postnasal, posterior internasal, prefrontal/frontonasal complex, 1st median ocular, canthal iii, 2nd loreal, and 3rd–5th supralabial (left)/(right); 2nd loreal shorter than 1st, approximately as high as wide (left)/(right), excluded from contact with supraocular by canthal iii (left)/(right); final loreal posteriorly bordering the upper and lower preoculars (left)/lower preocular (right); canthal iii wider than high (left)/(right), contacting 1st median ocular, anterior supraciliary, upper preocular, and 1st and 2nd loreals (left)/1st median ocular, anterior supraciliary, upper and lower preoculars, and 1st and 2nd loreals (right); 9 median oculars (left)/(right), 1st and 2nd contacting the prefrontal (left)/(right); 1 upper preocular (left)/(right); an irregular anterior supraciliary (left)/(right); 6 lateral oculars (left)/(right); 5 temporals (left)/(right); 2 suboculars (left)/(right); posterior subocular large and elongate (left)/(right); anterior subocular small (left)/(right); 11 (left)/10 (right) supralabials, 7 to level below center of eye (left)/(right); 11 infralabials (left)/(right), 7 to level below center of eye (left)/(right); mental small, followed by a single, larger postmental; 4 pairs of enlarged chin shields, followed by 1 pair of reduced chin shields; 1st pair in contact with one another; 3rd–5th pairs separated by 1–5 scales; 91 transverse rows of dorsal scales from interoccipital to base of tail; 93 transverse rows of ventral scales from mental to vent; 39 scales around midbody; 5 digits; finger lengths 3>4>2>5>1; 13 lamellae under longest finger (left)/(right); 50 total

lamellae on one hand; toe lengths 4>3>5>2>1; 18 (left)/19 (right) lamellae under longest toe; keelless and striate dorsal body and caudal scales; striate ventral scales; 173 total strigae counted on ten scales.

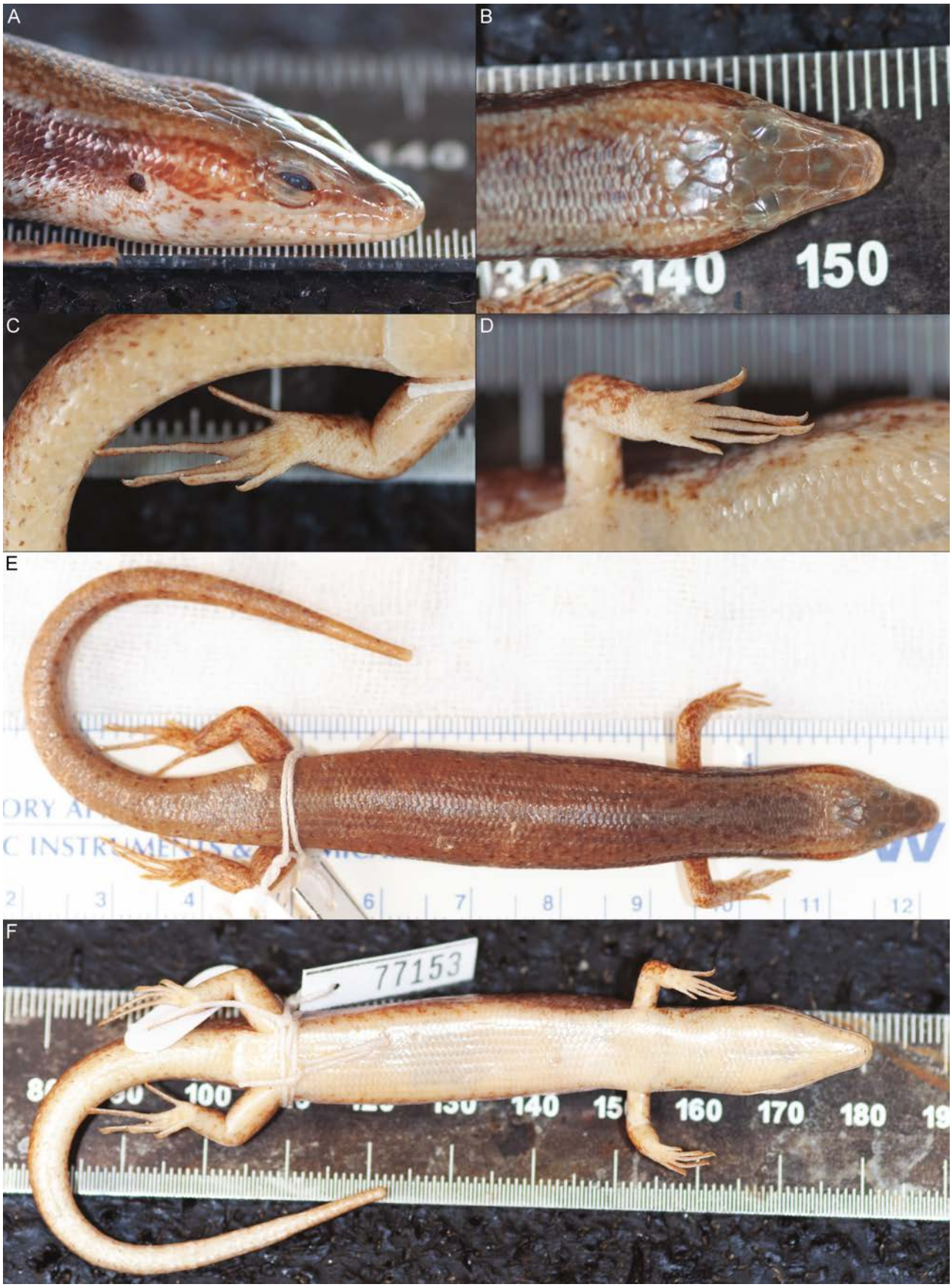

FIGURE 71. (A–F) *Panolopus nesobous* (MCZ R-77153, holotype), SVL 78.9 mm.

FIGURE 72. *Panolopus nesobous* (ANSP 38583, SBH 269457), in life. From Ile-a-Vache, Sud Department, Haiti. Photo by SBH.

Color (in alcohol): dorsal surface of head medium brown, patternless; lateral surfaces of head grading from medium brown to dark cream with darker brown eye masks; dorsal surfaces of the body are medium brown with some darker brown spots in longitudinal paramedian series and irregular darker brown flecks on body; dorsal surface of tail are paler brown than the body with some darker brown flecks; lateral areas grade from dark brown to yellow-cream with darker brown and off-white spots arranged in bars; dorsal surfaces of the limbs are medium brown with darker brown mottling; lateral and ventral areas of the limbs grading from medium brown to yellow-cream; ventral surfaces of the head, body, and tail are cream, patternless.

Variation. Much of the examined material resembles the holotype in dorsal pattern with irregular flecks or dots. In ANSP 38581, these dots are arranged vaguely into chevrons. All specimens have either longitudinal paramedian lines or dots in the longitudinal paramedian series. All specimens have dots arranged in bars in the lateral band. Measurements and other morphological data for the holotype and other examined material are presented in Table 1.

Distribution. *Panolopus nesobous* is distributed on Île-à-Vache of Haiti and in inland areas near Caye Michele at elevations of 0–1160 m (Fig. 50).

Ecology and conservation. No ecological data are associated with this species. We consider the conservation status of *Panolopus nesobous* to be Least Concern, based on IUCN Redlist criteria (IUCN 2023). It is likely a common species tolerant of some habitat disturbance, based on what is known of most species of *Panolopus*. However, it faces a primary threat of habitat destruction resulting from deforestation. A secondary threat is predation from introduced mammals, including the mongoose and black rats. Studies are needed to determine the health and extent of remaining populations and better understand the threats to the survival of the species.

Reproduction. No data on reproduction are available for this species.

Etymology. The species name (*nesobous*) is derived from the Greek *neso-* (island) and *bous* (cow) in reference to the type locality of this species on Île-à-Vache (Cow Island).

Remarks. Previously considered a subspecies of *Panolopus costatus*, herein we recognize *P. nesobous* to be a full species based on genetic and morphological differences. Additional specimens categorized as *P. costatus* from the range of *P. nesobous* should examined to determine if they are members of this species.

Panolopus nesobous was included in our genetic dataset and has significant support in both Bayesian and ML likelihood analyses at the crown node. The stem node that places *P. nesobous* outside of *P. costatus* and *P. oreistes* has a support value of 68% in our ML analysis and is not supported in our Bayesian analysis. Genomic data in Schools *et al.* (2022) placed *P. nesobous* outside of *P. costatus* and *P. oreistes* with a support value of 85% in their ML analysis, This relationship was not supported in their Bayesian analysis. Based on our timetree (Fig. 4), *P. nesobous* diverged from its closest relative 3.51 Ma, consistent with typical species of vertebrates (> 0.7 Ma; Hedges *et al.* 2015). *Panolopus nesobous* was recognized as a distinct species by our ASAP analysis.

***Panolopus oreistes* (Schwartz 1964)**
Dark Spotted Forest Lizard
(Fig. 73–74)

Diploglossus costatus oreistes Schwartz, 1964:25. Holotype: MCZ R-74940, collected by George Whiteman from Oriani, near Saltrou, Ouest department, Haiti, between 21 March and 20 June 1962 (18.317, -71.933; 1,544 m).
Celestus costatus oreistes—Schwartz & Henderson, 1988:96.
Celestus costatus oreistes—Schwartz & Henderson, 1991:367.
Celestus costatus oreistes—Hedges *et al.*, 2019:16.
Panolopus costatus oreistes—Schools & Hedges, 2021:230.

Material examined (n=53). DOMINICAN REPUBLIC. Barahona. KU 225401, 3 km N Enriquillo, 8 August 1975; KU 225410, 3 km N, 15 km SW Barahona, 20 June 1969. **Independencia.** ANSP 38609–12, Puerto Escondido, 20.8 km SE of, 23 July 1991; ANSP 38613–4, Puerto Escondido, 23.1 km SE of, 23 July 1991; ANSP 38615–21, Puerto Escondido, 23.9 km SE of, 25 July 1991; KU 225415, El Aguacate, 1969; SBH 192496, S. Blair Hedges, Richard Thomas, and Nicholas Plummer, 23.9 km SE of Puerto Escondido, 23 July 1991. **Pedernales.** ANSP 38598–606, Casetta Dos, Aceitillar, ca. 22 km N of, by road on ridge of Sierra de Bahoruco, 19 November 2009. **HAITI. Ouest.** ANSP 38585–96, S. Blair Hedges, Richard Thomas, Elizabeth Rochel, Eladio Fernandez, Berry, 19 November 2009; ANSP 38597, 1.0 km SW Berry, 19 November 2009; KU 225509, Peneau, 6 July 1962; KU 225513, 225515, Furcy, 8 July 1962; SBH 268567, 1.0 km SW Berry, 19 November 2009; SBH 268583, 268590, S. Blair Hedges, Richard Thomas, Elizabeth Rochel, Eladio Fernandez, Berry, 19 November 2009. **Sud-Est.** ANSP 38607–8, Morne D'Enfer, southwestern edge of plateau, 21 November 2011; KU 225520, Foret des Pins, 12 August 1962; KU 225522, Foret des Pins, 25 November 1972; KU 225531, Thiotte, 8 August 1976; MCZ R-74939, R-74940, R-74941, George Whiteman, Oriani, near Saltrou, 21 March–20 June 1962.

Diagnosis. *Panolopus oreistes* has (1) a dorsal pattern of irregular dots/dots in series/dots in chevrons, (2) head markings absent/present, (3) markings in the longitudinal paramedian area present, (4) dots arranged in bars in the lateral band present, (5) an adult SVL of 77.3–103 mm, (6) ventral scale rows, 80–104, (7) midbody scale rows, 35–43, (8) total lamellae on one hand, 39–55, (9) total strigae on ten scales, 155–267, (10) relative length of all digits on one hindlimb, 31.2–40.1 %, (11) relative distance between the angled subocular and mouth, 0.406–0.865 %, (12) relative eye length, 3.03–3.67 %, (13) relative forelimb length, 20.1–24.9 %, (14) relative ear width, 0.558–1.79 %, (15) relative rostral height, 1.82–2.88 %, (16) relative head length, 15.3–19.8 %, (17) relative mental width, 1.54–1.90 %, (18) relative postmental width, 2.18–3.19 %, (19) relative cloacal width, 7.13–8.78 %, (20) relative prefrontal width, 4.18–4.96 %, (21) relative largest supraocular width, 2.28–3.23 %, (22) relative longest finger length, 5.27–7.23 %, (23) relative distance between the ear and eye, 6.29–9.50 %, (24) relative head width, 66.1–85.0 %, (25) relative frontal width, 61.6–76.9 %, (26) relative nasal height, 0.878–1.06 %, (27) relative angled subocular height, 0.737–0.978 %, (28) relative distance between the eye and naris, 5.01–5.63 %, (29) relative canthal iii length, 1.61–2.16 %, (30) relative angled subocular width, 2.13–3.04 %, and (31) relative nasal length, 1.37–1.65 %. The species stem time is 2.43 Ma and the species crown time is 0.77 Ma (Fig. 4).

We distinguish *Panolopus oreistes* from the other species of *Panolopus* based on a complex of traits. From *Panolopus aenetergum*, we distinguish *P. oreistes* by the longitudinal paramedian lines (present versus absent), the relative length of digits on one hindlimb (31.2–40.1 versus 26.8), the relative prefrontal width (4.18–4.96 versus 4.15), the relative longest finger length (5.27–7.23 versus 4.83), the relative frontal width (61.6–76.9 versus 88.2), the relative nasal height (0.878–1.06 versus 1.15), the relative angled subocular height (0.737–0.978 versus 1.08), the relative distance between the eye and naris (5.01–5.63 versus 4.35), the relative angled subocular width (2.13–

3.04 versus 2.07), and the relative nasal width (1.37–1.65 versus 1.92). From *P. aporus*, we distinguish *P. oreistes* by the relative nasal height (0.878–1.06 versus 1.08–1.23). From *P. chalcorhabdus*, we distinguish *P. oreistes* by the relative nasal width (1.37–1.65 versus 1.70–2.01). From *P. costatus*, we distinguish *P. oreistes* by the area of the nasal scale by the SVL (1.06–1.57 versus 1.59–2.03) (see Remarks). From *P. curtissi*, we distinguish *P. oreistes* by the dorsal pattern (irregular dots/dots in series/dots in chevrons versus absent/irregular flecks), the dots arranged in bars in the lateral areas (present versus absent), the relative length of digits on one hindlimb (31.2–40.1 versus 20.8–28.1), and the relative longest finger length (5.27–7.23 versus 3.59–4.54). From *P. diastatus*, we distinguish *P. oreistes* by the dorsal pattern (irregular dots/dots in series/dots in chevrons versus absent/irregular flecks), the longitudinal paramedian lines (present versus absent), the relative length of digits on one hindlimb (31.2–40.1 versus 21.5–27.4), the relative longest finger length (5.27–7.23 versus 3.48–4.87), and the relative distance between the eye and naris (5.01–5.63 versus 4.06–4.94). From *P. emys*, we distinguish *P. oreistes* by the dorsal pattern (irregular dots/dots in series/ dots in chevrons versus absent/irregular flecks). From *P. hylonomus*, we distinguish *P. oreistes* by the dorsal pattern (irregular dots/dots in series/dots in chevrons versus absent/irregular flecks), the dots arranged in bars in the lateral areas (present versus absent), the adult SVL (77.3–103 versus 59.3–76.5), the relative length of digits on one hindlimb (31.2–40.1 versus 22.8–28.2), and the relative distance between the eye and naris (5.01–5.63 versus 4.03–4.98). From *P. lanceolatus* **sp. nov.**, we distinguish *P. oreistes* by the relative distance between the eye and naris (5.01–5.63 versus 4.58–4.98). From *P. lapierrae* **sp. nov.**, we distinguish *P. oreistes* by the relative length of digits on one hindlimb (31.2–40.1 versus 24.3–30.9), the relative mental width (1.54–1.90 versus 1.92–1.94), the relative longest finger length (5.27–7.23 versus 4.49–4.55), the relative frontal width (61.6–76.9 versus 77.6–79.0), and the relative nasal width (1.37–1.65 versus 1.81). From *P. leionotus*, we cannot distinguish *P. oreistes* based on our standard suite of characters (see Remarks). From *P. marcanoi*, we distinguish *P. oreistes* by the relative nasal height (0.878–1.06 versus 1.07–1.28). From *P. melanchrous*, we cannot distinguish *P. oreistes* based on our standard suite of characters (see Remarks). From *P. neiba*, we distinguish *P. oreistes* by the relative nasal width (1.37–1.65 versus 1.67–1.92). From *P. nesobous*, we distinguish *P. oreistes* by the relative mental width (1.54–1.90 versus 1.96–2.18), the relative nasal height (0.878–1.06 versus 1.12–1.14), and the relative nasal width (1.37–1.65 versus 1.69–1.71). From *P. psychonothes*, we distinguish *P. oreistes* by the relative nasal height (0.878–1.06 versus 1.12–1.32) and the relative nasal width (1.37–1.65 versus 1.68–1.94). From *P. saonae*, we distinguish *P. oreistes* by the dorsal pattern (irregular dots/dots in series/ dots in chevrons versus absent), the longitudinal paramedian lines (present versus absent), the relative length of digits on one hindlimb (31.2–40.1 versus 26.5–29.8), the relative mental width (1.54–1.90 versus 1.52), the relative prefrontal width (4.18–4.96 versus 4.14), the relative longest finger length (5.27–7.23 versus 5.01), the relative distance between the eye and naris (5.01–5.63 versus 6.43), and the relative nasal width (1.37–1.65 versus 1.69). From *P. semitaeniatus* **sp. nov.**, we distinguish *Panolopus oreistes* by the relative ear width (0.558–1.79 versus 1.90–2.30), the relative head width (66.1–85.0 versus 58.8–63.8), the relative nasal height (0.878–1.06 versus 1.08), the relative angled subocular height (0.737–0.978 versus 0.654), and the relative distance between the eye and naris (5.01–5.63 versus 4.61). From *P. unicolor* **sp. nov.**, we distinguish *P. oreistes* by the dorsal pattern (irregular dots/dots in series/dots in chevrons versus absent), the adult SVL (77.3–103 versus 67.6), the total strigae on ten scales (155–267 versus 144), the relative frontal width (61.6–76.9 versus 58.2), the relative nasal height (0.878–1.06 versus 1.15), and the relative nasal width (1.37–1.65 versus 2.00).

Description of holotype. MCZ R-74940. An adult; SVL 103 mm; tail slightly laterally compressed, broken in life, regenerated, 109 mm (106% SVL); axilla-to-groin distance 57.6 mm (55.9% SVL); forelimb length 23.2 mm (22.5% SVL); hindlimb length 31.7 mm (30.8% SVL); head length 20.0 mm (19.4% SVL); head width 14.3 mm (13.9% SVL); head width 71.5% head length; diameter of orbit 3.17 mm (3.08% SVL); horizontal diameter of ear opening 1.01 mm (0.981% SVL); vertical diameter of ear opening 1.58 mm (1.53% SVL); length of all toes on one foot 32.1 mm (31.2% SVL); shortest distance between angled subocular and lip 0.79 mm (0.767% SVL); shortest distance between the ocular and auricular openings 9.79 mm (9.50% SVL); largest supraocular width 2.83 mm (2.75% SVL); cloacal width 8.00 mm (7.77% SVL); mental width 1.90 mm (1.84% SVL); postmental width 3.29 mm (3.19% SVL); prefrontal width 5.11 mm (4.96% SVL); frontal width 70.4% frontal length; nasal height 1.05 mm (1.02% SVL); angled subocular height 0.86 mm (0.835% SVL); shortest distance between the eye and naris 5.54 mm (5.38% SVL); canthal iii width 1.75 mm (1.70% SVL); angled subocular width 2.44 mm (2.37% SVL); nasal width 1.54 mm (1.50% SVL); rostral 2.22X as wide as high, visible from above, not in contact with nasals, in contact with 1st supralabial and anterior internasal (left)/(right); anterior internasals are narrower than posterior ones; frontonasals, frontal, and prefrontal fused into a single large plate with a concave posterior margin, much

wider than long, bordered by posterior internasals, 1st loreals, 1st and 2nd median oculars, and the frontal; frontal longer than wide; a pair of frontoparietals, fused with frontal, separated by the posterior prolongation of the frontal and the interparietal plate; interparietal plate smaller than parietals and separating them, posteriorly touching the interoccipital, which is approximately as wide as long; parietal separated from supraoculars by 1st and 2nd temporals and frontoparietal (left)/1st temporal and frontoparietal (right); nasal single; nostril just posterior to suture between 1st and 2nd supralabials (left)/(right); 1 postnasal (left)/(right); 2 loreals (left)/(right); 1st loreal higher than wide (left)/(right), in contact with postnasal, posterior internasal, prefrontal/frontonasal complex, 1st median ocular, canthal iii, 2nd loreal, and 3rd–5th supralabial (left)/(right); 2nd loreal shorter than 1st, approximately as high as wide (left)/shorter than 1st, wider than high (right), excluded from contact with supraocular by canthal iii (left)/(right); final loreal posteriorly bordering the upper and lower preoculars (left)/(right); canthal iii wider than high (left)/(right), contacting 1st median ocular, anterior supraciliary, upper preocular, and 1st and 2nd loreals (left)/1st median ocular (fused), anterior supraciliary, upper preocular, and 1st and 2nd loreals (right); 10 (left)/9 (right) median oculars, 1st and 2nd contacting the prefrontal (left)/(right); 1 upper preocular (left)/(right); an irregular anterior supraciliary (left)/(right); 6 (left)/5 (right) lateral oculars; 5 temporals (left)/(right); 2 suboculars (left)/(right); posterior subocular large and elongate (left)/(right); anterior subocular small (left)/(right); 9 (left)/10 (right) supralabials, 6 (left)/7 (right) to level below center of eye; 9 (left)/10 (right) infralabials, 5 (left)/6 (right) to level below center of eye; mental small, followed by a single, larger postmental; 4 pairs of enlarged chin shields; 1st pair in contact with one another anteriorly, posteriorly separated by one scale; 2nd–4th pairs separated by 1–3 scales; 93 transverse rows of dorsal scales from interoccipital to base of tail; 100 transverse rows of ventral scales from mental to vent; 40 scales around midbody; 5 digits; finger lengths 3>4>2>5>1; 13 (right) lamellae under longest finger; 48 total lamellae on one hand; toe lengths 4>3>2>5>1; 18 (left)/20 (right) lamellae under longest toe; keelless and striate dorsal body and caudal scales; smooth to faintly striated ventral scales; 267 total strigae counted on ten scales.

Color (in alcohol): dorsal surface of head medium brown with several darker brown spots; lateral surfaces of head grading from medium brown to yellow-cream with darker brown eye masks and labial scales; dorsal surfaces of the body are gray-brown with markings in longitudinal paramedian series and faint darker brown spots arranged in vague herring bones farther down the dorsum; dorsal surface of tail same as the body; lateral areas grade from darker brown to dark cream with darker brown and off-white spots arranged in vertical bars; dorsal surfaces of the limbs are medium brown with darker brown mottling; lateral and ventral areas of the limbs grading to dark cream with reduced brown mottling; ventral surfaces of the head, body, and tail are orange-cream with darker spotting under the chest, head, and tail.

Variation. All of the examined material appears similar to the holotype in dorsal pattern and has either dots arranged in chevrons or dots occurring irregularly. Roughly half of the examined material has patternless heads whereas the other half displayed either darker outlines on head scale borders or dark, irregular markings on the head scales. All examined material have markings in the longitudinal paramedian series that range from dots in series, to broken longitudinal paramedian lines, to complete longitudinal paramedian lines. All animals of this species that we examined have dots arranged in bars in the lateral area. Measurements and other morphological data for the holotype and other examined material are presented in Table 1.

Distribution. *Panolopus oreistes* is distributed in southern Haiti and into the southeastern Dominican Republic at elevations of 0–2220 m (Fig. 49).

Ecology and conservation. No ecological data are associated with this species. We consider the conservation status of *Panolopus oreistes* to be Least Concern, based on IUCN Redlist criteria (IUCN 2023). It is likely a common species tolerant of some habitat disturbance, based on what is known of most species of *Panolopus*. However, it faces a primary threat of habitat destruction resulting from deforestation. A secondary threat is predation from introduced mammals, including the mongoose and black rats. Studies are needed to determine the health and extent of remaining populations and better understand the threats to the survival of the species.

Reproduction. Ovoviviparous, embryos observed in multiple specimens.

Etymology. The species name *oreistes* is derived from the Greek words *oreios*, meaning "mountain", and *stes*, meaning "dweller."

Remarks. Previously considered a subspecies of *Panolopus costatus*, herein we recognize *P. oreistes* to be a full species based on genetic and morphological differences. Additional specimens categorized as *P. costatus* from the range of *P. oreistes* should be examined to determine if they are members of this species.

FIGURE 73. (A–F) *Panolopus oreistes* (MCZ R-74940, holotype), SVL 103 mm.

FIGURE 74. *Panolopus oreistes* (ANSP 38608, SBH 269898), in life. From Morne D'Enfer, southwestern edge of plateau, Sud-Est Department, Haiti. Photo by SBH.

Panolopus oreistes and *P. costatus* cannot be morphologically separated based on our standard suite of characters; however, they can be separated by the area of the nasal scale by the SVL (1.06–1.57 [n=14] versus 1.59–2.03 [n=4]). *Panolopus oreistes* and *P. leionotus* cannot be distinguished based on our suite of morphological characters; however, both species are morphologically distinct from their respective closest relative (*P. costatus* and *P. semitaeniatus* **sp. nov.**, respectively). Additionally, *P. oreistes* and *P. leionotus* are genetically distinct (Fig. 3) and diverged 3.81 Ma (Fig. 4). Future studies should examine additional characters to morphologically diagnose *P. oreistes* and *P. leionotus*. *Panolopus oreistes* and *P. melanchrous* cannot be distinguished based on our suite of morphological characters and future studies should examine additional characters to morphologically diagnose those two species.

Panolopus oreistes was included in our genetic dataset and has significant support in both Bayesian and ML likelihood analyses at the crown node of the species and the stem node that places it as the closest relative to *P. costatus*. Based on our timetree (Fig. 4), *P. oreistes* diverged from its closest relative 2.43 Ma, consistent with typical species of vertebrates (> 0.7 Ma; Hedges *et al.* 2015). *Panolopus oreistes* was recovered as conspecific with *Panolopus aporus* in our ASAP analysis.

***Panolopus psychonothes* (Schwartz 1964)**

Constanza Forest Lizard
(Fig. 75)

Diploglossus costatus psychonothes Schwartz, 1964:32. Holotype: MCZ R-77156, collected by David C. Leber from 1 mi. S Constanza, La Vega province, Dominican Republic, on 30 June 1963 (18.893, -70.738; 1,164 m).
Celestus costatus psychonothes—Schwartz & Henderson, 1988:96.
Celestus costatus psychonothes—Schwartz & Henderson, 1991:367.
Celestus costatus psychonothes—Hedges *et al.*, 2019:16.
Panolopus costatus psychonothes—Schools & Hedges, 2021:230.

Material examined (n=19). DOMINICAN REPUBLIC. AMNH 16017–20, Rollo H. Beck, January 1917–June 1917. **Azua.** AMNH 16021–5, Rollo H. Beck, interior of Azua, 1917. **La Vega.** KU 225034–5, 7.2 mi S Constanza, 30 June 1963; KU 225643–8, 16 km SE Constanza, 25 December 1970; KU 225651, 17.2 km SE Constanza, 21 August 1973; MCZ R-77156, David C. Leber, 1 mi. S Constanza, 30 June 1963.

Diagnosis. *Panolopus psychonothes* has (1) a dorsal pattern of irregular dots/dots in series/dots in chevrons, (2) head markings absent/present, (3) markings in the longitudinal paramedian area absent/present, (4) dots arranged in bars in the lateral band absent/present, (5) an adult SVL of 70.9–97.2 mm, (6) ventral scale rows, 88–109, (7) midbody scale rows, 36–42, (8) total lamellae on one hand, 37–44, (9) total strigae on ten scales, 172–244, (10) relative length of all digits on one hindlimb, 26.5–33.1 %, (11) relative distance between the angled subocular and mouth, 0.505–1.03 %, (12) relative eye length, 2.74–3.87 %, (13) relative forelimb length, 17.4–23.8 %, (14) relative ear width, 0.954–2.31 %, (15) relative rostral height, 1.80–2.32 %, (16) relative head length, 15.9–19.5 %, (17) relative mental width, 1.47–2.91 %, (18) relative postmental width, 2.46–3.34 %, (19) relative cloacal width, 7.56–8.53 %, (20) relative prefrontal width, 3.89–4.75 %, (21) relative largest supraocular width, 1.92–2.68 %, (22) relative longest finger length, 4.89–5.81 %, (23) relative distance between the ear and eye, 6.79–8.29 %, (24) relative head width, 68.4–78.6 %, (25) relative frontal width, 66.5–81.0 %, (26) relative nasal height, 1.12–1.32 %, (27) relative angled subocular height, 0.803–0.952 %, (28) relative distance between the eye and naris, 4.00–5.62 %, (29) relative canthal iii length, 1.16–2.01 %, (30) relative angled subocular width, 2.01–2.44 %, and (31) relative nasal length, 1.68–1.94 %. No genetic data are available to estimate the species stem of crown time.

We distinguish *Panolopus psychonothes* from the other species of *Panolopus* based on a complex of traits. From *Panolopus aenetergum*, we distinguish *P. psychonothes* by the ventral scale rows (88–109 versus 80–86), the total strigae on ten scales (172–244 versus 267), the relative longest finger length (4.89–5.81 versus 4.83), the relative distance between the ear and eye (6.79–8.29 versus 8.40), the relative frontal width (66.5–81.0 versus 88.2), and the relative angled subocular height (0.803–0.952 versus 1.08). From *P. aporus*, we distinguish *P. psychonothes* by the relative largest supraocular width (1.92–2.68 versus 2.74–3.62). From *P. chalcorhabdus*, we distinguish *P. psychonothes* by the angled subocular width by the angled subocular height (2.37–2.72 versus 2.77–3.28) (see Remarks). From *P. costatus*, we distinguish *P. psychonothes* by the total lamellae on one hand (37–44 versus 49–58). From *P. curtissi*, we distinguish *P. psychonothes* by the dorsal pattern (irregular dots/dots in series/dots in chevrons versus absent/irregular flecks) and the relative longest finger length (4.89–5.81 versus 3.59–4.54). From *P. diastatus*, we distinguish *P. psychonothes* by the dorsal pattern (irregular dots/dots in series/dots in chevrons versus absent/irregular flecks) and the relative longest finger length (4.89–5.81 versus 3.48–4.87). From *P. emys*, we distinguish *P. psychonothes* by the dorsal pattern (irregular dots/dots in series/dots in chevrons versus absent/irregular flecks), the adult SVL (70.9–97.2 versus 99.0–113), the relative nasal height (1.12–1.32 versus 0.963–1.10), and the relative nasal width (1.68–1.94 versus 1.23–1.58). From *P. hylonomus*, we distinguish *P. psychonothes* by the dorsal pattern (irregular dots/dots in series/dots in chevrons versus absent/irregular flecks). From *P. lanceolatus* **sp. nov.**, we distinguish *P. psychonothes* by the relative nasal height (1.12–1.32 versus 0.904–1.06). From *P. lapierrae* **sp. nov.**, we distinguish *P. psychonothes* by the relative cloacal width (7.56–8.53 versus 8.55–8.81), the relative longest finger length (4.89–5.81 versus 4.49–4.55), the relative nasal height (1.12–1.32 versus 1.06–1.09), and the relative angled subocular width (2.01–2.44 versus 2.71). From *P. leionotus*, we distinguish *P. psychonothes* by the relative angled subocular width (2.01–2.44 versus 2.48–2.95). From *P. marcanoi*, we distinguish *P. psychonothes* by the relative angled subocular height (0.803–0.952 versus 0.505–0.793). From *P. melanchrous*, we distinguish *P. psychonothes* by the total lamellae on one hand (37–44 versus 47–58) and the relative nasal height (1.12–1.32 versus 0.897–0.952). From *P. neiba*, we distinguish *P. psychonothes* by the total lamellae on one hand (37–44 versus 45–49) and the relative nasal height (1.12–1.32 versus 0.963–1.08). From *P. nesobous*, we distinguish *P. psychonothes* by the total lamellae on one hand (37–44 versus 50–59), the relative length of digits on one hindlimb (26.5–33.1 versus 35.1), the relative largest supraocular width (1.92–2.68 versus 2.85–3.11), the relative longest finger length (4.89–5.81 versus 6.19–6.33), the relative frontal width (66.5–81.0 versus 60.8–63.5), the relative angled subocular height (0.803–0.952 versus 0.669–0.750), and the relative angled subocular width (2.01–2.44 versus 2.61–2.82). From *P. oreistes*, we distinguish *P. psychonothes* by the relative nasal height (1.12–1.32 versus 0.878–1.06) and the relative nasal width (1.68–1.94 versus 1.37–1.65). From *P. saonae*, we distinguish *P. psychonothes* by the dorsal pattern (irregular dots/dots in series/dots in chevrons versus absent), the relative postmental width (2.46–3.34 versus 2.43), the relative largest supraocular width (1.92–2.68 versus 2.77), the relative nasal height (1.12–1.32 versus 1.01), and the relative distance between the eye and naris (4.00–5.62 versus 6.43). From *P. semitaeniatus* **sp. nov.**,

we distinguish *P. psychonothes* by the relative rostral height (1.80–2.32 versus 2.41–2.63), the relative head width (68.4–78.6 versus 58.8–63.8), the relative nasal height (1.12–1.32 versus 1.08), the relative angled subocular height (0.803–0.952 versus 0.654), the relative angled subocular width (2.01–2.44 versus 2.62), and the relative nasal width (1.68–1.94 versus 1.51). From *P. unicolor* **sp. nov.**, we distinguish *P. psychonothes* by the dorsal pattern (irregular dots/dots in series/dots in chevrons versus absent), the adult SVL (70.9–97.2 versus 67.6), the total lamellae on one hand (37–44 versus 48), the total strigae on ten scales (172–244 versus 144), the relative length of digits on one hindlimb (26.5–33.1 versus 36.8), the relative largest supraocular width (1.92–2.68 versus 3.12), the relative longest finger length (4.89–5.81 versus 6.65), the relative frontal width (66.5–81.0 versus 58.2), the relative angled subocular width (2.01–2.44 versus 2.90), and the relative nasal width (1.68–1.94 versus 2.00).

Description of holotype. MCZ R-77156. An adult female; SVL 87.2 mm; tail nearly cylindrical, broken in life midway, regenerated, 62.0 mm (71.1% SVL); axilla-to-groin distance 52.5 mm (60.2% SVL); forelimb length 17.4 mm (20.0% SVL); hindlimb length 24.4 mm (28.0% SVL); head length 13.9 mm (15.9% SVL); head width 9.51 mm (10.9% SVL); head width 68.4% head length; diameter of orbit 2.39 mm (2.74% SVL); horizontal diameter of ear opening 0.93 mm (1.07% SVL); vertical diameter of ear opening 0.69 mm (0.791% SVL); length of all toes on one foot 24.7 mm (28.3% SVL); shortest distance between angled subocular and lip 0.44 mm (0.505% SVL); shortest distance between the ocular and auricular openings 6.09 mm (6.98% SVL); longest finger length 4.81 mm (5.52% SVL); largest supraocular width 1.67 mm (1.92% SVL); cloacal width 7.22 mm (8.28% SVL); mental width 2.54 mm (2.91% SVL); postmental width 2.38 mm (2.73% SVL); prefrontal width 3.39 mm (3.89% SVL); relative frontal width 73.1% frontal length; nasal height 1.15 mm (1.32% SVL); angled subocular height 0.83 mm (0.952% SVL); shortest distance between the eye and naris 3.49 mm (4.00% SVL); canthal iii width 1.01 mm (1.16% SVL); angled subocular width 1.97 mm (2.26% SVL); nasal width 1.69 mm (1.94% SVL); rostral 2.32X as wide as high, visible from above, not in contact with nasals, in contact with 1st supralabial and anterior internasal (left)/(right); anterior internasals are narrower than posterior ones; frontonasals and prefrontal fused into a single large plate with a slightly concave posterior margin, wider than long and divided into two scales, bordered by posterior internasals, 1st loreals, 1st median oculars, and the frontal; frontal longer than wide; a pair of frontoparietals, separated by the posterior prolongation of the frontal and the interparietal plate; interparietal plate smaller than parietals and separating them, posteriorly touching the interoccipital, which is wider than long; parietal separated from supraoculars by 1st and 2nd temporals and frontoparietal (left)/(right); nasal single; nostril above suture between 1st and 2nd supralabials (left)/(right); 1 postnasal (left)/(right); 2 loreals (left)/(right); 1st loreal higher than wide (left)/(right), in contact with postnasal, posterior internasal, prefrontal/frontonasal complex, 1st median ocular, canthal iii, 2nd loreal, and 3rd–4th supralabials (left)/(right); 2nd loreal shorter than 1st, approximately as high as wide (left)/(right), excluded from contact with supraocular by canthal iii (left)/(right); final loreal posteriorly bordering the lower preocular (left)/upper and lower preoculars (right); canthal iii wider than high (left)/(right), contacting 1st median ocular, anterior supraciliary, upper and lower preoculars, and 1st and 2nd loreals (left)/1st median ocular, anterior supraciliary, upper preocular, and 1st and 2nd loreals (right); 9 median oculars (left)/(right), 1st contacting the prefrontal (left)/(right); 1 upper preocular (left)/(right); an irregular anterior supraciliary (left)/(right); 6 (left)/5 (right) lateral oculars; 5 temporals (left)/(right); 2 suboculars (left)/(right); posterior subocular large and elongate (left)/(right); anterior subocular small (left)/(right); 10 supralabials (left)/(right), 6 to level below center of eye (left)/(right); 11 infralabials (left)/(right), 6 to level below center of eye (left)/(right); mental small, followed by a single, larger postmental; 4 pairs of enlarged chin shields, followed by 1 pair of reduced chin shields; 1st pair in contact with one another; 2nd–5th pairs separated by 1–5 scales; 101 transverse rows of dorsal scales from interoccipital to base of tail; 101 transverse rows of ventral scales from mental to vent; 40 scales around midbody; 5 digits; finger lengths 3>4>2>5>1; 10 lamellae under longest finger (left)/(right); 37 total lamellae on one hand; toe lengths 4>3>5>2>1; 16 (17th divided) (left)/15 (right) lamellae under longest toe; keelless and striate dorsal body and caudal scales; smooth-faint striations ventral scales; 188 total strigae counted on ten scales.

Color (in alcohol): dorsal surface of head pale tan, patternless; lateral surfaces of head grading from pale tan to cream with darker brown eye masks and other darker brown areas on the labial scales and sides of neck; dorsal surfaces of the body are gray-red with several darker brown, broken longitudinal paramedian lines that end before the forearms and darker brown spotting that covers the entirety of the back; dorsal surface of tail dark yellow-orange on the regenerated section, patternless; lateral areas grading from dark brown to yellow-cream with darker brown and off-white dots in bars; dorsal surfaces of the limbs are dark brown with paler cream spotting; lateral and ventral areas of the limbs fade to pale cream with some darker brown flecks; ventral surfaces of the head, body, and tail are

pale cream with darker streaking on the throat, darker spots on the tail, and some brown spotting towards the lateral areas.

FIGURE 75. (A–F) *Panolopus psychonothes* (MCZ R-77156, holotype), SVL 87.2 mm.

Variation. The majority of the examined material resembles the holotype in having irregular spots down the back. In some specimens the dots are arranged into broken chevrons. The majority of specimens have patternless heads whereas AMNH 16024 and AMNH 16019 have some darker borders to their head scale plates and several others have dark, irregular areas on their head scales. All specimens except for KU 225644 have markings in the longitudinal paramedian area. Most often these markings are complete longitudinal paramedian lines whereas some specimens have broken longitudinal paramedian lines or dots in series. KU 225651 possesses multiple

longitudinal paramedian lines. All specimens have dots arranged in bars in the lateral band. Measurements and other morphological data for the holotype and other examined material are presented in Table 1.

Distribution. *Panolopus psychonothes* is distributed in the Cordillera Central of the Dominican Republic at elevations of 1180–2360 m (Fig. 50). It has an extent of occurrence of ~280 km^2.

Ecology and conservation. Schwartz (1964) noted that three specimens were found under rocks in pastures or cut over and burned mountainsides. "When exposed by turning rocks, the lizards were so cold that it was a simple matter to collect them."

We consider the conservation status of *Panolopus psychonothes* to be Endangered B1ab(iii), based on IUCN Redlist criteria (IUCN 2023). It is likely a common species tolerant of some habitat disturbance, based on what is known of most species of *Panolopus*. However, it has a very small distribution, which is a concern. It also faces a primary threat of habitat destruction resulting from deforestation, especially given its distribution in the highly developed areas around Constanza. A secondary threat is predation from introduced mammals, including the mongoose and black rats. Studies are needed to determine the health and extent of remaining populations and better understand the threats to the survival of the species.

Reproduction. No data on reproduction are available for this species.

Etymology. The species name (*psychonothes*) means "torpid from the cold," in reference to the lethargy of the type specimens, which were easily collected from under rocks on a cold mountainside.

Remarks. Previously considered to be a subspecies of *Panolopus costatus*, we consider *P. psychonothes* to be a full species based on the morphological differences reported herein. *Panolopus psychonothes* and *P. chalcorhabdus* cannot be morphologically separated based on our standard suite of characters; however, they can be separated by the angled subocular width divided by the angled subocular height (2.37–2.72 [n=5] versus 2.77–3.28 [n=5]).

Additional museum specimens catalogued as *P. costatus* from within the distribution of *P. psychonothes* should be examined to determine if they are members of this species. *Panolopus psychonothes* is not included in our genetic dataset and future studies should be conducted using genetic or genomic data from this species.

Panolopus saonae (Schwartz 1971b)

Saona Forest Lizard
(Fig. 76)

Diploglossus costatus saonae Schwartz, 1971b:161. Holotype: CM 52285, collected by Sixto J. Incháustegui and locals on Isla Saona, La Altagracia province, Dominican Republic, in December 1968 (18.130, -68.736; 1 m).
Celestus costatus saonae—Schwartz & Henderson, 1988:96.
Celestus costatus saonae—Schwartz & Henderson, 1991:367.
Celestus costatus saonae—Hedges *et al.*, 2019:16.
Panolopus costatus saonae—Schools & Hedges, 2021:230.

Material examined (n=3). DOMINICAN REPUBLIC. La Altagracia. Saona Island. CM 52285, Sixto J. Incháustegui and locals, 0.5 km W Mano Juan, 29 December 1968; KU 226020, 225036, 0.5 km W Mano Juan, 29 December 1968.

Diagnosis. *Panolopus saonae* has (1) a dorsal pattern of absent, (2) head markings absent, (3) markings in the longitudinal paramedian area absent, (4) dots arranged in bars in the lateral band absent/present, (5) an adult SVL of 90.9–98.3 mm, (6) ventral scale rows, 92–95, (7) midbody scale rows, 35–39, (8) total lamellae on one hand, 40–42, (9) total strigae on ten scales, 212–284, (10) relative length of all digits on one hindlimb, 26.5–29.8 %, (11) relative distance between the angled subocular and mouth, 0.517–0.630 %, (12) relative eye length, 3.06–3.20 %, (13) relative forelimb length, 19.0–20.2 %, (14) relative ear width, 0.880–1.35 %, (15) relative rostral height, 2.15–2.46 %, (16) relative head length, 15.4–17.5 %, (17) relative mental width, 1.52 %, (18) relative postmental width, 2.43 %, (19) relative cloacal width, 8.20 %, (20) relative prefrontal width, 4.14 %, (21) relative largest supraocular width, 2.77 %, (22) relative longest finger length, 5.01 %, (23) relative distance between the ear and eye, 7.63 %, (24) relative head width, 73.5 %, (25) relative frontal width, 72.5 %, (26) relative nasal height, 1.01 %, (27) relative angled subocular height, 0.847 %, (28) relative distance between the eye and naris, 6.43 %, (29) relative canthal iii length, 1.99 %, (30) relative angled subocular width, 2.31 %, and (31) relative nasal length, 1.69 %. No genetic data are available to estimate the species stem or crown time.

FIGURE 76. (A–F) *Panolopus saonae* (CM 52285, holotype), SVL 90.9 mm.

Panolopus saonae has a larger relative eye to naris distance (6.43) than all other species of the genus. From *Panolopus aenetergum*, we distinguish *P. saonae* by the dorsal pattern (absent versus irregular dots), the ventral scale rows (92–95 versus 80–86), the relative distance between angled subocular and mouth (0.517–0.630 versus 0.717), and the relative eye length (3.06–3.20 versus 3.34). From *P. aporus*, we distinguish *P. saonae* by the relative mental width (1.52 versus 1.72–2.08), the relative prefrontal width (4.14 versus 4.18–4.53), the relative nasal height (1.01 versus 1.08–1.23), the relative distance between the eye and naris (6.43 versus 4.69–5.44), the relative width of canthal iii (1.99 versus 1.85–1.96), and the relative angled subocular width (2.31 versus 2.32–2.73). From *P. chalcorhabdus*, we distinguish *P. saonae* by the dorsal pattern (absent versus absent/irregular flecks/irregular dots),

the relative length of digits on one hindlimb (26.5–29.8 versus 31.3–36.0), the relative forelimb length (19.0–20.2 versus 20.4–23.7), the relative prefrontal width (4.14 versus 4.37–4.93), the relative longest finger length (5.01 versus 5.29–6.97), the relative distance between the eye and naris (6.43 versus 4.93–5.62), and the relative angled subocular width (2.31 versus 2.36–2.71). From *P. costatus*, we distinguish *P. saonae* by the total lamellae on one hand (40–42 versus 49–58), the relative length of digits on one hindlimb (26.5–29.8 versus 31.5–37.8), the relative mental width (1.52 versus 1.66–2.00), the relative longest finger length (5.01 versus 5.53–6.66), the relative frontal width (72.5 versus 56.2–67.4), the relative nasal height (1.01 versus 1.02–1.28), the relative distance between the eye and naris (6.43 versus 5.08–5.50), the relative width of canthal iii (1.99 versus 1.82–1.90), and the relative angled subocular width (2.31 versus 2.36–2.81). From *P. curtissi*, we distinguish *P. saonae* by the adult SVL (90.9–98.3 versus 64.1–85.5), the total lamellae on one hand (40–42 versus 32–39), the relative mental width (1.52 versus 1.60–2.09), the relative longest finger length (5.01 versus 3.59–4.54), the relative nasal height (1.01 versus 1.04–1.25), the relative distance between the eye and naris (6.43 versus 4.02–5.03), and the relative width of canthal iii (1.99 versus 1.75–1.93). From *P. diastatus*, we distinguish *P. saonae* by the adult SVL (90.9–98.3 versus 66.1–83.7), the relative cloacal width (8.20 versus 7.15–8.06), the relative largest supraocular width (2.77 versus 1.88–2.57), the relative longest finger length (5.01 versus 3.48–4.87), and the relative distance between the eye and naris (6.43 versus 4.06–4.94). From *P. emys*, we distinguish *P. saonae* by the adult SVL (90.9–98.3 versus 99.0–113), the relative cloacal width (8.20 versus 8.24–8.96), the relative longest finger length (5.01 versus 5.15–5.83), and the relative distance between the eye and naris (6.43 versus 4.37–5.19). From *P. hylonomus*, we distinguish *P. saonae* by the adult SVL (90.9–98.3 versus 59.3–76.5), the relative mental width (1.52 versus 1.63–2.11), the relative postmental width (2.43 versus 2.67–2.89), the relative prefrontal width (4.14 versus 4.23–4.87), the relative head width (73.5 versus 73.8–76.4), and the relative distance between the eye and naris (6.43 versus 4.03–4.98). From *P. lanceolatus* **sp. nov.**, we distinguish *P. saonae* by the longitudinal paramedian lines (absent versus present), the relative largest supraocular width (2.77 versus 2.20–2.71), the relative frontal width (72.5 versus 63.1–72.1), the relative distance between the eye and naris (6.43 versus 4.58–5.05), and the relative angled subocular width (2.31 versus 2.38–3.09). From *P. lapierrae* **sp. nov.**, we distinguish *P. saonae* by the adult SVL (90.9–98.3 versus 72.6–88.3), and the relative rostral height (2.15–2.46 versus 1.86–2.06). From *P. leionotus*, we distinguish *P. saonae* by the total lamellae on one hand (40–42 versus 43–48), the relative mental width (1.52 versus 1.67–2.02), the relative largest supraocular width (2.77 versus 1.94–2.50), the relative distance between the eye and naris (6.43 versus 4.46–5.61), the relative width of canthal iii (1.99 versus 1.55–1.89), and the relative angled subocular width (2.31 versus 2.48–2.95). From *P. marcanoi*, we distinguish *P. saonae* by the dorsal pattern (absent versus irregular dots/dots in chevrons), the head markings (absent versus present), the longitudinal paramedian lines (absent versus present), the adult SVL (90.9–98.3 versus 64.6–85.8), the relative mental width (1.52 versus 1.75–2.33), the relative postmental width (2.43 versus 2.46–3.24), the relative prefrontal width (4.14 versus 4.19–5.19), the relative nasal height (1.01 versus 1.07–1.28), the relative angled subocular height (0.847 versus 0.505–0.793), and the relative distance between the eye and naris (6.43 versus 4.68–5.82). From *P. melanchrous*, we distinguish *P. saonae* by the longitudinal paramedian lines (absent versus present), the total lamellae on one hand (40–42 versus 47–58), the relative length of digits on one hindlimb (26.5–29.8 versus 30.7–41.3), the relative postmental width (2.43 versus 2.71–3.38), the relative prefrontal width (4.14 versus 4.21–5.06), the relative longest finger length (5.01 versus 5.76–7.09), the relative frontal width (72.5 versus 61.3–71.4), the relative nasal height (1.01 versus 0.897–0.952), the relative distance between the eye and naris (6.43 versus 4.89–5.59), and the relative width of canthal iii (1.99 versus 1.67–1.94). From *P. neiba*, we distinguish *P. saonae* by the dorsal pattern (absent versus irregular flecks/dots in chevrons), the total lamellae on one hand (40–42 versus 45–49), the relative distance between angled subocular and mouth (0.517–0.630 versus 0.670–0.747), the relative mental width (1.52 versus 1.66–2.36), the relative prefrontal width (4.14 versus 4.41–5.49), the relative longest finger length (5.01 versus 5.61–6.66), the relative distance between the eye and naris (6.43 versus 4.51–5.01), the relative width of canthal iii (1.99 versus 1.51–1.95), and the relative angled subocular width (2.31 versus 2.34–2.83). From *P. nesobous*, we distinguish *P. saonae* by the dorsal pattern (absent versus irregular dots/dots in series), the longitudinal paramedian lines (absent versus present), the total lamellae on one hand (40–42 versus 50–59), the relative length of digits on one hindlimb (26.5–29.8 versus 35.1), the relative eye length (3.06–3.20 versus 3.41–3.63), the relative forelimb length (19.0–20.2 versus 23.3–25.1), the relative ear width (0.880–1.35 versus 1.39–1.60), and the relative head length (15.4–17.5 versus 17.9–19.8). From *P. oreistes*, we distinguish *P. saonae* by the dorsal pattern (absent versus irregular dots/dots in series/dots in chevrons), the longitudinal paramedian lines (absent versus present), the relative length of digits on one

hindlimb (26.5–29.8 versus 31.2–40.1), the relative mental width (1.52 versus 1.54–1.90), the relative prefrontal width (4.14 versus 4.18–4.96), the relative longest finger length (5.01 versus 5.27–7.23), the relative distance between the eye and naris (6.43 versus 5.01–5.63), and the relative nasal width (1.69 versus 1.37–1.65). From *P. psychonothes*, we distinguish *P. saonae* by the dorsal pattern (absent versus irregular dots/dots in series/dots in chevrons), the relative postmental width (2.43 versus 2.46–3.34), the relative largest supraocular width (2.77 versus 1.92–2.68), the relative nasal height (1.01 versus 1.12–1.32), and the relative distance between the eye and naris (6.43 versus 4.00–5.62). From *P. semitaeniatus* **sp. nov.**, we distinguish *P. saonae* by the SVL (90.9–98.3 versus 77.4–84.1), the total strigae on ten scales (212–284 versus 174–204), the relative length of digits on one hindlimb (26.5–29.8 versus 30.4–34.6), the relative distance between angled subocular and mouth (0.517–0.630 versus 0.666–0.808), the relative eye length (3.06–3.20 versus 3.27–3.61), the relative forelimb length (19.0–20.2 versus 21.3–23.8), the relative ear width (0.880–1.35 versus 1.90–2.30), the relative mental width (1.52 versus 1.69–2.09), the relative postmental width (2.43 versus 2.50–2.97), the relative prefrontal width (4.14 versus 4.38–4.94), the relative longest finger length (5.01 versus 5.17–6.05), and the relative head width (73.5 versus 58.8–63.8). From *P. unicolor* **sp. nov.**, we distinguish *P. saonae* by the longitudinal paramedian lines (absent versus present), the adult SVL (90.9–98.3 versus 67.6), the midbody scale rows (35–39 versus 40), the total strigae on ten scales (212–284 versus 144), the relative eye length (3.06–3.20 versus 3.38), the relative ear width (0.880–1.35 versus 1.60), and the relative head length (15.4–17.5 versus 17.8).

Description of holotype. CM 52285. An adult female; SVL 90.9 mm; tail nearly cylindrical, broken in life midway, regenerated, 83.8 mm (92.2% SVL); axilla-to-groin distance 52.4 mm (57.6% SVL); forelimb length 18.4 mm (20.2% SVL); hindlimb length 28.0 mm (30.8% SVL); head length 15.9 mm (17.5% SVL); head width 11.7 mm (12.9% SVL); head width 73.6% HL; diameter of orbit 2.78 mm (3.06% SVL); horizontal diameter of ear opening 0.80 mm (0.880% SVL); vertical diameter of ear opening 1.23 mm (1.35% SVL); length of all toes on one foot 27.1 mm (29.8% SVL); shortest distance between angled subocular and lip 0.47 mm (0.517% SVL); shortest distance between the ocular and auricular openings 6.94 mm (7.63% SVL); longest finger length 4.55 mm (5.01% SVL); largest supraocular width 2.52 mm (2.77% SVL); cloacal width 7.45 mm (8.20% SVL); mental width 1.38 mm (1.52% SVL); postmental width 2.21 mm (2.43% SVL); prefrontal width 3.76 mm (4.14% SVL); frontal width 72.5% frontal length; angled subocular width 2.10 mm (2.31% SVL); nasal width 1.54 mm (1.69% SVL); rostral 2.15X as wide as high, visible from above, not in contact with nasals, in contact with 1st supralabial and anterior internasal (left)/(right); anterior internasals are narrower than posterior ones; frontonasals and prefrontal fused into a single large plate with a slightly concave posterior margin, wider than long, bordered by posterior internasals, 1st loreals, 1st median oculars, and the frontal; frontal longer than wide; a pair of frontoparietals, separated by the posterior prolongation of the frontal and the interparietal plate; interparietal plate smaller than parietals and separating them, posteriorly touching the interoccipital, which is wider than long; parietal separated from supraoculars by 1st and 2nd temporals and frontoparietal (left)/1st and 2nd temporals (missing) and frontoparietal (right); nasal single; nostril above suture between 1st and 2nd supralabials (left)/(right); 1 postnasal (left)/(right); 2 loreals (left)/(right); 1st loreal higher than wide (left)/(right), in contact with postnasal, posterior internasal, prefrontal/frontonasal complex, 1st median ocular, canthal iii, 2nd loreal, and 3rd–4th supralabials (left)/(right); 2nd loreal shorter than 1st, approximately as high as wide (left)/(right), excluded from contact with supraocular by canthal iii (left)/(right); final loreal posteriorly bordering the lower and upper preoculars (left)/(right); canthal iii wider than high (left)/(right), contacting 1st median ocular, anterior supraciliary upper preocular, and 1st and 2nd loreals (left)/(right); 9 (left)/ missing several(right) median oculars, 1st contacting the prefrontal (left)/(right); 1 upper preocular (left)/(right); an irregular anterior supraciliary (left)/(right); 6 lateral oculars (left); 5 temporals (left); 2 suboculars (left)/(right); posterior subocular large and elongate (left)/(right); anterior subocular small (left)/(right); 9 supralabials (left)/(right), 6 to level below center of eye (left)/(right); 10 (left)/8 (right) infralabials, 6 to level below center of eye (left)/(right); mental small, followed by a single, larger postmental; 4 pairs of enlarged chin shields (damage on the left and several missing); 1st pair in contact with one another; 2nd–4th pairs separated by 1–3 scales; 92 transverse rows of dorsal scales from interoccipital to base of tail; 92 transverse rows of ventral scales from mental to vent; 35 scales around midbody; 5 digits; finger lengths 3>4>2>5>1; 10 lamellae under longest finger (left)/(right); 40 total lamellae on one hand; toe lengths 4>3>5>2>1; 17 lamellae under longest toe (left)/(right); keelless and striate dorsal body and caudal scales; smooth to faintly striated ventral scales; 212 total strigae counted on ten scales.

Color (in alcohol): dorsal surface of head medium brown, patternless; lateral surfaces of head grading from medium brown to cream with darker brown eye masks and markings on the labial scales; dorsal surfaces of the

body are medium brown, patternless; dorsal surface of tail the same as the body with several darker flecks; lateral areas grade from medium brown to cream with a darker brown lateral band with darker brown and off-white dots arranged in bars; dorsal surfaces of the limbs are darker brown with paler cream mottling; lateral and ventral areas of the limbs cream with several darker brown flecks; ventral surfaces of the head, body, and tail are cream with several darker brown flecks on the chest.

Variation. The material examined resembles the holotype in both the lack of a dorsal pattern and markings on the head scales. Only KU 226020 lacks dots arranged in bars in the lateral band. Measurements and other morphological data for the holotype and other examined material are presented in Table 1.

Distribution. *Panolopus saonae* is distributed on Isla Saona in southeastern Dominican Republic (Fig. 50). The elevational range of the island is 0–50 m.

Ecology and conservation. No ecological data are associated with this species. We consider the conservation status of *Panolopus saonae* to be Least Concern, based on IUCN Redlist criteria (IUCN 2023). It is likely a common species tolerant of some habitat disturbance, based on what is known of most species of *Panolopus*. Saona Island is a nature reserve with a currently reduced threat from human-caused habitat disturbance.

Reproduction. No data on reproduction are available for this species.

Etymology. The species name (*saonae*) is in reference to the island where it occurs.

Remarks. Previously, members of this species were considered to be a subspecies of *Panolopus costatus*. Herein, we recognize *P. saonae* to be a full species based on diagnostic morphological characteristics. *Panolopus saonae* is not included in our genetic dataset and future studies should be conducted using genetic or genomic data from this species.

***Panolopus semitaeniatus* sp. nov.**
Haitian Half-striped Forest Lizard
(Fig. 77–78)

Panolopus costatus—Schools & Hedges, 2021:230 (part).
Panolopus costatus leionotus—Schools & Hedges, 2021:230 (part).
Panolopus costatus—Landestoy *et al.*, 2022:205 (part).

Holotype. ANSP 38569, an adult female from the summit of Morne Boeuf, Artibonite Department, Haiti, collected by S. Blair Hedges, Tiffany Cloud, Miguel Landestoy, and Marcos Rodriguez on 23 November 2011 (19.07239, -72.25021; 1,780 m).

Paratypes (n=7). HAITI. Artibonite. ANSP 38570–72, S. Blair Hedges, Tiffany Cloud, Miguel Landestoy, and Marcos Rodriguez, the summit of Morne Boeuf, 23 November 2011; MCZ R-51434, Anthony Curtiss, Trou Farbour, 1–30 November 1942; SBH 269891–2, 269895, S. Blair Hedges, Tiffany Cloud, Miguel Landestoy, and Marcos Rodriguez, Morne Boeuf, 23 November 2011.

Diagnosis. *Panolopus semitaeniatus* **sp. nov.** has (1) a dorsal pattern of absent/irregular dots/dots in chevrons, (2) head markings absent/present, (3) markings in the longitudinal paramedian area absent/present, (4) dots arranged in bars in the lateral band absent/present, (5) an adult SVL of 84.1–109 mm, (6) ventral scale rows, 81–101, (7) midbody scale rows, 36–41, (8) total lamellae on one hand, 34–51, (9) total strigae on ten scales, 156–204, (10) relative length of all digits on one hindlimb, 30.4–37.0 %, (11) relative distance between the angled subocular and mouth, 0.666–0.826 %, (12) relative eye length, 3.38–3.77 %, (13) relative forelimb length, 20.8–25.6 %, (14) relative ear width, 1.47–1.90 %, (15) relative rostral height, 1.67–1.72 %, (16) relative head length, 16.3–17.9 %, (17) relative mental width, 1.65–1.75 %, (18) relative postmental width, 2.50–3.10 %, (19) relative cloacal width, 8.22–9.65 %, (20) relative prefrontal width, 4.38–4.81 %, (21) relative largest supraocular width, 2.59–2.96 %, (22) relative longest finger length, 5.17–6.72 %, (23) relative distance between the ear and eye, 6.69–7.42 %, (24) relative head width, 63.8–74.6 %, (25) relative frontal width, 71.0–76.5 %, (26) relative nasal height, 1.04–1.18 %, (27) relative angled subocular height, 0.654–0.844 %, (28) relative distance between the eye and naris, 4.61–5.61 %, (29) relative canthal iii length, 1.80–1.98 %, (30) relative angled subocular width, 2.45–2.71 %, and (31) relative nasal length, 1.46–1.62 %. The species stem time is 0.74 Ma and the species crown time is 0.01 Ma (Fig. 4).

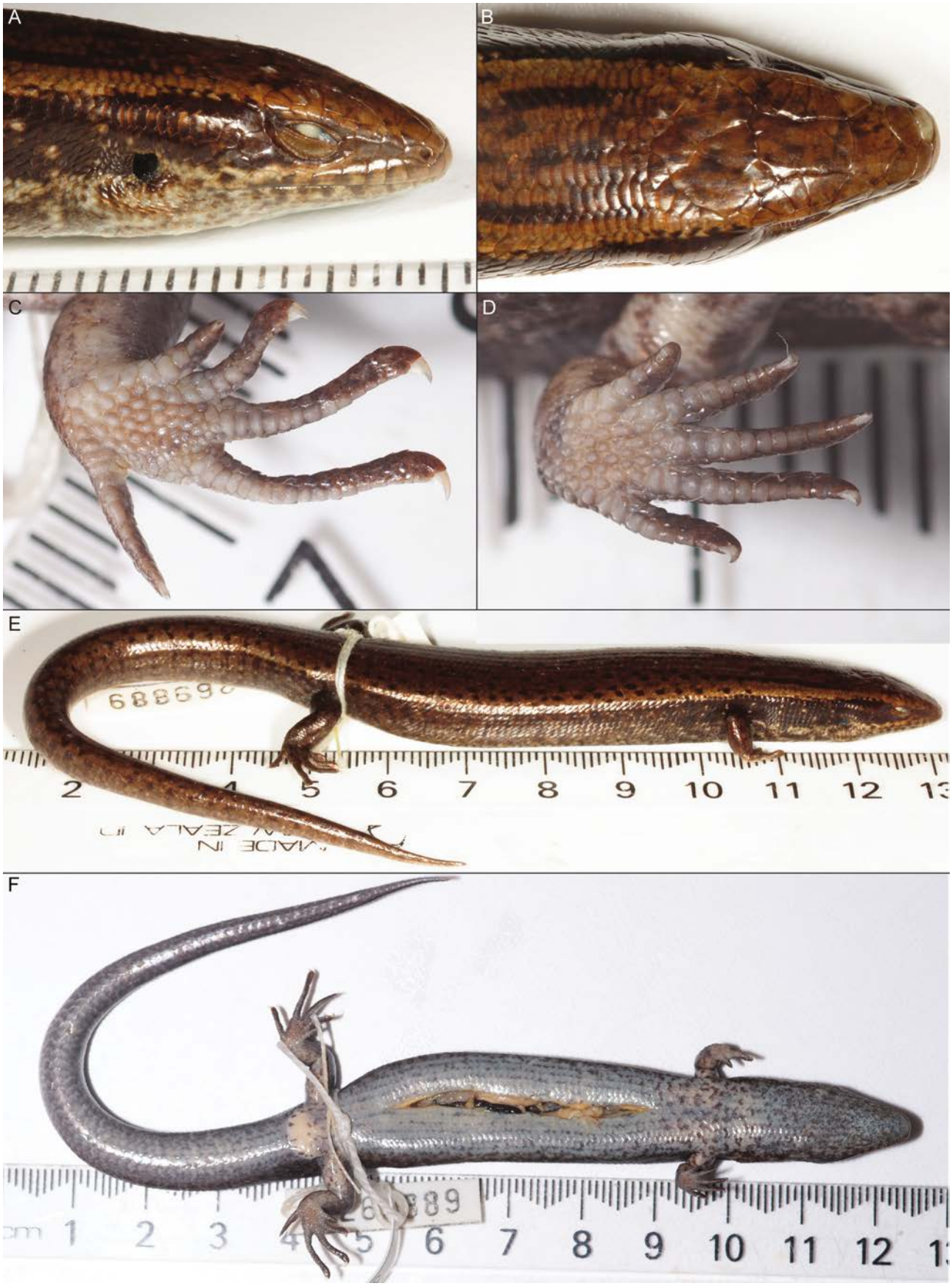

FIGURE 77. (A–F) *Panolopus semitaeniatus* **sp. nov.** (ANSP 38569, holotype), SVL 84.1 mm.

FIGURE 78. *Panolopus semitaeniatus* **sp. nov.** (ANSP 38570, SBH 269890), in life. From the summit of Morne Boeuf, Artibonite Department, Haiti. Photo by SBH.

Panolopus semitaeniatus **sp. nov.** has a smaller relative head width (58.8–63.8) than all other species of the genus. From *Panolopus aenetergum*, we distinguish *P. semitaeniatus* **sp. nov.** by the total strigae on ten scales (174–204 versus 267), the relative length of digits on one hindlimb (30.4–34.6 versus 26.8), the relative forelimb length (21.3–23.8 versus 20.6), the relative ear width (1.90–2.30 versus 1.29), the relative mental width (1.69–2.09 versus 1.63), the relative cloacal width (8.08–8.23 versus 7.60), the relative prefrontal width (4.38–4.94 versus 4.15), the relative largest supraocular width (2.59–3.32 versus 2.49), the relative longest finger length (5.17–6.05 versus 4.83), the relative distance between the ear and eye (6.64–7.90 versus 8.40), the relative head width (58.8–63.8 versus 76.4), the relative frontal width (63.6–76.5 versus 88.2), and the relative angled subocular height (0.654 versus 1.08). From *P. aporus*, we distinguish *P. semitaeniatus* **sp. nov.** by the relative ear width (1.90–2.30 versus 1.06–1.88), the relative rostral height (2.41–2.63 versus 2.01–2.40), the relative head width (58.8–63.8 versus 71.4–83.2), the relative distance between the eye and naris (4.61 versus 4.69–5.44), the relative width of canthal iii (1.80 versus 1.85–1.96), and the relative nasal width (1.51 versus 1.56–1.78). From *P. chalcorhabdus*, we distinguish *P. semitaeniatus* **sp. nov.** by the relative ear width (1.90–2.30 versus 1.26–1.65), the relative rostral height (2.41–2.63 versus 1.85–2.24), the relative head width (58.8–63.8 versus 65.0–76.3), the relative angled subocular height (0.654 versus 0.739–0.854), the relative distance between the eye and naris (4.61 versus 4.93–5.62), the relative width of canthal iii (1.80 versus 1.98–2.05), and the relative nasal width (1.51 versus 1.70–2.01). From *P. costatus*, we distinguish *P. semitaeniatus* **sp. nov.** by the total lamellae on one hand (34–46 versus 49–58), the relative rostral height (2.41–2.63 versus 1.78–2.26), the relative head width (58.8–63.8 versus 68.3–76.8), the relative distance between the eye and naris (4.61 versus 5.08–5.50), the relative width of canthal iii (1.80 versus 1.82–1.90), and the relative nasal width (1.51 versus 1.58–1.74). From *P. curtissi*, we distinguish *P. semitaeniatus* **sp. nov.** by the relative length of digits on one hindlimb (30.4–34.6 versus 20.8–28.1), the relative distance between angled subocular and mouth (0.666–0.808 versus 0.393–0.587), the relative forelimb length (21.3–23.8 versus 15.1–20.5), the relative longest finger length (5.17–6.05 versus 3.59–4.54), the relative head width (58.8–63.8 versus 68.3–78.1), and the relative angled subocular height (0.654 versus 0.708–1.19). From *P. diastatus*, we distinguish *P. semitaeniatus* **sp. nov.** by the relative length of digits on one hindlimb (30.4–34.6 versus 21.5–27.4), the relative distance between angled subocular and mouth (0.666–0.808 versus 0.00–0.614), the relative forelimb length (21.3–23.8 versus 16.2–20.1), the relative ear width (1.90–2.30 versus 0.667–1.43), the relative cloacal width (8.08–8.23 versus 7.15–8.06), the relative largest supraocular width (2.59–3.32 versus 1.88–2.57), the relative longest finger length (5.17–6.05 versus 3.48–4.87), and the relative head width (58.8–63.8 versus 69.4–74.8). From *P. emys*, we distinguish *P.*

semitaeniatus **sp. nov.** by the SVL (77.4–84.1 versus 99.0–113), the total strigae on ten scales (174–204 versus 238–311), the relative ear width (1.90–2.30 versus 0.756–1.75), the relative rostral height (2.41–2.63 versus 2.10–2.37), the relative cloacal width (8.08–8.23 versus 8.24–8.96), the relative prefrontal width (4.38–4.94 versus 3.99–4.36), the relative head width (58.8–63.8 versus 71.1–78.7), and the relative angled subocular height (0.654 versus 0.696–0.981). From *P. hylonomus*, we distinguish *P. semitaeniatus* **sp. nov.** by the SVL (77.4–84.1 versus 59.3–76.5), the relative length of digits on one hindlimb (30.4–34.6 versus 22.8–28.2), the relative forelimb length (21.3–23.8 versus 17.1–20.7), the relative rostral height (2.41–2.63 versus 1.72–2.28), the relative head width (58.8–63.8 versus 73.8–76.4), the relative angled subocular height (0.654 versus 0.690–1.13), and the relative width of canthal iii (1.80 versus 1.95–2.03). From *P. lanceolatus* **sp. nov.**, we distinguish *P. semitaeniatus* **sp. nov.** by the relative ear width (1.90–2.30 versus 0.770–1.35), the relative rostral height (2.41–2.63 versus 1.78–2.28), the relative head width (58.8–63.8 versus 68.0–77.6), and the relative nasal height (1.08 versus 0.904–1.06). From *P. lapierrae* **sp. nov.**, we distinguish *P. semitaeniatus* **sp. nov.** by the total strigae on ten scales (174–204 versus 228–231), the relative forelimb length (21.3–23.8 versus 18.5–20.6), the relative ear width (1.90–2.30 versus 0.929–1.58), the relative rostral height (2.41–2.63 versus 1.86–2.06), the relative cloacal width (8.08–8.23 versus 8.55–8.81), the relative longest finger length (5.17–6.05 versus 4.49–4.55), the relative head width (58.8–63.8 versus 77.7–78.1), and the relative frontal width (63.6–76.5 versus 77.6–79.0). From *P. leionotus*, we distinguish *P. semitaeniatus* **sp. nov.** by the SVL (77.4–84.1 versus 86.3–105), the relative rostral height (2.41–2.63 versus 1.79–2.36), the relative largest supraocular width (2.59–3.32 versus 1.94–2.50), the relative head width (58.8–63.8 versus 67.3–82.9), the relative angled subocular height (0.654 versus 0.750–1.33), and the relative nasal width (1.51 versus 1.59–2.01). From *P. marcanoi*, we distinguish *P. semitaeniatus* **sp. nov.** by the relative rostral height (2.41–2.63 versus 1.96–2.38), the relative head width (58.8–63.8 versus 68.4–77.9), the relative distance between the eye and naris (4.61 versus 4.68–5.82), and the relative nasal width (1.51 versus 1.64–1.96). From *P. melanchrous*, we distinguish *P. semitaeniatus* **sp. nov.** by the SVL (77.4–84.1 versus 93.2–124), the total lamellae on one hand (34–46 versus 47–58), the relative head width (58.8–63.8 versus 68.3–83.6), the relative nasal height (1.08 versus 0.897–0.952), the relative angled subocular height (0.654 versus 0.680–0.856), and the relative distance between the eye and naris (4.61 versus 4.89–5.59). From *P. neiba*, we distinguish *P. semitaeniatus* **sp. nov.** by the relative rostral height (2.41–2.63 versus 1.75–2.23), the relative head width (58.8–63.8 versus 67.9–78.4), the relative angled subocular height (0.654 versus 0.713–0.885), and the relative nasal width (1.51 versus 1.67–1.92). From *P. nesobous*, we distinguish *P. semitaeniatus* **sp. nov.** by the total lamellae on one hand (34–46 versus 50–59), the relative length of digits on one hindlimb (30.4–34.6 versus 35.1), the relative ear width (1.90–2.30 versus 1.39–1.60), the relative rostral height (2.41–2.63 versus 2.26–2.38), the relative longest finger length (5.17–6.05 versus 6.19–6.33), the relative distance between the ear and eye (6.64–7.90 versus 7.91–10.0), the relative head width (58.8–63.8 versus 71.2–76.4), and the relative frontal width (63.6–76.5 versus 60.8–63.5). From *P. oreistes*, we distinguish *P. semitaeniatus* **sp. nov.** by the relative ear width (1.90–2.30 versus 0.558–1.79), the relative head width (58.8–63.8 versus 66.1–85.0), the relative nasal height (1.08 versus 0.878–1.06), and the relative angled subocular height (0.654 versus 0.737–0.978), the relative distance between the eye and naris (4.61 versus 5.01–5.63). From *P. psychonothes*, we distinguish *P. semitaeniatus* **sp. nov.** by the relative rostral height (2.41–2.63 versus 1.80–2.32), the relative head width (58.8–63.8 versus 68.4–78.6), the relative nasal height (1.08 versus 1.12–1.32), the relative angled subocular height (0.654 versus 0.803–0.952), the relative angled subocular width (2.62 versus 2.01–2.44), and the relative nasal width (1.51 versus 1.68–1.94). From *P. saonae*, we distinguish *P. semitaeniatus* **sp. nov.** by the SVL (77.4–84.1 versus 90.9–98.3), the total strigae on ten scales (174–204 versus 212–284), the relative length of digits on one hindlimb (30.4–34.6 versus 26.5–29.8), the relative distance between angled subocular and mouth (0.666–0.808 versus 0.517–0.630), the relative eye length (3.27–3.61 versus 3.06–3.20), the relative forelimb length (21.3–23.8 versus 19.0–20.2), the relative ear width (1.90–2.30 versus 0.880–1.35), the relative mental width (1.69–2.09 versus 1.52), the relative postmental width (2.50–2.97 versus 2.43), the relative prefrontal width (4.38–4.94 versus 4.14), the relative longest finger length (5.17–6.05 versus 5.01), and the relative head width (58.8–63.8 versus 73.5). From *P. unicolor* **sp. nov.**, we distinguish *P. semitaeniatus* **sp. nov.** by the SVL (77.4–84.1 versus 67.6), the total lamellae on one hand (34–46 versus 48), the total strigae on ten scales (174–204 versus 144), the relative length of digits on one hindlimb (30.4–34.6 versus 36.8), the relative distance between angled subocular and mouth (0.666–0.808 versus 0.533), the relative ear width (1.90–2.30 versus 1.6), the relative cloacal width (8.08–8.23 versus 7.61), the relative longest finger length (5.17–6.05 versus 6.65), the relative head width (58.8–63.8 versus 70.8), and the relative frontal width (63.6–76.5 versus 58.2).

Description of holotype. ANSP 38569. An adult female; SVL 84.1 mm; tail nearly cylindrical, 107 mm (127% SVL); axilla-to-groin distance 46.6 mm (55.4% SVL); forelimb length 17.9 mm (21.3% SVL); hindlimb length 23.6 mm (28.1% SVL); head length 13.7 mm (16.3% SVL); head width 10.2 mm (12.1% SVL); head width 74.5% head length; diameter of orbit 2.84 mm (3.38% SVL); horizontal diameter of ear opening 1.60 mm (1.90% SVL); vertical diameter of ear opening 1.52 mm (1.81% SVL); length of all toes on one foot 25.5 mm (30.3% SVL); shortest distance between angled subocular and lip 0.56 mm (0.666% SVL); shortest distance between the ocular and auricular openings 5.69 mm (6.77% SVL); longest finger length 4.35 mm (5.17% SVL); largest supraocular width 2.18 mm (2.59% SVL); cloacal width 6.91 mm (8.22% SVL); mental width 1.42 mm (1.69% SVL); postmental width 2.10 mm (2.50% SVL); prefrontal width 3.68 mm (4.38% SVL); frontal width 76.5% frontal length; nasal height 0.91 mm (1.08% SVL); angled subocular height 0.55 mm (0.654% SVL); shortest distance between the eye and naris 3.88 mm (4.61% SVL); canthal iii width 1.51 mm (1.80% SVL); angled subocular width 2.20 mm (2.62% SVL); nasal width 1.27 mm (1.51% SVL); rostral 2.27X as wide as high, visible from above, not in contact with nasals, in contact with 1st supralabial and anterior internasal (left)/(right); anterior internasals are narrower than posterior ones; frontonasals and prefrontal fused into a single large plate with a slightly concave posterior margin, wider than long, bordered by posterior internasals, 1st loreals, 1st and 2nd median oculars, and the frontal; frontal much longer than wide; a pair of frontoparietals (left fused with frontal), separated by the posterior prolongation of the frontal and the interparietal plate; interparietal plate smaller than parietals and separating them, posteriorly touching the interoccipital, which is approximately as wide as long; parietal separated from supraoculars by 1st–3rd temporals and frontoparietal (left)/1st and 2nd temporals and frontoparietal (right); nasal single; nostril above suture between 1st and 2nd supralabials (left)/(right); 1 postnasal (left)/(right); 2 loreals (left)/(right); 1st loreal higher than wide (left)/(right), in contact with postnasal, posterior internasal, prefrontal/frontonasal complex, 1st median ocular, canthal iii, 2nd loreal, and 3rd–4th supralabials (left)/(right); 2nd loreal shorter than 1st, wider than high (left)/(right), excluded from contact with supraocular by canthal iii (left)/(right); 2nd loreal posteriorly bordering the upper and lower preoculars (left)/(right); canthal iii wider than high (left)/(right), contacting 1st median ocular, anterior supraciliary, upper preocular, and 1st and 2nd loreals (left)/(right); 10 median oculars (left)/(right), 1st and 2nd contacting the prefrontal (left)/(right); 1 upper preocular (left)/(right); an irregular anterior supraciliary (left)/(right); 6 lateral oculars (left)/(right); 6 (left)/5 (right) temporals; 1 (left)/2 (right) suboculars; posterior subocular large and elongate (left)/(right); anterior subocular small (right); 10 supralabials (left)/(right), 6 to level below center of eye (left)/(right); 10 infralabials (left)/(right), 6 to level below center of eye (left)/(right); mental small, followed by a single, larger postmental; 4 pairs of enlarged chin shields, followed by 1 unpaired chin shield (right); 1st pair in contact with one another anteriorly, posteriorly separated by one scale; 2nd–4th pairs separated by 1–3 scales; 93 transverse rows of dorsal scales from interoccipital to base of tail; 100 transverse rows of ventral scales from mental to vent; 37 scales around midbody; 5 digits; finger lengths 3>4>2>5>1; 11 lamellae under longest finger (left); 45 total lamellae on one hand; toe lengths 4>3>5>2>1; 17 (left)/18 (right) lamellae under longest toe; dorsal body and caudal scales striate, some with a very faint median keel; smooth ventral scales; 204 total strigae counted on ten scales.

Color (in alcohol): dorsal surface of head deep brown with darker brown mottling; lateral surfaces of head grading from deep brown to gray-white with darker brown eye masks and dark brown mottling on every surface; dorsal surfaces of the body are deep brown with two dark brown longitudinal paramedian lines end before the forearms, entire dorsum covered in irregular dark brown spots; dorsal surface of tail the same as the body with the dark brown dots arranged into lines; lateral areas dark brown with some small irregular off-white dots; dorsal surfaces of the limbs are dark brown, with dark gold mottling; lateral and ventral areas of the limbs fade to gray-white with dark brown mottling; ventral surfaces of the head, body, and tail are pale gray with dark brown mottling that is most apparent by the forelimbs and sides of body, disappears on the tail, which is dark gray.

Variation. The majority of the examined material resembles the holotype with a dorsal pattern of irregular dots or flecks. In some specimens these markings are arranged into broken chevrons. MCZ R-51434 is unique in lacking a dorsal pattern. The majority of the examined material has patternless heads except for ANSP 38572, which has darker outlines on heads scale borders, and the holotype, which has irregular, dark markings on its head scales. All specimens except for MCZ R-51434 have markings in the longitudinal paramedian area. These markings range from dots in series to broken longitudinal paramedian lines to complete longitudinal paramedian lines. Measurements and other morphological data for the holotype and other examined material are presented in Table 1.

Distribution. *Panolopus semitaeniatus* **sp. nov.** is known from on and near Morne Boeuf in central Haiti at elevations of 160–1780 m (Fig. 49). It has an extent of occurrence of ~990 km^2.

Ecology and conservation. SBH and team visited Morne Boeuf by helicopter for about 24 hours on 23 November 2011. The specimens were collected in and around rotting logs near the summit of Morne Boeuf. No standing primary forest remained at the time of collection, but it appeared to have been cut down only within a decade or two prior to the visit, and logs from large trees were still present on the rocks and ground. We consider the conservation status of *Panolopus semitaeniatus* **sp. nov.** to be Endangered B1ab(iii), based on IUCN Redlist criteria (IUCN 2023). It faces a primary threat of habitat destruction (deforestation) from agriculture and charcoaling. Secondary threats to this species include predation from introduced predators, including the mongoose and black rats. Studies are needed to determine the health of any remaining populations and threats to the survival of the species. Captive-breeding programs should be considered.

Reproduction. No data on reproduction are available for this species.

Etymology. The species name (*semitaeniatus*) is a feminine adjective derived from the Latin *semi* (half) and *taenia* (ribbon, stripe), hence half-striped, referring to the majority of specimens displaying broken longitudinal paramedian lines or dots in the longitudinal paramedian series as opposed to complete longitudinal paramedian lines.

Remarks. Upon collection, several animals of this species were identified as *Panolopus leionotus*. Others were more generally referred to as *P. costatus*, with no subspecies designation. One, MCZ R-51434, was referred to as *P. costatus curtissi*. Additional museum specimens collected from this region and catalogued as *P. costatus* or *P. curtissi* should be examined to determine if they are members of *P. semitaeniatus* **sp. nov.**

Panolopus semitaeniatus **sp. nov.** is included in our genetic dataset and has significant support in both Bayesian and ML likelihood analyses at the crown node of the species and the stem node that places it as the closest relative to *P. leionotus*. Based on our timetree (Fig. 4), *P. semitaeniatus* **sp. nov.** diverged from its closest relative 0.74 Ma, consistent with typical species of vertebrates (> 0.7 Ma; Hedges *et al.* 2015). We recognize *P. semitaeniatus* **sp. nov.** as a distinct species based on the multiple morphological characters that separate it from its closest relative (*P. leionotus*). *Panolopus semitaeniatus* **sp. nov.** was recovered as conspecific with *Panolopus leionotus* and *Panolopus neiba* in our ASAP analysis.

***Panolopus unicolor* sp. nov.**

Unicolored Forest Lizard
(Fig. 79)

Panolopus curtissi hylonomus—Schools & Hedges, 2021:250 (part).
Panolopus curtissi hylonomus—Schools *et al.* 2022:42 (part).
Panolopus curtissi hylonomus—Landestoy *et al.*, 2022: 222 (part).

Holotype. ANSP 38647, an adult from 14.8 N, 7.8 km SE Cruce de Ocoa on dirt road, at Martinez, near La Palma, San José de Ocoa province, Dominican Republic, collected by Richard Thomas, Manuel Leal, and Herman Dominici on 10 July 1993 (18.46, -70.45; 675 m).

Diagnosis. *Panolopus unicolor* **sp. nov.** has (1) a dorsal pattern of absent, (2) head markings absent, (3) markings in the longitudinal paramedian area present, (4) dots arranged in bars in the lateral band present, (5) an adult SVL of 67.6 mm, (6) ventral scale rows, 93, (7) midbody scale rows, 40, (8) total lamellae on one hand, 48, (9) total strigae on ten scales, 144, (10) relative length of all digits on one hindlimb, 36.8 %, (11) relative distance between the angled subocular and mouth, 0.533 %, (12) relative eye length, 3.38 %, (13) relative forelimb length, 23.5 %, (14) relative ear width, 1.60 %, (15) relative rostral height, 2.23 %, (16) relative head length, 17.8 %, (17) relative mental width, 1.73 %, (18) relative postmental width, 2.80 %, (19) relative cloacal width, 7.61 %, (20) relative prefrontal width, 4.69 %, (21) relative largest supraocular width, 3.12 %, (22) relative longest finger length, 6.65 %, (23) relative distance between the ear and eye, 7.61 %, (24) relative head width, 70.8 %, (25) relative frontal width, 58.2 %, (26) relative nasal height, 1.15 %, (27) relative angled subocular height, 0.814 %, (28) relative distance between the eye and naris, 5.52 %, (29) relative canthal iii length, 1.79v, (30) relative angled subocular width, 2.90 %, and (31) relative nasal length, 2.00 %. The species stem time is 0.85 Ma and no data are available to estimate the species crown time (Fig. 4).

FIGURE 79. (A–F) *Panolopus unicolor* **sp. nov.** (ANSP 38647, holotype), SVL 67.6 mm.

Panolopus unicolor **sp. nov.** has a smaller relative frontal width (58.2) and a lower number of total strigae on ten scales (144) than most species of the genus. The species also has a larger relative length of digits on one hindlimb (36.8) than most species of the genus. The only known specimen of *P. unicolor* **sp. nov.** is a small adult specimen, which may contribute to a bias towards larger measurements. From *Panolopus aenetergum*, we distinguish *P. unicolor* **sp. nov.** by the dorsal pattern (absent versus irregular dots), the longitudinal paramedian lines (present

versus absent), the total strigae on ten scales (144 versus 267), and the relative frontal width (58.2 versus 88.2). From *P. aporus*, we distinguish *P. unicolor* **sp. nov.** by the adult SVL (67.6 versus 77.8–100), the total strigae on ten scales (144 versus 150–235), the relative length of digits on one hindlimb (36.8 versus 27.7–33.7), the relative cloacal width (7.61 versus 7.92–8.86), the relative prefrontal width (4.69 versus 4.18–4.53), the relative longest finger length (6.65 versus 4.57–5.72), the relative head width (70.8 versus 71.4–83.2), the relative frontal width (58.2 versus 61.7–75.1), the relative distance between the eye and naris (5.52 versus 4.69–5.44), the relative width of canthal iii (1.79 versus 1.85–1.96), the relative angled subocular width (2.90 versus 2.32–2.73), and the relative nasal width (2.00 versus 1.56–1.78). From *P. chalcorhabdus*, we distinguish *P. unicolor* **sp. nov.** by the adult SVL (67.6 versus 71.9–95.4), the total strigae on ten scales (144 versus 184–233), the relative length of digits on one hindlimb (36.8 versus 31.3–36.0), the relative cloacal width (7.61 versus 7.74–9.08), the relative largest supraocular width (3.12 versus 2.52–2.86), the relative frontal width (58.2 versus 62.5–80.8), the relative width of canthal iii (1.79 versus 1.98–2.05),and the relative angled subocular width (2.90 versus 2.36–2.71). From *P. costatus*, we distinguish *P. unicolor* **sp. nov.** by the adult SVL (67.6 versus 83.6–107), the total lamellae on one hand (48 versus 49–58), the total strigae on ten scales (144 versus 158–217), the relative distance between angled subocular and mouth (0.533 versus 0.582–0.916), the relative prefrontal width (4.69 versus 3.97–4.67), the relative largest supraocular width (3.12 versus 1.93–3.01), the relative distance between the eye and naris (5.52 versus 5.08–5.50), the relative width of canthal iii (1.79 versus 1.82–1.90), the relative angled subocular width (2.90 versus 2.36–2.81), and the relative nasal width (2.00 versus 1.58–1.74). From *P. curtissi*, we distinguish *P. unicolor* **sp. nov.** by the dots arranged in bars in the lateral areas (present versus absent), the midbody scale rows (40 versus 32–38), the total lamellae on one hand (48 versus 32–39), the total strigae on ten scales (144 versus 165–260), the relative length of digits on one hindlimb (36.8 versus 20.8–28.1), the relative forelimb length (23.5 versus 15.1–20.5), the relative postmental width (2.80 versus 2.07–2.72), the relative prefrontal width (4.69 versus 3.96–4.68), the relative largest supraocular width (3.12 versus 1.88–2.98), the relative longest finger length (6.65 versus 3.59–4.54), the relative frontal width (58.2 versus 65.4–83.1), the relative distance between the eye and naris (5.52 versus 4.02–5.03), the relative angled subocular width (2.90 versus 2.26–2.76), and the relative nasal width (2.00 versus 1.44–1.82). From *P. diastatus*, we distinguish *P. unicolor* **sp. nov.** by the longitudinal paramedian lines (present versus absent), the midbody scale rows (40 versus 33–39), the total lamellae on one hand (48 versus 35–41), the total strigae on ten scales (144 versus 169–234), the relative length of digits on one hindlimb (36.8 versus 21.5–27.4), the relative eye length (3.38 versus 2.71–3.32), the relative forelimb length (23.5 versus 16.2–20.1), the relative ear width (1.60 versus 0.667–1.43), the relative prefrontal width (4.69 versus 3.74–4.61), the relative largest supraocular width (3.12 versus 1.88–2.57), the relative longest finger length (6.65 versus 3.48–4.87), the relative distance between the eye and naris (5.52 versus 4.06–4.94), the relative angled subocular width (2.90 versus 1.93–2.86), and the relative nasal width (2.00 versus 1.41–1.77). From *P. emys*, we distinguish *P. unicolor* **sp. nov.** by the adult SVL (67.6 versus 99.0–113), the total strigae on ten scales (144 versus 238–311), the relative length of digits on one hindlimb (36.8 versus 28.9–35.2), the relative forelimb length (23.5 versus 18.5–23.4), the relative cloacal width (7.61 versus 8.24–8.96), the relative prefrontal width (4.69 versus 3.99–4.36), the relative largest supraocular width (3.12 versus 2.01–2.89), the relative longest finger length (6.65 versus 5.15–5.83), the relative head width (70.8 versus 71.1–78.7), the relative frontal width (58.2 versus 67.7–74.5), the relative nasal height (1.15 versus 0.963–1.10), the relative distance between the eye and naris (5.52 versus 4.37–5.19). From *P. hylonomus*, we distinguish *P. unicolor* **sp. nov.** by the dots arranged in bars in the lateral areas (present versus absent), the midbody scale rows (40 versus 33–39), the total lamellae on one hand (48 versus 34–47), the total strigae on ten scales (144 versus 169–222), the relative length of digits on one hindlimb (36.8 versus 22.8–28.2), the relative forelimb length (23.5 versus 17.1–20.7), the relative cloacal width (7.61 versus 7.98–8.57), the relative largest supraocular width (3.12 versus 2.65–2.90), the relative longest finger length (6.65 versus 4.47–5.27), the relative head width (70.8 versus 73.8–76.4), the relative frontal width (58.2 versus 64.0–74.5), the relative distance between the eye and naris (5.52 versus 4.03–4.98), the relative width of canthal iii (1.79 versus 1.95–2.03), and the relative angled subocular width (2.90 versus 1.61–2.75). From *P. lanceolatus* **sp. nov.**, we distinguish *P. unicolor* **sp. nov.** by the adult SVL (67.6 versus 78.5–104), the total strigae on ten scales (144 versus 186–234), the relative length of digits on one hindlimb (36.8 versus 28.4–35.9), the relative distance between angled subocular and mouth (0.533 versus 0.567–0.704), the relative ear width (1.60 versus 0.770–1.35), the relative postmental width (2.80 versus 2.36–2.66), the relative cloacal width (7.61 versus 8.01–8.76), the relative prefrontal width (4.69 versus 3.97–4.55), the relative largest supraocular width (3.12 versus 2.20–2.71), the relative longest finger length (6.65 versus 4.76–6.36), the relative frontal width (58.2

versus 63.1–72.1), the relative nasal height (1.15 versus 0.904–1.06), the relative distance between the eye and naris (5.52 versus 4.58–5.05), and the relative nasal width (2.00 versus 1.48–1.95). From *P. lapierrae* **sp. nov.**, we distinguish *P. unicolor* **sp. nov.** by the adult SVL (67.6 versus 72.6–88.3), the midbody scale rows (40 versus 33–38), the total lamellae on one hand (48 versus 38–47), the total strigae on ten scales (144 versus 228–231), the relative length of digits on one hindlimb (36.8 versus 24.3–30.9), the relative distance between angled subocular and mouth (0.533 versus 0.620–0.725), the relative forelimb length (23.5 versus 18.5–20.6), the relative ear width (1.60 versus 0.929–1.58), the relative rostral height (2.23 versus 1.86–2.06), the relative mental width (1.73 versus 1.92–1.94), the relative cloacal width (7.61 versus 8.55–8.81), the relative prefrontal width (4.69 versus 4.73–4.75), the relative largest supraocular width (3.12 versus 1.91–2.77), the relative longest finger length (6.65 versus 4.49–4.55), the relative distance between the ear and eye (7.61 versus 7.78–8.43), the relative head width (70.8 versus 77.7–78.1), the relative frontal width (58.2 versus 77.6–79.0), the relative nasal height (1.15 versus 1.06–1.09), the relative angled subocular height (0.814 versus 0.838–0.978), the relative distance between the eye and naris (5.52 versus 5.21), the relative angled subocular width (2.90 versus 2.71), and the relative nasal width (2.00 versus 1.81). From *P. leionotus*, we distinguish *P. unicolor* **sp. nov.** by the adult SVL (67.6 versus 86.3–105), the total strigae on ten scales (144 versus 191–266), the relative length of digits on one hindlimb (36.8 versus 25.4–34.1), the relative cloacal width (7.61 versus 8.03–8.69), the relative largest supraocular width (3.12 versus 1.94–2.50), the relative longest finger length (6.65 versus 4.58–6.10), and the relative frontal width (58.2 versus 68.7–81.2). From *P. marcanoi*, we distinguish *P. unicolor* **sp. nov.** by the dorsal pattern (absent versus irregular dots/dots in chevrons), the head markings (absent versus present), the total lamellae on one hand (48 versus 36–44), the relative length of digits on one hindlimb (36.8 versus 26.3–31.9), the relative mental width (1.73 versus 1.75–2.33), the relative frontal width (58.2 versus 59.0–73.0), the relative angled subocular height (0.814 versus 0.505–0.793), and the relative nasal width (2.00 versus 1.64–1.96). From *P. melanchrous*, we distinguish *P. unicolor* **sp. nov.** by the adult SVL (67.6 versus 93.2–124), the total strigae on ten scales (144 versus 168–413), the relative frontal width (58.2 versus 61.3–71.4), the relative nasal height (1.15 versus 0.897–0.952), and the relative angled subocular width (2.90 versus 2.28–2.82). From *P. neiba*, we distinguish *P. unicolor* **sp. nov.** by the dorsal pattern (absent versus irregular flecks/dots in chevrons), the adult SVL (67.6 versus 77.9–102), the total strigae on ten scales (144 versus 179–239), the relative length of digits on one hindlimb (36.8 versus 29.5–36.6), the relative distance between angled subocular and mouth (0.533 versus 0.670–0.747), the relative largest supraocular width (3.12 versus 2.06–3.04), the relative frontal width (58.2 versus 63.3–74.0), the relative nasal height (1.15 versus 0.963–1.08), the relative distance between the eye and naris (5.52 versus 4.51–5.01), the relative angled subocular width (2.90 versus 2.34–2.83), and the relative nasal width (2.00 versus 1.67–1.92). From *P. nesobous*, we distinguish *P. unicolor* **sp. nov.** by the dorsal pattern (absent versus irregular dots/dots in series) and the total lamellae on one hand (48 versus 50–59). From *P. oreistes*, we distinguish *P. unicolor* **sp. nov.** by the dorsal pattern (absent versus irregular dots/dots in series/dots in chevrons), the adult SVL (67.6 versus 77.3–103), the total strigae on ten scales (144 versus 155–267), the relative frontal width (58.2 versus 61.6–76.9), the relative nasal height (1.15 versus 0.878–1.06), and the relative nasal width (2.00 versus 1.37–1.65). From *P. psychonothes*, we distinguish *P. unicolor* **sp. nov.** by the dorsal pattern (absent versus irregular dots/dots in series/dots in chevrons), the adult SVL (67.6 versus 70.9–97.2), the total lamellae on one hand (48 versus 37–44), the total strigae on ten scales (144 versus 172–244), the relative length of digits on one hindlimb (36.8 versus 26.5–33.1), the relative largest supraocular width (3.12 versus 1.92–2.68), the relative longest finger length (6.65 versus 4.89–5.81), the relative frontal width (58.2 versus 66.5–81.0), the relative angled subocular width (2.90 versus 2.01–2.44), and the relative nasal width (2.00 versus 1.68–1.94). From *P. saonae*, we distinguish *P. unicolor* **sp. nov.** by the longitudinal paramedian lines (present versus absent), the adult SVL (67.6 versus 90.9–98.3), the midbody scale rows (40 versus 35–39), the total strigae on ten scales (144 versus 212–284), the relative eye length (3.38 versus 3.06–3.20), the relative ear width (1.60 versus 0.880–1.35), and the relative head length (17.8 versus 15.4–17.5). From *P. semitaeniatus* **sp. nov.**, we distinguish *P. unicolor* **sp. nov.** by the SVL (67.6 versus 77.4–84.1), the total lamellae on one hand (48 versus 34–46), the total strigae on ten scales (144 versus 174–204), the relative length of digits on one hindlimb (36.8 versus 30.4–34.6), the relative distance between angled subocular and mouth (0.533 versus 0.666–0.808), the relative ear width (1.6 versus 1.90–2.30), the relative cloacal width (7.61 versus 8.08–8.23), the relative longest finger length (6.65 versus 5.17–6.05), the relative head width (70.8 versus 58.8–63.8), and the relative frontal width (58.2 versus 63.6–76.5).

Description of holotype. ANSP 38647. An adult; SVL 67.6 mm; tail nearly cylindrical, broken in life midway, regenerated, 55.6 mm (82.2% SVL); axilla-to-groin distance 37.9 mm (56.1% SVL); forelimb length 15.8 mm

(23.4% SVL); hindlimb length 22.7 mm (33.6% SVL); head length 12.0 mm (17.8% SVL); head width 8.50 mm (12.6% SVL); head width 70.8% head length; diameter of orbit 2.28 mm (3.37% SVL); horizontal diameter of ear opening 1.08 mm (1.60% SVL); vertical diameter of ear opening 0.88 mm (1.30% SVL); length of all toes on one foot 24.9 mm (36.8% SVL); shortest distance between angled subocular and lip 0.36 mm (0.533% SVL); shortest distance between the ocular and auricular openings 5.14 mm (7.60% SVL); longest finger length 4.49 mm (6.64% SVL); largest supraocular width 2.11 mm (3.12% SVL); cloacal width 5.14 mm (7.60% SVL); mental width 1.17 mm (1.73% SVL); postmental width 1.89 mm (2.80% SVL); prefrontal width 3.17 mm (4.69% SVL); frontal width 58.2% frontal length; nasal height 0.78 mm (1.15% SVL); angled subocular height 0.55 mm (0.814% SVL); shortest distance between the eye and naris 3.73 mm (5.52% SVL); canthal iii width 1.21 mm (1.79% SVL); angled subocular width 1.96 mm (2.90% SVL); nasal width 1.35 mm (2.00% SVL); rostral 2.23X as wide as high, visible from above, not in contact with nasals, in contact with 1st supralabial and anterior internasal (left)/(right); anterior internasals are narrower than posterior ones; frontonasals and prefrontal fused into a single large plate with a concave posterior margin, wider than long, bordered by posterior internasals, 1st loreals, 1st median oculars, and the frontal; frontal longer than wide; a pair of frontoparietals, separated by the posterior prolongation of the frontal and the interparietal plate; interparietal plate smaller than parietals and separating them, posteriorly touching the interoccipital, which is wider than long; parietal separated from supraoculars by 1st and 2nd temporals and frontoparietal (left)/(right); nasal single; nostril above suture between 1st and 2nd supralabials (left)/(right); 1 postnasal (left)/(right); 2 loreals (left)/(right); 1st loreal higher than wide (left)/(right), in contact with postnasal, posterior internasal, prefrontal/frontonasal complex, 1st median ocular, canthal iii, 2nd loreal, and 3rd–4th supralabials (left)/(right); 2nd loreal shorter than 1st, approximately as high as wide (left)/(right), excluded from contact with supraocular by canthal iii (left)/(right); final loreal posteriorly bordering the lower preocular (left)/(right); canthal iii wider than high (left)/(right), contacting 1st median ocular, anterior supraciliary, upper and lower preoculars, and 1st and 2nd loreals (left)/(right); 9 median oculars (left)/(right), 1st contacting the prefrontal (left)/(right); 1 upper preocular (left)/(right); an irregular anterior supraciliary (left)/(right); 6 lateral oculars (left)/(right); 5 temporals (left)/(right); 2 suboculars (left)/(right); posterior subocular large and elongate (left)/(right); anterior subocular small; 9 supralabials (left)/(right), 6 to level below center of eye (left)/(right); 10 (left)/9 (right) infralabials, 6 to level below center of eye (left)/(right); mental small, followed by a single, larger postmental; 4 pairs of enlarged chin shields, followed by 1 pair of reduced chin shields; 1st pair in contact with one another; 2nd–5th pairs separated by 1–5 scales; 96 transverse rows of dorsal scales from interoccipital to base of tail; 93 transverse rows of ventral scales from mental to vent; 40 scales around midbody; 5 digits; finger lengths 3>4>2>5>1; 12 lamellae under longest finger (left)/(right); 48 total lamellae on one hand; toe lengths 4>3>2>5>1; 16 (left)/17 (right) lamellae under longest toe; dorsal body and caudal scales keelless and striate; striate ventral scales; 144 total strigae counted on ten scales.

Color (in alcohol): dorsal surface of head medium gray, patternless; lateral surfaces of head grading from medium gray to cream with darker brown eye masks and markings on the labial scales; dorsal surfaces of the body are the same medium gray as the head with several dark brown flecks in the longitudinal paramedian area; dorsal surface of tail the same as the body except on the regenerated section, which is yellow; lateral areas grade from medium gray to cream with dark and pale dots arranged in bars in the lateral band; dorsal surfaces of the limbs are pale brown with darker brown mottling; lateral and ventral areas of the limbs grade to patternless cream; ventral surfaces of the head, body, and tail are patternless cream with several darker brown flecks under the chin.

Variation. No other specimens are known. Measurements and other morphological data for the holotype and other examined material are presented in Table 1.

Distribution. The only representative of *Panolopus unicolor* **sp. nov.** was collected near Cruce de Ocoa in the southcentral region of the Dominican Republic at 680 m (Fig. 49).

Ecology and conservation. Upon collection, the ravine in which the specimen was collected had "lots of native vegetation" and "even some very tall trees."

We consider the conservation status of *Panolopus unicolor* to be Least Concern, based on IUCN Redlist criteria (IUCN 2023). It is likely a common species tolerant of some habitat disturbance, based on what is known of most species of *Panolopus*. However, it is known from only a single specimen, and it faces a primary threat of habitat destruction resulting from deforestation. A secondary threat is predation from introduced mammals, including the mongoose and black rats. Studies are needed to determine the health and extent of remaining populations and better understand the threats to the survival of the species.

Reproduction. No data on reproduction are available for this species.

Etymology. The species name (*unicolor*) is a nominative singular masculine adjective, referring to the absence of a pattern on the dorsum of the holotype and only known specimen of this species.

Remarks. Only one individual of this species has ever been collected. No museum collection has specimens categorized as either *P. curtissi* or *P. costatus* from the nearby region, prompting the need for additional field surveys of the surrounding area to confirm the continued existence of this species. *Panolopus unicolor* **sp. nov.** is included in our genetic dataset and has significant support in both Bayesian and ML analyses at the stem node that places it as the closest relative to *P. hylonomus*. Based on our timetree (Fig. 4), *P. unicolor* **sp. nov.** diverged from its closest relative 0.85 Ma, consistent with typical species of vertebrates (> 0.7 Ma; Hedges *et al.* 2015). We recognize *P. unicolor* **sp. nov.** as a distinct species because of the multiple morphological traits that separate it from *P. hylonomus. Panolopus unicolor* was recognized as a distinct species by our ASAP analysis.

Genus *Sauresia* Gray, 1852

Long-headed Four-toed Forest Lizards
(Fig. 80)

Sauresia Gray, 1852:282. Type species: *Sauresia sepsoides* Gray, 1852:282, by original designation.
Embryopus Weinland, 1863:135. Type species: *Embryopus habichii* Weinland, 1863:135, by original designation.

Diagnosis. Species of *Sauresia* have (1) a dorsal pattern of absent/irregular flecks/irregular dots/lineate/mottled, (2) head markings absent/present, (3) markings in the longitudinal paramedian area absent/present, (4) dots arranged in bars in the lateral band absent, (5) an adult SVL of 49.3–72.0 mm, (6) ventral scale rows, 101–129, (7) mid-body scale rows, 31–42, (8) total lamellae on one hand, 14–19, (9) total strigae on ten scales, 78–150, (10) relative length of all digits on one hindlimb, 10.5–15.1 %, (11) relative distance between the angled subocular and mouth, 0.00–0.473 %, (12) relative eye length, 2.14–3.40 %, (13) relative forelimb length, 9.14–13.6 %, (14) relative ear width, 0.294–1.17 %, (15) relative rostral height, 1.45–2.73 %, (16) relative head length, 12.3–16.3 %, (17) relative mental width, 1.21–2.05 %, (18) relative postmental width, 1.92–2.76 %, (19) relative cloacal width, 5.11–7.18 %, (20) relative prefrontal width, 3.01–4.29 %, (21) relative largest supraocular width, 1.57–2.63 %, (22) relative longest finger length, 1.69–2.86 %, (23) relative distance between the ear and eye, 5.91–8.03 %, (24) relative head width, 64.7–83.1 %, (25) relative frontal width, 69.1–94.4 %, (26) relative nasal height, 0.706–1.17 %, (27) relative angled subocular height, 0.778–1.64 %, (28) relative distance between the eye and naris, 2.67–3.77 %, (29) relative canthal iii length, 0.943–1.82 %, (30) relative angled subocular width, 1.54–2.55 %, and (31) relative nasal length, 0.942–1.62 %. Notably, *Sauresia* possesses four digits (as opposed to five), a trait also observed in *Wetmorena.*

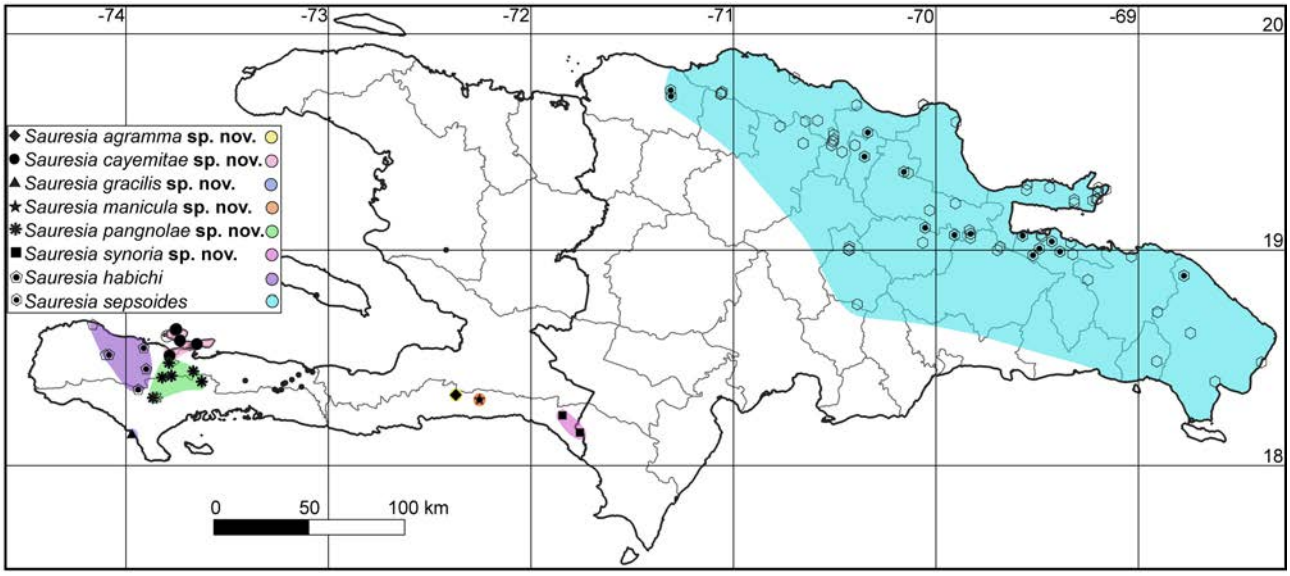

FIGURE 80. Map showing the distribution of *Sauresia*. Hollow symbols indicate unexamined records assignable to species. Small black dots indicate unexamined museum records not assignable to species.

Content. Eight species (Table 3): *Sauresia agramma* **sp. nov.**, *Sauresia cayemitae* **sp. nov.**, *Sauresia gracilis* **sp. nov.**, *Sauresia habichi*, *Sauresia manicula* **sp. nov.**, *Sauresia pangnolae* **sp. nov.**, *Sauresia sepsoides*, and *Sauresia synoria* **sp. nov.**

Distribution: *Sauresia* is only known from Hispaniola but is notably absent from the driest parts of the island, including northwestern Haiti and some areas in the southern Dominican Republic.

***Sauresia agramma* sp. nov.**
Denfer Four-toed Forest Lizard
(Fig. 81–82)

Sauresia sepsoides—Schwartz & Henderson, 1991:463 (part).
Celestus sepsoides—Hedges *et al.*, 2019:17 (part).
Sauresia sepsoides—Schools & Hedges, 2021:231 (part).
Sauresia sepsoides—Landestoy *et al.*, 2022: 205 (part).

Holotype. ANSP 38688, an adult female from Morne D'Enfer (southwestern edge of plateau), Sud-Est Department, Haiti, collected by S. Blair Hedges, Tiffany Cloud, Miguel Landestoy, and Marcos Rodriguez on 21 November 2011 (18.33005, -72.37095; 1433 m).

Paratypes (n=3). HAITI. Sud-Est. ANSP 38685–7, S. Blair Hedges, Tiffany Cloud, Miguel Landestoy, and Marcos Rodriguez, Morne D'Enfer (southwestern edge of plateau), 21 November 2011.

Diagnosis. *Sauresia agramma* **sp. nov.** has (1) a dorsal pattern of absent, (2) head markings absent/present, (3) markings in the longitudinal paramedian area absent/present, (4) dots arranged in bars in the lateral band absent, (5) a maximum SVL of 53.8–69.1 mm, (6) ventral scale rows, 121–127, (7) midbody scale rows, 37–39, (8) total lamellae on one hand, 17, (9) total strigae on ten scales, 103–138, (10) relative length of all digits on one hindlimb, 11.3–14.9 %, (11) relative distance between the angled subocular and mouth, 0.217–0.262 %, (12) relative eye length, 2.30–3.16 %, (13) relative forelimb length, 10.2–13.6 %, (14) relative ear width, 0.576–0.709 %, (15) relative rostral height, 1.92–2.12 %, (16) relative head length, 13.6–15.2 %, (17) relative mental width, 1.61–2.05 %, (18) relative postmental width, 2.30–2.70 %, (19) relative cloacal width, 6.09–6.82 %, (20) relative prefrontal width, 3.02–3.98 %, (21) relative largest supraocular width, 1.87–2.47 %, (22) relative longest finger length, 2.11–2.86 %, (23) relative distance between the ear and eye, 6.93–7.86 %, (24) relative head width, 69.7–74.6 %, (25) relative frontal width, 80.2–81.9 %, (26) relative nasal height, 0.883–1.02 %, (27) relative angled subocular height, 0.912–1.13 %, (28) relative distance between the eye and naris, 2.98–3.75 %, (29) relative canthal iii length, 1.17–1.30 %, (30) relative angled subocular width, 2.07–2.47 %, and (31) relative nasal length, 1.36–1.57 %. The species stem time is 1.58 Ma and the species crown time is 0.00 Ma (Fig. 4).

We distinguish *Sauresia agramma* **sp. nov.** from the other species of *Sauresia* based on a complex of traits. From *Sauresia cayemitae* **sp. nov.**, we distinguish *S. agramma* **sp. nov.** by the ventral scale rows (121–127 versus 101–119), and the relative distance between the ear and eye (6.93–7.86 versus 6.02–6.88). From *S. gracilis* **sp. nov.**, we distinguish *S. agramma* **sp. nov.** by the dorsal pattern (absent versus mottled/lineate), the adult SVL (53.8–69.1 versus 51.1), the ventral scale rows (121–127 versus 103), the midbody scale rows (37–39 versus 36), the total lamellae on one hand (17 versus 18), the total strigae on ten scales (103–138 versus 100), the relative rostral height (1.92–2.12 versus 1.90), the relative head length (13.6–15.2 versus 15.7), the relative postmental width (2.30–2.70 versus 2.76), the relative cloacal width (6.09–6.82 versus 7.18), the relative longest finger length (2.11–2.86 versus 1.96), the relative head width (69.7–74.6 versus 67.6), the relative frontal width (80.2–81.9 versus 82.9), the relative width of canthal iii (1.17–1.30 versus 1.82), the relative angled subocular width (2.07–2.47 versus 1.96), and the relative nasal width (1.36–1.57 versus 1.33). From *S. habichi*, we distinguish *S. agramma* **sp. nov.** by the total lamellae on one hand (17 versus 18–19), the relative distance between angled subocular and mouth (0.217–0.262 versus 0.000594–0.201), the relative head width (69.7–74.6 versus 77.7–78.6), the relative frontal width (80.2–81.9 versus 71.8–77.5), the relative angled subocular width (2.07–2.47 versus 1.67–2.03), and the relative nasal width (1.36–1.57 versus 0.942–1.12). From *S. manicula* **sp. nov.**, we distinguish *S. agramma* **sp. nov.** by the relative distance between angled subocular and mouth (0.217–0.262 versus 0.168–0.188), the relative rostral height (1.92–2.12 versus 1.89–1.90), the relative postmental width (2.30–2.70 versus 2.13–2.16), the relative angled subocular width (2.07–2.47 versus 1.81–2.01), and the relative nasal width (1.36–1.57 versus 1.19–1.29). From *S.*

pangnolae **sp. nov.**, we distinguish *S. agramma* **sp. nov.** by the ventral scale rows (121–127 versus 104–119). From *S. sepsoides*, we distinguish *S. agramma* **sp. nov.** by the ventral scale rows (121–127 versus 104–119). From *S. synoria* **sp. nov.**, we distinguish *S. agramma* **sp. nov.** by the midbody scale rows (37–39 versus 34–36), the relative frontal width (80.2–81.9 versus 82.0–94.4), and the relative nasal width (1.36–1.57 versus 1.13–1.35).

Description of holotype. ANSP 38688. An adult female; SVL 64.8 mm; tail nearly cylindrical, broken in life, 37.8 mm (58.3% SVL); axilla-to-groin distance 44.4 mm (68.5% SVL); forelimb length 7.14 mm (11.0% SVL); hindlimb length 12.0 mm (18.5% SVL); head length 8.91 mm (13.8% SVL); head width 6.21 mm (9.58% SVL); head width 69.7% head length; diameter of orbit 1.49 mm (2.30% SVL); horizontal diameter of ear opening 0.43 mm (0.664% SVL); vertical diameter of ear opening 0.39 mm (0.602% SVL); length of all toes on one foot 7.94 mm (12.3% SVL); shortest distance between angled subocular and lip 0.17 mm (0.262% SVL); shortest distance between the ocular and auricular openings 4.49 mm (6.93% SVL); longest finger length 1.49 mm (2.30% SVL); largest supraocular width 1.23 mm (1.90% SVL); cloacal width 3.96 mm (6.11% SVL); mental width 1.04 mm (1.60% SVL); postmental width 1.49 mm (2.30% SVL); prefrontal width 2.16 mm (3.33% SVL); frontal width 80.2% frontal length; nasal height 0.66 mm (1.02% SVL); angled subocular height 0.68 mm (1.05% SVL); shortest distance between the eye and naris 2.10 mm (3.24% SVL); canthal iii width 0.76 mm (1.17% SVL); angled subocular width 1.34 mm (2.07% SVL); nasal width 1.02 mm (1.57% SVL); rostral 2.12X as wide as high, visible from above, not in contact with nasals, in contact with 1st supralabial and anterior internasal (left)/(right); anterior internasals are narrower than posterior ones; frontonasals and prefrontal fused into a single large plate with a slightly concave posterior margin, wider than long, bordered by posterior internasals, 1st loreals, 1st median oculars, and the frontal; frontal much longer than wide; a pair of frontoparietals, separated by the posterior prolongation of the frontal and the interparietal plate; interparietal plate larger than parietals and separating them, posteriorly touching the interoccipital, which is wider than long; parietal separated from supraoculars by 1st and 2nd temporals and frontoparietal (left)/(right); nasal single; nostril just posterior to suture between 1st and 2nd supralabials (left)/(right); 1 postnasal (left)/(right); 2 loreals (left)/(right); 1st loreal higher than wide (left)/(right), in contact with postnasal, posterior internasal, prefrontal/frontonasal complex, 1st median ocular, canthal iii, 2nd loreal, and 3rd supralabial (left)/(right); 2nd loreal shorter than 1st, higher than wide (left)/(right), excluded from contact with supraocular by canthal iii (left)/(right); 2nd loreal posteriorly bordering the lower preocular (left)/(right); canthal iii wider than high (left)/(right), contacting 1st median ocular, anterior supraciliary, lower preocular, and 1st and 2nd loreals (left)/1st median ocular, anterior supraciliary, upper and lower preoculars, and 1st and 2nd loreals (right); 9 median oculars (left)/(right), 1st contacting the prefrontal (left)/(right); 1 upper preocular (left)/(right); an irregular anterior supraciliary (left)/(right); 6 lateral oculars (left)/(right); 5 temporals (left)/(right); 2 suboculars (left)/(right); posterior subocular large and elongate (left)/(right); anterior subocular small (left)/(right); 9 supralabials (left)/(right), 5 to level below center of eye (left)/(right); 9 infralabials (left)/(right), 5 to level below center of eye (left)/(right); mental small, followed by a single, larger postmental; 4 pairs of enlarged chin shields; 1st and 2nd pairs in contact with one another; 3rd pair in contact with one another anteriorly, posteriorly separated by one scale; 3rd–4th pairs separated by 1–2 scales; 114 transverse rows of dorsal scales from interoccipital to base of tail; 126 transverse rows of ventral scales from mental to vent; 37 scales around midbody; 4 digits; finger lengths 3>2>4>1; 5 (left)/6 (right) lamellae under longest finger; 17 total lamellae on one hand; toe lengths 3>4>2>1; 12 (left)/10 (right) lamellae under longest toe; keelless and striate dorsal body and caudal scales; smooth ventral scales; 138 total strigae counted on ten scales.

Color (in alcohol): dorsal surface of head deep brown with darker brown mottling; lateral surfaces of head grading from deep brown to white-gray, patternless; dorsal surfaces of the body are dark brown, with darker brown mottling on the neck; dorsal surface of tail dark brown, patternless; lateral areas grade from dark brown to cream, patternless; dorsal surfaces of the limbs are dark brown with paler brown mottling; lateral and ventral areas of the limbs fade to yellow-cream with some darker brown mottling on the sides; ventral surfaces of the head, body, and tail are yellow-cream with some darker brown mottling under the throat and the tail.

Variation. The material examined of this species is similar to the holotype in lacking a dorsal pattern other than several specimens that have mottling in the longitudinal paramedian area. The majority of the specimens have darker outlines on their internasal and prefrontal scales. All specimens lack longitudinal paramedian lines. Measurements and other morphological data for the holotype and other examined material are presented in Table 1.

Distribution. *Sauresia agramma* **sp. nov.** is known only from the type series that was collected from Morne D'Enfer in the east-central region of the Tiburon Peninsula of Haiti at an elevation of 1433 m (Fig. 80). It has an extent of occurrence of ~90 km^2.

FIGURE 81. (A–F) *Sauresia agramma* **sp. nov.** (ANSP 38688, holotype), SVL 64.8 mm.

Ecology and conservation. Individuals were found under objects (rocks, logs) on the ground. We consider the conservation status of *Sauresia agramma* **sp. nov.** to be Critically Endangered B1ab(iii), based on IUCN Redlist criteria (IUCN 2023). It faces a primary threat from habitat destruction from agriculture and charcoaling. The Massif de la Selle (including Morne D'Enfer) and Haiti in general are heavily deforested with < 1% of primary forest remaining in the country (Hedges *et al.* 2018). Secondary threats to this species include predation from introduced predators, including the mongoose and black rats. Studies are needed to determine the health of any remaining populations and threats to the survival of the species. Captive-breeding programs should be undertaken, because eradication of introduced mammalian predators is currently not possible on large islands.

Reproduction. No data on reproduction are available for this species.

Etymology. The species name (*agramma*) is a feminine noun derived from the Latin and Greek prefix *a-* (away from, without) and the Greek noun *gramma* (line), referring to the absence of lines on the dorsum of this species.

Remarks. Morne D'Enfer is one of the most remote areas in the Massif de la Selle of Haiti, rarely visited by biologists because of difficulty of access. It is a high plateau at the western end of La Visite National Park and

harbors probably the largest remaining stands of primary hardwood forest in the mountain range, although even that is small. SBH visited it by helicopter for about 24 hours on 21 November 2011. The team found four individuals in forest close to the campsite. Despite the protected status of the area (national park), no rangers provide protection and evidence of recent clear-cutting and charcoal production was abundant.

FIGURE 82. (A–B) *Sauresia agramma* **sp. nov.** (ANSP 38687, SBH 269900), in life. From Morne D'Enfer, south-western edge of plateau, Sud-Est Department, Haiti. Photos by SBH.

Sauresia agramma **sp. nov.** is included in our genetic dataset and has significant support in both Bayesian and ML likelihood analyses at the crown node of the species and the stem node that places it as the closest relative to *S. manicula* **sp. nov.** and *S. synoria* **sp. nov.** Based on our timetree (Fig. 4), *S. agramma* diverged from its closest relative 1.58 Ma, consistent with typical species of vertebrates (> 0.7 Ma; Hedges *et al.* 2015). We recognize *S. agramma* **sp. nov.** as a distinct species based on the multiple morphological traits that separate it from its closest relatives (*S. manicula* **sp. nov.** and *S. synoria* **sp. nov.**). *Sauresia agramma* **sp. nov.** was recovered as conspecific with *Sauresia sepsoides* in our ASAP analysis.

***Sauresia cayemitae* sp. nov.**
Cayemite Four-toed Forest Lizard
(Fig. 83–84)

Sauresia sepsoides—Schwartz & Henderson, 1988:162 (part).
Sauresia sepsoides—Schwartz & Henderson, 1991:463 (part).
Celestus sepsoides—Hedges *et al.*, 2019:17 (part).
Sauresia sepsoides—Schools & Hedges, 2021:231 (part).
Sauresia sepsoides—Landestoy *et al.*, 2022: 205 (part).

Holotype. ANSP 38691, an adult female from 5.0 km South of Pestel, collected by Richard Thomas and Manuel Leal on 25 May 1991.

Paratypes (n=11). Grande'Anse. ANSP 38673, S. Blair Hedges, Tiffany Cloud, Miguel Landestoy, Grande Cayemite (helipad-camp), 19 June 2012; ANSP 38674–7, S. Blair Hedges, Tiffany Cloud, Miguel Landestoy, Grande Cayemite (waypoint 166), 19 June 2012; KU 227730–1, Presqu'ile des Baraderes, ca Grand Boucan, 1971; KU 227740–1, KU 227746, Ile Grande Cayemite, ca Anse-a-Macon, 1971; SBH 274212, Grande Cayemite (waypoint 166).

Diagnosis. *Sauresia cayemitae* **sp. nov.** has (1) a dorsal pattern of absent/irregular flecks/lineate, (2) head markings absent/present, (3) markings in the longitudinal paramedian area present, (4) dots arranged in bars in the lateral band absent, (5) an adult SVL of 47.8–58.1 mm, (6) ventral scale rows, 101–119, (7) midbody scale rows, 31–37, (8) total lamellae on one hand, 15–19, (9) total strigae on ten scales, 84–104, (10) relative length of all digits on one hindlimb, 11.5–14.0 %, (11) relative distance between the angled subocular and mouth, 0.0558–0.473 %, (12) relative eye length, 2.14–2.90 %, (13) relative forelimb length, 9.65–12.5 %, (14) relative ear width, 0.294–1.17 %, (15) relative rostral height, 1.65–2.73 %, (16) relative head length, 13.0–15.6 %, (17) relative mental width, 1.46–1.78 %, (18) relative postmental width, 2.27–2.51 %, (19) relative cloacal width, 5.59–6.24 %, (20) relative prefrontal width, 3.11–3.64 %, (21) relative largest supraocular width, 1.67–2.25 %, (22) relative longest finger length, 2.36–2.65 %, (23) relative distance between the ear and eye, 6.02–6.88 %, (24) relative head width, 68.5–77.1 %, (25) relative frontal width, 71.3–83.1 %, (26) relative nasal height, 0.792–0.951 %, (27) relative angled subocular height, 0.740–1.02 %, (28) relative distance between the eye and naris, 2.86–3.51 %, (29) relative canthal iii length, 1.07–1.30 %, (30) relative angled subocular width, 1.88–2.17 %, and (31) relative nasal length, 1.06–1.46 %. The species stem time is 1.19 Ma and the species crown time is 0.18 Ma (Fig. 4).

We distinguish *Sauresia cayemitae* **sp. nov.** from the other species of *Sauresia* based on a complex of traits. From *Sauresia agramma* **sp. nov.**, we distinguish *S. cayemitae* **sp. nov.** by the ventral scale rows (101–119 versus 121–127) and the relative distance between the ear and eye (6.02–6.88 versus 6.93–7.86). From *S. gracilis* **sp. nov.**, we distinguish *S. cayemitae* **sp. nov.** by the relative eye length (2.14–2.90 versus 2.97), the relative head length (13.0–15.6 versus 15.7), the relative postmental width (2.27–2.51 versus 2.76), the relative cloacal width (5.59–6.24 versus 7.18), the relative prefrontal width (3.11–3.64 versus 3.81), the relative largest supraocular width (1.67–2.25 versus 2.44), the relative longest finger length (2.36–2.65 versus 1.96), the relative distance between the ear and eye (6.02–6.88 versus 7.63), the relative head width (68.5–77.1 versus 67.6), the relative nasal height (0.792–0.951 versus 0.998), and the relative width of canthal iii (1.07–1.30 versus 1.82). From *S. habichi*, we distinguish *S. cayemitae* **sp. nov.** by the ventral scale rows (101–119 versus 122–125), the midbody scale rows (31–37 versus 38–41), and the relative head width (68.5–77.1 versus 77.7–78.6). From *S. manicula* **sp. nov.**, we distinguish *S. cayemitae* **sp. nov.** by the adult SVL (47.8–58.1 versus 59.6–69.0), the ventral scale rows (101–119 versus 121–129), the total strigae on ten scales (84–104 versus 119–150), the relative postmental width (2.27–2.51 versus 2.13–2.16), and the relative longest finger length (2.36–2.65 versus 2.20–2.21). From *S. pangnolae* **sp. nov.**, we distinguish *S. cayemitae* **sp. nov.** by the relative prefrontal width (3.11–3.64 versus 3.70–3.83) and the relative distance between the ear and eye (6.02–6.88 versus 6.94–7.46). From *S. sepsoides*, we cannot distinguish *S. cayemitae* **sp. nov.** based on our standard suite of characters (see Remarks). From *S. synoria* **sp. nov.**, we distinguish *S. cayemitae* **sp. nov.** by the frontal width by the SVL (3.11–3.75 versus 3.78–4.32) (see Remarks).

Description of holotype. ANSP 38691. An adult female; SVL 58.1 mm; tail nearly cylindrical, 58.0 mm (99.8% SVL); axilla-to-groin distance 39.0 mm (67.1% SVL); forelimb length 7.29 mm (12.5% SVL); hindlimb length 11.7 mm (20.1% SVL); head length 8.02 mm (13.8% SVL); head width 5.91 mm (10.2% SVL); head width 73.7% head length; diameter of orbit 1.49 mm (2.56% SVL); horizontal diameter of ear opening 0.41 mm (0.706% SVL);

vertical diameter of ear opening 0.30 mm (0.516% SVL); length of all toes on one foot 7.80 mm (13.4% SVL); shortest distance between angled subocular and lip 0.09 mm (0.155% SVL); shortest distance between the ocular and auricular openings 3.90 mm (6.71% SVL); longest finger length 1.33 mm (2.29% SVL); largest supraocular width 1.31 mm (2.25% SVL); cloacal width 3.51 mm (6.04% SVL); mental width 0.85 mm (1.46% SVL); postmental width 1.42 mm (2.44% SVL); prefrontal width 1.90 mm (3.27% SVL); frontal width 73.0% frontal length; nasal height 0.46 mm (0.792% SVL); angled subocular height 0.43 mm (0.740% SVL); shortest distance between the eye and naris 2.04 mm (3.51% SVL); canthal iii width 0.62 mm (1.07% SVL); angled subocular width 1.22 mm (2.10% SVL); nasal width 0.73 mm (1.26% SVL); rostral 1.88X as wide as high, visible from above, not in contact with nasals, in contact with 1st supralabial and anterior internasal (left)/(right); anterior internasals are narrower than posterior ones; frontonasals and prefrontal fused into a single large plate with a straight posterior margin, much wider than long, bordered by posterior internasals, canthal iii, 1st median oculars, and the frontal; frontal longer than wide; a pair of frontoparietals, separated by the posterior prolongation of the frontal and the interparietal plate; interparietal plate smaller than parietals and separating them, posteriorly touching the interoccipital, which is wider than long; parietal separated from supraoculars by 1st and 2nd temporals and frontoparietal (left)/(right); nasal single; nostril just posterior to suture between 1st and 2nd supralabials (left)/(right); 1 postnasal (left)/(right); 2 loreals (left)/(right); 1st loreal higher than wide (left)/(right), in contact with postnasal, posterior internasal, canthal iii, 2nd loreal, and 3rd–4th supralabials (left)/(right); 2nd loreal shorter than 1st, higher than wide (left)/(right), excluded from contact with supraocular by canthal iii (left)/(right); final loreal posteriorly bordering the lower preocular (left)/(right); canthal iii wider than high (left)/(right), contacting 1st median ocular, anterior superciliary, upper and lower preoculars, posterior internasal, prefrontal/frontonasal complex, and 1st and 2nd loreals (left)/1st median ocular, anterior superciliary, upper and lower preoculars, posterior internasal, prefrontal/frontonasal complex, and 1st and 2nd loreals,(right); 10 (left)/11 (right) median oculars, 1st contacting the prefrontal (left)/(right); 1 upper preocular (left)/(right); an irregular anterior superciliary (left)/(right); 6 lateral oculars (left)/(right); 6 temporals (left)/(right); 2 suboculars (left)/(right); posterior subocular large and elongate (left)/(right); anterior subocular(s) small (left)/(right); 9 (left)/10 (right) supralabials, 5 (left)/6 (right) to level below center of eye; 9 (left)/6 (right) infralabials, 9 (left)/6 (right) to level below center of eye; mental small, followed by a single, larger postmental; 4 pairs of enlarged chin shields; 1st pair in contact with one another; 2nd–4th pairs separated by 1–2 scales; 115 transverse rows of dorsal scales from interoccipital to base of tail; 116 transverse rows of ventral scales from mental to vent; 37 scales around midbody; 4 digits; finger lengths 3>2>4>1; 7 (left)/ 6 (right) lamellae under longest finger; 19 total lamellae on one hand; toe lengths 3>2>4>1; 12 (left)/(right) lamellae under longest toe; keelless and striate dorsal body and caudal scales; smooth ventral scales; 84 total strigae counted on ten scales.

Color (in alcohol): dorsal surface of head medium brown, covered in darker brown mottling; lateral surfaces of head grading from medium brown to cream with darker brown mottling, especially on the labial scales and around the eye; dorsal surfaces of the body are medium brown with darker areas in the center of the scales giving a lineate appearance; dorsal surface of tail dark brown, patternless; lateral areas grade from dark brown to cream; dorsal surfaces of the limbs are medium brown, patternless; lateral and ventral areas of the limbs fade to an orange-cream, patternless; ventral surfaces of the head, body, and tail are orange-cream with darker brown mottling under the chin and tail.

Variation. Roughly half of the examined material has a dorsal pattern of multiple longitudinal paramedian lines that extend down the dorsum. The other half of examined material lacks a dorsal pattern. ANSP 38673 also shows some irregular flecks on its dorsum. KU 227746 has a patternless head, whereas all other specimens have darker outlines on their internasal scales and ANSP 38673 and ANSP 38677 both have irregular darker areas on their head. All specimens lack dots arranged in bars in their lateral areas. Measurements and other morphological data for the holotype and other examined material are presented in Table 1.

Distribution. *Sauresia cayemitae* **sp. nov.** is known from Ile Grande Cayemite and the north-central coast of the Tiburon Peninsula of Haiti at elevations of 40–350 m (Fig. 80). It has an extent of occurrence of ~210 km^2.

Ecology and conservation. No ecological data are associated with this species. We consider the conservation status of *Sauresia cayemitae* **sp. nov.** to be Endangered B1ab(iii), based on IUCN Redlist criteria (IUCN 2023). It faces a primary threat from habitat destruction caused by agriculture and charcoaling. Haiti, in general, is heavily deforested with < 1% of the nation's primary forest remaining (Hedges *et al.* 2018). Secondary threats to this species include predation from introduced predators, including the mongoose and black rats. Studies are needed to determine the health of any remaining populations and threats to the survival of the species.

FIGURE 83. (A–F) *Sauresia cayemitae* **sp. nov.** (ANSP38691, holotype), SVL 58.1 mm.

Reproduction. A litter size of two was recorded in this species (SBH, field data).

Etymology. The species name *cayemitae* is a Latin, feminine, genitive noun, in reference to the presence of this species on Grande Cayemite Island, Haiti.

Remarks. Previously, this species was considered to be a member of *Sauresia sepsoides*. Additional material in museum collections currently catalogued as *S. sepsoides* from in or near the distribution of *S. cayemitae* **sp. nov.** should be examined to determine if they represent additional material of *Sauresia cayemitae* **sp. nov.**

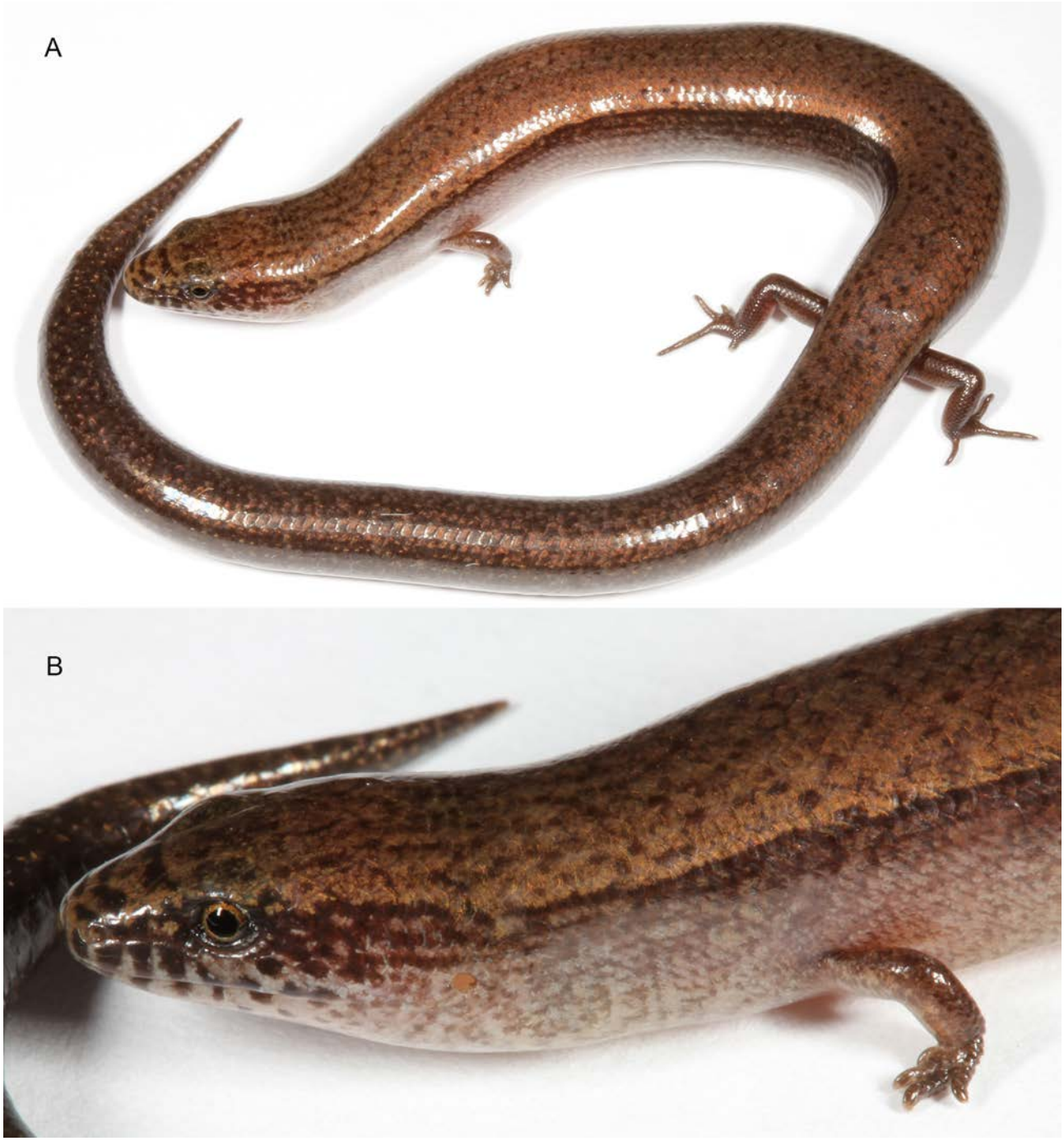

FIGURE 84. (A–B) *Sauresia cayemitae* **sp. nov.** (ANSP 38673, SBH 274050), in life. From Grande Cayemite, Grand'Anse Department, Haiti. Photos by SBH.

Sauresia cayemitae **sp. nov.** and *S. synoria* **sp. nov.** cannot be morphologically separated based on our standard suite of characters; however, they can be separated by the frontal width by the SVL (3.11–3.75 [n=7] versus 3.78–4.32 [n=2]). *Sauresia cayemitae* **sp. nov.** and *S. sepsoides* cannot be distinguished based on our suite of morphological characters; however, these species are not each other's closest relative, are genetically distinct from one another (Fig. 3), and have been diverged for 4.98 My (Fig. 4). In addition, *Sauresia cayemitae* **sp. nov.** possesses guanine at site 108 of the CytB gene while *Sauresia sepsoides* possesses adenine. *Sauresia cayemitae* **sp. nov.** also possesses thymine at site 141 of the CytB gene while *Sauresia sepsoides* possesses adenine. Future studies should examine additional characters to morphologically diagnose *Sauresia cayemitae* **sp. nov.** and *S. sepsoides.*

Sauresia cayemitae **sp. nov.** is included in our genetic dataset and has significant support in both Bayesian and ML likelihood analyses at the crown node of the species and the stem node that places it as the closest relative to *S.*

habichi. Based on our timetree (Fig. 4), *S. cayemitae* **sp. nov.** is separated from *S. habichi* by 1.19 Ma, consistent with typical species of vertebrates (> 0.7 Ma; Hedges *et al.* 2015). We recognize it as a distinct species because of the multiple morphological traits that separate it from *S. habichi*. *Sauresia cayemitae* **sp. nov.** was recovered as conspecific with *Sausesia habichi* in our ASAP analysis.

***Sauresia gracilis* sp. nov.**
Slender Four-toed Forest Lizard
(Fig. 85)

Sauresia sepsoides—Schwartz & Henderson, 1988:162 (part).
Sauresia sepsoides—Schwartz & Henderson, 1991:463 (part).
Celestus sepsoides—Henderson & Powell, 2009:105 (part).
Celestus sepsoides—Hedges *et al.*, 2019:17 (part).
Sauresia sepsoides—Schools & Hedges, 2021:231 (part).
Sauresia sepsoides—Landestoy *et al.*, 2022: 205 (part).

Holotype. USNM 328852, an adult from 10.3 km NW of Port Salut, Sud Department, Haiti, collected by S. Blair Hedges and Richard Thomas on 28 October 1984 (18.1419, -73.9711; 10 m).

Diagnosis. *Sauresia gracilis* **sp. nov.** has (1) a dorsal pattern of mottled/lineate, (2) head markings absent, (3) markings in the longitudinal paramedian area present, (4) dots arranged in bars in the lateral band absent, (5) a maximum SVL of 51.1 mm, (6) ventral scale rows, 103, (7) midbody scale rows, 36, (8) total lamellae on one hand, 18, (9) total strigae on ten scales, 100, (10) relative length of all digits on one hindlimb, 13.8 %, (11) relative distance between the angled subocular and mouth, 0.254 %, (12) relative eye length, 2.97 %, (13) relative forelimb length, 10.8 %, (14) relative ear width, 0.665 %, (15) relative rostral height, 1.90 %, (16) relative head length, 15.7 %, (17) relative mental width, 1.76 %, (18) relative postmental width, 2.76 %, (19) relative cloacal width, 7.18 %, (20) relative prefrontal width, 3.81 %, (21) relative largest supraocular width, 2.44 %, (22) relative longest finger length, 1.96 %, (23) relative distance between the ear and eye, 7.63 %, (24) relative head width, 67.6 %, (25) relative frontal width, 82.9 %, (26) relative nasal height, 0.998 %, (27) relative angled subocular height, 0.958 %, (28) relative distance between the eye and naris, 3.15 %, (29) relative canthal iii length, 1.82 %, (30) relative angled subocular width, 1.96 %, and (31) relative nasal length, 1.33 %. The species stem time is 4.21 Ma and no data are available to estimate the species crown time (Fig. 4).

Sauresia gracilis **sp. nov.** has a larger relative postmental width (2.76), relative cloacal width (7.18), and relative canthal iii length (1.82) than all other species of the genus. The only known specimen of *S. gracilis* **sp. nov.** is a small adult specimen, which may contribute to a bias towards larger measurements.

From *Sauresia agramma* **sp. nov.**, we distinguish *S. gracilis* **sp. nov.** by the dorsal pattern (mottled/lineate versus absent), the adult SVL (51.1 versus 53.8–69.1), the ventral scale rows (103 versus 121–127), the midbody scale rows (36 versus 37–39), the total lamellae on one hand (18 versus 17), the total strigae on ten scales (100 versus 103–138), the relative rostral height (1.90 versus 1.92–2.12), the relative head length (15.7 versus 13.6–15.2), the relative postmental width (2.76 versus 2.30–2.70), the relative cloacal width (7.18 versus 6.09–6.82), the relative longest finger length (1.96 versus 2.11–2.86), the relative head width (67.6 versus 69.7–74.6), the relative frontal width (82.9 versus 80.2–81.9), the relative width of canthal iii (1.82 versus 1.17–1.30), the relative angled subocular width (1.96 versus 2.07–2.47), and the relative nasal width (1.33 versus 1.36–1.57). From *S. cayemitae* **sp. nov.**, we distinguish *S. gracilis* **sp. nov.** by the relative eye length (2.97 versus 2.14–2.90), the relative head length (15.7 versus 13.0–15.6), the relative postmental width (2.76 versus 2.27–2.51), the relative cloacal width (7.18 versus 5.59–6.24), the relative prefrontal width (3.81 versus 3.11–3.64), the relative largest supraocular width (2.44 versus 1.67–2.25), the relative longest finger length (1.96 versus 2.36–2.65), the relative distance between the ear and eye (7.63 versus 6.02–6.88), the relative head width (67.6 versus 68.5–77.1), the relative nasal height (0.998 versus 0.792–0.951), and the relative width of canthal iii (1.82 versus 1.07–1.30). From *S. habichi*, we distinguish *S. gracilis* **sp. nov.** by the head markings (absent versus present), the adult SVL (51.1 versus 51.9–63.3), the ventral scale rows (103 versus 122–125), the midbody scale rows (36 versus 38–41), the relative length of digits on one hindlimb (13.8 versus 11.2–13.1), the relative distance between angled subocular and mouth (0.254 versus 0.000594–0.201), the relative eye length (2.97 versus 2.22–2.95), the relative head length (15.7 versus 13.3–15.0),

the relative postmental width (2.76 versus 2.11–2.34), the relative cloacal width (7.18 versus 5.86–6.68), the relative largest supraocular width (2.44 versus 1.96–2.23), the relative longest finger length (1.96 versus 2.26–2.71), the relative distance between the ear and eye (7.63 versus 6.64–7.30), the relative head width (67.6 versus 77.7–78.6), the relative frontal width (82.9 versus 71.8–77.5), and the relative width of canthal iii (1.82 versus 1.10–1.41). From *S. manicula* **sp. nov.**, we distinguish *S. gracilis* **sp. nov.** by the dorsal pattern (mottled/lineate versus absent), the ventral scale rows (103 versus 121–129), the midbody scale rows (36 versus 37–38), and the total lamellae on one hand (18 versus 15–17). From *S. pangnolae* **sp. nov.**, we distinguish *S. gracilis* **sp. nov.** by the dorsal pattern (mottled/lineate versus absent/irregular dots), the adult SVL (51.1 versus 53.8–66.7), the ventral scale rows (103 versus 104–119), the relative forelimb length (10.8 versus 11.4–12.6), the relative ear width (0.665 versus 0.681–1.11), the relative head length (15.7 versus 13.0–15.4), the relative postmental width (2.76 versus 2.04–2.47), the relative cloacal width (7.18 versus 6.07–6.81), the relative longest finger length (1.96 versus 2.29–2.54), the relative distance between the ear and eye (7.63 versus 6.94–7.46), the relative head width (67.6 versus 70.8–78.2), the relative frontal width (82.9 versus 69.6–81.5), the relative width of canthal iii (1.82 versus 1.09–1.51), the relative angled subocular width (1.96 versus 2.16–2.39), and the relative nasal width (1.33 versus 1.38–1.62). From *S. sepsoides*, we distinguish *S. gracilis* **sp. nov.** by the ventral scale rows (103 versus 104–119), the relative postmental width (2.76 versus 1.92–2.61), the relative cloacal width (7.18 versus 5.11–6.77), and the relative width of canthal iii (1.82 versus 0.943–1.62). From *S. synoria* **sp. nov.**, we distinguish *S. gracilis* **sp. nov.** by the dorsal pattern (mottled/lineate versus absent), the adult SVL (51.1 versus 53.5–72.0), the ventral scale rows (103 versus 114–127), the relative length of digits on one hindlimb (13.8 versus 10.5–12.3), the relative eye length (2.97 versus 2.47–2.94), the relative mental width (1.76 versus 1.21–1.70), the relative postmental width (2.76 versus 2.09–2.75), the relative cloacal width (7.18 versus 5.62–6.94), the relative prefrontal width (3.81 versus 3.01–3.30), the relative largest supraocular width (2.44 versus 1.57–1.91), the relative head width (67.6 versus 70.8–76.0), and the relative width of canthal iii (1.82 versus 0.943–1.31).

Description of holotype. USNM 328852. An adult; SVL 51.1 mm; tail nearly cylindrical, broken, 5.65 mm (11.1% SVL); axilla-to-groin distance 33.1 mm (64.8% SVL); forelimb length 5.54 mm (10.8% SVL); hindlimb length 10.4 mm (20.4% SVL); head length 8.03 mm (15.7% SVL); head width 5.43 mm (10.6% SVL); head width 67.6% head length; diameter of orbit 1.52 mm (2.97% SVL); horizontal diameter of ear opening 0.34 mm (0.665% SVL); vertical diameter of ear opening 0.25 mm (0.489% SVL); length of all toes on one foot 7.07 mm (13.8% SVL); shortest distance between angled subocular and lip 0.13 mm (0.254% SVL); shortest distance between the ocular and auricular openings 3.90 mm (7.63% SVL); longest finger length 1.00 mm (1.96% SVL); largest supraocular width 1.25 mm (2.45% SVL); cloacal width 3.67 mm (7.18% SVL); mental width 0.90 mm (1.76% SVL); postmental width 1.41 mm (2.76% SVL); prefrontal width 1.95 mm (3.82% SVL); frontal width 82.9% frontal length; nasal height 0.510 mm (0.998% SVL); angled subocular height 0.49 mm (0.959% SVL); shortest distance between the eye and naris 1.61 mm (3.15% SVL); canthal iii width 0.93 mm (1.82% SVL); angled subocular width 1.00 mm (1.96% SVL); nasal width 0.68 mm (1.33% SVL); rostral 1.90X as wide as high, visible from above, not in contact with nasals, in contact with 1st supralabial and anterior internasal (left)/(right); anterior internasals are narrower than posterior ones; frontonasals and prefrontal fused into a single large plate with a straight posterior margin, much wider than long, bordered by posterior internasals, 1st loreals, 1st median oculars, and the frontal; frontal longer than wide; a pair of frontoparietals, separated by the posterior prolongation of the frontal and the interparietal plate; interparietal plate smaller than parietals and separating them, posteriorly touching the interoccipital, which is wider than long; parietal separated from supraoculars by 1st and 2nd temporals and frontoparietal (left)/(right); nasal single; nostril just posterior to suture between 1st and 2nd supralabials (left)/(right); 1 postnasal (left)/(right); 2 loreals (left)/(right); 1st loreal higher than wide (left)/(right), in contact with postnasal, posterior internasal, prefrontal/frontonasal complex, 1st median ocular, canthal iii, 2nd loreal, and 3rd supralabial (left)/(right); 2nd loreal shorter than 1st, higher than wide (left)/(right), excluded from contact with supraocular by canthal iii (left)/(right); 2nd loreal posteriorly bordering the lower preocular (left)/(right); canthal iii wider than high (left)/(right), contacting 1st median ocular, anterior supraciliary, upper and lower preoculars, and 1st and 2nd loreals (left)/(right); 10 (left)/9 (right) median oculars, 1st contacting the prefrontal (left)/(right); 1 upper preocular (left)/(right); an irregular anterior supraciliary (left)/(right); 6 lateral oculars (left)/(right); 5 temporals (left)/(right); 2 (left)/3 (right) suboculars; posterior subocular large and elongate (left)/(right); anterior subocular small (left)/(right); 10 supralabials (left)/(right), 6 to level below center of eye (left)/(right); 8 (left)/9 (right) infralabials, 5 (left)/6 (right) to level below center of eye; mental small, followed by a single, larger post mental; 4 pairs of enlarged chin shields; 1st pair in contact with one another; 2nd–4th

pairs separated by 1–2 scales; 99 transverse rows of dorsal scales from interoccipital to base of tail; 103 transverse rows of ventral scales from mental to vent; 36 scales around midbody; 4 digits; finger lengths 3>2>4>1; 5 (left)/6 (right) lamellae under longest finger; 18 total lamellae on one hand; toe lengths 3>2>4>1; 9 lamellae under longest toe (left)/(right); keelless and striate dorsal body and caudal scales; smooth ventral scales; 100 total strigae counted on ten scales.

FIGURE 85. (A–F) *Sauresia gracilis* **sp. nov.** (USNM 328852, holotype), SVL 51.1 mm.

Color (in alcohol): dorsal surface of head rusty brown with some darker brown mottling; lateral surfaces of head grading from rusty brown to dark cream with darker brown eye masks and spotting on the labial scales; dorsal surfaces of the body are rusty brown with darker areas in the center of scales, giving a lineate appearance that is most prominent around the neck; dorsal surface of tail the same as the body; lateral areas grade from dark brown to dark cream; dorsal surfaces of the limbs are dark brown; lateral and ventral areas of the limbs grading from dark brown to yellow-cream; ventral surfaces of the head, body, and tail are yellow-cream with some darker brown mottling especially under the chin and posteriorly, where it becomes the predominant color on the tail.

Variation. No other specimens are known. Measurements and other morphological data for the holotype are presented in Table 1.

Distribution. *Sauresia gracilis* **sp. nov.** is known only from the type specimen, which was collected on the southwestern coast of the Tiburon Peninsula of Haiti at an elevation of 10 m (Fig. 80). It has an extent of occurrence of ~40 km^2.

Ecology and conservation. The holotype of this species was collected during the day under an object in leaf litter. SBH has visited this region of the type locality (not necessarily the specific location) on many occasions in the intervening 40 years and has not found another specimen. It likely is very localized and secretive.

We consider the conservation status of *Sauresia gracilis* **sp. nov.** to be Critically Endangered B1ab(iii), based on IUCN Redlist criteria (IUCN 2023). It faces a primary threat from habitat destruction resulting from agriculture and charcoaling. Haiti, in general, is heavily deforested with < 1% of the nation's primary forest remaining (Hedges *et al.* 2018). Secondary threats to this species include predation from introduced predators, including the mongoose and black rats. Studies are needed to determine the health of any remaining populations and threats to the survival of the species. Captive-breeding programs should be undertaken, because eradication of introduced mammalian predators is currently not possible on large islands.

Reproduction. No data on reproduction are available for this species.

Etymology. The species name (*gracilis*) is a Latin nominative singular adjective meaning "slender," alluding to the thin body shape and unusually low number of midbody scale rows in the holotype and only known representative of this species.

Remarks. Previously, this species was considered to be a member of *Sauresia sepsoides*. Additional material in museum collections currently catalogued as *S. sepsoides* from in or near the distribution of *S. gracilis* **sp. nov.** should be examined to determine if they represent additional material of *S. gracilis* **sp. nov.** This species is represented in our genetic dataset and the stem node places it outside of *S. agramma* **sp. nov.**, *S. manicula* **sp. nov.**, *S. sepsoides*, and *S. synoria* **sp. nov.** is significantly supported in our ML and Bayesian analyses. Based on our timetree (Fig. 4), *S. gracilis* **sp. nov.** diverged from its closest relative 4.21 Ma, consistent with typical species of vertebrates (> 0.7 Ma; Hedges *et al.* 2015). Our ASAP analysis also recognized *S. gracilis* **sp. nov.** as a distinct species.

***Sauresia habichi* (Weinland 1863)**

Stout Four-toed Forest Lizard
(Fig. 86–87)

Embryopus Habichii—Weinland, 1863:135. Holotype: ZMB 1310, Collected by D. F. Weinland at Jérémie, Grand'Anse department, Haiti, in 1857–58.
Sauresia sepsoides—Schwartz & Henderson, 1988:162 (part).
Sauresia sepsoides—Schwartz & Henderson, 1991:463 (part).
Celestus sepsoides—Hedges *et al.*, 2019:17 (part).
Sauresia sepsoides—Schools & Hedges, 2021:231 (part).
Sauresia sepsoides—Landestoy *et al.*, 2022: 205 (part).

Material examined (n=11). HAITI. **Grand'Anse.** ANSP 38681–83, an adult from 8.0 km S of Marche Leon, collected by S. Blair Hedges, Manuel Leal, Richard Thomas, and Nicholas Plummer on 28 May 1991 (18.51678, -74.08311; 435 m); KU 227597–99, ca 3 km (airline) SW Corail, 20 March 1966 (18.54806, -73.91232); KU 227802–03 (ca 7.5 km (airline) SSE Roseau, ca 2 km W La Bastille on 20 March 1966 (18.35407, -73.9395); MCZ R-74595, R-74598, David O. Hill, Trou-Bois on Jeremie Road, 1 January 1963; ZMB 1301, David Friedrich Weinland, Jeremie, 1857–1858.

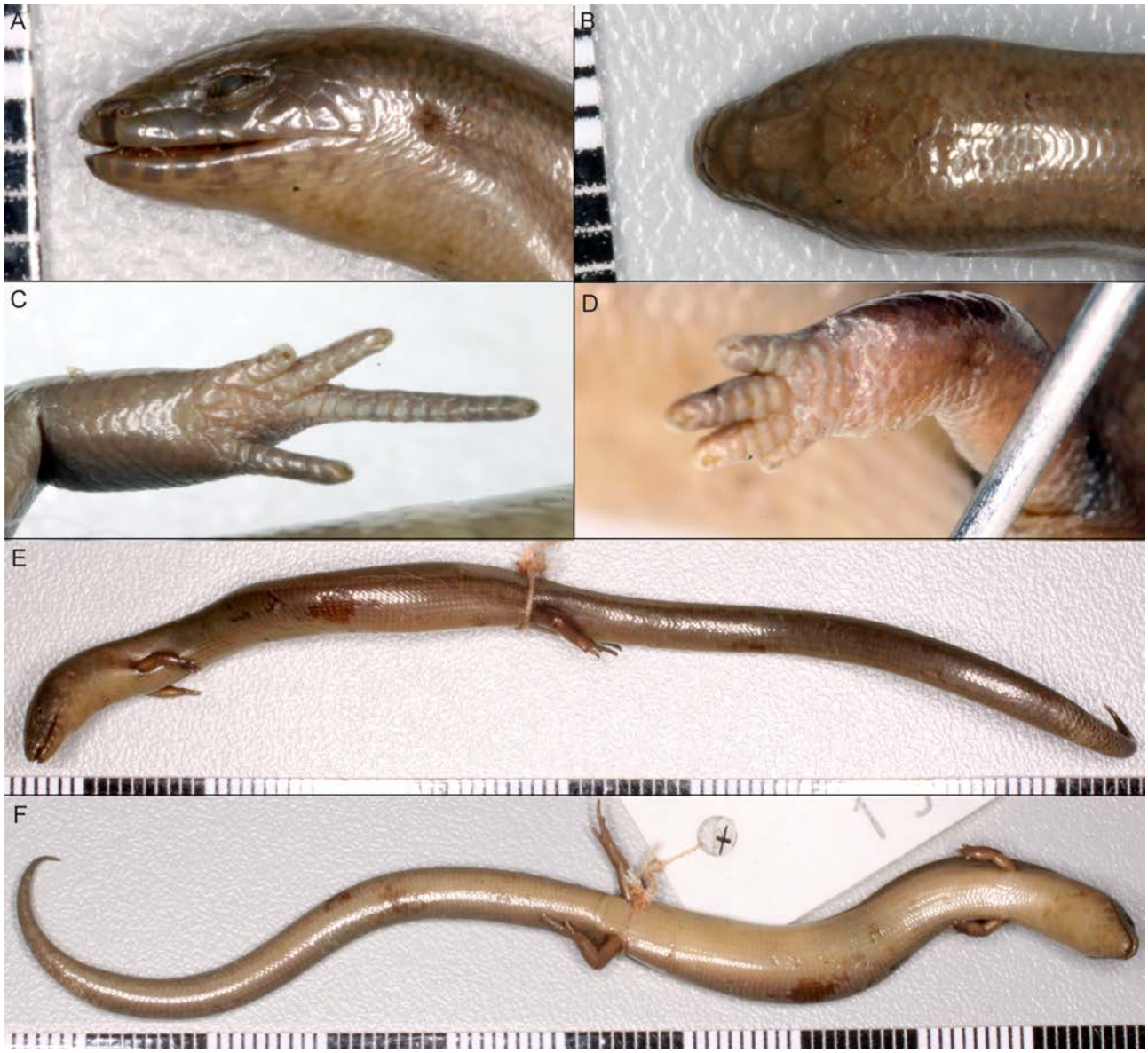

FIGURE 86. (A–F) *Sauresia habichi* (ZMB 1310, holotype), SVL 50.8 mm.

Diagnosis. *Sauresia habichi* has (1) a dorsal pattern of absent/lineate, (2) head markings present, (3) markings in the longitudinal paramedian area absent/present, (4) dots arranged in bars in the lateral band absent, (5) a maximum SVL of 51.9–63.3 mm, (6) ventral scale rows, 122–125, (7) midbody scale rows, 38–41, (8) total lamellae on one hand, 18–19, (9) total strigae on ten scales, 89–113, (10) relative length of all digits on one hindlimb, 11.2–13.1 %, (11) relative distance between the angled subocular and mouth, 0.000594–0.201 %, (12) relative eye length, 2.22–2.95 %, (13) relative forelimb length, 9.84–13.1 %, (14) relative ear width, 0.364–0.996 %, (15) relative rostral height, 1.83–2.42 %, (16) relative head length, 13.3–15.0 %, (17) relative mental width, 1.49–1.82 %, (18) relative postmental width, 2.11–2.34 %, (19) relative cloacal width, 5.86–6.68 %, (20) relative prefrontal width, 3.39–3.96 %, (21) relative largest supraocular width, 1.96–2.23 %, (22) relative longest finger length, 2.26–2.71 %, (23) relative distance between the ear and eye, 6.64–7.30 %, (24) relative head width, 77.7–78.6 %, (25) relative frontal width, 71.8–77.5 %, (26) relative nasal height, 0.890–1.11 %, (27) relative angled subocular height, 0.909–1.42 %, (28) relative distance between the eye and naris, 3.04–3.59 %, (29) relative canthal iii length, 1.10–1.41 %, (30) relative angled subocular width, 1.67–2.03 %, and (31) relative nasal length, 0.942–1.12 %. The species stem time is 1.19 Ma and the species crown time is 0.00 Ma (Fig. 4).

We distinguish *Sauresia habichi* from the other species of *Sauresia* based on a complex of traits. From *S. agramma* **sp. nov.**, we distinguish *S. habichi* by the total lamellae on one hand (18–19 versus 17), the relative

distance between angled subocular and mouth (0.000594–0.201 versus 0.217–0.262), the relative head width (77.7–78.6 versus 69.7–74.6), the relative frontal width (71.8–77.5 versus 80.2–81.9), the relative angled subocular width (1.67–2.03 versus 2.07–2.47), and the relative nasal width (0.942–1.12 versus 1.36–1.57). From *S. cayemitae* **sp. nov.**, we distinguish *S. habichi* by the ventral scale rows (122–125 versus 101–119), the midbody scale rows (38–41 versus 31–37), and the relative head width (77.7–78.6 versus 68.5–77.1). From *S. gracilis* **sp. nov.**, we distinguish *S. habichi* by the head markings (present versus absent), the adult SVL (51.9–63.3 versus 51.1), the ventral scale rows (122–125 versus 103), the midbody scale rows (38–41 versus 36), the relative length of digits on one hindlimb (11.2–13.1 versus 13.8), the relative distance between angled subocular and mouth (0.000594–0.201 versus 0.254), the relative eye length (2.22–2.95 versus 2.97), the relative head length (13.3–15.0 versus 15.7), the relative postmental width (2.11–2.34 versus 2.76), the relative cloacal width (5.86–6.68 versus 7.18), the relative largest supraocular width (1.96–2.23 versus 2.44), the relative longest finger length (2.26–2.71 versus 1.96), the relative distance between the ear and eye (6.64–7.30 versus 7.63), the relative head width (77.7–78.6 versus 67.6), the relative frontal width (71.8–77.5 versus 82.9), and the relative width of canthal iii (1.10–1.41 versus 1.82). From *S. manicula* **sp. nov.**, we distinguish *S. habichi* by the total lamellae on one hand (18–19 versus 15–17), the total strigae on ten scales (89–113 versus 119–150), the relative longest finger length (2.26–2.71 versus 2.20–2.21), the relative frontal width (71.8–77.5 versus 81.5), and the relative nasal width (0.942–1.12 versus 1.19–1.29). From *S. pangnolae* **sp. nov.**, we distinguish *S. habichi* by the ventral scale rows (122–125 versus 104–119), the relative angled subocular width (1.67–2.03 versus 2.16–2.39), and the relative nasal width (0.942–1.12 versus 1.38–1.62). From *S. sepsoides*, we distinguish *S. habichi* by the ventral scale rows (122–125 versus 104–119), the midbody scale rows (38–41 versus 34–37), and the relative nasal width (0.942–1.12 versus 1.16–1.60). From *S. synoria* **sp. nov.**, we distinguish *S. habichi* by the midbody scale rows (38–41 versus 34–36), the relative prefrontal width (3.39–3.96 versus 3.01–3.30), the relative largest supraocular width (1.96–2.23 versus 1.57–1.91), the relative head width (77.7–78.6 versus 70.8–76.0), the relative frontal width (71.8–77.5 versus 82.0–94.4), and the relative nasal width (0.942–1.12 versus 1.13–1.35).

Description of holotype (from detailed photographs). ZMB 1301. An adult; SVL 50.8; tail nearly cylindrical; head length 6.92 mm (13.6% SVL); head width 5.50 mm (10.8% SVL); head width 79.5% head length; diameter of orbit 1.14 mm (2.24% SVL); horizontal diameter of ear opening 0.32 mm (0.630% SVL); shortest distance between angled subocular and lip 0.10 mm (0.197% SVL); shortest distance between the ocular and auricular openings 3.69 mm (67.26% SVL); largest supraocular width 0.92 mm (1.81% SVL); mental width 0.89 mm (1.75% SVL); postmental width 1.25 mm (2.46% SVL); prefrontal width 1.93 mm (3.80% SVL); nasal height 0.56 mm (1.10% SVL); angled subocular height 0.71 mm (1.40% SVL); shortest distance between the eye and naris 1.80 mm (3.54% SVL); canthal iii width 0.58 mm (1.14% SVL); angled subocular width 0.95 mm (1.87% SVL); nasal width 0.55 mm (1.08% SVL); rostral 1.86X as wide as high, visible from above, not in contact with nasals, in contact with 2nd supralabial and anterior internasal (left), in contact with 1st supralabial and anterior internasal (right); anterior internasals are narrower than posterior ones; frontonasals and prefrontal fused into a single large plate with a slightly concave posterior margin, much wider than long, bordered by posterior internasals, 1st loreals, 1st median oculars, and the frontal; frontal longer than wide; a pair of frontoparietals, separated by the posterior prolongation of the frontal and the interparietal plate; interparietal plate smaller than parietals and separating them, posteriorly touching the interoccipital, which is almost as wide as long; nasal single; nostril just posterior to suture between 1st and 2nd supralabials (left)/(right); 1 postnasal (left)/(right); 2 loreals (left)/(right); 1st loreal higher than wide (left)/(right); canthal iii wider than high (left)/(right); 2 suboculars (left)/(right); posterior subocular large and elongate (left)/(right); anterior subocular small (left)/(right); 10/9 supralabials (left)/(right), 6/5 to level below center of eye (left)/(right); mental small, followed by a single, larger postmental; 4 pairs of enlarged chin shields; 1st pair in contact with one another; 2nd–4th pairs separated by 1–2 scales; 4 digits; 6 lamellae under longest finger (right); 19 total lamellae on one hand (right); 12 lamellae under longest toe (left).

Color (in alcohol): dorsal surface of head pale brown with darker brown outlines that are most pronounced on the internasal scales and prefrontal plate; lateral surfaces of head grading from pale brown to cream; dorsal surfaces of the body are medium brown with some darker brown mottling on the back of the neck; dorsal surface of tail medium brown, patternless; lateral areas grade from dark brown to cream; dorsal surfaces of the limbs are dark brown, patternless; lateral and ventral areas of the limbs fade to orange-cream, patternless; ventral surfaces of the head, body, and tail are an orange-cream with darker brown mottling under the head.

FIGURE 87. (A–F) *Sauresia habichi* (ANSP 38683, representative specimen), SVL 50.5 mm.

Description of a representative specimen. ANSP 38683. An adult; SVL 50.5 mm; tail nearly cylindrical, broken in life near tip, regenerated, 69.9 mm (138% SVL); axilla-to-groin distance 32.6 mm (64.6% SVL); forelimb length 6.61 mm (13.1% SVL); hindlimb length 9.27 mm (18.4% SVL); head length 7.16 mm (14.2% SVL); head width 5.63 mm (11.0% SVL); head width 78.6% head length; diameter of orbit 1.21 mm (2.40% SVL); horizontal diameter of ear opening 0.34 mm (0.673% SVL); vertical diameter of ear opening 0.30 mm (0.594% SVL); length of all toes on one foot 6.63 mm (13.1% SVL); shortest distance between angled subocular and lip 0.03 mm (0.0594% SVL); shortest distance between the ocular and auricular openings 3.41 mm (6.75% SVL); longest finger length 1.37 mm (2.71% SVL); largest supraocular width 1.05 mm (2.08% SVL); cloacal width 3.07 mm (6.08% SVL); mental width 0.92 mm (1.82% SVL); postmental width 1.18 mm (2.34% SVL); prefrontal width 2.00 mm (3.96% SVL); frontal width 74.0% frontal length; nasal height 0.46 mm (0.911% SVL); angled subocular height 0.50 mm (0.990% SVL); shortest distance between the eye and naris 1.58 mm (3.13% SVL); canthal iii width 0.67 mm (1.33% SVL); angled subocular width 1.25 mm (2.48% SVL); nasal width 0.87 mm (1.72% SVL); rostral 2.42X as wide as high, visible from above, not in contact with nasals, in contact with 1st supralabial and anterior internasal (left)/(right); anterior internasals are narrower than posterior ones; frontonasals and prefrontal fused into a single large plate with a concave posterior margin, much wider than long, bordered by posterior internasals, 1st loreals, 1st median oculars, and the frontal; frontal longer than wide; a pair of frontoparietals, separated by the posterior prolongation of the frontal and the interparietal plate; interparietal plate slightly smaller than parietals and separating them, posteriorly touching the interoccipital, which is wider than long; parietal separated from supraoculars by 1st and 2nd temporals and frontoparietal (left)/(right); nasal single; nostril just posterior to suture between 1st and 2nd supralabials (left)/(right); 1 postnasal (left)/(right); 2 loreals (left)/(right); 1st loreal higher than wide (left)/(right), in contact with postnasal, posterior internasal, prefrontal/frontonasal complex, 1st median ocular, canthal iii, upper and lower preoculars, and 3rd–4th supralabials (left)/postnasal, posterior internasal, prefrontal/frontonasal complex, 1st median ocular, canthal iii, 2nd loreal, and 3rd–4th supralabials (right); final loreal posteriorly bordering the lower preocular and canthal iii (left)/(right); canthal iii wider than high (left)/(right), contacting 1st median ocular, anterior supraciliary, upper and lower preoculars, and loreal 1 (left)/(right); 9 median oculars (left)/(right), 1st contacting the prefrontal (left)/(right); 1 upper preocular (left)/(right); an irregular anterior supraciliary (left)/(right); 6 lateral oculars (left)/(right); 6 temporals (left)/(right); 2 suboculars (left)/(right); posterior subocular large and elongate (left)/(right); anterior subocular small (left)/(right); 9 supralabials (left)/(right), 5 to level below center of eye (left)/(right); 9 infralabials (left)/(right), 6 to level below center of eye (left)/(right); mental small, followed by a single, larger postmental; 4 pairs of enlarged chin shields; 1st pair in contact with one another; 2nd–4th pairs separated by 1–2 scales; 114 transverse rows of dorsal scales from interoccipital to base of tail; 124 transverse rows of ventral scales from mental to vent; 38 scales around midbody; 4 digits; finger lengths 3>2>4>1; 6 lamellae under longest finger (left)/(right); 19 total lamellae on one hand; toe lengths 3>2>4>1; 11 lamellae under longest toe (left)/(right); keelless and striate dorsal body and caudal scales; smooth ventral scales; 89 total strigae counted on ten scales.

Color (in alcohol): dorsal surface of head pale brown with darker brown mottling and darker brown outlines on the internasal scales and prefrontal plate; lateral surfaces of head grading from pale brown to cream with darker brown markings around the eyes and on the infralabial scales; dorsal surfaces of the body are medium brown with darker red-brown areas in the center of scales; dorsal surface of tail dark brown, patternless; lateral areas grade from dark brown to cream; dorsal surfaces of the limbs are medium brown, patternless; lateral and ventral areas of the limbs fade to orange-cream, patternless; ventral surfaces of the head, body, and tail are orange-cream with darker brown mottling under the head and tail.

Variation. The majority of the examined material resembles the holotype in having multiple faded longitudinal paramedian lines that extend down the dorsum. MCZ R-74598 and MCZ R-74595 are both patternless. All specimens have darker outlines on their internasal scales. Measurements and other morphological data for the holotype and other examined material are presented in Table 1.

Distribution. *Sauresia habichi* is known from the west-central region of the Tiburon Peninsula of Haiti at elevations ranging from near sea level (holotype at Jérémie) to 1420 m (Fig. 80).

Ecology and conservation. No ecological data are associated with this species. We consider the conservation status of *Sauresia habichi* to be Endangered B1ab(iii), based on IUCN Redlist criteria (IUCN 2023). It faces a primary threat from habitat destruction resulting from agriculture and charcoaling. Haiti, in general, are heavily deforested with < 1% of the nation's primary forest remaining (Hedges *et al*. 2018). Secondary threats to this species include predation from other introduced predators, including the mongoose and black rats. Studies are needed to determine the health of any remaining populations and threats to the survival of the species.

Reproduction. No data on reproduction are available for this species.

Etymology. David Friedrich Weinland described this species in honor of Edward Habich of Boston, a friend who accompanied him during his six-month visit to Jérémie, Haiti, in 1857–1858 (Weinland 1858).

Remarks. Previously, this species was considered to be *Sauresia sepsoides*. Additional material in museum collections currently catalogued as *S. sepsoides* from in or near the distribution of *S. habichi* should be examined to determine if they represent additional material of *S. habichi*.

Sauresia habichi is included in our genetic dataset and has significant support in both Bayesian and ML likelihood analyses at the crown node of the species and the stem node that places it as the closest relative to *S. cayemitae* **sp. nov.** Based on our timetree (Fig. 4), *S. habichi* diverged from its closest relative 1.19 Ma, consistent with typical species of vertebrates (> 0.7 Ma; Hedges *et al.* 2015). We recognize it as a distinct species because of the multiple morphological traits that separate it from its closest relative (*S. sepsoides*). *Sausesia habichi* was recovered as conspecific with *Sauresia cayemitae* **sp. nov.** in our ASAP analysis.

***Sauresia manicula* sp. nov.**
Small-footed Four-toed Forest Lizard
(Fig. 88)

Sauresia sepsoides—Schwartz & Henderson, 1988:162 (part).
Sauresia sepsoides—Schwartz & Henderson, 1991:463 (part).
Celestus sepsoides—Hedges *et al.*, 2019:17 (part).
Sauresia sepsoides—Schools & Hedges, 2021:231 (part).
Sauresia sepsoides—Landestoy *et al.*, 2022: 205 (part).

Holotype. ANSP 38667, an adult from Berry, Ouest Department, Haiti, collected by S. Blair Hedges, Richard Thomas, Elizabeth Rochel, and Eladio Fernandez on 21 November 2009 (18.30795, -72.25389; 1,630 m).

Paratypes (n=3). HAITI. Ouest. ANSP 38668–9, S. Blair Hedges, Richard Thomas, Elizabeth Rochel, and Eladio Fernandez, Berry, 21 November 2009; SBH 268588, S. Blair Hedges, Richard Thomas, Elizabeth Rochel, and Eladio Fernandez, Berry, 21 November 2009.

Diagnosis. *Sauresia manicula* **sp. nov.** has (1) a dorsal pattern of absent, (2) head markings absent/present, (3) markings in the longitudinal paramedian area present, (4) dots arranged in bars in the lateral band absent, (5) a maximum SVL of 59.6–69.0 mm, (6) ventral scale rows, 121–129, (7) midbody scale rows, 37–38, (8) total lamellae on one hand, 15–17, (9) total strigae on ten scales, 119–150, (10) relative length of all digits on one hindlimb, 11.2–12.1 %, (11) relative distance between the angled subocular and mouth, 0.168–0.188 %, (12) relative eye length, 2.29–2.32 %, (13) relative forelimb length, 11.5–11.9 %, (14) relative ear width, 0.604–0.870 %, (15) relative rostral height, 1.89–1.90 %, (16) relative head length, 13.1–14.3 %, (17) relative mental width, 1.48–1.67 %, (18) relative postmental width, 2.13–2.16 %, (19) relative cloacal width, 5.30–6.41 %, (20) relative prefrontal width, 3.32–3.62 %, (21) relative largest supraocular width, 1.86–2.01 %, (22) relative longest finger length, 2.20–2.21 %, (23) relative distance between the ear and eye, 6.76–7.49 %, (24) relative head width, 72.9–82.8 %, (25) relative frontal width, 81.5 %, (26) relative nasal height, 0.772–1.09 %, (27) relative angled subocular height, 0.923–1.25 %, (28) relative distance between the eye and naris, 2.89–3.17 %, (29) relative canthal iii length, 1.06–1.43 %, (30) relative angled subocular width, 1.81–2.01 %, and (31) relative nasal length, 1.19–1.29 %. The species stem time is 0.78 Ma and the species crown time is 0.00 Ma (Fig. 4).

We distinguish *Sauresia manicula* **sp. nov.** from the other species of *Sauresia* based on a complex of traits. From *Sauresia agramma* **sp. nov.**, we distinguish *S. manicula* **sp. nov.** by the relative distance between angled subocular and mouth (0.168–0.188 versus 0.217–0.262), the relative rostral height (1.89–1.90 versus 1.92–2.12), the relative postmental width (2.13–2.16 versus 2.30–2.70), the relative angled subocular width (1.81–2.01 versus 2.07–2.47), and the relative nasal width (1.19–1.29 versus 1.36–1.57). From *S. cayemitae* **sp. nov.**, we distinguish *S. manicula* **sp. nov.** by the adult SVL (59.6–69.0 versus 47.8–58.1), the ventral scale rows (121–129 versus 101–119), the total strigae on ten scales (119–150 versus 84–104), the relative postmental width (2.13–2.16 versus 2.27–2.51), and the relative longest finger length (2.20–2.21 versus 2.36–2.65). From *S. gracilis* **sp. nov.**, we distinguish *S. manicula* **sp. nov.** by the dorsal pattern (absent versus mottled/lineate), the ventral scale rows (121–129 versus 103), the midbody scale rows (37–38 versus 36), and the total lamellae on one hand (15–17 versus 18). From *S. habichi*,

we distinguish *S. manicula* **sp. nov.** by the total lamellae on one hand (15–17 versus 18–19), the total strigae on ten scales (119–150 versus 89–113), the relative longest finger length (2.20–2.21 versus 2.26–2.71), the relative frontal width (81.5 versus 71.8–77.5), and the relative nasal width (1.19–1.29 versus 0.942–1.12). From *S. pangnolae* **sp. nov.**, we distinguish *S. manicula* **sp. nov.** by the ventral scale rows (121–129 versus 104–119), the total strigae on ten scales (119–150 versus 78–109), the relative eye length (2.29–2.32 versus 2.56–3.02), the relative prefrontal width (3.32–3.62 versus 3.70–3.83), the relative longest finger length (2.20–2.21 versus 2.29–2.54), the relative angled subocular width (1.81–2.01 versus 2.16–2.39), and the relative nasal width (1.19–1.29 versus 1.38–1.62). From *S. sepsoides*, we distinguish *S. manicula* **sp. nov.** the ventral scale rows (121–129 versus 104–119) and the relative eye length (2.29–2.32 versus 2.46–3.40). From *S. synoria* **sp. nov.**, we distinguish *S. manicula* **sp. nov.** by the midbody scale rows (37–38 versus 34–36), the total strigae on ten scales (119–150 versus 84–111), the relative eye length (2.29–2.32 versus 2.47–2.94), the relative prefrontal width (3.32–3.62 versus 3.01–3.30), and the relative frontal width (81.5 versus 82.0–94.4).

Description of holotype. ANSP 38667. An adult; SVL 69.0 mm; tail nearly cylindrical, broken in life near tip, regenerated, 70.1 mm (102% SVL); axilla-to-groin distance 46.2 mm (67.0% SVL); forelimb length 7.93 mm (11.5% SVL); hindlimb length 13.1 mm (19.0% SVL); head length 9.83 mm (14.2% SVL); head width 8.14 mm (11.8% SVL); head width 82.8% head length; diameter of orbit 1.58 mm (2.29% SVL); horizontal diameter of ear opening 0.60 mm (0.870% SVL); vertical diameter of ear opening 0.57 mm (0.826% SVL); length of all toes on one foot 8.32 mm (12.1% SVL); shortest distance between angled subocular and lip 0.13 mm (0.188% SVL); shortest distance between the ocular and auricular openings 5.17 mm (7.49% SVL); longest finger length 1.52 mm (2.20% SVL); largest supraocular width 1.39 mm (2.01% SVL); cloacal width 4.42 mm (6.41% SVL); mental width 1.15 mm (1.67% SVL); postmental width 1.49 mm (2.16% SVL); prefrontal width 2.50 mm (3.62% SVL); frontal width 81.5% frontal length; nasal height 0.75 mm (1.09% SVL); angled subocular height 0.86 mm (1.25% SVL); shortest distance between the eye and naris 2.19 mm (3.17% SVL); canthal iii width 0.99 mm (1.43% SVL); angled subocular width 1.39 mm (2.01% SVL); nasal width 0.89 mm (1.29% SVL); rostral 1.90X as wide as high, barely visible from above, not in contact with nasals, in contact with 1st supralabial and anterior internasal (left)/(right); anterior internasals are narrower than posterior ones; frontonasals and prefrontal fused into a single large plate with a straight posterior margin, much wider than long, bordered by posterior internasals, 1st loreals, 1st median oculars, and the frontal; frontal longer than wide; a pair of frontoparietals, separated by the posterior prolongation of the frontal and the interparietal plate; interparietal plate slightly smaller than parietals and separating them, posteriorly touching the interoccipital, which is wider than long; parietal separated from supraoculars by 1st and 2nd temporals, additional scale posterior to frontoparietal 1st temporals, and frontoparietal (left)/1st and 2nd temporals and frontoparietal (right); nasal single; nostril just posterior to suture between 1st and 2nd supralabials (left)/(right); 1 postnasal (left)/(right); 2 loreals (left)/(right); 1st loreal higher than wide (left)/(right), in contact with postnasal, posterior internasal, prefrontal/frontonasal complex, 1st median ocular, canthal iii, 2nd loreal, and 3rd–4th supralabials (left)/(right); 2nd loreal shorter than 1st, higher than wide (left)/(right), excluded from contact with supraocular by canthal iii (left)/(right); second loreal posteriorly bordering the upper and lower preoculars (left)/lower preocular (right); canthal iii wider than high (left)/(right), contacting 1st median ocular, anterior supraciliary, upper preocular, and 1st and 2nd loreals (left)/1st median ocular, anterior supraciliary, upper and lower preoculars, and 1st and 2nd loreals (right); 10 median oculars (left)/(right), 1st contacting the prefrontal (left)/(right); 1 upper preocular (left)/(right); an irregular anterior supraciliary (left)/(right); 7 lateral oculars (left)/(right); 6 (left)/7 (right) temporals; 2 (left)/3 (right) suboculars; posterior subocular large and elongate (left)/(right); anterior subocular small (left)/(right); 9 (left)/10 (right) supralabials, 5 to level below center of eye (left)/(right); 8 (left)/9 (right) infralabials, 5 to level below center of eye (left)/(right); mental small, followed by a single, larger postmental; 4 pairs of enlarged chin shields; 1st pair in contact with one another; 2nd pair in contact with one another anteriorly, posteriorly separated by one scale; 2nd–4th pairs separated by 1–2 scales; 125 transverse rows of dorsal scales from interoccipital to base of tail; 128 transverse rows of ventral scales from mental to vent; 37 scales around midbody; 4 digits; finger lengths 3>2>4>1; 5 lamellae under longest finger (left)/(right); 17 total lamellae on one hand; toe lengths 3>2>4>1; 11 lamellae under longest toe (left)/(right); keelless and striate dorsal body and caudal scales; smooth ventral scales; 150 total strigae counted on ten scales.

Color (in alcohol): dorsal surface of head medium brown with some darker brown mottling; lateral surfaces of head grading from medium brown to orange-tan with cream outlines on the labial scales; dorsal surfaces of the body are paler brown than the head with slightly darker areas on the interiors of scales, giving a lineate appearance; dorsal surface of tail slightly darker brown than the body, patternless; lateral areas grade from dark brown to creamy

orange; dorsal surfaces of the limbs are dark brown with some paler brown mottling on the upper limb; lateral and ventral areas of the limbs fade to creamy orange, patternless; ventral surfaces of the head, body, and tail are creamy orange with some medium brown mottling under the throat.

FIGURE 88. (A–F) *Sauresia manicula* **sp. nov.** (ANSP 38667, holotype), SVL 69.0 mm.

Variation. The examined material resembles the holotype in having mottling in the longitudinal paramedian area and faint lines extending down the dorsum. Several specimens possess darker outlines on their internasal scales. All specimens lack dots arranged in bars in the lateral area. Measurements and other morphological data for the holotype and other examined material are presented in Table 1.

Distribution. *Sauresia manicula* **sp. nov.** is known only from the locality of the type series, which was collected from the east-central region of the Tiburon Peninsula of Haiti at an elevation of 1630 m (Fig. 80). It has an extent of occurrence of ~90 km^2.

Ecology and conservation. No ecological data are associated with this species. We consider the conservation status of *Sauresia manicula* **sp. nov.** to be Critically Endangered B1ab(iii), based on IUCN Redlist criteria (IUCN 2023). It faces a primary threat from habitat destruction resulting from agriculture and charcoaling. Haiti, in general, is heavily deforested with < 1% of the nation's primary forest remaining (Hedges *et al.* 2018). Secondary threats to this species include predation from introduced predators, including the mongoose and black rats. Studies are needed to determine the health of any remaining populations and threats to the survival of the species. Captive-breeding programs should be undertaken, because eradication of introduced mammalian predators is currently not possible on large islands.

Reproduction. No data on reproduction are available for this species.

Etymology. The species name (*manicula*) is a Latin feminine nominative singular noun meaning small hand, in reference to the relatively small hands and feet in these lizards.

Remarks. Previously, this species was considered to be *Sauresia sepsoides*. Additional material in museum collections currently catalogued as *S. sepsoides* from in or near the distribution of *S. manicula* **sp. nov.** should be examined to determine if they represent additional material of *S. manicula* **sp. nov.**

Sauresia manicula **sp. nov.** is included in our genetic dataset and has significant support in both Bayesian and ML likelihood analyses at the crown node of the species and the stem node that places it as the closest relative to *S. synoria* **sp. nov.** Based on our timetree (Fig. 4), *S. manicula* **sp. nov.** diverged from its closest relative 0.78 Ma, consistent with typical species of vertebrates (> 0.7 Ma; Hedges *et al.* 2015). We recognize *S. manicula* **sp. nov.** as a distinct species based on the multiple morphological traits that separate it from its closest relative (*S. synoria* **sp. nov.**). *Sauresia manicula* **sp. nov.** was recovered as conspecific with *Sauresia synoria* **sp. nov.** in our ASAP analysis.

***Sauresia pangnolae* sp. nov.**
Pangnol Four-toed Forest Lizard
(Fig. 89–90)

Sauresia sepsoides—Schwartz & Henderson, 1988:162 (part).
Sauresia sepsoides—Schwartz & Henderson, 1991:463 (part).
Celestus sepsoides—Hedges *et al.*, 2019:17(part).
Sauresia sepsoides—Schools & Hedges, 2021:231 (part).
Sauresia sepsoides—Landestoy *et al.*, 2022: 205 (part).

Holotype. ANSP 38684, an adult female from Morne Bois Pangnol, Nippes Department, Haiti, collected by S. Blair Hedges, Tiffany Cloud, Sarah Hanson, and Miguel Landestoy on 20 June 2012 (18.41869, -73.77512; 1,170 m).

Paratypes (n=10). HAITI. Grand'Anse. ANSP 38690, Richard Thomas and Manuel Leal, 11.8 km S of Pestel, 25 May 1991. **Nippes**. ANSP 38663–4, S. Blair Hedges, Nicholas Plummer, Manuel Leal, Richard Thomas, and locals, 8.0 km SSW of Baraderes, 7 June 1991. **Sud.** KU 227822, Camp Perrin, 26 July 1962 (18.31667, -73.86667); KU 227823, 227827–8, 4.5 mi N Camp Perrin, 26–27 June 1979 (18.41118, -73.821); KU 227837–8, 227842, 11.8 mi N Cavaillon, 27 July 1976.

Diagnosis. *Sauresia pangnolae* **sp. nov.** has (1) a dorsal pattern of absent/irregular dots, (2) head markings absent/present, (3) markings in the longitudinal paramedian area absent/present, (4) dots arranged in bars in the lateral band absent, (5) a maximum SVL of 53.8–66.7 mm, (6) ventral scale rows, 104–119, (7) midbody scale rows, 35–42, (8) total lamellae on one hand, 14–19, (9) total strigae on ten scales, 78–109, (10) relative length of all digits on one hindlimb, 11.6–14.3 %, (11) relative distance between the angled subocular and mouth, 0.129–0.259 %, (12) relative eye length, 2.56–3.02 %, (13) relative forelimb length, 11.4–12.6 %, (14) relative ear width, 0.681–1.11 %, (15) relative rostral height, 1.73–2.27 %, (16) relative head length, 13.0–15.4 %, (17) relative mental width, 1.23–1.90 %, (18) relative postmental width, 2.04–2.47 %, (19) relative cloacal width, 6.07–6.81 %, (20) relative prefrontal width, 3.70–3.83 %, (21) relative largest supraocular width, 1.77–2.63 %, (22) relative longest finger length, 2.29–2.54 %, (23) relative distance between the ear and eye, 6.94–7.46 %, (24) relative head width,

70.8–78.2 %, (25) relative frontal width, 69.6–81.5 %, (26) relative nasal height, 0.945–1.05 %, (27) relative angled subocular height, 0.862–1.64 %, (28) relative distance between the eye and naris, 2.86–3.70 %, (29) relative canthal iii length, 1.09–1.51 %, (30) relative angled subocular width, 2.16–2.39 %, and (31) relative nasal length, 1.38–1.62 %. The species stem time is 4.66 Ma and the species crown time is 0.65 Ma (Fig. 4).

We distinguish *Sauresia pangnolae* **sp. nov.** from the other species of *Sauresia* based on a complex of traits. From *Sauresia agramma* **sp. nov.**, we distinguish *S. pangnolae* **sp. nov.** by the ventral scale rows (104–119 versus 121–127). From *S. cayemitae* **sp. nov.**, we distinguish *S. pangnolae* **sp. nov.** by the relative prefrontal width (3.70–3.83 versus 3.11–3.64) and the relative distance between the ear and eye (6.94–7.46 versus 6.02–6.88). From *S. gracilis* **sp. nov.**, we distinguish *S. pangnolae* **sp. nov.** by the dorsal pattern (absent/irregular dots versus mottled/lineate), the adult SVL (53.8–66.7 versus 51.1), the ventral scale rows (104–119 versus 103), the relative forelimb length (11.4–12.6 versus 10.8), the relative ear width (0.681–1.11 versus 0.665), the relative head length (13.0–15.4 versus 15.7), the relative postmental width (2.04–2.47 versus 2.76), the relative cloacal width (6.07–6.81 versus 7.18), the relative longest finger length (2.29–2.54 versus 1.96), the relative distance between the ear and eye (6.94–7.46 versus 7.63), the relative head width (70.8–78.2 versus 67.6), the relative frontal width (69.6–81.5 versus 82.9), the relative width of canthal iii (1.09–1.51 versus 1.82), the relative angled subocular width (2.16–2.39 versus 1.96), and the relative nasal width (1.38–1.62 versus 1.33). From *S. habichi*, we distinguish *S. pangnolae* **sp. nov.** by the ventral scale rows (104–119 versus 122–125), the relative angled subocular width (2.16–2.39 versus 1.67–2.03), and the relative nasal width (1.38–1.62 versus 0.942–1.12). From *S. manicula* **sp. nov.**, we distinguish *S. pangnolae* **sp. nov.** by the ventral scale rows (104–119 versus 121–129), the total strigae on ten scales (78–109 versus 119–150), the relative eye length (2.56–3.02 versus 2.29–2.32), the relative prefrontal width (3.70–3.83 versus 3.32–3.62), the relative longest finger length (2.29–2.54 versus 2.20–2.21), the relative angled subocular width (2.16–2.39 versus 1.81–2.01), and the relative nasal width (1.38–1.62 versus 1.19–1.29). From *S. sepsoides*, we cannot distinguish *S. pangnolae* **sp. nov.** based on our standard suite of characters (see Remarks). From *S. synoria* sp. nov., we distinguish *S. pangnolae* **sp. nov.** by the relative ear width (0.681–1.11 versus 0.361–0.670), the relative prefrontal width (3.70–3.83 versus 3.01–3.30), the relative frontal width (69.6–81.5 versus 82.0–94.4), and the relative nasal width (1.38–1.62 versus 1.13–1.35).

Description of holotype. ANSP 38684. An adult female; SVL 66.1 mm; tail nearly cylindrical, 43.6 mm (66.0% SVL); axilla-to-groin distance 43.5 mm (65.8% SVL); forelimb length 7.54 mm (11.4% SVL); hindlimb length 10.4 mm (15.7% SVL); head length 8.62 mm (13.0% SVL); head width 6.74 mm (10.2% SVL); head width 78.2% head length; diameter of orbit 1.69 mm (2.56% SVL); horizontal diameter of ear opening 0.45 mm (0.681% SVL); vertical diameter of ear opening 0.48 mm (0.726% SVL); length of all toes on one foot 7.67 mm (11.6% SVL); shortest distance between angled subocular and lip 0.12 mm (0.182% SVL); shortest distance between the ocular and auricular openings 4.59 mm (6.94% SVL); longest finger length 1.53 mm (2.31% SVL); largest supraocular width 1.17 mm (1.77% SVL); cloacal width 4.20 mm (6.35% SVL); mental width 0.81 mm (1.23% SVL); postmental width 1.57 mm (2.38% SVL); frontal width 69.6% frontal length; nasal height 0.65 mm (0.983% SVL); angled subocular height 0.57 mm (0.862% SVL); shortest distance between the eye and naris 1.89 mm (2.86% SVL); angled subocular width 1.53 mm (2.31% SVL); nasal width 0.91 mm (1.38% SVL); rostral 1.81X as wide as high, visible from above, not in contact with nasals, in contact with 1st supralabial and anterior internasal (left)/(right); anterior internasals are narrower than posterior ones; frontonasals and prefrontal fused into a single large plate with a concave posterior margin, much wider than long, bordered by posterior internasals, 1st loreals, 1st median oculars, and the frontal; frontal longer than wide; a pair of frontoparietals, separated by the posterior prolongation of the frontal and the interparietal plate; interparietal plate smaller than parietals and separating them, posteriorly touching the interoccipital, which is wider than long; parietal separated from supraoculars by 1st and 2nd temporals and frontoparietal (left)/(right); nasal single; nostril just posterior to suture between 1st and 2nd supralabials (left)/(right); 1 postnasal (left)/(right); 2 (left)/3 (right) loreals; 1st loreal higher than wide (left)/small(right), in contact with postnasal, posterior internasal, prefrontal/frontonasal complex, 1st median ocular, canthal iii, 2nd loreal, and supralabial 4 (left); 2nd loreal shorter than 1st, higher than wide (left)/higher than wide, in contact with posterior internasal, prefrontal/frontonasal complex, 1st median ocular, canthal iii, and 1st and 3rd loreals (right), excluded from contact with supraocular by canthal iii (left)/; large, irregular, excluded from contact with median oculars by canthal iii (right); final loreal posteriorly bordering the lower preocular (left)/(right); canthal iii wider than high (left)/small (right), contacting 1st median ocular (fused with anterior supraciliary), 2 upper preoculars, lower preocular, and 1st and 2nd loreals (left)/1st median ocular (fused with anterior supraciliary) and 2nd and 3rd loreals (right); 10 median oculars

(left)/(right), 1st contacting the prefrontal (left)/(right); 2 (left)/1 (right) upper preoculars; anterior supraciliary fused with 1st median ocular (left)/irregular (right); 7 lateral oculars (left)/(right); 6 temporals (left)/(right); 2 suboculars (left)/(right); posterior subocular large and elongate (left)/(right); anterior subocular small (left)/(right); 12 (left)/11 (right) supralabials, 6 to level below center of eye (left)/(right); 9 infralabials (left)/(right), 6 to level below center of eye (left)/(right); mental small, followed by a single, larger postmental; 4 pairs of enlarged chin shields, followed by 1 pair of reduced chin shields; 1st pair in contact with one another anteriorly, posteriorly separated by one scale; 2nd–5th pairs separated by 1–5 scales; 127 transverse rows of dorsal scales from interoccipital to base of tail; 128 transverse rows of ventral scales from mental to vent; 42 scales around midbody; 4 digits; finger lengths 3>2>4>1; 5 lamellae under longest finger (left)/(right); 17 total lamellae on one hand; toe lengths 3>2>4>1; 11 (left)/10 (right) lamellae under longest toe; keelless and striate dorsal body and caudal scales; smooth ventral scales; 92 total strigae counted on ten scales.

Color (in alcohol): dorsal surface of head dark gray-brown with darker brown mottling; lateral surfaces of head grading from dark gray-brown to pale cream with darker spots of brown, especially prominent on the labials; dorsal surfaces of the body are medium gray-brown with darker areas in the center of scales, giving a lineate appearance that is most prominent around the neck, which has a checkered appearance; dorsal surface of tail dark gray-brown, patternless; lateral areas are dark brown with paler brown to cream mottling giving the appearance of diagonal lines, especially on the sides of the neck; dorsal surfaces of the limbs are dark brown with paler cream spots; lateral and ventral areas of the limbs fade to pale cream with medium brown mottling; ventral surfaces of the head, body, and tail are pale cream color with large medium brown spots under the chin and medium gray-brown mottling on the tail.

Variation. The majority of the examined material resembles the holotype with no dorsal pattern other than mottling in the longitudinal paramedian area. KU 227828, KU 227842, and KU 227837 have a dorsal pattern of irregular dots. Most specimens show some degree of mottling in the longitudinal paramedian area whereas several others (including ANSP 38664 and ANSP 38663) have multiple faint longitudinal paramedian lines extending down their dorsums. All specimens either lack dots arranged in bars in the lateral band or this area appears mottled. Measurements and other morphological data for the holotype and other examined material are presented in Table 1.

Distribution. *Sauresia pangnolae* **sp. nov.** is known primarily from the mountainous interior of the Tiburon Peninsula east of Macaya National Park. The current delimitation of the range corresponds largely to the region of Morne Bois Pangnol. The elevational range is 420–1170 m (Fig. 80). The extent of occurrence is ~500 km^2.

Ecology and conservation. No ecological data are associated with this species. Haiti National Trust is currently working to protect the primary forest habitat on Morne Bois Pangnol, where this species was found, by having it declared it a National Park by Haiti and then managing the area and restoring native forest (Haiti National Trust 2024). However, it currently has no protection.

We consider the conservation status of *Sauresia pangnolae* **sp. nov.** to be Endangered B1ab(iii), based on IUCN Redlist criteria (IUCN 2023). It faces a primary threat from habitat destruction caused by agriculture and charcoaling. The Bois Pangnol region and Haiti in general, are heavily deforested with < 1% of the nation's primary forest remaining (Hedges *et al.* 2018). Secondary threats to this species include predation from introduced predators, including the mongoose and black rats. Studies are needed to determine the health of any remaining populations and threats to the survival of the species.

Reproduction. A litter size of two was recorded in this species (SBH, field data).

Etymology. The species name (*pangnolae*) is a feminine genitive singular noun referring to the distribution of this species in the region of Morne Bois Pangnol.

Remarks. Previously, this species was considered to be *Sauresia sepsoides*. Additional material in museum collections currently catalogued as *S. sepsoides* from in or near the distribution of *S. pangnolae* should be examined to determine if they represent additional material of *Sauresia pangnolae* **sp. nov.**

Sauresia pangnolae **sp. nov.** and *S. sepsoides* cannot be distinguished based on our suite of morphological characters; however, these species are not each other's closest relative, are genetically distinct from one another (Fig. 3), and have been diverged for 4.98 My (Fig. 4). In addition, *Sauresia pangnolae* **sp. nov.** possesses adenine at site 201 of the CytB gene while *Sauresia sepsoides* possesses guanine. *Sauresia pangnolae* **sp. nov.** also possesses thymine at site 228 of the CytB gene while *Sauresia sepsoides* possesses cytosine.

FIGURE 89. (A–F) *Sauresia pangnolae* **sp. nov.** (ANSP 38684, holotype), SVL 66.1 mm.

FIGURE 90. (A–B) *Sauresia pangnolae* **sp. nov.** (ANSP 38684, SBH 274213), SVL 66.1 mm, in life. From Morne Bois Pangnol, Nippes Department, Haiti. Photos by SBH.

Sauresia pangnolae **sp. nov.** is included in our genetic dataset and has significant support in both Bayesian and ML likelihood analyses at the crown node of the species. The stem node that places *S. pangnolae* **sp. nov.** as the closest relative of *S. habichi* and *S. cayemitae*, has a significant support value in our ML analysis, and a support value of 74% in our Bayesian analysis. Based on our timetree (Fig. 4), *S. pangnolae* **sp. nov.** diverged from its closest relative 4.66 Ma, consistent with typical species of vertebrates (> 0.7 Ma; Hedges *et al.* 2015). This species also occurs in sympatry with *S. sepsoides* in the area 5–12 km S Pestel. *Sauresia pangnolae* **sp. nov.** was recognized as a distinct species by our ASAP analysis.

***Sauresia sepsoides* Gray, 1852**
Eastern Four-toed Forest Lizard
(Fig. 91–92)

Sauresia sepsoides Gray, 1852:282. Holotype: BMNH 1946.8.29.29, collected by M. Salle on "St. Domingo" (no specific locality on the island of Hispaniola, see below).
Sauresia sepsoides—Boulenger, 1885:295.
Sauresia sepsoides—Barbour, 1930:100.
Sauresia sepsoides—Barbour, 1935:123.
Sauresia sepsoides—Barbour, 1937:139.
Sauresia (*Celestus*) *sepsoides*—Schmidt, 1921:16.
Sauresia sepsoides—Cochran, 1941:256.
Sauresia sepsoides—Greer, 1967:95.
Sauresia sepsoides—Schwartz & Henderson, 1991:463.
Celestus sepsoides—Henderson & Powell, 2009:105.
Celestus sepsoides—Hedges *et al.*, 2019:17.
Sauresia sepsoides—Schools & Hedges, 2021:231.
Sauresia sepsoides—Landestoy *et al.*, 2022: 205.

Material examined. (n=41). BMNH 1946.8.29.29, M. Salle, St. Domingo. **DOMINICAN REPUBLIC. Duarte.** Hispaniola. ANSP 38665–6, Richard Thomas, Manuel Leal, and Herman Dominicia, Batez Piedra, on west side of Rio Pazabo, 13 July 1993; SBH 193149, Herman Dominicia and Richard Thomas, southern slopes of Loma Quita Espuela, 16 July 1993. **Hato Mayor.** ANSP 38692–6, Dan Rabosky, Richard Thomas, 5.0 km airline SW Sabana de la Mar, 5 August 2001; ANSP 38697–702, Andres Perez, Dan Rabosky, and Richard Thomas, 7.8 km S of Sabana de la Mar, 2 August 2001; SBH 266963–75, A Perez, D Rabosky, and R Thomas, Loma del Fresca, 5.7 km airline SW Sabana de la Mar, 3 August 2001. **La Altagracia.** ANSP 38678, S. Blair Hedges, Richard Thomas, and Nicholas Plummer, 7.5 km W of La Zanga, at Rio Maimon, 20 July 1991. **Los Tabucos.** ANSP 38706–9, Richard Thomas, 8.8 km N, thence 0.5 km W Tenares, Salcedo, 21 July 1993. **Monte Plata.** ANSP 38679–80, Richard Thomas, 4.3 km N of Majagual, 13 July 1993. **Salcedo.** ANSP 38703–5, Richard Thomas, 23.2 km N of thence 4.5 km W Tenares, = 0.2 km E Jaiba, 21 July 1993. **Sanchez Ramirez.** ANSP 38670–2, Richard Thomas and Manuel Leal, 8.6 km NE of, thence 8.1 km east Cotui, =El Aguacate, 11 July 1993.

Diagnosis. *Sauresia sepsoides* has (1) a dorsal pattern of absent/mottled/irregular flecks, (2) head markings absent/present, (3) markings in the longitudinal paramedian area absent/present, (4) dots arranged in bars in the lateral band absent, (5) an adult SVL of 50.7–65.9 mm, (6) ventral scale rows, 104–119, (7) midbody scale rows, 34–37, (8) total lamellae on one hand, 14–19, (9) total strigae on ten scales, 83–119, (10) relative length of all digits on one hindlimb, 10.6–15.1 %, (11) relative distance between the angled subocular and mouth, 0.00–0.427 %, (12) relative eye length, 2.46–3.40 %, (13) relative forelimb length, 9.48–12.5 %, (14) relative ear width, 0.428–1.01 %, (15) relative rostral height, 1.45–2.49 %, (16) relative head length, 13.1–16.3 %, (17) relative mental width, 1.32–1.97 %, (18) relative postmental width, 1.92–2.61 %, (19) relative cloacal width, 5.11–6.77 %, (20) relative prefrontal width, 3.02–4.29 %, (21) relative largest supraocular width, 1.61–2.48 %, (22) relative longest finger length, 1.69–2.37 %, (23) relative distance between the ear and eye, 6.13–8.03 %, (24) relative head width, 64.7–83.1 %, (25) relative frontal width, 69.1–93.3 %, (26) relative nasal height, 0.706–1.17 %, (27) relative angled subocular height, 0.778–1.25 %, (28) relative distance between the eye and naris, 2.99–3.77 %, (29) relative canthal iii length, 0.943–1.62 %, (30) relative angled subocular width, 1.54–2.55 %, and (31) relative nasal length, 1.16–1.60 %. The species stem time is 2.46 Ma and the species crown time is 1.09 Ma (Fig. 4).

We distinguish *Sauresia sepsoides* from the other species of *Sauresia* based on a complex of traits. From *Sauresia agramma* **sp. nov.**, we distinguish *S. sepsoides* by the ventral scale rows (104–119 versus 121–127). From *S. cayemitae* **sp. nov.**, we cannot distinguish *S. sepsoides* based on our standard suite of characters (see Remarks). From *S. gracilis sp. nov.*, we distinguish *S. sepsoides* by the ventral scale rows (104–119 versus 103), the relative postmental width (1.92–2.61 versus 2.76), the relative cloacal width (5.11–6.77 versus 7.18), and the relative width of canthal iii (0.943–1.62 versus 1.82). From *S. habichi*, we distinguish *S. sepsoides* by the ventral scale rows (104–119 versus 122–125), the midbody scale rows (34–37 versus 38–41), and the relative nasal width (1.16–1.60 versus 0.942–1.12). From *S. manicula* **sp. nov.**, we distinguish *S. sepsoides* by the ventral scale rows (104–119 versus 121–129) and the relative eye length (2.46–3.40 versus 2.29–2.32). From *S. pangnolae* **sp. nov.**, we cannot

distinguish *S. sepsoides* based on our standard suite of characters (see Remarks). From *S. synoria* **sp. nov.**, we cannot distinguish *S. sepsoides* (see Remarks).

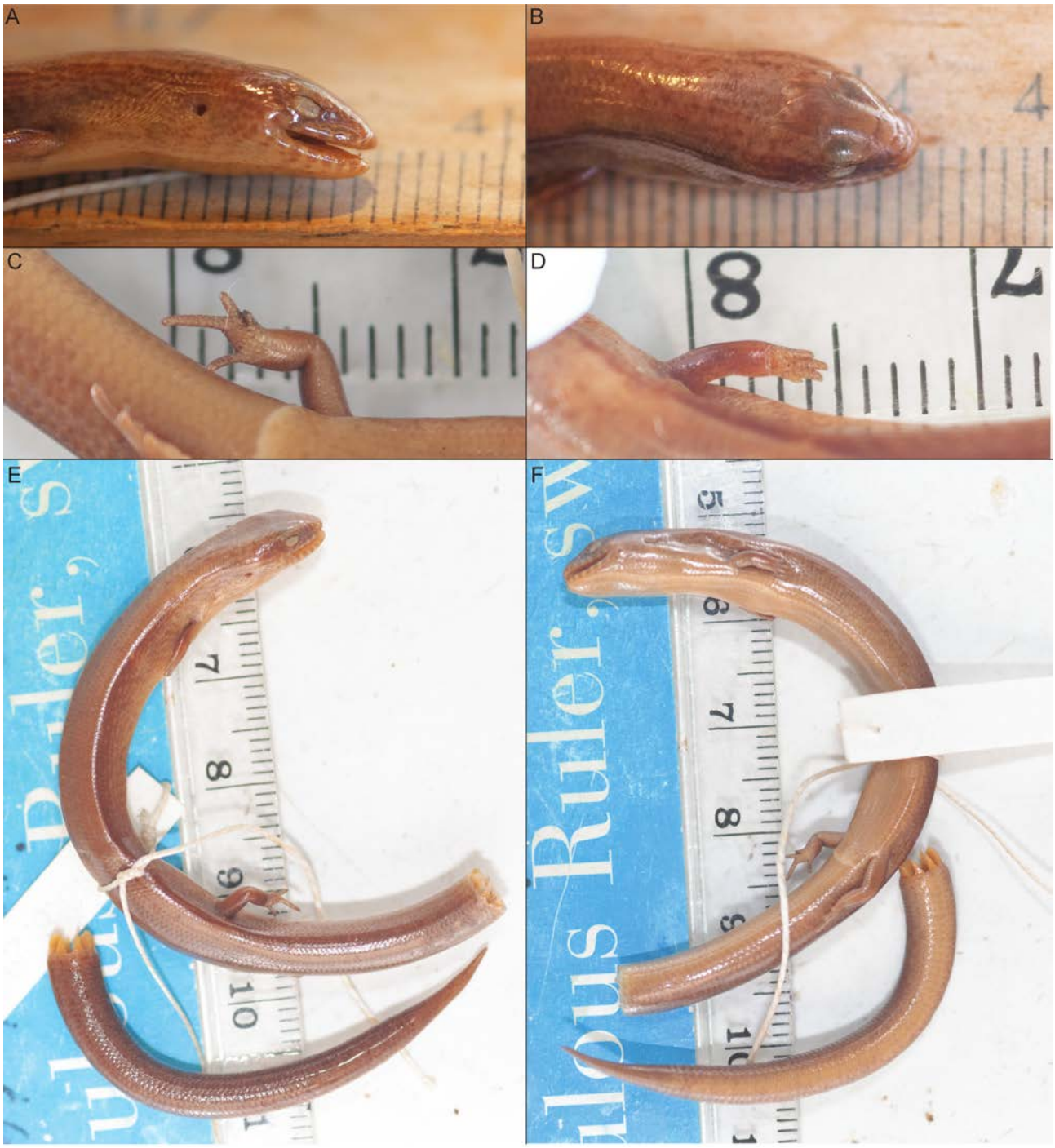

FIGURE 91. (A–F) *Sauresia sepsoides* (BMNH 1946.8.29.29, holotype), SVL 56.2 mm.

Description of holotype. BMNH 1946.8.29.29. An adult; SVL 56.2 mm; tail cylindrical, broken, also broken in life and regenerated, 77.2 mm (137% SVL); axilla-to-groin distance 37.0 mm (65.8% SVL); forelimb length 5.87 mm (10.4% SVL); hindlimb length 10.3 mm (18.3% SVL); head length 8.34 mm (14.8% SVL); head width 6.47 mm (11.5% SVL); head width 77.6% head length; diameter of orbit 1.46 mm (2.60% SVL); horizontal diameter of ear opening 0.45 mm (0.801% SVL); vertical diameter of ear opening 0.43 mm (0.765% SVL); length of all toes on one foot 5.98 mm (10.6% SVL); shortest distance between angled subocular and lip 0.24 mm (0.427% SVL); shortest distance between the ocular and auricular openings 3.98 mm (7.08% SVL); longest finger length 1.33 mm (2.37% SVL); largest supraocular width 1.31 mm (2.33% SVL); cloacal width 3.51 mm (6.25% SVL); prefrontal

width 1.90 mm (3.38% SVL); nasal height 0.66 mm (1.17% SVL); angled subocular height 0.70 mm (1.25% SVL); shortest distance between the eye and naris 1.99 mm (3.54% SVL); canthal iii width 0.53 mm (0.943% SVL); angled subocular width 1.16 mm (2.06% SVL); nasal width 0.71 mm (1.26% SVL); rostral 1.90X as wide as high, visible from above, not in contact with nasals, in contact with 1st supralabial and anterior internasal (left)/(right); anterior internasals are narrower than posterior ones; frontonasals and prefrontal fused into a single large plate with a convex posterior margin, much wider than long, bordered by posterior internasals, 1st loreals, 1st median oculars, and the frontal; frontal longer than wide; a pair of frontoparietals, separated by the posterior prolongation of the frontal and the interparietal plate; interparietal plate approximately the size of parietals and separating them, posteriorly touching the interoccipital, which is wider than long; parietal separated from supraoculars by 1st and 2nd temporals and frontoparietal (left)/(right); nasal single; nostril just posterior to suture between 1st and 2nd supralabials (left)/(right); 1 postnasal (left)/(right); 2 loreals (left)/(right); 1st loreal higher than wide (left)/(right), in contact with postnasal, posterior internasal, prefrontal/frontonasal complex, 1st median ocular, canthal iii, 2nd loreal, and the 3rd supralabials (left)/(right); 2nd loreal shorter than 1st, higher than wide (left)/(right), excluded from contact with supraocular by canthal iii (left)/(right); final loreal posteriorly bordering the upper and lower preoculars (left)/(right); canthal iii wider than high (left)/(right), contacting 1st median ocular, anterior supraciliary, upper and lower preoculars, and 1st and 2nd loreals (left)/1st median ocular, anterior supraciliary, upper preocular, and 1st and 2nd loreals (right); 8 (left)/10 (right) median oculars, 1st contacting the prefrontal (left)/(right); 1 upper preocular (left)/(right); an irregular anterior supraciliary (left)/(right); 6 lateral oculars (left)/(right); 6 temporals (left)/(right); 2 suboculars (left)/(right); posterior subocular large and elongate (left)/(right); anterior subocular small (left)/(right); 9 supralabials (left)/(right), 5 to level below center of eye (left)/(right); 8 (left)/9 (right) infralabials, 5 (left)/6 (right) to level below center of eye; mental small, followed by a single, larger postmental; 4 pairs of enlarged chin shields; 1st pair in contact with one another; 2nd pair in contact with one another anteriorly, posteriorly separated by one scale; 3rd–4th pairs separated by 1–2 scales; 103 transverse rows of dorsal scales from interoccipital to base of tail; 107 transverse rows of ventral scales from mental to vent; 35 scales around midbody; 4 digits; finger lengths 3>2>4>1; 5 lamellae under longest finger (left)/(right); 16 total lamellae on one hand; toe lengths 3>4>2>1; 9 (left)/11 (right) lamellae under longest toe; keelless and striate dorsal body and caudal scales; smooth ventral scales.

Color (in alcohol): dorsal surface of head medium brown with some darker brown mottling; lateral surfaces of head grading from medium brown to dark tan; dorsal surfaces of the body are medium brown with some mottling on neck; dorsal surface of tail same as body; lateral areas darker brown with mottling near the forelimb; dorsal surfaces of the limbs are same as lateral areas; lateral and ventral areas of the limbs fade to deep yellow; ventral surfaces of the head, body, and tail are deep yellow, patternless.

Variation. Members of this species have more pronounced longitudinal paramedian lines and lineate patterns than the holotype, which is faded; however, the majority of other specimens resemble the holotype in scalation. The majority of examined specimens have darker outlines on their head scale borders and several have dark markings on their head. No specimens have dots arranged in bars in the lateral band. Measurements and other morphological data for the holotype and other examined material are presented in Table 1.

Distribution. *Sauresia sepsoides* is distributed across the eastern and northeastern Dominican Republic at elevations of 30–820 m (Fig. 80). It has an extent of occurrence of ~15,230 km^2.

Ecology and conservation. Past literature accounts of ecological data for this species conflate multiple species and therefore cannot be used. We consider the conservation status of *Sauresia sepsoides* to be Least Concern, based on IUCN Redlist criteria (IUCN 2023). Species in this genus can be common in places, tolerant of some habitat disturbance, and this one has a wide distribution. However, it faces a primary threat of habitat destruction resulting from deforestation. A secondary threat is predation from introduced mammals, including the mongoose and black rats. Studies are needed to determine the health and extent of remaining populations and better understand the threats to the survival of the species.

Reproduction. Past literature accounts of reproductive data for this species conflate multiple species and therefore cannot be used.

Etymology. The species name *sepsoides* was coined by Gray to mean "similar to *Seps*," referring to a genus known at the time for skinks with reduced limbs. Historically, the name *Seps* has been associated with limb-reduced lizards, a usage that dates back to Linnaeus with the species *Lacerta seps*. The term has even older roots in Latin, where "seps" referred to small, venomous snakes or lizards, stemming from the Greek word sepein, which means "to putrefy."

FIGURE 92. *Sauresia sepsoides* (SBH 267756), in life. From ca. 1 km SW Los Limones, Monte Plata Province, Dominican Republic. Photograph by SBH.

Remarks. Herein, we divide what was previously considered the single species *Sauresia sepsoides* into eight species. Future studies should examine additional museum specimens catalogued as *S. sepsoides* to determine their correct taxonomic identification. The locality for the holotype of this species was reported as "St. Domingo," referred to the entire island of Hispaniola and not to the city of Santo Domingo, Dominican Republic. In the mid-nineteenth Century, the island was often called either "St. Domingo" or "Hayti," and sometimes "San Domingo" or "Saint Dominique."

Sauresia sepsoides and *S. pangnolae* **sp. nov.** cannot be distinguished based on our suite of morphological characters; however, these species are not each other's closest relative, are genetically distinct from one another (Fig. 3), and have been diverged for 4.98 My (Fig. 4). In addition, *Sauresia pangnolae* **sp. nov.** possesses adenine at site 201 of the CytB gene while *Sauresia sepsoides* possesses guanine. *Sauresia pangnolae* **sp. nov.** also possesses thymine at site 228 of the CytB gene while *Sauresia sepsoides* possesses cytosine. *Sauresia sepsoides* and *S. cayemitae* **sp. nov.** cannot be distinguished based on our suite of morphological characters; however, these species are not each other's closest relative, are genetically distinct from one another (Fig. 3), and have been diverged for 4.98 My (Fig. 4). In addition, *Sauresia cayemitae* **sp. nov.** possesses guanine at site 108 of the CytB gene while *Sauresia sepsoides* possesses adenine. *Sauresia cayemitae* **sp. nov.** also possesses thymine at site 141 of the CytB gene while *Sauresia sepsoides* possesses adenine. *Sauresia sepsoides* and *S. synoria* **sp. nov.** cannot be distinguished based on our suite of morphological characters; however, these species are not each other's closest relative, are genetically distinct from one another (Fig. 3), and have been diverged for 2.46 My (Fig. 4). Multiple characters distinguish *S. synoria* **sp. nov.** and its closest relative, *S. manicula* **sp. nov.** In addition, *Sauresia synoria* **sp. nov.** possesses thymine at site 105 of the CytB gene while *Sauresia sepsoides* possesses cytosine. *Sauresia synoria* **sp. nov.** also possesses guanine at site 108 of the CytB gene while *Sauresia sepsoides* possesses adenine.

Sauresia sepsoides **sp. nov.** is included in our genetic dataset and has significant support in both Bayesian and ML likelihood analyses at the crown node of the species and the stem node that places it as the closest relative to the group containing *S. agramma* **sp. nov.**, *S. manicula* **sp. nov.**, and *S. synoria* **sp. nov.** Based on our timetree (Fig. 4), *S. sepsoides* diverged from its closest relative 2.46 Ma, consistent with typical species of vertebrates (> 0.7 Ma;

Hedges *et al*. 2015). *Sauresia sepsoides* was recovered as conspecific with *Sauresia agramma* **sp. nov.** in our ASAP analysis.

***Sauresia synoria* sp. nov.**
Borderland Four-toed Forest Lizard
(Fig. 93–94)

Sauresia sepsoides—Schwartz & Henderson, 1988:162 (part).
Sauresia sepsoides—Schwartz & Henderson, 1991:463 (part).
Celestus sepsoides—Hedges *et al.*, 2019:17 (part).
Sauresia sepsoides—Schools & Hedges, 2021:231 (part).
Sauresia sepsoides—Landestoy *et al.*, 2022: 205 (part).

Holotype. ANSP 38689, an adult male from 22 km N Pedernales (at the Rio Mulito), Pedernales province, Dominican Republic, collected by S. Blair Hedges and Richard Thomas on 26 June 1985 (18.1544, -71.7581; 274 m).

Paratypes (n=3). DOMINICAN REPUBLIC. Pedernales. SBH 160343, Richard Thomas and S. Blair Hedges, Pedernales, 22 km N at Rio Mulito, 6 June 1985. **HAITI. Sud-Est.** MCZ R-131326–7, George Whiteman, Thiotte on road to Sal Trou, 1–31 March 1972.

Diagnosis. *Sauresia synoria* **sp. nov.** has (1) a dorsal pattern of absent, (2) head markings absent/present, (3) markings in the longitudinal paramedian area present, (4) dots arranged in bars in the lateral band absent, (5) a maximum SVL of 53.5–72.0 mm, (6) ventral scale rows, 114–127, (7) midbody scale rows, 34–36, (8) total lamellae on one hand, 16–18, (9) total strigae on ten scales, 84–111, (10) relative length of all digits on one hindlimb, 10.5–12.3 %, (11) relative distance between the angled subocular and mouth, 0.0561–0.472 %, (12) relative eye length, 2.47–2.94 %, (13) relative forelimb length, 9.14–11.9 %, (14) relative ear width, 0.361–0.670 %, (15) relative rostral height, 1.82–1.94 %, (16) relative head length, 12.3–15.9 %, (17) relative mental width, 1.21–1.70 %, (18) relative postmental width, 2.09–2.75 %, (19) relative cloacal width, 5.62–6.94 %, (20) relative prefrontal width, 3.01–3.30 %, (21) relative largest supraocular width, 1.57–1.91 %, (22) relative longest finger length, 1.75–2.52 %, (23) relative distance between the ear and eye, 5.91–7.81 %, (24) relative head width, 70.8–76.0 %, (25) relative frontal width, 82.0–94.4 %, (26) relative nasal height, 0.754–1.09 %, (27) relative angled subocular height, 0.880–1.22 %, (28) relative distance between the eye and naris, 2.67–3.61 %, (29) relative canthal iii length, 0.943–1.31 %, (30) relative angled subocular width, 1.82–2.30 %, and (31) relative nasal length, 1.13–1.35 %. The species stem time is 0.78 Ma and no data are available to estimate the species crown time (Fig. 4).

We distinguish *Sauresia synoria* **sp. nov.** from the other species of *Sauresia* based on a complex of traits. From *Sauresia agramma* **sp. nov.**, we distinguish *S. synoria* **sp. nov.** by the midbody scale rows (34–36 versus 37–39), the relative frontal width (82.0–94.4 versus 80.2–81.9), and the relative nasal width (1.13–1.35 versus 1.36–1.57). From *S. cayemitae* **sp. nov.**, we distinguish *S. synoria* **sp. nov.** by the frontal width by the SVL (3.78–4.32 versus 3.11–3.75) (see Remarks). From *S. gracilis* **sp. nov.**, we distinguish *S. synoria* **sp. nov.** by the dorsal pattern (absent versus mottled/lineate), the adult SVL (53.5–72.0 versus 51.1), the ventral scale rows (114–127 versus 103), the relative length of digits on one hindlimb (10.5–12.3 versus 13.8), the relative eye length (2.47–2.94 versus 2.97), the relative mental width (1.21–1.70 versus 1.76), the relative postmental width (2.09–2.75 versus 2.76), the relative cloacal width (5.62–6.94 versus 7.18), the relative prefrontal width (3.01–3.30 versus 3.81), the relative largest supraocular width (1.57–1.91 versus 2.44), the relative head width (70.8–76.0 versus 67.6), and the relative width of canthal iii (0.943–1.31 versus 1.82). From *S. manicula* **sp. nov.**, we distinguish *S. synoria* **sp. nov.** by the midbody scale rows (34–36 versus 37–38), the total strigae on ten scales (84–111 versus 119–150), the relative eye length (2.47–2.94 versus 2.29–2.32), the relative prefrontal width (3.01–3.30 versus 3.32–3.62), and the relative frontal width (82.0–94.4 versus 81.5). From *S. pangnolae* **sp. nov.**, we distinguish *S. synoria* **sp. nov.** by the relative ear width (0.361–0.670 versus 0.681–1.11), the relative prefrontal width (3.01–3.30 versus 3.70–3.83), the relative frontal width (82.0–94.4 versus 69.6–81.5), and the relative nasal width (1.13–1.35 versus 1.38–1.62). From *S. habichi*, we distinguish *S. synoria* **sp. nov.** by the midbody scale rows (34–36 versus 38–41), the relative prefrontal width (3.01–3.30 versus 3.39–3.96), the relative largest supraocular width (1.57–1.91 versus 1.96–2.23), the relative head width (70.8–76.0 versus 77.7–78.6), the relative frontal width (82.0–94.4 versus 71.8–77.5), and the relative nasal width (1.13–1.35 versus 0.942–1.12). From *S. sepsoides*, we cannot distinguish *S. synoria* **sp. nov.** (see Remarks).

FIGURE 93. (A–F) *Sauresia synoria* **sp. nov.** (ANSP 38689, holotype), SVL 53.5 mm.

Description of holotype. ANSP 38689. An adult male; SVL 53.5 mm; tail nearly cylindrical, broken, 3.01 mm (5.63% SVL); axilla-to-groin distance 36.2 mm (67.7% SVL); forelimb length 6.38 mm (11.9% SVL); hindlimb length 9.51 mm (17.8% SVL); head length 7.61 mm (14.2% SVL); head width 5.74 mm (10.7% SVL); diameter of orbit 1.57 mm (2.93% SVL); horizontal diameter of ear opening 0.32 mm (0.598% SVL); vertical diameter

of ear opening 0.18 mm (0.336% SVL); length of all toes on one foot 6.56 mm (12.3% SVL); shortest distance between angled subocular and lip 0.03 mm (0.0561% SVL); shortest distance between the ocular and auricular openings 3.58 mm (6.69% SVL); longest finger length 1.35 mm (2.52% SVL); largest supraocular width 1.02 mm (1.91% SVL); cloacal width 3.23 mm (6.04% SVL); mental width 0.82 mm (1.53% SVL); postmental width 1.12 mm (2.09% SVL); prefrontal width 1.69 mm (3.16% SVL); frontal width 94.4% frontal length; nasal height 0.52 mm (0.972% SVL); angled subocular height 0.55 mm (1.03% SVL); shortest distance between the eye and naris 1.76 mm (3.29% SVL); canthal iii width 0.51 mm (0.953% SVL); angled subocular width 1.19 mm (2.22% SVL); nasal width 0.72 mm (1.35% SVL); rostral 1.93X as wide as high, visible from above, not in contact with nasals, in contact with 1st supralabial and anterior internasal (left)/(right); anterior internasals are narrower than posterior ones; frontonasals and prefrontal fused into a single large plate with a convex posterior margin, much wider than long, bordered by posterior internasals, 1st loreal (left), 1st median oculars, and the frontal; frontal longer than wide; a pair of frontoparietals, separated by the posterior prolongation of the frontal and the interparietal plate; interparietal plate slightly smaller than parietals and separating them, posteriorly touching the interoccipital, which is longer than wide; parietal separated from supraoculars by 1st and 2nd temporals and frontoparietal (left)/(right); nasal single; nostril just posterior to suture between 1st and 2nd supralabials (left)/above suture between 1st and 2nd supralabials (right); 1 postnasal (left)/(right); 2 loreals (left)/(right); 1st loreal higher than wide (left)/(right), in contact with postnasal, posterior internasal, prefrontal/frontonasal complex, 1st median ocular, canthal iii, 2nd loreal, and 3rd and 4th supralabials (left)/postnasal, posterior internasal, canthal iii, 2nd loreal, and 3rd–4th supralabials (right); 2nd loreal shorter than 1st, higher than wide (left)/(right), excluded from contact with supraocular by canthal iii (left)/(right); 2nd loreal posteriorly bordering the lower preocular (left)/upper and lower preoculars (right); canthal iii wider than high (left)/(right), contacting 1st median ocular, anterior supraciliary, upper and lower preoculars, and 1st and 2nd loreals (left)/1st median ocular, anterior supraciliary, upper preocular, posterior internasal, and 1st and 2nd loreals (right); 9 median oculars (left)/(right), 1st contacting the prefrontal (left)/(right); 1 upper preocular (left)/(right); an irregular anterior supraciliary (left)/(right); 6 lateral oculars (left)/(right); 5 temporals (left)/(right); 2 suboculars (left)/(right); posterior subocular large and elongate (left)/(right); anterior subocular small (left)/(right); 8 supralabials (left)/(right), 5 to level below center of eye (left)/(right); 8 infralabials (left)/(right), 4–6 (left)/5 (right) to level below center of eye; mental small, followed by a single, larger postmental; 4 pairs of enlarged chin shields; 1st–2nd pairs in contact with one another; 3rd pair in contact with one another anteriorly, posteriorly separated by one scale; 4th pair separated by 1–2 scales; 108 transverse rows of dorsal scales from interoccipital to base of tail; 126 transverse rows of ventral scales from mental to vent; 35 scales around midbody; 4 digits; finger lengths 3>2>4>1; 6 lamellae under longest finger (left)/(right); 17 total lamellae on one hand; toe lengths 3>2>4>1; 11 (left)/10 (right) lamellae under longest toe; keelless and striate dorsal body and caudal scales; smooth ventral scales.

Color (in alcohol): dorsal surface of head medium brown with darker brown areas on scale borders; lateral surfaces of head grading from medium brown to an orange-cream with darker brown areas extending from the nasal scale to past the eye with some cream borders on scales; dorsal surfaces of the body are medium brown with darker areas in the middle of many scales giving a lineate appearance; dorsal surface of tail the same medium brown as the head with darker areas in the middle of many scales giving a lineate appearance; lateral areas grade from dark brown to orange-cream; dorsal surfaces of the limbs are medium brown, patternless; lateral and ventral areas of the limbs fade to orange cream; ventral surfaces of the head, body, and tail are yellow-cream color with medium brown mottling.

Variation. The majority of the examined material lacks a dorsal pattern other than mottling on the back of the neck. In the holotype and SBH 160343, multiple faded longitudinal paramedian lines extend down the dorsum. Both the holotype and SBH 160343 possess darker outlines on head scale borders whereas the heads are patternless in the other specimens. All specimens lack dots arranged in bars in the lateral area. Measurements and other morphological data for the holotype are presented in Table 1.

Distribution. *Sauresia synoria* **sp. nov.** is known only from the locality of the type series, which was collected in extreme southeastern Haiti and extreme southwestern Dominican Republic, where it was collected at an elevation of 270 m (Fig. 80). It has an extent of occurrence ~250 km^2.

Ecology and conservation. Little ecological information is associated with the type species other than the holotype was collected during the day and the paratype was collected at night under a rock.

We consider the conservation status of *Sauresia synoria* **sp. nov.** to be Endangered B1ab(iii), based on IUCN Redlist criteria (IUCN 2023). It faces a primary threat of habitat destruction resulting from agriculture and

charcoaling. Haiti is heavily deforested with < 1% of the nation's primary forest remaining, and the Dominican Republic also has suffered habitat loss (Hedges *et al.* 2018). Secondary threats to this species include predation from introduced predators, including the mongoose and black rats. Studies are needed to determine the health of any remaining populations and threats to the survival of the species.

FIGURE 94. *Sauresia synoria* **sp. nov.** (SBH 160343), in life. From 22 km N Pedernales at Rio Mulito, Pedernales Province, Dominican Republic. Photograph by SBH.

Reproduction. Litter size two (live mass of litter, 0.53 g) (SBH, field data).

Etymology. The species name (*synoria*) is a noun, from the Greek, meaning "borderland," in reference to this species' range extending into both the Dominican Republic and Haiti.

Remarks. Previously, this species was considered to be *Sauresia sepsoides*. Additional material in museum collections currently catalogued as *S. sepsoides* from in or near the distribution of *S. synoria* **sp. nov.** should be examined to determine if they represent this species.

Sauresia synoria and *S. cayemitae* cannot be morphologically separated based on our standard suite of characters; however, they can be separated by the frontal width by the SVL (3.78–4.32 [n=2] versus 3.11–3.75 [n=7]). *Sauresia synoria* **sp. nov.** and *S. sepsoides* cannot be distinguished based on our suite of morphological characters; however, these species are not each other's closest relative, are genetically distinct from one another (Fig. 3), and have been diverged for 2.46 My (Fig. 4). Multiple characters distinguish *S. synoria* **sp. nov.** and its closest relative, *S. manicula* **sp. nov.** In addition, *Sauresia synoria* **sp. nov.** possesses thymine at site 105 of the CytB gene while *Sauresia sepsoides* possesses cytosine. *Sauresia synoria* **sp. nov.** also possesses guanine at site 108 of the CytB gene while *Sauresia sepsoides* possesses adenine.

Sauresia synoria **sp. nov.** is included in our genetic dataset and has significant support in both Bayesian and ML analyses at the stem node that places it as the closest relative to *S. manicula* **sp. nov.** Based on our timetree (Fig. 4), *S. synoria* **sp. nov.** diverged from its closest relative 0.78 Ma, consistent with typical species of vertebrates (> 0.7 Ma; Hedges *et al.* 2015). We recognize *S. synoria* **sp. nov.** as a distinct species based on the multiple morphological traits that separate it from *S. manicula* **sp. nov**. *Sauresia synoria* **sp. nov.** was recovered as conspecific with *Sauresia manicula* **sp. nov.** in our ASAP analysis.

Genus *Wetmorena* (Cochran 1927)
Short-headed Four-toed Forest Lizards
(Fig. 95)

Wetmorena Cochran, 1927:91. Type species. *Wetmorena haetiana* Cochran, 1927:91, by original designation.

Diagnosis. Species of *Wetmorena* have (1) a dorsal pattern of absent/irregular dots/dots in series/lineate, (2) head markings absent/present, (3) markings in the longitudinal paramedian area absent/present, (4) dots arranged in bars in the lateral band absent, (5) a maximum SVL of 46.9–102 mm, (6) ventral scale rows, 100–126, (7) mid-body scale rows, 27–43, (8) total lamellae on one hand, 14–26, (9) total strigae on ten scales, 73–153, (10) relative length of all digits on one hindlimb, 9.44–19.7 %, (11) relative distance between the angled subocular and mouth, 0.00–0.600 %, (12) relative eye length, 2.07–3.74 %, (13) relative forelimb length, 8.05–17.2 %, (14) relative ear width, 0.00–0.634 %, (15) relative rostral height, 1.58–2.58 %, (16) relative head length, 12.1–14.1 % (or not applicable), (17) relative mental width, 1.40–2.24 %, (18) relative postmental width, 1.75–3.05 %, (19) relative cloacal width, 4.69–7.64 %, (20) relative prefrontal width, 3.26–4.60 %, (21) relative largest supraocular width, 1.62–2.97 %, (22) relative longest finger length, 1.44–5.35 %, (23) relative distance between the ear and eye, 5.80–6.61 % (or not applicable), (24) relative head width, 64.0–77.5 % (or not applicable), (25) relative frontal width, 73.6–114 %, (26) relative nasal height, 0.712–1.24 %, (27) relative angled subocular height, 0.851–1.52 %, (28) relative distance between the eye and naris, 2.25–5.20 %, (29) relative canthal iii length, 0.481–1.33 %, (30) relative angled subocular width, 1.55–2.47 %, and (31) relative nasal length, 0.803–1.95 %. Notably, *Wetmorena* possesses four digits (as opposed to five), a trait also observed in *Sauresia*.

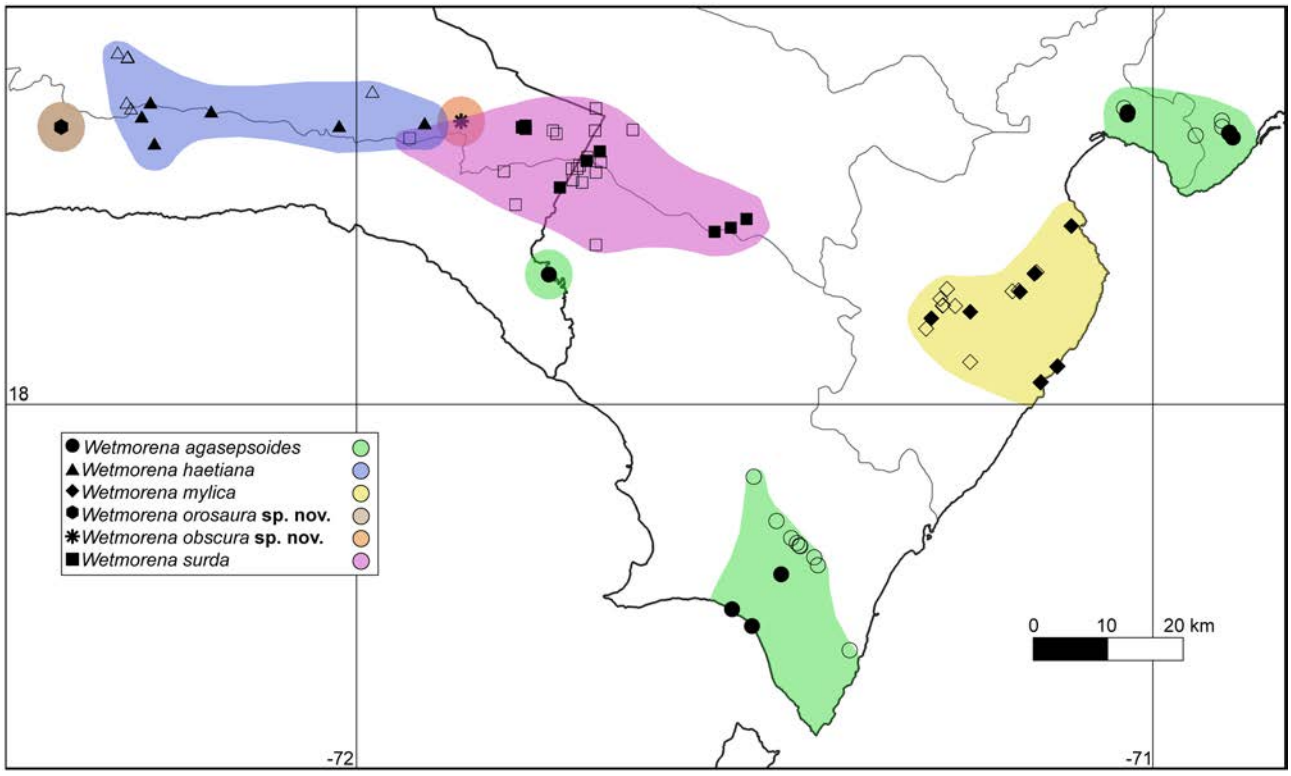

FIGURE 95. Map showing the distribution of *Wetmorena*. Hollow symbols indicate unexamined records assignable to species.

Content. Six species (Table 3): *Wetmorena agasepsoides*, *W. haetiana*, *W. mylica*, *W. obscura* **sp. nov.**, *W. orosaura* **sp. nov.**, and *W. surda*.

Distribution. *Wetmorena* occurs only on Hispaniola, primarily in upland areas of the Massif de la Selle (Haiti) and the Sierra de Bahoruco and Sierra Martin Garcia (Dominican Republic), but also in adjacent lowlands of the Barahona Peninsula.

***Wetmorena agasepsoides* (Thomas 1971)**
Serpentine Forest Lizard
(Fig. 96–97)

Diploglossus agasepsoides Thomas, 1971:2. Holotype: USNM 166964, collected by Richard Thomas from Barreras, Azua province, Dominican Republic, on 22 July 1969 (18.3228, -70.9042; 155 m).
Sauresia agasepsoides—Schwartz & Henderson, 1988:162.
Sauresia agasepsoides—Schwartz & Henderson, 1991:462.
Celestus agasepsoides—White & Powell, 1996:1.
Celestus agasepsoides—Hedges *et al.*, 2019:16.
Wetmorena agasepsoides—Schools & Hedges, 2021:232.
Wetmorena agasepsoides—Landestoy *et al.*, 2022: 205.

Material examined (n=10). DOMINICAN REPUBLIC. Azua. KU 93387, Barreras, 25 July 1969; USNM 166963, Barreras, 22 July 1969; USNM 166964, Richard Thomas, Barreras, 22 July 1969. **Barahona.** ANSP 38712, S. Blair Hedges and Richard Thomas, Canoa, 0.3 km S, 13.5 km E (airline), 19 June 1985; ANSP 38713–4, Richard Thomas and S. Blair Hedges, Canoa, 13.7 km due E (airline), 19 June 1985. **Pedernales.** ANSP 38710–1, S. Blair Hedges, Richard Thomas, and locals, Bucan Detwi, 6 January 1998; ANSP 38715, Richard Thomas and S. Blair Hedges, 14.5 km S of Los Arroyos, 12 August 1983; ANSP 38716, Richard Thomas and locals, Troudiye, Richard Thomas and locals, 6 January 1998.

Diagnosis. *Wetmorena agasepsoides* has (1) a dorsal pattern of absent, (2) head markings absent/present, (3) markings in the longitudinal paramedian area absent/present, (4) dots arranged in bars in the lateral band absent, (5) a maximum SVL of 49.1–58.6 mm, (6) ventral scale rows, 110–121, (7) midbody scale rows, 27–31, (8) total lamellae on one hand, 14–17, (9) total strigae on ten scales, 94–153, (10) relative length of all digits on one hindlimb, 9.44–11.2 %, (11) relative distance between the angled subocular and mouth, 0.00–0.224 %, (12) relative eye length, 2.22–3.11 %, (13) relative forelimb length, 8.05–9.58 %, (14) relative ear width, 0.292–0.634 %, (15) relative rostral height, 1.58–2.58 %, (16) relative head length, 12.1–14.4 %, (17) relative mental width, 1.40–1.66 %, (18) relative postmental width, 1.75–2.30 %, (19) relative cloacal width, 4.69–6.57 %, (20) relative prefrontal width, 2.77–3.35 %, (21) relative largest supraocular width, 1.66–2.07 %, (22) relative longest finger length, 1.44–2.01 %, (23) relative distance between the ear and eye, 5.80–6.61 %, (24) relative head width, 64.0–77.5 %, (25) relative frontal width, 74.9–94.4 %, (26) relative nasal height, 0.712–0.933 %, (27) relative angled subocular height, 0.851–1.09 %, (28) relative distance between the eye and naris, 2.25–3.27 %, (29) relative canthal iii length, 0.481–0.970 %, (30) relative angled subocular width, 1.55–2.36 %, and (31) relative nasal length, 0.803–1.55 %. The species stem time is 4.75 Ma and the species crown time is 0.54 Ma (Fig. 4).

Wetmorena agasepsoides has a smaller relative forelimb length (8.05–9.58) and relative longest finger length (1.44–2.01) than all other species of the genus. This species also has a larger relative auricular length (0.292–0.634) than all other species of the species. Notably, *W. agasepsoides* possesses external auricular openings while all other species of the genus lack this trait.

From *Wetmorena haetiana*, we distinguish *W. agasepsoides* by the adult SVL (49.1–58.6 versus 78.3–102), the midbody scale rows (27–31 versus 34–39), the total lamellae on one hand (14–17 versus 18–26), the relative length of digits on one hindlimb (9.44–11.2 versus 13.0–18.2), the relative forelimb length (8.05–9.58 versus 12.4–15.7), the relative ear width (0.292–0.634 versus 0.00), the relative prefrontal width (2.77–3.35 versus 3.44–4.60), and the relative longest finger length (1.44–2.01 versus 2.65–3.63). From *W. mylica*, we distinguish *W. agasepsoides* by the adult SVL (49.1–58.6 versus 76.0–98.2), the midbody scale rows (27–31 versus 37–41), the relative forelimb length (8.05–9.58 versus 10.5–14.3), the relative ear width (0.292–0.634 versus 0.00), and the relative longest finger length (1.44–2.01 versus 2.43–2.95). From *W. obscura* **sp. nov.**, we distinguish *W. agasepsoides* by the dorsal pattern (absent versus lineate), the midbody scale rows (27–31 versus 35–36), the total lamellae on one hand (14–17 versus 20–21), the total strigae on ten scales (94–153 versus 73–83), the relative length of digits on one hindlimb (9.44–11.2 versus 13.8–16.2), the relative distance between angled subocular and mouth (0.00–0.224 versus 0.295–0.426), the relative forelimb length (8.05–9.58 versus 13.6–16.3), the relative ear width (0.292–0.634 versus 0.00), the relative mental width (1.40–1.66 versus 1.72–2.24), the relative postmental width (1.75–2.30 versus 2.49–3.05), the relative prefrontal width (2.77–3.35 versus 4.03–4.58), the relative longest finger length (1.44–2.01 versus 4.08–5.35), and the relative distance between the eye and naris (2.25–3.27 versus 3.68–5.01). From *W. orosaura* **sp. nov.**, we distinguish *W. agasepsoides* by the dorsal pattern (absent versus lineate/irregular

dots), the adult SVL (49.1–58.6 versus 59.6–68.0), the midbody scale rows (27–31 versus 33–41), the total lamellae on one hand (14–17 versus 22–26), the relative length of digits on one hindlimb (9.44–11.2 versus 18.6–19.7), the relative forelimb length (8.05–9.58 versus 16.9–17.2), the relative ear width (0.292–0.634 versus 0.00), the relative postmental width (1.75–2.30 versus 2.31–2.68), the relative cloacal width (4.69–6.57 versus 6.69–6.88), the relative prefrontal width (2.77–3.35 versus 3.85–4.11), the relative largest supraocular width (1.66–2.07 versus 2.27–2.39), the relative longest finger length (1.44–2.01 versus 3.86–4.46), the relative nasal height (0.712–0.933 versus 1.07–1.16), the relative angled subocular height (0.851–1.09 versus 1.22–1.45), the relative distance between the eye and naris (2.25–3.27 versus 3.37–3.91), and the relative width of canthal iii (0.481–0.970 versus 1.14–1.26). From *W. surda*, we distinguish *W. agasepsoides* by the dorsal pattern (absent versus irregular dots/dots in series/lineate), the adult SVL (49.1–58.6 versus 62.5–81.9), the total lamellae on one hand (14–17 versus 18–21), the relative forelimb length (8.05–9.58 versus 11.3–13.9), the relative ear width (0.292–0.634 versus 0.00), the relative prefrontal width (2.77–3.35 versus 3.47–3.91), the relative longest finger length (1.44–2.01 versus 2.12–2.98), and the relative width of canthal iii (0.481–0.970 versus 1.17–1.33).

Description of holotype. USNM 166964. An adult; SVL 58.6 mm; tail nearly cylindrical, broken in life midway, regenerated, 43.8 mm (74.7% SVL); axilla-to-groin distance 42.0 mm (71.7% SVL); forelimb length 13.0 mm (22.2% SVL); hindlimb length 8.44 mm (14.4% SVL); head length 7.10 mm (12.1% SVL); head width 5.50 mm (9.39% SVL); head width 77.5% head length; diameter of orbit 1.30 mm (2.22% SVL); horizontal diameter of ear opening 0.24 mm (0.410% SVL); vertical diameter of ear opening 0.35 mm (0.597% SVL); length of all toes on one foot 5.71 mm (9.74% SVL); shortest distance between angled subocular and lip 0.13 mm (0.222% SVL); shortest distance between the ocular and auricular openings 3.41 mm (5.82% SVL); longest finger length 0.99 mm (1.69% SVL); largest supraocular width 0.97 mm (1.66% SVL); cloacal width 3.19 mm (5.44% SVL); prefrontal width 1.62 mm (2.76% SVL); frontal width 94.4% frontal length; nasal height 0.43 mm (0.734% SVL); angled subocular height 0.57 mm (0.973% SVL); shortest distance between the eye and naris 1.32 mm (2.25% SVL); canthal iii width 0.42 mm (0.717% SVL); angled subocular width 0.91 mm (1.55% SVL); nasal width 0.47 mm (0.802% SVL); rostral 1.58X as wide as high, visible from above, not in contact with nasals, in contact with 1st supralabial and anterior internasal (left)/(right); anterior internasals are slightly narrower than posterior ones; frontonasals and prefrontal fused into a single large plate with a straight posterior margin, much wider than long, bordered by posterior internasals, 1st loreals, 1st median oculars, and the frontal; frontal longer than wide; a pair of frontoparietals, separated by the posterior prolongation of the frontal and the interparietal plate; interparietal plate slightly larger than parietals and separating them, posteriorly touching the interoccipital, which is wider than long; parietal separated from supraoculars by 1st and 2nd temporals and frontoparietal (left)/(right); nasal single; nostril just posterior to suture between 1st and 2nd supralabials (left)/(right); 1 postnasal (left)/(right); 1 loreal (left)/(right); postnasal, posterior internasal, prefrontal/frontonasal complex, frontal, 1st median ocular, upper and lower preoculars, and the 3rd and 4th supralabials (left)/(right); 9 median oculars (left)/(right), 1st contacting the prefrontal (left)/(right); 2 (left)/2 (right) upper preoculars; an irregular anterior supraciliary (left)/(right); 6 lateral oculars (left)/(right); 5 temporals (left)/(right); 2 suboculars (left)/(right); posterior subocular large and elongate (left)/(right); anterior subocular small (left)/(right); 8 supralabials (left)/(right), 5 to level below center of eye (left)/(right); 8 (left)/9 (right) infralabials, 5 to level below center of eye (left)/(right); mental small, followed by a single postmental of equal size; 4 pairs of enlarged chin shields; 1st pair in contact with one another; 106 transverse rows of dorsal scales from interoccipital to base of tail; 114 transverse rows of ventral scales from mental to vent; 29 scales around midbody; 4 digits; finger lengths 3>2>4>1; 5 lamellae under longest finger (left)/(right); 23 total lamellae on one hand; toe lengths 3>2>4>1; 11 (left)/10 (right) lamellae under longest toe; keelless and striate dorsal body and caudal scales; smooth ventral scales; 106 total strigae counted on ten scales.

Color (in alcohol): dorsal surface of head medium brown with some darker brown mottling; lateral surfaces of head grading from medium brown to pale tan with darker brown eye masks and spots on the labial scales; dorsal surfaces of the body are medium brown with darker areas in the center of the scales giving a lineate appearance; dorsal surface of tail the same as the body, regenerated section is bright yellow; dorsal surfaces of the limbs are orange-brown; lateral and ventral areas of the limbs fade to orange-cream with some pale brown mottling; ventral surfaces of the head, body, and tail are gray-tan with some darker mottling on the throat.

Variation. The majority of the examined material resembles the holotype in having a dorsal pattern of faded lines extending down the dorsum. USNM 166963 is completely patternless, whereas KU 93387 is patternless other than several irregular flecks on the neck. ANSP 38715 and ANSP 38714 have patternless heads, whereas the other

examined specimens have dark outlines on their head scales. KU 93387 and USNM 166963 also have darker, irregular areas on their heads. All specimens lack dots arranged in bars in the longitudinal paramedian area. Measurements and other morphological data for the holotype and other examined material are presented in Table 1.

FIGURE 96. (A–F) *Wetmorena agasepsoides* (USNM 166964, holotype), SVL 58.6 mm.

Distribution. *Wetmorena agasepsoides* is distributed in three southwestern areas of the Dominican Republic at elevations of 10–750 m (Fig. 95). It has an extent of occurrence of ~2,600 km^2.

Ecology and conservation. Little has been recorded of the ecological habits of *Wetmorena agasepsoides*. Individuals have been collected under rocks and other surface debris (Thomas 1971; Schwartz & Henderson 1991; White *et al.* 1992). A stomach content analysis of this species showed that its diet mostly consists of invertebrates

including beetles, beetle larvae and pupae, crickets, roaches, flies, ants, and centipedes (White *et al.* 1992). Thomas (1971) suspected that the Sierra de Martín García population is a geographic isolate, as the surrounding areas were mostly xeric cactus scrub as opposed to the mesic forest on the Sierra de Martín García.

The IUCN Redlist (IUCN 2023) considers the conservation status of *Wetmorena agasepsoides* to be Endangered B1ab(iii) "due to its limited distribution (with an extent of occurrence of 2509 km^2), occurrence in two locations and ongoing threats from agriculture expansion and wood extraction." The original description also reported that areas surrounding the type locality had already been heavily cut for charcoal (Thomas 1971). Studies are needed to determine the health of remaining populations and threats to the survival of the species. Captive-breeding programs should be undertaken, because eradication of introduced mammalian predators is currently not possible on large islands.

Reproduction. No data on reproduction are available for this species.

Etymology. The name *agasepsoides* is derived from the Greek *aga* (meaning "very") and *sepsoides*, in reference to the elongate species *Sauresia sepsoides*, considered by Thomas (1971) to be its closest relative. Hence, it refers to the very elongate habitus of this species. See the etymology for *Sauresia sepsoides* for additional information on the origin of the word "*sepsoides*."

Remarks. When described, *Wetmorena agasepsoides* was considered a close relative of *Sauresia sepsoides*, likely because of the presence of ears (Thomas 1971). *Wetmorena agasepsoides* is included in our genetic dataset and has significant support in both Bayesian and ML analyses at the crown node that defines it as a species. The stem node that places *W. agasepsoides* as the closest relative to *W. obscura* **sp. nov.** has a support value of 66% in our ML analysis and is not supported in our Bayesian analysis. Using genomic data, Schools *et al.* (2022) placed *W. agasepsoides* as the outgroup to all other species of *Wetmorena* with significant support in both ML and Bayesian analyses. Based on our timetree (Fig. 4), *Wetmorena agasepsoides* diverged from its closest relative (*W. obscura* **sp. nov.**) 4.75 Ma, consistent with typical species of vertebrates (> 0.7 Ma; Hedges *et al.* 2015). *Wetmorena agasepsoides* was recognized as a distinct species by our ASAP analysis.

FIGURE 97. *Wetmorena agasepsoides* (ANSP 38713), SVL 57.6 mm, in life. From 13.7 km due E Canoa, Barahona Province, Dominican Republic. Photograph by SBH.

***Wetmorena haetiana* (Cochran 1927)**

Stout Earless Forest Lizard
(Fig. 98–99)

Wetmorena haetiana Cochran, 1927:91. Holotype: USNM 72600, collected by Dr. A. Wetmore on Morne Cabaio, Ouest department, Haiti, on 10 April 1927 (18.3569, -72.2589; 2,241 m).
Wetmorena haetiana—Barbour, 1930:100.
Wetmorena haetiana—Barbour, 1935:123.
Wetmorena haetiana—Barbour, 1937:140.
Wetmorena haetiana—Cochran, 1941:259.
Wetmorena haetianus—Schwartz & Henderson, 1988:197.
Wetmorena haetianus—Schwartz & Henderson, 1991:553.

Celestus haetianus—Hedges *et al.*, 2019:17.
Wetmorena haetiana—Schools & Hedges, 2021:232.
Wetmorena haetiana—Landestoy *et al.*, 2022: 205.

Material examined (n=38). HAITI. Ouest. ANSP 38717–8, S. Blair Hedges, Richard Thomas, Elizabeth Rochel, Eladio Fernandez, Berry, 19 November 2009; ANSP 38719–22, S. Blair Hedges, Richard Thomas, Elizabeth Rochel, Eladio Fernandez, Morne Cardineau, 18 November 2009; ANSP 38726, S. Blair Hedges, Richard Thomas, Elizabeth Rochel, Eladio Fernandez, Morne La Visite, Sink hole in P. La Visite next to ridge crest, 19 November 2009; ANSP 38743, S. Blair Hedges, southeast of Pic La Selle, 20 November 2011; ANSP 38744–5, S. Blair Hedges, Richard Thomas, Elizabeth Rochel, Eladio Fernandez, Waterfall in Parc La Visite, 18 November 2009; SBH 268542–3, Morne Cardineau; SBH 268564, Morne La Visite, Sink hole in P. La Visite next to ridge crest; USNM 72600–1, USNM 72604 Dr. A. Wetmore, Morne Cabaio (= Morne du Cibao), Massif de la Selle, 10 April 1927. **Sud-Est.** ANSP 38727–42, S. Blair Hedges, Tiffany Cloud, Miguel Landestoy, Marcos Rodriguez, Southeast of Pic La Selle, 20 November 2011; SBH 269929–30, Pic La Selle Sud-Ouest. **Barahona.** KU 79722–5, 24 km SW Barahona, 2 August 1963.

FIGURE 98. (A–F) *Wetmorena haetiana* (USNM 72600, holotype), SVL 95.0 mm.

Diagnosis. *Wetmorena haetiana* has (1) a dorsal pattern of absent/irregular dots/lineate, (2) head markings absent/present, (3) markings in the longitudinal paramedian area absent/present, (4) dots arranged in bars in the lateral band absent, (5) a maximum SVL of 78.3–102 mm, (6) ventral scale rows, 100–126, (7) midbody scale rows, 34–39, (8) total lamellae on one hand, 18–26, (9) total strigae on ten scales, 96–144, (10) relative length of all digits

on one hindlimb, 13.0–18.2 %, (11) relative distance between the angled subocular and mouth, 0.135–0.600 %, (12) relative eye length, 2.53–3.74 %, (13) relative forelimb length, 12.4–15.7 %, (14) relative ear width, 0.00 %, (15) relative rostral height, 1.62–2.48 %, (16) relative head length, not applicable, (17) relative mental width, 1.45–1.78 %, (18) relative postmental width, 2.16–2.82 %, (19) relative cloacal width, 6.26–7.64 %, (20) relative prefrontal width, 3.44–4.60 %, (21) relative largest supraocular width, 1.99–2.38 %, (22) relative longest finger length, 2.65–3.63 %, (23) relative distance between the ear and eye, not applicable, (24) relative head width, not applicable, (25) relative frontal width, 75.6–97.3 %, (26) relative nasal height, 0.777–1.19 %, (27) relative angled subocular height, 0.940–1.52 %, (28) relative distance between the eye and naris, 3.02–5.20 %, (29) relative canthal iii length, 0.800–1.14 %, (30) relative angled subocular width, 1.71–2.39 %, and (31) relative nasal length, 1.47–1.92 %. The species stem time is 2.76 Ma and the species crown time is 0.00 Ma (Fig. 4).

We distinguish *Wetmorena haetiana* from the other species of *Wetmorena* based on a complex of traits. From *Wetmorena agasepsoides*, we distinguish *W. haetiana* by the adult SVL (78.3–102 versus 49.1–58.6), the midbody scale rows (34–39 versus 27–31), the total lamellae on one hand (18–26 versus 14–17), the relative length of digits on one hindlimb (13.0–18.2 versus 9.44–11.2), the relative forelimb length (12.4–15.7 versus 8.05–9.58), the relative ear width (0.00 versus 0.292–0.634), the relative prefrontal width (3.44–4.60 versus 2.77–3.35), and the relative longest finger length (2.65–3.63 versus 1.44–2.01). From *W. mylica*, we cannot distinguish *W. haetiana* based on our standard suite of characters, although Schwartz (1965) was correct that *W. haetiana* has a dark brown venter whereas *W. mylica* has a cream venter. From *W. obscura* **sp. nov.**, we distinguish *W. haetiana* by the adult SVL (78.3–102 versus 46.9–61.1), the total strigae on ten scales (96–144 versus 73–83), the relative longest finger length (2.65–3.63 versus 4.08–5.35). From *W. orosaura* **sp. nov.**, we distinguish *W. haetiana* by the adult SVL (78.3–102 versus 59.6–68.0), the relative length of digits on one hindlimb (13.0–18.2 versus 18.6–19.7), the relative forelimb length (12.4–15.7 versus 16.9–17.2), and the relative longest finger length (2.65–3.63 versus 3.86–4.46). From *W. surda*, we distinguish *W. haetiana* by the relative width of canthal iii (0.800–1.14 versus 1.17–1.33).

Description of holotype. USNM 72600. An adult; SVL 85.0 mm; tail nearly cylindrical, 60.2 mm (70.8% SVL); axilla-to-groin distance 48.3 mm (56.8% SVL); forelimb length 13.0 mm (15.3% SVL); hindlimb length 22.6 mm (2.66% SVL); head width 12.7 mm (14.9% SVL); diameter of orbit 3.18 mm (3.74% SVL); horizontal diameter of ear opening 0.00 mm (0.00% SVL); vertical diameter of ear opening 0.00 mm (0.00% SVL); length of all toes on one foot 15.5 mm (18.2% SVL); shortest distance between angled subocular and lip 0.51 mm (0.600% SVL); longest finger length 2.70 mm (3.18% SVL); largest supraocular width 1.87 mm (2.20% SVL); cloacal width 6.49 mm (7.64% SVL); mental width 1.37 mm (1.61% SVL); postmental width 2.40 mm (2.82% SVL); prefrontal width 3.91 mm (4.60% SVL); frontal width 87.1% frontal length; nasal height 0.97 mm (1.14% SVL); angled subocular height 1.04 mm (1.22% SVL); shortest distance between the eye and naris 4.42 mm (5.20% SVL); canthal iii width 0.88 mm (1.04% SVL); angled subocular width 2.03 mm (2.39% SVL); nasal width 1.56 mm (1.84% SVL); rostral 2.09X as wide as high, barely visible from above, not in contact with nasals, in contact with 1st supralabial and anterior internasal (left)/(right); anterior internasals are slightly wider than posterior ones; frontonasals and prefrontal fused into a single large plate with a slightly concave posterior margin, much wider than long, bordered by posterior internasals, 1st loreals, 1st median oculars, and the frontal; frontal longer than wide; a pair of frontoparietals, separated by the posterior prolongation of the frontal and the interparietal plate; interparietal plate smaller than parietals and separating them, posteriorly touching the interoccipital, which is wider than long; parietal separated from supraoculars by 1st and 2nd temporals and frontoparietal (left)/(right); nasal single; nostril above suture between 1st and 2nd supralabials (left)/(right); 1 postnasal (left)/(right); 2 loreals (left)/(right); 1st loreal higher than wide (left)/(right), in contact with postnasal, posterior internasal, prefrontal/frontonasal complex, 1st median ocular, canthal iii, 2nd loreal, and 3rd supralabial (left)/(right); 2nd loreal shorter than 1st, higher than wide (left)/(right), excluded from contact with supraocular by canthal iii (left)/(right); final loreal posteriorly bordering the upper and lower preoculars (left)/(right); canthal iii barely wider than high (left)/(right), contacting 1st median ocular, anterior supraciliary, upper preocular, and 1st and 2nd loreals (left)/(right); 11 (left)/10 (right) median oculars, 1st contacting the prefrontal (left)/(right); 1 upper preocular (left)/(right); an irregular anterior supraciliary (left)/(right); 6 lateral oculars (left)/(right); 5 temporals (left)/(right); 2 suboculars (left)/(right); posterior subocular large and elongate (left)/(right); anterior subocular small (left)/(right); 9 supralabials (left)/(right), 5 to level below center of eye (left)/(right); 10 (left)/9 (right) infralabials, 5–6 (left)/6 (right) to level below center of eye; mental small, followed by a single, larger postmental; 4 pairs of enlarged chin shields; 1st pair in contact with one another; 2nd–4th pairs separated by 1–2 scales; 114 transverse rows of dorsal scales from interoccipital to base of tail; 116 transverse

rows of ventral scales from mental to vent; 40 scales around midbody; 4 digits; finger lengths 3>2>4>1; 7 (left)/8 (right) lamellae under longest finger; 23 total lamellae on one hand; toe lengths 3>2>4>1; 11 (left)/11 (two are fused) (right) lamellae under longest toe; keelless and striate dorsal body and caudal scales; smooth ventral scales; 106 total strigae counted on ten scales.

FIGURE 99. (A–B) *Wetmorena haetiana* (ANSP 38727, SBH 269913), in life. From southeast of Pic La Selle, Sud-Est Department, Haiti. Photograph by SBH.

Color (in alcohol): dorsal surface of head medium brown with some darker brown mottling; lateral surfaces of head grading from medium brown to pale tan with darker brown eye masks and spots on the labial scales; dorsal surfaces of the body are medium brown with some darker brown flecks, most prominent on the neck; dorsal surface of tail medium brown with some darker brown mottling and flecks that form lines; lateral areas are darker brown

with cream spots; dorsal surfaces of the limbs are dark brown with cream spots; lateral and ventral areas of the limbs do not grade but the cream spots disappear; ventral surfaces of the head, body, and tail are dark brown with cream spots that fade down the tail.

Variation. The dorsal pattern of this species is variable. Several specimens lack a dorsal patten entirely, whereas specimens such as ANSP 38731 have mottling on their entire dorsum. The majority of specimens have irregular dots that extend along their entire dorsum, occasionally occurring as an extension of the longitudinal paramedian lines or in multiple series. Almost every specimen of this species has darker outlines on their head scale borders and more than half have dark, irregular areas on their head scales. Markings in the longitudinal paramedian area range from being completely absent to irregular dots to dots in series to broken and complete longitudinal paramedian lines. Many specimens have dots that occur in the lateral band; however, they are not comparable to the dots arranged in bars in the other genera (particularly *Panolopus*). Measurements and other morphological data for the holotype and other examined material are presented in Table 1.

Distribution. *Wetmorena haetiana* is distributed in the Massif de la Selle in southeastern Haiti at elevations of 1330–2250 m (Fig. 95). It has an extent of occurrence of ~710 km^2.

Ecology and conservation. Past literature accounts of ecological data for this species conflate multiple species and therefore cannot be used.

We consider the conservation status of *Wetmorena haetiana* to be Endangered B1ab(iii), based on IUCN Redlist criteria (IUCN 2023). It faces a primary threat from habitat destruction resulting from agriculture and charcoaling. Haiti is heavily deforested with < 1% of the nation's primary forest remaining (Hedges *et al.* 2018). Secondary threats to this species include predation from introduced predators, including the mongoose and black rats. Studies are needed to determine the health of any remaining populations and threats to the survival of the species.

Reproduction. Past literature accounts of reproductive data for this species conflate multiple species and therefore cannot be used.

Etymology. The species name (*haetiana*) refers to this species' distribution in Haiti.

Remarks. Although *Wetmorena haetiana* and *W. mylica* differ only in ventral coloration, they are not closest relatives, are genetically distinct from one another (Fig. 3), and have been diverged for 5.57 My (Fig. 4).

Wetmorena haetiana is included in our genetic dataset and has significant support in both Bayesian and ML likelihood analyses at the crown node of the species and the stem node that places it as the closest relative of *W. orosaura* **sp. nov.** Based on our timetree (Fig. 4), *Wetmorena haetiana* diverged from that species 2.76 Ma, consistent with typical species of vertebrates (> 0.7 Ma; Hedges *et al.* 2015). *Wetmorena haetiana* also occurs in sympatry with *W. orosaura* **sp. nov.** Our ASAP analysis recognized *W. haetiana* as a distinct species.

Wetmorena mylica (Schwartz 1965)

Barahona Earless Forest Lizard
(Fig. 100–101)

Wetmorena haetiana mylica Schwartz, 1965:45. Holotype: MCZ R-77049, collected by David C. Leber and A. Thomas from 24 km SW Barahona, Barahona province, Dominican Republic, on 2 August 1963.
Wetmorena haetiana mylica—Schwartz & Henderson, 1991:553.
Celestus haetianus mylica—Henderson & Powell, 2009:103.
Celestus haetianus mylicus—Hedges *et al.*, 2019:17.

Material examined (n=26). DOMINICAN REPUBLIC. Barahona. AMNH 92086–7, D. C. Leber & Richard Thomas, 8 km NE Las Auyamas, 28 July 1963; AMNH 92088, D. C. Leber & Richard Thomas, 24 km SW Barahona, 2 August 1963; KU 228144–50, 24 km SW Barahona, 2 August 1963; MCZ R-77049, David C. Leber, A. Thomas, 24 km SW Barahona, 2 August 1963; USNM 150554–7, Barahona, 24 km SW of, 2 August 1963; USNM 328854–5, 328857, 328863, 328865, 328871–2, 328875–6, 328878, 328881, Richard Thomas and S. Blair Hedges, 15.3 km S, 6.7 km E (road) of Cabral, 16 August 1284.

Diagnosis. *Wetmorena mylica* has (1) a dorsal pattern of absent/irregular dots, (2) head markings absent/present, (3) markings in the longitudinal paramedian area absent/present, (4) dots arranged in bars in the lateral band absent, (5) a maximum SVL of 76.0–98.2 mm, (6) ventral scale rows, 112–126, (7) midbody scale rows, 37–41, (8) total lamellae on one hand, 16–23, (9) total strigae on ten scales, 84–105, (10) relative length of all digits on one

FIGURE 100. (A–F) *Wetmorena mylica* (MCZ R-77049, holotype), SVL 85.3 mm.

FIGURE 101. *Wetmorena mylica* (USNM 328895, SBH 160207), in life. From ca. 2 km S Tejunde, Barahona Province, Dominican Republic. Photograph by SBH.

hindlimb, 9.62–15.5 %, (11) relative distance between the angled subocular and mouth, 0.00–0.504 %, (12) relative eye length, 2.13–2.97 %, (13) relative forelimb length, 10.5–14.3 %, (14) relative ear width, 0.00 %, (15) relative rostral height, 1.76–2.37 %, (16) relative head length, not applicable, (17) relative mental width, 1.34–1.95 %, (18) relative postmental width, 2.02–2.91 %, (19) relative cloacal width, 5.90–7.07 %, (20) relative prefrontal width, 3.26–4.01 %, (21) relative largest supraocular width, 1.62–2.97 %, (22) relative longest finger length, 2.43–2.95 %, (23) relative distance between the ear and eye, not applicable, (24) relative head width, not applicable, (25) relative frontal width, 84.8–114 %, (26) relative nasal height, 0.850–1.13 %, (27) relative angled subocular height, 1.09–1.50 %, (28) relative distance between the eye and naris, 3.10–3.67 %, (29) relative canthal iii length, 0.956–1.15 %, (30) relative angled subocular width, 1.74–2.29 %, and (31) relative nasal length, 1.23–1.65 %. The species stem time is 4.25 Ma and the species crown time is 0.43 Ma (Fig. 4).

We distinguish *Wetmorena mylica* from the other species of *Wetmorena* based on a complex of traits. From *Wetmorena agasepsoides*, we distinguish *W. mylica* by the dorsal pattern (absent/irregular dots versus absent), the adult SVL (76.0–98.2 versus 49.1–58.6), the midbody scale rows (37–41 versus 27–31), the relative forelimb length (10.5–14.3 versus 8.05–9.58), the relative ear width (0.00 versus 0.292–0.634), and the relative longest finger length (2.43–2.95 versus 1.44–2.01). From *W. haetiana*, we cannot distinguish *W. mylica* based on our standard suite of characters, but the two taxa can be separated by ventral coloration: dark brown in *W. haetiana* versus cream in *W. mylica*, as noted by Schwartz (1965). From *W. obscura* **sp. nov.**, we distinguish *W. mylica* by the dorsal pattern (absent/irregular dots versus lineate), the adult SVL (76.0–98.2 versus 46.9–61.1), the ventral scale rows (112–126 versus 108–111), the midbody scale rows (37–41 versus 35–36), the total strigae on ten scales (84–105 versus 73–83), the relative prefrontal width (3.26–4.01 versus 4.03–4.58), the relative longest finger length (2.43–2.95 versus 4.08–5.35), the relative frontal width (84.8–114 versus 73.6–81.9), and the relative distance between the eye and naris (3.10–3.67 versus 3.68–5.01). From *W. orosaura* **sp. nov.**, we distinguish *W. mylica* by the adult SVL (76.0–98.2 versus 59.6–68.0), the relative length of digits on one hindlimb (9.62–15.5 versus 18.6–19.7), the relative eye length (2.13–2.97 versus 3.04–3.56), the relative forelimb length (10.5–14.3 versus 16.9–17.2), the relative longest finger length (2.43–2.95 versus 3.86–4.46), and the relative frontal width (84.8–114 versus 80.0–84.6). From *W. surda*, we distinguish *W. mylica* by the relative width of canthal iii (0.956–1.15 versus 1.17–1.33).

Description of holotype. MCZ R-77049. An adult male; SVL 85.3 mm; tail nearly cylindrical, 100 mm (117% SVL); axilla-to-groin distance 53.6 mm (62.8% SVL); forelimb length 11.0 mm (12.9% SVL); hindlimb length 17.2 mm (20.2% SVL); head width 11.8 mm (13.8% SVL); diameter of orbit 2.39 mm (2.80% SVL); horizontal diameter of ear opening 0.00 mm (0.00% SVL); vertical diameter of ear opening 0.00 mm (0.00% SVL); length of all toes on one foot 10.8 mm (12.7% SVL); shortest distance between angled subocular and lip 0.43 mm (0.504% SVL); longest finger length 2.33 mm (2.73% SVL); largest supraocular width 2.53 mm (2.97% SVL); cloacal width 6.03 mm (7.07% SVL); mental width 1.66 mm (1.95% SVL); postmental width 2.48 mm (2.91% SVL); prefrontal width 3.42 mm (4.01% SVL); frontal width 114% frontal length; nasal height 0.96 mm (1.13% SVL); angled subocular height 1.28 mm (1.50% SVL); shortest distance between the eye and naris 3.00 mm (3.52% SVL); canthal iii width 0.83 mm (0.973% SVL); angled subocular width 1.95 mm (2.29% SVL); nasal width 1.41 mm (1.65% SVL); rostral 1.91X as wide as high, visible from above, not in contact with nasals, in contact with 1st supralabial and anterior internasal (left)/(right); anterior internasals are narrower than posterior ones; frontonasals and prefrontal fused into a single large plate with a slightly concave posterior margin, wider than long, bordered by posterior internasals, 1st loreals, 1st median oculars, and the frontal; frontal approximately as long as wide; a pair of frontoparietals, separated by the posterior prolongation of the frontal and the interparietal plate; interparietal plate smaller than parietals and separating them, posteriorly touching the interoccipital, which is wider than long; parietal separated from supraoculars by 1st and 2nd temporals and frontoparietal (left)/1st and 2nd temporals and frontoparietal (irregular) (right); nasal single; nostril above suture between 1st and 2nd supralabials (left)/(right); 1 postnasal (left)/(right); 2 loreals (left)/(right); 1st loreal higher than wide (left)/(right), in contact with postnasal, posterior internasal, prefrontal/frontonasal complex, 1st median ocular, canthal iii, 2nd loreal, and 3rd–4th supralabials (left)/(right); 2nd loreal shorter than 1st, higher than wide (left)/(right), excluded from contact with supraocular by canthal iii (left)/(right); final loreal posteriorly bordering the upper and lower preoculars (left)/(right); canthal iii wider than high (left)/(right), contacting 1st median ocular, anterior supraciliary, upper preocular, and 1st and 2nd loreals (left)/(right); 9 median oculars (left)/(right), 1st contacting the prefrontal (left)/(right); 1 upper preocular (left)/(right); an irregular anterior supraciliary (left)/(right); 6 (left)/5 (right) lateral oculars; 5 (left)/7 (right) temporals; 2 suboculars (left)/(right); posterior subocular large and elongate (left)/(right); anterior subocular small (left)/(right); 9 supralabials (left)/(right), 5 to level below center of eye (left)/(right); 9 (left)/10 (right) infralabials, 6 to level below center of eye (left)/(right); mental small, followed by a single, larger postmental; 4 pairs of enlarged chin shields; 1st pair in contact with one another; 2nd–4th pairs separated by 1–3 scales; 107 transverse rows of dorsal scales from interoccipital to base of tail; 113 transverse rows of ventral scales from mental to vent; 39 scales around midbody; 4 digits; finger lengths 3>2>1>4; 6 (left)/7 (right) lamellae under longest finger; 23 total lamellae on one hand; toe lengths 3>2>4>1; 12 (left) lamellae under longest toe; keelless and striate dorsal body and caudal scales; smooth ventral scales; 105 total strigae counted on ten scales.

Color (in alcohol): dorsal surface of head dark gold with darker brown mottling and darker brown areas on scale borders; lateral surfaces of head grading from dark gold to faded dark brown with some cream spots on the sides of the throat and dark brown eye masks; dorsal surfaces of the body are medium brown with two darker brown longitudinal paramedian lines that end before the forearms in addition to many small, dark brown, irregular spots; dorsal surface of tail medium brown covered in small, dark brown, irregular spots; lateral areas grade from dark brown to dark cream with off-white mottling; dorsal surfaces of the limbs are dark brown with some paler cream spotting; lateral and ventral areas of the limbs fade to pale cream with heavy, dark brown spotting; ventral surfaces of the head, body, and tail are cream with heavy dark brown spotting that becomes the dominant color on the underside of the tail.

Variation. The majority of the examined material resembles the holotype in having irregular dots or flecks on their dorsum whereas a minority of specimens lack a pattern on their dorsum other than longitudinal paramedian markings. Several specimens have patternless heads whereas a majority possess darker outlines on their head scale borders and/or irregular darker markings on their head scales. AMNH 92087 and AMNH 92088 lack longitudinal paramedian markings whereas the markings in other specimens range from dots in series to small or broken lines to multiple thin lines. The dots in the lateral band appear mottled, as opposed to arranged in bars. Measurements and other morphological data for the holotype and other examined material are presented in Table 1.

Distribution. *Wetmorena mylica* is distributed on the eastern coast of the Sierra de Baoruco in the Dominican Republic at elevations of 40–1390 m (Fig. 95). It has an extent of occurrence of extent of occurrence of ~520 km^2.

Ecology and conservation. No ecological data are associated with this species. We consider the conservation

status of *Wetmorena mylica* to be Endangered B1ab(iii), based on IUCN Redlist criteria (IUCN 2023). It faces a primary threat from habitat destruction resulting from agriculture and urbanization. Secondary threats to this species include predation from introduced predators, including the mongoose and black rats. Studies are needed to determine the health of any remaining populations and threats to the survival of the species.

Reproduction. A litter size of four was recorded in this species (SBH, field data).

Etymology. The species name (*mylica*) is derived from the Greek *mylikos* (mill), in reference to the type locality (an abandoned mahogany sawmill).

Remarks. Previously regarded as a subspecies of *Wetmorena haetiana*, herein we recognize *W. mylica* as a full species based on genetic and morphological differences. This species occurs at much lower elevations than other species (e.g., *W. haetiana* and *W. surda*). Schwartz (1965) suggested that extreme deforestation in the other areas is the reason, whereas some lower-elevation habitat of *W. mylica* is still intact.

Although *Wetmorena mylica* and *W. haetiana* differ only in ventral coloration, they are not closest relatives, are genetically distinct from one another (Fig. 3), and have been diverged for 5.57 My (Fig. 4).

Wetmorena mylica was included in our genetic dataset and has significant support in both Bayesian and ML analyses at the crown node. The stem node that places *W. mylica* within *Wetmorena* has a support value of 65% in our ML analysis and is not supported in our Bayesian analysis. Schools *et al.* (2022) used genomic data to place *W. mylica* outside of *W. haetiana* and *W. surda* with significant support values in ML and Bayesian analyses. Based on our timetree (Fig. 4), *Wetmorena mylica* diverged from its closest relative 4.25 Ma, consistent with typical species of vertebrates (> 0.7 Ma; Hedges *et al.* 2015). *Wetmorena mylica* was recognized as a distinct species by our ASAP analysis.

***Wetmorena obscura* sp. nov.**
Long-fingered Earless Forest Lizard
(Fig. 102)

Wetmorena haetiana surda—Schwartz, 1965:41 (part).
Wetmorena haetiana surda—Schwartz & Henderson, 1991:553 (part).
Celestus haetianus surdus—Hedges *et al*., 2019:17 (part).

Holotype. USNM 328904, a juvenile from Gros Cheval (ca. 15 km W of, via logging roads, NE slope of Pic La Selle), collected by S. Blair Hedges and Richard Thomas on 18 November 1984 (18.3367, -71.8686; 2,020 m).

Paratypes (n=2). HAITI. Sud-Est. USNM 328905–6, same locality, date, and collectors as holotype.

Diagnosis. *Wetmorena obscura* **sp. nov.** has (1) a dorsal pattern of lineate, (2) head markings present, (3) markings in the longitudinal paramedian area present, (4) dots arranged in bars in the lateral band absent, (5) a maximum SVL of 46.9–61.1 mm, (6) ventral scale rows, 108–111, (7) midbody scale rows, 35–36, (8) total lamellae on one hand, 20–21, (9) total strigae on ten scales, 73–83, (10) relative length of all digits on one hindlimb, 13.8–16.2 %, (11) relative distance between the angled subocular and mouth, 0.295–0.426 %, (12) relative eye length, 2.65–3.13 %, (13) relative forelimb length, 13.6–16.3 %, (14) relative ear width, 0.00 %, (15) relative rostral height, 1.72–2.22 %, (16) relative head length, not applicable, (17) relative mental width, 1.72–2.24 %, (18) relative postmental width, 2.49–3.05 %, (19) relative cloacal width, 6.26–6.69 %, (20) relative prefrontal width, 4.03–4.58 %, (21) relative largest supraocular width, 1.70–2.54 %, (22) relative longest finger length, 4.08–5.35 %, (23) relative distance between the ear and eye, not applicable, (24) relative head width, not applicable, (25) relative frontal width, 73.6–81.9 %, (26) relative nasal height, 0.753–1.24 %, (27) relative angled subocular height, 0.999–1.29 %, (28) relative distance between the eye and naris, 3.68–5.01 %, (29) relative canthal iii length, 0.835–0.980 %, (30) relative angled subocular width, 1.82–2.17 %, and (31) relative nasal length, 1.41–1.57 %. The species stem time is 4.75 Ma and the species crown time is 0.00 Ma (Fig. 4).

Wetmorena obscura **sp. nov.** has a lower number of total strigae on ten scales (73–83) than all other species of the genus. From *Wetmorena agasepsoides*, we distinguish *W. obscura* **sp. nov.** by the dorsal pattern (lineate versus absent), the midbody scale rows (35–36 versus 27–31), the total lamellae on one hand (20–21 versus 14–17), the total strigae on ten scales (73–83 versus 94–153), the relative length of digits on one hindlimb (13.8–16.2 versus 9.44–11.2), the relative distance between angled subocular and mouth (0.295–0.426 versus 0.00–0.224), the relative forelimb length (13.6–16.3 versus 8.05–9.58), the relative ear width (0.00 versus 0.292–0.634), the relative

mental width (1.72–2.24 versus 1.40–1.66), the relative postmental width (2.49–3.05 versus 1.75–2.30), the relative prefrontal width (4.03–4.58 versus 2.77–3.35), the relative longest finger length (4.08–5.35 versus 1.44–2.01), and the relative distance between the eye and naris (3.68–5.01 versus 2.25–3.27). From *W. haetiana*, we distinguish *W. obscura* **sp. nov.** by the adult SVL (46.9–61.1 versus 78.3–102), the total strigae on ten scales (73–83 versus 96–144), and the relative longest finger length (4.08–5.35 versus 2.65–3.63). From *W. mylica*, we distinguish *W. obscura* **sp. nov.** by the dorsal pattern (lineate versus absent/irregular dots), the adult SVL (46.9–61.1 versus 76.0–98.2), the ventral scale rows (108–111 versus 112–126), the midbody scale rows (35–36 versus 37–41), the total strigae on ten scales (73–83 versus 84–105), the relative prefrontal width (4.03–4.58 versus 3.26–4.01), the relative longest finger length (4.08–5.35 versus 2.43–2.95), the relative frontal width (73.6–81.9 versus 84.8–114), and the relative distance between the eye and naris (3.68–5.01 versus 3.10–3.67). From *W. orosaura* **sp. nov.**, we distinguish *W. obscura* **sp. nov.** by the total lamellae on one hand (20–21 versus 22–26), the total strigae on ten scales (73–83 versus 92–98), the relative length of digits on one hindlimb (13.8–16.2 versus 18.6–19.7), the relative distance between angled subocular and mouth (0.295–0.426 versus 0.206–0.285), the relative forelimb length (13.6–16.3 versus 16.9–17.2), the relative width of canthal iii (0.835–0.980 versus 1.14–1.26), and the relative angled subocular width (1.82–2.17 versus 2.21–2.47). From *W. surda*, we distinguish *W. obscura* **sp. nov.** by the adult SVL (46.9–61.1 versus 62.5–81.9), the total strigae on ten scales (73–83 versus 84–123), the relative prefrontal width (4.03–4.58 versus 3.47–3.91), the relative longest finger length (4.08–5.35 versus 2.12–2.98), and the relative width of canthal iii (0.835–0.980 versus 1.17–1.33).

Description of holotype. USNM 328904. An adult; SVL 61.1 mm; tail nearly cylindrical, broken, 25.4 mm (41.6% SVL); axilla-to-groin distance 37.3 mm (61.0% SVL); forelimb length 8.29 mm (13.6% SVL); hindlimb length 12.3 mm (20.1% SVL); head width 7.34 mm (12.0% SVL); diameter of orbit 1.62 mm (2.65% SVL); horizontal diameter of ear opening 0.00 mm (0.00% SVL); vertical diameter of ear opening 0.00 mm (0.00% SVL); length of all toes on one foot 8.80 mm (14.4% SVL); shortest distance between angled subocular and lip 0.18 mm (0.295% SVL); longest finger length 2.49 mm (4.08% SVL); largest supraocular width 1.04 mm (1.70% SVL); cloacal width 4.09 mm (6.69% SVL); mental width 1.20 mm (1.96% SVL); prefrontal width 2.52 mm (4.12% SVL); frontal width 81.9% frontal length; nasal height 0.46 mm (0.753% SVL); angled subocular height 0.79 mm (1.29% SVL); shortest distance between the eye and naris 3.06 mm (5.01% SVL); canthal iii width 0.51 mm (0.835% SVL); angled subocular width 1.11 mm (1.82% SVL); nasal width 0.96 mm (1.57% SVL); rostral 1.72X as wide as high, barely visible from above, not in contact with nasals, in contact with 1st supralabial and anterior internasal (left)/(right); anterior internasals are narrower than posterior ones; frontonasals and prefrontal fused into a single large plate with a straight posterior margin, wider than long, bordered by posterior internasals, 1st loreals, 1st median oculars, and the frontal; frontal longer than wide; a pair of frontoparietals (missing on the right), separated by the posterior prolongation of the frontal and the interparietal plate; interparietal plate smaller than parietals and separating them, posteriorly touching the interoccipital, which is wider than long; parietal separated from supraoculars by 1st and 2nd temporals and frontoparietal (left)/(right); nasal single; nostril just posterior to suture between 1st and 2nd supralabials (left)/(right); 1 postnasal (left)/(right); 2 loreals (left)/(right); 1st loreal higher than wide (left)/(right), in contact with postnasal, posterior internasal, prefrontal/frontonasal complex, 1st median ocular, canthal iii, 2nd loreal, and 3rd supralabials (left)/(right); 2nd loreal shorter than 1st, higher than wide (left)/(right), excluded from contact with supraocular by canthal iii (left)/(right); 2nd loreal posteriorly bordering the lower preocular (left)/(right); canthal iii wider than high (left)/(right), contacting 1st median ocular, anterior supraciliary, upper preocular, and 1st and 2nd loreals (left)/(right); 9 median oculars (left)/(right), 1st contacting the prefrontal (left)/(right); 1 upper preocular (left)/(right); an irregular anterior supraciliary (left)/(right); 6 lateral oculars (left)/(right); 5 temporals (left)/(right); 2 suboculars (left)/(right); posterior subocular large and elongate (left)/(right); anterior subocular small (left)/(right); 9 supralabials (left)/(right), 5 to level below center of eye (left)/(right); 9 infralabials (left)/(right), 6 to level below center of eye (left)/(right); mental small, followed by 2 post mentals, the first small and the second large; 4 pairs of enlarged chin shields; 1st pair in contact with one another; 2nd–4th pairs separated by 1–3 scales; 112 transverse rows of dorsal scales from interoccipital to base of tail; 108 transverse rows of ventral scales from mental to vent; 35 scales around midbody; 4 digits; finger lengths 3>2>4>1; 6 lamellae under longest finger (left)/(right); 20 total lamellae on one hand; toe lengths 3>2>4>1; 11 lamellae under longest toe (left)/(right); keelless and striate dorsal body and caudal scales; smooth ventral scales; 83 total strigae counted on ten scales.

Color (in alcohol): dorsal surface of head gray-brown with darker brown areas on scale borders and in irregular spots; lateral surfaces of head grading from gray-brown to faded gray-brown with darker brown eye masks and

areas on the labial scales; dorsal surfaces of the body are gray-brown with darker brown spots arranged in broken longitudinal paramedian lines that continue as multiple lines down the back; dorsal surface of tail the same as the body; lateral areas grade from dark brown to gray with paler spots; dorsal surfaces of the limbs are dark brown with paler mottling; lateral and ventral areas of the limbs grade to pale brown with darker mottling; ventral surfaces of the head, body, and tail are pale gray-brown covered in dark brown mottling that becomes heavier posteriorly.

FIGURE 102. (A–F) *Wetmorena obscura* **sp. nov.** (USNM 328904, holotype), SVL 61.1 mm.

Variation. The two USNM paratypes (USNM 328905–6) resemble the holotype in pattern and scalation. All specimens have head markings in the form of a darker outline on head scale borders. USNM 328904 also has dark, irregular areas on its head scales. The dots arranged in bars in the lateral band are either absent or appear as mottling. Measurements and other morphological data for the holotype and other examined material are presented in Table 1.

Distribution. *Wetmorena obscura* **sp. nov.** is known only from the locality of the type series, which was collected in southeastern Haiti at an elevation of 2020 m (Fig. 95). It has an extent of occurrence of ~90 km^2.

Ecology and conservation. The type series was collected under rocks in pine forest (SBH, field data). We consider the conservation status of *Wetmorena obscura* **sp. nov.** to be Critically Endangered B1ab(iii), based on IUCN Redlist criteria (IUCN 2023). It faces a primary threat from habitat destruction resulting from agriculture and charcoaling. Haiti is heavily deforested with < 1% of nation's primary forest remaining (Hedges *et al.* 2018). Secondary threats to this species include predation from introduced predators, including the mongoose and black rats. Studies are needed to determine the health of any remaining populations and threats to the survival of the species.

Reproduction. No data on reproduction are available for this species.

Etymology. The species name (*obscura*) is a Latin feminine singular adjective meaning "dark" in reference to the dark color of this species.

Remarks. Previously regarded as *Wetmorena haetiana surda*, we recognize *W. obscura* **sp. nov.** as a full species based on its genetic and morphological distinctiveness. Additional specimens in museum collections catalogued as *W. haetiana* or *W. haetiana surda* should be examined to determine if they are additional specimens of this species.

Wetmorena obscura **sp. nov.** is included in our genetic dataset and has significant support in both Bayesian and ML likelihood analyses at the crown node. The stem node that places *W. obscura* **sp. nov.** as the closest relative of *W. agasepsoides* has a support value of 66% in our ML analysis and is not supported in our Bayesian analysis. Using genomic data, Schools *et al.* (2022) placed *W. agasepsoides* as the outgroup to all other species of *Wetmorena* with significant support in both ML and Bayesian analyses. Based on our timetree (Fig. 4), *W. obscura* **sp. nov.** diverged from its closest relative (*W. agasepsoides*) 4.75 Ma, consistent with typical species of vertebrates (> 0.7 Ma; Hedges *et al.* 2015). Although not scored in our suite of diagnostic characters, *W. obscura* has the darkest dorsal color of the genus *Wetmorena*. *Wetmorena obscura* **sp. nov.** was recovered as conspecific with *Wetmorena surda* in our ASAP analysis.

***Wetmorena orosaura* sp. nov.**
Denfer Earless Forest Lizard
(Fig. 103–104)

Wetmorena haetiana haetiana—Schools & Hedges, 2021:232 (part).
Wetmorena haetiana haetiana—Landestoy *et al.*, 2022: 205 (part).

Holotype. ANSP 38725, an adult male from Morne D'Enfer (southwestern edge of plateau), Sud-Est Department, Haiti, collected by S. Blair Hedges, Tiffany Cloud, Miguel Landestoy, and Marcos Rodriguez on 21 November 2011 (18.330052, -72.37095; 1,433 m).

Paratypes (n=3) HAITI. Sud-Est. ANSP 38723–4, SBH 269864, same locality and data as the holotype.

Diagnosis. *Wetmorena orosaura* **sp. nov.** has (1) a dorsal pattern of lineate/irregular dots, (2) head markings absent/present, (3) markings in the longitudinal paramedian area present, (4) dots arranged in bars in the lateral band absent, (5) a maximum SVL of 59.6–68.0 mm, (6) ventral scale rows, 110–125, (7) midbody scale rows, 33–41, (8) total lamellae on one hand, 22–26, (9) total strigae on ten scales, 92–98, (10) relative length of all digits on one hindlimb, 18.6–19.7 %, (11) relative distance between the angled subocular and mouth, 0.206–0.285 %, (12) relative eye length, 3.04–3.56 %, (13) relative forelimb length, 16.9–17.2 %, (14) relative ear width, 0.00 %, (15) relative rostral height, 1.85–2.31 %, (16) relative head length, not applicable, (17) relative mental width, 1.61–1.93 %, (18) relative postmental width, 2.31–2.68 %, (19) relative cloacal width, 6.69–6.88 %, (20) relative prefrontal width, 3.85–4.11 %, (21) relative largest supraocular width, 2.27–2.39 %, (22) relative longest finger length, 3.86–4.46 %, (23) relative distance between the ear and eye, not applicable, (24) relative head width, not applicable, (25) relative frontal width, 80.0–84.6 %, (26) relative nasal height, 1.07–1.16 %, (27) relative angled subocular height, 1.22–1.45 %, (28) relative distance between the eye and naris, 3.37–3.91 %, (29) relative canthal iii length, 1.14–1.26 %, (30) relative angled subocular width, 2.21–2.47 %, and (31) relative nasal length, 1.50–1.95 %. The species stem time is 2.76 Ma and the species crown time is 0.41 Ma (Fig. 4).

Wetmorena orosaura **sp. nov.** has a larger relative length of digits on one hindlimb (18.6–19.7) and relative forelimb length (16.9–17.2) than all other species of the genus. From *Wetmorena agasepsoides*, we distinguish *W. orosaura* **sp. nov.** by the dorsal pattern (lineate/irregular dots versus absent), the adult SVL (59.6–68.0 versus 49.1–58.6), the midbody scale rows (33–41 versus 27–31), the total lamellae on one hand (22–26 versus 14–17), the relative length of digits on one hindlimb (18.6–19.7 versus 9.44–11.2), the relative forelimb length (16.9–17.2 versus 8.05–9.58), the relative ear width (0.00 versus 0.292–0.634), the relative postmental width (2.31–2.68 versus 1.75–2.30), the relative cloacal width (6.69–6.88 versus 4.69–6.57), the relative prefrontal width (3.85–4.11 versus 2.77–3.35), the relative largest supraocular width (2.27–2.39 versus 1.66–2.07), the relative longest finger length (3.86–4.46 versus 1.44–2.01), the relative nasal height (1.07–1.16 versus 0.712–0.933), the relative angled subocular height (1.22–1.45 versus 0.851–1.09), the relative distance between the eye and naris (3.37–3.91 versus 2.25–3.27),

and the relative width of canthal iii (1.14–1.26 versus 0.481–0.970). From *W. haetiana*, we distinguish *W. orosaura* **sp. nov.** by the adult SVL (59.6–68.0 versus 78.3–102), the relative length of digits on one hindlimb (18.6–19.7 versus 13.0–18.2), the relative forelimb length (16.9–17.2 versus 12.4–15.7), and the relative longest finger length (3.86–4.46 versus 2.65–3.63). From *W. mylica*, we distinguish *W. orosaura* **sp. nov.** by the adult SVL (59.6–68.0 versus 76.0–98.2), the relative length of digits on one hindlimb (18.6–19.7 versus 9.62–15.5), the relative eye length (3.04–3.56 versus 2.13–2.97), the relative forelimb length (16.9–17.2 versus 10.5–14.3), the relative longest finger length (3.86–4.46 versus 2.43–2.95), and the relative frontal width (80.0–84.6 versus 84.8–114). From *W. obscura* **sp. nov.**, we distinguish *W. orosaura* **sp. nov.** by the total lamellae on one hand (22–26 versus 20–21), the total strigae on ten scales (92–98 versus 73–83), the relative length of digits on one hindlimb (18.6–19.7 versus 13.8–16.2), the relative distance between angled subocular and mouth (0.206–0.285 versus 0.295–0.426), the relative forelimb length (16.9–17.2 versus 13.6–16.3), the relative width of canthal iii (1.14–1.26 versus 0.835–0.980), and the relative angled subocular width (2.21–2.47 versus 1.82–2.17). From *W. surda*, we distinguish *W. orosaura* **sp. nov.** by the total lamellae on one hand (22–26 versus 18–21), the relative length of digits on one hindlimb (18.6–19.7 versus 10.7–14.4), the relative eye length (3.04–3.56 versus 2.07–2.83), the relative forelimb length (16.9–17.2 versus 11.3–13.9), the relative largest supraocular width (2.27–2.39 versus 1.73–2.06), the relative longest finger length (3.86–4.46 versus 2.12–2.98), and the relative nasal height (1.07–1.16 versus 0.828–1.06).

Description of holotype. ANSP 38725. An adult male; SVL 68.0 mm; tail nearly cylindrical, broken in life midway, regenerated, 46.0 mm (67.6% SVL); axilla-to-groin distance 41.0 mm (60.3% SVL); forelimb length 11.5 mm (16.9% SVL); hindlimb length 17.0 mm (25.0% SVL); head width 8.50 mm (12.5% SVL); diameter of orbit 2.07 mm (3.04% SVL); horizontal diameter of ear opening 0.00 mm (0.00% SVL); vertical diameter of ear opening 0.00 mm (0.00% SVL); length of all toes on one foot 13.4 mm (19.7% SVL); shortest distance between angled subocular and lip 0.14 mm (0.206% SVL); longest finger length 2.89 mm (4.25% SVL); largest supraocular width 1.59 mm (2.34% SVL); cloacal width 4.55 mm (6.69% SVL); mental width 1.13 mm (1.66% SVL); postmental width 1.79 mm (2.63% SVL); prefrontal width 2.62 mm (3.85% SVL); frontal width 80.0% frontal length; nasal height 0.79 mm (1.16% SVL); angled subocular height 0.83 mm (1.22% SVL); shortest distance between the eye and naris 2.43 mm (3.57% SVL); canthal iii width 0.83 mm (1.22% SVL); angled subocular width 1.68 mm (2.47% SVL); nasal width 1.13 mm (1.66% SVL); rostral 2.31X as wide as high, visible from above, not in contact with nasals, in contact with 1st supralabial and anterior internasal (left)/(right); anterior internasals are narrower than posterior ones; frontonasals and prefrontal fused into a single large plate with an irregular posterior margin, much wider than long, bordered by posterior internasals, 1st loreals, 1st median oculars, and the frontal; frontal longer than wide; a pair of frontoparietals, separated by the posterior prolongation of the frontal and the interparietal plate; interparietal plate smaller than parietals and separating them, posteriorly touching the interoccipital, which is wider than long; parietal separated from supraoculars by 1st and 2nd temporals and frontoparietal (left)/(right); nasal single; nostril above suture between 1st and 2nd supralabials (left)/(right); 1 postnasal (left)/(right); 2 loreals (left)/(right); 1st loreal higher than wide (left)/(right), in contact with postnasal, posterior internasal, prefrontal/frontonasal complex, 1st median ocular, canthal iii, 2nd loreal, and 3rd supralabial (left)/(right); 2nd loreal shorter than 1st, higher than wide (left)/(right), excluded from contact with supraocular by canthal iii (left)/(right); final loreal posteriorly bordering the upper and lower preoculars (left)/(right); canthal iii wider than high (left)/(right), contacting 1st median ocular, anterior supraciliary, upper preocular, and 1st and 2nd loreals (left)/(right); 10 (left)/9 (right) median oculars, 1st contacting the prefrontal (left)/(right); 2 upper preoculars (left)/(right); an irregular anterior supraciliary (left)/(right); 6 lateral oculars (left)/(right); 5 temporals (left)/(right); 2 suboculars (left)/(right); posterior subocular large and elongate (left)/(right); anterior subocular small (left)/(right); 9 supralabials (left)/(right), 5 to level below center of eye (left)/(right); 10 infralabials (left)/(right), 5–6 (left)/5 (right) to level below center of eye; mental small, followed by a single, larger postmental; 4 pairs of enlarged chin shields, followed by 1 pair of reduced chin shields; 1st pair in contact with one another anteriorly, posteriorly separated by one scale; 2nd–5th pairs separated by 1–6 scales; 110 transverse rows of dorsal scales from interoccipital to base of tail; 124 transverse rows of ventral scales from mental to vent; 40 scales around midbody; 4 digits; finger lengths 3>2>4>1; 7 lamellae under longest finger (left)/(right); 24 total lamellae on one hand; toe lengths 3>2>4>1; 10 (left)/11 (right) lamellae under longest toe; keelless and striate dorsal body and caudal scales; smooth ventral scales; 98 total strigae counted on ten scales.

Color (in alcohol): dorsal surface of head gray-brown with darker brown areas on scale borders; lateral surfaces of head grading from gray-brown to muted gray-brown with cream spots around the labial scales; dorsal surfaces of the body are gray-brown with darker brown spots arranged in broken longitudinal paramedian lines and other irregular dark brown spots down the length of the back; dorsal surface of tail the same gray-brown as the body with

darker brown spots; lateral areas grade from dark brown to faded gray with cream spots arranged in lines; dorsal surfaces of the limbs are dark brown with some bronze spots; lateral and ventral areas of the limbs fade to muted gray-brown; ventral surfaces of the head, body, and tail are muted gray-brown with large, irregular cream spots down the length.

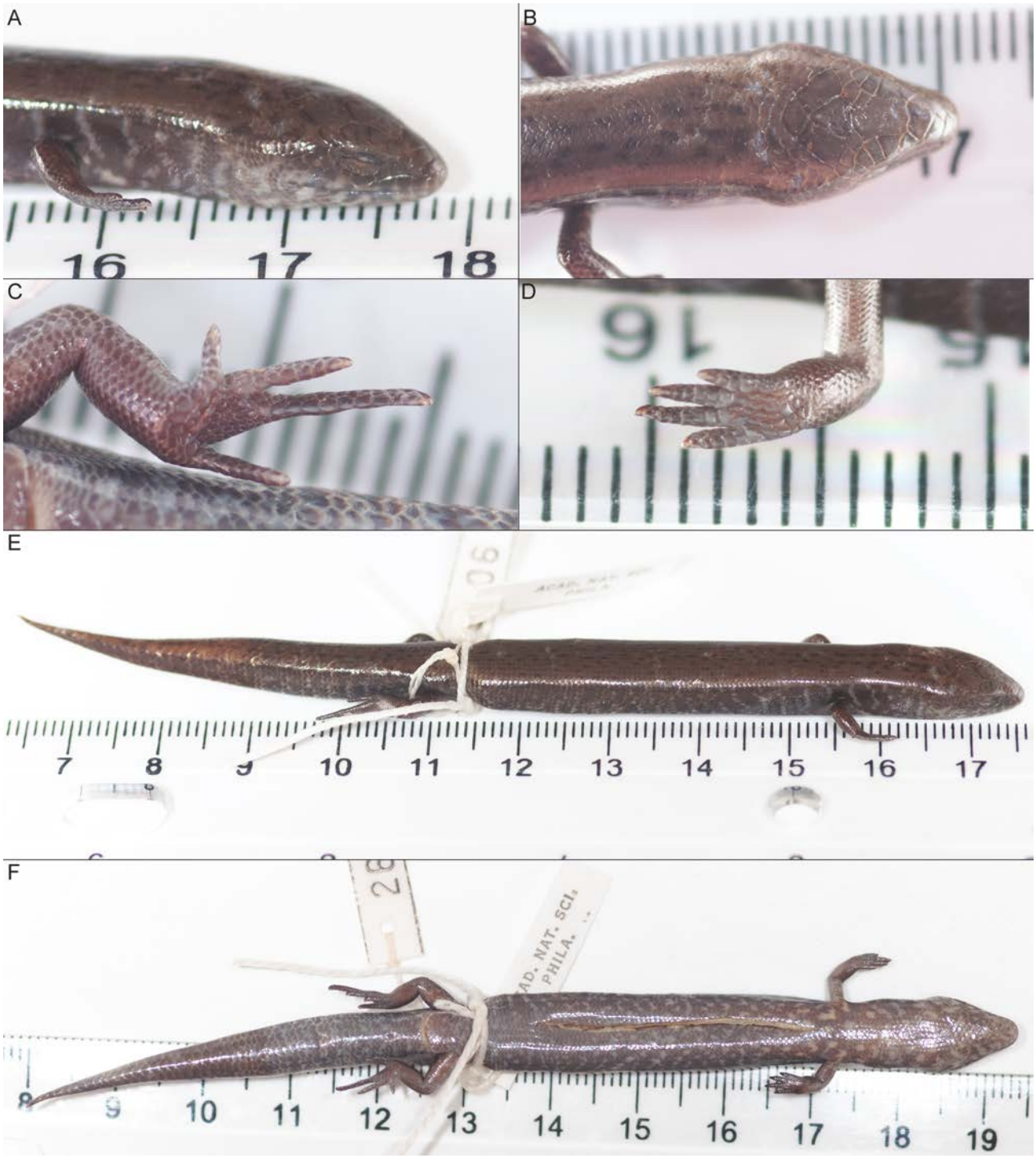

FIGURE 103. (A–F) *Wetmorena orosaura* **sp. nov.** (ANSP 38725, holotype), SVL 68.0 mm.

Variation. The majority of the material examined resembles the holotype in having irregular dots that extend along the entire dorsum. SBH 269864 has a reduced dorsal pattern that appears almost lineate. ANSP 38724 has a patternless head, whereas all other specimens have darker outlines on their head scales. ANSP 38723 has dark, irregular areas on its head scales in addition to darker outlines on the scale borders. All specimens have dots arranged in bars in the lateral line except for SBH 269864. Measurements and other morphological data for the holotype and other examined material are presented in Table 1.

Distribution. *Wetmorena orosaura* **sp. nov.** is known only from the type locality on Morne D'Enfer, the western extension of the Massif de la Selle of Haiti, at an elevation of 1433 m (Fig. 95). It has an extent of occurrence of ~90 km^2.

FIGURE 104. (A–B) *Wetmorena orosaura* **sp. nov.** (ANSP 38723, SBH 269904), in life. From Morne D'Enfer, southwestern edge of plateau, Sud-Est Department, Haiti. Photos by SBH.

Ecology and conservation. This species occurs within La Visite National Park, but tree-cutting in the park continues unabated (Hedges *et al.* 2018) and therefore no current protection exists for this species. No ecological data are associated with *Wetmorena orosaura* **sp. nov.** We consider the conservation status of *Wetmorena orosaura* **sp. nov.** to be Critically Endangered B1ab(iii), based on IUCN Redlist criteria (IUCN 2023). It faces a primary threat from habitat destruction resulting from agriculture and charcoaling. Haiti is heavily deforested with < 1% of the nation's primary forest remaining (Hedges *et al.* 2018). Secondary threats to this species include predation from introduced predators, including the mongoose and black rats. Studies are needed to determine the health of any remaining populations and threats to the survival of the species.

Reproduction. No data on reproduction are available for this species.

Etymology. The species name (*orosaura*) is a feminine noun derived from the Greek *oros* (mountain) and *saura* (lizard), referring to the distribution of the species on Morne D'Enfer (Fig. 95).

Remarks. We recognize *W. orosaura* **sp. nov.** as a full species based on genetic and morphological distinctiveness. Additional surveys of the area and of specimens in museum collections catalogued as *W. haetiana* should be examined to determine if they are this species.

Wetmorena orosaura **sp. nov.** was included in our genetic dataset and has significant support in both Bayesian and ML likelihood analyses at the crown node of the species and the stem node that places it as the closest relative to *W. haetiana*. *Wetmorena orosaura* **sp. nov.** diverged from *W. haetiana* 2.76 Ma (Fig. 4), consistent with typical species of vertebrates (> 0.7 Ma; Hedges *et al.* 2015). *Wetmorena orosaura* **sp. nov.** occurs within 9 km of *W. haetiana* localities and may be sympatric with that species. *Wetmorena orosaura* **sp. nov.** was recognized as a distinct species by our ASAP analysis.

Wetmorena surda (Schwartz 1965)

Striped Earless Forest Lizard
(Fig. 105–106)

Wetmorena haetiana surda Schwartz, 1965:41. Holotype: MCZ R-77040, collected by Ron F. Klinikowski and locals in Foret de Pins on 8 December 1962 (18.32939911, -71.79250336; 1,711 m).
Wetmorena haetiana surda—Schwartz & Henderson, 1991:553.
Celestus haetianus surdus—Hedges *et al.*, 2019:17.

Material examined (n=33). DOMINICAN REPUBLIC. Independencia. ANSP 38746–7, SBH 192540, S. Blair Hedges, Richard Thomas, and Nicholas Plummer, 23.1 km SE of Puerto Escondido, 23 July 1991; ANSP 38748–54, S. Blair Hedges, Richard Thomas, and Nicholas Plummer, 23.9 km SE of Puerto Escondido, 23 July 1991. **Pedernales.** USNM 328897–99, S. Blair Hedges and Richard Thomas, 10.3 km S of El Aguacate on Haitian border road, 13 August 1983; USNM 328900, S. Blair Hedges and Richard Thomas, 6.6 km S of El Aguacate on Haitian border road, 13 August 1983. **HAITI. Ouest.** Hispaniola. AMNH 92079–85, R. F. Klinikowski, Foret des Pins, 12 August 1962; MCZ R-77040, Ron F. Klinikowski and locals, Foret de Pins, 8 December 1962; USNM 150548–53, Foret des Pins, 12 August 1862. **Sud-Est.** KU 228366, Foret des Pins, 30 June 1962; KU 228370–3, Foret des Pins, 12 August 1962.

Diagnosis. *Wetmorena surda* has (1) a dorsal pattern of irregular dots/dots in series/lineate, (2) head markings absent/present, (3) markings in the longitudinal paramedian area present, (4) dots arranged in bars in the lateral band absent, (5) a maximum SVL of 62.5–81.9 mm, (6) ventral scale rows, 100–124, (7) midbody scale rows, 31–43, (8) total lamellae on one hand, 18–21, (9) total strigae on ten scales, 84–123, (10) relative length of all digits on one hindlimb, 10.7–14.4 %, (11) relative distance between the angled subocular and mouth, 0.0151–0.520 %, (12) relative eye length, 2.07–2.83 %, (13) relative forelimb length, 11.3–13.9 %, (14) relative ear width, 0.00 %, (15) relative rostral height, 1.72–2.28 %, (16) relative head length, not applicable, (17) relative mental width, 1.49–1.96 %, (18) relative postmental width, 1.81–2.93 %, (19) relative cloacal width, 5.89–7.23 %, (20) relative prefrontal width, 3.47–3.91 %, (21) relative largest supraocular width, 1.73–2.06 %, (22) relative longest finger length, 2.12–2.98 %, (23) relative distance between the ear and eye, not applicable, (24) relative head width, not applicable, (25) relative frontal width, 81.1–89.7 %, (26) relative nasal height, 0.828–1.06 %, (27) relative angled subocular height, 0.944–1.52 %, (28) relative distance between the eye and naris, 3.04–3.71 %, (29) relative canthal iii length, 1.17–1.33 %, (30) relative angled subocular width, 1.93–2.31 %, and (31) relative nasal length, 1.26–1.54 %. The species stem time is 4.25 Ma and the species crown time is 1.77 Ma (Fig. 4).

We distinguish *Wetmorena surda* from the other species of *Wetmorena* based on a complex of traits. From *Wetmorena agasepsoides*, we distinguish *W. surda* by the dorsal pattern (irregular dots/dots in series/lineate versus absent), the adult SVL (62.5–81.9 versus 49.1–58.6), the total lamellae on one hand (18–21 versus 14–17), the relative forelimb length (11.3–13.9 versus 8.05–9.58), the relative ear width (0.00 versus 0.292–0.634), the relative prefrontal width (3.47–3.91 versus 2.77–3.35), the relative longest finger length (2.12–2.98 versus 1.44–2.01), and the relative width of canthal iii (1.17–1.33 versus 0.481–0.970). From *W. haetiana*, we distinguish *W. surda* by the

relative width of canthal iii (1.17–1.33 versus 0.800–1.14). From *W. mylica*, we distinguish *W. surda* by the relative width of canthal iii (1.17–1.33 versus 0.956–1.15). From *W. obscura* **sp. nov.**, we distinguish *W. surda* by the adult SVL (62.5–81.9 versus 46.9–61.1), the total strigae on ten scales (84–123 versus 73–83), the relative prefrontal width (3.47–3.91 versus 4.03–4.58), the relative longest finger length (2.12–2.98 versus 4.08–5.35), and the relative width of canthal iii (1.17–1.33 versus 0.835–0.980). From *W. orosaura* **sp. nov.**, we distinguish *W. surda* by the total lamellae on one hand (18–21 versus 22–26), the relative length of digits on one hindlimb (10.7–14.4 versus 18.6–19.7), the relative eye length (2.07–2.83 versus 3.04–3.56), the relative forelimb length (11.3–13.9 versus 16.9–17.2), the relative largest supraocular width (1.73–2.06 versus 2.27–2.39), the relative longest finger length (2.12–2.98 versus 3.86–4.46), and the relative nasal height (0.828–1.06 versus 1.07–1.16).

Description of holotype. MCZ R-77040. An adult female; SVL 78.8 mm; tail nearly cylindrical, broken in life near tip, regenerated, 67.1 mm (85.2% SVL); axilla-to-groin distance 52.8 mm (67.0% SVL); forelimb length 9.16 mm (11.6% SVL); hindlimb length 15.7 mm (19.9% SVL); head width 10.1 mm (12.8% SVL); diameter of orbit 2.10 mm (2.66% SVL); horizontal diameter of ear opening 0.00 mm (0.00% SVL); vertical diameter of ear opening 0.00 mm (0.00% SVL); length of all toes on one foot 9.41 mm (11.9% SVL); shortest distance between angled subocular and lip 0.23 mm (0.292% SVL); longest finger length 2.35 mm (2.98% SVL); largest supraocular width 1.36 mm (1.73% SVL); cloacal width 5.70 mm (7.23% SVL); mental width 1.38 mm (1.75% SVL); postmental width 2.31 mm (2.93% SVL); prefrontal width 2.97 mm (3.77% SVL); frontal width 86.9% frontal length; nasal height 0.82 mm (1.04% SVL); angled subocular height 1.20 mm (1.52% SVL); shortest distance between the eye and naris 2.53 mm (3.21% SVL); canthal iii width 0.96 mm (1.22% SVL); angled subocular width 1.52 mm (1.93% SVL); nasal width 0.99 mm (1.26% SVL); rostral 1.72X as wide as high, visible from above, not in contact with nasals, in contact with 1st supralabial and anterior internasal (left)/(right); anterior internasals are slightly narrower than posterior ones; frontonasals and prefrontal fused into a single large plate with a straight posterior margin, wider than long, bordered by posterior internasals, 1st loreals, 1st median oculars, and the frontal; frontal longer than wide; a pair of frontoparietals, separated by the posterior prolongation of the frontal and the interparietal plate; interparietal plate approximately the size of parietals and separating them, posteriorly touching the interoccipital, which is approximately as wide as long; parietal separated from supraoculars by 1st and 2nd temporals and frontoparietal (left)/(right); nasal single; nostril above suture between 1st and 2nd supralabials (left)/(right); 1 postnasal (left)/(right); 2 loreals (left)/(right); 1st loreal higher than wide (left)/(right), in contact with postnasal, posterior internasal, prefrontal/frontonasal complex, 1st median ocular, canthal iii, 2nd loreal, and 3rd–5th supralabial (left)/postnasal, posterior internasal, prefrontal/frontonasal complex, 1st median ocular, canthal iii, 2nd loreal, and 3rd supralabial (right); 2nd loreal shorter than 1st, higher than wide (left)/(right), excluded from contact with supraocular by canthal iii (left)/(right); final loreal posteriorly bordering the upper and lower preoculars (left)/(right); canthal iii wider than high (left)/(right), contacting 1st median ocular, anterior supraciliary, upper preocular, and 1st and 2nd loreals (left)/(right); 9 median oculars (left)/(right), 1st contacting the prefrontal (left)/(right); 1 upper preocular (left)/(right); an irregular anterior supraciliary (left)/(right); 6 lateral oculars (left)/(right); 5 temporals (left)/(right); 2 suboculars (left)/(right); posterior subocular large and elongate (left)/(right); anterior subocular small (left)/(right); 9 supralabials (left)/(right), 5 to level below center of eye (left)/(right); 9 (left)/8 (right) infralabials, 6 (left)/5 (right) to level below center of eye; mental small, followed by a single, larger postmental; 4 pairs of enlarged chin shields; 1st pair in contact with one another; 2nd–4th pairs separated by 1–3 scales; 110 transverse rows of dorsal scales from interoccipital to base of tail; 114 transverse rows of ventral scales from mental to vent; 38 scales around midbody; 4 digits; finger lengths 2>3>4>1; 6 lamellae under longest finger (left)/(right); 20 total lamellae on one hand; toe lengths 3>2>4>1; 12 (left)/11 (right) lamellae under longest toe; keelless and striate dorsal body and caudal scales; smooth ventral scales; 122 total strigae counted on ten scales.

Color (in alcohol): dorsal surface of head dark gold with some darker brown areas and darker brown areas on scale borders; lateral surfaces of head grading from dark gold to orange-cream with darker brown eye masks and other darker brown areas on the labial scales and sides of neck; dorsal surfaces of the body are reddish gray with two dark brown, almost complete longitudinal paramedian lines that extend onto the tail and additional spots arranged into 5–6 rows; dorsal surface of tail same as body; lateral areas grade from red-brown to orange-cream with darker orange mottling; dorsal surfaces of the limbs are dark brown with paler cream spotting; lateral and ventral areas of the limbs fade to pale cream with heavy darker brown spotting; ventral surfaces of the head, body, and tail are cream with heavy dark brown spotting that becomes the dominant color on the underside of the tail.

FIGURE 105. (A–F) *Wetmorena surda* (MCZ R-77040, holotype), SVL 78.7 mm.

FIGURE 106. *Wetmorena surda* (USNM 328897, SBH 101404), in life. From 10.3 km S of El Aguacate on border road, Pedernales Province, Dominican Republic. Photograph by SBH.

Variation. The dorsal pattern of the material examined resembles the holotype in having pronounced longitudinal paramedian lines and dots that are extensions of those longitudinal paramedian lines continuing down the dorsum. Many specimens have other dots that occur irregularly or in addition to the longitudinal paramedian series on their dorsums. All specimens other than ANSP 38748, SBH 192540, USNM 150550, and USNM 150551 have patterned heads. Most specimens have both darker outlines on their head scales in addition to dark, irregular areas on their heads. This species lacks dots arranged in bars in the lateral band, dots appear as mottling when they do occur on the lateral area. Measurements and other morphological data for the holotype and other examined material are presented in Table 1.

Distribution. *Wetmorena surda* is distributed in the Massif de la Selle in extreme southeastern Haiti and the adjacent Sierra de Baoruco of the Dominican Republic at elevations of 670–2270 m (Fig. 95). It has an extent of occurrence of ~640 km^2.

Ecology and conservation. Animals were collected under rocks in pine and hardwood forests (SBH, field data). We consider the conservation status of *Wetmorena surda* to be Endangered B1ab(iii), based on IUCN Redlist criteria (IUCN 2023). It faces a primary threat from habitat destruction resulting from agriculture and charcoaling. Haiti is heavily deforested with < 1% of the nation's primary forest remaining (Hedges *et al.* 2018). The forests in the Sierra de Baoruco are in better condition, but have some pressure from deforestation as well. Secondary threats to this species include predation from introduced predators, including the mongoose and black rats, although less of a problem at higher elevations. Studies are needed to determine the health of any remaining populations and threats to the survival of the species.

Reproduction. A litter size of four was recorded in a female of this species weighing 4.2 g live (SBH, field data).

Etymology. The species name is the Latin word for deaf, referring to the lack of external ear openings in this species (Schwartz 1965).

Remarks. Previously regarded as a subspecies of *Wetmorena haetiana*, we recognize *W. surda* as a full species based on genetic and morphological distinctiveness. Museum specimens catalogued as *W. haetiana* or *W. haetiana surda* should be examined to determine if they are additional specimens of this species.

Wetmorena surda is represented in our genetic dataset with the crown node defining it as a species having a significant support value in our ML analysis and a support value of 92% in our Bayesian analysis. The stem node that places *W. surda* as the closest relative to *W. mylica* has a support value of 65% in our ML analysis and is not supported in our Bayesian analyses. Based on our timetree (Fig. 4), *W. surda* diverged from its closest relative 4.25 Ma, consistent with typical species of vertebrates (> 0.7 Ma; Hedges *et al.* 2015). *Wetmorena surda* was recovered as conspecific with *Wetmorena obscura* **sp. nov.** in our ASAP analysis.

Of special interest is the unexpected population subdivision within this species (Fig. 4). The three populations sampled are approximately as divergent as some full species of forest lizards (1.02–1.77 Ma) and yet are geographically close to one another. The population southeast of Puerto Escondido on the high central area of the Sierra de Baoruco not far from Casetta Dos, is about 20 km from the other two populations. The latter are both on the border with Haiti, about 5 km from each other and only about 10 km from Forêt des Pins, Haiti. These high levels of genetic divergence and close proximity suggest that hidden species remain unresolved within *W. surda*, which will require the examination of more genetic data and specimens to resolve.

Discussion

Phylogenetic relationships

We have revised the taxonomy of diploglossid lizards based on a re-evaluation of morphological characters in concert with a new molecular phylogeny.

Genera and large clades. Several generic relationships differ between our phylogeny and the phylogeny used by Schools *et al.* (2022) that was generated with genomic data. Our phylogeny (Fig. 3) places *Panolopus* and *Celestus* as sister taxa with significant support in our ML and Bayesian analyses. Schools *et al.* (2022) placed *Panolopus* and *Comptus* as sister taxa with significant support values in both ML and Bayesian analyses. Schools *et al.* (2022) also placed the group containing *Sauresia* and *Wetmorena* as the outgroup to the other celestines included in the dataset with significant support in both the ML and Bayesian analyses. Our phylogeny places *Caribicus* as the outgroup to the other celestines included in the dataset with significant support in both ML and Bayesian analyses.

The differences between our tree and that of Schools *et al.* (2022) likely stem from the different datasets used to generate them. The bulk of the alignment used in Schools *et al.* (2022) was made up of genomic data (UCEs). The alignment used in these analyses contained 64,669 base pairs. For the work presented herein, we used genetic data in a nine-gene alignment (6,948 base pairs in length). Genomic data are ideal for delimiting genus-level relationships because of the high resolution that it can provide at basal nodes (Liimatainen *et al.* 2022; Schools *et al.* 2022). A comparison between the nine-gene dataset of Schools & Hedges (2021) and the genomic dataset of (Schools *et al.* 2022: Table 4) shows that the genomic phylogeny has higher support values at nodes that determine the relationships between genera. In light of this, the relationships between genera determined by genomic data should be favored over those determined with nine genes.

Our nine-gene phylogeny shows that within the celestine radiation, the seven included genera diverged from their closest relatives 10.5–7.50 Ma (Fig. 4), and the earliest divergence within a genus was 7.77 Ma. Therefore, all of the genera arose in the Miocene and had begun diversification before the close of the Miocene. Timing similar to these dates has been reported among other Caribbean genera of lizards, including skinks (Hedges & Conn 2012).

Species groups and small clades. In *Caribicus*, we lacked genetic data from *C. anelpistus*, one of the three species of this genus. Given the morphological similarities, *C. anelpistus* likely is the closest relative of *C. warreni*, the other species of large-bodied Neotropical forest lizard in this genus. The subspecies that previously fell under *Celestus crusculus*, *Comptus stenurus*, *Panolopus costatus*, and *Panolopus curtissi* often do not form monophyletic groups. The taxonomy that we introduce herein corrects these instances of non-monophyly.

Within the genus *Celestus*, the pairing of *C. hesperius* **sp. nov.** and *C. jamesbondi* **sp. nov.** is unusual in that the two closely related species are separated not only by a large distributional gap of at least 110 km, but in that gap is the distribution of the species (*C. crusculus*), with which they had been confused, now shown to be only distantly related (Figs. 3–4). Also, two extinct or possibly extinct species, *C. striatus* and *C. occiduus*, both appearing "golden" in coloration to their describer (Gray) two centuries ago, apparently are close relatives despite their structural difference and adaptation to different niches (tree-dwelling and swamp-dwelling, respectively). The evolutionary history of *Celestus*, which has been difficult to study because of the 19th Century decimation by the mongoose, is now in better focus, but more work needs to be done for complete resolution.

Within *Comptus*, the relationships of the species are now well-established (Fig. 3–4). Two well-defined groups exist: the *stenurus* Group (*C. arboreus* **sp. nov.** and *C. stenurus*) and the *weinlandi* Group (*C. alloeides*, *C. badius*, *C. maculatus*, and *C. weinlandi*). The former is distributed on the South Paleoisland of Hispaniola and the latter on the North Paleoisland or derived (*C. badius* and *C. maculatus*) from the North Paleoisland by dispersal.

Within *Panolopus*, the relationships of the species are not as well-established as in *Comptus* (Fig. 3–4).

Nonetheless, they also show a strong influence of paleogeography. The *costatus* Group (*P. costatus, P. nesobous,* and *P. oreistes*) occurs on the South Paleoisland, with *P. nesobous* tentatively assigned to that group because of its weakly supported node (Figs. 3–4). We assign the remaining species, forming a well-supported cluster, to the *curtissi* Group (*Panolopus aenetergum, P. aporus, P. chalcorhabdus, P. curtissi, P. diastatus, P. emys, P. hylonomus, P. lanceolatus* **sp. nov.**, *P. lapierrae* **sp. nov.**, *P. leionotus, P. marcanoi, P. melanchrous, P. neiba, P. psychonothes, P. saonae, P. semitaeniatus* **sp. nov.**, and *P. unicolor* **sp. nov.**). We emphasize that this species group has no relationship to the taxonomy of *P. curtissi* and its subspecies as previously defined, because this new group contains taxa formerly assigned to *P. costatus,* a species (*sensu stricto*) not even included in this group. All but a single species (*P. aporus*) in the *curtissi* Group occur on the North Paleoisland, although one locality of *P. curtissi* is on the South Paleoisland (Fig. 50). More sequence data will be needed to further resolve the relationships within *Panolopus*.

Within *Sauresia*, the relationships of the species are now well-established (Fig. 3–4). Two well-defined groups exist: the *sepsoides* Group (*S. alinea* **sp. nov.**, *S. gracilis* **sp. nov.**, *S. manicula* **sp. nov.**, *S. sepsoides*, and *S. synoria* **sp. nov.**) and the *habichi* Group (*S. cayemitae* **sp. nov.**, *S. habichi*, and *S. pangnolae* **sp. nov**.). *Sauresia pangnolae* **sp. nov.** is included in the *habichi* Group with significant support in our ML analysis and a support value of 74% in our Bayesian analysis. This placement also is geographically consistent with other members in the group. More sequence data will be needed to further resolve this relationship in *Sauresia*. Additionally, because of the small size and burrowing nature of lizards in this genus, a high likelihood exists that additional species of *Sauresia* remain to be identified.

Within *Wetmorena*, the majority of species included in our analyses are well resolved; however, additional sequence data will be needed to further resolve the relationships between several species within the genus. Our phylogeny lends additional support to the inclusion of *Wetmorena agasepsoides* in this genus, instead of the genus *Sauresia* in which it was previously included. Previous phylogenies support the position of *W. agasepsoides* that we found here (Schools & Hedges 2021; Landestoy *et al.* 2022; Schools *et al.* 2022).

In our study, we recognize the complexity of distinguishing between interspecific and intraspecific variations, particularly in cases where species divergence times are close to the threshold of intraspecific divergence. The delineation of species in these borderline cases was achieved through a comprehensive analysis of genetic, morphological, and ecological data. While divergence times alone might suggest potential conspecificity, the integration of multiple lines of evidence provided a more nuanced understanding, supporting the recognition of these taxa as distinct species. Future research with larger sample sizes and additional genetic markers could further clarify these relationships and potentially refine our taxonomic conclusions.

Stem divergence dates between all sequenced celestine species range from 8.59–0.74 Ma in our phylogeny. The older end of this range (8.59 Ma) is when *Guarocuyus jaraguanus*, the only species in *Guarocuyus*, diverged from other species. After this divergence time, the next oldest split occurred 6.83 Ma between *Caribicus darlingtoni* and *C. warreni*. The youngest measured divergence time (0.74 Ma) was between *Panolopus leionotus* and *P. semitaeniatus* **sp. nov.** The modal stem divergence time of only the 12 sequenced celestine species that are newly described here (1.68 Ma) was not much less than that of all 41 sequenced celestine species in our tree (2.73 Ma). Our youngest pair of sympatric species (*Panolopus neiba*/*P. leionotus*) diverged 1.23 Ma, which provides additional support for the recognition of species with divergence times of that age or older.

Evolution and biogeography

Previous works have indicated that two dispersal events occurred from a South American point of origin resulting in the presence of diploglossids in the Caribbean, one leading to diploglossines and the other to celestines (Schools & Hedges 2021; Schools *et al.* 2022). The most recent of those studies, using genomic data, timed the celestine dispersal event to 44.1–10.3 Ma (Schools *et al.* 2022). Subsequent dispersals among Caribbean islands likely occurred via the same mechanism, over-water dispersal on flotsam and carried by ocean currents, as discussed elsewhere (Hedges *et al.* 1992; Hedges 1996, 2001, 2006; Ali & Hedges 2021, 2024). According to our analyses and this same logic, subsequent dispersals within Celestinae (Fig. 4) occurred from Hispaniola to Jamaica (7.50–5.58 Ma, leading to the Jamaican *Celestus*), Hispaniola to Navassa Island (3.52 Ma–present, leading to *Comptus badius*), and Hispaniola to Cayman Brac (2.43 Ma–present, leading to *Comptus maculatus*).

Schools *et al.* (2022) tested multiple biogeographic models to determine the method of colonization of the Caribbean for diploglossids and to determine how subsequent dispersal events between islands took place. The favored model from their analyses suggested that the dispersal events that resulted in the current distribution of Caribbean diploglossids were via flotsam that floated in the direction of the currents. Several relationships in our

phylogeny support this finding. Most notably, *Celestus macrotus* is the closest relative of all Jamaican *Celestus*, as would be expected given dispersal from Hispaniola of an ancestral species. The location of *Celestus macrotus* on the Hispaniola South Paleoisland further supports this finding. Additionally, the distribution of *Comptus badius* and *C. maculatus*, both on islands that are farther west than the other members of *Comptus* on Hispaniola, also suggests that over water dispersal events took place. In this case, it is interesting that those two species are both derived from the primarily North Paleoisland clade (*Comptus alloeides* and *C. weinlandi*) instead of the closer South Paleoisland clade (*C. arboreus* and *C. stenurus*). However, this is often the case with over-water dispersal on flotsam, which is determined by water currents and not necessarily by proximity of landmasses.

Ecology and behavior

The "cryptozoic" lives led by many diploglossid species have resulted in a lack of ecological studies (Lotzkat *et al.* 2016). However, Schools *et al.* (2022) used a combination of morphology, primary literature reports, and statistics to assign the then defined species of diploglossids to ecomorph categories. These ecomorph categories included Grass Ecomorph, Ground Ecomorph, Rock Ecomorph, Soil Ecomorph, Swamp Ecomorph, and Tree Ecomorph (Table 4). Both the Soil Ecomorph and the Tree Ecomorph occur at multiple points in the phylogeny, indicating the presence of convergent evolution.

Celestus macrolepis and *C. occiduus* are the only two members of the Swamp Ecomorph, and they are both likely extinct as a result of the mongoose. Similarly, one of the Caribbean representatives of the Tree Ecomorph (*C. striatus*) is represented by only three specimens and has not been recorded since the 1971 description of *C. fowleri* (synonymized herein with *C. striatus*), although it was photographed in the 1990s (see above). However, the arboreal nature of *C. striatus* might have helped it elude introduced predators such as the mongoose (Schools *et al.* 2022), elusive species and extinctions such as these have made studying several of the more unique ecomorphs in Caribbean diploglossids very difficult.

The Ground Ecomorph contains the majority of Caribbean diploglossid species, with the bulk of *Celestus*, *Comptus*, and *Panolopus* falling into this group. Schools *et al.* (2022) suggested a reason to further subdivide this ecomorph, in part because some species (e.g., *Comptus badius*, *Celestus microblepharis*), have eyes, digits, and reduced limbs suggesting that they occupy a semi-fossorial niche, and one case (*C. badius*) was observed living and moving within leaf litter debris on the forest floor. They suggested that those species should be placed in a Leaf Litter Ecomorph, intermediate between the Ground and Soil Ecomorphs. Herein (Table 4) we place those two species in the Leaf Litter Ecomorph, which should be used for other diploglossids, as noted by Schools *et al.* (2022). Additional ecological information on celestine species will help refine these categories in the future.

TABLE 4. List of ecomorphs and the respective assignments of Caribbean celestines.

Ecomorph	Species
Ground	*Caribicus anelpistus*, *Caribicus darlingtoni*, *Caribicus warreni*, *Celestus barbouri*, *Celestus capitulatus* **sp. nov.**, *Celestus crusculus*, *Celestus hesperius* **sp. nov.**, *Celestus hewardi*, *Celestus jamesbondi* **sp. nov.**, *Celestus macrotus*, *Celestus molesworthi*, *Celestus oligolepis* **sp. nov.**, *Comptus maculatus*, *Panolopus aenetergum*, *Panolopus aporus*, *Panolopus chalcorhabdus*, *Panolopus curtissi*, *Panolopus diastatus*, *Panolopus emys*, *Panolopus hylonomus*, *Panolopus lanceolatus* **sp. nov.**, *Panolopus lapierrae* **sp. nov.**, *Panolopus leionotus*, *Panolopus marcanoi*, *Panolopus melanchrous*, *Panolopus neiba*, *Panolopus psychonothes*, *Panolopus saonae*, *Panolopus semitaeniatus* **sp. nov.**, *Panolopus unicolor* **sp. nov.**
Leaf Litter	*Celestus microblepharis*, *Comptus badius*
Soil	*Sauresia agramma* **sp. nov.**, *Sauresia cayemitae* **sp. nov.**, *Sauresia gracilis* **sp. nov.**, *Sauresia habichi*, *Sauresia manicula* **sp. nov.**, *Sauresia pangnolae* **sp. nov.**, *Sauresia sepsoides*, *Sauresia synoria* **sp. nov**., *Wetmorena agasepsoides*, *Wetmorena haetiana*, *Wetmorena mylica*, *Wetmorena obscura* **sp. nov.**, *Wetmorena orosaura* **sp. nov.**, *Wetmorena surda*
Swamp	*Celestus macrolepis*, *Celestus occiduus*
Tree	*Celestus duquesneyi*, *Celestus striatus*, *Comptus alloeides*, *Comptus arboreus* **sp. nov.**, *Comptus stenurus*, *Comptus weinlandi*, *Guarocuyus jaraguanus*, *Panolopus costatus*, *Panolopus nesobous*, *Panolopus oreistes*

Reproduction

All Caribbean species of diploglossids either are, or presumed to be, ovoviviparous. As in other Caribbean lizards, a

positive correlation appears to exist between body size and litter size (Hedges & Conn 2012). *Caribicus anelpistus* and *C. warreni* have the largest litter sizes, with a litter size of 34 recorded for *C. warreni* (Lawler & Norris 1979) and two adult female *C. anelpistus* giving birth to 42 young (Schwartz *et al.* 1979). Smaller lizards, such as those in *Sauresia*, are reported to have litter sizes of one or two (Greer 1967; SBH, field data). Additional studies are needed to learn more about the reproductive cycles of celestines.

Conservation

We consider 32 of the 58 endemic Caribbean celestine species to be threatened with extinction, based on IUCN Redlist criteria (IUCN 2023). Of those species, fourteen (24%) are Critically Endangered, seventeen (29%) are Endangered, and one (2%) is Vulnerable. This large proportion (54%) of threatened species is more than twice as high as the average (21%) for reptiles (Cox *et al*. 2022). Of the Critically Endangered species, three are extinct or possibly extinct, and strong evidence indicates that deforestation and introduced predators (mainly the Small Indian Mongoose [*Urva auropunctata*]) are largely responsible for the decimation of the Caribbean islands diploglossid fauna (Fig. 107). Most species appear to require primary (undisturbed) forest, but some species do not and are tolerant of human disturbance and therefore are treated here as Least Concern. Nonetheless, species that are tolerant of habitat disturbance are still likely to be affected by introduced predators such as the mongoose and black rats. Besides consideration of habitat quality (primary forest versus disturbed) and the effect of introduced predators, we mention a third consideration in the accounts related to abundance: common or rare, which are subjective terms. Although we generally consider species that are tolerant of habitat disturbance to be "common," they likely still have been affected by introduced predators, lowering their abundance. Therefore, species of Least Concern should be monitored, as well as threatened species, to determine if they are declining because of predation by introduced predators.

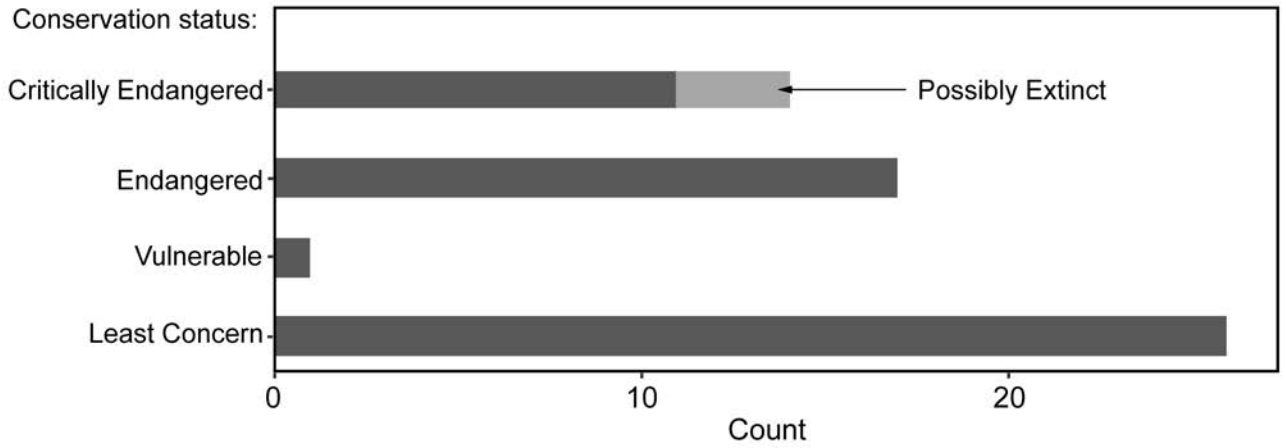

FIGURE 107. Summary graph on the IUCN conservation status of the 59 endemic Caribbean celestine species, according to IUCN (2023) criteria.

The decline of primary forest in the Caribbean because of human activities (Hedges *et al.* 2018) continues to destroy habitat of Caribbean diploglossids. Remaining primary forest in Haiti accounts for <1% of the total land area, and remaining primary forest in the Dominican Republic is estimated to be ~5% (Hedges & Conn 2012; Hedges *et al.* 2018). Although national parks and other protected areas exist in these countries, deforestation still takes place within their boundaries, meaning that they offer little to no protection.

The Small Indian Mongoose has been considered the major cause of Caribbean reptile extinctions and extirpations since shortly after its introduction (Barbour 1910, 1930; Henderson 1992; Breuil 2002; Powell & Henderson 2005; Lorvelec *et al.* 2007; Daltry 2009; Lewis *et al.* 2011; Hedges & Conn 2012). Notably, Hedges & Conn (2012) showed evidence that the effect of the mongoose is much more detrimental than that of other unspecified anthropogenic effects, persecution by humans, predation by other introduced species, and the effects of island size.

Although the introduction of the Small Indian Mongoose has had the most detrimental effect on Caribbean lizards, other introduced predators including rats, cats, dogs, pigs, and opossums also have had negative effects on Caribbean reptiles (Lowe *et al.* 2000; Daltry 2009; Hedges & Conn 2012). The ground-dwelling and diurnal habits of Caribbean diploglossids render them especially susceptible to mongoose predation and predation from other

introduced species. Species that can climb trees are in the minority. Whether these species have escaped extinction because of this adaptation is unknown, because most are rare.

Future studies incorporating additional morphological and genetic data will further clarify the diversity and phylogeny of diploglossid lizards. Further sampling efforts, particularly on Hispaniola and Jamaica, are needed to provide information on the current population status of many of these species. Sampling efforts such as these, particularly undertaken in traditionally under sampled or remote areas, are likely to result in the discovery of additional diploglossid species that may bring further resolution to the phylogeny of diploglossid lizards. This insight, especially concerning the relationships of species and populations, will provide a basis for additional studies on the ecology, evolution, and biogeography of this family.

Conclusions and recommendations

The taxonomy of diploglossid lizards, particularly the Caribbean species, has a long and muddled history. A lack of diagnostic morphological characters has caused persistent issues at the generic level; however, genetic data have recently clarified these relationships, leading to a more stable and functional taxonomy (Schools & Hedges 2021). Nevertheless, additional confusion has remained at the species level, addressed in this revision of the subfamily Celestinae. Our introduction of 17 new species and the elevation of 17 taxa from synonymy more accurately represents the genetic and morphological diversity of celestines. This revision also has more than doubled the number of recognized Caribbean celestine species, increasing that number from 24 to 58. This work will also provide future researchers with a systematic framework to explore ecological, evolutionary, and biogeographic questions concerning Caribbean celestine species that otherwise would not have been possible to ask.

Sadly, the majority of species are threatened with extinction and three species may already be extinct. Of the species that are not currently threatened with extinction, future studies should focus on incorporating genetic or genomic data from throughout their ranges to determine if additional species warrant recognition. All species should be monitored for threats to their survival, including those that are now deemed Least Concern. We believe that this work provides further evidence that the fauna of the Caribbean islands is unique, fragile, and understudied, and remains threatened by continued disturbance of habitats, including deforestation and predation from introduced mammals.

Acknowledgments

For the loan of specimens, access to collections, permission to photograph specimens, gift of tissue samples, or for providing information on specimens, we thank Ned Gilmore and Ted Daeschler, The Academy of Natural Sciences of Drexel University (ANSP), Philadelphia; Patrick Campbell, Colin McCarthy, and Jeff Streicher, The Natural History Museum (BMNH), London; Stevie Kennedy-Gold, Museum of Comparative Zoology, Harvard University (MCZ), Cambridge; Nicolas Vidal, National Museum of Natural History (MNHN), Paris; Byron S. Wilson, University of the West Indies, Jamaica; Jeremy Jacobs, Esther Langan, Roy W. McDiarmid, Robert Wilson, W. Ronald Heyer, Addison Wynn, and George R. Zug, National Museum of Natural History (USNM), Washington, D.C; Rafe Brown and Ana Mota, The University of Kansas Biodiversity Institute and Natural History Museum (KU), Lawrence, Kansas, USA. We thank our reviewers for comments on the manuscript. We thank the technical team at Daicel Arbor Biosciences, especially Jennifer Klunk and Tianying Lan, for their successful efforts in getting historical DNA sequence from our samples, and assistance with bioinformatics. SBH thanks his students, staff, and colleagues for providing assistance on expeditions since the 1980s, including Yvonne Arias, Philippe Bayard, Tiffany Cloud, Ronald Crombie, Arnaud Dupuy, Eladio Fernandez, Sarah Hanson, Jessie Haspil, Carla Hass, Matthew Heinicke, Richard Highton, Sixto Inchaustegui, Anderson Jean, Miguel Landestoy, Manuel Leal, Allison Loveless, Einar Madsen, Carlos Martinez, Nicholas Plummer, Jennifer Pramuk, Jessica Preston, Daniel Rabosky, Elisabeth Rochel, Florence Sergile, Richard Thomas, Joel Timyan, Michael Tracy, Lyonel Valbrun, and Byron Wilson; Stephanie Dennison, Carla Hass, Joanna Hofstaedter, Adrienne Kasprowicz, Allison Loveless, Angela Marion, Kathleen McGrath, Jessica Preston, Elisabeth Rochel, and Jennifer Stella for providing analytical and laboratory assistance; Robert W. Henderson for making available the research materials of Albert Schwartz; and the governments of the Cayman Islands, the Dominican Republic, the Republic of Haiti, and Jamaica for collecting and export permits. This research was supported by funding from the United States National Science Foundation (8307115, 8906325, 9123556,

9525775, 9615643, and 0918891), the Critical Ecosystems Partnership Fund (HAI/62132), and Temple University to S. Blair Hedges. Finally, SBH gives special thanks to Richard Thomas, who accompanied him on countless trips to the islands to collect amphibians and reptiles, including many celestine lizards.

References cited

Ali, J.R., & Hedges, S.B. (2021) Colonizing the Caribbean: New geological data and an updated land-vertebrate colonization record challenge the GAARlandia land-bridge hypothesis. *Journal of Biogeography*, 48 (11), 2699–2707. https://doi.org/10.1111/jbi.14234

Ali, J.R., & Hedges, S.B. (2024) Paleogeography of the Aves Ridge and its potential role as a bio-colonization pathway linking South America and the Greater Antilles in the mid-Cenozoic. *Earth-Science Reviews*, 254, 104823. https://doi.org/10.1016/j.earscirev.2024.104823

Ahrenfeldt, R.H. (1954) Identification of the Amphibia and Reptilia recorded in Jamaica by Hans Sloane (1688–89). *Copeia*, 1954 (2), 105–111.

Barba-Montoya, J., Tao, Q., & Kumar, S. (2021) Assessing rapid relaxed-clock methods for phylogenomic dating. *Genome Biology and Evolution*, 13 (11), evab251. https://doi.org/10.1093/gbe/evab251

Barbour, T. (1910) Notes on the herpetology of Jamaica. *Bulletin of the Museum of Comparative Zoology*, 52, 273–301.

Barbour, T. (1922) *An annotated list of the Amphibia and Reptilia of Jamaica*. Handbook of Jamaica, for 1922. 666–669 pp.

Barbour, T. (1930) A list of Antillean reptiles and amphibians. *Zoologica, New York*, 11, 61–116.

Barbour, T. (1935) Second list of Antillean reptiles and amphibians. *Zoologica, New York*, 19, 77–142.

Barbour, T. (1937) Third list of Antillean reptiles and amphibians. *Bulletin of the Museum of Comparative Zoology*, 82, 77–166.

Boulenger, G.A. (1885) *Catalogue of the Lizards in the British Museum. Vol. 2*. Taylor & Francis, London, 497 pp.

Boulenger, G.A. (1900) Description of a new Lizard from Jamaica. *Journal of Natural History*, 6 (32), 193–194.

Breuil, M. (2002) Histoire naturelle des Amphibiens et Reptiles terrestres de l'Archipel Guadeloupéen: Guadeloupe et dépendances, Saint-Martin, Saint-Barthélemy. *Patrimoines naturels IEGB, SPN MNHN*, 54, 1–339.

Browne, P. (1789) *The Civil and Natural History of Jamaica*. B. White and Son, London, 503 pp.

Cochran, D.M. (1927) A new genus of anguid lizards from Haiti. *Proceedings of the Biological Society of Washington*, 40, 91–92.

Cochran, D.M. (1939) Diagnoses of three new lizards and a frog from the Dominican Republic. *Proceedings of the New England Zoölogical Club*, 18, 1–3.

Cochran, D.M. (1941) The herpetology of Hispaniola. *Bulletin of the United States National Museum*, 177, 1–398. https://doi.org/10.5962/bhl.part.14437

Cockerell, T.D.A. (1894) A Little Known Jamaican Naturalist, Dr. Anthony Robinson. *The American Naturalist*, 28 (333), 775–780.

Cooper, W. & Bradley, K. (2009) Prey chemical discrimination by a diploglossine lizard, the giant Hispaniolan galliwasp (*Celestus warreni*). *Amphibia-Reptilia*, 30 (1), 135–140.

Cope, E.D. (1861) Descriptions of reptiles from tropical America and Asia. *Proceedings of the Academy of Natural Sciences of Philadelphia*, 12 (1860), 368–374.

Cope, E.D. (1862a) Contributions to Neotropical saurology. *Proceedings of the Academy of Natural Sciences of Philadelphia*, 14, 176–188.

Cope, E.D. (1862b) On the genera *Panolopus*, *Centropyx*, *Aristelliger* and *Sphaerodactylus*. *Proceedings of the Academy of Natural Sciences of Philadelphia*, 13 (1861), 494–500.

Cope, E.D. (1865) Third contribution to the herpetology of tropical America. *Proceedings of the Academy of Natural Sciences of Philadelphia*, 17, 185–198.

Cope, E.D. (1868) An examination of the Reptilia and Batrachia obtained by the Orton Expedition to Ecuador and the Upper Amazon, with notes on other species. *Proceedings of the Academy of Natural Sciences of Philadelphia*, 20, 96–140.

Cope, E.D. (1879) Eleventh contribution to the herpetology of tropical America. *Proceedings of the American Philosophical Society*, 18 (104), 261–277.

Cousens, P.N. (1956) Notes on the Jamaican and Cayman Island lizards of the genus *Celestus*. *Brevoria*, 56, 1–6.

Cox, N., Young, B.E., Bowles, P., Fernandez, M., Marin, J., Rapacciuolo, G., Böhm, M., Brooks, TM, Hedges, S.B., Hilton-Taylor, C., Hoffmann, M., Jenkins, R.K.B., Tognelli, M.F., Alexander, G.J., Allison, A., Ananjeva, N.B., Auliya, M., Avila, L.J., Chapple, D.G., Cisneros-Heredia, D.F., Cogger, H.G., Colli, G.R., de Silva, A., Eisemberg, C.C., Els, J., Fong, G.A., Grant, T.D., Hitchmough, R.A., Iskandar, D.T. Kidera, N., Martins, M., Meiri, S., Mitchell, N.J., Molur, S., Nogueira, C.C., Ortiz, J.C., Penner, J., Rhodin, A.G.J., Rivas, G.A., Rödel, M.O., Roll, U., Sanders, K.L., Santos-Barrera, G., Shea, G.M., Spawls, S., Stuart, B.L., Tolley, K.A., Trape, J.F., Vidal, M.A., Wagner, P., Wallace, B.P. & Xie, Y. (2022) A global reptile assessment highlights shared conservation needs of tetrapods. *Nature*, 605 (7909), 285–290. https://doi.org/10.1038/s41586-022-04664-7

Crombie, R.I. (1999) Jamaica. *In*: Crother, B.I. (Ed.), *Caribbean amphibians and reptiles*. Academic Press, San Diego, USA, pp. 63–92.
Daltry, J.C. (2009) *The Status and Management of Saint Lucia's Forest Reptiles and Amphibians. Technical Report No. 2 to the National Forest Demarcation and Bio-Physical Resource Inventory Project*. FCG International Ltd, Helsinki, 129 pp.
De Jesus, N., Marte, C., Espinal, R.J. & Incháustegui, S.J. (2023) Rediscovery of the Altagracia Giant Galliwasp (*Caribicus anelpistus*) at Villa Altagracia, Dominican Republic. *Reptiles & Amphibians*, 30 (1), e20611–e20611.
Dennison, S.L. (2010) Molecular phylogeny and biogeography of Neotropical lizards of the family Diploglossidae. Honors Thesis, Pennsylvania State University, University Park, Pennsylvania. 110 pp.
Duméril, A.M.C., & Bibron, G. (1839) *Erpétologie Générale on Histoire Naturelle Complète des Reptiles. Vol.5*. Roret/Fain et Thunot, Paris, 871 pp.
Dunn, E.R. (1939) Zoological results of the George Vanderbilt South Pacific Expedition of 1937. Part III. The lizards of Malpelo Island, Colombia. *Notulae Naturae, Academy of Natural Sciences of Philadelphia*, 4, 1–3.
Etheridge, R. (1965) Fossil lizards from the Dominican Republic. *Quarterly Journal of the Florida Academy of Sciences*, 28 (1), 83–105.
Franz, R. & Cordier, D. (1986) *Herpetofaunas of the National Parks of Haiti.* Florida Museum of Natural History, University of Florida, USAID/Haiti, Port au Prince, 16 pp.
Fürbringer, M. (1900) Zur Vergleichenden Anatomie des Brustschulterapparates und der Schultermuskeln. *Janaische Zeitschrift für Naturwissenschaf*, 34, 215–718.
https://doi.org/10.5962/bhl.title.52377
Garman, S. (1887) On West Indian Geckonidae and Anguide. *Bulletin of the Essex Institute*, 19, 17–24.
Garman, S. (1888) Reptiles and batrachians form the Caymans and the Bahamas. *Bulletin of the Essex Institute*, 20, 1–13.
Genbank. (2020) *GenBank*. National Institutes of Health, Bethesda, Maryland. Available from: http://www.ncbi.nlm.nih.gov/genbank/ (accessed 16 December 2020)
Gosse, P.H. (1851) *A Naturalist's Sojourn in Jamaica*. Longman, Brown, Green, and Longmans, London, 552 pp.
Grant, C. (1940a). II. The reptiles. *In*: Lynn, W.G. & Grant, C. (Eds.), *The Herpetology of Jamaica*. The Institute of Jamaica, Kingston, pp. 61–148.
Grant, C. (1940b) Notes on the reptiles and amphibians of Jamaica, with diagnoses of new species and subspecies. *In*: *Jamaica Today*. Hazell, Watson, and Viney, London and Aylesbury, pp. 151–157.
Grant, C. (1951) The specific characters of the Celesti, with description of a new species of *Celestus* (Sauria: Anguidae). *Copeia*, 1951 (1), 67–69.
https://doi.org/10.2307/1438056
Gray, J.E. (1825) A synopsis of the genera of reptiles and Amphibia, with a description of some new species. *Annals of Philosophy*, 10, 193–217.
Gray, J.E. (1839) Catalogue of the slender-tongued saurians, with descriptions of many new genera and species. *Annals & Magazine of Natural History*, Series 1, 2 (11), 331–337.
https://doi.org/10.1080/00222933909512395
Gray, J.E. (1845) *Catalogue of the specimens of lizards in the collections of the British Museum*. British Museum, London, xxvii + 289 pp.
Gray, J.E. (1852) Description of *Sauresia*, a new genus of Scincidae from St. Domingo. *Annals and Magazine of Natural History*, 10 (58), 281–282.
https://doi.org/10.1080/03745485609495697
Greer, A.E. (1967) Notes on the mode of reproduction in anguid lizards. *Herpetologica*, 23 (2), 94–99.
Hallermann, J. & Böhme, W. (2002) On giant anguids from the West Indies with special reference to *Celestus warreni* (Schwartz, 1970) and its relatives from Hispaniola (Reptilia: Squamata: Anguidae). *Mitteilungen aus dem Hamburgischen Zoologischen Museum und Institut*, 99, 169–178.
Hass, C.A., Maxson, L.R. & Hedges, S.B. (2001) Relationships and divergence times of West Indian amphibians and reptiles: Insights from albumin immunology. *In*: Woods, C.A. & Sergile, F.E. (Eds.), *Biogeography of the West Indies: Patterns and Perspectives. 2nd Edition*. CRC Press, Boca Raton, Florida, pp. 15–33.
https://doi.org/10.1201/9781420039481-11
Hedges, S.B. (1996) Historical biogeography of West Indian vertebrates. *Annual Review of Ecology and Systematics*, 27 (1), 163–196.
Hedges, S.B. (2001) Caribbean biogeography: an outline. *In*: Woods, C.A. & Sergile, F.E. (Eds.), *Biogeography of the West Indies: Patterns and Perspectives. 2nd Edition*. CRC Press, Boca Raton, Florida, pp. 15–33.
https://doi.org/10.1146/annurev.ecolsys.27.1.163
Hedges, S.B. (2006) Paleogeography of the Antilles and the origin of West Indian terrestrial vertebrates. *Annals of the Missouri Botanical Garden*, 93, 231–244.
https://doi.org/10.3417/0026-6493(2006)93[231:POTAAO]2.0.CO;2
Hedges, S.B. (2008). Caribherp: amphibians and reptiles of Caribbean islands. Available from: http://www.caribherp.org/ (Accessed 24 November 2008. Pennsylvania State University)
Hedges, S.B. (2013) Caribmap: a mobile-friendly web resource for Caribbean maps that facilitates quantitative historical analysis. *Journal of Map and Geography Libraries*, 9 (3), 350–360.

Hedges, S.B. (2024) Caribherp: amphibians and reptiles of Caribbean islands. Available from: http://www.caribherp.org/ (Accessed 1 January 2024. Center for Biodiversity, Temple University)
Hedges, S.B., Cohen, W.B., TiMan, J. & Yang, Z. (2018) Haiti's biodiversity threatened by nearly complete loss of primary forest. *Proceedings of the National Academy of Sciences*, 115 (46), 11850–11855. https://doi.org/10.1073/pnas.1809753115
Hedges, S.B. & Conn, C.E. (2012) A new skink fauna from Caribbean islands (Squamata, Mabuyidae, Mabuyinae). *Zootaxa*, 3288 (1), 1–244. https://doi.org/10.11646/zootaxa.3288.1.1
Hedges, S.B., Duellman, W.E. & Heinicke, M.P. (2008) New World direct-developing frogs (Anura: Terrarana): molecular phylogeny, classification, biogeography, and conservation. *Zootaxa*, 1737 (1), 1–182. https://doi.org/10.11646/zootaxa.1737.1.1
Hedges, S.B., Hass, C.A. & Maxson, L.R. (1992) Caribbean biogeography: molecular evidence for dispersal in West Indian terrestrial vertebrates. *Proceedings of the National Academy of Sciences*, 89 (5), 1909–1913. https://doi.org/10.1073/pnas.89.5.1909
Hedges, S.B., Marin, J., Suleski, M., Paymer, M. & Kumar, S. (2015) Tree of life reveals clock-like speciation and diversification. *Molecular Biology and Evolution*, 32 (4), 835–845. https://doi.org/10.1093/molbev/msv037
Hedges, S.B., Powell, R., Henderson, R.W., Hanson, S. & Murphy, J.C. (2019) Definition of the Caribbean Islands biogeographic region, with checklist and recommendations for standardized common names of amphibians and reptiles. *Caribbean Herpetology*, 67, 1–53. https://doi.org/10.31611/ch.67
Hedges, S.B. & Shah, P. (2003) Comparison of mode estimation methods and application in molecular clock analysis. *BMC Bioinformatics*, 4 (31), 1–11.
Henderson, R.W. (1992) Consequences of predator introductions and habitat destruction on amphibians and reptiles in the post Columbus West Indies. *Caribbean Journal of Science*, 28 (1–2), 1–10.
Henderson, R.W. & Powell, R. (2009) *Natural History of West Indian Reptiles and Amphibians*. University Press of Florida, Gainesville, Florida, 495 pp.
Incháustegui, S.J., Schwartz, A. & Henderson, R.W. (1985) Hispaniolan giant *Diploglossus* (Sauria, Anguidae): description of a new species and notes on the ecology of *D. warreni*. *Amphibia-Reptilia*, 6 (2), 195–201.
IUCN. (2023) *IUCN Redlist of Threatened Species*. Available from: http://www.iucnredlist.org/ Gland, Switzerland: International Union for the Conservation of Nature (accessed 13 November 2023).
Kumar, S. (2022) Embracing green computing in molecular phylogenetics. *Molecular biology and evolution*, 39 (3), msac043. https://doi.org/10.1093/molbev/msac043
Kumar, S., Stecher, G., Li, M., Knyaz, C. & Tamura, K. (2018) MEGA X: molecular evolutionary genetics analysis across computing platforms. *Molecular Biology and Evolution*, 35 (6), 1547–1549. https://doi.org/10.1093/molbev/msy096
Landestoy, M., Schools, M. & Hedges, S.B. (2022) A new genus and species of Caribbean forest lizard (Diploglossidae; Celestinae) from southern Hispaniola. *Zootaxa*, 5219 (3), 201–226.
Lawler, H.E. & Norris, C. (1979) Breeding the Haitian giant galliwasp, *Diploglossus warreni* (Sauria: Anguidae) at the Knoxville Zoological Park. In: *Third Annual Symposium on Captive Propagation and Husbandry*, pp. 73–79.
Lewis, D.S., Veen, R.V. & Wilson, B.S. (2011) Conservation implications of Small Indian Mongoose (*Herpestes auropunctatus*) predation in a hotspot within a hotspot: the Hellshire Hills, Jamaica. *Biological Invasions*, 13 (1), 25–33. https://doi.org/10.1007/s10530-010-9781-0
Lorvelec, O., Pascal, M., Pavis, C. & Feldmann, P. (2007) Amphibians and reptiles of the French West Indies: inventory, threats and conservation. *Applied Herpetology*, 4 (2), 131–161.
Lotzkat, S., Hertz, A. & Köhler, G. (2016) A new species of *Celestus* (Squamata: Anguidae) from western Panama. *Mesoamerican Herpetology*, 3, 962–975. https://doi.org/10.1163/157075407780681356
Lowe, S., Browne, M., Boudjelas, S. & De Poorter, M. (2000) *100 of the World's Worst Invasive Alien Species: A Selection from the Global Invasive Species Database*. Invasive Species Specialist Group (ISSG), a specialist group of the Species Survival Commission (SSC) of the World Conservation Union (IUCN), Gland, Switzerland, 12 pp.
McGinnity, D. (2002) The conservation initiative for giant galliwasps at Nashville Zoo: A preliminary account. *International Zoo News*, 396–403.
Minh, B.Q., Schmidt, H.A., Chernomor, O., Schrempf, D., Woodhams, M.D., Von Haeseler, A. & Lanfear, R. (2020) IQ-TREE 2: new models and efficient methods for phylogenetic inference in the genomic era. *Molecular Biology and Evolution*, 37 (5), 1530–1534. https://doi.org/10.1093/molbev/msaa015
Ober, L.D. (1970) Reproduction in the anguid lizard, *Diploglossus curtissi aporus* Schwartz. *Herpetologica*, 26 (2), 275–275.
Oppel, M. (1811) *Die Ordnungen, Familien und Gattungen der reptilien, als Prodrom einer Naturgeschichte derselben*. Joseph Lindauer, Munich, 86 pp. https://doi.org/10.5962/bhl.title.4911

Peters, J.A. & Donoso-Barros, R. (1970) Catalogue of the Neotropical Squamata: Part II. Lizards and amphisbaenians. *Bulletin of the United States National Museum*, 297, 1–347. https://doi.org/10.5479/si.03629236.297.1
Powell, R. (1999) Herpetology of Navassa Island, West Indies. *Caribbean Journal of Science*, 35, 1–13.
Powell, R. & Henderson, R.W. (2003) The taxonomic and conservation status of giant Hispaniolan *Celestus* (Anguidae). *Caribbean Journal of Science*, 39, 237–240.
Powell, R. & Henderson, R.W. (2005) Conservation status of Lesser Antillean reptiles. *Iguana*, 12 (2), 3–17.
Puillandre, N., Brouillet, S. & Achaz, G. (2021) ASAP: assemble species by automatic partitioning. *Molecular Ecology Resources*, 21 (2), 609–620.
QGIS. (2020) QGIS Geographic Information System. Open Source Geospatial Foundation Project. Available from: http://qgis.org (accessed 20 August 2020)
Renesto, S. & Dalla Vecchia, F.M. (2000) The unusual dentition and feeding habits of the prolacertiform reptile *Langobardisaurus* (Late Triassic, Northern Italy). *Journal of Vertebrate Paleontology*, 20 (3), 622–627. https://doi.org/10.1671/0272-4634(2000)020[0622:TUDAFH]2.0.CO;2
Ronquist, F., Teslenko, M., van der Mark, P., Ayres, D.L., Darling, A., Höhna, S., Larget, B., Liu, L., Suchard, M.A. & Huelsenbeck, J.P. (2012) MRBAYES 3.2: Efficient Bayesian phylogenetic inference and model selection across a large model space. *Systematic Biology*, 61 (3), 539–542. https://doi.org/10.1093/sysbio/sys029
Sangermano, F., Bol, L., Galvis, P., Gullison, R.E., Hardner, J. & Ross, G.S. (2015) Habitat suitability and protection status of four species of amphibians in the Dominican Republic. *Applied Geography*, 63, 55–65.
Savage, J.M. & Lips, K.R. (1993) A review of the status and biogeography of the lizard genera *Celestus* and *Diploglossus* (Squamata: Anguidae), with description of two new species from Costa Rica. *Revista de Biología Tropical*, 41, 817–842.
Savage, J.M., Lips, K.R., & Ibáñez, D. (2008) A new species of *Celestus* from west-central Panama, with consideration of the status of the genera of the Anguidae: Diploglossinae (Squamata). *Revista de Biología Tropical*, 56 (2), 845–859.
Schmidt, K.P. (1921) Notes on the herpetology of Santo Domingo. *Bulletin of the AMNH*, 44, article 2.
Schools, M. & Hedges, S.B. (2021). Phylogenetics, classification, and biogeography of the Neotropical forest lizards (Squamata, Diploglossidae). *Zootaxa*, 4974 (2), 201–257. https://doi.org/10.11646/zootaxa.4974.2.1
Schools, M., Kasprowicz, A. & Hedges, S.B. (2022) Phylogenomic data resolve the historical biogeography and ecomorphs of Neotropical forest lizards (Squamata, Diploglossidae). *Molecular Phylogenetics and Evolution*, 175, 107577.
Schwartz, A. (1964) *Diploglossus costatus* Cope (Sauria, Anguidae) and its relatives in Hispaniola. *Reading Public Museum and Art Gallery*, 13, 1–57.
Schwartz, A. (1965) Two new subspecies of the anguid lizard *Wetmorena* from Hispaniola. *Proceedings of the Biological Society of Washington*, 78, 39–48.
Schwartz, A. (1970) A new species of large *Diploglossus* (Sauria: Anguidae) from Hispaniola. *Proceedings of the Biological Society of Washington*, 82 (60), 777–788.
Schwartz, A. (1971a) A new species of bromeliad-inhabiting galliwasp (Sauria: Anguidae) from Jamaica. *Breviora*, 371, 1–10.
Schwartz, A. (1971b) Two new subspecies of *Diploglossus costatus* from Hispaniola (Sauria, Anguidae). *Journal of Herpetology*, 161–165.
Schwartz, A., Graham, E.D. Jr. & Duval, J.J. (1979) A new species of *Diploglossus* (Sauria: Anguidae) from Hispaniola. *Proceedings of the Biological Society of Washington*, 92, 1–9.
Schwartz, A. & Henderson, R.W. (1988) West Indian amphibians and reptiles: a checklist. *Milwaukee Public Museum Contributions to Biology and Geology*, 74, 1–264.
Schwartz, A. & Henderson, R.W. (1991) *Amphibians and reptiles of the West Indies: descriptions, distributions, and natural history*. University of Florida Press, Gainesville, Florida, 720 pp.
Schwartz, A. & Inchaustegui, S.I. (1976) A new species of *Diploglossus* (Reptilia, Lacertilia, Anguidae) from Hispaniola. *Journal of Herpetology*, 10, 241–246. https://doi.org/10.2307/1562985
Schwartz, A. & Jacobs, J.F. (1989) A new subspecies of *Celestus costatus* (Sauria: Anguidae) from the República Dominicana. *Journal of Herpetology*, 193–195.
Seidel, M.E. & Franz, R. (1994) Amphibians and reptiles (exclusive of marine turtles) of the Cayman Islands. In: Brunt, M.A., Davis, J.E. (Eds.), *The Cayman Islands: natural history and biogeography.* Dordrecht, The Netherlands, Kluwer, pp. 407–433.
Shaw, G. (1802) *General zoology or systematic natural history. Vol. 3*. Thomas Davison, London, viii + 312 pp.
Sloane, H. (1725) *A voyage to the islands of Madera, Barbados, Nieves, St. Christophers, and Jamaica with the natural history of the herbs and trees, four-footed beasts, fishes, birds, insects, reptiles etc. of the last of those islands, vol. 2.* Christophers and Jamaica, 2, 1707–1725.
Strahm, M.H. & Schwartz, A. (1977) Osteoderms in the anguid lizard subfamily Diploglossinae and their taxonomic importance. *Biotropica*, 9, 58–72. https://doi.org/10.2307/2387862
Sukumaran, J. & Knowles, L.L. (2017) Multispecies coalescent delimits structure, not species. *Proceedings of the National*

Academy of Sciences, 114 (7), 1607–1612.
Tamura, K., Battistuzzi, F.U., Billing-Ross, P., Murillo, O., Filipski, A. & Kumar, S. (2012) Estimating divergence times in large molecular phylogenies. *Proceedings of the National Academy of Sciences*, 109 (47), 19333–19338.
Thomas, R. (1966) A reassessment of the herpetofauna of Navassa Island. *Journal of the Ohio Herpetological Society*, 5 (3), 73–89.
https://doi.org/10.2307/1562610
Thomas, R. (1971) A new species of *Diploglossus* (Sauria: Anguidae) from Hispaniola. *Occasional papers of the Museum of Zoology Louisiana State University*, 1 (40), 1–9.
Thomas, R. & Hedges, S.B. (1989) A new *Celestus* (Sauria: Anguidae) from the Chaine de La Selle of Haiti. *Copeia*, 4, 886–891.
https://doi.org/10.2307/1445973
Underwood, G. (1959). A new Jamaican galliwasp (Sauria, Anguidae). *Brevoria*, 102, 1–13.
Vidal, N. & Hedges, S.B. (2005) The phylogeny of squamate reptiles (lizards, snakes, and amphisbaenians) inferred from nine nuclear protein-coding genes. *Comptes Rendus Biologies*, 328 (10–11), 1000–1008.
https://doi.org/10.1016/j.crvi.2005.10.001
Vidal, N. & Hedges, S.B. (2009) The molecular evolutionary tree of lizards, snakes, and amphisbaenians. *CR Biologies*, 332 (2–3), 129–139.
Weinland, D.F. (1858) Zoology of Hayti. *American Journal of Science and Arts*, 76, 210–214.
Weinland, D.F. (1863) Beschreibung und Abbildung von drei neuen Sauriern (*Embryopus Habichii* und *Amphisbaena innocens* von Haiti, und *Brachymeles Leuckartii* von Neuholland). *Abhandlungen der Senckenbergischen Naturforschenden Gesellschaft*, 4, 132–145.
White, L.R. & Powell, R. (1996) *Celestus agasepsoides*. *Catalogue of American Amphibians and Reptiles*, 627, 1–2.
White, L.R., Powell, R., Parmerlee, J.S., Lathrop, A. & Smith, D.D. (1992) Food habits of three syntopic reptiles from the Barahona Peninsula, Hispaniola. *Journal of Herpetology*, 26 (4), 518–520.
Wiens, J.J., Brandley, M.C. & Reeder, T.W. (2006) Why does a trait evolve multiple times within a clade? Repeated evolution of snakeline body form in squamate reptiles. *Evolution*, 60 (1), 123–141.
https://doi.org/10.1111/j.0014-3820.2006.tb01088.x
Wilson, B.S. & Vogel, P. (2000) A survey of the herpetofauna of the Hellshire Hills, Jamaica, including the rediscovery of the Blue-tailed Galliwasp (*Celestus duquesneyi* Grant). *Caribbean Journal of Science*, 36 (3/4), 244–249.

APPENDIX 1. Specimens and sequences used in the molecular analyses.

Genbank numbers are listed for CytB, ND2, and 12S rRNA. Genes that were previously submitted as a part of Schools & Hedges (2021) or Landestoy *et al.* 2022 can be found in the appendices of those papers. Three sequences contain a higher percentage of ambiguous sites than Genbank can accept. Those CytB sequences, obtained from *Celestus macrolepis 1* and *Sauresia sepsoides 28* respectively, are:

TATGCCTAATTATCCAAATCCTAACAGGACTATTCTTGGCCATAC[31N's]ATCAATCGCACATATCTGCC
GAGATGTACAATANGGTTGACTTCTA[21N's]GCCTCAATGTTTTTCTTCTGCATTTATTTCCACATTGGA
CGAGGAATCTACTATGGCTCATACCTA[156N's]GTTCACTGAACATGAGGGGGATTTGCCATCGACAAC
GCAACTCTGACTCGATTCTTTACATTACACTTC[227N's]GACCCATTAGTAACCCCACCACACATTAAAC
CTGAATGATACTTCCTATTCGCCTATGCAATCCTACGCTCAATTCCTAACAAAATCGGAGGCGTCCTT

and:
AAAAACTTGATACACAGGGACTATTATACTATTACTTCTAATAGCCACAGCATTCCTAGGATATGTACTT
CCCTGAGGAYAAATATCCTTCTGAGGTGCAACCGTCATCACCAACCTACTATCAGCCCTCCCAT[206N's]
TATACCTACAAAGACCTGCTTGGAATCACGCTATTCATAATAGTACTTACAACACTCAC[75N's]TAAGCC
CGAATGATACTTCTTATTCGCCTATGCAATCTTACGCTCCATCCCTAACAAAATTGGAGGGGTCMT.

The ND2 sequence for *Panolopus aporus 2* is:

ACCATTCTTATAATTAATTTAGCCATTGGCACAATTATCACCATATCAAGCCACCACTGACTACTAGCAT
GAATAGGCTTAGAACTAAATACCCTTGCCATCCTACCAATCATCTCAAAAATCCACCACCCCCGAGCCA
CAGAAGCCTCAACCAAATACTTTTTAACACAAGCAGCAGCATCCGCCCTAATCCTATTCTCAAGCTCA
CTCAACGCCCAAAGCACCGGACAGTGAAATATTCTCGACCTTAACAATCAAATATCAAAAACATTAAT
TACCATAGCACTGGGAATAAAACTAGGACTTGCACCAGCCCACTTCTGACTCCCAGAAGTATTACAAG
GTGCCTCACTTACAACCTCCCTAATCATTGTTACCTGACAAAAACTAGCACCAACATCTCTACTTTACC
TGACATGAAATCAAATCTCACCAACAATCATCACCCTAATAGGCGCACTATCAGTAATTGTAGGCGGAC
TAGGGGGACTCAACCAAACTCAAATGCGAAAAATCATCGCCTACTCATCAATCGCCCACCTAGGATGA
ATGGCCACAATTATATCTAAATCCAACAAACTAGCCCTACTAAACCTAACAATGTATATTATTATTACCTC
ATCATTGATACTATCGCTAATTTTCTTCTACACAAAAACAATCCTAGACCTAACCACTATATGAACCGCA
TCACCAACACTCACCATAATAACTATAACAACACTACTATCATTAGGAGGGCTTCCTCCCCTGGCCGGC
TTTATCCCAAAATGGTTAACCTTGGAAGTACTAATAAACCATAACTCAACAACCCTAGCAACCGCACTA
GCACTCTCCACACTATTAAGCCTATTTTTCTACTTACGACTATCCTATTCAATAGCCGT.

Locality data are summarized below. Specimen vouchers (if known), laboratory numbers ("SBH", if voucher is not available), and localities of samples used in molecular analyses. NA = not applicable (sequence not obtained).

Caribicus darlingtoni. 1–3: USNM 328805–07 (Dom. Rep., La Vega, ca. 37 km SE of Constanza via new road to San Jose de Ocoa; 18.7056, -70.5981). ***Caribicus warreni.*** 1: SBH 194521 (Voucher not available; Dom. Rep., Puerto Plata, presumably the region of Puerto Plata). 2: ANSP 38501 (Haiti, locality not available). ***Celestus barbouri.*** 1: ANSP 38503 (Jamaica, Trelawny, 0.5 km N of Windsor; 18.3579, -77.6482). 2: USNM 328153 (Jamaica, Trelawny, vicinity of Quick Step). ***Celestus capitulatus* sp. nov.** 1–2: USNM 328168–69 (Jamaica, St. Elizabeth, Knoxwood; 18.00363, -77.74490). 3: USNM 328157 (Jamaica, Westmoreland, 4.5 km W of Old Hope, at Little Bay; 18.22033, -78.26636). ***Celestus crusculus*.** 1–4: USNM 328159–60, 328166–7 (Jamaica, Trelawny, 0.3 km W of Duncans, jct. with Silver Sands road). 5: ANSP 38504 (Jamaica, Trelawny, 0.3 km W Duncans, jct with Silver Sands access road). 6: USNM 328186 (Jamaica, St. Catherine, 5.6 km SW of Braeton (in Hellshire Hills, at Hellshire Beach; 17.89784, -76.89407). ***Celestus duquesneyi.*** 1: SBH 267952 (Voucher not available; Jamaica, St. Catherine, Hellshire Hills). ***Celestus hesperius* sp. nov.** 1–2: USNM 328154–55 (Jamaica, Hanover, 3.2 km SE of Content). 3: USNM 328156 (Jamaica, Westmoreland, 5.3 km N of Town Head). ***Celestus hewardi.*** 1: SBH 267097 (Voucher not available; Jamaica, Manchester, Mandeville). ***Celestus jamesbondi* sp. nov.** 1: USNM 328170 (Jamaica, Clarendon, Jackson's Bay, on beach at the hunting club). 2: SBH 171439 (Voucher not available; Jamaica, St. Mary, 6.2 km W of Oracabessa; 18.40805, -76.99293). 3: SBH 274324 (Voucher not available; Jamaica, St.

Mary, 1.7 miles ESE Mango Valley; 18.38088, -76.97265). 4: USNM 328172 (Jamaica, St. Mary, vicinity of town of Jack's River; 18.37546, -76.93952). 5: USNM 328173 (Jamaica, St. Mary, ca. 1.6 km S of Oracabessa, on road to Jacks River; 18.38642, -76.94306). 6–7: USNM 328174–75 (Jamaica, St. Mary, 6.2 km W of Oracabessa; 18.40805, -76.99293). 8: USNM 328176 (Jamaica, St. Mary, Salt Gut, vicinity of Boscobel Airport [E side]; 18.40379, -76.96941). 9: USNM 328177 (Jamaica, St. Mary, 2.9 km N of Port Maria; 18.38939, -76.89576). 10–13: USNM 328180, 328182, 328183–84 (Jamaica, St. Mary, ca. 6.4 km S of Port Maria; chevrons). ***Celestus macrolepis.*** 1: BMNH 1946.8.3.82 (no locality; restricted here to Jamaica). ***Celestus macrotus.*** 1–2: MALT 00796, 00799 (Dom. Rep., P.N. Sierra de Bahoruco, ESE Caseta Loma de Toro (Helipuerto); 18.28718, -71.71251). 3: (Dom. Rep., Bahoruco). 4: ANSP 38505 (Haiti, Sud-Est, Southeast of Pic La Selle; 18.32887, -72.02184). 5: ANSP 38506 (Haiti, Ouest, southeast of Pic La Selle; 18.32887, -72.02184). ***Celestus molesworthi.*** 1: USNM 328144 (Jamaica, Portland, 1.3 km WSW of Section, on road to Hardwar Gap). 2: SBH 274634 (Voucher not available; Jamaica, Portland, 1.0 km S by road Manchioneal; 18.03653, -76.27861). 3: SBH 274632 (Voucher not available; Jamaica, St. Thomas, 5.9 km W Trinity Ville by road; 17.98239, -76.5666). ***Celestus occiduus.*** 1: BMNH XV.115.A. 2: MNHN 0.2855. ***Celestus oligolepis*** **sp. nov.** 1: USNM 328158 (Jamaica, Westmoreland, 7.0 km WSW of Old Hope; 18.2232, -78.2861). ***Celestus striatus*****.** 1: BMNH 1946.8.8.3 (no locality; restricted here to Jamaica). 2: MCZ R-125601 (Jamaica, Trelawny Forest; 18.3520, -77.64782). ***Comptus alloeides.*** 1: USNM 328830 (Dom. Rep., Maria Trinidad Sanchez, 4 km SE of Nagua; 19.3481, -69.8244). ***Comptus arboreus*** **sp. nov.** 1–3: ANSP 38538–40 (Haiti, Grand'Anse, Belandier, 5.0 km N of Dame Marie; 18.58568, -74.40762). 4: SBH 191945 (Haiti, Grand'Anse, 0.8 km E of Dame-Marie; 18.55925, -74.41550). 5: SBH 269065 (Voucher not available; Haiti, Grand'Anse, Bourdon, 9.2 km E of Ause D'Hainalt; 18.48225, -74.36113). 6: ANSP 38543 (Haiti, Grand'Anse, 1.5 km N of Carcasse; 18.3852, -74.44755). 7: SBH 274478 (Voucher not available; Haiti, Sud, Morne Grand Bois, east slope; 18.374, -74.29661). ***Comptus badius.*** 1–2: SBH 194963–64 (Voucher not available; United States Caribbean, Navassa Island). ***Comptus maculatus.*** 1–5: ANSP 38507–11 (Cayman Islands, Cayman Brac, West End, Tiara Beach Hotel and surrounding area; 19.7192, -79.8263). 6: ANSP 38512 (Cayman Islands, Cayman Brac, 1.2 km E of West End; 19.698, -79.8696). 7: SBH 266526 (Voucher not available; Cayman Islands, Cayman Brac, 0.7 km E Hawkesbill Bay on A7, ~10 km E West End, 1.7 km E Ashton Reid Drive; 19.7142, -79.7864). ***Comptus stenurus.*** 1: ANSP 38546 (Haiti, Sud, Caye Madeline; 18.32419, -74.00949). 2–3: ANSP 38544–45 (Haiti, Sud, 8.6 km SW of Carretour Joute, near Riviere la Source on the Presquille de Port Salut; 18.07109, -73.89951). 4–5: SBH 269019–20 (Voucher not available; Haiti, Sud, Port Salut Gumbwa near Ça Vilason; 18.04923, -73.7887). 6: SBH 267494 (Voucher not available; Haiti, Sud, Île-à-Vache; 18.10379, -73.69400), 7: SBH 269017 (Voucher not available; Haiti, Sud, St. Jean, near Cabalice; 18.05023, -73.86208) 8–9: USNM 328837–38 (Haiti, Grand'Anse, between Rampe des Lions and Bois Sec, 6.5–1.5 km S and 0.1–4.5 km E Marche Leon; 18.50430, -74.0972). 10: USNM 328836 (Haiti, Grand'Anse, between Rampe des Lions and Bois Sec, 6.5–1.5 km S and 0.1–4.5 km E Marche Leon; 18.50430, -74.0972). ***Comptus weinlandi.*** 1: ANSP 38541 (Haiti, Nord'Ouest, Bombardopolis; 19.69135, -73.34209). 2: ANSP 38542 (Haiti, Artibonite, 11.8 km W of Ça Soleil; 19.46955, -72.77713). 3: ANSP 38547 (Dom. Rep., Independencia, 5.1 km NW of La Descubierta; 18.5711, -71.7549). 4: ANSP 38549 (Haiti, Ouest, 10.1 km ENE of Petionville, 18.51893, -72.20856). 5–7: ANSP 38551–52, 38554 (Haiti, Ouest, 18.7 km E of Thomaseau; 18.67476, -72.00285). 8: SBH 102918 (Voucher not available; Dom. Rep., Independencia, 1 km E Tierra Nueva; 18.58432, -71.89993). 9: SBH 102958 (Voucher not available; Locality not available). 10: SBH 191622 (Voucher not available; Haiti, Ouest, 18.7 km E of Thomaseau; 18.67476, -72.00285). 11–12: SBH 192406, 192408 (Voucher not available; Haiti, Artibonite, 11.8 km W of Ça Soleil; 19.46955, -72.77713). 13: SBH 192424 (Voucher not available; Haiti, Ouest, 10.1 km ENE of Petionville; 18.51893, -72.20856). 14–15: SBH 194492–93 (Voucher not available; Dom. Rep., Independencia, 5.1 km NW of La Descubierta; 18.57316, -71.75415). 16: USNM 328781 (Haiti, Ouest, Soliette; 18.43, -71.92). 17–20: SBH 266682–85 (Voucher not available; Dom. Rep., Independencia, La Zurza; 18.39965, -71.57266). 21: USNM 328808 (Dom. Rep., Barahona, 16 km ESE of Canoa; 18.3125, -71.0417). 22: MALT 00551 (Dom. Rep., Patio Americo, Guille Sanquitin). 23–26: ANSP 38516–19 (Dom. Rep., Hato Mayor, Loma del Fresca, 5.7 km airline SW of Sabana de la Mar; 18.27942, -71.40496). 27: ANSP 38524 (Dom. Rep., Hato Mayor, 7.8 km S of Sabana de la Mar; 18.9883, -69.38955). 28: ANSP 38528 (Dom. Rep., El Siebo, 5 km airline W of Sabana de Nisibon; 18.953, -68.8605). 29–30: ANSP 38529–30 (Dom. Rep., Duarte, 10.1 km NE of San Francisco de Macoris; 19.34473, -70.18077). 31–32: ANSP 38532–33 (Dom. Rep., Salcedo, 23.2 km N thence 4.5 km W of [= 0.2 km E Jaiba] Tenares; 19.5445, -70.3362). 33–35: ANSP 38534–35, 38537 (Dom. Rep., Los Tabucos, 8.8 km N thence 0.5 km W of Tenares; 19.4324, -70.3525). 36: SBH 267796 (Voucher not available; Dom. Rep., Hato Mayor, unnamed

beach near Cueva Infierno and Cueva del Angel; 19.08605, -69.50572). 37: SBH 267776 (Voucher not available; Dom. Rep., Hato Mayor, 14.1 km W El Valle; 19.00655, -69.48888). 38: USNM 328761 (Dom. Rep., Hato Mayor, ca. 15 km W of El Valle, on road to Trepada Alta; 18.9758, -69.5205). 39: USNM 328762 (Dom. Rep., Hato Mayor, 7 km E of Sabana de La Mar; 19.0314, -69.3264). 40–47: USNM 328812–19 (Dom. Rep., Hato Mayor, 1.7 km W of Sabana de la Mar; 19.0531, -69.4028), 48: USNM 328831 (Dom. Rep., Maria Trinidad Sanchez, 4 km SE of Nagua; 19.3481, -69.8244). 49: USNM 328832 (Dom. Rep., Samaná, 6 km SSW of Las Galeras; 19.2433, -69.2053). 50: USNM 328847 (Dom. Rep., Hato Mayor, 9.5 km W (airline) of Sabana de La Mar, in Los Haitises; 19.0606, -69.4758). ***Guarocuyus jaraguanus.*** 1–7: MNHNSD 23.3912–15, IIBZHER00001, IIBZHER00003–04 (Dom. Rep., Perdernales, Parque Nacional Jaragua, Laguna de Oviedo, Cayo de las Iguanas; 17.73205, -71.37126). ***Panolopus aporus.*** 1: MALT 00516 (Dom. Rep., P.N. Sierra de Bahoruco, Los Arroyos, frente a caseta; 18.25995, -71.74291). 2: MALT 00809 (Dom. Rep., Barahona, Paraíso, Cruce Platón-La Malanga). 3–4: ANSP 38624–25 (Dom. Rep., Pedernales, Bucan Detwi; 17.73462, -71.50335). 5–6: ANSP 38628–29 (Dom. Rep., Pedernales, Pedernales town, in palm grove; 18.029, -71.7471). 7: ANSP 38630 (Haiti, Sud-Est, Southeast of Pic La Selle; 18.32388, -72.0264). 8: ANSP 38631 (Haiti, Sud-Est, Southeast of Pic La Selle; 18.32887, -72.021842). 9: SBH 102611 (Voucher not available; Dom. Rep., Pedernales, 6.4 km SW, 0.7 km SE [road] of Juancho; 17.8358, -71.3439). 10: SBH 194833 (Voucher not available; Dom. Rep., Pedernales, Bucan Detwi; 17.73462, -71.50335). 11: SBH 266164 (Voucher not available; Dom. Rep., Barahona, ca. 2 km NW Paraiso; 18.00071, -71.18476). 12: SBH 269908 (Voucher not available; Haiti, Sud-Est, Southeast of Pic La Selle; 18.32388, -72.0264). 13–14: SBH 269910–11 (Voucher not available; Haiti, Sud-Est, Southeast of Pic La Selle; 18.32887, -72.021842). 15: USNM 328742 (Dom. Rep., Barahona, ca. 4–5 km S, 2.7 km W of Barahona, via coast road and road to Filipinas; 18.1619, -71.0967). 16: USNM 328743 (Dom. Rep., Barahona, ca. 4.5 km S, 4.0 km W of Barahona, via coast road and road to Filipinas; 18.1531, -71.1025). 17: USNM 328744 (Dom. Rep., Barahona, 15 km SSW of La Guazara; 18.1333, -71.1667). 18–20: USNM 328766–68 (Dom. Rep., Pedernales, Juancho; 17.8564, -71.295). 21–23: USNM 328770–72 (Dom. Rep., Pedernales, Los Arroyos; 18.2308, -71.7564). 24: USNM 328793 (Dom. Rep., Barahona, 11.3 km S of Barahona; 18.1267, -71.0731). 25–26: USNM 328799–800 (Dom. Rep., Pedernales, 6.4 km SW, 0.7 km SE [road] of Juancho; 17.8358, -71.3439). ***Panolopus costatus.*** 1: ANSP 38559 (Haiti, Grand'Anse, 17.0 km S of Beaumont; 18.38472, -73.87569). 2: ANSP 38560 (Haiti, Sud, 11.6 km NW of Les Anglais, on Morne Grand Bois; 18.37417, -74.29928). 3: ANSP 38561 (Haiti, Sud, ca. 1 km NE of Tiburon; 18.32913, -74.38797). 4: SBH 268974 (Voucher not available; Haiti, Sud, ca. 1km NE Tiburon; 18.32913, -74.38797). 5: SBH 269064 (Voucher not available; Haiti, Grand'Anse, 6.2 km E (source cacao) Ause D'Hainalt; 18.4887, -74.3815). 6: SBH 274063 (Voucher not available; Haiti, Nippes, Morne Bois Pangnol; 18.41869, -73.77512). 7: SBH 274477 (Voucher not available; Haiti, Sud, Morne Grand Bois; 18.37329, -74.29288). 8: USNM 328773 (Haiti, Grand'Anse, vicinity of Castillion; 18.52, -74.1). 9: USNM 328780 (Haiti, Grand'Anse, 3 km SW of Castillion; 18.4975, -74.1201). 10: ANSP 38558 (Haiti, Grand'Anse, Abricots [outskirts]; 18.64783, -74.30721). ***Panolopus curtissi.*** 1: ANSP 38632 (Dom. Rep., Independencia, 5.1 km NW of La Descubierta; 18.5711, -71.7549). 2: SBH 194494 (Voucher not available; Dom. Rep., 5.1 km NW of Independencia; 18.5711, -71.7549). 3: SBH 269302 (Voucher not available; Haiti, Ouest; 18.9343, -72.63568). 4: SBH 269305 (Voucher not available; Haiti, Artibonite; 18.94918, -72.66465). 5–7: ANSP 38633–35 (Haiti, Artibonite, Gonave; 18.91220, -73.05222). ***Panolopus diastatus.*** 1–4: ANSP 38643–46 (Haiti, Nord'Ouest, Mole St. Nicolas; 19.80583, -73.37556). 5: SBH 194603 (Voucher not available; Haiti, Nord'Ouest, Bombardopolis; 19.69135, -73.34209). ***Panolopus hylonomus.*** 1: SBH 267793 (Dom. Rep., Altagracia, ca. 2 km S of Juanillo). ***Panolopus lapierrae*** **sp. nov.** 1: ANSP 38578 (Haiti, Artibonite, Ça Soleil, 11.8 km W of; 19.46955, -72.77713). ***Panolopus leionotus.*** 1–3: ANSP 38562, 38564–65 (Dom. Rep., Baoruco, ca. 5 km N of Apolinar Perdomo; 18.593, -71.3979). 4: ANSP 38566 (Dom. Rep., 1.6 mi NNE El Azul San Juan; 18.717, -71.413). 5–6: ANSP 38567–68 (Dom. Rep., Baoruco, Loma Monte Bonito; 18.60139, -71.39056). 7–9: ANSP 38573–74, 38577 (Dom. Rep., Elias Pina, 0.6 km NE of Rosa de la Piedra; 18.77689, -71.7157). 10: SBH 194362 (Voucher not available; Dom. Rep., Baoruco, ca. 5 km N of Apolinar Perdomo; 18.593, -71.3979). 11: SBH 266313 (Dom. Rep., Elias Pina, 0.6 km NE of Rosa de la Piedra; 18.77689, -71.7157). 12–13: USNM 328752–53 (Dom. Rep., Elias Pina, 17 km N of Cacique Enriquillo; 18.7069, -71.7703). ***Panolopus marcanoi.*** 1–4: ANSP 38650–52, 38657 (Dom. Rep., Santiago, Valle de Bao; 19.0685, -71.0361). 5: ANSP 38648 (Dom. Rep., Santiago, La Lagunas; 19.1512, -71.0102). 6: ANSP 38649 (Dom. Rep., Santiago, Loma los Banaderos, east slope; 19.1177, -71.0362). ***Panolopus neiba.*** 1–3: USNM 328745, 328747–48 (Dom. Rep., Elias Pina, ca. 24 km N of Los Pinos; 18.6919, -71.78). 4–6: USNM 328749–51 (Dom. Rep., Elias Pina, ca. 27 km N of Los Pinos; 18.6994, -71.7694). 7: USNM 328746 (Dom.

Rep., Elias Pina, ca. 24 km N of Los Pinos; 18.6919, -71.78). 8: ANSP 38579 (Dom. Rep., Independencia, ca. 7 km W of Los Pinos by road; 18.60033, -71.80859). 9–11: USNM 328754–56 (Dom. Rep., Elias Pina, 17 km N of Cacique Enriquillo; 18.7069, -71.7703). 12: USNM 328765 (Dom. Rep., Independencia, 6.2 km N, 4.0 km W [airline] of Descubierta; 18.6241, -71.774). ***Panolopus nesobous.*** 1: ANSP 38582 (Haiti, Sud, 10.7 km WNW of Les Platons Citadel, Caye Michel previously called Caye Paul; 18.33160, -74.02244). 2–3: ANSP 38580–81 (Haiti, Sud, 10.7 km WNW of Les Platons Citadel, Caye Michel previously called Caye Paul; 18.33160, -74.02244). 4: ANSP 38583 (Haiti, Sud, Île-à-Vache; 18.10516, -73.69288). 5: SBH 269117 (Voucher not available; Haiti, Sud, Plaine Formon near Caye Michel; 18.32420, -74.025814). ***Panolopus oreistes.*** 1: ANSP 38585 (Haiti, Ouest, Berry; 18.30795, -72.25389). 2: SBH 268567 (Haiti, Ouest, 1.0 km SW of Berry; 18.30854, -72.72079). 3–7: ANSP 38598–602 (Dom. Rep., Pedernales, Casetta Dos, 22 km N of Aceitillar, by road on ridge of Sierra de Bahoruco; 18.2125, -71.53417). 8–9: ANSP 38607–08 (Haiti, Sud-Est, Morne D'Enfer, southwestern edge of plateau; 18.33005, -72.37095). 10: ANSP 38615 (Dom. Rep., Independencia, 23.9 km SE of Puerto Escondido; 18.21, -71.53). 11: SBH 269898 (Voucher not available; Haiti, Sud-Est, Morne D'Enfer, southwestern edge of plateau; 18.33005, -72.37095). 12: USNM 328792 (Haiti, Sud-Est, 9.5 km E of Jacmel; 18.22706, -72.44959). ***Panolopus semitaeniatus*** **sp. nov.** 1–4: ANSP 38569–72 (Haiti, Artibonite, Morne Boeuf; 19.07239, -72.25021). 5–7: SBH 269891–92, 269895 (Haiti, Artibonite, Morne Boeuf; 19.07239, -72.25021). ***Panolopus unicolor*** **sp. nov.** 1: ANSP 38647 (Dom. Rep., Peravia, Cruce de Ocoa, 14.8 N, 7.8 km SE on dirt road, at Martinez near La Palma; 18.46, -70.45). ***Sauresia agramma*** **sp. nov.** 1–4: ANSP 38685–88 (Haiti, Sud-Est, Morne D'Enfer, southwestern edge of plateau; 18.33005, -72.37095). ***Sauresia cayemitae*** **sp. nov.** 1–3: ANSP 38674–76 (Haiti, Grand'Anse, Grande Cayemite (waypoint 166); 18.63562, -73.75175). 4: SBH 274212 (Haiti, Grand'Anse, Grande Cayemite (waypoint 166); 18.63562, -73.75175). 5: ANSP 38673 (Haiti, Grand'Anse, Grande Cayemite (helipad-camp); 18.63316, -73.75524). 6: ANSP 38691 (Haiti, Grand'Anse, 5.0 km S of Pestel; 18.51329, -73.78463). ***Sauresia gracilis*** **sp. nov.** 1: USNM 328852 (Haiti, Sud, 10.3 km NW of Port Salut; 18.1419, -73.9711). ***Sauresia habichi.*** 1–2: ANSP 38681, 38683 (Haiti, Marche Leon, 8.0 km S of Grand'Anse; 18.51678, -74.08311). ***Sauresia manicula*** **sp. nov.** 1–2: ANSP 38667–68 (Haiti, Ouest, Berry; 18.30795, -72.25389). ***Sauresia pangnolae*** **sp. nov.** 1: ANSP 38690 (Haiti, Grand'Anse, 5.0 km S of Pestel; 18.47942, -73.78744). 2: ANSP 38684 (Haiti, Nippes, Morne Bois Pangnol; 18.41869, -73.77512). 3: ANSP 38663 (Haiti, Grand'Anse, 8.0 km SSW of Baraderes; 18.44032, -73.66756). 4: ANSP 38664 (Haiti, Grand'Anse, 8.0 km SSW of Baraderes; 18.44032, -73.66756). ***Sauresia sepsoides***: 1: SBH 267773 (Dom. Rep., Hato Mayor, 14.1 km W El Valle; 19.00655, -69.48888). 2–3: SBH 267780–81 (Dom. Rep., Parque Nacional Los Haitises, 1.2 km S Naranjo Arriba; 19.06667, -69.57127). 4: USNM 328846 (Dom. Rep., Hato Mayor, 9.5 km W (airline) of Sabana de La Mar, in Los Haitises; 19.0606, -69.4758). 5–6: USNM 328850–51 (Dom. Rep., Hato Mayor, ca. 15 km W of El Valle, on road to Trepada Alta; 18.9758, -69.5205). 7: ANSP 38678 (Dom. Rep., La Altagracia, 7.5 km W of La Zanga (at Rio Maimon); 18.8807, -68.7749). 8: ANSP 38666 (Dom. Rep., Duarte, Batez Piedra, on west side of Rio Pazabo, 19.06997, -69.90815). 9–11: ANSP 38670–72 (Dom. Rep., Sanchez Ramirez, 8.6 km NE of, thence 8.1 km east (=El Aguacate) Cotui; 19.1037, -70.0531). 12: ANSP 38680 (Dom. Rep., Monte Plata, 4.3 km N of Majagual; 19.07539, -69.82842). 13–15: ANSP 38706–08 (Dom. Rep., Los Tabucos, 8.8 km N, thence 0.5 km W (Salcedo) Tenares; 19.4324, -70.3525). 16: ANSP 38709 (Dom. Rep., Los Tabucos, 8.8 km N, thence 0.5 km W (Salcedo) Tenares; 19.4324, -70.3525). 17: SBH 193149 (Dom. Rep., Duarte, Southern slopes of Loma Quita Espuela; 19.3627, -70.15819). 18: SBH 266746 (Dom. Rep., Monte Plata, Los Limones, footpath N of town). 19–21: SBH 266748–50 (Dom. Rep., Monte Plata, 3 km S Los Limones). 22: SBH 266754 (Dom. Rep., Monte Plata, 6 km S Los Limones). 23–27: SBH 267754–58 (Dom. Rep., Monte Plata, ca. 1 km SW Los Limones; 19.01932, -69.73766). 28: BMNH 1946.8.29.29 (St. Domingo). ***Sauresia synoria*** **sp. nov.** 1: SBH 160343 (Dom. Rep., Pedernales 22 km N Pedernales, at Rio Mulito; 18.1544, -71.7581). ***Wetmorena agasepsoides.*** 1: ANSP 38711 (Dom. Rep., Pedernales, Bucan Detwi; 17.73462, -71.50335). 2: SBH 194660 (Dom. Rep., Pedernales, ca. 5 km SW of Los Tres Charcos, ca. 0.5 km NW Fondo de Paradise; 17.79667, -71.46667). 3: ANSP 38712 (Dom. Rep., Barahona, 0.3 km S, 13.5 km E (airline) Canoa; 18.3448, -71.032). 4: SBH 102690 (Dom Rep., Barahona, 3.0 km E of Canoa). ***Wetmorena haetiana.*** 1: ANSP 38718 (Haiti, Ouest, Berry; 18.30795, -72.25389). 2–5: ANSP 38719–22 (Haiti, Ouest, Morne Cardineau; 18.34615, -72.18256). 6: ANSP 38726 (Haiti, Ouest, Morne La Visite, Sink hole in P. La Visite next to ridge crest; 18.34737, -72.2835). 7–10: ANSP 38727, 38729, 38734, 38736 (Haiti, Sud-Est, Southeast of Pic La Selle; 18.32887, -72.02184). 11–16: ANSP 38728, 38730–33, 38735 (Haiti, Sud-Est, Southeast of Pic La Selle; 18.32887, -72.02184). 17: ANSP 38743 (Haiti, Ouest, southeast of Pic La Selle; 18.33225, -71.91447). 18: ANSP 38745 (Haiti, Ouest, Waterfall in Parc La Visite; 18.34014, -72.26983). 19: SBH 268542 (Haiti, Ouest, Morne Cardineau; 18.34615, -

72.18256). 20: SBH 268564 (Haiti, Ouest, Morne La Visite, Sink hole in P. La Visite next to ridge crest; 18.34737, -72.2835). ***Wetmorena mylica*.** 1: USNM 328862 (Dom. Rep., Barahona, 15.3 km S, 6.7 km E (road) of Cabral; 18.1094, -71.2292). 2: USNM 328889 (Dom. Rep., Barahona, ca. 2 km S of Tejunde, on N slope of Loma Pie de Palo; 18.1333, -71.1667). 3: USNM 328859 (Dom. Rep., Barahona, 15.3 km S, 6.7 km E (road) of Cabral; 18.1094, -71.2292). 4: USNM 328858 (Dom. Rep., Barahona, 15.3 km S, 6.7 km E (road) of Cabral; 18.1094, -71.2292). ***Wetmorena obscura* sp. nov.** 1–2: USNM 328904–05 (Haiti, Sud-Est, ca. 15 km W of Gros Cheval via logging roads, NE slope of Pic La Selle; 18.3367, -71.8686). ***Wetmorena orosaura* sp. nov.** 1: ANSP 38724 (Haiti, Sud-Est, Morne D'Enfer, southwestern edge of plateau; 18.330052, -72.37095). 2–5: ANSP 38723, 38725, SBH 269902–03 (Haiti, Sud-Est, Morne D'Enfer, southwestern edge of plateau; 18.33005, -72.37095). ***Wetmorena surda*.** 1: MALT 00801 (Sierra de Bahoruco, ESE Caseta Loma de Toro (Helipuerto); 18.28718, -71.71251). 2–4: SBH 266704–05, 266707 (Dom. Rep., Pedernales, N Los Arroyos; 18.2579, -71.7446). 5–6: ANSP 38749, SBH 192496 (Dom. Rep., Independencia, 23.9 km SE of Puerto Escondido; 18.21, -71.53). 7–9: USNM 328897, 328899–900 (Dom. Rep., Pedernales, 10.3 km S of El Aguacate, on Haitian border road; 18.2897, -71.7111).

			Genbank Accession Number		
Species	**Laboratory Number**	**Specimen Voucher**	**CytB**	**ND2**	**12s**
Caribicus darlingtoni 1	SBH 161686	USNM 328805	PP566315	PP557047	PP599887
Caribicus darlingtoni 2	SBH 161687	USNM 328806	MW824662	MW824717	MW824918
Caribicus darlingtoni 3	SBH 161688	USNM 328807	PP566316	PP557048	PP599888
Caribicus warreni 1	SBH 194521	Voucher not available	MW824663	MW824718	MW824910
Caribicus warreni 2	SBH 172914	ANSP 38501	PP566317	PP557049	PP599889
Celestus barbouri 1	SBH 190678	ANSP 38503	PP566320	Na	Na
Celestus barbouri 2	SBH 161122	USNM 328153	MW824664	MW824719	MW824914
Celestus capitulatus ***sp. nov.*** *1*	SBH 103448	USNM 328168	PP566329	PP557058	PP599891
Celestus capitulatus ***sp. nov.*** *2*	SBH 103449	USNM 328169	MW824668	MW824723	Na
Celestus capitulatus ***sp. nov.*** *3*	SBH 172440	USNM 328157	PP566340	PP557069	Na
Celestus crusculus 1	SBH 172439	USNM 328159	PP566339	PP557068	PP599900
Celestus crusculus 2	SBH 161123	USNM 328160	MW824667	MW824722	Na
Celestus crusculus 3	SBH 101577	USNM 328166	PP566326	PP557056	Na
Celestus crusculus 4	SBH 101578	USNM 328167	PP566327	PP557057	Na
Celestus crusculus 5	SBH 190695	ANSP 38504	PP566342	PP557071	Na
Celestus crusculus 6	SBH 171607	USNM 328186	PP566338	PP557067	PP599899
Celestus duquesneyi 1	SBH 267952	Voucher not available	MW824672	MW824727	MW824913
Celestus hesperius ***sp. nov.*** *1*	SBH 101572	USNM 328154	MW824665	MW824720	MW824915
Celestus hesperius ***sp. nov.*** *2*	SBH 101573	USNM 328155	PP566325	PP557055	PP599890
Celestus hesperius ***sp. nov.*** *3*	SBH 101554	USNM 328156	PP566323	PP557054	Na
Celestus hewardi 1	SBH 267097	Voucher not available	MW824673	MW824728	MW824912
Celestus jamesbondi ***sp. nov.*** *1*	SBH 103586	USNM 328170	PP566330	PP557059	PP599892
Celestus jamesbondi ***sp. nov.*** *2*	SBH 171439	Voucher not available	PP566332	PP557061	PP599894
Celestus jamesbondi ***sp. nov.*** *3*	SBH 274324	Voucher not available	PP566343	Na	Na
Celestus jamesbondi ***sp. nov.*** *4*	SBH 101570	USNM 328172	PP566324	Na	Na
Celestus jamesbondi ***sp. nov.*** *5*	SBH 101615	USNM 328173	PP566328	Na	Na
Celestus jamesbondi ***sp. nov.*** *6*	SBH 172438	USNM 328174	MW824669	MW824724	Na
Celestus jamesbondi ***sp. nov.*** *7*	SBH 171606	USNM 328175	PP566337	PP557066	PP599898
Celestus jamesbondi ***sp. nov.*** *8*	SBH 161124	USNM 328176	PP566331	PP557060	PP599893
Celestus jamesbondi ***sp. nov.*** *9*	SBH 172442	USNM 328177	PP566341	PP557070	PP599901
Celestus jamesbondi ***sp. nov.*** *10*	SBH 171601	USNM 328180	PP566333	PP557062	PP599895
Celestus jamesbondi ***sp. nov.*** *11*	SBH 171603	USNM 328182	PP566334	PP557063	PP599896
Celestus jamesbondi ***sp. nov.*** *12*	SBH 171604	USNM 328183	PP566335	PP557064	PP599897

Celestus jamesbondi ***sp. nov.*** *13*	SBH 171605	USNM 328184	PP566336	PP557065	Na
Celestus macrolepis 1	Na	BMNH 1946.8.3.82	See above	PP557075	Na
Celestus macrotus 1	Na	MALT 00796	PP566318	PP557050	Na
Celestus macrotus 2	Na	MALT 00799	PP566319	PP557051	Na
Celestus macrotus 3	SBH 269438	Voucher not available	PP566347	PP557076	Na
Celestus macrotus 4	SBH 269912	ANSP 38505	PP566348	PP557077	PP599902
Celestus macrotus 5	SBH 269931	ANSP 38506	MW824674	MW824729	Na
Celestus molesworthi 1	SBH 172465	USNM 328144	MW824671	MW824726	Na
Celestus molesworthi 2	SBH 274634	Voucher not available	PP566344	PP557072	Na
Celestus molesworthi 3	SBH 274632	Voucher not available	MW824670	MW824725	Na
Celestus occiduus 1	Na	BMNH XV.115.A	PP566350	PP557079	Na
Celestus occiduus 2	Na	MNHN 0.2855	PP566349	PP557078	Na
Celestus oligolepis ***sp. nov.*** *1*	SBH 172441	USNM 328158	MW824666	MW824721	Na
Celestus striatus 1	Na	BMNH 1946.8.8.3	PP566351	PP557080	Na
Celestus striatus 2	Na	MCZ R-125601	PP566345	PP557073	Na
Comptus alloeides 1	SBH 103083	USNM 328830	MW824677	MW824731	MW824919
Comptus arboreus ***sp. nov.*** *1*	SBH 269043	ANSP 38538	PP566360	PP557087	PP599907
Comptus arboreus ***sp. nov.*** *2*	SBH 269044	ANSP 38539	PP566361	PP557088	PP599908
Comptus arboreus ***sp. nov.*** *3*	SBH 269045	ANSP 38540	MW824678	MW824732	Na
Comptus arboreus ***sp. nov.*** *4*	SBH 191945	Voucher not available	PP566359	Na	Na
Comptus arboreus ***sp. nov.*** *5*	SBH 269065	Voucher not available	PP566363	PP557090	PP599910
Comptus arboreus ***sp. nov.*** *6*	SBH 269047	ANSP 38543	PP566362	PP557089	PP599909
Comptus arboreus ***sp. nov.*** *7*	SBH 274478	Voucher not available	PP566364	Na	Na
Comptus badius 1	SBH 194963	Voucher not available	PP566352	PP557081	Na
Comptus badius 2	SBH 194964	Voucher not available	MW824675	MW824730	MW824911
Comptus maculatus 1	SBH 266527	ANSP 38507	MW824676	Na	MW824899
Comptus maculatus 2	SBH 266550	ANSP 38508	PP566355	PP557083	PP599903
Comptus maculatus 3	SBH 266551	ANSP 38509	PP566356	PP557084	PP599904
Comptus maculatus 4	SBH 266552	ANSP 38510	PP566357	PP557085	PP599905
Comptus maculatus 5	SBH 266553	ANSP 38511	PP566358	PP557086	PP599906
Comptus maculatus 6	SBH 266528	ANSP 38512	PP566354	PP557082	Na
Comptus maculatus 7	SBH 266526	Voucher not available	PP566353	Na	Na
Comptus stenurus 1	SBH 269100	ANSP 38546	PP566401	Na	Na
Comptus stenurus 2	SBH 192253	ANSP 38544	PP566395	PP557115	Na
Comptus stenurus 3	SBH 192254	ANSP 38545	PP566396	PP557116	Na
Comptus stenurus 4	SBH 269019	Voucher not available	PP566399	Na	Na
Comptus stenurus 5	SBH 269020	Voucher not available	PP566400	PP557119	PP599919
Comptus stenurus 6	SBH 267494	Voucher not available	PP566397	PP557117	Na
Comptus stenurus 7	SBH 269017	Voucher not available	PP566398	PP557118	PP599918
Comptus stenurus 8	SBH 103901	USNM 328837	PP566393	PP557112	Na
Comptus stenurus 9	SBH 103902	USNM 328838	PP566394	PP557114	Na
Comptus stenurus 10	SBH 103900	USNM 328836	MW824679	MW824733	Na
Comptus weinlandi 1	SBH 194610	ANSP 38541	PP566417	Na	Na
Comptus weinlandi 2	SBH 192405	ANSP 38542	PP566409	PP557124	PP599923
Comptus weinlandi 3	SBH 194504	ANSP 38547	PP566416	PP557131	Na
Comptus weinlandi 4	SBH 192423	ANSP 38549	PP566412	PP557127	Na

Comptus weinlandi 5	SBH 191591	ANSP 38551	PP566405	PP557122	PP599921
Comptus weinlandi 6	SBH 191592	ANSP 38552	PP566406	Na	Na
Comptus weinlandi 7	SBH 191594	ANSP 38554	PP566407	Na	Na
Comptus weinlandi 8	SBH 102918	Voucher not available	PP566402	Na	Na
Comptus weinlandi 9	SBH 102958	Voucher not available	PP566403	PP557120	Na
Comptus weinlandi 10	SBH 191622	Voucher not available	PP566408	PP557123	PP599922
Comptus weinlandi 11	SBH 192406	Voucher not available	PP566410	PP557125	Na
Comptus weinlandi 12	SBH 192408	Voucher not available	PP566411	PP557126	Na
Comptus weinlandi 13	SBH 192424	Voucher not available	PP566413	PP557128	Na
Comptus weinlandi 14	SBH 194492	Voucher not available	PP566414	PP557129	Na
Comptus weinlandi 15	SBH 194493	Voucher not available	PP566415	PP557130	Na
Comptus weinlandi 16	SBH 103607	USNM 328781	PP566404	PP557121	PP599920
Comptus weinlandi 17	SBH 266682	Voucher not available	PP566418	PP557132	PP599924
Comptus weinlandi 18	SBH 266683	Voucher not available	PP566419	PP557133	PP599925
Comptus weinlandi 19	SBH 266684	Voucher not available	PP566420	PP557134	Na
Comptus weinlandi 20	SBH 266685	Voucher not available	PP566421	PP557135	Na
Comptus weinlandi 21	SBH 102712	USNM 328808	MW824680	MW824734	Na
Comptus weinlandi 22	Na	MALT 00551	PP566322	PP557053	Na
Comptus weinlandi 23	SBH 266999	ANSP 38516	PP566386	Na	Na
Comptus weinlandi 24	SBH 267000	ANSP 38517	PP566387	PP557109	Na
Comptus weinlandi 25	SBH 267002	ANSP 38518	PP566388	PP557110	Na
Comptus weinlandi 26	SBH 267003	ANSP 38519	PP566389	PP557111	Na
Comptus weinlandi 27	SBH 266951	ANSP 38524	PP566385	Na	Na
Comptus weinlandi 28	SBH 267065	ANSP 38528	PP566390	Na	Na
Comptus weinlandi 29	SBH 193191	ANSP 38529	PP566378	PP557103	PP599913
Comptus weinlandi 30	SBH 193192	ANSP 38530	PP566379	PP557104	PP599914
Comptus weinlandi 31	SBH 193216	ANSP 38532	PP566383	Na	PP599916
Comptus weinlandi 32	SBH 193217	ANSP 38533	PP566384	PP557108	PP599917
Comptus weinlandi 33	SBH 193197	ANSP 38534	PP566380	PP557105	PP599915
Comptus weinlandi 34	SBH 193198	ANSP 38535	PP566381	PP557106	Na
Comptus weinlandi 35	SBH 193200	ANSP 38537	PP566382	PP557107	Na
Comptus weinlandi 36	SBH 267796	Voucher not available	PP566392	PP557113	Na
Comptus weinlandi 37	SBH 267776	Voucher not available	PP566391	Na	Na
Comptus weinlandi 38	SBH 102371	USNM 328761	PP566373	Na	Na
Comptus weinlandi 39	SBH 102388	USNM 328762	PP566374	PP557099	Na
Comptus weinlandi 40	SBH 101247	USNM 328812	PP566365	PP557091	Na
Comptus weinlandi 41	SBH 101248	USNM 328813	PP566366	PP557092	Na
Comptus weinlandi 42	SBH 101249	USNM 328814	PP566367	PP557093	Na
Comptus weinlandi 43	SBH 101250	USNM 328815	PP566368	PP557094	Na
Comptus weinlandi 44	SBH 101251	USNM 328816	PP566369	PP557095	Na
Comptus weinlandi 45	SBH 101252	USNM 328817	PP566370	PP557096	Na
Comptus weinlandi 46	SBH 101253	USNM 328818	PP566371	PP557097	Na
Comptus weinlandi 47	SBH 101254	USNM 328819	PP566372	PP557098	Na
Comptus weinlandi 48	SBH 103084	USNM 328831	PP566377	PP557102	PP599912
Comptus weinlandi 49	SBH 103075	USNM 328832	PP566376	PP557101	PP599911
Comptus weinlandi 50	SBH 102389	USNM 328847	PP566375	PP557100	Na

Guarocuyus jaraguanus 1	Na	MNHNSD 23.3912	OP413939	OP413932	OP413939
Guarocuyus jaraguanus 2	Na	MNHNSD 23.3913	OP413938	OP413931	OP413910
Guarocuyus jaraguanus 3	Na	MNHNSD 23.3914	OP413937	OP413930	OP413909
Guarocuyus jaraguanus 4	Na	MNHNSD 23.3915	OP413940	OP413934	OP413913
Guarocuyus jaraguanus 5	Na	IIBZHER00001	Na	OP413933	OP413912
Guarocuyus jaraguanus 6	Na	IIBZHER00003	OP413936	OP413929	OP413908
Guarocuyus jaraguanus 7	Na	IIBZHER00004	OP413935	OP413928	OP413907
Panolopus aporus 1	Na	MALT 00516	PP566321	PP557052	Na
Panolopus aporus 2	Na	MALT 00809	Na	See above	Na
Panolopus aporus 3	SBH 194832	ANSP 38624	PP566495	PP557170	Na
Panolopus aporus 4	SBH 194838	ANSP 38625	PP566497	PP557172	Na
Panolopus aporus 5	SBH 267509	ANSP 38628	PP566498	Na	Na
Panolopus aporus 6	SBH 267510	ANSP 38629	PP566499	Na	Na
Panolopus aporus 7	SBH 269907	ANSP 38630	PP566500	PP557173	PP599954
Panolopus aporus 8	SBH 269909	ANSP 38631	PP566502	PP557175	PP599956
Panolopus aporus 9	SBH 102611	Voucher not available	PP566484	PP557163	Na
Panolopus aporus 10	SBH 194833	Voucher not available	PP566496	PP557171	Na
Panolopus aporus 11	SBH 266164	Voucher not available	PP566422	Na	Na
Panolopus aporus 12	SBH 269908	Voucher not available	PP566501	PP557174	PP599955
Panolopus aporus 13	SBH 269910	Voucher not available	PP566503	PP557176	PP599957
Panolopus aporus 14	SBH 269911	Voucher not available	PP566504	PP557177	PP599958
Panolopus aporus 15	SBH 102716	USNM 328742	PP566489	PP557167	Na
Panolopus aporus 16	SBH 102706	USNM 328743	PP566485	PP557164	Na
Panolopus aporus 17	SBH 160291	USNM 328744	PP566494	Na	Na
Panolopus aporus 18	SBH 102707	USNM 328766	PP566486	PP557165	PP599952
Panolopus aporus 19	SBH 102708	USNM 328767	PP566487	Na	Na
Panolopus aporus 20	SBH 102709	USNM 328768	PP566488	PP557166	PP599953
Panolopus aporus 21	SBH 102914	USNM 328770	PP566490	PP557168	Na
Panolopus aporus 22	SBH 102915	USNM 328771	PP566491	Na	Na
Panolopus aporus 23	SBH 102916	USNM 328772	PP566492	Na	Na
Panolopus aporus 24	SBH 102930	USNM 328793	PP566493	PP557169	Na
Panolopus aporus 25	SBH 102609	USNM 328799	PP566483	PP557162	Na
Panolopus aporus 26	SBH 102610	USNM 328800	MW824699	MW824746	MW824917
Panolopus costatus 1	SBH 192260	ANSP 38559	PP566431	PP557143	PP599934
Panolopus costatus 2	SBH 269458	ANSP 38560	PP566435	Na	PP599937
Panolopus costatus 3	SBH 268996	ANSP 38561	PP566433	PP557145	PP599936
Panolopus costatus 4	SBH 268974	Voucher not available	PP566432	PP557144	PP599935
Panolopus costatus 5	SBH 269064	Voucher not available	PP566434	Na	Na
Panolopus costatus 6	SBH 274063	Voucher not available	PP566436	Na	Na
Panolopus costatus 7	SBH 274477	Voucher not available	PP566437	Na	Na
Panolopus costatus 8	SBH 103805	USNM 328773	PP566429	PP557141	PP599932
Panolopus costatus 9	SBH 104113	USNM 328780	PP566430	PP557142	PP599933
Panolopus costatus 10	SBH 192054	ANSP 38558	MW824693	MW824740	MW824901
Panolopus curtissi 1	SBH 194503	ANSP 38632	MW824700	MW824747	Na
Panolopus curtissi 2	SBH 194494	Voucher not available	PP566477	Na	Na
Panolopus curtissi 3	SBH 269302	Voucher not available	PP566478	Na	Na

Panolopus curtissi 4	SBH 269305	Voucher not available	PP566479	Na	Na
Panolopus curtissi 5	SBH 269339	ANSP 38633	PP566480	Na	Na
Panolopus curtissi 6	SBH 269347	ANSP 38634	PP566481	PP557160	Na
Panolopus curtissi 7	SBH 269348	ANSP 38635	PP566482	PP557161	PP599951
Panolopus diastatus 1	SBH 194553	ANSP 38643	PP566505	PP557178	PP599959
Panolopus diastatus 2	SBH 194554	ANSP 38644	PP566506	Na	Na
Panolopus diastatus 3	SBH 194555	ANSP 38645	PP566507	Na	Na
Panolopus diastatus 4	SBH 194580	ANSP 38646	MW824701	MW824748	Na
Panolopus diastatus 5	SBH 194603	Voucher not available	PP566508	Na	Na
Panolopus hylonomus 1	SBH 267793	Voucher not available	PP566509	Na	Na
Panolopus lapierrae ***sp. nov.*** *1*	SBH 192428	ANSP 38578	MW824696	MW824743	MW824902
Panolopus leionotus 1	SBH 194363	ANSP 38562	PP566452	PP557151	PP599943
Panolopus leionotus 2	SBH 194365	ANSP 38564	PP566453	Na	Na
Panolopus leionotus 3	SBH 194391	ANSP 38565	PP566456	Na	Na
Panolopus leionotus 4	SBH 266286	ANSP 38566	MW824694	MW824741	Na
Panolopus leionotus 5	SBH 194366	ANSP 38567	PP566454	Na	Na
Panolopus leionotus 6	SBH 194367	ANSP 38568	PP566455	Na	Na
Panolopus leionotus 7	SBH 266312	ANSP 38573	PP566457	Na	Na
Panolopus leionotus 8	SBH 266314	ANSP 38574	PP566459	Na	Na
Panolopus leionotus 9	SBH 266321	ANSP 38577	PP566460	PP557152	PP599944
Panolopus leionotus 10	SBH 194362	Voucher not available	PP566451	PP557150	PP599942
Panolopus leionotus 11	SBH 266313	Voucher not available	PP566458	Na	Na
Panolopus leionotus 12	SBH 161498	USNM 328752	PP566446	Na	Na
Panolopus leionotus 13	SBH 161499	USNM 328753	PP566447	Na	Na
Panolopus marcanoi 1	SBH 193279	ANSP 38650	PP566510	PP557179	PP599960
Panolopus marcanoi 2	SBH 193280	ANSP 38651	PP566511	PP557180	PP599961
Panolopus marcanoi 3	SBH 193281	ANSP 38652	PP566512	Na	Na
Panolopus marcanoi 4	SBH 193286	ANSP 38657	MW824703	MW824749	MW824903
Panolopus marcanoi 5	SBH 193309	ANSP 38648	PP566513	PP557181	PP599962
Panolopus marcanoi 6	SBH 193323	ANSP 38649	PP566514	Na	Na
Panolopus neiba 1	SBH 102923	USNM 328745	PP566439	PP557147	PP599939
Panolopus neiba 2	SBH 102925	USNM 328747	PP566441	PP557149	PP599941
Panolopus neiba 3	SBH 102926	USNM 328748	PP566442	Na	Na
Panolopus neiba 4	SBH 102927	USNM 328749	PP566443	Na	Na
Panolopus neiba 5	SBH 102928	USNM 328750	PP566444	Na	Na
Panolopus neiba 6	SBH 102929	USNM 328751	PP566445	Na	Na
Panolopus neiba 7	SBH 102924	USNM 328746	PP566440	PP557148	PP599940
Panolopus neiba 8	SBH 267615	ANSP 38579	PP566461	Na	Na
Panolopus neiba 9	SBH 161500	USNM 328754	PP566448	Na	Na
Panolopus neiba 10	SBH 161501	USNM 328755	PP566449	Na	Na
Panolopus neiba 11	SBH 161502	USNM 328756	PP566450	Na	Na
Panolopus neiba 12	SBH 102922	USNM 328765	PP566438	PP557146	PP599938
Panolopus nesobous 1	SBH 192263	ANSP 38582	PP566464	Na	Na
Panolopus nesobous 2	SBH 192261	ANSP 38580	PP566462	PP557153	PP599945
Panolopus nesobous 3	SBH 192262	ANSP 38581	PP566463	PP557154	PP599946
Panolopus nesobous 4	SBH 269457	ANSP 38583	MW824697	MW824744	Na

Panolopus nesobous 5	SBH 269117	Voucher not available	PP566465	Na	Na
Panolopus oreistes 1	SBH 268573	ANSP 38585	PP566473	Na	PP599947
Panolopus oreistes 2	SBH 268567	Voucher not available	PP566472	Na	Na
Panolopus oreistes 3	SBH 267554	ANSP 38598	PP566467	Na	Na
Panolopus oreistes 4	SBH 267555	ANSP 38599	PP566468	Na	Na
Panolopus oreistes 5	SBH 267556	ANSP 38600	PP566469	Na	Na
Panolopus oreistes 6	SBH 267557	ANSP 38601	PP566470	Na	Na
Panolopus oreistes 7	SBH 267558	ANSP 38602	PP566471	Na	Na
Panolopus oreistes 8	SBH 269896	ANSP 38607	PP566474	PP557157	PP599948
Panolopus oreistes 9	SBH 269897	ANSP 38608	PP566475	PP557158	PP599949
Panolopus oreistes 10	SBH 192480	ANSP 38615	PP566466	PP557155	Na
Panolopus oreistes 11	SBH 269898	Voucher not available	PP566476	PP557159	PP599950
Panolopus oreistes 12	SBH 104408	USNM 328792	MW824698	MW824745	MW824916
Panolopus semitaeniatus ***sp. nov.*** *1*	SBH 269889	ANSP 38569	PP566423	Na	PP599926
Panolopus semitaeniatus ***sp. nov.*** *2*	SBH 269890	ANSP 38570	MW824695	MW824742	Na
Panolopus semitaeniatus ***sp. nov.*** *3*	SBH 269893	ANSP 38571	PP566426	PP557138	PP599929
Panolopus semitaeniatus ***sp. nov.*** *4*	SBH 269894	ANSP 38572	PP566427	PP557139	PP599930
Panolopus semitaeniatus ***sp. nov.*** *5*	SBH 269891	Voucher not available	PP566424	PP557136	PP599927
Panolopus semitaeniatus ***sp. nov.*** *6*	SBH 269892	Voucher not available	PP566425	PP557137	PP599928
Panolopus semitaeniatus ***sp. nov.*** *7*	SBH 269895	Voucher not available	PP566428	PP557140	PP599931
Panolopus unicolor ***sp. nov.*** *1*	SBH 193037	ANSP 38647	MW824702	Na	Na
Sauresia agramma ***sp. nov.*** *1*	SBH 269778	ANSP 38685	PP566550	PP557156	Na
Sauresia agramma ***sp. nov.*** *2*	SBH 269899	ANSP 38686	PP566551	Na	PP599965
Sauresia agramma ***sp. nov.*** *3*	SBH 269900	ANSP 38687	PP566552	Na	PP599966
Sauresia agramma ***sp. nov.*** *4*	SBH 269901	ANSP 38688	PP566553	Na	PP599967
Sauresia cayemitae ***sp. nov.*** *1*	SBH 274113	ANSP 38674	PP566555	Na	Na
Sauresia cayemitae ***sp. nov.*** *2*	SBH 274211	ANSP 38675	MW824705	MW824752	Na
Sauresia cayemitae ***sp. nov.*** *3*	SBH 274224	ANSP 38676	PP566557	PP557215	Na
Sauresia cayemitae ***sp. nov.*** *4*	SBH 274212	Voucher not available	PP566556	PP557214	Na
Sauresia cayemitae ***sp. nov.*** *5*	SBH 274050	ANSP 38673	PP566554	PP557213	Na
Sauresia cayemitae ***sp. nov.*** *6*	SBH 191850	ANSP 38691	PP566520	PP557185	Na
Sauresia gracilis ***sp. nov.*** *1*	SBH 103643	USNM 328852	PP566518	PP557184	Na
Sauresia habichi 1	SBH 191913	ANSP 38681	PP566522	PP557187	PP599963
Sauresia habichi 2	SBH 191915	ANSP 38683	PP566523	PP557188	PP599964
Sauresia manicula ***sp. nov.*** *1*	SBH 268585	ANSP 38667	MW824704	MW824751	Na
Sauresia manicula ***sp. nov.*** *2*	SBH 268586	ANSP 38668	PP566549	PP557212	Na
Sauresia pangnolae ***sp. nov.*** *1*	SBH 191851	ANSP 38690	PP566521	PP557186	Na
Sauresia pangnolae ***sp. nov.*** *2*	SBH 274213	ANSP 38684	MW824706	MW824753	Na
Sauresia pangnolae ***sp. nov.*** *3*	SBH 192312	ANSP 38663	PP566515	Na	Na
Sauresia pangnolae ***sp. nov.*** *4*	SBH 192313	ANSP 38664	PP566524	PP557189	Na
Sauresia sepsoides 1	SBH 267773	Voucher not available	PP566546	PP557209	Na
Sauresia sepsoides 2	SBH 267780	Voucher not available	PP566547	PP557210	Na
Sauresia sepsoides 3	SBH 267781	Voucher not available	PP566548	PP557211	Na
Sauresia sepsoides 4	SBH 102369	USNM 328846	MW824707	MW824754	MW824920
Sauresia sepsoides 5	SBH 102383	USNM 328850	PP566516	PP557182	Na
Sauresia sepsoides 6	SBH 102384	USNM 328851	PP566517	PP557183	Na

Sauresia sepsoides 7	SBH 192469	ANSP 38678	PP566525	PP557190	Na
Sauresia sepsoides 8	SBH 193093	ANSP 38666	PP566529	PP557194	Na
Sauresia sepsoides 9	SBH 193040	ANSP 38670	PP566526	PP55719	Na
Sauresia sepsoides 10	SBH 193041	ANSP 38671	PP566527	PP557192	Na
Sauresia sepsoides 11	SBH 193042	ANSP 38672	PP566528	PP557193	Na
Sauresia sepsoides 12	SBH 193116	ANSP 38680	PP566530	PP557195	Na
Sauresia sepsoides 13	SBH 193201	ANSP 38706	PP566532	PP557197	Na
Sauresia sepsoides 14	SBH 193202	ANSP 38707	PP566533	PP557198	Na
Sauresia sepsoides 15	SBH 193203	ANSP 38708	PP566534	PP557199	Na
Sauresia sepsoides 16	SBH 193204	ANSP 38709	PP566535	PP557200	Na
Sauresia sepsoides 17	SBH 193149	Voucher not available	PP566531	PP557196	Na
Sauresia sepsoides 18	SBH 266746	Voucher not available	PP566536	PP557201	Na
Sauresia sepsoides 19	SBH 266748	Voucher not available	PP566537	Na	Na
Sauresia sepsoides 20	SBH 266749	Voucher not available	PP566538	PP557202	Na
Sauresia sepsoides 21	SBH 266750	Voucher not available	PP566539	PP557203	Na
Sauresia sepsoides 22	SBH 266754	Voucher not available	PP566540	PP557204	Na
Sauresia sepsoides 23	SBH 267754	Voucher not available	PP566541	PP557205	Na
Sauresia sepsoides 24	SBH 267755	Voucher not available	PP566542	PP557206	Na
Sauresia sepsoides 25	SBH 267756	Voucher not available	PP566543	PP557207	Na
Sauresia sepsoides 26	SBH 267757	Voucher not available	PP566544	PP557208	Na
Sauresia sepsoides 27	SBH 267758	Voucher not available	PP566545	Na	Na
Sauresia sepsoides 28	Na	BMNH 1946.8.29.29	See above	PP557216	Na
Sauresia synoria ***sp. nov.*** *1*	SBH 160343	Voucher not available	PP566519	Na	Na
Wetmorena agasepsoides 1	SBH 194830	ANSP 38711	PP566560	Na	PP599968
Wetmorena agasepsoides 2	SBH 194660	Voucher not available	PP566559	Na	Na
Wetmorena agasepsoides 3	SBH 160191	ANSP 38712	MW824713	MW824756	MW824904
Wetmorena agasepsoides 4	SBH 102690	Voucher not available	PP566558	Na	Na
Wetmorena haetiana 1	SBH 268593	ANSP 38718	PP566568	PP557224	PP599971
Wetmorena haetiana 2	SBH 268538	ANSP 38719	PP566561	PP557217	PP599969
Wetmorena haetiana 3	SBH 268539	ANSP 38720	PP566562	PP557218	Na
Wetmorena haetiana 4	SBH 268540	ANSP 38721	PP566563	PP557219	Na
Wetmorena haetiana 5	SBH 268541	ANSP 38722	PP566564	PP557220	Na
Wetmorena haetiana 6	SBH 268563	ANSP 38726	PP566566	PP557222	PP599970
Wetmorena haetiana 7	SBH 269913	ANSP 38727	PP566574	PP557229	PP599977
Wetmorena haetiana 8	SBH 269915	ANSP 38729	PP566576	PP557231	PP599979
Wetmorena haetiana 9	SBH 269920	ANSP 38734	PP566581	Na	PP599984
Wetmorena haetiana 10	SBH 269922	ANSP 38736	PP566583	PP557236	PP599986
Wetmorena haetiana 11	SBH 269914	ANSP 38728	PP566575	PP557230	PP599978
Wetmorena haetiana 12	SBH 269916	ANSP 38730	PP566577	PP557232	PP599980
Wetmorena haetiana 13	SBH 269917	ANSP 38731	PP566578	Na	PP599981
Wetmorena haetiana 14	SBH 269918	ANSP 38732	PP566579	PP557233	PP599982
Wetmorena haetiana 15	SBH 269919	ANSP 38733	PP566580	PP557234	PP599983
Wetmorena haetiana 16	SBH 269921	ANSP 38735	PP566582	PP557235	PP599985
Wetmorena haetiana 17	SBH 269932	ANSP 38743	PP566584	PP557237	PP599987
Wetmorena haetiana 18	SBH 268568	ANSP 38745	MW824714	MW824757	Na
Wetmorena haetiana 19	SBH 268542	Voucher not available	PP566565	PP557221	Na

Wetmorena haetiana 20	SBH 268564	Voucher not available	PP566567	PP557223	Na
Wetmorena mylica 1	SBH 102550	USNM 328862	PP566586	PP557239	PP599989
Wetmorena mylica 2	SBH 160201	USNM 328889	PP566587	PP557240	PP599990
Wetmorena mylica 3	SBH 102547	USNM 328859	PP566585	PP557238	PP599988
Wetmorena mylica 4	SBH 102546	USNM 328858	MW824715	MW824758	MW824921
Wetmorena obscura ***sp. nov.*** *1*	SBH 104418	USNM 328904	PP566590	PP557243	PP599991
Wetmorena obscura ***sp. nov.*** *2*	SBH 104419	USNM 328905	PP566591	PP557244	PP599992
Wetmorena orosaura ***sp. nov.*** *1*	SBH 269905	ANSP 38724	PP566572	Na	PP599975
Wetmorena orosaura ***sp. nov.*** *2*	SBH 269904	ANSP 38723	PP566571	PP557227	PP599974
Wetmorena orosaura ***sp. nov.*** *3*	SBH 269906	ANSP 38725	PP566573	PP557228	PP599976
Wetmorena orosaura ***sp. nov.*** *4*	SBH 269902	Voucher not available	PP566569	PP557225	PP599972
Wetmorena orosaura ***sp. nov.*** *5*	SBH 269903	Voucher not available	PP566570	PP557226	PP599973
Wetmorena surda 1	Na	MALT 00801	PP566346	PP557074	Na
Wetmorena surda 2	SBH 266704	Voucher not available	PP566594	PP557246	Na
Wetmorena surda 3	SBH 266705	Voucher not available	PP566595	Na	Na
Wetmorena surda 4	SBH 266707	Voucher not available	PP566596	PP557247	Na
Wetmorena surda 5	SBH 192486	ANSP 38749	PP566592	PP557245	Na
Wetmorena surda 6	SBH 192496	Voucher not available	PP566593	Na	Na
Wetmorena surda 7	SBH 101404	USNM 328897	PP566588	PP557241	Na
Wetmorena surda 8	SBH 101406	USNM 328899	MW824716	MW824759	Na
Wetmorena surda 9	SBH 101407	USNM 328900	PP566589	PP557242	Na

APPENDIX 2. Specimens used in the morphological analyses.

Caribicus anelpistus (n=8). KU 227505–11 (Dom. Rep., San Cristobal, Villa Altagracia, Ingenio Catarey, 'Come Hombre'; 18.66667, -70.16666), USNM 197336 (Dom. Rep., San Cristobal, Villa Altagracia, Ingenio Catarey, 'Come Hombre'; 18.6864, -70.1778). ***Caribicus darlingtoni*** (n=17). MALT 00988–91, 00997 (Dom. Rep., La Vega, Constanza, 16.9 km SSE of), MCZ R-44374–76 (Dom. Rep., Valle Nuevo; 18.809, -70.682), USNM 107563–64 (Dom. Rep., Valle Nuevo; 18.8, -70.6833), USNM 328801–04 (Dom. Rep., La Vega, 36.7 km SE Constanza via old road to San Jose de Ocoa; 8.7175, -70.6011), USNM 328805–07 (Dom. Rep., La Vega ca. 37 km SE of Constanza via new road to San Jose de Ocoa; 18.7056, -70.5981). ***Caribicus warreni*** (n=14). AMNH 103215 (Haiti, Tortue Island, Palmiste; 20.05491, -72.79248), ANSP 38501 (Haiti, locality not available), ANSP 38502 (Dom. Rep., locality not available [pet trade]), KU 227530 (Haiti, Nord-Ouest, Tortue Island, Palmiste; 20.01667, -72.73333) USNM 197369 (Dom. Rep., Puerto Plata, Comedero; 19.8183, -71.0617), MNHNSD 723–25, 727–29, 731, USNM 59435 (Haiti, Nord-Ouest, Riviere des Barres), 1 unnumbered specimen. ***Celestus barbouri*** (n=14). ANSP 38503 (Jamaica, Trelawny, Windsor, 0.5 km N of; 18.3579, -77.6482), BMNH 1965.234–35 (one of the series) (Jamaica, St. Ann, Spur Tree, Manchester, Mt Diabolo), BMNH 1936.12.1.110 (Jamaica, St. Elizabeth, Springfield), MCZ R-45169 (Jamaica, Mandeville; 18.04168, -77. 50714), USNM 38949–50 (Jamaica, Manchester, Mandeville), USNM 328145–47 (Jamaica, Trelawny, Quick Step, ca. 0.8 km N of), USNM 328148–49, USNM 328151–53 (Jamaica, Trelawny, vicinity of Quick Step). ***Celestus capitulatus*** **sp. nov.** (n=36). AMNH 72365, 139138–39 (Jamaica, 1 mi S of Black River; 18.02468, -77.85169), BMNH 1938.4.13.8 (Jamaica, Alligator Pond, south coast; 17.87113, -77.56495), BMNH 1970.1717 (Jamaica, Westmoreland, Negril Hill, Holmes Bay; 18.25068, -78.30011), BMNH 1970.1713 (Jamaica, Booby Cay; 18.338120, -78.34763), BMNH 1970.1718 (Jamaica, Westmoreland, North of Springfield; 18.17965, -77.87171), BMNH 1970.1721–24 (one of series) (Jamaica, Alligator Pond; 17.87113, -77.56495), BMNH 1970.1719 (Jamaica, St. Elizabeth, Black River; 18.03372, -77.85692), BMNH 1970.1715–16 (Jamaica, Westmoreland, Negril; 18.26819, -78.34709), KU 229232–33 (Jamaica, Westmoreland, 2 mi SW Old Hope), KU 229244 (Jamaica, Westmoreland, 0.3 mi NW Whitehouse), KU 229250–51 (Jamaica, Westmoreland, 0.5 mi SE Whitehouse), KU 229252–58, 229260 (Jamaica, Westmoreland, 0.7 mi NW Bluefields), KU 229273–74 (Jamaica, Westmoreland, 0.1 mi N Beeston Spring), KU 229275–76 (Jamaica, Westmoreland, 3 mi N Kilmarnoch), KU 229277, 229279–82 (Jamaica, St Elizabeth, 3 mi SE Whitehouse), USNM 328168 (Jamaica, St. Elizabeth, Knoxwood), USNM 328157, 328169 (Jamaica, Westmoreland, 4.5 km W of Old Hope [at Little Bay]). ***Celestus crusculus*** (n=26). ANSP 38504 (Jamaica, Trelawny, 0.3 km W Duncans, jct with Silver Sands access road; 18.47105, -77.53887), BMNH 1940.3.11.69 (Jamaica, Constant Springs; 18.05851, -76.78692), BMNH 1970.1714 (Jamaica, St. Ann, Runaway Bay; 18.45657, -77.32621), BMNH 1954.1.2.37, 1965.129, 1965.135, 1965.139 (Jamaica, St. Andrews, Mona; 18.01077, -76.74763), BMNH 1970.1726 (Jamaica, Red Hills; 18.07397, -76.86104), BMNH 1970.1727 (Jamaica, Papine, St. Andrew; 18.01156, -76.73633), MCZ R-6051 (Jamaica, Kingston; 18, -76.8), MCZ R-45163, R-45166–67 (Jamaica, Mandeville; 18.04168, -77.50714), USNM 108220–22 (Jamaica, Manchester, Mandeville), USNM 328159–67 (Jamaica, Trelawny, Duncans, 0.3 km W jct with Silver Sands access road); 18.47105, -77.53887), USNM 328186 (Jamaica, St. Catherine, 5.6 km SW of Braeton, at Hellshire Beach in Hellshire Hills). ***Celestus duquesneyi*** (n=1). MCZ R-45194 (Jamaica, Portland Point;17.75573, -77.16471). ***Celestus hesperius*** (n=3). USNM 328154–55 (Jamaica, Hanover, Content, 3.2 km SE of; 18.351, -77.991), USNM 328156 (Jamaica, Westmoreland, Town Head, 5.3 km N of). ***Celestus hewardi*** (n=23). BMNH 1938.4.13.6 (Jamaica, Mandeville; 18.03359, -77.50431), BMNH 1946.8.7.99 (Jamaica), BMNH 1845.12.27.6–8 (one of series) (Jamaica), KU 226546 (Jamaica, Trelawny, Duncans), KU 226549–50 (Jamaica, Westmoreland, 6.9 mi SSE Darliston). MCZ R-45173, R-45177, R-127906–07 (Jamaica, Manchester, Mandeville; 18.04168, -77.50714), USNM 102651 (Jamaica, Kensworth), USNM 108231, 108234, 108238 (Jamaica, Manchester, Mandeville), USNM 108329–35 (Jamaica, St. James, 5 mi W of Montego Bay), USNM 251918 (Jamaica, Windsor, 1.1 mi NW of Trelawny; 18.3722, -77.6583), USNM 251919 (Jamaica, St. Ann, 1.5 mi NE of Orange Valley). ***Celestus jamesbondi*** **sp. nov.** (n=41). AMNH 107325–29 (Jamaica, St. Mary's, 2 mi W Port Maria, Dowling's house; 18.36705, -76.91180), KU 229363 (Jamaica, St. Mary, 6.1 mi W Oracabessa), KU 229364–65 (Jamaica, St. Mary, 0.6 mi S Spring Valley), KU 229366 (Jamaica, St. Mary, 4.3 mi W, thence 1 mi S Oracabessa), KU 229368 (Jamaica, St. Mary, 8.6 mi WNW Anotto Bay), KU 229369–70 (Jamaica, St. Mary, 3.3 mi W, thence 1.4 mi S Oracabessa), KU 229371–72 (Jamaica, St. Mary, 2.8 mi W Oracabessa), KU 229373 (Jamaica, St. Mary, 4.7 mi E Ocho Rios), KU 229374 (Jamaica, St. Mary, 2.5 mi N Port Maria), KU 229375–76 (Jamaica, St. Mary, 3.2 mi E Oracabessa), KU 229377 (Jamaica, St. Mary, 2.8

mi E Oracabessa), KU 229378 (Jamaica, St. Mary, 2 mi E Oracabessa), KU 229379 (Jamaica, St. Mary, 2.8 mi E Oracabessa), MCZ R-45149–50 (Jamaica, None Such, 6 mi SE of; 18.28333, -76.90000), MCZ R-45152–53 (Jamaica, St. Mary, Brimmer Hall, 4 miles S. of Port Maria; 18.34499, -76.91498), MCZ R-45154–55 (Jamaica, St. Mary, N Port Maria; 18.36849, -76.88946), USNM 328170 (Jamaica, Clarendon, Jackson's Bay, on beach at the hunting club), USNM 328171 (Jamaica, Clarendon, ca. 1.6 km ESE of Jackson's Bay [at entrance to Jackson's Bay Caves]), USNM 328172 (Jamaica, St. Mary, vicinity of town of Jack's River), USNM 328173 (Jamaica, St. Mary, ca. 1.6 km S of Oracabessa, on road to Jacks River), USNM 328174–75 (Jamaica, St. Mary, 6.2 km W of Oracabessa), USNM 328176 (Jamaica, St. Mary, Salt Gut, vicinity of Boscobel Airport [E side]), USNM 328177–79 (Jamaica, St. Mary, 2.9 km N of Port Maria), USNM 328180, 328182–84 (Jamaica, St. Mary, ca. 6.4 km S of Port Maria). ***Celestus macrolepis*** (n=2). BMNH 1946.8.3.82 (no locality; restricted here to Jamaica), BMNH 1961.1851 (Jamaica). ***Celestus macrotus*** (n=7). ANSP 38505 (Haiti, Sud-Est, Southeast of Pic La Selle; 18.32887, -72.02184), ANSP 38506 (Haiti, Ouest, southeast of Pic La Selle; 18.32887, -72.02184), MALT 00796–99 (Dom. Rep., Pedernales, 7 km NNE of Los Arroyos, helipad at Loma del Toro), USNM 286917 (Haiti, Ouest, ca. 15 km W of Gros Cheval by logging roads, northeastern slope of Morne La Selle in the Massif de la Selle; 18.3509, -71.9020). ***Celestus microblepharis*** (n=1). MCZ R-55764 (Jamaica, St. Mary, Boscobel; 18.40406, -76.96879). ***Celestus molesworthi*** (n=11). BMNH 1970.1747 (Jamaica, St. Thomas, Trinityville, Half a Bottle Trail; 17.96078, -76.521861), BMNH 1965.194, BMNH 1970.1731–36 (one of series), BMNH 1970.1737 (Jamaica, St. Thomas, Morant Point; 17.92033, -76.18015), BMNH 1970.1741 (Jamaica, Portland, Priestman's River; 18.13437, -76.33726), MCZ R-45184–85 (Jamaica, Kingston; 18.01788, -76.80990), USNM 108158–59 (Jamaica, Portland, 1 mi S of Buff Bay), USNM 117672 (Jamaica, St. Andrew, Clydesdale), USNM 326600 (Jamaica, St. Thomas, 4.8 mi N of Hordley). ***Celestus occiduus*** (n=6). ANSP 9776, BMNH 1970.1816, BMNH XV.115.A, MCZ R-131774 (Jamaica), USNM 73272 (Jamaica, St. Elizabeth, Balaclava), USNM 102652 (Jamaica, Manchester, Kensworth, near Newport). ***Celestus oligolepis*** **sp. nov.** (n=1). USNM 328158 (Jamaica, Westmoreland, 7.0 km WSW of Old Hope; 18.2232, -78.2861). ***Celestus striatus*** (n=3). BMNH 1946.8.8.3 (no locality; restricted here to Jamaica), KU 226528 (Jamaica, Trelawny, Windsor), MCZ R-125601 (Jamaica, Trelawny Forest; 18.35195, -77.64782). ***Comptus alloeides*** (n=44). AMNH 27748 (Dom. Rep., Samaná), AMNH 38376–77, 39877–80, 40261–62, 40264, 40267–68, 40396, 40402, 40404, 40980, 40982–83 (Dom. Rep., Samaná; 19.20308, -69.33877), ANSP 40232 (Dom. Rep., Samaná, Laguna), MCZ R-44398 (Dom. Rep., Sanchez; 19.00000, -70.66667), MCZ R-77152 (Dom. Rep., Samaná, 6 km E. Sanchez; 19.22330, -69.56140), KU 226555 (Dom. Rep., Samaná, 13 km W Samaná; 19.205, -69.433), KU 226556 (Dom. Rep., Samaná, 6 km W Samaná; 19.24, -69.36), KU 226557–60 (Dom. Rep., Samaná, 8 km W Samaná; 19.196, -69.379), KU 226561 (Dom. Rep., Samaná, 13 km W Samaná; 19.205, -69.433), KU 226562 (Dom. Rep., Samaná, 6 km E Sanchez; 19.227, -69.562), KU 226563 (Dom. Rep., Samaná, 11 km E Sanchez; 19.221, -69.515), KU 226564–69 (Dom. Rep., Samaná, 14 km E Sanchez; 19.221, -69.515), USNM 61931–32 (Dom. Rep., Samaná, near Laguna), USNM 62363–64 (Dom. Rep., Samaná, Sanchez), USNM 66760–61 (Dom. Rep., Samaná, Peninsula de Samaná; 19.25, -69.4167), USNM 66975–76 (Dom. Rep., Samaná, Laguna, 6 mi NE of Samaná, Samaná Peninsula; 19.2358, -69.2006). ***Comptus arboreus*** **sp. nov.** (n=9). ANSP 38538–40 (Haiti, Grand'Anse, Belandier, 5.0 km N of Dame Marie; 18.58569, -74.40762), ANSP 38543 (Haiti, Grand'Anse, 1.5 km N of Carcasse; 18.3852, -74.44755), KU 227117–18 (Haiti, Grand'Anse, ca 5 km (airline) S Dame Marie; 18.51371, -74.42333), SBH 191945–46 (Haiti, Grand'Anse, 0.8 km E of Dame-Marie; 18.55925, -74.41550), SBH 269065 (Grand'Anse, Bourdon (9.2 km E Ause D'Hainalt); 18.48225, -74.36113). ***Comptus badius*** (n=6). AMNH 17079, 120486–87 (Navassa Island), USNM 25817–18, 157378 (Navassa Island; 18.4028, -75.0125). ***Comptus maculatus*** (n=9). ANSP 38507 (Cayman Islands, Cayman Brac, 0.7 km E Hawkesbill Bay on A7, ~10 km E West End, 1.7 km E Ashton Reid Drive; 19.7142, -79.7864), ANSP 38508–11 (Cayman Islands, Cayman Brac, West End, Tiara Beach Hotel and surrounding area; 19.7192, -79.8263), ANSP 38512 (Cayman Islands, Cayman Brac, 1.2 km E of West End; 19.698, -79.8696), MCZ R-6231 (Cayman Islands, Cayman Brac; 19.71828, -79.80774), SBH 266554 (Cayman Islands, Cayman Brac, West End, Tiara Beach Hotel and surrounding area; 19.7192, -79.8263), USNM 107973 (Cayman Islands, Cayman Brac; 19.7181, -79.8083). ***Comptus stenurus*** (n=14). ANSP 38544–45 (Haiti, Sud, Carretour Joute, 8.6 km SW of, near Riviere la Source on the Presquille de Port Salut; 18.07109, -73.89951), ANSP 38546 (Haiti, Sud, Caye Madeline; 18.32419, -74.00949), ANSP 38550 (Haiti, Sud, Port Salut Gumbwa near Ça Vilason; 18.04923, -73.7887), BMNH 1964.309–10 (Haiti, Sud, Camp Perrin), KU 227167 (Dom. Rep., Sud, 4.5 mi N Camp Perrin, 18.41118, -73.821), MCZ R-3612 (Haiti, Jeremie; 18.63894, -74.11529), MCZ R-119419–20 (Haiti, Castillon; 19.68333, -72.36667), MCZ R-133108–09 (Haiti, Sud, St Croix, 7-8 mi NE Paillant; 18.44610, -73.11000),

SBH 269020 (Haiti, Sud, Port Salut Gumbwa, near Ca Vilason; 18.04923, -73.7887), SBH 267494 (Haiti, Sud, Île-à-Vache; 18.10379, -73.69400). ***Comptus weinlandi*** (n=53). ANSP 38513–14 (Dom. Rep., Hato Mayor, El Valle, 5.6 km airline W of; 18.97525, -69.43195), ANSP 38515–22 (Dom. Rep., Hato Mayor, Loma del Fresca, Sabanade la Mar 5.7 km airline SW of; 18.27942, -71.40496), ANSP 38523 (Dom. Rep., El Seibo, Nisibon, 4.2 km N, 8.4 km W of [airline], at Playa Cucharera [= beach W Punta Limon]; 18.9936, -68.87), ANSP 38524–27 (Dom. Rep., Hato Mayor, Sabana de la Mar, 7.8 km S of; 18.9883, -69.38955), ANSP 38528 (Dom. Rep., El Siebo, Sabana de Nisibon, 5 km airline W of; 18.953, -68.8605), ANSP38529–31 (Dom. Rep., Duarte, San Francisco de Macoris, 10.1 km NE of; 19.34473, -70.18077), ANSP 38532–33 (Dom. Rep., Salcedo, Tenares, 23.2 km N thence 4.5 km W of [= 0.2 km E Jaiba]; 19.5445, -70.3362), ANSP 38534–37 (Dom. Rep., Los Tabucos, Tenares, 8.8 km N thence 0.5 km W of; 19.4324, -70.3525), ANSP 38541 (Haiti, Nord'Ouest, Bombardopolis; 19.69135, -73.34209), ANSP 38542 (Haiti, Artibonite, Ça Soleil, 11.8 km W of; 19.46955, -72.77713), ANSP 38547–48 (Dom. Rep., Independencia, La Descubierta, 5.1 km NW of; 18.5711, -71.7549), ANSP 38549 (Haiti, Ouest, Petionville, 10.1 km ENE of,18.51893, -72.20856), ANSP 38551–54 (Haiti, Ouest, Thomaseau, 18.7 km E of; 18.67476, -72.00285), MCZ R-126742 (Dom. Rep., 15 km S Nagua; 19.27970, -69.82670), MCZ R-163165 (Haiti, l'Ouest, Mariani (on Port-au-Prince to Leogane road); 18.55000, -72.60000), SBH 191620, 191649–50 (Haiti, Ouest, Thomazeau 18.1 km E of; 18.67268, -72.00621), SBH 191622–24 (Haiti, Ouest, Thomaseau, 18.7 km E of; 18.67476, -72.00285), SBH 192406, 192408 (Haiti, Artibonite, Ça Soleil, 11.8 km W of; 19.46955, -72.77713), SBH 192424 (Haiti, Ouest, Petionville, 10.1 km ENE of,18.51893, -72.20856), SBH 193218 (Dom. Rep., Salcedo, Tenares, 23.2 km N thence 4.5 km W of [= 0.2 km E Jaiba]; 19.5445, -70.3362), SBH 194492–93 (Dom. Rep., Independencia, La Descubierta, 5.1 km NW of; 18.5711, -71.7549), SBH 267001 (Dom. Rep., Hato Mayor, Loma del Fresca, Sabanade la Mar 5.7 km airline SW of; 18.27942, -71.40496), SBH 267017, 267031 (Dom. Rep., Hato Mayor, Sabana de la Mar, 7.8 km S of; 18.9883, -69.38955), USNM 10260 (Dom. Rep., Puerto Plata, Puerto Plato (= San Felipe de Puerto Plata); 19.7947, -70.6989), USNM 12145 (Haiti, Ouest, Port-au-Prince, within 25 mi of; 18.5383, -72.3344). ***Guarocuyus jaraguanus*** (n=19). IIBZ-HER00001–08, MNHNSD 23.3912–16, 23.3934–37 (Dom. Rep., Pedernales, Parque Nacional Jaragua, Laguna de Oviedo Cayo de las Iguanas), MNHNSD 23.3948–49 (Dom. Rep., Pedernales, Laguna de Oviedo, Cayo Pei). ***Panolopus aenetergum*** (n=1). USNM 197323 (Dom. Rep., La Altagracia, Isla Catalinita, just south of central part of island, inland; 18.1928, -68.64). ***Panolopus aporus*** (n=41). AMNH 92798 (Dom. Rep., Pedernales, 5 mi NE Oviedo; 17.82645, - 71.35501), ANSP 38623–27 (Dom. Rep., Pedernales, Bucan Detwi; 17.73462, -71.50335), ANSP 38628–29 (Dom. Rep., Pedernales, Pedernales town, in palm grove; 18.029, -71.7471), ANSP 38630 (Haiti, Sud-Est, Southeast of Pic La Selle; 18.32388, -72.0264), ANSP 38630 (Haiti, Sud-Est, Southeast of Pic La Selle; 18.32887, -72.02184), KU 79827 (Dom. Rep., Barahona, 5 km NE Enriquillo; 17.93194, -71.19996), KU 226021–23, (Dom. Rep., Pedernales, 13.1 mi SW Enriquillo; 17.786, -71.379), KU 226024, 226027–28 (Dom. Rep., Barahona, 0.5 mi NE Caleton; 17.93847, -71.19463), KU 226041–42 (Dom. Rep., Pedernales, 13.1 mi SW Enriquillo; 17.79390, -71.37530), MCZ R-77159 (Dom. Rep., Pedernales, 13.1 mi SW Enriquillo; 17.79390, -71.37530), SBH 269908 (Haiti, Sud-Est, Pic La Selle Sud-Ouest; 18.32388, -72.0264), SBH 269910–11 (Haiti, Sud-Est, Pic La Selle Sud-Ouest; 18.32887, -72.02184), USNM 328742 (Dom. Rep., Barahona, ca. 4–5 km S, 2.7 km W of Barahona via coast road and road to Filipinas; 18.1619, -71.0967), USNM 328743 (Dom. Rep., Barahona, ca. 4.5 km S, 4.0 km W of Barahona via coast road and road to Filipinas; 18.1531, -71.1025), USNM 328744 (Dom. Rep., Barahona, 15 km SSW of La Guazara; 18.1333, -71.1667), USNM 328766–68 (Dom. Rep., Pedernales, Juancho; 17.8564, -71.295), USNM 328769–72, (Dom. Rep., Pedernales, Los Arroyos; 18.2308, -71.7564), USNM 328793 (Dom. Rep., Barahona, 11.3 km S of Barahona; 18.1267, -71.0731), USNM 328794–800 (Dom. Rep., Pedernales, 6.4 km SW, 0.7 km SE [road] of Juancho; 17.8358, -71.3439). ***Panolopus charlcorhabdus*** (n=8). KU 225001 (Dom. Rep., La Altagracia, 0.9 mi SE El Macao; 18.75741, -68.54029), KU 225002 (Dom. Rep., La Romana, 8 km E La Romana; 18.41667, -68.89095), KU 225003 (Dom. Rep., La Altagracia, 3.2 mi W Higuey; 18.61667, -68.7488), KU 225076–77 (Dom. Rep., La Altagracia, mouth Rio Chavon, W side; 18.4, -68.894), KU 225078–79 (Dom. Rep., La Altagracia, 3.3 mi SE El Macao; 18.754, -68.501), MCZ R-77158 (Dom. Rep., La Romana, 0.9 mi. SE El Macas; 18.42787, -68.97425). ***Panolopus costatus*** (n=24). ANSP 38558 (Haiti, Grand'Anse, Abricots [outskirts]; 18.64783, -74.30721), ANSP 38559 (Haiti, Grand'Anse, 17.0 km S of Beaumont; 18.38472, -73.87569), ANSP 38560 (Haiti, Sud, 11.6 km NW of Les Anglais, on Morne Grand Bois; 18.37417, -74.29928), ANSP 38561 (Haiti, Sud, ca. 1 km NE of Tiburon; 18.32913, -74.38797), KU 225088 (Haiti, Grand'Anse, 7 mi W Jeremie; 18.64097, -74.22092), KU 225089, 225091 (Haiti, Grand'Anse, btw La Foret and Jeremie; 18.644, -74.153), KU 225116–17 (Haiti, Grand'Anse, ca 3 km (airline) SW Corail; 18.54806, -73.91232), KU 225171, 225173 (Haiti, Grand'Anse, Castillon to ca 2 km

S Castillon; 18.50763, -74.1), MCZ-3606 (Haiti, Jeremie; 18.63894, -74.11529), MCZ R-134262–64 (Haiti, Sud, St Croix, 7-8 mi NE Paillant; 18.44610, -73.11000), SBH 268974 (Haiti, Sud, ca. 1 km NE Tiburon; 18.32913, -74.38797), SBH 269064 (Haiti, Grand'Anse, 6.2 km E Ause D'Hainalt, source cacao; 18.4887, -74.3815), USNM 328773, 328775–79 (Haiti, Grand'Anse, Castillion; 18.52, -74.1), USNM 328780 (Haiti, Grand'Anse, 3 km SW of Castillion; 18.4975, -74.1201). ***Panolopus curtissi*** (n=18). ANSP 38632 (Dom. Rep., Independencia, 5.1 km NW of La Descubierta; 18.5711, -71.7549), ANSP 38633–35 (Haiti, Artibonite, La Gonave, near Richard, along coast road; 18.91220, -73.05222), KU 226192 (Haiti, Artibonite, Pierre Payen, 9 mi S St Marc; 19, -72.73333), KU 226242–43 (Haiti, Ouest, 10.1 km SE Montrouis; 18.88548, -72.63219), KU 226248 (Haiti, Ouest, 0.3 mi S Terre Rouge; 18.5623, -74.25), KU 226253 (Dom. Rep., Independencia, 2 km E Boca de Cachon; 18.555, -71.82078), SBH 194494 (Dom. Rep., Independencia, 5.1 km NW of La Descubierta; 18.5711, -71.7549), MCZ R-80800 (Haiti, Gonave Island, Pointe-a-Roquettes; 18.77920, -73.05810), USNM 117265 (Haiti, Ouest, Trou Caiman; 18.6564, -72.1442), USNM 117266–68, 117337–38, 129399 (Haiti, Trou Forban; 18.92, -72.65). ***Panolopus diastatus*** (n=16). AMNH 49816 (Haiti, N part of Haiti, near intersection of Jean Rabel and Port a l'Ecu Road), ANSP38636–40 (Haiti, Nord'Ouest, Bombardopolis; 19.69135, -73.34209), ANSP 38641–42 (Haiti, Nord'Ouest, about 3.5 mi SW of Bombardopolis, on S facing slope of Morne Tony; 19.65806, -73.36672), ANSP 38643–46 (Haiti, Nord'Ouest, Mole St. Nicolas; 19.80583, -73.37556), MCZ R-63395, MCZ R-63402, R-63400 (Haiti, Bombardopolis; 19.67849, -73.33289), MCZ R-63412 (Haiti, Mole St. Nicolas; 19.80477, -73.37529). ***Panolopus emys*** (n=20). KU 225005–06, 225008–17 (Haiti, Nord-Ouest, ca Palmiste, Tortue Island, 20.018, -72.725), MCZ R-119382 (Haiti, Nord-Ouest, Tortue Island, Palmiste; 20.018, -72.725), MCZ R-119396–98 (Haiti, Nord-Ouest, Tortue Island, Palmiste; 20.018, -72.725), USNM 167300, 167316–18 (Haiti, Nord-Ouest, Palmiste; 20.018, -72.725). ***Panolopus hylonomus*** (n=12). AMNH 49771 (Dom. Rep., at caves near Rio Chavon, E of La Romana), AMNH 92799 (Dom. Rep., Distrito Nacional, 7 mi E Boca Chica; 18.40452, - 69.52073), KU 226274 (Dom. Rep., La Altagracia, 0.5 mi NW Boca de Yuma; 18.38847, -68.60538), KU 226275–76 (Dom. Rep., La Altagracia, 4 mi SE San Rafael del Yuma; 18.39221, -68.62358), KU 226281–82 (Dom. Rep., La Altagracia, Juanillo; 18.483, -68.395), KU 226387 (Dom. Rep., La Altagracia, 1.2 km SSW Punta Cana; 18.50498, -68.37278), MCZ R-75028–29 (Dom. Rep., La Altagracia, Juanilo; 18.46970, -68.40190), MCZ R-77160 (Dom. Rep., La Romana, 0.5 mi. N. Boca de Yuma; 18.38190, -68.61190), USNM 259954 (Dom. Rep., La Altagracia, Punta Palmillas, "Caldera" Pigeon shooting camp on Lagoon E of; 18.2, -68.75). ***Panolopus lanceolatus*** **sp. nov.** (n=9). KU 226436–39 (Haiti, Artibonite, 1.2 mi W Ennery; 19.48333, -72.50173), MCZ R-190691–92 (Haiti, Nord, first and only major intersection between Ennery and Plaisance, couple hundred meters E on intersecting road; 19.52387, -72.45154), MCZ R-63383–84 (Haiti, Dondon; 19.52560, -72.23920), MCZ R-63386 (Haiti, Jean Bernard between Cap Haitien and Grande Riviere du Nord; 19.70030, -72.17670). ***Panolopus lapierrae*** **sp. nov.** (n=5). ANSP 38578 (Haiti, Artibonite, 11.8 km W of Ça Soleil; 19.46955, -72.77713), KU 226257–58, 226261 (Haiti, Artibonite, 7.6 mi W Ça Soleil; 19.49377, -72.76905), SBH 192407 (Haiti, Artibonite, 11.8 km W of Ça Soleil; 19.46955, -72.77713). ***Panolopus leionotus*** (n=20). AMNH 92796 (Dom. Rep., Azua, 5 km S Padre las Casas; 18.69912, -70.92983), ANSP 38562–65 (Dom. Rep., Baoruco, Apolinar Perdomo, ca. 5 km N of; 18.593, -71.3979), ANSP 38566 (Dom. Rep., San Juan, 1.6 mi NNE El Azul; 18.717, -71.413), ANSP 38567–68 (Dom. Rep., Baoruco, Loma Monte Bonito; 18.60139, -71.39056), ANSP 38573–77 (Dom. Rep., Elias Pina, Rosa de la Piedra, 0.6 km NE of; 18.77689, -71.7157), KU 225018–19 (Dom. Rep., San Juan, 15 km SE San Juan; 18.69822, -71.0654), MCZ R-77154 (Dom. Rep., San Juan, 15 km E. San Juan; 18.73250, -71.11860), SBH 266286 (Dom. Rep., San Juan, 1.6 mi NNE El Azul; 18.717, -71.413), SBH 266313 (Dom. Rep., Elias Pina, Rosa de la Piedra, 0.6 km NE of; 18.77689, -71.7157), USNM 328752–53 (Dom. Rep., Elisa Pina, 17 km N Cacique Enriquillo (31 km N of Los Pinos); 18.7069, -71.7703). ***Panolopus marcanoi*** (n=23). ANSP 38648 (Dom. Rep., Santiago, La Lagunas; 19.1512, -71.0102), ANSP 38649 (Dom. Rep., Santiago, Loma los Banaderos, east slope; 19.1177, -71.0362), ANSP 38650–62 (Dom. Rep., Santiago, Valle de Bao; 19.0685, -71.0361), KU 226551–54 (Dom. Rep., Santiago, Valle de Bao, Cordillera Central (rd to Pico Duarte); 19.08333, -71.03333), SBH 193288–89, SBH 193293 (Dom. Rep., Santiago, Valle de Bao; 19.0685, -71.0361), USNM 197299 (Dom. Rep., Santiago, Valle de Bao; 19.0833, -71.0333). ***Panolopus melanchrous*** (n=80). AMNH 38378–85, 39876, 40258, 40260, 40263, 40265–66, 40272, 40393–95 40397–401, 40403, 40405, 44745–52, 44825, 44827–28 (Dom. Rep., Samaná; 19.20308, - 69.33877), AMNH 39361 (Dom. Rep., Samaná, Roja Cabo), AMNH 40231 (Dom. Rep., Samaná, Laguna), AMNH 40945, 40947–48, 40950–54, 40956–58, 40960–61, 40967, 40969–72 (Dom. Rep., La Bracita [=Los Bracitos]), AMNH 40975 (Dom. Rep., Paso Bajito; 19.06498, -70.60383), AMNH 40981 (Samaná, Samaná; 19.20308, -69.33877), KU 225021 (Dom. Rep., Puerto Plata, 3 km NE Sosua; 19.78583, -70.49643), KU

225028 (Dom. Rep., La Vega, Dom. Rep., 7 km E Paso Bajito), KU 225232 (Dom. Rep., Espaillat, 10 mi N San Victor; 19.61205, -70.51667), KU 225255 (Dom. Rep., Hato Mayor, 2.3 mi N El Valle), KU 225261, 225263, 225266 (Dom. Rep., La Altagracia, Playa El Coco, 46 km N Higuey), KU 225298–300 (Dom. Rep., Samaná, 7.6 mi NE Sanchez), KU 225311 (Dom. Rep., Samaná, 5.1 mi NW El Limon), KU 225313–14 (Dom. Rep., La Vega, 12 km NE Jarabacoa), KU 225315 (Dom. Rep., La Vega, 4 km S La Vega), KU 225318 (Dom. Rep., La Vaga, 1.5 km W Jayaco), KU 225321 (Dom. Rep., Puerto Plata, 0.25 km NW Sabaneta de Yasica; 19.66826, -70.38502), KU 225348 (Dom. Rep., Santiago, 0.5 mi SE Pedro Garcia; 19.59486, -70.64458), MCZ R-77157 (Dom. Rep., Espaillat, 8 km E. Gaspar Hernandez; 19.63170, -70.22000), USNM 62361 (Dom. Rep., Sanchez), USNM 65780 (Dom. Rep., Hato Mayor, Las Canitas; 19.0136, -69.2625), USNM 66678 (Dom. Rep., El Seibo, Guarabo), USNM 66679 (Dom. Rep., El Seibo, Jovero (= Miches); 18.9822, -69.0481). ***Panolopus neiba*** (n=27). AMNH 92797 (Dom. Rep., San Rafael, 15 km SW Elias Pina; 18.7999, -71.70147), ANSP 38579 (Dom. Rep., Independencia, ca. 7 km W of Los Pinos by road; 18.60033, -71.80860), KU 79826 (Dom. Rep., Elias Pina, 15 km S Comendador; 18.776, -71.719), KU 225030–31 (Dom. Rep., Elias Pina, 14 km SW Hondo Valle; 18.691, -71.746), KU 225353–54 (Dom. Rep., Independencia, Sabana Real, 0.7 mi W, 17.7 mi N La Descubierta; 18.63333, -71.80000), KU 225356–58 (Dom. Rep., Independencia, Sabana Real, 14 km N Los Pinos; 18.63333, -71.80000), MCZ R-77155 (Dom. Rep., San Rafael, 19 km SW Hando Valle; 18.682, -71.788), MCZ R-171776–77 (Dom. Rep., Baoruco, Alto de la Pena, stream just off the path from El Aguacate (La Venta) to Sabana del Silencio; 18.633333, -71.46667), USNM 328745–48 (Elias Pina, ca. 24 km N of Los Pinos; 18.6919, -71.78), USNM 328749–51 (Dom. Rep., Elias Pina, ca. 27 km N of Los Pinas; 18.6994, -71.7694), USNM 328754–56 (Dom. Rep., 17 km N of Cacique Enriquillo; 18.7069, -71.7703), USNM 328759 (Dom. Rep., Elias Pina, 13 km N of Cacique Enriquillo; 18.6936, -71.7747), USNM 328763 (Dom. Rep., Independencia, 9 km N of Cacique Enriquillo; 18.6783, -71.7883), USNM 328764 (Dom. Rep., Independencia, 7 km N of Cacique Enriquillo; 18.6742, -71.7731), USNM 328765 (Dom. Rep., Independencia, La Descubierta, 4.0 km W (airline) of 6.2 km N; 18.6241, -71.774). ***Panolopus nesobous*** (n=8). ANSP 38580–82 (Haiti, Sud, 10.7 km WNW of Les Platons Citadel, Caye Michel previously called Caye Paul; 18.33160, -74.02244), ANSP 38583 (Haiti, Sud, Île-à-Vache; 18.10516, -73.69288), KU 225032–33 (Haiti, Sud, Ile-a-Vache western end; 18.109, -73.706), MCZ R-77153 (Haiti, Sud, Ile-a-Vache, western end; 18.10560, -73.70810), SBH 269117 (Haiti, Sud, Plaine Formon near Caye Michel; 18.32420, -74.02581). ***Panolopus oreistes*** (n=53). ANSP 38585–96 (Haiti, Ouest, Berry; 18.30795, -72.25390), ANSP 38597 (Haiti, Ouest, 1.0 km SW of Berry; 18.30854, -72.72079), ANSP 38598–606 (Dom. Rep., Pedernales, Casetta Dos, ca. 22 km N of Aceitillar, by road on ridge of Sierra de Bahoruco; 18.2125, -71.53417), ANSP 38607–08 (Haiti, Sud-Est, Morne D'Enfer, southwestern edge of plateau; 18.33005, -72.37095), ANSP 38609–12 (Dom. Rep., Independencia, 20.8 km SE of Puerto Escondido; 18.2251, -71.5003), ANSP 38613–14 (Dom. Rep., Independencia, 23.1 km SE of Puerto Escondido; 18.2204, -71.5102), ANSP 38615–21 (Dom. Rep., Independencia, 23.9 km SE of Puerto Escondido; 18.21, -71.53), KU 225401 (Dom. Rep., 3 km N Enriquillo Barahona; 17.92711, -71.23333), KU 225410 (Dom. Rep., Barahona, 3 km N, 15 km SW Barahona; 18.15611, -71.14639), KU 225415 (Dom. Rep., Independencia, El Aguacate; 18.33333, -71.70000), KU 225509 (Dom. Rep., Ouest, Peneau), KU 225513, 225515 (Haiti, Ouest, Furcy; 18.41667, -72.30000), KU 225520, 225522 (Haiti, Sud-Est, Foret des Pins; 18.33167, -71.78778), KU 225531 (Haiti, Sud-Est, Thiotte; 18.25, -71.85000), MCZ R-74939, MCZ R-74940–41 (Haiti, Sud-Est, Oriani, nr Saltrou; 18.30000, -71.85000), SBH 192496 (Dom. Rep., Independencia, 23.9 km SE of Puerto Escondido; 18.21, -71.53), SBH 268567 (Haiti, Ouest, 1.0 km SW of Berry; 18.30854, -72.72079). SBH 268583, 268590 (Haiti, Ouest, Berry; 18.30795, -72.25390). ***Panolopus psychonothes*** (n=19). AMNH 16017–20 (Santo Domingo), AMNH 16021–25 (Dom. Rep., Azua, interior of Azua), KU 225034–35 (Dom. Rep., La Vega, 7.2 mi S Constanza; 18.845, -70.75), KU 225643–48 (Dom. Rep., La Vega, 16 km SE Constanza; 18.84, -70.7), KU 225651 (Dom. Rep., La Vega, 17.2 km SE Constanza; 18.828, -70.705), MCZ R-77156 (Dom. Rep., La Vega, 1 mi. S Constanza; 18.89310, -70.73220). ***Panolopus saonae*** (n=3). CM 52285 (Dom. Rep., Isla saonae, 0.5 mi. W Mano Juan; 18.13406, -68.72078), KU 226020, 225036 (Dom. Rep., Isla saonae, 0.5 mi. W Mano Juan; 18.13406, -68.72078). ***Panolopus semitaeniatus*** **sp. nov.** (n=8). ANSP 38569–72 (Haiti, Artibonite, Morne Boeuf; 19.07239, -72.25021), MCZ R-51434 (Haiti, Trou Farbou; 19.00000, -72.41667), SBH 269891–92, 269895 (Haiti, Artibonite, Morne Boeuf; 19.07239, -72.25021). ***Panolopus unicolor*** **sp. nov.** (n=1). ANSP 38647 (Dom. Rep., Perovia, 14.8 N, 7.8 km SE Cruce de Ocoa on dirt road; 18.46, -70.45). ***Sauresia agramma*** **sp. nov.** (n=4). ANSP 38685–88 (Haiti, Sud-Est, Morne D'Enfer, southwestern edge of plateau; 18.33005, -72.37095). ***Sauresia cayemitae*** **sp. nov.** (n=12). ANSP 38673 (Haiti, Grand'Anse, Grande Cayemite (helipad-camp); 18.63316, -73.75524), ANSP 38674–77 (Haiti, Grand'Anse, Grande Cayemite; 18.63562, -

73.75175), ANSP 38691 (Haiti, Grand'Anse, Pestel (5.0 km S of); 18.51329, -73.78463), KU 227730–31 (Haiti, Grand'Anse, Presqu'ile des Baraderes, ca Grand Boucan: 18.56667, -73.65000), KU 227740–41, 227746 (Haiti, Grand'Anse, Ile Grande Cayemite, ca Anse-a-Macon; 18.58333, -73.73333); SBH 274212 (Haiti, Grand'Anse, Grande Cayemite (waypoint 166); 18.63562, -73.75175). ***Sauresia gracilis* sp. nov.** (n=1). USNM 328852 (Haiti, Sud, 10.3 km NW of Port Salut; 18.1419, -73.9711). ***Sauresia habichi*** (n=11). ANSP 38681–83 (Haiti, Grand'Anse, Marche Leon, 8.0 km S of Grand'Anse; 18.51678, -74.08311), KU 227597–99 (Haiti, Grand'Anse, Corail (ca 3 km (airline) SW of); 18.54806, -73.91232), KU 227802–03 (Haiti, Grand'Anse, Roseau (ca 7.5 km (airline) SSE of, ca 2 km W of La Bastille; 18.35407, -73.9395), MCZ R-74595, R-74598 (Haiti, Trou-Bois on Jeremie Road; 18.45000, -73.90000), ZMB 1310 (Haiti, Jeremie). ***Sauresia manicula* sp. nov.** (n=4). ANSP 38667–69 (Haiti, Ouest, Berry; 18.30795, -72.25389), SBH 268588 (Haiti, Ouest, Berry; 18.30795, -72.253894). ***Sauresia pangnolae* sp. nov.** (n=11). ANSP 38684 (Haiti, Nippes, Morne Bois Pangnol; 18.41869, -73.77512), ANSP 38663–64 (Haiti, Grand'Anse, 8.0 km SSW of Baraderes; 18.44032, -73.66756), ANSP 38690 (Haiti, Grand'Anse, 5.0 km S of Pestel; 18.47942, -73.78744), KU 227822 (Haiti, Sud, Camp Perrin; 18.31667, -73.86667), KU 227823, 227827–28 (Haiti, Sud, 4.5 mi N Camp Perrin; 18.41118, -73.821), KU 227837–38, KU 227842 (Haiti, Sud, 11.8 mi N Cavaillon; 18.39199, -73.62571). ***Sauresia sepsoides*** (n=41). ANSP 38665–66 (Dom. Rep., Duarte, Batez Piedra on west side of Rio Pazabo; 19.06997, -69.90815), ANSP 38670–72 (Dom. Rep., Sanchez Ramirez, 8.6 km NE thence 8.1 km E of Cotui; 19.1037, -70.0531), ANSP 38678 (Dom. Rep., La Altagracia, 7.5 km W of La Zanga, at Rio Maimon; 18.8807, -68.7749), ANSP 38679–80 (Dom. Rep., Monte Plata, 4.3 km N of Majagual; 19.07539, -69.82842), ANSP 38692–96 (Dom. Rep., Hato Mayor, 5.0 km [airline] SW of Sabana de la Mar; 19.03968, -69.42737), 38697–702 (Dom. Rep., Hato Mayor, 7.8 km S of Sabana de la Mar; 18.9883, -69.38955), ANSP38703–05 (Dom. Rep., Salcedo, 23.2 km N, thence 4.5 km W of [= 0.2 km E Jaiba] Tenares; 19.5445, -70.3362), ANSP 38706–09 (Dom. Rep., Los Tabucos, 8.8 km N thence 0.5 km W of Tenares; 19.4324, -70.3525), BMNH 1946.8.29.29 (St. Domingo), SBH 193149 (Dom. Rep., Duarte, southern slopes of Loma Quita Espuela; 19.3627, -70.15819), SBH 266963–75 (Dom. Rep., Hato Mayor, 5.7 km airline SW Sabana de la Mar Loma del Fresca; 18.27942, -71.40496). ***Sauresia synoria* sp. nov.** (n=4). ANSP 38689 (Dom. Rep., Pedernales, at the Rio Mulito, 22 km N; 18.1544, -71.7581), MCZ R-131326–27 (Haiti, Thiotte on road to Sal Trou; 18.23470, -71.84440), SBH 160343 (Dom. Rep., Pedernales, at the Rio Mulito, 22 km N; 18.1544, -71.7581). ***Wetmorena agasepsoides*** (n=10). ANSP 38710–11 (Dom. Rep., Pedernales, Bucan Detwi; 17.73462, -71.50335), ANSP 38712 (Dom. Rep., Barahona, 0.3 km S, 13.5 km E airline Canoa; 18.3448, -71.032), ANSP 38713–14 (Dom. Rep., Barahona, 13.7 km due E [airline] of Canoa; 18.3477, -71.0314), ANSP 38715 (Dom. Rep., Pedernales, 14.5 km S of Los Arroyos; 18.1541, -71.7585), ANSP 38716 (Dom. Rep., Pedernales, Troudiye; 17.7548, -71.5284), KU 93387 (Dom. Rep., Azua, Barreras; 18.31667, -70.90000), USNM 166963–64 (Dom. Rep., Azua, Barreras; 18.3228, -70.9042). ***Wetmorena haetiana*** (n=38). ANSP 38717–18 (Haiti, Ouest, Berry; 18.30795, -72.25389), ANSP 38719–22 (Haiti, Ouest, Morne Cardineau; 18.34615, -72.18256), ANSP 38726 (Haiti, Ouest, Morne La Visite; 18.34737, 72.2835), ANSP 38727–42 (Haiti, Sud-Est, Pic La Selle; 18.32887, -72.02184), ANSP 38743 (Haiti, Ouest, southeast of Pic La Selle;18.33225, -71.91447), ANSP 38744–45 (Haiti, Ouest, waterfall in Parc La Visite; 18.3401, -72.26983), KU 79722–25 (Dom. Rep., Barahona, 24 km SW Barahona; 18.025, -71.141), SBH 268542–43 (Haiti, Ouest, Morne Cardineau; 18.34615, -72.18256), SBH 268564 (Haiti, Ouest, Morne La Visite; 18.34737, 72.2835), SBH 269929–30 (Haiti, Sud-Est, Pic La Selle; 18.32887, -72.02184), USNM 72600–01, 72604 (Ouest, Morne Cabaio (= Morne du Cibao), Massif de la Selle; 18.3569, -72.2589). ***Wetmorena mylica*** (n=26). AMNH 92086–87 (Dom. Rep., Barahona, 8 km NE Las Auyamas; 18.10173, -71.27814), AMNH 92088 (Dom. Rep., Barahona, 24 km SW Barahona; 18.02574, -71.14044), KU 228144–50 (Dom. Rep., Barahona, 24 km SW Barahona; 18.025, -71.141), MCZ R-77049 (Dom. Rep., Barahona, 24 km SW Barahona; 18.15500, -71.14860), USNM 150554–57 (Dom. Rep., Barahona, 24 km SW Barahona; 18.155, -71.1486), USNM 328854–55, 328857, 328863, 328865, 328871–72, 328875–76, 328878, 328881 (Dom. Rep., Barahona, 15.3 km S, 6.7 km E (road) of Cabral; 18.1094, -71.2292). ***Wetmorena obscura* sp. nov.** (n=3) USNM 328904–06 (Haiti, Sud-Est, ca. 15 km W of Gros Cheval, via logging roads, NE slope of Pic La Selle); 18.3367, -71.8686). ***Wetmorena orosaura* sp. nov.** (n=4). ANSP 38723–25 (Haiti, Sud-Est, Morne D'Enfer, southwestern edge of plateau; 18.33005, -72.37095), SBH 269864 (Haiti, Sud-Est, Morne D'Enfer, southwestern edge of plateau; 18.33005, -72.37095). ***Wetmorena surda*** (n=33). AMNH 92079–85 (Haiti, Ouest, Foret des Pins; 18.33167, -71.78778), ANSP 38748–54 (Dom. Rep., Independencia, 29.7 km SE of Puerto Escondido; 18.2051, -71.5503), ANSP 38746–47 (Dom. Rep., Independencia, Puerto Escondido; 18.2204, -71.5102), KU 228366, KU 228370–73 (Haiti, Sud-Est, Foret des Pins; 18.33167, -71.78778), MCZ R-77040 (Haiti, Ouest, Foret de Pins; 18.32940, -

71.79250), SBH 192540 (Dom. Rep., Independencia, Puerto Escondido; 18.2204, -71.5102), USNM 150548–53 (Haiti, Ouest, Forêt des Pins; 18.3278, -71.7875), USNM 328897–99 (Dom. Rep., Pedernales, 10.3 km S of El Aguacate, on Haitian border road; 18.2897, -71.7111), USNM 328900 (Dom. Rep., Pedernales, 6.6 km S of El Aguacate (on Haitian border road); 18.3008, -71.6944).